

1  
9  
9  
4

Abstracts

# URSI RADIO SCIENCE MEETING

A  
B  
S  
T  
R  
A  
C  
T  
S  
&  
P  
R  
O  
G  
R  
A  
M



JUNE 19-24, 1994

UNIVERSITY OF WASHINGTON  
SEATTLE, WASHINGTON USA

224

~~235~~

**NATIONAL ACADEMIES OF SCIENCE AND ENGINEERING  
NATIONAL RESEARCH COUNCIL  
OF THE UNITED STATES**

**INTERNATIONAL UNION OF RADIO SCIENCE**



**RADIO SCIENCE MEETING**

**JUNE 19-24, 1994**

**PROGRAM AND ABSTRACTS**

**THE UNIVERSITY OF WASHINGTON  
SEATTLE, WASHINGTON**



## **STEERING COMMITTEE**

### **CHAIR**

Gary E. Miller

### **VICE CHAIR AND URSI TECHNICAL PROGRAM CHAIR**

Akira Ishimaru

### **AP-S TECHNICAL PROGRAM CHAIR**

Leung Tsang

### **AP-S TECHNICAL PROGRAM**

#### **VICE CHAIR**

W. Preston Geren

### **EXHIBITS**

Yasuo Kuga

### **FINANCE**

David B. Peterson

### **INTERNATIONAL LIAISON**

Lisa Zurk

### **LOCAL ARRANGEMENTS**

Shira Broschat

### **PUBLICATIONS AND STUDENT PAPER CONTEST**

Chi Hou Chan

### **PUBLICITY**

Dale Winebrenner

### **REGISTRATION**

Yasuo Kuga

Craig Clayton

### **SECRETARY**

Richard J. Coe

### **SHORT COURSES**

John Sahr

Thomas Seliga

Roland Svensson

### **WORKSHOPS**

V.K. Tripathi

### **MEMBERS AT LARGE**

Tom Blakney

Robert Olsen

Irene Peden

### **CONFERENCE MANAGEMENT**

Jan Kvamme

## **THE UNITED STATES NATIONAL COMMITTEE FOR URSI**

### **CHAIRMAN**

David C. Chang

### **SECRETARY**

Susan K. Avery

### **VICE CHAIRMAN**

Dr. Charles M. Rush

### **IMMEDIATE PAST CHAIRMAN**

Chalmers M. Butler

## **URSI TECHNICAL PROGRAM COMMITTEE**

### **URSI TECHNICAL PROGRAM CHAIR**

Akira Ishimaru

### **URSI REVIEWERS**

Chi Hou Chan

Don Dudley

Bob Gardner

E.V. Jull

Yasuo Kuga

Henry Lai

James Lin

M. Kanda

J.W. Mink

Robert G. Olsen

C. Ramon

Jeff Young

## Table of Contents

Session	Title	Page
M-J8	Random Media I.....	1
M-U3	Numerical Methods I.....	13
M-U4	EMC/EMI and Noise.....	25
M-U5	Microstrip Lines.....	35
M-U6	Scattering I.....	47
M-J1	Random Media II.....	57
M-U1	Mesh Truncation Techniques for PDE's.....	69
M-U7	Electromagnetic Theory.....	77
M-U8	Numerical Methods II.....	89
M-U9	Antenna Measurements.....	101
M-U10	High Frequency Methods.....	109
M-U11	Propagation and Antennas.....	115
M-U12	Circuits and Devices for Micro and Millimeter Waves.....	123
M-U13	Time Domain Analysis I.....	129
M-U14	Scattering II.....	135
T-J2	Rough Surface Scattering I.....	147
T-U15	Absorbing Boundary Conditions and MEI.....	159
T-U16	EM Field Measurements.....	171
T-U17	Microwave and Millimeter Wave Devices I.....	181
T-U18	Scattering III.....	193
T-J3	Wave Propagation and Scattering (Honoring Akira Ishimaru).....	205
T-U19	Microstrip Antennas.....	219
T-U20	Antennas I.....	231
T-U21	Impulse Radar Measurements.....	243
T-U22	Inverse Problems.....	255

T-U23	Physical Characteristics of EM Field in Biological Media.....	267
T-U24	Microwave and Millimeter Wave Devices II.....	275
T-U25	Time Domain Analysis II.....	287
W-P1	Plenary Session .....	299
W-J4	Rough Surface Scattering II.....	301
W-J5	Nonlinear Electromagnetism.....	311
W-U26	Time Domain Analysis III.....	319
W-U27	Waveguides I.....	331
W-U28	Wedges and Spheroids .....	341
W-U29	Electronic Devices and Waveguides.....	351
W-U30	Microstrip Analysis.....	357
W-U31	Radio Wave Propagation for PCS.....	363
Th-J6	Rough Surface Scattering III.....	371
Th-U32	A Tribute to Roger F. Harrington.....	379
Th-U33	Measurements for Dielectric Measurements.....	389
TH-U34	Finite Element / Boundary Element.....	399
TH-U35	Antennas II.....	411
TH-U36	Chiral Medium .....	423
TH-U38	Periodic Surfaces.....	435
Th-J7	Random Media & Rough Surface Scattering.....	445
Th-U37	Fundamentals of Active and Passive Polarimetry.....	451
TH-U39	Waveguides II .....	461
Th-U40	Medical Applications of Radiofrequency Fields.....	471
TH-U41	Antennas III.....	483

MONDAY AM JOINT SPECIAL SESSION M-J8

Room: HUB 310

RANDOM MEDIA I

Chairs: S.M. Flatté, University of California; L.C. Andrews, University of Central Florida

Organizers: S. Broschat, Washington State University; A. Ishimaru, University of Washington

- 8:20 Frequency Decorrelation of Intensity Scintillations-Influence of Refractive Modulation 2  
\*B. Rickett, Univ. of California at San Diego
- 8:40 Numerical Solution of the Fourth Moment Equation and Comparison with the MATE Data 3  
\*C. Macaskill, Univ. of Sydney; T.E. Ewart, J..G. Ballard, Univ. of Washington
- 9:00 Numerical Simulation of Optical Waves Through Atmospheric Turbulence; Moments and 4  
PDFs of Log-Irradiance  
\*S.M. Flatté, Univ. of California at Santa Cruz; C. Bracher, Univ. of California at San  
Diego; G.-Y. Wang, Univ. of California at Santa Cruz
- 9:20 Propagation of Pulses in a Waveguide Filled with a Random Medium 5  
\*S.M. Flatté, J.A. Colosi, C. Bracher, Univ. of California, Santa Cruz
- 9:40 Path-Integral Results for Irradiance Moments in the Asymptotic Regime 6  
\*G.-Y. Wang, S. Flatté, Univ. of California; R. Dashen, Univ. of California at San Diego
- 10:00 Break
- 10:20 Double Passage of a Gaussian Beam Wave Through Atmospheric Turbulence 7  
\*L.C. Andrews, Univ. of Central Florida; W.B. Miller, J.C. Ricklin, Battlefield  
Environment Directorate
- 10:40 Effects of a Modified Spectral Model on the Spatial Coherence of a Laser Beam 8  
C.Y. Young, L.C. Andrews, Univ. of Central Florida
- 11:00 Quadruple Refraction of HF-Waves in the Ionosphere 9  
\*S. Yano, Kochi National College of Technology; A. Ishimaru, Univ. of Washington; T.  
Ogawa, Science Laboratory International
- 11:20 Dual-Parameter Methods of Radar Turbulence Detection 10  
\*F.J. Yanovsky, Kiev Inst. of Civil Aviation Engineering
- 11:40 Some Results of Sounding of Thunderstorm and Hail Clouds by Dual-Polarization 11  
Airborne Radar  
A. Shupiatsky, Central Aerological Observatory; F.J. Yanovsky, Kiev Inst. of Civil  
Aviation Engineering

## Frequency Decorrelation of Intensity Scintillations - Influence of Refractive Modulation.

Barney Rickett  
Electrical and Computer Engineering Dept.,  
University of California at San Diego

The correlation function of intensity fluctuations (scintillations) versus frequency is studied for a phase screen with the dispersive properties of a plasma, under conditions that the strength of scintillation is strong but not very strong. The correlation function is evaluated numerically as a function of the strength of scintillation, using the theoretical analysis of Codona et al. (Radio Sci., vol 21, 815, 1986). The standard approximation for strong scintillation is that the correlation of intensity is the square of the correlation of electric field (second moment), after first removing the effect of refraction. The cross spectrum given by equation (32) of Codona et al. gives a more precise formulation, which includes the influence of refractive phase gradients on the scale of the scattering disk. The correlation function of intensity, computed via the Fourier transform of the cross spectrum, is displayed versus the scaled frequency difference. The scaling removes the first order dependence on the strength of scattering. The result shows how the computation approaches the standard asymptotic result, as the strength of scattering increases. The effect is a decorrelation over a narrower frequency difference than in the asymptotic limit.

Simulations of scattering from a screen are also presented, which support this analysis, and show that the extra decorrelation is due to frequency dependent displacements of the diffraction pattern, due to the frequency dependence of the angles of refraction. These refractive displacements are modelled and a simplified theory is formulated which gives results in agreement with the formal analysis. This simplified refractive modulation model is then used to estimate the typical bias in the interpretation of cross correlation functions based on the standard asymptotic formula. The ratio of the true characteristic decorrelation bandwidth to the asymptotic result is plotted versus  $u$ , which is the strength of scintillation defined as the ratio of the Fresnel scale to the field coherence scale.

Applications to scintillation in the interplanetary and interstellar plasma are discussed. For the interplanetary case observations are made of strong scintillation for lines of sight near the Sun, corresponding to  $u$  values in the range 1 to 5. For the interstellar case observations of pulsars show very fine structure versus frequency, indicating  $u$  in the range 10-1000. When pulsars signals are displayed as dynamic spectra they often show diffractive features which drift in time versus frequency. The refractive modulation model is also used to predict the typical slopes of such drifting features.

**Numerical Solution of the Fourth Moment Equation and  
Comparison with the MATE Data**

**C. Macaskill \***

School of Mathematics and Statistics  
University of Sydney  
NSW 2006 Australia

**T.E. Ewart and J.G. Ballard**

Applied Physics Laboratory  
College of Ocean and Fishery Sciences  
University of Washington  
Seattle, Washington 98105

The fourth moment equation for intensity fluctuations has been extensively studied. Approximate analytical solutions have been available for over ten years, and there have been many numerical solutions of the equation since the early 1970's. However, when detailed comparisons are made with experimental data, such as that obtained in the MATE acoustical fluctuations experiment, it is found that there are some differences; this is particularly apparent when looking at the cross-frequency coherence, i.e. the cross-correlation between acoustic signals of different frequencies propagating through the same medium at the same time.

Corrections to the analytical approximations are very hard to evaluate, particularly when a realistic description of the medium, such as that encountered at MATE, is introduced. In addition, it is known that the analytical approximations do not accurately describe the cross-frequency problem. Numerical solutions suffer from the difficulty that extremely high resolution is required to resolve the fourth moment, and this is especially true when the scintillation index, or covariance of the intensity, is large. Recently Uscinski and co-workers, in a series of papers, have demonstrated that adaptive grid methods can be used to dramatically increase the numerical resolution without too great a computing time penalty, and hence they obtain very accurate results for idealized random media in the very strong fluctuation regime. These methods work just as well for the cross-frequency problem.

In the present paper we apply similar techniques to the solution of the fourth moment equation, but extend the methods to deal with a realistic description of the internal waves and finestructure encountered in MATE. We present results for the cross-frequency problem and discuss the dependence of these results on the precise details of the model used to describe the medium.

## Numerical simulation of optical waves through atmospheric turbulence; Moments and PDFs of log-irradiance

Stanley M. Flatté\*, Charles Bracher, and Guang-Yu Wang  
Physics Department, University of California, Santa Cruz, CA, 95064

Optical propagation through atmospheric turbulence is calculated by numerical simulation. The turbulence spectrum in the neighborhood of the inner scale is taken to be that described by Hill (R. Hill, *Waves in Random Media* 2, 179-201, 1992) as representing the real atmosphere. Distributions of irradiance are used to determine the first few moments and the probability density function (PDF) of irradiance and log-irradiance as a function of turbulence strength and inner scale. As turbulence strength increases, the irradiance variance is known to rise to a peak and then slowly fall toward the asymptotic value of unity. Our simulations cover the region from zero strength to a strength that is well past the peak. Irradiance variance as a function of turbulence strength and inner scale are compared with experiment for both a point source and an incident plane wave, and excellent agreement is found. There are no free parameters in this comparison, as the experiments included independent measurements of both turbulence strength and inner scale (M.E. Gracheva, A.S. Gurvich, S.O. Lomadze, V.I. Pokasov, and A.S. Khrupin. *Radiophys. Quantum Electron.* 17, 83-87, 1974; A. Consortini, F. Cochetti. J.H. Churnside, and R.J. Hill, *J. Opt. Soc. Am. A* 10, 2354-2362, 1993; S.M. Flatté, G.Y. Wang, and J.M. Martin, *J. Opt. Soc. Am. A* 10, 2363-2370, 1993) This comparison is made in the saturated region, just beyond the peak in variance (as a function of turbulence strength). The moments and PDFs of log-irradiance for an incident plane wave are presented and compared with the K-distribution and the distribution obtained by convolving the exponential distribution with the log-normal distribution. The PDF of log-irradiance for a point source in the strong-fluctuation regime is calculated and compared with experiment, and excellent agreement is found.

## Propagation of pulses in a waveguide filled with a random medium

S. M. Flatté\*, J. A. Colosi, and C. Bracher  
Physics Department University of California, Santa Cruz, CA 95064

The ocean is a waveguide for acoustic waves (the sound channel) and superposed on this waveguide are small-scale fluctuations known as internal waves. To a good approximation the propagation can be considered two-dimensional (depth and range). Tomography of the ocean is carried out by sending pulses over a megameter or more and measuring the variations in their travel time. A recent one-megameter acoustic pulse transmission experiment in the Pacific transmitted 10-ms-wide pulses to a 3000-m vertical array of hydrophones (T. Duda, S. M. Flatté, J. A. Colosi, B.D. Cornuelle, J.A. Hildebrand, W.S. Hodgkiss, Jr., P.F. Worcester, B.M. Howe, J.A. Mercer, and R.C. Spindel. *J. Acoust. Soc. Am.* 92, 939-955, 1992). The experiment revealed unexpected fluctuations on received wavefronts, including a dominant rapid variation, called the broadband fluctuation, with time scales less than 10 minutes and spatial scales of less than 60 m; a distinct break-down of the geometrical optics wavefront pattern and broadening of the wavefront near the transmission finalé; and a coherent wavefront motion with a timescale near the semi-diurnal tidal period. We have carried out parabolic-equation numerical simulations which utilize environmental data and which take into account internal-wave-induced sound-speed perturbations obeying the Garrett-Munk spectral model. We show that the effects of internal waves can account for the broadband fluctuations, the breakdown of the geometrical optics pattern, and the wavefront broadening. Tidal period coherent fluctuations are observed, strongly suggesting the influence of an internal tide during the experiment.

## Path-Integral Results for Irradiance Moments in the Asymptotic Regime

Guang-Yu Wang\* and Stanley Flatté

*Department of Physics  
University of California, Santa Cruz, CA 95064*

Roger Dashen

*Department of Physics  
University of California at San Diego, La Jolla, CA 92093*

Path-integral methods for calculating the moments of both irradiance and log-irradiance are discussed. These quantities cannot be expressed in closed analytical form and approximation methods are required. One interpretation of the path integral is the representation of the propagation problem in terms of an infinite number of phase screens. This interpretation makes it easier to identify approximations and also serves as the base for many numerical approaches. Using a recently developed asymptotic scheme (R.Dashen and G.-Y. Wang. *Optics Letters*, V17,91-93,1992) and cluster expansion techniques, we are able to obtain quantitative predictions of various moments in the strong scattering regime. This provides a precise method for studying the probability distribution functions.

Asymptotic results for various moments of intensity and log intensity, up to third orders, are presented for both plane incident waves and spherical waves from a point source that propagate through Kolmogorov power-law media with or without inner-scale cutoffs. These results give significantly better estimates of the scintillation index than previous asymptotic results. They also help to clarify the theoretical status of various distribution functions, such as the K-distribution, the distribution of convolving the exponential distribution with the log-normal distribution, etc. Sources of error and corrections of these distributions may also be estimated from our results.

With recent large-scale numerical simulations (based on path-integral techniques), we are able to numerically study the irradiance statistics in the strong scattering regime. Comparisons between asymptotic results and numerical simulations are presented. The combination of numerical simulations and asymptotic expansions provides global quantitative descriptions of the entire scattering regime.

## DOUBLE PASSAGE OF A GAUSSIAN BEAM WAVE

L. C. Andrews  
Department of Mathematics and  
Department of Electrical and Computer Engineering  
University of Central Florida, Orlando, FL 32816

W. B. Miller and J. C. Ricklin  
Battelfield Environment Directorate  
U.S. Army Research Laboratory  
White Sands Missile Range, NM 88002

### ABSTRACT

Tractable analytic expressions are developed for the mean intensity of the double passage of a Gaussian beam wave scattered by a reflector of finite dimensions. Limiting cases of a point reflector and infinite plane reflector are shown to reduce to established results. In the strictly backward direction the dependence on inner scale of these statistical quantities is similar to that of the scintillation index of a single passage Gaussian beam. All calculations are performed in the weak fluctuation regime and based on a modified spectrum for refractive-index fluctuations that includes effects of inner and outer scale as well as a high wave number "bump."

## **EFFECTS OF A MODIFIED SPECTRAL MODEL ON THE SPATIAL COHERENCE OF A LASER BEAM**

C.Y. Young and L.C. Andrews

Department of Mathematics, University of Central Florida  
Orlando, FL 32816

General expressions are derived for the mutual coherence function (MCF) and wave structure function (WSF) of a lowest-order Gaussian beam wave propagating through atmospheric turbulence. These expressions, based on weak fluctuation theory and a modified spectrum of refractive-index fluctuations characterized by a high wave number bump, are compared with recent findings based on the (modified) von Karman spectrum. The MCF is also derived by the parabolic equation method using a quadratic approximation for the structure function of a plane wave. The implied beam spot size and radius of curvature from the parabolic equation method are used to develop "effective" beam parameters that account for additional diffraction effects due to turbulence and permit the weak turbulence expression for the degree of coherence to formally extend into the strong fluctuation regime.

In general, we found that the implied beam spreading based on the modified spectrum is only slightly greater than that predicted by conventional spectral models except in the strong fluctuation regime. However, there is significant difference in the implied spatial coherence predicted by the modified spectrum. Specifically, the implied spatial coherence length based on conventional spectral models is greater than that based on the modified spectrum whenever the Fresnel zone size is larger than the initial beam radius. For a focused beam, however, the predicted coherence length based on conventional models is less than that for the modified spectrum when the Fresnel zone size is much smaller than the initial beam radius. When the Fresnel zone and initial beam radius are of comparable size, the presence of a spectral bump appears to have minimal effect on spatial coherence.

## QUADRUPLE REFRACTION OF HF-WAVES IN THE IONOSPHERE

Sazanami Yano,\* Department of Electrical Engineering  
Kochi National College of Technology, Monobe, Nankoku, Kochi 783, Japan

Akira Ishimaru, Department of Electrical Engineering, FT-10  
University of Washington, Seattle, Washington 98195, USA

Toshio Ogawa, Science Laboratory International  
2C, Sunset Building, 1510-1 Kamobe, Kochi 780, Japan

**Abstract.** The radio waves transmitted from standard frequency and time signal stations have deep fading phenomena made by the interference of two or more waves before and after the sunrise. The cause, by which an source wave is separated into two or more waves, is estimated the double refraction in the ionosphere. The wave path is divided into four routes in maximum by the quadruple refraction. The waves on each path have different frequencies shifted by the Doppler effect in the ionosphere. The frequency variation of the waves shows a C-shaped form in the frequency-time diagram when the ionospheric electron density increase and an inverse C-shaped form when it decreases. The C-shaped frequency variation is made by the double refraction of a source wave. Similarly, the quadruple refraction of the wave makes a  $\Sigma$ -shaped frequency variation at the sunrise time. We have measured the  $\Sigma$ -shaped frequency-time diagram produced from the standard frequency and time signals transmitted from the station of JJY (Nazaki in Japan) 637 km away. We have also measured a Z-shaped frequency variation, but this may be equivalent to the lower part of the  $\Sigma$ -shaped variation.

We propose an analysis method using the geometrical optics approximation and derive theoretically some conditions for the ionospheric electron density to make the  $\Sigma$ -shaped variation in the frequency. The theoretically calculated  $\Sigma$ -shaped variations in the frequency of the waves, which are made by the quadruple refraction and shifted by the Doppler effect at the sunrise, show good agreement with the measured variations.

Figure 1(a) and (b) show the measured  $\Sigma$ -shaped frequency variation and the calculated variation, respectively.

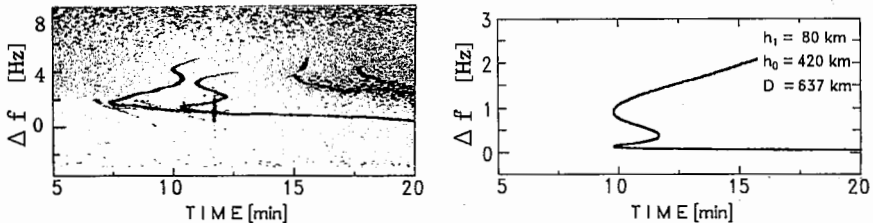


Fig.1 The  $\Sigma$ -shaped frequency variation produced by quadruple refraction and the Doppler effect. (a) Measured on 8 MHz of JJY. (b) Calculated for the ionosphere with the bottom height of 80 km and the maximum electron-density-height of 420 km.

## **Dual-Parameter Methods of Radar Turbulence Detection**

**Felix J. Yanovsky**

Professor of the Kiev Institute of Civil Aviation Engineering,

Doctor of Science

Kiev, Ukraine

### **Abstract**

The statistic models of radar signals reflected from turbulent areas in clouds and precipitation are discussed. Thus using of generalized Rice distribution and robust estimations of amplitude and coefficient of an interperiod correlation provided a mean for carrying out the synthesis of the turbulent areas detection's complex algorithm adapted for a noise level. This algorithm provides moderate turbulence detection with 0.9 detection probability and 0.1 probability of false alarm.

Other synthesized optimum algorithm of an after-detector turbulent areas finding based on a Markoff model of echo. Proposed algorithm provides moderate turbulence detection in clouds and precipitation with high detection probability and relatively small value of false alarm probability. However the main advantage of the given method is a possibility to operate using small samples, for example 10 or even 5 pulses. Such samples can be obtained easily by airborne weather radar.

Comparative analysis of this and some other algorithms is given in this report.

**Some Results of Sounding of  
Thunderstorm and Hail Clouds  
by Dual-Polarization Airborne Radar**

**Professor Arcady Shupiatsky**  
Central Aerological Observatory  
Dolgoprudny, Moscow Region, Russia

**Professor Felix J. Yanovsky**  
Kiev Institute of Civil Aviation Engineering  
Kiev, Ukraine

**Abstract**

The theoretical study carried out made it possible to obtain mathematical patterns showing the kind of dependencies of the polarization parameters on a shape, phase structure and orientation of diffusing particles. These results show that statistical peculiarities of polarization characteristics of radar signals may be used to determine zones of icing, hail, and electric activities in clouds.

Algorithms of hail and icing areas detection were synthesized by authors. These algorithms were realized on the base of airborne weather radar "Groza M-154" with polarization controlled aerial which has been worked out and patented.

The data obtained as a result of experiments carried out with the help of groundbased and airborne polarimetric radar are given and discussed in this report. The analysis of experiment results shows correspondence with the theoretical ideas.

There have also been discussed the possibility of creating airborne operative devices detecting the areas in clouds with high icing probability, hail, and increased electric activities.



## MONDAY AM URSI-B SESSION M-U3

Room: Savery 249

### NUMERICAL METHODS I

Chairs: J.R.Mautz, Syracuse University; K. Umashankar, University of Illinois at Chicago

8:20	Symmetric Pairs of Moment Solutions as Opposed to Unsymmetric Ones <i>*J.R. Mautz, Syracuse University</i>	14
8:40	Electric- and Magnetic-Field Volume-Surface Integral Equations for 3-D Inhomogeneous Scatterers <i>*A.D. Yaghjian, R.W. Wang, Department of the Air Force</i>	15
9:00	Domain Decomposition in the Electromagnetic Analysis of Large Two- and Three-Dimensional Structures on Serial and Parallel Computer Architectures <i>*C.T. Spring, A.C. Cangellaris, Univ. of Arizona</i>	16
9:20	A Domain Decomposition Method for the Solution of the Wave Equation <i>B. Stupfel, Univ. of Illinois; J. Guillem, Commissariat à l'Énergie Atomique</i>	17
9:40	Numerical Analysis of Electromagnetic Scattering by Electrically Large Three Dimensional Objects Using Spatial Decomposition Technique <i>*K. Umashankar, S. Laxpati, S. Kawalko, Univ. of Illinois at Chicago</i>	18
10:00	Break	
10:20	Iterative Solution of Dense MoM or Hybrid BEM/FEM Linear Systems Arising from 3D Scattering Problems. A Treatment of Multiple Incident Electromagnetic Fields <i>*P. Soudais, Univ. of Illinois/Chicago (for Office National d'Etudes et de Recherches Aerospatiales)</i>	19
10:40	A Sparsely Preconditioned Block GMRES Iterative Solver for Dense Complex Matrices <i>W.E. Boyse, *A. E. Seidl, Lockheed Palo Alto Research Laboratories</i>	20
11:00	Computation of the Capacitance of Manhattan Patches Using an Efficient Implementation of a GBGM-FFT Algorithm <i>E. Drake, *F. Medina, M. Horno, Univ. of Seville</i>	21
11:20	Solution of Integral Equations in Electromagnetics by Adaptive Wavelet Expansion and Multilevel Iteration Method <i>X. Zhu, G.-W. Pan, Univ. of Wisconsin-Milwaukee</i>	22
11:40	A 3D Moment Method Code Based on Fast Multipole <i>B. Dembart, B. Yip, The Boeing Company</i>	23
12:00	Numerical Results Using IML and a New CFIE <i>*F.X. Canning, Rockwell International</i>	24

## Symmetric Pairs of Moment Solutions as Opposed to Unsymmetric Ones

Joseph R. Mautz

Department of Electrical and Computer Engineering  
Syracuse University, Syracuse, NY 13244-1240

Consider the problem of obtaining a numerical approximation to the functional  $\rho = \langle f, h \rangle$  where  $f$  satisfies

$$Lf = g \quad (1)$$

Here,  $g$  and  $h$  are known functions,  $L$  is a linear operator, and  $\langle f, h \rangle$  is the symmetric product of  $f$  with  $h$ . Let  $w$  be the function that satisfies

$$L^a w = h \quad (2)$$

where  $L^a$  is the adjoint of  $L$ . Using (2) and the definition of the adjoint operator, one obtains  $\rho = \langle Lf, w \rangle$ . Using the method of moments to solve (1) for  $f$ , one obtains  $f \approx \tilde{f}$  where  $\tilde{f}$  is the moment approximation to  $f$ . Let  $\tilde{w}$  be the moment approximation to the solution  $w$  of (2) obtained by using the same expansion and testing functions. Let  $\hat{w}$  be the moment approximation to the solution  $w$  of (2) obtained by testing with these expansion functions and expanding with these testing functions. In other words, the expansion and testing functions for  $\tilde{w}$  are respectively the expansion and testing functions for  $\tilde{f}$ , but the expansion and testing functions for  $\hat{w}$  are respectively the testing and expansion functions for  $\tilde{f}$ . The coupled pair of moment solutions  $(\tilde{f}, \tilde{w})$  is called an unsymmetric pair and the pair  $(\tilde{f}, \hat{w})$  is called a symmetric pair. The pair  $(\tilde{f}, \hat{w})$  is obtained through symmetric use of two sets of functions. That is, each set is used once for expansion and once for testing.

A functional of  $\tilde{f}$  and  $\hat{w}$  is variational if it reduces to the quantity of interest  $\langle Lf, w \rangle$  when  $(\tilde{f}, \hat{w}) = (f, w)$  and is stationary there. If there is a sequence of moment solutions  $\{\tilde{f}, \hat{w}\}$  that converges to  $(f, w)$ , then  $\langle L\tilde{f}, \hat{w} \rangle$  is variational. However,  $\langle L\tilde{f}, \tilde{w} \rangle$  is not necessarily variational when there is a sequence of moment solutions  $\{\tilde{f}, \tilde{w}\}$  that converges to  $(f, w)$ . Therefore, one is advised to use symmetric pairs of moment solutions rather than unsymmetric ones.

Consider, for example, the circular cylindrical surface ( $\rho = a$ ,  $0 \leq \phi < 2\pi$ ,  $-\infty \leq z \leq \infty$ ) where  $a = 0.6\lambda$  where  $\lambda$  is the wavelength. For (1), let the electric current  $\hat{z}f$  on this surface produce the electric field  $-\hat{z}g$  there. The electric field operator is self-adjoint. For (2), let the electric current  $\hat{z}w$  on the cylindrical surface produce the electric field  $-\hat{z}h$  there. The functions  $g$  and  $h$  are chosen and sequences  $\{\tilde{f}, \tilde{w}\}$  and  $\{\tilde{f}, \hat{w}\}$  of coupled moment solutions are constructed so that both  $\{\tilde{f}, \tilde{w}\}$  and  $\{\tilde{f}, \hat{w}\}$  converge to  $(f, w)$  and so that  $\langle L\tilde{f}, \hat{w} \rangle$  is variational but  $\langle L\tilde{f}, \tilde{w} \rangle$  is not. Plots will be shown.

**ELECTRIC- AND MAGNETIC-FIELD VOLUME-SURFACE  
INTEGRAL EQUATIONS FOR 3-D INHOMOGENEOUS  
SCATTERERS**

Arthur D. Yaghjian\* and Rose W. Wang  
Electromagnetics Directorate, Rome Laboratory  
Hanscom AFB, MA 01731, USA

Conventional electric-field and magnetic-field volume integral equations encounter numerical instabilities when applied to high-contrast scatterers using pulse basis functions and point matching (A.F. Peterson, Proc. IEEE, 1431-1441, 1991). For two-dimensional (2-D) problems Jin, Liepa and Tai (JEWA, 573-588, 1988) have derived TE and TM volume-surface integral equations that yield stable solutions to scattering from inhomogeneous cylinders when solved using pulse basis functions and point matching. In this paper, we derive the following analogous electric-field and magnetic-field volume-surface integral equations (VSIE's) for three-dimensional (3-D) inhomogeneous scatterers:

$$-\mathbf{E}_i + \mathbf{E} = \int_{V^-} \left[ k_0^2(\epsilon_r - 1)\mathbf{E}\psi - \frac{\nabla' \epsilon_r \cdot \mathbf{E}}{\epsilon_r} \nabla' \psi \right] dV' \\ + \int_{S^-} (\epsilon_r - 1)(\hat{\mathbf{n}}' \cdot \mathbf{E}) \nabla' \psi dS' - (\epsilon_r - 1) \frac{(\hat{\mathbf{n}} \cdot \mathbf{E}) \hat{\mathbf{n}}}{2} \quad (1)$$

$$-\epsilon_r \mathbf{H}_i + \mathbf{H} = \int_{V^-} \left[ k_0^2(\epsilon_r - 1)\mathbf{H}\psi - \mathbf{H} \left( \frac{\nabla' \epsilon_r}{\epsilon_r} \cdot \nabla' \psi \right) + \mathbf{H} \times \left( \frac{\nabla' \epsilon_r}{\epsilon_r} \times \nabla' \psi \right) \right] dV' \\ + \int_{S^-} (\epsilon_r - 1)[\mathbf{H}(\hat{\mathbf{n}}' \cdot \nabla' \psi) - \mathbf{H} \times (\hat{\mathbf{n}}' \times \nabla' \psi)] dS' - (\epsilon_r - 1) \frac{\mathbf{H}}{2} \quad (2)$$

where  $\psi(\mathbf{r}, \mathbf{r}')$  is the free space Green's function,  $\mathbf{E}$  and  $\mathbf{H}$  are the total electromagnetic fields, and the observation point  $\mathbf{r}$  lies in the volume  $V$  of the scatterer. For the sake of simplicity, the permeability of the scatterer has been set equal to the free-space value, so that (1) and (2) apply only to dielectric scatterers with relative permittivity  $\epsilon_r(\mathbf{r})$ , which can vary throughout the scatterer. The last terms in (1) and (2) are present only if the observation point  $\mathbf{r}$  lies on the surface  $S^-$  of the scatterer of volume  $V^-$ . In that case the surface integrals in (1) and (2) are principal-value integrals. The superscript "-" on  $V^-$  in (1) and (2) indicates that the volume integration only approaches the surface of the scatterer where  $\epsilon_r$  is discontinuous. If there are surfaces within the scatterer across which  $\epsilon_r$  is also discontinuous, the surface integrals in (1) and (2) must extend over these surfaces as well. When the observation points are not on a surface of discontinuity so that the last terms in (1) and (2) are absent, and when the scatterer is composed of homogeneous regions so that the  $\nabla \epsilon_r$  terms in (1) and (2) are zero, these volume-surface integral equations reduce to those introduced by Wust *et al.* (IEEE Trans. Biomedical Engineering, 745-759, 1993). For 2-D problems (1) and (2) reduce to the TM and TE volume-surface integral equations, respectively, of Jin, Liepa and Tai. Uniqueness of solution is proven for the VSIE's, (1) and (2), at all frequencies. Finally, numerical solutions to (1) and (2) are shown that indicate the numerical stability of these equations, even for large permittivities, when using simple pulse basis functions and point matching.

DOMAIN DECOMPOSITION IN THE ELECTROMAGNETIC ANALYSIS  
OF LARGE TWO- AND THREE-DIMENSIONAL STRUCTURES  
ON SERIAL AND PARALLEL COMPUTER ARCHITECTURES

C. T. Spring\* and A. C. Cangellaris  
Department of Electrical and Computer Engineering  
University of Arizona, Tucson, AZ 85721

The domain decomposition method, a technique for the rigorous and computationally efficient analysis of electrically large structures, is implemented for the electromagnetic modeling of two- and three-dimensional structures. The idea behind the method is to decompose the structure into smaller regions before any numerical modeling is done. Numerical solutions are computed in each region separately due to basis excitations on the partitions subdividing the large structure into regions. Then, field continuity at the partitions is invoked to solve for the total field.

Domain decomposition offers a number of benefits in tackling large problems. Each region can be solved with the most suitable numerical technique, with different techniques permitted in different regions. By working with smaller problem spaces in the individual regions, the numerical mesh generation for finite techniques is greatly simplified. This also diminishes the ill-conditioning, and subsequent round-off error, associated with very large matrices. Accuracy and efficiency are increased by avoiding multiple analysis of repetitious regions; this is especially useful in analyzing periodic or nearly periodic structures. The decomposition approach is also ideally suited for parallel processing. Domain decomposition offers at least two levels of parallelism, while the finite element technique used in the numerical modeling has many additional levels of parallelism that can be exploited. Examples from a two-dimensional parallel code on the Connection Machine illustrate these points.

Three-dimensional examples of domain decomposition for guided problems are numerically analyzed with finite element techniques. The three-dimensional problem also introduces a simple and elegant formulation of the Helmholtz equation that is free from the spurious modes from vector parasites noted in other finite element formulations. Rather than adding divergence free "penalty" terms to the double curl vector equation, the basic Helmholtz equation is applied to each vector component, which assures divergence free solutions. Boundary terms are considered carefully in such a way that the three components become coupled.

## A DOMAIN DECOMPOSITION METHOD FOR THE SOLUTION OF THE WAVE EQUATION

Bruno Stupfel and Jérôme Guillem  
Centre d'Études de Limeil-Valenton, Commissariat à l'Énergie Atomique.  
94195 Villeneuve St Georges cedex, France.

The solution of open region scattering problems involving inhomogeneous objects may be performed through the use of the finite element technique which requires enclosing the scatterer by an outer boundary on which an absorbing boundary condition (ABC) is applied. Domain decomposition methods are particularly attractive when the size of the domain to be meshed and, consequently, the number of unknowns, is too large for the memory storage available; moreover, the corresponding iterative algorithm is parallelizable.

Després (Ph.D. thesis, Paris, 1991) proposed a method in which the subdomains are parallelepipeds. The propagation of waves through the boundaries between adjacent subdomains is ensured by a transmission condition (TC) which involves the values, on these boundaries, of the normal derivative of the field as well as the values of the field itself. On the outer boundary  $S$  of the entire computational domain, a zero order Engquist-Majda ABC is implemented. He showed, analytically, that the resulting algorithm always converges.

The domain decomposition technique presented here has the following characteristics: in order to minimize the size of the domain to be meshed,  $S$  is conformal to the object, and the ABC is the one proposed by Stupfel (IEEE-AP digest, Ann Arbor, 1993). The subdomains circumscribe the object in an "oignon" like structure. The TC is derived from the above mentioned ABC, and both can be of order 0, 1 or 2; if the order 0 is used and the boundaries are parallelepipedic, then a particular form of Després' method is obtained.

We evaluate the efficiency of this technique by first solving in closed-form the scattering problem by a perfectly conducting infinite circular cylinder. Then the case of a perfectly conducting infinite cylinder of triangular cross section coated with materials is considered. We show that, for a given order of the ABC, the number of iterations required to solve these problems with a given accuracy is the lowest when the order of the TC is the highest. In terms of memory storage requirements, this domain decomposition method compares favourably with a combined finite element-integral equation technique where the integral equation is directly prescribed on the surface of the object.

NUMERICAL ANALYSIS OF ELECTROMAGNETIC SCATTERING  
BY ELECTRICALLY LARGE THREE DIMENSIONAL OBJECTS  
USING SPATIAL DECOMPOSITION TECHNIQUE

Korada Umashankar\*, Sharad Laxpati and Stephen Kawalko  
Department of Electrical Engineering and Computer Science  
University of Illinois at Chicago  
Chicago, Illinois 60680

The boundary value integro-differential equations and method of moments numerical technique is widely utilized for the study of electromagnetic scattering by three dimensional arbitrary shaped conducting, penetrable and loaded objects. Even though, this direct approach is elegant, as far as its application to analyze three dimensional electrically large object is concerned, it inherently suffers from wide range of computational limitations. The method of moments system matrix is, in general, complex valued, full and dense requiring impractical demand on computer storage and time resources. In addition to operational numerical errors and ill-conditioning involved in the solution of large scale matrix equation, the direct numerical technique bears progressive degradation of accuracy of the near-field solution as the size of the system matrix increases.

The apparent computational limitations with the direct integro-differential equation formulation and the method of moments has prompted an alternative numerical solution procedure based on the spatial decomposition technique. Using rigorous electromagnetic equivalence, the spatial decomposition technique virtually divides a three dimensional electrically large object into a multiplicity of sub-zones. It permits the maximum size of the method of moments system matrix that need be inverted to be strictly limited within error bounds, regardless of the electrical size of the large scattering conducting and dielectric object being modeled. The requirement on the computer resources is of order  $(N)$ , where  $N$  is the number of spatial sub-zones and each sub-zone is electrically small spanning in the order of few wavelengths. Numerical examples related to bistatic and monostatic radar cross section are reported along with validation to demonstrate applicability of the spatial decomposition technique to study electromagnetic scattering by electrically-large three dimensional conducting and dielectric objects.

# **Iterative Solution of Dense MoM or Hybrid BEM/FEM Linear Systems Arising from 3D Scattering Problems. A Treatment of Multiple Incident Electromagnetic Fields.**

Paul SOUDAIS<sup>+</sup>

ONERA B.P. 72 92322 Chatillon Cedex FRANCE

This paper deals with an iterative solution technique that has been developed for use in the solution of a 3D electromagnetism problem discretized by a hybrid Boundary Element Method/Finite Element Method (BEM/FEM). The problem was to compute the electromagnetic fields scattered by a bounded object illuminated by an electromagnetic wave. The propagation of electromagnetic waves inside the scatterer was taken into account by the harmonic Maxwell equations. The propagation in the unbounded outer space was taken into account by integral equations. A coupled variational formulation was developed (J.J. ANGÉLINI, C. SOIZE, P. SOUDAIS, IEEE Trans. on Antennas and Propagat., 41, pp.66-76, Jan. 1993). The mathematical formulation has been constructed in order to obtain a symmetric matrix with positive real part for the discretized problem. Therefore an efficient iterative method can be used.

Iterative techniques are interesting alternatives to direct Gaussian elimination especially given the very large problems that are of present and future interest and given the increasing use of parallel computers. But the efficiency of iterative techniques may be compromised if the solution is required for multiple incident electromagnetic waves.

We present a new strategy to deal with this problem. The approximate solutions for the  $k_p$  systems are constructed from a single set of the search vectors. At a given step, the new search vector is defined in order to improve in particular the approximate solution that shows the worst residual. This method was developed for the generalized conjugate residual algorithm. It gave rise to a multi-GCR algorithm (MGCR).

Several validations on complex 3D scatterers are presented. They validate the iterative solution for a single excitation and up to 360 excitations. The 360 solutions are computed with MGCR in the time of the GCR solution for 9 right-hand sides. The MGCR solution of this 360 excitations requires a fourth of the arithmetic operations required by Gaussian elimination.

(+) Presently on a leave as a Visiting Researcher at the University of Illinois, Chicago.

# A Sparsely Preconditioned Block GMRES Iterative Solver for Dense Complex Matrices

William E. Boyse and Andrew A. Seidl\*  
Lockheed Palo Alto Research Laboratories  
3251 Hanover Street  
Palo Alto, CA 94304-1191

## Abstract

Scattering computations from large objects using the method of moments (MOM) requires the solution of a large dense general complex matrix for many right hand side (RHS) vectors. This is typically accomplished by performing an LU factorization followed by forward reduction and back substitution for each solution. However, today iterative methods are being used more and more for this time consuming task.

While there are generalizations of most conjugate gradient type algorithms which are appropriate for general complex matrices, the most reliable "iterative" method is the generalized minimum residual (GMRES) method. The word "iterative" is quoted because this is not an iterative method in the strictest sense since the work and storage increase with each iteration. However, GMRES is effective for these problems if properly used.

Our principal in using GMRES is to obtain convergence in the fewest possible iterations, before problems arise. Continued iterations can result in loss of orthogonality of the residuals causing slowed convergence and excessive storage and computation involved when many residuals are kept. Several techniques are used to accelerate the convergence of this algorithm.

First, a sparse preconditioner, i.e. approximate LU factorization, is used. The computation of this preconditioner is numerically stable and takes much less time to compute and use than the full LU factorization. Second, solving blocks of RHS's simultaneously accelerates convergence further. Finally, the computed Krylov space for one block of RHS vectors may be used to solve other blocks, providing additional solutions with no matrix multiplies.

Numerical examples, on large MOM problems, are presented showing the performance of the method. These examples show the effectiveness of preconditioning and block size on convergence and the ability to obtain additional solutions using the same Krylov space.

## Computation of the Capacitance of Manhattan Patches Using an Efficient Implementation of a GBGM-FFT Algorithm

E. Drake, F. Medina\*, M. Horno

Microwave Group. Department of Electronics and Electromagnetism  
University of Seville

Avda. Reina Mercedes s/n. 41012 SEVILLA (SPAIN)

The accurate determination of the capacitance of printed finite size conductors embedded in a layered dielectric/semiconducting medium is of paramount importance in the analysis and design of microwave integrated circuits and devices. The electrostatic analysis of this type of structures can be carried out by solving the integral equation for the free surface charge density on the conductors. Different versions of both the moments method and the Rayleigh-Ritz method are the most commonly used techniques for this purpose (e.g. Z.Q. Ning et al., IEEE-ED, 34, 644-649, March 1987; C.H. Chan et al., IEEE-MTT, 36, 96-105, Jan. 1988). Most of the works on this subject concerns the analysis of rectangular, circular and elliptical patches on which the charge densities can be expanded in terms of a set of entire domain basis functions. However, more complex geometries are also of interest. In particular, configurations which can be split into rectangular subregions (Manhattan patches) are very common.

The configuration considered in this work is a Manhattan patch embedded in a layered substrate with lateral walls of periodic repetition (unit cell). This problem is conveniently formulated by using the spectral domain Galerkin method with subdomain rectangular pulses as basis functions. The application of this technique leads to a large system of linear equations whose entries keep the convolution nature of the integral kernel. To solve this system, we propose an efficient implementation of an iterative algorithm (the generalized biconjugate gradient method -GBGM-) in conjunction with FFT for exploiting the convolution property. This iterative technique was successfully applied to the analysis of two-dimensional problems (Drake et al., IEEE-MTT, 40, 652-658, April 1992). Special attention is paid to the obtaining of an efficient means to compute the infinite-array spatial Green's function. Direct computation by two-dimensional inverse FFT is not efficient. Therefore, an specific asymptotic treatment has been programmed.

The GBGM-FFT algorithm has been implemented by a FORTRAN-77 code in a CONVEX computer. The reliability of this computer code to compute the capacitance of Manhattan metallizations has been conveniently tested with available data. Although the periodic array of infinite patches is the case solved exactly, a single Manhattan patche can also be analyzed with the present method by placing the periodic repetition walls far enough. In addition, the extension of the method to the analysis of coupled multipatches configurations is straightforward.

# **Solution of Integral Equations in Electromagnetics by Adaptive Wavelet Expansion and Multilevel Iteration Method**

Xiaojun Zhu and Guang-Wen Pan  
The Laboratory for Signal Propagation  
The University of Wisconsin-Milwaukee, WI 53201

In this presentation, a combined wavelet expansion and multilevel iteration method is developed to solve integral equations in electromagnetic problems. The wavelet expansion method renders the continuous operator equations into a set of discrete matrix equations with very sparse coefficient matrices, while the multilevel iteration method is employed to solve the matrix equations.

The Meyer-Lamarric wavelets are used to expand the operators. With polynomial decompositions of the wavelets, the method is as easy as the Galerkin's method with a basis of the same order. The sparse coefficient matrices are obtained by using the fast wavelet transform. An adaptive algorithm has been developed by choosing the resolution levels according to the regularity of the solution.

The matrix equation obtained from the wavelet expansion is solved by multilevel iteration method (also called multigrid method). This method is characterized by two steps: fine level relaxation and coarse level correction. It is based on the low pass property of the iterative relaxation schemes. By projecting the low frequency components of the errors on the fine level onto coarse level and iterating on the coarse level, a much faster convergence can be obtained.

Since both the wavelet expansion and multigrid method share the same property of multi-resolution, and the wavelet expansion method discretizes the operators into matrices in a sequence of resolution levels, much computing effort can be saved when the resulting matrix equations are solved by multigrid method. In this work, the full multigrid V-cycle (FMV) and other multigrid schemes are employed. Gauss-Seidel, Jacobi, projection method, and the successive over-relaxation methods are used, their performances are studied and compared. Finally the combined method is applied to several examples.

## A 3D Moment Method Code based on Fast Multipole

B. Dembart, E. Yip

The Boeing Company  
Seattle Wa. 98124

A 3D electromagnetic scattering code has been built based on the method of moments. The methods included a preconditioned iterative solver and the fast multipole method (FMM). The Generalized Minimum Residual Method (GMRES) has been selected as the iterative solver. The preconditioner is based on sparse matrix techniques.

The FMM permits theoretical computational complexity of  $O(n \log(n))$ , where  $n$  is the number of expansion coefficients. The memory requirement is also  $O(n \log(n))$ . The scattering object is enclosed in a cube which is bisected along each edge to produce 8 subcubes. Each subcube is again bisected. The process continues until the cubes produced have edge length of half of a wavelength. The implementation of the FMM is based on signature functions for each of the cubes. Outer signature functions are computed at the finest level; then translations and interpolations are used to compute signature functions on the larger cubes. The outer signature functions are converted to inner signature functions at the coarsest level by the translator operators. Inner signature functions for smaller cubes are computed by filtering and translation. Far fields are computed by integrating the product of the inner signature functions with the test signature functions. Near fields are computed using conventional moment method techniques.

The code implements EFIE, MFIE and CFIE.

Comparison with the Mie series solutions demonstrates the accuracy of the method. Timing results demonstrates the  $O(n \log(n))$  complexity.

## NUMERICAL RESULTS USING IML AND A NEW CFIE

Francis X. Canning  
Rockwell Science Center  
1049 Camino Dos Rios  
Thousand Oaks, CA 91360

The Impedance Matrix Localization (IML) method has been used to replace the usual full moment method matrix by a sparse matrix of the same dimension. Later work developed a new Combined Field Integral Equation (CFIE). This resulted from expressing the EFIE and the MFIE matrices in the IML basis and testing functions, multiplying the EFIE matrix by a diagonal matrix, and then adding the MFIE matrix (F. X. Canning, Radio Science, March-April 1994). The result was that for closed conducting bodies matrix elements describing propagation from the interior are now negligible. This new form has many interesting properties for numerical work which are explored here.

The resulting matrix is highly sparse, since now peaks within the matrix occur only for fields incident from the exterior. The sparse approximate inverse previously found for general IML problems is highly efficient for this problem. Indeed, for convex bodies the matrix is banded and numerical results are presented showing a factor time linear in  $N$ . The matrix also has many other desirable properties. For example, the condition number is examined as the exact combination of EFIE and MFIE is changed slightly. The accuracy of numerical results for the scattered field is considered as a function of the tolerance used to approximate very small matrix elements by zero. The method used here to generate the matrix elements is an adaptive quadrature using the IML basis and testing functions. Thus, we also consider how the accuracy of the scattered field varies as the number of basis functions per wavelength varies. The advantages of using such smooth basis functions become evident, as does the speed of the matrix generation.

## MONDAY AM URSI-E SESSION M-U4

Room: Savery 211

### EMC/EMI AND NOISE

- Chairs: J.L. ter Haseborg, Technical University Hamburg-Harburg; R. Gardner, Phillips Laboratory
- 8:20 EMC Measures Against Transients on Telecommunication Lines 26  
\*J.L. ter Haseborg, Technical Univ. Hamburg-Harburg; F. Wolf, C. Plath Company for Nautical Electronics
- 8:40 Examination of Electromagnetic Interference to Civil Aviation CPS Receivers 27  
\*Y.E. Yang, M.A. Tassoudji, H.T. Ewe, J.A. Kong, Massachusetts Inst. of Technology; G.J. Markey, Federal Aviation Administration
- 9:00 Transfer Impedance and Transfer Admittance for Multiconductor Transmission Lines-Measurement Results 28  
\*T. Kasdepke, J.L. ter Haseborg, Technical Univ. Hamburg-Harburg
- 9:20 A Fast Method for EMI/EMC Prediction 29  
\*X. Yuan, D. Sun, Z.J. Cendes, Carnegie Mellon Univ.
- 9:40 Calculation of Far Zone Electromagnetic Fields Radiated from Structures in Multilayer Printed Circuit Boards 30  
\*G. Aguirre, L. Vakanas, A.C. Cangellaris, Univ. of Arizona
- 10:00 Break
- 10:20 Power Line Magnetic Field Including the Catenary Effect and Electric Field Including Absorbing Boundary Conditions 31  
\*R.D. Nevels, A.V. Mamishev, B.D. Russell, Texas A&M Univ.
- 10:40 Electromagnetic Analysis of Simultaneous Switching Noise in High-Speed Digital Systems Using FDTD Method and Spice Models for CMOS Inverters 32  
\*Y.-S. Tsuei, A.C. Cangellaris, J.L. Prince, Univ. of Arizona
- 11:00 Modelling of Nonlinear Response of Object to the Influencer of Powerful EMP 33  
S.I. Gridchin, Kharkov Technical Univ.; \*V.V. Knyazev, Res. & Eng. Inst. Molniya; A.E. Serebryannikov, Ukrainian Academy of Science
- 11:20 Diversity Combiner Performance Under Correlated Noise in Mobile Radio 34  
M. Kalkan, Istanbul Technical Univ.; F. Kerestecioglu, Bogazici Univ.

## **EMC measures against transients on telecommunication lines**

**J.L. ter Haseborg\***

Technical University Hamburg-Harburg  
Department of Measurement Engineering/EMC  
21071 Hamburg, Germany

**F. Wolf**

C. Plath Company for Nautical Electronics  
20097 Hamburg, Germany

Typical EMC measures against interfering electromagnetic fields and currents are grounding, shielding, wiring, filters and EMC-qualified arrangement of sensitive as well as of radiation emitting components in a circuit. In many cases the installation of filters will be necessary if the application of the other measures mentioned above is not sufficient.

Transient voltages and currents which are characterized by extreme short rise times and high peak values, which are much higher than the amplitudes of the line signals, often require the application of filters in terms of nonlinear protection circuits. The realization of these protection circuits is strongly dependent on the application i. e. on the type of the line to be protected (e. g. power supply line or telecommunication line). Here protection circuits for telecommunication lines will be discussed.

Generally terminations of telecommunication lines are more sensitive than terminations of power supply lines. Therefore in case of telecommunication lines often multistage protection circuits combined with linear filters are required which often additionally have to attenuate interfering pulses generated by responding nonlinear protective components e. g. gas arresters. As already mentioned before in other papers protection circuits for telecommunication lines i. e. RF transmission lines have to be developed in such a manner that on the one hand interfering transients are suppressed sufficiently and on the other hand the line signals are influenced negligibly by the nonlinear protective components.

It will be shown and discussed that e. g. responding gas arresters may generate steep pulses which have been suppressed effectively by means of a band-pass filter as linear filter. The complete protection unit has been developed for a VHF-receiving system. Measurement results in the time domain will show the efficiency of this measure. In addition measurements in the frequency domain will be presented representing the compatibility of suppressor diodes as nonlinear components for comparatively sensitive line terminations to be protected.

## Examination of Electromagnetic Interference to Civil Aviation GPS Receivers

Y. E. Yang\*, M. A. Tassoudji, H. T. Ewe, J. A. Kong  
Massachusetts Institute of Technology, Cambridge, Massachusetts 02139  
G. J. Markey  
Federal Aviation Administration, Washington, DC 20591

Global Positioning System (GPS) is the newest navigational system deployed by the United States Department of Defense. Using total of 21 to 24 satellites, they provide three-dimensional position and time information to everywhere in the world. Following the success in military applications, a wide range of commercial services and products have been developed. Among others probably the most ambitious task is undertaken by the civil aviation community, who hope to use GPS receiver in the future aircraft precision landing system. Experiments have been conducted to demonstrate the potential of achieving accuracy comparable to today's landing systems. In addition, researchers have begun to investigate system issues for implementation, such as integrity, reliability and continuity-of-service.

Statistics of aircraft accidents show that the relatively short landing process is a very critical period. Therefore, it is important to have the highest degree of continuity-of-service by electronic navigational aid. The low power level of GPS signal makes it particularly vulnerable to electromagnetic interference, which might cause the loss of required continuity. In this study, experimental investigation of civil aviation GPS receiver susceptibility to electromagnetic interference is conducted. A commercial GPS receiver mounted on the roof of a building was subject to on-channel and off-channel CW and narrow-band noise with varying power levels. The interfering signal was sent through the open air. Besides readout on the front panel, we relied on a PC to continuously record GPS data and warning flag throughout the process. Taking the receiver front-end as the reference point, we obtain the interference level that renders the GPS receiver incapable of decoding position data. This level is converted to antenna receiving power, from which we estimate the effective radiation power (ERP) level required for interferers at a distance. The variation of this interference threshold with GPS signal strength as the latter varies in time is also calculated.

Our preliminary estimation based on the measurement data of test units indicates that an on-channel (at L1 frequency 1575.42 MHz) interferer of approximately 20dBm ERP may pose problems for a GPS receiver within 40 nmi. This modest level of interference appears easy to create. At 10 MHz above the L1 frequency, the estimated threshold is roughly 50dB above the on-channel case, which might still be of concern at shorter range. These results, though of limited scope, not only are useful for establishing interference prevention schemes, but also point to the need to investigate auxiliary systems to cope with interference.

## **Transfer Impedance and Transfer Admittance for Multiconductor Transmission Lines - Measurement Results**

**T. Kasdepke, J.-L. ter Haseborg**

Department of Measurement Engineering/EMC  
Technical University Hamburg-Harburg  
21071 Hamburg, Germany

Due to the increasing concentration of different electric and electronic equipment in a limited space, the analysis of disturbing currents on transmission lines becomes a matter of great importance. One useful procedure for estimating the propagation of interferences on cables is given by the multiconductor transmission line theory.

A large number of methods for estimating the primary line parameters exists. For shielded multiconductor transmission lines also the coupling parameters between the cable shield and the inner conductors - the transfer impedance and the transfer admittance - have to be well known. There exists no general relation in order to calculate these parameters for this type of cables. All known relations are only valid for coaxial cables.

Furthermore most of the standardized measurement procedures are only valid for coaxial cables. If multiconductor cables are investigated, mostly all the inner conductors are short circuited at both ends of the line and it is treated as a coaxial system. So only one value can be obtained for the whole system. But for a multiconductor cable the coupling parameters will be different for each inner conductor.

In accordance with IEC 96-1 and Kley ("Measuring the coupling parameters of shielded cables," IEEE Trans. on EMC, Feb.1993) measurement results for magnitude and phase of the coupling parameters will be presented.

For this measurements, the line is supposed to be a two conductor line with a special characteristic impedance and a special characteristic propagation constant. These data are dependent on the position of the analysed line in the cable bundle and on the termination of the other inner conductors. The influence of the terminating network on the measurement results will be discussed in detail.

# A Fast Method for EMI/EMC Prediction

Xingchao Yuan\*, Din Sun, and Zoltan Cendes  
Ansoft Corporation  
Pittsburgh, PA 15129

As the speed and processing power of modern electronic devices increases, electromagnetic interference and electromagnetic compatibility (EMI/EMC) becomes increasingly important for electronic designers. Practical EMI/EMC problems are often very complex in terms of problem geometry, material properties, physical sizes, and frequency ranges. Among many numerical techniques available, the finite element method is particularly suitable for this task. This is because the finite element method handles complicated geometries and material types very naturally.

In order to address EMI/EMC problems effectively, we must address two key problems. One is the need for accurate radiation boundary conditions to model wave propagation into infinite space. The other is the need for a way to quickly generate solutions over a very wide bandwidth.

To address the first problem, we incorporate second order vector radiation boundary conditions with high-order tangential finite vector finite elements. The implementation is very efficient because the symmetry of the finite element matrix is preserved and the radiation boundary may be placed very close to the scatterer—typically less than a quarter of the wavelength away. Finally, in contrast with many other methods, the radiation boundary does not have to be a sphere but rather can be made conformal to the geometry.

To address the second problem, we present a new method called AWEfem that combines the finite element method with asymptotic waveform evaluation which provides the frequency response of the device over broad bandwidth. Unlike traditional frequency domain methods, this method allows the problem to be solved at one frequency and uses Taylor series expansions and Pade approximations to approximate the solution at other frequencies. Over a typically bandwidth, it requires one matrix LU decomposition and twenty forward/backward substitutions. This is at least one order of magnitude faster than traditional point by point frequency sweep methods. Furthermore, the new method predicts device resonances and nulls analytically. It is therefore very accurate and reliable for EMI/EMC predictions that are required over a wide bandwidth.

The method is validated and compared to other available solutions and experiments by using a number of examples.

## CALCULATION OF FAR ZONE ELECTROMAGNETIC FIELDS RADIATED FROM STRUCTURES IN MULTILAYER PRINTED CIRCUIT BOARDS

G. Aguirre\*, L. Vakanas, and A. C. Cangellaris  
Center for Electronic Packaging Research  
Department of Electrical and Computer Engineering  
University of Arizona, Tucson, AZ 85721

Radiated emissions from printed circuit boards (PCB) become an important issue as digital circuitry speed, density, and complexity increase in modern electronic systems. Fast calculation of such emissions with engineering accuracy is essential for rapid and EMI-sound PCB layout design. This paper presents a method for calculating the far zone electromagnetic fields radiated from exposed multiple transmission lines (MTL) in a multi-layer printed circuit board. As compared to full-wave tools, the proposed method offers expediant and reasonably accurate calculation of radiated emission levels above PCBs across a specified frequency band. For special cases, the fields from wires extending from the PCB can also be found. A brief summary of the proposed method follows.

The electromagnetic fields for each exposed MTL is found by assuming that each point on the MTL radiates like an horizontal electric dipole above a stratified media. The dipole moments at each point are found by using the fact that the current distribution along the MTLs is the summation of forward and reverse traveling waves. A coupled transmission line analysis, based on scattering parameters, allows the calculation of all the modal currents on the MTL. The far zone fields are then obtained by integrating the expressions for the dipole field over the length of the lines weighted with the appropriate dipole strength. To calculate the radiation for electrically short wires that may be attached to the PCB, the extended wire is replaced by a capacitor connected to ground. The value of the capacitor is calculated from a three-dimensional capacitance extractor. The current through the capacitor is used as the maximum value of a current distribution along the wire that is tapered linearly to zero from the connected end of the wire to the open end of the wire. The electric field is found by assuming the wire radiates in free space.

The details of the mathematical formulation will be presented. The validity of the method is demonstrated by comparing results to those obtained by using full-wave tools for several simple interconnect models. Results from modeling of complex interconnect structures will be vied to demonstrate the computational efficiency of the method.

## **Power Line Magnetic Field Including the Catenary Effect and Electric Field Including Absorbing Boundary Conditions**

R. D. Nevels,\* A. V. Mamishev, B. D. Russell  
Department of Electrical Engineering  
Texas A&M University  
College Station, Texas 77843

An accurate determination of the electric and magnetic fields near a power line is necessary for a number of reasons. For example, in order to avoid possible health effects due to power line electromagnetic fields and to stem public criticism, several states have instituted regulations that limit field intensities on transmission line rights-of-way. A prediction of the right-of-way distances which will comply with state requirements for various power line conductor configurations has therefore become a necessity during the new power line design phase. Another example is that it is useful to know the field amplitude in close proximity to power lines in order to determine safety limits for maintenance workers.

While the literature is generally well developed on the subject of field calculation for power lines, the models tend to assume that the wire is straight. A more accurate description is that along its length a power line is a periodic catenary. The effect of the catenary on the field amplitude is significant. For example, the horizontal component of the magnetic field can vary as much as 40% one meter above ground level between the position of the support beam and the center of the catenary.

In this paper we will present a method for analytical/numerical evaluation of the magnetic field of a power line including the effect of the catenary and the ground image component. Comparison will be made with field measurements. It will be shown that significant differences exist between the magnetic fields obtained by a straight wire and a wire containing a catenary and that the measured field closely correlates with that of the catenary model.

Also in this talk we will give a brief presentation of electric field calculations. When trees, foliage or buildings are in the vicinity of a power line, a quasistatic approach is taken whereby Laplace's equation is solved numerically by the finite-difference method. We will show computed results for the case of a single line in the vicinity of a tree and a building. Emphasis will be placed on the newly developed absorbing boundary conditions for Laplace's equation. It will be shown that while these conditions can be successfully implemented in an iterative procedure, convergence acceleration by the overrelaxation method does not appear to be possible.

ELECTROMAGNETIC ANALYSIS OF SIMULTANEOUS SWITCHING NOISE  
IN HIGH-SPEED DIGITAL SYSTEMS  
USING FD-TD METHOD AND SPICE MODELS FOR CMOS INVERTERS

Yuh-Sheng Tsuei\*, Andreas C. Cangellaris, and John L. Prince  
Center for Electronic Packaging Research  
Department of Electrical and Computer Engineering  
University of Arizona, Tucson, AZ 85721

Simultaneous Switching Noise (SSN) is a voltage drop at the chip-package power distribution connections due to the "parasitic" inductance provided by the connections and the associated power/ground planes. SSN effects become increasingly important as driver speeds increase and power supply voltages drop. Accurate prediction of SSN is critical for the reliable operation of state-of-the-art and future high-speed digital systems.

This paper proposes a rigorous electromagnetic model for the full-wave analysis of SSN effects. The proposed method combines a Finite-Difference Time-Domain (FD-TD) based Maxwell's equations solver with SPICE circuit models for the nonlinear drivers to perform the electromagnetic modeling. Through detail modeling of all geometric and material characteristics of the package, the model accounts explicitly for all parasitics associated with power/ground connections and chip-to-package interfaces. Consequently, all electromagnetic effects associated with the specific geometry and material characteristics (e.g., the type of chip-to-package connection, the characteristics of the connections to the power and ground planes) are modeled rigorously.

Complete SPICE models are properly incorporated in the FD-TD algorithm in order to account for the CMOS inverters used as drivers. Issues associate with the stable incorporation of these models in the FD-TD code will be discussed. Indeed, the emphasis of the paper will be on the issue whether a direct utilization of SPICE *within* the FD-TD code is possible.

The numerical results will emphasize switching noise modeling in a realistic single chip package. Comparisons of the results obtained using this method with results calculated using SPICE will be presented. The purpose of such comparisons will be to indicate up to what speeds SPICE-based simulations using transmission line representations of the interconnects remains accurate and when does rigorous electromagnetic modeling becomes necessary.

MODELLING OF NONLINEAR RESPONSE OF OBJECT TO THE  
INFLUENCE OF POWERFUL EMP

Sergei I. Gridchin  
Kharkov Technical University, Kharkov, Ukraine  
Vladimir V.Knyazev  
Res.&Eng.Institute "Molniya", Kharkov, Ukraine  
Andrey E.Serebryannikov  
Radio Astronomy Institute, Ukrainian Academy of Science, Kharkov, Ukraine

The problem of construction of generalized mathematical model of objects (units and elements) whose behavior is characterized by the nonstationary and nonlinear physical-chemical processes arising in them is of great practical interest. This paper suggests a general approach, based on the use of functional Voltaire series. It considers the response of radio electronic device to the action of powerful EMP. The action of powerful EMP has a complex character and it is practically impossible to differentiate the influence of different factors. In this situation the representation of object in the form of "black box" with the whole combination of internal bonds with several inputs and one output can be considered as a natural approach to the modelling.

The sources of disturbances, whose effect is equivalent to the effects produced by the powerful EMP on a system are connected to the inputs of a "black box". The reaction of a concrete element to the disturbances, measured during experiment, serves as an output. At present the authors have implemented the algorithm and computational programs for the case of one input. Nonlinear model of a system is prescribed by the operator  $A: H \rightarrow Y$ , where  $H$  and  $Y$  are normalized spaces. The problem of identification is reduced to one related to the determination of  $h \in H$  by the known element  $y \in Y$  from the equation

$$Ah = y. \quad (1)$$

Naturally, the input and output values are measured with some error. Therefore, in reality the approximated expression is used instead of exact one (1). The solution of approximated equation can be used instead of (1) only in case when regularizator exist.

The operator  $A$  is prescribed by Voltaire polynomial. Further the problem of nonlinear identification is solved by the method of least squares and is reduced to the problem related to finding of Voltaire nuclei's  $h_1, \dots, h_m$  by the measurements of input  $x(t)$  and output  $y(t)$  signals. The projection method of solution has been applied. A system of linear independent functions  $\varphi_p(\tau)$ ,  $p=1 \dots m$ , that could be orthogonal, can be selected. Using the expansion of unknown nuclei's  $h$  by the Fourier basis we obtained linear parametric model of object relatively Fourier coefficient. The measurement of  $x(t)$  and  $y(t)$  signals is discrete with some step, therefore the continuous model is replaced by the discrete one that has the form  $Y=WB$  (where  $Y$  is a vector of  $y$  measurements' results,  $W$  is a matrix of  $x$  measurements' results,  $B$  is a vector of  $h$  nuclei's expansion coefficients).

The method of singular expansion with the use of numeric realization of SVD procedure has been used for the solution of linear algebraic equations set. The given mathematical apparatus allowed for the development of algorithm and identification program that allowed for the construction of the mathematical model of protective devices for the protection of radio electronic equipment from over voltages.

# Diversity Combiner Performance under Correlated Noise in Mobile Radio

Mine Kalkan

*Istanbul Technical University, Dept. of Space Sciences and Technology, Maslak 80626  
Istanbul, Turkey*

Feza Kerestecioglu

*Boğaziçi University, Dept. of Electrical-Electronics Eng., Bebek, Istanbul 80815, Turkey*

## Abstract

The conventional discussion on diversity has referred to the additive noise as having the characteristics of front-end receiver noise which is independent among diversity branches. However, in many applications, including those of mobile radio, noise arises also from the sources external to the receiving system. In fact, in the frequencies that mobile radio systems use, man-made noise level exceeds that of the receiver noise. In this case the received noise may be highly correlated in all diversity branches. This is of considerable importance for the maximal ratio diversity combining schemes where the signal-to-noise ratio (SNR) at the system output would be affected by the noise correlation. In such cases, the weighting coefficients maximizing the output SNR of a maximal-ratio predetection combiner in the uncorrelated case are no longer optimal.

In this paper a statistical model to determine the order of spatial noise correlation at urban-area base stations is devised. Optimal weighting coefficients for a maximal-ratio combiner with two-branch space diversity are then derived under conditions of correlated noise. The analysis has shown that correlation in branch noise can be used to improve the maximal-ratio combiner performance.

It is shown that the noise correlation would be determined by the mean and the width of the incoming direction of noise. When mean incoming direction of noise is about in-line with the diversity array axis, branch noises will be highly correlated. Results also indicate that branch noises will be significantly correlated up to antenna separations of  $20\lambda$  for angular widths up to  $30^\circ$ , and of  $10\lambda$  for a  $45^\circ$  sector. Note that spacings of  $15-20\lambda$  would be needed to achieve independent signal fading when high-elevation base antennas are used.

In the paper optimal weighting coefficients presented for correlated branch noise are used to obtain the cumulative distribution function of the combined SNR. Based on this result, it is shown that correlated branch noise can be used to improve the maximal-ratio combiner performance by dynamically adjusting the weightings. As an example, for a noise correlation of 0.8, one finds the combined signal to be 2.6 dB better than that of uncorrelated case for 98% of time. At the 99.9% reliability level the improvement over the uncorrelated case is 2.2 dB.

MONDAY AM URSI-B SESSION M-U5

Room: HUB 106

MICROSTRIP LINES

Chairs: S.M. El-Ghazaly, Arizona State University; M.I. Aksun, Bilkent University

- 8:20 Finite Difference Analysis of Cylindrical Microstrip Transmission Lines 36  
\*A. Z. Elsherbeni, Y. Ying, C. E. Smith, Univ. of Mississippi
- 8:40 Experimental Verification of a Leaky Dominant Mode on Microstrip Line with an Isotropic Substrate 37  
D. Nghiem, J.T. Williams, D.R. Jackson, Univ. of Houston; A.A. Oliner, Polytechnic Univ.
- 9:00 Crosstalk Between Microstrip Transmission Lines 38  
\*D. A. Hill, K. H. Cavcey, United States Department of Commerce
- 9:20 Analysis of Higher Order Modes of Stripline Field Applicators 39  
\*D.J. Infante, D.P. Nyquist, Michigan State Univ.
- 9:40 Characterization of Via Holes in Microstrip Geometries 40  
M.I. Aksun, Bilkent Univ.; R. Mittra, Univ. of Illinois at Urbana-Champaign
- 10:00 Break
- 10:20 Single and Two-Layer Quasi-TEM Surface-Impedance Approaches for the Analysis of Ohmic Losses in Multilayer and Multiconductor MMIC Lines 41  
\*J. Aguilera, R. Marqués, M. Horno, Univ. of Seville
- 10:40 Accelerated Quasi-TEM Analysis of Multilayered Non-Coplanar Multiconductor Lines with Polygonal Cross Section Conductors 42  
\*G. Plaza, F. Mesa, M. Horno, Univ. of Seville
- 11:00 Analysis of Microstrip Lines on Multilayered Ferrimagnetic Substrates 43  
\*K. Sun, Jackson State Univ.
- 11:20 Characterization of Discontinuities by the Method of Lines Using Matched Load Terminations 44  
B. Le Menn, M. Drissi, J. Citerne, LCST/INSA; T. Follet, S.A.T.
- 11:40 Control of Slow Wave Propagation on Suspended Microstrip Line 45  
A.K. Verma, A. Bhupal, Univ. of Delhi, South Campus

## FINITE DIFFERENCE ANALYSIS OF CYLINDRICAL MICROSTRIP TRANSMISSION LINES

A. Z. Elsherbeni\*, Y. Ying, and C. E. Smith  
Electrical Engineering Department  
University of Mississippi  
University, MS 38677

### ABSTRACT

Single and coupled microstrip lines are the basis of most microwave and millimeter integrated circuits including directional couplers, filters, delay lines, etc. Numerous papers have pursued the analysis, design, and applications of single and coupled planar microstrip lines. However, the analysis and design of microstrip lines conformed on circular or elliptical dielectric (single or multi-layer) substrates have not been explored as extensively. The analysis of these non-planar microstrip transmission lines is of increased importance in applications where the circuit must conform to surfaces on aeroplanes, missiles, and other vehicles.

In this paper, single and coupled microstrip lines conformed to a cylindrical boundary along with layers of dielectric substrate and/or superstrate of finite width is considered. The effects of the thickness of the strip lines are also considered in this investigation. A finite width dielectric substrate and/or superstrate provides a very practical design in many microwave and millimeter applications and antenna designs. For the coupled lines, a notch between the conducting transmission lines is also introduced in order to alter the coupling or crosstalk between the lines. This geometrical arrangement provides less coupling between the transmission lines and the surrounding transmission lines or any other microwave devices.

The infinite domain surrounding the transmission line is terminated at an artificial circular boundary. At this boundary a second order approximate boundary condition is used to truncate the domain of solution. The finite difference method, with non-uniform mesh, is then used to analyze this transmission line in a region bounded by the artificial boundary and the inner cylindrical grounded core. The assumption of having a shielding (perfectly conducting grounded circular boundary) in place of the artificial boundary is also considered in our computations in order to show the effects of the assumed approximate procedure at the artificial boundary. The potential distribution, self and mutual capacitances, odd and even phase velocities, and line impedance of single and coupled lines are computed to show the effects of the line parameters on its quasi-TEM characteristics.

## EXPERIMENTAL VERIFICATION OF A LEAKY DOMINANT MODE ON MICROSTRIP LINE WITH AN ISOTROPIC SUBSTRATE

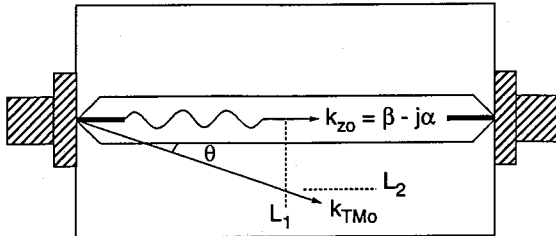
David Nghiem, Jeffery T. Williams, David R. Jackson,  
and Arthur A. Oliner<sup>†</sup>

Department of Electrical Engineering  
University of Houston  
Houston, TX 77204-4793

<sup>†</sup>Weber Research Institute  
Polytechnic University  
Brooklyn, NY 11201

Recently, the surprising discovery was made that a leaky dominant mode exists at high frequencies in addition to, and independently of, the customary bound dominant mode on a conventional microstrip line with an isotropic substrate (D. Nghiem et al., 1992 IEEE MTT-S Symp. Digest, pp. 491-494). This leaky mode has a strip current and a field distribution near the strip that are both similar to those of the customary bound dominant mode, but has a complex propagation constant  $k_{z0} = \beta - j\alpha$ . The attenuation constant  $\alpha$  corresponds to leakage into the fundamental  $TM_0$  surface wave on the grounded substrate. The main purpose of this talk is to demonstrate experimentally the existence of this newly discovered leaky mode at high frequencies. This is done in two ways. First, field-probe measurements are used, which demonstrate the expected improper field behavior of the leaky mode away from the strip, and which allow for a direct determination of the phase constant  $\beta$  and the leakage constant  $\alpha$  of the leaky mode. Secondly, it is demonstrated from direct  $S_{12}$  measurements how the existence of the leaky mode is responsible for increased attenuation along the line and destructive interference with the bound mode.

The figure below shows the setup for performing the measurements. The line  $L_2$  lies within the region of leakage, defined by the leakage angle  $\theta$ . Field measurements along this line directly yield  $\beta$  and  $\alpha$ . A measurement of the leakage angle  $\theta$ , made by probing the field along the line  $L_1$ , is also used to determine  $\beta$  from the relation  $\theta = \cos^{-1}(\beta/k_{TM_0})$ , where  $k_{TM_0}$  is the propagation wavenumber of the  $TM_0$  surface wave. Preliminary results show a good agreement between calculated and measured results for  $\beta$  (within 3%) and  $\alpha$  (within 10%).



## CROSSTALK BETWEEN MICROSTRIP TRANSMISSION LINES

D.A. Hill,<sup>\*</sup> K.H. Cavcey, and R.T. Johnk  
Electromagnetic Fields Division  
National Institute of Standards and Technology  
Boulder, CO 80303

In dense circuits, electromagnetic coupling (crosstalk) between closely spaced signal lines limits interconnect performance (L.B. Gravelle and P.R. Wilson, IEEE Trans. Electromag. Compat. 34, 109-116, 1992) and becomes an important aspect of circuit design. In this talk we analyze crosstalk between a pair of weakly coupled microstrip transmission lines located on a single substrate, but the techniques are applicable to more general geometries.

We first consider a pair of identical, parallel microstrip lines that support two dominant modes, even and odd. The propagation constants and characteristic impedances of the these two modes are obtained by solving the multiconductor transmission line equations (J.C. Isaacs and N.A. Strakhov, Bell Sys. Tech. J. 52, 101-115, 1973). The near-end and far-end crosstalk are then obtained directly in terms of these quantities.

For more general microstrip geometries, we review two first-order perturbation techniques that neglect multiple interactions between lines, but do not require that the lines be parallel. The potential method (J.M. Dunn, L.C. Howard, and K. Larsen, IEEE Trans. Microwave Theory Tech., 41, 1287-1293, 1993) introduces two source terms, proportional to the scalar potential and the magnetic vector potential produced by the driven line, that excite the undriven line. We show that these two terms are equivalent to the mutual capacitance and mutual inductance terms in classical multiconductor transmission line theory. The induced EMF method (R.G. Olsen, IEEE Trans. Electromag. Compat. 26, 79-83, 1984) integrates the electric field of the driven line along the undriven line in the same manner as performed in classical antenna theory. We show that this method is equivalent to the potential method. Both methods have the advantage that the spacings of the two lines are not required to be electrically small as in classical transmission line theory.

To confirm our calculations, we performed near-end and far-end crosstalk measurements on a pair of microstrip lines for frequencies from 50 MHz to 5 GHz. Good agreement with theory was obtained in both amplitude and phase up to about 3 GHz, the upper frequency limit for which the quasi-static analysis of the microstrips was valid.

## ANALYSIS OF HIGHER ORDER MODES OF STRIPLINE FIELD APPLICATORS

D. Infante\* and D. P. Nyquist  
Department of Electrical Engineering  
Michigan State University  
E. Lansing, MI 48824

Stripline structures have found increasing use in areas such as integrated circuit devices and the electromagnetic characterization of materials. Because of its symmetric structure, the stripline lends itself well to analysis for in-band operation. In spite of this fact, little has been documented about higher order modes on the stripline. Knowledge of the cutoff frequencies of higher order modes is critical for designing broad band field applicators for material measurements.

To determine the cutoff frequencies of the higher order modes a Hertzian potential Green's function is established for the region between two parallel plates using Sommerfeld integrals and assuming that a generalized impressed current is suspended in the space between the plates. This Green's function is then specialized to the stripline by enforcing boundary conditions for tangential fields on a stripline structure. This results in an electric field integral equation (EFIE) for currents on the stripline

$$\hat{t} \cdot (k^2 + \nabla \nabla) \int_S \vec{G}(\vec{r}|\vec{r}') \vec{K}(\vec{r}') ds' = -j\omega \epsilon \hat{t} \cdot \vec{E}^i(\vec{r}) \quad (1)$$

where  $\vec{G}$  is the Green's function,  $\vec{E}^i$  is the impressed field,  $\vec{K}(\vec{r}')$  is the surface current on the center conductor,  $k$  is the wavenumber and  $\epsilon$  is the permittivity of the guiding region,  $\hat{t}$  is a unit tangent vector, and  $S$  encompasses the center conductor. Guided mode solutions for this EFIE are determined by Fourier transforming on the axial variable and examining the resulting EFIE

$$\hat{t} \cdot (k^2 + \vec{\nabla} \vec{\nabla}) \int_{-a}^a \vec{g}_\zeta(\vec{\rho}|\vec{\rho}') \cdot \vec{k}_p(x') dx' = 0 \quad (2)$$

where  $\vec{\nabla}$  is the transform domain gradient operator,  $\vec{g}$  is the transform domain Green's function,  $\vec{k}_p$  is the transform domain current, and the center conductor is defined to extend from  $-a$  to  $a$ . Equation (2) has solutions only for discrete values of  $\zeta$  which are the propagation constants for the guided wave modes. The EFIE is converted to matrix form via the method of moments. The resulting homogeneous matrix equation has non-trivial solutions only for discrete  $\zeta = \zeta_p$ . The  $\zeta_p$  are determined by numerically rooting the determinantal equation.

This paper will discuss a full-wave integral equation formulation for stripline currents and propagation constants.

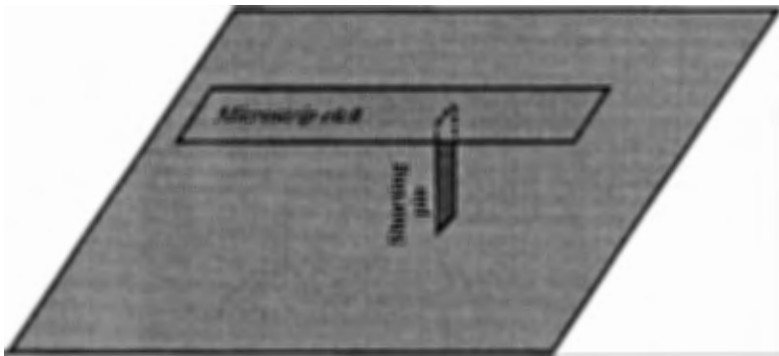
## CHARACTERIZATION OF VIA HOLES IN MICROSTRIP GEOMETRIES

M. I. Aksun  
Bilkent University  
Dept. of Elect. and Electronics Eng.  
06533 Ankara-Turkey

R. Mittra  
Electromagnetic Communication Lab.  
University of Illinois at Urbana-Champaign  
Urbana, IL. 61801

Via holes, also called shorting pins in some applications, are found in a number of microstrip structures, e.g., microstrip patch antennas, and etches on multilayered substrates and superstrates. For the case of a microstrip patch antenna, the shorting pins are used to modify the antenna pattern and to realize dual-frequency operation. For the multilayer case, the interconnections between the etches residing on different layers are accomplished by using the vias.

Microstrip antennas with some shorting pins have been investigated in the past by using the cavity model which, though computationally very efficient, is not sufficiently rigorous for some applications. In contrast, the interconnect problem in a multilayered microstrip geometry has been modeled by employing numerically rigorous and versatile techniques, e.g., the Finite Difference Time Domain and the Finite Element Method, both of which are, unfortunately, computationally very expensive. Recently, the Method of Moments has been successfully applied in conjunction with the closed-form Green's functions to microstrip geometries with substrates and superstrates that are strictly confined to a single plane, and has been found to be very efficient for analyzing these structures in comparison to the conventional MoM/ spectral domain approach. The objective of this paper is to extend the closed-form Green's function analysis to non-planar structures by applying it to the shorting pin geometry depicted in the accompanying figure below. Both the horizontal and vertical electric dipole Green's functions are needed for the analysis of this type of geometry and the derivation of these Green's functions in closed forms, as well as the use of the discontinuous basis functions in the MoM procedure, are discussed in the paper. Numerical results illustrating the application of the method are included in the paper.



GROUND PLANE

## Single and two-layer Quasi-TEM Surface-impedance Approaches for the Analysis of Ohmic Losses in Multilayer and Multiconductor MMIC Lines

José Aguilera\*, Ricardo Marqués and Manuel Horno  
Microwave Group. Department of Electronics and Electromagnetism  
University of Seville  
Avda. Reina Mercedes s/n. 41012 SEVILLA (SPAIN)

The thickness of metallizations in Monolithic Microwave Integrated Circuits (MMIC) lines prevents the use of strong skin effect based techniques – such as the incremental inductance rule – for the analysis of conductor losses. On the other hand, the use of a quasi-TEM approach is suggested by the small optical length of MMICs lines at the usual operating frequencies (G.L. Matthaei et al., IEEE-MTT, 38, pp. 1031–1035, 1990). The suitability of quasi-TEM spectral domain analysis in MMIC lines has been discussed in (M. Horno et al., IEEE-MTT, 38, pp. 1059–1068, 1990). This analysis includes substrate dielectric and magnetic anisotropy, as well as substrate losses. In (R. Marqués et al., MOTL, 6, pp. 391–394, 1993) a quasi-TEM method is proposed to incorporate the effects of the finite conductivity of the metallizations, using a single-layer surface impedance model. The limitations of this method are not in the quasi-TEM analysis (for the usual MMIC frequencies and dimensions) but in the choice of the surface impedance definition at the strips: computed results have shown to be very sensitive to this parameter. Moreover, the strip thickness effects were not directly considered.

In the present paper a two-plate model is considered to solve the above deficiencies. The proposed model replaces the conductor by two surface impedance plates. The thickness of the strip is directly incorporated to the surface impedance definition, which becomes unambiguous. Then both, the ohmic losses and the thickness effect are taken into account. The use of the spectral domain technique make possible to extend the method to multiconductor and/or anisotropic lines straightforwardly.

The proposed method has been tested with both, theoretical and experimental data, showing a good agreement with them. Once the method was tested, it was used for the study of the suitability of the different surface-impedance definitions in the frame of the single-layer model. Although the single-layer model, with a careful choice of the surface impedance definition, seems to be useful for attenuation constant calculations in simple configurations, the two layers model ensures a good accuracy for both the attenuation and phase constants, without ambiguity in the choice of the surface impedance. Slow wave structures, including conductor, semiconductor and/or magnetic losses, have been also analysed using the proposed two-plates model.

## Accelerated Quasi-TEM Analysis of Multilayered Non-coplanar Multiconductor Lines with Polygonal Cross Section Conductors.

Gonzalo Plaza\*, Francisco Mesa, Manuel Horno  
Microwave Group. Department of Electronics and Electromagnetics  
University of Seville  
Avda. Reina Mercedes s/n. 41012 SEVILLA (SPAIN)

In the last few years, the analysis of multilayered multiconductor lines with arbitrary cross section conductors has found an increasing interest (C.J. Railton et al., IEEE-MTT, 38, pp. 1017-1022, Aug. 1990; F. Olyslager et al., IEEE-MTT, 41, pp. 79-88, June 1993). One of the motivations of this interest is the geometry of the conductors used in MMIC and some interconnecting systems. For example, in MMIC technology, the strip thickness may be as large as a 30% of the strip width (C.J. Railton et al., IEEE-MTT, 38, pp. 1017-1022, Aug. 1990). Moreover, due to the manufacturing process, the conductors approximately present trapezoidal cross sections (F.E. Gardiol, Proc. IEE, 135, pp. 145-157, June 1988). On the other hand, accuracy and short CPU time are two features required for computer codes for the analysis of those lines if they have to be used in a CAD environment. This communication is a contribution to this research line.

In this work, general multilayered non-coplanar multiconductor transmission lines with arbitrarily shaped (polygonal) conductors are analyzed under the quasi-TEM approach. Polygonal cross section conductors are modeled following the idea presented by the authors in (G. Plaza et al., MOTL, 2, pp. 257-260, July 1989): conductors are replaced by a suitable number of equipotential zero thickness planar strips. Once this substitution has been made, one can employ spectral domain formulation to solve the problem. However, numerical efficiency of this technique should be meaningfully enhanced to obtain a practical computer code. One the essential aspects stressed in this work has been the improvement of the computational efficiency. This goal has been achieved by using a proper analytical preprocessing of the spectral integrals arising in the solution of the problem. The Prony's method has been employed to obtain the asymptotic behavior of the Green's function. Quasi-analytical methods have been developed to compute the spectral tails in order to reduce CPU time as much as possible. In addition, the spectral tails for high order basis functions (i.e., greater than 1) have been obtained by means of recurrence formulae thus providing additional CPU time reduction and numerical stability. It is also interesting than anisotropic and certain gyromagnetic materials are considered as possible substrates.

A FORTRAN computer code has been written based on the aforementioned study. This code can analyze general multilayered multiconductor transmission lines on PC's, providing high accuracy results in short CPU time.

## ANALYSIS OF MICROSTRIP LINES ON MULTILAYERED FERRIMAGNETIC SUBSTRATES

Kunquan Sun  
Department of Technology/IA  
Jackson State University, Jackson, MS 39217

During the recent years the progress has been made in the growth and deposition of magnetic films on semiconductors in conjunction with metals and dielectrics. As a result of this progress, there is a great interest in the characteristics of microstrip transmission lines on magnetic substrates because of their applications in monolithic microwave integrated circuits (MIC). The work presented here is to study the dispersion characteristics of microstrip lines on multilayered magnetic structures, which have shown the feature of wider bandwidth in the device applications.

This study uses the spectral-domain technique with multilayered YIG/GGG/YIG as a substrate. A general formulation is obtained to relate the arbitrary coefficients of TE and TM modes in each region to the currents, which are flowing on the metal strip; by imposing the boundary conditions at each interface of the layered structure. Then, the spectral-domain Green's functions are determined. The basis functions are chosen to expand the currents and are ensured to satisfy the required edge conditions. Galerkin's method is applied in the spectral-domain along with Parseval's theorem, and the resultant system matrix equation is solved for the propagation constant at each frequency by setting the determinant of the system matrix equation equal to zero.

Numerical computations have been performed for double layered YIG structure with the applied dc magnetic field normal to the film plane. It is found that the separation between the two YIG slabs has a strong effect on the dispersion curves. Effects of width of the strip and thickness of YIG slabs on the dispersion characteristics are also studied. Further study is undergoing to investigate the field distribution across the strip.

# CHARACTERIZATION OF DISCONTINUITIES BY THE METHOD OF LINES USING MATCHED LOAD TERMINATIONS

**B. Le Menn, M. Drissi, J.Citerne and T. Follet<sup>(1)</sup>**  
 LCST / INSA , CNRS URA 834, 35043 RENNES Cedex  
 (1) Div.Télécom., S.A.T., B.P.370, 75626 PARIS Cedex 13, France

Recent research has proved that the Method Of Lines (M.O.L.) is useful and efficient to modelize planar discontinuities. Unfortunately, the scattering matrix calculation is often achieved by terminating the outports with open or short-circuits, or by using different excitations, which makes it difficult to extract accurately the reflection coefficients due to very high standing wave ratios.

In this paper, the M.O.L. is extended to characterize planar discontinuities with matched load ends. These loads are achieved through the use of absorbing boundary conditions at the microstrip outputs. The applied absorbing boundaries are similar to those developed to simulate open boundaries on the wall sides of a shielded microstrip structure (A. Dreher & R. Pregla, IEEE Microwave and Guided Wave Let. vol. 1, No.6, June 91). When using this technique for shielded discontinuities, the reflection coefficient is obtained from only one current distribution. In order to get the  $S_{22}$  and  $S_{12}$  parameters, once  $S_{21}$  obtained, it is proceeded in the same way after inversion of the load and the source.

Fig.2 shows the current distribution along the circuit element described in fig.1, when ended by a matched load. The higher the discretization is, the better the adaptation. One can obtain respectively 30 dB and 40 dB return losses for 12 and 30 lines of discretization per wavelength. As an example, the developed technique is applied to characterize a step discontinuity. To illustrate the convergence, the reflection coefficient is presented in fig.3 ( $W_2/W_1=2, W_1/h=1, \epsilon_r=10$ ) for different discretizations. A good agreement can be observed when comparing the results to those from N.H.L. Koster & R.H. Jansen (IEEE MTT, vol.34, No. 2, Feb. 86).

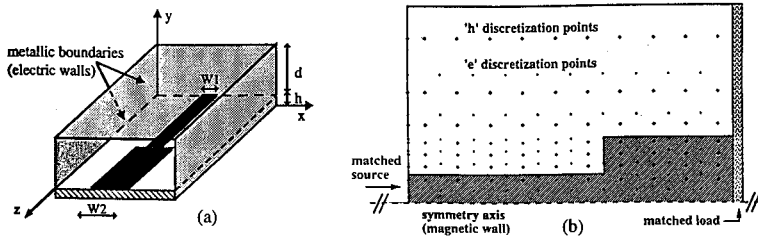


Fig.1.(a),(b) Description of a two-dimensionally discretized shielded microstrip step-in-width discontinuity

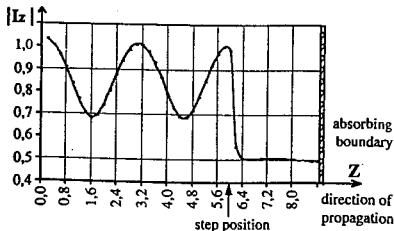


Fig.2 Magnitude of  $I_z$  along the microstrip step discontinuity described in fig.1

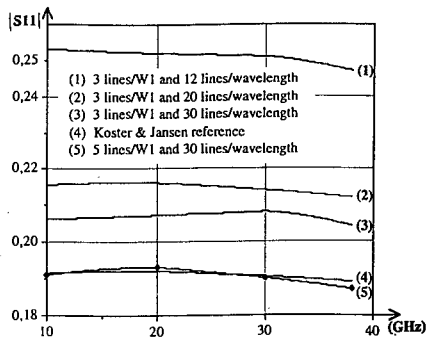


Fig.3

# Control of Slow wave Propagation on Suspended Microstrip Line

A.K.Verma and Annapoorna Bhupal

Deptt. of Electronic Science, University of Delhi, South Campus,  
New Delhi-110021, India

## Abstract:

The Slow wave phenomenon has been reported by several authors on the semi conducting substrate with passivation layer by using full wave analysis [P.K.Gib and A.Balanis, MTT, 92, 2148-2154]. The slow wave has been used for design of delay line. However, static variational technique has not been used for such analysis. By defining complex effective permittivity  $\epsilon_{eff}^* = \frac{c}{c_0}$  of the composite substrate structure [A.K.Verma and A.Bhupal, APMC, 1993, Australia] and single layer reduction (SLR) technique [A.K.Verma and G.Sadr, MTT, 91, 1587-1591], we have converted the composite lossy substrate structure into an equivalent single layer lossy structure. Real part of the  $\epsilon_{eff}^*$  provides dielectric mode and slow wave-mode. From the same formulation dielectric loss of the slow wave mode has also been obtained. The method has been used for analysing slow wave on the suspended microstrip structure fig. (1) for the purpose of getting variable phase velocity of slow wave by controlling the airgap. Thus by controlling airgap delay line of required nature and low loss can be obtained as shown in fig (2) and fig (3). Fig(2) and fig(3) also show comparison of our present model against full wave analysis within 1%. The proposed method is fast for CAD purpose and is suitable for synthesis of delay line on semi conducting substrate with and without airgap.

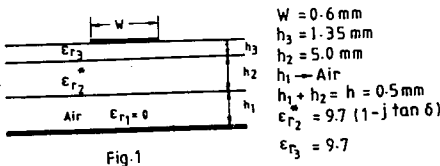


Fig.1

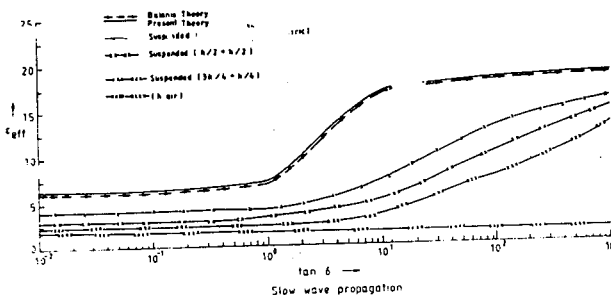


Fig 2

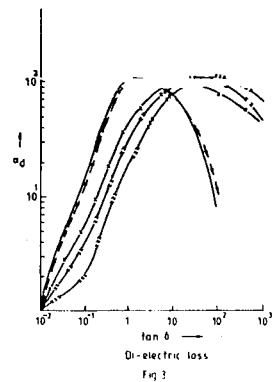


Fig 3



## MONDAY AM URSI-B SESSION M-U6

Room: HUB 309

### SCATTERING I

- Chairs: T.A. Pankaskie, The Boeing Company; S.R. Laxpati, University of Illinois at Chicago
- 8:20 Combined Complex Multipole Beam-Method of Moments Approach to Scattering Problems 48  
\*A. Boag, \*E. Michielssen, R. Mittra, Univ. of Illinois
- 8:40 Co-Pol and Cross-Pol Radar Cross-Sections for a Missile-Like Body with an Impedance Patch 49  
S.F. Kawalko, \*S.R. Laxpati, P.L.E. Uslenghi, Univ. of Illinois at Chicago
- 9:00 Scattering by a Conducting Spherical Shell with Multi Slots of Arbitrary Shapes and Sizes 50  
\*R.A. Said, A. Sebak, G.E. Bridges, Univ. of Manitoba
- 9:20 Suppression of Creeping Waves on Coated Cylinders by Anisotropic Coating 51  
\*T.A. Pankaskie, The Boeing Company; R.G. Olsen, Washington State Univ.
- 9:40 Resonant Frequencies of Dielectric Objects by the Phase Matching Method 52  
D.J. Taylor, Naval Research Laboratory; H. Überall, The Catholic Univ. of America
- 10:00 Break
- 10:20 Material Properties and Scattering Predictions of Thin Chaff Sheets 53  
\*R. C. Baucke, GE Aircraft Engines
- 10:40 ARCHAEOPTERYX: a Parallel Software Package for High-Frequency RCS Predictions of Complex Targets 54  
M. Calamia, M. Fallai, A. Naldini, \*S. Selleri, R. Cecchini, Univ. of Florence
- 11:00 [Paper withdrawn]
- 11:20 3D-Bistatic RCS-Calculations by IEM and PO 55  
\*E. Kemptner, M. Ruppel, German Aerospace Research Establishment DLR
- 11:40 3D-Monostatic RCS-Calculations by IEM, PO and PTD 56  
\*E. Kemptner, D. Klement, V. Stein, German Aerospace Research Establishment DLR

## Combined Complex Multipole Beam—Method of Moments Approach to Scattering Problems

Amir Boag\*, Eric Michielssen, and Raj Mittra  
Electromagnetic Communication Laboratory  
University of Illinois, Urbana, IL 61801

The conventional approach to formulating the problem of electromagnetic scattering using the method of moments (MoM) is to employ subdomain basis functions to represent the surface currents on the body. This approach often requires the use of ten or more unknowns per linear wavelength, and thus leads to relatively large matrices even for moderately-sized scatterers. In addition, the resulting generalized impedance matrix is typically dense, owing to a strong coupling between the subdomain basis and testing functions, even when they are remotely separated from each other. However, it is well-known from asymptotic solutions of canonical problems, that the wave interactions between the smooth parts of the scatterer are essentially local. A new technique, called the Complex Multipole Beam (CMB) approach, has been recently introduced by the authors (A. Boag & R. Mittra, 856-859, *Proc. IEEE AP-S. Intl. Symp.*, 1993). The strategy followed in this method is to expand the scattered fields in terms of beams, generated by a judiciously selected set of multipole sources located in the complex space. These beams are very similar to the Gabor basis functions when sampled at the boundary of the scatterer. Thanks to the use of smooth expansion functions, the CMB approach has the advantage over the MoM in terms of the number of unknowns, typical figures being less than four per linear wavelength. This results in an order of magnitude reduction of the number of unknowns required to model three-dimensional scatterers. In addition, the CMB algorithm gives rise to matrix systems that are essentially banded, making the storage requirements and the computational complexity of  $O(N)$ ,  $N$  being the number of unknowns.

The MoM is the most widely-used technique for analyzing electromagnetic scattering thanks largely to its applicability to a nearly unrestricted class of target geometries consisting of arbitrarily shaped surfaces with possible wire attachments. On the other hand, in its original form, the CMB approach was designed for application to the problem of scattering from large smooth bodies. The hybrid approach proposed herein attempts to optimally combine the MoM with the CMB algorithm, thereby allowing for a flexible geometrical description of arbitrarily-shaped targets while retaining the overall efficiency of the CMB approach. In the hybrid CMB-MoM algorithm, the complex multipole beam representation is designed to represent the fields scattered from the smooth parts of the surfaces, while conventional MoM basis functions are employed only on those parts of the scatterer that do not permit an accurate representation of the scattered field on the boundary by the complex multipoles. This is the case near sharp edges, grooves, parts of the structure with small radii of curvature, and wires. Following this hybrid expansion of the fields, a matrix equation in terms of the unknown expansion coefficients is obtained by point matching the boundary conditions on the surface of the scatterer. Since the bulk of the surface area of practical scatterers is typically smooth, the hybrid algorithm retains the desirable characteristics of the CMB method in terms of the number of unknowns, efficiency of the matrix element calculations, and bandedness of the resulting matrix equation. The presentation will begin by surveying the basic CMB approach and then go on to describe the application of the combined formulation to arbitrary scatterers.

## CO-POL AND CROSS-POL RADAR CROSS-SECTIONS FOR A MISSILE-LIKE BODY WITH AN IMPEDANCE PATCH

S. F. Kawalko, S. R. Laxpati \* and P. L. E. Uslenghi  
Department of Electrical Engineering and Computer Science, (M/C 154)  
University of Illinois at Chicago  
851 S. Morgan Street  
Chicago, IL 60607-7053

This paper will present some results on the scattering of a linearly polarized plane electromagnetic wave by an impedance scatterer consisting of a body of revolution to which one or more thin fins are attached. The shape of the fins is restricted to a simple rectangular plate with a small nonzero thickness. The surface impedance is allowed to vary in a stepwise manner over the entire surface of the scatterer. Previously, results for the bistatic radar cross-section for such a scatterer have been reported by the authors [ICEAA 1993, Torino, Italy, September 1993].

Using a linear ( $HV$ ) polarization basis, the relation between the incident and scattered electric fields can be written as follows:

$$\begin{pmatrix} E_H^s \\ E_V^s \end{pmatrix} = \begin{pmatrix} a_{HH} & a_{HV} \\ a_{VH} & a_{VV} \end{pmatrix} \begin{pmatrix} E_H^i \\ E_V^i \end{pmatrix}$$

If polarization is taken into account, four radar cross-sections can be defined as follows:

$$\sigma_{ij} = \lim_{r \rightarrow \infty} 4\pi r^2 |a_{ij}|^2, \quad i = H, V; \quad j = H, V$$

The radar cross-sections  $\sigma_{HH}$  and  $\sigma_{VV}$  relate the reflectivity of a scatterer illuminated by an  $H$ -polarized and  $V$ -polarized incident fields, respectively, as seen by the same polarization and are called the co-polarized (co-pol) radar cross-sections. The radar cross-sections  $\sigma_{VH}$  and  $\sigma_{HV}$  relate the reflectivity of a scatterer illuminated by an  $H$ -polarized and  $V$ -polarized incident fields, respectively, but seen by the other polarization and are called the cross-polarized (cross-pol) radar cross-sections.

The problem is formulated in terms of an electric field integral equation for the vector electric surface current density. The integral equation is solved using an implementation of the method of moments which uses parametric surface elements, Hermite expansion functions and delta function testing. The far scattered electric field is numerically obtained from the solution for the electric surface current density. The co-pol and cross-pol radar cross-sections are obtained from these values for the far scattered electric field.

Results for several missile-shaped scatterers are presented. The co-pol and cross-pol radar cross-sections for a scatterer with fins is compared to one without fins. Also, a comparison is made between the radar cross-sections for a scatterer with fins and a constant surface impedance and the same scatterer with various impedance patches.

# SCATTERING BY A CONDUCTING SPHERICAL SHELL WITH MULTI SLOTS OF ARBITRARY SHAPES AND SIZES

R.A. Said\*, A. Sebak, and G.E. Bridges  
Department of Electrical and Computer Engineering  
University of Manitoba  
Winnipeg, Manitoba R3T 5V6, CANADA

As other separable problems, the electromagnetic scattering by complete spherical bodies has been treated extensively in the literature where both exact and approximate solutions have been presented. When these bodies are no longer separable due to the presence of one or more apertures, the scattering characteristics are drastically changed and an exact solution is more difficult to formulate. To overcome this difficulty, approximate solutions are sought using classical GTD approach or physical optics reasoning. A more accurate solution can be obtained using boundary value approach, however the solution is not completely analytic due to unavailable orthogonal set of expansion functions over the boundary of the unseparable body.

This paper presents a general formulation of the scattering by a thin conducting spherical shell with multi slots of different shapes and sizes as shown in Fig. 1. The problem is treated using boundary value approach where the fields inside and outside the shell are expressed in terms of Hansen vector wave functions with unknown expansion coefficients. To approximate the expansion coefficients, the least-square error method is applied to the equations resulting from applying the fields boundary conditions at the surface of the spherical shell. Numerical results will be presented in the form of amplitude patterns for the aperture fields and radar cross-section.

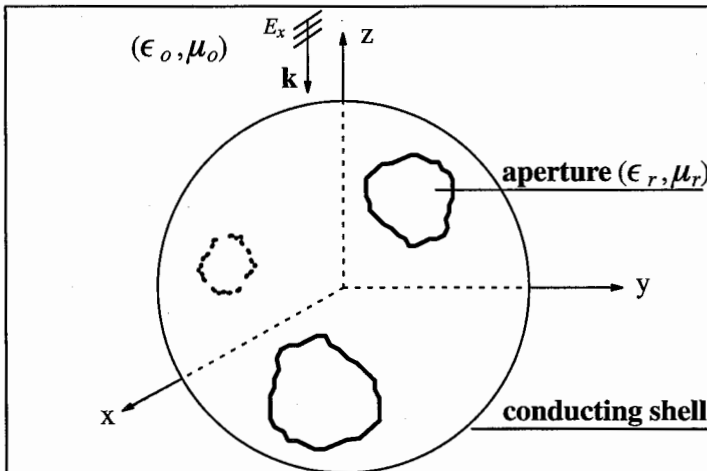


Fig. 1. Spherical conducting shell with multi slots of different shapes and sizes.

## **Suppression of Creeping Waves on Coated Cylinders by Anisotropic Coating**

T. A. Pankaskie \*  
The Boeing Co.  
P.O. Box 3999, M/S 2T-40  
Seattle, WA. 98124-2499

R. G. Olsen  
School of Electrical Engineering and Computer Science  
Washington State University  
Pullman, WA. 99164-2752

Conducting cylinders with material coatings can, in many instances, support slowly attenuated creeping waves. When present, these creeping waves contribute significantly to the radar cross-section, particularly in the backscatter region. Examination of the polarization dependence of these creeping waves shows that if there is a creeping wave in the E-Polarization, for a given configuration, then there will not be one in the H-Polarization. Conversely, if there is a creeping wave in the H-Polarization then there will not be one in the E-Polarization. Anisotropy in the material coating the cylinder can be used to alter this relationship such that a creeping wave may exist in either both or neither polarization. Numerical results demonstrate these ideas.

In order to confirm the numerical results, an experiment was conducted. A conducting cylinder was coated with an artificial anisotropic dielectric. The coating was constructed of a solid sheet of dielectric material into which small holes were drilled on a hexagonal grid covering the entire sheet. The spacing of the holes was kept to a fraction of a wavelength with the host dielectric constant, hole size, and spacing determining the anisotropy of the composite sheet. The coating properties were analyzed by using Homogenization Theory (Olsen & Vanhoff, J. of Ap. Phy, Vol 69, pp 2497-2503) and verified by waveguide measurement of a sample of the material. Bistatic radar cross-section measurements were made using an H.P. 8510 network analyzer. Comparisons between measurement results and theory are presented. Despite the limitations of the experiment, there was good agreement between experiment and theory.

## Resonant frequencies of Dielectric Objects by the Phase Matching Method

Douglas J. Taylor

Signature Technology Office, Code 4050  
Naval Research Laboratory, Washington, DC 20375

Herbert Überall

Physics Department, The Catholic University of America  
Washington, DC 20064

The natural frequencies of dielectric or perfectly conducting objects can be excited during the scattering process and have been analyzed in terms of surface waves generated that return in phase over a geodesic path. This principle can and has been applied to arbitrary shapes to predict electromagnetic and acoustic scattering resonances. Mathematically, a resonance condition exists in the following form,

$$\oint \frac{ds}{\lambda(\omega, s)} = \frac{1}{2\pi} \oint k(\omega, s) ds = m + \frac{n'}{4}$$

where at resonance ( $\omega$ ), a surface wave with a local wavelength  $\lambda(\omega, s)$  and propagation constant  $k(\omega, s)$  traversing a geodesic path accumulates phase such that the total closed path is  $m$  integral wavelengths with  $n'$  jumps of  $1/4$  wavelength for each caustic encountered. Validation of and use of this principle to predict the complex resonances of non spherical, perfectly conducting objects have been quite successful. The results presented here are the first attempt to use the phase matched surface wave method to predict resonances of penetrable dielectric objects which are not spherical, or amenable to series solution.

A homogeneous lossless dielectric,  $\epsilon=2.56$ , circular cylinder with hemispherical endcaps was selected because it is continuously deformable from a sphere, allowing the movement of known spherical resonances to be tracked as a function of the cylindrical body length. The real parts of the complex electromagnetic resonant frequencies of this object were computed using the phase matching condition determined from the optical path length accumulated by a surface wave propagating over a closed path on the surface. A 'Bohr Sommerfeld' resonance condition exists, for this geometry, when this optical path length is exactly  $n + 1/2$  wavelengths long, where  $n$  is an integer. An approximate solution for the optical path length is obtained using the surface wave propagation constants for the  $HE_{11}$  mode on an infinite length cylinder and phase velocities determined from dielectric sphere resonances. These results are compared to the real part of the complex resonant frequencies computed numerically from the zeros of the impedance matrix of a body of revolution, magnetic field integral equation (HFIE) method. Only the  $m = 0$  modes are studied.

## Material Properties and Scattering Predictions of Thin Chaff Sheets

R. Craig Baucke  
GE Aircraft Engines  
1 Neumann Way M/D G104  
Cincinnati, OH 45215-6301  
(513) 243-4830

Thin, paper-like sheets containing a quasi-random loading of short, carbon-loaded fibers are used as resistive/conductive layers in RF shielding and absorbing applications. Typically, these sheets (herein called chaff sheets) are modeled as resistive or impedance layers in 2D and 3D moment method models. However, good resistive or impedance models can be difficult to create from measured data. Analytical scattering prediction is difficult due to the quasi-random placement of the carbon fibers which yields an arrangement of connected and unconnected fibers.

In this work, a resistive thin wire method of moments code is developed in order to predict the scattering from chaff sheets. In this code, multiple resistive thin wires are placed in a plane, and the interconnections between the fibers are determined. The scattering from the sheet is computed using a traditional MoM approach (piecewise linear expansion and testing functions). Junction basis functions are included to ensure current continuity between connected fibers.

The statistical behavior of sheets of various amounts of fiber loading is determined from a large population of moment method runs. Phenomena difficult to quantify by measurement, such as depolarization properties, are studied with this code. The effect of material changes in the carbon fibers are studied, such as changing the fiber diameter and the resistivity of the fibers. Models created for chaff sheets using this MoM code are compared to models created from measured data.

## **ARCHAEOPTERYX: a parallel software package for high-frequency RCS predictions of complex targets**

M. Calamia, M. Fallai, A. Naldini, S. Selleri\*  
Department of Electrical Engineering, University of Florence  
Via C. Lombroso 6/17, I-50134 Florence, Italy

R. Cecchini  
Department of Physics, University of Florence  
Largo E. Fermi 2, I-50127 Florence, Italy

These last few years have been characterized by a raising interest in numerical methods devoted to the prediction of the radar cross section (RCS) of complex objects. These codes are now feasible thanks to the increasing power of machines and are developed by companies and universities alike.

The main characteristic of the ARCHAEOPTERYX program, compared to the existing codes, is that it is structured so that it can be executed on a parallel ACPU machine, loosely coupled. The implementation is on a network of IBM-compatible PCs which uses the interconnection software PVM - Parallel Virtual Machine System 3.1 (A.L. Beguelin *et al.*, 1993). The code is modular and can be very easily implemented on parallel machines with different architectures. The PC network system was chosen for its simplicity, its low cost/performance ratio, and thus allowing an easy industrial implementation. The choice of a modular parallel code was made to allow easy insertions of future improvements in the evaluation of contributions from single modules and to obtain a relatively low computing time for calculating the RCS or special contributions to the scattered field even for very complex objects.

The code is organized in four principal steps, some of which benefit most from the parallel architecture: a) decomposition of the target in canonical components (the description of each canonical component is made analytically or numerically, with a CAD program); b) evaluation of the interactions among different components (multiple reflections with masking); c) evaluation of the field scattered from every component; d) sum of all the contributions. For what concerns the previous point c) the code evaluates the field scattered from large surfaces applying the Physical Optics approximation (both for conducting and absorbing coated surfaces, these latter are treated by impedance boundary conditions) together with the incremental diffraction coefficients (G. Pelosi *et al.*, IEEE Trans. AP, vol. 10, 1992). Contributions from inlets are also considered. The user interface has been implemented with particular attention and it allows a continuous control over each phase of the RCS simulation.

### 3D-BISTATIC RCS-CALCULATIONS BY IEM AND PO

*E. Kemptner\*, M. Ruppel*

German Aerospace Research Establishment DLR

The bistatic RCS of cylindrical objects is calculated using two computer codes based on different methods. The first one is the well-known **NEC-2** based on the *Integral-Equation-Method (IEM)*. The treated objects are modeled by wires as well as by patches. The second one is a new code called **BISTRO**. It has been developed at DLR and is based on the *Physical Optics (PO)*.

Both codes are used to calculate the scattered fields of perfectly conducting cylinders. Different shapes have been investigated, for example circular, elliptical, ogival and airfoil-like. The dimensions are of several wavelengths which can still be handled by NEC-2. PO as a high-frequency approximation needs much less CPU-time than IEM. For both methods the convergence of the results as a function of mesh-width is investigated.

For validation of the theoretical results the bistatic RCS of appropriate test bodies were measured at an *indoor range* using a frequency of 94 GHz with far-field conditions. The separation angle was varied from 8° to 180°, which includes the region of forward-scattering. Finally, the IEM solutions, PO results and experimental data are compared. Similarities and differences are shown and discussed.

### 3D-MONOSTATIC RCS-CALCULATIONS BY IEM, PO AND PTD

E. Kemptner\*, D. KLEMENT, V. STEIN

German Aerospace Research Establishment DLR

3D-objects such as an elliptic cylinder and an airfoil are treated theoretically by the *Integral-Equation-Method (IEM)*, *Physical Optics (PO)* and *Physical Theory of Diffraction (PTD)*. The dimensions of the objects are in the order of several wavelengths.

The computer code for the PO as well as for the PTD is *SIGMA*. For this code the objects have to be modeled by flat panels and the surface may be perfectly conducting or coated with one or more dielectric layers. A hidden-surface- as well as a double-reflection-algorithm is included. To treat edge diffraction effects equivalent edge currents based on the PTD may be used optionally.

Since PO and PTD are approximate methods the results are compared with those of the IEM, using the code *NEC-2*. The objects mentioned are modeled by wires as well as by patches.

A comparison and discussion of the monostatic RCS-results of perfectly conducting bodies calculated by these three methods is presented. Investigations on the stability and convergence lead to conclusions concerning accuracy and efficiency (CPU-time).

## MONDAY PM JOINT SPECIAL SESSION M-J1

Room: HUB 310

### RANDOM MEDIA II

Chairs: R. Lang, The George Washington University; K.H. Ding, Massachusetts Institute of Technology

Organizers: S. Broschat, Washington State University; A. Ishimaru, University of Washington

- |      |  |      |
|------|--|------|
| 1:20 | An Innovative Hybrid Experimental/Theoretical Technique for Modelling Radar Scatter from Random Media<br><i>*J.R. Kendra, K. Sarabandi, F.T. Ulaby, Univ. of Michigan</i>                      | 58   |
| 1:40 | Comparison of Microwave Scattering Models of Vegetation<br><i>S.S. Saatchi, M. Moghaddam, K. McDonald, S. Durden, California Inst. of Technology</i>   | 59   |
| 2:00 | Nonlinear Inverse Scattering Applied to Calculation of the Effective Permittivity of Random Collections of Scatterers<br><i>*M. Moghaddam, B. Houshmand, Univ. of California, Los Angeles</i>  | 60   |
| 2:20 | Volume and Rough Surface Scattering Contributions to the Bistatic Scattering Characteristics of Highly Dense Randomly Distributed Cylinders<br><i>C. Clayton, Y. Kuga, Univ. of Washington</i> | 61   |
| 2:40 | Poynting's Theorem and Electromagnetic Wave Multiple Scattering in Dense Media Near Resonance<br><i>Y.N. Barabanenkov, Russian Academy of Sciences; L.M. Zurk, Univ. of Washington</i>         | 62   |
| 3:00 | Break  |      |
| 3:20 | Mismatched Boundary Effects on Diffusion of Beam Waves in Discrete Random Media<br><i>S. Ito, Toyo Univ.</i>   | 63   |
| 3:40 | Phase Preserving Modeling of Evolution of Clutter Spectra in the Time Domain<br><i>*L.B. Felsen, L. Carin, Polytechnic Univ.</i>   | 64   |
| 4:00 | Anderson Localization of Electromagnetic Waves in a Random Non-Reciprocal Waveguide<br><i>A.R. McGurn, Western Michigan Univ.; A.A. Maradudin, Univ. of California</i>                         | 65   |
| 4:20 | Acoustic Volume Scattering from Ocean Sediments<br><i>*D.R. Jackson, Univ. of Washington</i>   | 66   |
| 4:40 | Wave Scattering from a Conducting Target in Random Media<br><i>M. Tateiba, H. Koga, Z.Q. Meng, Kyushu Univ..</i>   | AP-S |
| 5:00 | Monte Carlo Simulations of the Extinction Rate of Densely Packed Spheres Based on Solution of Maxwell's Equations<br><i>L. Zurk, L. Tsang, Univ. of Washington.</i>                            | AP-S |
| 5:20 | Exact Solution of the Equations for Electromagnetic Scattering in Random Media<br><i>*A.I. Timchenko, Ukrainian Academy of Sciences</i>  | 67   |

# **An Innovative Hybrid Experimental/Theoretical Technique for Modelling Radar Scatter from Random Media**

**John R. Kendra\*, Kamal Sarabandi, and F. T. Ulaby**  
Radiation Laboratory  
Department of Electrical Engineering and Computer Science  
The University of Michigan  
Ann Arbor, MI 48109-2122

## **Abstract**

Scattering from random media has long been an active area of research due to potential applications in many radar remote sensing problems. The main stumbling blocks are related to dense and non-tenuous volume scattering media, in which near-field effects appear to be important and the concept of a discrete scatterer may be dubious. The present work describes an innovative hybrid experimental/theoretical technique for dealing with volume scattering phenomena, which is designed to circumvent the obstacles mentioned above. To begin with, it is assumed that the scattering behavior of the medium is described by the standard equation of transport from radiative transfer. Unlike conventional radiative transfer theory, however, the phase matrix and the extinction matrix are not calculated using single-scatter theory, which has been shown to be invalid for dense media. Instead, these quantities, which are the fundamental quantities governing scattering, are allowed to exist as unknowns. For the case of snow, at frequencies of 10 GHz and below, wherein the scattering albedo is expected to be small, a first order solution is derived. The unknown quantities in this formulation, the elements of the extinction and phase matrices, are then retrieved for the particular material under investigation by direct inversion using fully polarimetric backscatter measurements. Knowledge of these quantities amounts to a characterization of the material, so that they may be used in the mathematical machinery of radiative transfer to predict scattering for general configurations of the medium. The validity of this technique is demonstrated through examples including field radar measurements of artificial snow of various depths, and also laboratory experiments involving layers of silica gravel.

# COMPARISON OF MICROWAVE SCATTERING MODELS OF VEGETATION

*S. Saatchi, M. Moghaddam, K. McDonald, and S. Durden*  
*Jet Propulsion Laboratory*  
*California Institute of Technology*  
*4800 Oak Grove Drive*  
*Pasadena, California 91109*  
*phone: (818) 354-1051, Fax: (818) 393-6943*

During the last few years, there have been substantial advances in using radar remote sensing techniques for monitoring vegetation canopies in general and forest canopies in particular. Interpretation of the radar images over forest canopies is contingent particularly upon the understanding of scattering processes and their relative importance in the total radar backscatter data. Microwave vegetation models are the means for simulating the radar data and deriving useful information about the scattering mechanism and consequently the biophysical characteristics of the forest canopy.

In modeling the scattering for forest canopies at microwave frequencies, several scattering mechanisms are usually taken into account: 1) crown volume scattering, 2) trunk volume scattering, 3) surface scattering from forest floor, 4) trunk-surface interaction, 5) trunk-crown interaction, 6) crown-ground interaction. Understanding the behavior of each scattering component for various forest canopies is dependent on the derivation of the models and the underlying assumptions. A majority of the models are discrete scattering models where the vegetation canopy can be viewed as an ensemble of randomly distributed scatterers (leaves, branches, and trunks) in one or many layers.

In this study, three commonly used discrete scattering models, distorted Born approximation (DBA), Born approximation (BA) and radiative transfer theory (RT), are compared. The DBA and BA models are formulated according to a field theory point of view and the RT model as an intensity or transport theory. In all three models, each scattering mechanism is formulated explicitly so that its relative contribution to the total backscattering coefficient can be analyzed. The models are used to simulate polarimetric radar data over coniferous and deciduous forests by using the same input parameters. The model simulations are then analyzed to check the effect of canopy parameters and the importance of scattering mechanisms. The results are also compared with radar images at P-, L-, and C-bands in order to assess the validity of the model comparisons.

*This work has been performed at the Jet Propulsion Laboratory, California Institute of Technology under contract with National Aeronautics and Space Administration.*

NONLINEAR INVERSE SCATTERING APPLIED  
TO CALCULATION OF THE EFFECTIVE PERMITTIVITY OF  
RANDOM COLLECTIONS OF SCATTERERS

M. Moghaddam\*<sup>1</sup> and B. Houshmand<sup>2</sup>  
<sup>1</sup> Jet Propulsion Laboratory  
California Institute of Technology  
4800 Oak Grove Drive  
Pasadena, CA 91109

<sup>2</sup> Department of Electrical Engineering  
University of California at Los Angeles  
Los Angeles, CA 90024

ABSTRACT

The effective dielectric constant of a random mixture of two-dimensional scatterers is found by a combination of forward and inverse scattering techniques. Without loss of generality in either the forward solution or inversion, we will assume that the scatterers have circular cross sections. The method is based on calculating the scattered field of the mixture using an arbitrary source configuration (normal plane wave incidence for convenience), and using the results, in a statistical sense, in an inverse scattering solution to retrieve a single scatterer. This scatterer is a cylinder with the same support as the mixture, and produces the same scattered field. The field is found by averaging the scattered fields due to many arrangements of the random mixture with given permittivity, radius, and location distributions. This would be similar to a Monte Carlo simulation. Previously, we have reported the results of this approach for the case where the dielectric constant distribution of the scatterers is such that the effective scatterer is weak. In this case, although the multiple scattering effects may need to be included in the forward solution, the inversion can be carried out using a linear algorithm, e.g., diffraction tomography. To obtain the forward solution that includes all the multiple scattering effects, we use the recently developed T-matrix type algorithms by Chew et al. (e.g., see Chew, W. C., *Waves and Fields in Inhomogeneous Media*. New York: Van Nostrand Reinhold, 1990). In this work, we consider the case where the scatterers are not weak, and hence nonlinear inversion must be carried out. We use the Born iterative method whereby Born-type iterations are carried out on the source-type integral equation for the scattered field. Although each iteration is linearized, the final solution is that of the nonlinear inversion problem. The forward and inverse scattering algorithms will be briefly discussed, and results from mixtures with various parameters will be presented.

This work was performed in part by the Jet Propulsion Laboratory, California Institute of Technology, under a contract from the National Aeronautics and Space Administration.

**VOLUME AND ROUGH SURFACE SCATTERING CONTRIBUTIONS TO THE  
BISTATIC SCATTERING CHARACTERISTICS OF HIGHLY DENSE  
RANDOMLY DISTRIBUTED CYLINDERS**

Craig Clayton and Yasuo Kuga

Department of Electrical Engineering, FT-10

University of Washington

Seattle, Washington 98195

Telephone: (206) 543-2159 Fax: (206) 543-3842

**Abstract**

Bistatic scattering characteristics of highly dense media are important in many areas of remote sensing, such as millimeter-wave scattering from snow and ice. The scattering characteristics of highly dense media are dependent on the size of the particles and the source wavelength used.

To study the fundamental characteristics of electromagnetic wave interactions with highly dense media, we conducted extensive experiments using millimeter-wave bistatic radar and dielectric cylinders of different sizes and concentrations. By studying the cylindrical case, we are able to compare the effects of both volume and rough surface scattering. Experimental data have been obtained for size parameter  $ka$  of 2.4-3.1 and 4.7-6.2 with fractional volume densities of 5, 10, 30, and 50% in addition to the highly dense case. Attenuation constant measurements were also obtained for the cases stated above and will be presented.

It is shown that for large  $ka$ , the dense scattering characteristics are volume in nature and exhibit characteristics similar to that of a single cylinder. For small  $ka$ , the dense case is predominantly volume scattering, but the packed case exhibits much different behavior. It will be shown that it is a combination of rough surface and volume scattering. The experimental results are compared with second-order radiative transfer theory and a Monte Carlo simulation of wave scattering from 1-D rough dielectric surfaces.

# POYNTING'S THEOREM and ELECTROMAGNETIC WAVE MULTIPLE SCATTERING in DENSE MEDIA NEAR RESONANCE

Yu. N. Barabanenkov

Institute of Radioengineering and  
Electronics of the Russian  
Academy of Sciences, Mohovaya  
11, 103907 Moscos, GSP-3, Russia

L. Zurk

Applied Physics Lab, University of  
Washington, 1013 NE 40th, Seattle,  
WA 98105, USA (206) 685-8623

## Abstract

Electromagnetic wave multiple scattering theory in random media has to be energetically consistent. Usually this property is verified for a single frequency wave field applying the time averaged Poynting's theorem. In the framework of the Dyson and Bethe-Salpeter equations for electric wave field, the optical relation (theorem) is thus obtained between the tensor mass operator, the intensity operator and the averaged Greens function. In a dense medium near Mie resonance the electromagnetic energy within a dielectric sphere may be much greater compared with that of a sphere of the same radius of the background medium (Bott A. and Zdunkowski W., J. Opt. Soc. Am, A.4, 1361, 1987). To include this resonance phenomenon in the general electromagnetic wave multiple scattering theory in dense media we apply the time Fourier transform to the Poynting's theorem for a non-steady electromagnetic wave field. Using a two frequency domain we prove an identity between the electric and the magnetic energy density in a random medium ("virial" theorem). This virial theorem permits us to establish a close connection between the Poynting's theorem and the two frequency Ward identity of the type (Barabanenkov Yu. N. and Ozrin V. D., Phys. Lett. A154, 38, 1991) that generalizes the optical theorem. On the basis of the two frequency Ward identity we derive a modified nonstationary radiative transfer equation for the tensor radiant intensity which has the usual form but with a wave energy transport velocity (Van Albada M.P., Van Tiggelen B.A., Lagendijk A. and Tip A. Phys. Rev. Lett. 66, 3132, 1991) instead of the group velocity. We consider the solutions of the obtained equation for pulse transmitted through the optically thin and thick slabs to discuss the pulse propagation experiment (Kuga Y., Rice D.J. and Ishimaru A. PIERS Symposium, July 12-16, 1993) comparing the wave energy transport velocity with the energy arrival velocity that is measured directly in the time-domain.

# MISMATCHED BOUNDARY EFFECTS ON DIFFUSION OF BEAM WAVES IN DISCRETE RANDOM MEDIA

Shigeo Ito

Department of Electrical and Electronic Engineering  
Faculty of Engineering, Toyo University, Kawagoe, 350 Japan

The multiple scattering effect on propagation characteristics of optical waves in discrete random media has been studied in great detail. Its accurate knowledge is important for the development of communications and remote sensing systems, and also for diagnostics of biological media. One mathematical approach to such problems is to solve the radiative transfer equation, but the general solution is difficult to obtain. For very large optical depths, the diffusion approximation to the radiative transfer equation is useful for analyzing the optical wave propagation. This approximation has been applied to pulse propagation in clouds and fog, and analytical expressions have been derived for the pulse intensity for plane and beam waves. For continuous beam waves, on the other hand, the range of the validity of diffusion theory has been examined in comparison of theoretical calculations with experimental data (Ishimaru et al., *J. Opt. Soc. Am.*, 71, 131-136, 1983). However, the diffuse surface reflection at a boundary has not been taken into account in the calculation of the diffuse intensity.

In this paper the three-dimensional diffusion of a continuous narrow beam wave in discrete random media is discussed for a large optical depth. The boundary conditions are employed for surfaces where the diffuse reflection occurs. An analytical expression is first derived for the average diffuse intensity in terms of the sum of the residual values under practical situations of interest. We then discuss the dependence of the scattering parameters such as the mean cosine of the scattering angle and the single scattering albedo on the diffuse intensity in the radial direction.

The effects of mismatched boundary is shown to increase the diffuse intensity when the single scattering albedo is equal to unity. However, the spatial spreading of beam waves for nonabsorption only slightly increases with an increase in the mean cosine of the scattering angle. For larger optical depths, the spatial spreading is more sensitive to a very small change in the single scattering albedo. A comparison with previously reported Monte Carlo and experimental results on the beam width is also discussed to ascertain the validity of the analytic solution obtained here.

## **Phase Preserving Modeling of Evolution of Clutter Spectra in the Time Domain**

L.B. Felsen and L. Carin  
Department of Electrical Engineering  
Polytechnic University  
Brooklyn, NY 11201

Frequency domain (FD) scattering from irregular environments is usually characterized by statistical measures which smooth out phase coherent wave processes and apply globally over extended regions of the environment. Under short-pulse (SP) time domain (TD) conditions with high spatial-temporal resolution, individual scatterers in the irregular ensemble initially contribute isolated returns at the observer. Global effects appear in the return signal only at later times when multiple interactions between scatterers have had a chance to develop. As a first step toward a systematic study of how clutter spectra evolve from individual scatterings we have considered a two-dimensional plane-wave-excited model environment comprising a finite collection of perfectly conducting, infinitely long, flat strips which can be located and tilted arbitrarily. FD and TD numerical reference data generated for unperturbed, smoothly perturbed and randomly perturbed periodic realizations has been subjected to phase space (configuration-spectrum) processing via windowed Fourier as well as multiresolution transforms which extract wave phenomenology from the data. This has been compared with analytic asymptotic models that parametrize these scattering scenarios in terms of FD and TD self-consistent combinations of individual element returns, global or local Bragg spectra tied to global or local periodicity, and edge diffractions from the truncations. Throughout, these signatures are obtained with strict retention of phases and time delays, even for each randomly perturbed realization. Various examples illustrate the phase space footprints left by each wave process in each model configuration. Of special interest are target-in-clutter modelings wherein the target is fixed while the clutter changes during various realizations; here, the SP-TD regime has distinct advantages with respect to target-clutter separation. TD statistical information can be assembled by applying statistical measures to an ensemble of these realizations, but this has not yet been done.

**Anderson Localization of Electromagnetic Waves  
in a Random Non-Reciprocal Waveguide**

Arthur R. McGurn

Department of Physics

Western Michigan University

Kalamazoo, MI 49008

and

Alexei A. Maradudin

Department of Physics

University of California

Irvine, CA 92717

**Abstract**

The localization length for electromagnetic waves in a waveguide containing a random non-reciprocal media is computed. Specifically, the waveguide is formed from two parallel perfectly conducting plates and between the plates is a random layered system composed of vacuum and semiconducting slabs. The widths of the vacuum and semiconducting slabs are randomly disordered and the system is made to be non-reciprocal by the application of an external constant magnetic field. The localization length is computed as a function of frequency, disorder and applied magnetic field intensity. The localization length is found to exhibit an asymmetry for electromagnetic waves incident from different directions on the waveguide structure.

## Acoustic Volume Scattering from Ocean Sediments

Darrell R. Jackson  
Applied Physics Laboratory  
College of Ocean and Fishery Sciences  
University of Washington  
Seattle, WA 98105

It has become evident that acoustic scattering from the ocean bottom is often due to volume inhomogeneities rather than to sediment-water interface roughness. Because sediment volume scattering is weak, several investigators have applied perturbation theory to this problem. We consider some of the consequences of the perturbation treatment, including half-space effects, correlations between density and compressibility fluctuations, and higher-order scattering. In this work, sediment volume scattering is described in terms of an interface scattering cross section per unit area. This approach is justified when the acoustic penetration depth is small compared to the source and receiver altitudes.

Fits to backscatter data as a function of frequency are used to constrain the spectra for compressibility and density fluctuations. The approximate frequency independence of the backscattering cross section and sediment acoustic  $Q$  suggest that sediment inhomogeneities can be approximated as fractal with dimension four. This, in turn, implies that very small-scale fluctuations are dominant. The final constraint is provided by geoacoustic data showing that sound speed fluctuations are much smaller than density fluctuations. This implies strong anticorrelation between density and compressibility fluctuations. With these constraints, it is possible to make predictions for bistatic scattering with no free parameters.

As density and compressibility fluctuations scatter sound with monopole and dipole patterns, respectively, correlations between these two fluctuations impart an interesting bistatic angular dependence. This dependence is further complicated by refractive effects at the interface. In "slow" sediments (sound speed less than the water sound speed), forward scattering in the specular direction is not particularly strong owing to suppression by the assumed compressibility-density anticorrelation. Fast sediments, however, display a peak in the specular direction for incidence angles greater than the critical value, owing to the combined effects of evanescence and inhomogeneity spectral behavior. Historical data agree in some respects with these predictions, but have insufficient resolution and angular coverage to provide a rigorous test.

# Exact Solution of the Equations for Electromagnetic Scattering in Random Media

A.I. Timchenko

Institute for Radiophysics and Electronics  
Ukrainian Academy of Sciences  
Proscura 12, Kharkov, 310085, Ukraine

## Abstract

The scattering of the electromagnetic waves in the random media is investigated. The equations for the mean Green's function and the corresponding second moment are derived by using a technique of the variational derivations for the averaging.

Such equations usually extend into an infinite system which doesn't contain the variational derivations. The most commonly used approximation for the solution this system is the nonlinear-approximated equation for the mean Green's function. However, this form of the equation and corresponding approximation for the equations for second moment include only the part multiple-scattering terms and don't provide sufficient accuracy in some cases.

This paper presents the exact analytic solutions of the equations with the variational derivations, obtained for unbounded random media.

The exact solution for the mean Green's function has been used for considering some interesting cases, for example, anomalously large-scale fluctuations whose correlation function possesses a singular spectrum. It is shown that the Green's function submits a super-exponential attenuation law, which is distinguished from that in the Bourret approximation.

From second moment exact solution the expression for scattering intensity was obtained and its angular distribution was investigated. It is shown that in vicinity of the coherent backscattering peak the angular spectrum differs from that predicted by the diffusion theory if the random inhomogeneities are represented with isotropically centers.

In general, the obtained expressions for the mean Green's function and the second moment allow to analyze the effect of the multiple scattering in dense media, localization, backscattering enhancement, etc.



MONDAY PM URSI-B SPECIAL SESSION M-U1

Room: Kane 220

MESH TRUNCATION TECHNIQUES FOR PDE'S

Chairs: R. Mittra, University of Illinois; A. Cangellaris, University of Arizona

Organizers: R. Mittra, University of Illinois; A. Cangellaris, University of Arizona

- 1:20 Introduction and General Remarks on ABCs  
*R. Mittra, Univ. of Illinois; A. Cangellaris, Univ. of Arizona*
- 1:40 Review of the MEI Approach 70  
*\*R. Pous, Polytechnic Univ. of Catalonia*
- 2:00 A Study of Mesh Truncation in Radar Cross Section Computations 71  
*\*L. Muth, J. Gary, National Inst. of Standards and Technology*
- 2:20 A Theoretical Study of Numerical Absorbing Boundary Conditions 72  
*B. Stupfel, Centre d'Études de Limeil-Valenton; R. Mittra, Univ. of Illinois at Urbana-Champaign*
- 2:40 A Numerical Absorbing Boundary Condition for Finite Difference and Finite Element Analysis of Open Structures 73  
*\*A. Boag, A. Boag, R. Mittra, Univ. of Illinois; \*Y. Leviatan, Technion*
- 3:00 Break
- 3:20 Discussion
- 4:00 Performance of Bayliss-Turkel Type Radiation Conditions Applied on a Conformal Outer Boundary 74  
*D. A. Mohamed, Military Technical College, Egyptian Air Defense; \*R. Janaswamy, Naval Postgraduate School*
- 4:20 Electrostatic Solution for Open-Region Three-Dimensional Arbitrarily-Shaped Conducting Bodies via the FEM/MEI Method 75  
*\*J. H. Henderson, S. M. Rao, Auburn Univ.*

## REVIEW OF THE MEI APPROACH

R. Pous

Antennas-Microwave-Radar Group, TSC Dept.  
ETSETB, Polytechnic University of Catalonia.  
P.O. Box 30002, 08080 Barcelona, SPAIN.

### ABSTRACT

One of the main differences between the Measured Equation of Invariance and the Absorbing Boundary Conditions is that the former uses the Green function of the structure to derive the mesh truncation coefficients. In the FD analysis of printed structures the Green function of the grounded dielectric slab must be used. For this we rely on the techniques employed in the MoM solution to this type of problems. Since in most cases the MEI does not require the computation of the Green function in the same plane as the source, the calculation converges more rapidly. For this reason, the asymptotic expressions, singularity extraction techniques, and approximations usually employed in the MoM calculation must be reconsidered in terms of their MEI computational efficiency.

One of the open questions about the MEI approach is the choice of metrons. Recently, a lot of work has been done trying different sets of functions, and looking for the criteria to choose them.

In this presentation, we will discuss how the FD and MoM techniques are used in the MEI solution of printed antennas and circuits, and will present some numerical results. We will also present some numerical results comparing the performance of different sets of metrons in different types of applications.

## A Study of Mesh Truncation in Radar Cross Section Computations

Lorant Muth\* and John Gary  
National Institute of Standards and Technology  
Boulder, CO 80303

A comparison of two methods of mesh termination in the computation of the radar cross section is given. One of the methods is due to Mei, and the second is due to Keller and Givoli. Both these methods are used to terminate meshes obtained in finite difference and finite element approximations of the Helmholtz equation in a small domain containing the scatterer. The use of an absorbing outer boundary is critical to both methods. In the first method, called the *measured equations of invariance* (MEI) technique (R. Pous, Ph. D. thesis, University of California at Berkeley, 1992), a set of physically realizable currents on the surface of the scatterer is used to derive the coefficients of the linear relationship postulated to exist on three boundary points and one interior point independent of the details of the solution. It is thought that this boundary condition at the exterior domain will pass, without reflection, the scattered waves generated by any incident radiation. The second method is due to Keller and Givoli (J. Keller and D. Givoli, *Jour Comp Phys*, 82:172-192, 1989). Here a relation between the solution and its normal derivative (a Dirichlet-Neumann map), which is exactly satisfied by outgoing waves, is used as the outer boundary condition.

To demonstrate the accuracy of the method of solution and mesh termination, the computed radar cross sections are compared to the exact analytic solutions for a plane wave scattered from a two-dimensional infinite perfectly conducting cylinder. The accuracy of the computed radar cross section as a function of the bistatic angle is studied as the mesh size and distance of the boundary from the scattering surface is varied for both methods. The condition number of the linear system resulting from the discretization is studied. Possible explanations for observed residuals are presented, and improvements to the MEI boundary conditions are explored.

## A THEORETICAL STUDY OF NUMERICAL ABSORBING BOUNDARY CONDITIONS

Bruno Stupfel<sup>†§</sup> and Raj Mittra<sup>§</sup>

<sup>†</sup> Centre d'Études de Limeil-Valenton, Commissariat à l'Énergie Atomique.  
94195 Villeneuve St Georges cedex, France.

<sup>§</sup> Electromagnetic Communication Laboratory, University of Illinois.  
Urbana, IL 61801-2991

In a recent paper, Mei, Pous, Chen and Liu have introduced the Measured Equation of Invariance (MEI) as an approach to solving scattering problems using the finite difference method. The authors postulated that the value of the field at a node  $M_0$  on the mesh boundary  $S$  may be written as

$$u(M_0) = \sum_{i=1}^N c_i u(M_i) \quad (1)$$

where  $M_i$  denote the  $N$  neighboring nodes of  $M_0$ . The coefficients  $c_i$  are computed by solving the linear system of equations derived by inserting outgoing wave functions  $u$  in (1). These wave functions are generated by using  $N$  "metrons", that are essentially entire domain basis functions for current distributions on the scatterer. In a more recent publication, Gordon, Mittra, Glisson and Michielssen have shown that the relationship between the neighbor nodes could be used as a numerical absorbing boundary condition (NABC) in a FEM formulation and that the field  $u$  in (1) could be efficiently derived by using line sources.

In this paper, we demonstrate, analytically, that when the  $c_i$  in (1) are determined by using plane wave fields or line sources, then the resulting NABC becomes equivalent to many of the existing ABCs as the distance  $h$  between the nodes  $M_i$  tends to 0. Both regularly and irregularly distributed nodes, that may be situated either on a single or double layer, are investigated, and locally planar as well as locally circular boundaries are considered. For instance, it is shown that, for planar  $S$  and plane wave incident fields, the NABC yields Engquist-Majda or Higdon's ABCs as  $h \rightarrow 0$ , depending upon the location of the nodes and the angles of incidence of the waves. It is also shown that the order of the ABC is directly related to  $N$ .

We note, however, that the value of the normal derivative of  $u$  on  $S$ , i.e.  $\partial_n u$ , is required in order to compute the RCS of the scatterer. We show that a first order finite difference approximation for  $\partial_n u$  is not complete when  $N \geq 2$ . This prompts us to investigate the validity of the modified NABC,  $\partial_n u(M_0) = \sum_{i=0}^{N-1} c_i u(M_i)$ , proposed by Li, Cendes and Yuan. Following the same lines than those previously described, we demonstrate once again the equivalence between the above NABC and the existing ABCs as  $h \rightarrow 0$ .

## A Numerical Absorbing Boundary Condition for Finite Difference and Finite Element Analysis of Open Structures

Amir Boag\*, Alona Boag, and Raj Mittra  
Electromagnetic Communication Laboratory  
University of Illinois, Urbana, IL 61801

Yehuda Leviatan  
Electrical Engineering Department  
Technion, Haifa 32000, Israel

The Finite Difference/Finite Element Methods (FD/FEM) are often preferred over the Method of Moments (MoM) for problems involving inhomogeneous materials or complex geometries. The use of these methods for scattering and radiation problems requires one to couple, explicitly, the FD/FEM computational domain to the unbounded free space external to the mesh region. The FD/FEM solution can either be matched to a modal expansion, or be combined with the MoM (also referred to as the Boundary Element Method) to satisfy the radiation condition. Both ways lead to non-local boundary conditions that are exact, albeit at the expense of spoiling the sparsity of the matrices generated in these formulations. This has prompted many workers to search for an alternative, viz., to develop a local boundary condition which has relatively little effect on the sparsity of the FD/FEM matrices. Notable contributions in this area have been made by a number of authors including Bayliss and Turkel, and Engquist and Majda. A review paper describing the theoretical developments and the results of a comparative study of Absorbing Boundary conditions (ABCs) has been published by Mittra and Ramahi (Differential Methods in Electromagnetic Scattering, J.A. Kong & M.A. Morgan, eds., 133-173, Elsevier, 1989). They have shown in this paper that, for a circular outer boundary, the Bayliss-Turkel ABC works well for lower-order cylindrical harmonics that are propagating in nature, but it becomes inaccurate for the higher-order harmonics that are either close to or beyond cutoff. Attempts to alleviate this problem have not been successful to-date, and the development of an accurate boundary condition for mesh truncation, that does not exact a very heavy price by requiring that the truncation boundary be removed far away from the outer boundary of the scatterer, has remained an elusive goal.

The method followed in this paper begins by posing the problem of deriving the ABC as that of determining a numerical relationship that links the value of the field at the boundary grid point to those at the number of neighboring points, and this number itself is determined in a systematic manner in the process of the derivation of the boundary condition. The numerical relationship, referred to as the numerical absorbing boundary condition (NABC), is derived by imposing the conditions that the NABC must be satisfied to within a certain tolerance, by *all* of the *outgoing* wave components impinging on the boundary from its interior. In that sense the MEI technique (K.K. Mei et al., *Proc. IEEE AP-S. Intl. Symp.*, 2047-2050, 1992) for truncation of FD mesh can be shown to be a restricted case of the NABC method. The number of adjacent boundary nodes that are to be coupled to a given boundary node is determined by using the criteria that the satisfaction of the outgoing field condition be at least as accurate as the satisfaction of the field equations at the internal nodes (nodes away from the boundary), and that the discrimination against the *incoming* waves be at least as high as the set desired value. The number of coupled nodes on the boundary depends, of course, on the separation distance between the outer boundary of the object and the truncation boundary of the FD/FEM mesh, and also on the mesh density itself. Numerical examples that illustrate the derivation and application of the NABC will be included in the presentation.

## Performance of Bayliss-Turkel Type Radiation Conditions Applied on a Conformal Outer Boundary

Darwish A. Mohamed<sup>1</sup>

Ramakrishna Janaswamy<sup>2,\*</sup>

<sup>1</sup>Egyptian Air Defense, Military Technical College, Alexandria, Egypt

<sup>2</sup>Code EC/Js, Naval Postgraduate School, Monterey, CA 93943

An efficient PDE solution of the Helmholtz equation in open regions such as encountered in antennas and scattering entails the use of radiation conditions on a terminating boundary. Several radiation conditions on circular boundaries have been proposed (Bayliss, Gunzburger and Turkel, *SIAM J Appl Math* (42), 430-451, 1982; Engquist and Majda, *Commn Pure Appl Math* (32), 313-357, 1979). These when combined with finite methods such as finite difference and finite element produce sparse matrices enabling a rapid solution. Generalization of the Bayliss-Turkel (B-T) type radiation conditions to non-circular boundaries can be carried out by means of coordinate transformations (Janaswamy, *Microwave Optical Tech Letters*, (5), 393-395, 1992). For the method to be effective, the radiation conditions must be applied to the far-zone field, although some have proposed that the B-T conditions can be applied directly on the object surface itself by simply replacing the distance variable with the radius of curvature and the angle variable with the normalized arc length (Kriegsmann, *et al.*, *IEEE Trans Antennas Propagat*, (35), 153-161, 1987). The accuracy of the solution depends on the distance of the boundary from the object, size, shape and composition of the object, among other things. Prompted by the lack of sufficient guidelines, Mei (Mei *et al.*, *Joint APS/URSI Symposium*, Chicago, 1992) proposed a novel method, known as the Measured Equation of Invariance (MEI), whereby, discrete conditions are generated directly using the near-zone fields. Using these, the terminating boundary can be brought very close to the object.

In this presentation, we will examine the accuracy of B-T conditions when applied on a conformal boundary very close to a conducting object. Our objective is to show, by comparison with the MEI method, that the B-T conditions are *not* adequate in this case, particularly for non-convex shaped objects. Results are shown for typical geometries such as circular, square, rectangular, and re-entrant cylinders.

# Electrostatic Solution for Open-Region Three-Dimensional Arbitrarily-Shaped Conducting Bodies via the FEM/MEI Method

**John H. Henderson\* and S. M. Rao**  
Department of Electrical Engineering  
200 Broun Hall  
Auburn University, Alabama, USA 36849-5201

The finite element method (FEM) using tetrahedral elements has a number of advantages that make it suitable for the numerical solution of electrostatics problems. Tetrahedrals can easily conform to arbitrarily-shaped, three-dimensional geometries, the technique handles inhomogeneities well, and strict FEM results in a sparse system matrix, and thus, less demand on computer memory and CPU resources. However, the handling of open-region problems with strict FEM requires the gridding of all space, which is unfeasible. Currently, this is circumvented by one of several means. A very large area surrounding the object can be gridded, and the voltage at the problem-space boundaries forced to zero. This results in a very large number of elements, and does not provide a solution as accurate, or as efficient, as moment methods. The boundary may be placed on, or close to, the object, truncating the problem space. The voltage at the boundary may be assumed to be that due to canonical geometries, which often proves to be a poor approximation, or the boundary may be dealt with by augmenting the FEM with a variation of method of moments on the boundary, a solution that destroys the sparsity of the matrix, and thus eliminates one of the primary advantages of the FEM.

In this work, a method is presented, originally proposed by Mei, by which the finite element technique is augmented to solve for the electrostatic fields due to a three-dimensional, arbitrarily-shaped, conducting body in such a manner as to preserve the sparseness of the system matrix while allowing the problem space to be truncated as close to the object as two layers of elements. Numerical results are presented that demonstrate the effectiveness of this technique.



MONDAY PM URSI-B SESSION M-U7

Room: Kane 130

ELECTROMAGNETIC THEORY

Chairs: N. Engheta, University of Pennsylvania; T. Senior, University of Michigan

- 1:20 On the Relationship Between Fractional Integration / Differentiation and Green's Functions  
in Certain Electromagnetic Problems 78  
\*N. Engheta, Univ. of Pennsylvania
- 1:40 Electromagnetic Fields in Source Regions of Anisotropic Media 79  
\*W. S. Weiglhofer, Univ. of Glasgow; A. Lakhtakia, Pennsylvania State Univ.
- 2:00 Green's Function Representations Involving Differentiation in Source-Point Coordinates 80  
\*L.W. Pearson, Clemson Univ.
- 2:20 Singularity Extraction from the Green's Function for Vertical Current Enclosed in Non  
Homogeneous Shielded Structure 81  
H. Ghali, Ain Shams Univ.; J. Citerne, INSA; V.F. Hanna, CNET/PAB
- 2:40 Generalized Boundary Conditions and Babinet Principles for Scalar Fields 82  
\*T.B.A. Senior, Univ. of Michigan
- 3:00 Break
- 3:20 Higher Order Impedance Boundary Conditions, Ratio of Polynomials and Surface Waves:  
an Insight 83  
D. Hoppe, \*Y. Raymat-Samii, Univ. of California Los Angeles
- 3:40 Hybrid Beam Mode Representation for Guided Propagation 84  
\*E. Heyman, A. Goldberg, Tel-Aviv Univ.
- 4:00 Electromagnetic Localized Waves in Lossy Media 85  
\*R. Donnelly, Memorial Univ.; R.W. Ziolkowski, Univ. of Arizona
- 4:20 Geometrical Optics, Geometric Phase, and Mode Connection 86  
\*K. Suchy, Univ. of Düsseldorf
- 4:40 Application of Treatment of Lorentz Type Resonance to Induced Emission Property in  
Spatial Network and FDTD Methods for Vector Potential and Hertz Vector 87  
\*N. Yoshida, Hokkaido Univ.

# ON THE RELATIONSHIP BETWEEN FRACTIONAL INTEGRATION/DIFFERENTIATION AND GREEN'S FUNCTIONS IN CERTAIN ELECTROMAGNETIC PROBLEMS

Nader Engheta

Moore School of Electrical Engineering  
University of Pennsylvania  
Philadelphia, Pennsylvania 19104, U.S.A.

Fractional calculus, which deals with the study of mathematical operators involving differentiation and/or integration of general (fractional) orders (i.e., not necessarily positive integers) has been the subject of research in pure and applied mathematics, particularly applied analysis [A. C. McBride and G. F. Roach (eds.), *Fractional Calculus*, research Notes in Mathematics, Pitman Advanced Pub., Boston, 1985, and K. B. Oldham and J. Spanier, *The Fractional Calculus*, Academic Press, New York, 1974]. Continuous dimensionality was also considered in von Neumann algebra which has been important in mathematical treatment and connection of some areas of mathematics with statistical mechanics.

Clearly differential and integral operators are key elements in analyzing mathematical properties of various physical phenomena in many branches of science. In such fields, a general question can be asked with regards to potential use of the concept of fractional calculus in describing physical observables: What will happen if one generalizes the conventional concept of integer differentiation and integration in these physical phenomena to the non-integer (fractional) counterparts? For instance, in electrodynamics, differential and integral operators are used on vector field quantities. What will result if one expands the concept of conventional differentiation into fractional differentiation in electrodynamical problems? For instance, to describe interaction of waves with fractal interface, Le Méhauté *et al.* introduced the idea of impedance with non-integer dimension, and they have suggested some fractional operators between electric and magnetic fields [A. Le Méhauté, *et al.*, "Ondes en Milieu Fractal Application à la Caractérisation des Milieux Hétérogènes," *Revue Scientifique et Technique de la Défense*, 1er trimestre, pp. 23-33, 1992., and A. Le Méhauté and F. Heliodore, "Introduction to Fractional Derivatives in Electromagnetism: Fractal Approach of Waves/Fractal Interface Interactions," *Progress in Electromagnetics Research Symposium (PIERS,89)*, p. 183, 1989]. Furthermore, the idea of fractional calculus was used to describe certain aspects of electrostatic fields near sharp edges [N. Engheta, "On the role of non-integral (fractional) calculus in electrodynamics," *1992 IEEE AP-SIURSI International Symposium*, Chicago, Illinois, July 17-20, 1992, Vol. URSI Digest, p. 163.]

In this talk, we will present and discuss some of our recent work on novel relationships between fractional integrations/differentiations and the Green's functions in certain source configurations and boundary geometries in electromagnetic problems. Some novel and interesting aspects of this type of formulation of electromagnetic problems will be mentioned. Physical insights into some of these results will be provided.

## Electromagnetic fields in source regions of anisotropic media

W S Weiglhofer<sup>1\*</sup> and A Lakhtakia<sup>2</sup>

<sup>1</sup> Department of Mathematics, University of Glasgow, Glasgow G12 8QW  
Scotland, Great Britain; email: werner@maths.glasgow.ac.uk

<sup>2</sup> Department of Engineering Science and Mechanics,  
Pennsylvania State University, University Park, PA 16802-1401, USA

In one of the most widely used techniques in electromagnetic field problems the electric field is represented in terms of the dyadic Green function (of the electric type) by virtue of the relation

$$\mathbf{E}(\mathbf{x}) = \int_{V'} d^3\mathbf{x}' \overline{\mathbf{G}}(\mathbf{x}, \mathbf{x}') \cdot \mathbf{J}(\mathbf{x}'). \quad (1)$$

In (1),  $\mathbf{E}(\mathbf{x})$  is the electric field,  $\mathbf{J}(\mathbf{x}')$  is the electric current density and  $\overline{\mathbf{G}}(\mathbf{x}, \mathbf{x}')$  is the dyadic Green function. The integration extends over the region  $V'$  where  $\mathbf{J}$  is nonzero. While (1) is valid everywhere it is essential to realize however, that for  $\mathbf{x} \in V'$ , i.e., when the field point lies in the source region, great care must be taken when evaluating the integral because of the singular behaviour of the integrand as  $\mathbf{x} \rightarrow \mathbf{x}'$ . A large body of literature exists which deals with the proper evaluation of the integral occurring in (1) when  $\mathbf{x} \in V'$ . All of these investigations are however restricted to the isotropic medium and extensions to anisotropic media have been lacking so far.

Here, we make some progress towards the near-field or singularity structure of the dyadic Green function for two types of media: a general (electrically) anisotropic medium and a simple uniaxial bianisotropic medium. Having obtained the expressions for the singularity behaviour of the dyadic Green function, we proceed to apply these relations to find some general results on the effective properties of homogenized particulate composites.

## Green's Function Representations Involving Differentiation in Source-Point Coordinates

L. Wilson Pearson  
Department of Electrical and Computer Engineering  
Clemson University  
Clemson, SC 29634-0915  
pearson@eng.clemson.edu

The source-region completeness of Green's function representations has received substantial attention concomitant with the development of numerical integral equation solutions over the last twenty years. (c.f. R.E. Collin, *Field Theory of Guided Waves*, 2nd. ed., C.T. Tai, *Dyadic Green's Functions in Electromagnetic Theory*, 2nd ed.). Many workers in numerical methods employ potential theory in deriving field expressions in order to ensure correct source-region field representations. A noteworthy example of this is the so-called mixed-potential formulation developed by Wilton and his coworkers.

It is constructive to view field computation through Green's functions in four categories as schematized in the table below:

	Vector Eigenfunction	Scalarized
<b>Potential-Based</b>		Harrington, Butler, Wilton, etc.
<b>Direct-Field</b>	Hansen, Tai, Collin, etc.	Levine & Schwinger, Felsen & Marcuvitz, etc.

Historically, direct-field formulations emerged first—a natural consequence of early interest in far-field computations using analytical and asymptotic methods. Source-region completeness is not an issue in the far field case: it emerged as an issue only as numerical methods gave rise to the need to compute fields on a scattering obstacle in the process of constructing a numerical solution to the scattering problem. The applications of Green's functions in numerical solution brought under scrutiny source-region completeness in the case indicated in the lower left box in the table above, and the recent works by Tai and by Collin cited above have brought clarity to the completeness issue where significant confusion had existed before.

Those who approached numerical solutions through potential-based field computations could deal with source-region issues in a direct explicit fashion because it emerges naturally in the (explicit) electrostatic term that appears in potential formulations (either as a  $\nabla\nabla \cdot \mathbf{A}$  term or a  $\nabla\Phi$  term). The scalarization of potential based formulation is generally the straightforward separation of vectors and dyadics into scalar components. Hence, in a three-dimensional problem, one would need to deal with nine components of a dyadic, albeit with some commonality in the scalar PDEs arising.

The direct field scalarization introduced by Levine and Schwinger (*Comm. Pure and Appl. Math.*, v. III, 1950) has several attractive features. (1) All field components are generally expressible in terms of two scalar PDE solutions. (2) The spectral summation is one dimension lower than the spatial dimension of the geometry under consideration. (3) And, as a consequence of (2), the development of a given Green's function lends itself naturally to alternative representations to enhance convergence of the spectral summation in different circumstances. (The alternative representation ideas are developed to a high level of refinement in Felsen and Marcuvitz's work *Radiation and Scattering of Waves*.)

However, source-region representations associated with the Levine and Schwinger approach has received less attention than for the other formulations tabulated above. The PDEs of the L&S formulation involve source-point differentiation, and must be treated with exceeding care in order that the fields in the source region be represented correctly. Mayes and his coworkers (c.f. Mayes and Hanson, *Radio Science*, 1978, pp. 49-58) have addressed some relevant issues.

The author's presentation addresses the source-region completeness issue from a fundamental level in the L&S formulation.

**Singularity Extraction from the Green's Function  
for Vertical Current Enclosed  
in Non Homogeneous Shielded Structure**

H. GHALI\*, J. CITERNE\*\* and V. FOUAD HANNA\*\*\*

\*Faculty of Engineering, Ain Shams University, Cairo-EGYPT

\*\*INSA, Rennes-FRANCE

\*\*\*CNET/PAB, Issy-Les-Moulineaux, FRANCE

**Abstract**

The most important problem encountered in the analysis of three dimensional shielded discontinuities using the electric field integral equation technique (EFIE) is the determination of the electric field Green's function singularity especially for vertical current components. The integration of this singularity, when the moment method is applied, represents the diagonal terms of the impedance matrix from which the discontinuity scattering parameters are obtained. Existing techniques for singularity integration calculation are based on using the principal value of this integration in addition to the source dyadic term which accounts for the eliminated surface containing the singular point. The main difficulty of this technique lies in the choice of the eliminated surface shape and consequently the convergence of the principal value integration. In this paper, the Green's function for the potential vector of a vertical current component is determined in terms of the eigenvectors for the three dimensional differential operators. For the two operators in the horizontal plane, the eigenvectors are those similar to a homogenous structure (empty cavity). Using this fact, the Helmholtz equation reduces to a one dimensional second order differential equation in the vertical variable containing the singularity. By solving this differential equation, subjected to the boundary conditions at interfaces, the delta Dirac function in this variable can be determined in terms of the resulting eigenvectors. The Green's function is now obtained as a triple summation of possible eigenvectors for three operators, hence, the electric field Green's function is obtained by a simple transformation. The resulting form of the Green's function can be integrated directly eliminating the need of using the principal value approach.

GENERALIZED BOUNDARY CONDITIONS  
AND BABINET PRINCIPLES FOR SCALAR FIELDS

Thomas B.A. Senior  
Radiation Laboratory  
Dept. of Electrical Engineering and Computer Science  
University of Michigan, Ann Arbor MI 48109-2122

Generalized boundary conditions are characterized by the presence of field derivatives of higher order than the first, and are designed to improve the simulation of the material properties of the surface. A rather general class of conditions is described and the constraints necessary to ensure a unique solution of the boundary value problem are then derived. A special case is that of a planar surface for which a Babinet principle may exist. Just as a first order boundary condition gives rise to two related transition conditions describing membranes which are complementary in the sense of Babinet's principle (T.B.A. Senior, *J. Acoust. Soc. Amer.* 58, 501-503, 1975), so it is with the present class of boundary condition. The corresponding membranes are defined, and the resulting Babinet principle connecting the fields in the two problems encompasses all other known forms.

Commission B, June 1994

## Higher Order Impedance Boundary Conditions, Ratio of Polynomials and Surface Waves: An Insight

D. Hoppe and Y. Rahmat-Samii\*  
Department of Electrical Engineering  
University of California Los Angeles  
Los Angeles, CA 90024-1594

Applications of Impedance Boundary Conditions have received considerable attention in last fifty years. The main usage of these boundary conditions is that they provide significant simplification in the electromagnetic analysis of coated objects. Originally, the Standard Impedance Boundary Conditions (SIBC) were used. However, it was found that the SIBC fails very notably for off-normal incidence angles. Next, different forms of the Higher Order Impedance Boundary Conditions (HOIBC) were introduced and used. It has been shown that these HOIBC's have markedly improved the SIBC for off-normal incidence situations and objects with complex coatings. The key issue in the application of the HOIBC's is the determination of proper relationship among the tangential components of the electric and magnetic fields on the surface of coated objects.

Recently, Hoppe and Rahmat-Samii [IEEE Trans. Antennas & Propag., Vol. 40, Dec. 1992] presented a novel spectral method for the determination of the proper spatial relationships among the tangential components of the electric and magnetic fields on the surface of coated objects. The method is based on four steps namely: (a) determination of the exact impedance boundary condition in the spectral domain, (b) approximation of the exact spectral domain impedance by ratio of polynomials with unknown coefficients, (c) determination of the unknown coefficients by matching the exact and approximate spectral impedance, (d) conversion of the approximate spectral domain impedance into a spatial differential equation using the Fourier Transform.

In this presentation, results are shown for several different coated materials with different thicknesses to demonstrate how the "Ratio of Polynomial" approximations allow for an excellent approximation of the exact spectral impedance representation. In particular, attention will be focused on the important issue of the determination of the range of applicability for off-normal incidence situations and their extensions into the surface wave regions. The methodology described in this presentation will also allow one to check the "goodness" of the HOIBC before applying it to a particular scattering problem of interest. Representative examples will be used to examine the domain of the applicability of the HOIBC's.

## HYBRID BEAM MODE REPRESENTATION FOR GUIDED PROPAGATION

Ehud Heyman\* and Ariel Goldberg

Tel-Aviv University, Dept. of Electrical Engineering — Physical Electronics

Tel-Aviv 69978, Israel

Fax: +972-3-6423508, E-mail: heyman@eng.tau.ac.il

Guided propagation has different features in the near and in the far Fresnel zones of the guiding structure. In the near zone, the field maintains the local characteristics of the source, as expressed most efficiently by the ray representation. In the far zone, on the other hand, the field gradually adapts to the global characteristics of the waveguide and has the structure of guided modes. The interplay between the local ray, and the global mode representations has been formalized uniformly, and most generally, by Felsen's hybrid ray mode representation that proves the spectral equivalence between groups of rays and modes. Thus the most fundamental representation at a given range is obtained if the spectral components that still maintain the local features of the source are described by rays, whereas those that have already been adapted to the global guiding environment are described by modes. This representation has also been used in order to replace transitional ray fields (e.g., near caustics) by an equivalent group of modes.

In the hybrid beam mode representation presented here, we use Norris theorem [A. Norris, J. Opt. Soc. Am. A, 3, 205-210, 1986] to describe the field by a spectrum of Gaussian beams (actually complex source beams) emanating radially from the source in all directions and propagating along the ray trajectories. The beam field is readily calculated by solving the wave equation in a ray-centered coordinate system. We then show how a group of these beam basis function can be replaced by a spectrally equivalent group of modes. We therefore describe the field by an appropriately parametrized hybrid combination of modes and beams. The former account essentially for those spectral components that have already been adapted to the guiding environment, while the latter account for the spectral components that still maintain the local features of the source (usually the near axis component). The beam representation has certain advantages over the ray representation: It avoids the need to solve the two point problems and to calculate all the rays that pass exactly through any given observation point. Instead one tracks beams that pass *near*, but not necessarily *through*, the observation point. The beam propagators are also insensitive to ray transition regions and also to small artifacts of a numerically approximated medium. It therefore combines the algorithmical ease of the ray representation with the uniform features of the spectral representation.

In the present paper the hybrid beam mode representation is developed, and investigated numerically for the canonical problem of plane parallel waveguide.

## Electromagnetic Localized Waves in Lossy Media

Rod Donnelly\*  
Faculty of Engineering &  
Applied Science  
Memorial University  
St. John's, Nfld.  
CANADA A1B 3X5

Richard W. Ziolkowski  
Electrical & Computer  
Engineering Department  
University of Arizona  
Tucson, Arizona 85721

Recently there has been a renewed interest in electromagnetic pulse propagation in lossy media. The ability to launch focussed electromagnetic pulses in a lossy medium has applications in remote sensing, nondestructive evaluation of materials, and hyperthermia treatment of cancerous tissue. In this paper we show how one can design so called *Localized Wave* [LW] pulses for a lossy environment. The LW pulses were first discovered as focussed solutions of the homogeneous wave equation. They propagate in a fixed direction, and possess an arbitrary degree of focussing transverse to this direction.

The design of lossy medium LW solutions is carried out in phase space, i.e. the spacetime Fourier transform domain. Basically, one chooses the Fourier transform of a lossy medium LW as a generalized function whose support is a line lying on a particular surface, together with an arbitrary weighting. The line determines the propagation behaviour, whereas the weighting function determines the degree of focussing of the pulse; one thus has control over the degree of focussing. Examples of closed form spacetime lossy medium LW pulses will be given. Additionally, because the pulses are designed in phase space, we also present examples of pulses whose spacetime behaviour is determined only after numerical integration. The propagation and focussing characteristics of these pulses will be discussed and demonstrated graphically.

## Geometrical optics, geometric phase, and mode connection

Kurt Suchy

Institute for Theoretical Physics, University of Düsseldorf, Germany

Maxwell's curl equations together with the constitutive relations are transformed with the generalized eikonal ansatz

$$\begin{bmatrix} \mathbf{E} \\ \mathbf{H} \end{bmatrix} = \sum_{\beta} e^{i\phi_{\beta}} \mathbf{f}_{\beta} \quad \text{into} \quad \sum_{\beta} e^{i\phi_{\beta}} \left[ \mathbf{M} \left( i + \overleftrightarrow{\partial} + \frac{\overleftarrow{\partial}}{2} \right) - \frac{\partial \mathbf{C}}{\partial t} \right]_{\mathbf{K}=\mathbf{K}_{\beta}} \cdot \mathbf{f}_{\beta} = 0$$

with the  $6 \times 6$ -matrices

$$\mathbf{M} := \begin{bmatrix} \omega\epsilon + i\sigma & \mathbf{k} \times \mathbf{l} \\ -\mathbf{k} \times \mathbf{l} & \omega\mu \end{bmatrix} \quad \text{and} \quad \mathbf{C} := \begin{bmatrix} \epsilon & 0 \\ 0 & \mu \end{bmatrix},$$

the four-vectors

$$\mathbf{X} := \mathbf{x} + t\mathbf{g}_t =: \mathbf{X}_T + \tau\mathbf{g}_\tau, \quad \text{and} \quad \mathbf{K} := \mathbf{k} - \omega\mathbf{g}^t = \frac{\partial\phi}{\partial\mathbf{X}} = \nabla\phi + \frac{\partial\phi}{\partial t}\mathbf{g}^t =: \mathbf{K}_T + \lambda\mathbf{g}^\tau,$$

and the scalar operators

$$\overleftrightarrow{\partial} := \frac{\overleftarrow{\partial}}{\partial\mathbf{K}} \cdot \frac{\overrightarrow{\partial}}{\partial\mathbf{X}} \quad \text{and} \quad \overleftarrow{\partial} := \frac{\overleftarrow{\partial}^2}{\partial\mathbf{K} \partial\mathbf{K}} : \frac{\partial}{\partial\mathbf{X}} \mathbf{K}$$

With  $\widehat{\mathbf{f}}_{\alpha}$  and  $\widehat{\mathbf{f}}_{\beta} = \mathbf{f}_{\beta}/\alpha_{\beta}$  as suitably normalized left- and right-eigenvectors of  $\mathbf{M}$  one obtains the set of amplitude transport equations

$$\mathbf{W}_{\alpha\beta} \cdot \frac{\partial\alpha_{\beta}}{\partial\mathbf{X}} + \Gamma_{\alpha\beta} \alpha_{\beta} = 0 \quad \text{with} \quad \mathbf{W}_{\alpha\beta} = \delta_{\alpha\beta} \frac{d\mathbf{X}_{\beta}}{d\tau} + \overset{\circ}{O}(\lambda_{\alpha} - \lambda_{\beta})$$

and the coefficients

$$\Gamma_{\alpha\beta} = \frac{\delta_{\alpha\beta}}{2} \frac{\partial}{\partial\mathbf{X}} \cdot \frac{d\mathbf{X}_{\beta}}{d\tau} + \widehat{\mathbf{f}}_{\alpha} \cdot \frac{d}{d\tau} (\mathbf{M}_L \cdot \widehat{\mathbf{f}}_{\beta}) + O(\lambda_{\alpha} - \lambda_{\beta}).$$

The first term describes the geometric spreading, the second one the geometric phase. The latter dominates in the vicinity of a mode connection point  $\tau_{\alpha\beta}$  where two eigenvalues  $\lambda_{\alpha}$  and  $\lambda_{\beta}$  coalesce to  $\lambda_{\alpha\beta}$  as

$$\lambda_{\alpha} - \lambda_{\alpha\beta} \sim |\tau - \tau_{\alpha\beta}|^{\nu} \sim \lambda_{\beta} - \lambda_{\alpha\beta}, \quad \text{leading to} \quad \Gamma_{\alpha\beta} \approx -\frac{\nu}{\tau - \tau_{\alpha\beta}} (1 - \delta_{\alpha\beta})$$

and therefore to the system of amplitude transport equations

$$\frac{d}{d\tau} \begin{bmatrix} a_{\alpha} \\ a_{\beta} \end{bmatrix} = \frac{\nu}{\tau - \tau_{\alpha\beta}} \begin{bmatrix} 0 & 1 \\ 1 & 0 \end{bmatrix} \begin{bmatrix} a_{\alpha} \\ a_{\beta} \end{bmatrix} =: \frac{\nu}{\tau - \tau_{\alpha\beta}} \overset{\circ}{A}(\tau) \cdot \mathbf{a}(\tau).$$

Its transfer matrix  $\mathbf{A}(\tau_2, \tau_1)$  for  $\tau_2 - \tau_{\alpha\beta} = \tau_{\alpha\beta} - \tau_1$ , viz.

$$\mathbf{A}_{\nu}(\tau_2, \tau_1) = \cos \nu\pi \overset{\circ}{1} - i \sin \nu\pi \overset{\circ}{A}, \quad \text{is unitary.}$$

For  $\nu = 1/2$  it represents the phase jumps at a caustic.

**APPLICATION OF TREATMENT OF LORENTZ TYPE RESONANCE TO  
INDUCED EMISSION PROPERTY IN SPATIAL NETWORK AND FD-TD  
METHODS FOR VECTOR POTENTIAL AND HERTZ VECTOR**

Norinobu Yoshida  
Department of Electrical Engineering  
Hokkaido University, Sapporo 060 Japan

In the analysis of electromagnetic fields, easiness in treating many types of medium conditions, such as active, dispersive, anisotropic, and nonlinear properties, is an essentially important factor. I have already proposed the treatment of dispersive medium conditions in the Spatial Network Method (SNM) for both the vector potential and the Hertz vector in the three-dimensional space and on the time domain. [N.Yoshida; "Adaptation of Spatial Network for Vector Potential to Electromagnetic Fields with Medium Conditions", *Abstract of 1993 Radio Science Meeting*, pp. 270 (1993)]. In the treatment by the vector potential, the continuity law between equivalent currents holds physically for not the current but the electric or magnetic flux. Therefore, the equivalent elements at each node corresponds directly to the polarization. This fact gives the simpler formulation than that in the conventional SNM for the Maxwell's equation because of needless of differentiating procedure to obtain the current variables. Furthermore, the use of polarization has intimacy with the mechanism of the dipoles in the medium, which is the macroscopic or classic interpretation of the quantum mechanism.

In this paper, it is shown that formulation for the Lorentz type resonance property can be applied to the treatment of the induced emission, that is, the basic characteristics for the maser and the laser, by using the negative polarizability correspondent to the negative temperature property due to the inverse distribution of dipole moments. In the figure, the amplification variations for a supposed parameter model are shown as a function of the frequency normalized by the resonance frequency at the distance of 15-22.5 wavelengths.

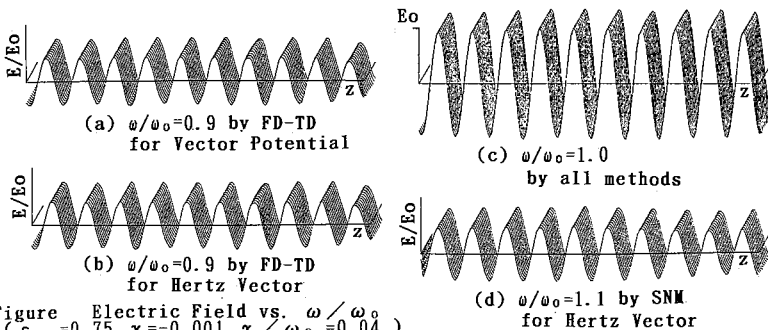


Figure Electric Field vs.  $\omega/\omega_0$   
( $\epsilon_s = 0.75$ ,  $\chi = -0.001$ ,  $\gamma/\omega_0 = 0.04$ )



MONDAY PM URSI-B SESSION M-U8

Room: Kane 110

NUMERICAL METHODS II

Chairs: Y. Leviatan, Technion-Israel Institute of Technology; A. Boag, University of Illinois

1:20	A Surface Integral Equation Formulation Based on Radiation Currents <i>*P.M. Goggans, A.W. Glisson, Univ. of Mississippi</i>	90
1:40	The Singularity in the Solution of Hallen's Equation <i>*R.C. Booton, Jr., Univ. of Colorado at Boulder</i>	91
2:00	Analysis of Dielectric Resonator-Microstrip Filters by the Method of Moments <i>*M. Yousefi, S.K. Chaudhuri, Univ. of Waterloo</i>	92
2:20	Electromagnetic Scattering Analysis Using a Model of Dipoles Located in Complex Space <i>E. Erez, Kibbutz Ein Hashofet; *Y. Leviatan, Technion-Israel Inst. of Technology</i>	93
2:40	Analysis of Slot Antennas Fed by Stripline in Rectangular Waveguide Below Cutoff <i>C.L. Levinson, C.M. Butler, Clemson Univ.</i>	94
3:00	Break	
3:20	Analysis of Bodies of Revolution Whose Generating ARCs Possess Junctions <i>*Z. Qiu, C.M. Butler, Clemson Univ.</i>	95
3:40	Penetration Through Small Apertures: Some Two Dimensional Examples <i>*J.D. Shumpert, C.M. Butler, Clemson Univ.</i>	96
4:00	A Dual-Method Approach for Solving Radiative Transport Equation in a Plane-Parallel Geometry <i>T.-L. Wu, *H.-W. Chang, National Sun Yat-sen Univ.</i>	97
4:20	A Spurious TLM Mode and its Effect on Equivalence of the FDTD and TLM Methods <i>M. Celuch-Marcysiak, W.K. Gwarek, Warsaw Univ. of Technology</i>	98
4:40	Numerical Restrictions for a Green's Function Solution <i>*M. Y. Andrawis, South Dakota State Univ.; W. A. Davis, Virginia Polytechnic Inst. and State Univ.</i>	99

## A SURFACE INTEGRAL EQUATION FORMULATION BASED ON RADIATION CURRENTS

P. M. Goggans\* and A. W. Glisson

University of Mississippi  
Department of Electrical Engineering  
University, MS 38677

This paper presents a new surface integral equation formulation for accurately calculating the equivalent surface currents on material bodies in regions where the radiation currents are small. This formulation is particularly useful in the determining the electromagnetic field scattered by objects with low contrast. Low contrast materials are characterized by a relative permittivity and relative permeability close to unity.

When used in conjunction with a numerical integral equation solution, the conventional surface integral equation formulations can result in a poor estimate of the field scattered by a low contrast object. The poor performance of the standard formulations is due at least partly to their being cast in terms of the total equivalent current on the boundary surface of the scattering body. Only a portion of the total equivalent current gives rise to the scattered field. When this portion is small (as in the case of low contrast scatterers), errors in the radar cross section (RCS) calculation can occur. The new integral equation formulation is cast only in terms of the portion of the total current that gives rise to the scattered field; hence, the new formulation avoids this problem.

Although its main application appears to be in treating low contrast scatterers, the radiation current formulation is also useful for accurately determining the equivalent currents on general material bodies in regions of the surface where the radiation currents are small. Unlike other low-contrast formulations, the radiation current formulation works for high contrast scatterers as well as low contrast scatterers.

Examples generated using the new integral equation formulation are presented for two-dimensional objects. The numerical integral equation solution results are verified by comparison with series solution results for circular cylindrical objects.

## THE SINGULARITY IN THE SOLUTION OF HALLEN'S EQUATION

Richard C. Booton, Jr.

Center for Microwave/ Millimeter-Wave Computer-Aided Design

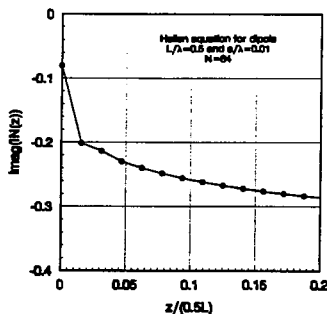
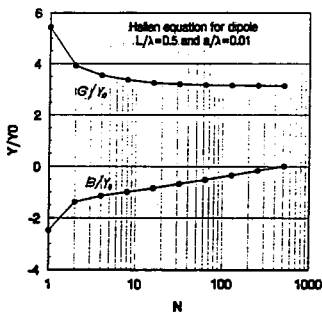
Department of Electrical and Computer Engineering

University of Colorado

Boulder, CO 80309-0425

The solution of Hallen's equation for the current in a center-fed dipole with an infinitesimal gap is known theoretically [T.T. Wu, "Introduction to linear antennas", in *Antenna Theory*, McGraw-Hill, 1969] to contain a logarithmic singularity at the origin. A number of numerical solutions of this equation, however, have been presented that apparently show no sign of this singularity. Calculations for a finite gap [T. Do-Nhat, R.H. MacPhie, "On the effect of gap width on the admittance of solid circular cylindrical dipoles", *IEEE Trans. Antennas and Propagat.*, vol. 37, no. 12, December 1989] do show a steadily increasing susceptance as the gap is decreased.

A sequence of numerical computations performed to investigate this matter is presented. The moment-method with triangular basis functions and point matching was utilized. As expected theoretically, as the number of basis functions is increased the conductance converges. The susceptance, however, continues to increase with no sign of convergence, as shown in the first figure. The susceptance appears from such graphs to be a linear function of the logarithm of the number of basis functions, with the slope increasing as the cylinder radius is increased. The effect is quite noticeable for a cylinder radius of 0.01 wavelengths, but for a radius of 0.001 wavelengths the effect is easy to overlook, although clearly it is present. In addition, careful examination of the numerical solutions shows that the imaginary part of the input current does not seem to belong to the same curve as the rest of the imaginary current values, as shown in the second figure. Again, this is what would be expected from a logarithmic singularity in the imaginary component of the current.



# Analysis of Dielectric Resonator-Microstrip Filters by the Method of Moments

M. Yousefi\*, and S.K. Chaudhuri

Dept. of E&CE, University of Waterloo, Waterloo, Ont., Canada, N2L 3G1

## Abstract

A mixed potential integral equation (MPIE) is proposed to solve the interaction between a dielectric resonator (DR) and a microstrip circuit. The coupling between a DR and a nearby metallization with an arbitrary shape can be modeled by solving this integral equation. Method of Moments (MoM) has been employed to solve the integral equation. For this integral equation, a Green's function is developed in a layered medium *in the presence of DR*. The unknown current distribution on the metallization is then obtained via solving the integral equation. Since the presence of the DR has been taken into account in the Green's function, this versatile and efficient method allows one to directly calculate the  $S$  matrix of the circuit as well as its coupling parameters and gives a clear qualitative insight of the behavior of DR-microstrip interactions. The flexibility of the method to analyze DR on a generally shaped metallization, and its computational advantages over methods like "FE" is demonstrated through the design of a band-pass DR-microstrip circuit shown in Figure 1. The calculated  $S$  matrix of the DR band-pass filter is presented. Also the current distribution on the metallization with and without the DR show the filtering mechanism of the DR filter very clearly. The time-efficiency of the method in conjunction with its versatility makes it a suitable choice for CAD softwares.

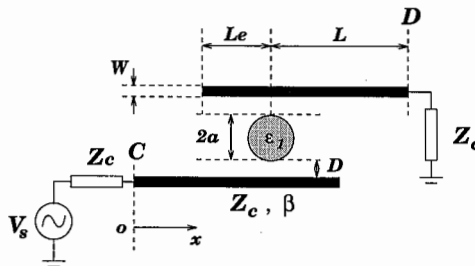


Figure 1: A band-pass DR filter.

# Electromagnetic Scattering Analysis Using a Model of Dipoles Located in Complex Space

Eitan Erez  
Kibbutz Ein Hashofet, Israel

Yehuda Leviatan\*  
Department of Electrical Engineering  
Technion-Israel Institute of Technology  
Haifa 32000, Israel

Fictitious current-models have been applied extensively in recent years to a variety of time-harmonic electromagnetic wave scattering problems. This paper is introducing an extension of the current-model technique which facilitates the solution to problems subsuming scatterers that contain a variety of length-scales.

The proposed extension is in tune with the current-model technique philosophy of using simple current sources the fields of which are analytically derivable. It amounts to letting the coordinates of part of the source centers assume complex values. Positioned in complex space, the simple current sources radiate beam-type fields which are more localized and are better approximations of the scattering from the smooth expanses of the structure. The coordinates of the other source centers can retain their conventional real values or have only a relatively small imaginary constituent. These latter current sources are used, of course, to approximate the fields in the vicinity of the more rapidly varying expanses of the structure.

The new approach is applied to analyze electromagnetic scattering by an object comprising two adjacent perfectly conducting spheres of different size and by a perfectly conducting oblate spheroid. It is found to render the solution computationally more effective at the expense of only a slight increase in its complexity.

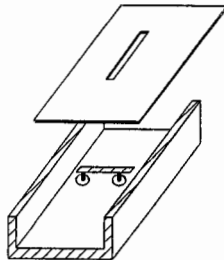
## ANALYSIS OF SLOT ANTENNAS FED BY STRIPLINE IN RECTANGULAR WAVEGUIDE BELOW CUTOFF

Catherine L. Levinson and Chalmers M. Butler  
ECE Department  
Clemson University  
Clemson, SC 29634-0915

The stripline-fed slot array is a low-profile antenna comprising an array of narrow, finite-length slots coupled to a stripline. In the structure of interest, the trace of the stripline actually resides in a rectangular waveguide formed by the slotted ground plane and a U-shaped trough as illustrated below. The stripline can be fed from below (as illustrated) or at its edges. Undesirable, propagating, rectangular waveguide modes could be excited by electric currents on bottom feeds or by equivalent magnetic currents in the slot, but the design dimensions are such that all the rectangular waveguide modes are evanescent, or cut off.

Measurements and numerical results will be presented for a single element that is fed and loaded from the edge, fed and loaded from the bottom, or fed from the edge and loaded from the bottom, or vice versa. Numerical modelling has shown that at frequencies above the mode cutoffs the slot is tightly coupled to the rectangular waveguide modes. Most of the power is then lost to these modes instead of being coupled and radiated to the exterior region. At frequencies below the waveguide cutoff, however, little power is lost to these modes. Hence, the array element is designed so that the guide cutoff frequencies are all above the operating frequency band.

Coupled integral equations are derived and solved for the electric currents on the stripline trace and feeds and for the equivalent magnetic currents in the slot. The method used to numerically evaluate the sums found in the Green's function for a dipole in a rectangular waveguide is described along with convergence tests. Data illustrating input admittance and far-zone fields are presented.



## ANALYSIS OF BODIES OF REVOLUTION WHOSE GENERATING ARCS POSSESS JUNCTIONS

Zhiqiang Qiu\* and Chalmers M. Butler  
Department of Electrical and Computer Engineering  
Clemson University, Clemson, SC 29634-0915

Interest in this paper focuses upon the electromagnetic analysis of a body of revolution (*bor*) whose generating arc possesses junctions. The excitation of the structure can be due to one of several sources: electric or magnetic dipoles, distributions of specified currents, incident plane waves, or antenna-type sources on the body. One can think of such a structure being created in the usual way by rotating a generating arc through  $2\pi$  radians, but with the generating arc in this case being one which has a junction of three or more sub-arcs. An example would be a body with a thin outer shell (conducting) and with partitions inside formed by the generating arc's "appendages."

Coupled integro-differential equations are derived for the current induced on the structure, with full account taken of the junctions in the generating arc and the associated coupling. Effectively, Kirchhoff's current law is enforced on the  $t$  component of the surface current at the arc junctions by techniques similar to what is done in the case of thin-wire junctions. No special conditions are needed on the  $\phi$  component of current at the junction to ensure proper behavior. In the usual way for *bors*, coupled integro-differential equations are formulated for the  $m$  Fourier series coefficients of the current components, with the Fourier coefficients of the components of incident electric field serving as forcing functions. These coupled equations are solved numerically for the  $m$  coefficients of the two components of the current.

The electric current induced on a *bor* shell and on its exterior appendages by a specified incident field are determined to demonstrate the effectiveness of the analysis. The same is done for interior arc appendages which form cavities within the shell. In this latter case, interior fields are computed and compared with fields determined by other techniques. Data are presented to illustrate the behavior of shell currents on a sphere with exterior "skirts" and a hollow cylinder with inside partitions.

## PENETRATION THROUGH SMALL APERTURES: SOME TWO DIMENSIONAL EXAMPLES

John D. Shumpert\* and Chalmers M. Butler  
Department of Electrical and Computer Engineering  
Clemson University, Clemson, SC 29634-0915 USA

Interest in this paper focuses upon some of the difficulties in the computation of penetration through small apertures in closed conducting surfaces. The traditional approach of treating the body as a scatterer and solving for the field that penetrates a conducting surface through a small aperture by summing the incident and the scattered field is straight-forward but can lead to very very inaccurate or even meaningless results. This is demonstrated by means of simple examples. Two alternate methods that enable one to solve for the penetration but which do not suffer the inherent inaccuracies of the so-called scatterer method can be formulated. These alternate methods do yield accurate results but they fail at interior resonances of the body.

The first alternate scheme depends upon solving for the aperture field directly and then determining the penetrated field from knowledge of the aperture field. The second alternate scheme is based upon a theorem which allows one to change the excitation of the structure from the known source or incident field to an equivalent surface current placed in the aperture. The penetrated field is then determined by a procedure similar to that of the scatterer method but without the inherent inaccuracies. Unfortunately, as mentioned above, the two alternate methods are susceptible to interior resonances and the pertinent equations must be reformulated so that they remain valid over the entire spectrum of interest. This is done by appealing to the so-called combined field or combined source formulation, which do lead to integral equations valid at all frequencies.

Often, when characterizing unwanted penetration, one must determine the maximum interior field which frequently occurs at the frequency for which the un-altered integral equations fail, *i.e.*, at the interior resonances. Of course, these are not true resonances because such resonances cannot occur in a cavity having a hole through which energy can leak. Nevertheless, the original equations fail at the frequencies for which penetration data are needed and, hence, the alternate methods are warranted.

The principles alluded to above are illustrated by determining currents and penetrated fields for several cylindrical shells with slots. The inaccuracies of the scatterer method are demonstrated and the alternate methods are shown to yield accurate penetrated field. Failure at interior resonances is also demonstrated by example as are the integral equation remedies.

**A DUAL-METHOD APPROACH FOR SOLVING RADIATIVE TRANSPORT  
EQUATION IN A PLANE-PARALLEL GEOMETRY**

Tzuoh-Luen Wu and Hung-Wen Chang\*  
Institute of Electro-Optics, National Sun Yat-sen University  
Kaohsiung, Taiwan, Republic of China 80424

Many numerical studies have been conducted on solving the radiative transport equation in a plane-parallel geometry. There are two different approaches to the problem. The first approach treats the radiative, plane-parallel problem as a boundary value problem. The method looks for solutions which satisfy the radiative transfer equation as well as the given boundary conditions. These methods include eigen-function expansion of the vector differential equations, spherical harmonic expansion of specific intensity (in various orders), matrix exponential method and many other approximation techniques such as the Monte-Carlo simulation and the finite-different approximation.

The other approach treats the radiative, plane-parallel problem as an initial value problem. This method solves for the reflection (R) and transmission (T) matrices of the specific intensities. The matrices R and T satisfy a pair of nonlinear matrix differential equations called matrix Riccati equations each having a simple initial condition. The method can be combined with the doubling method which gives the new R and T of twice the original thickness in terms of the old R and T. With R and T matrices and the incoming specific intensity vectors (boundary conditions), one can easily calculate the transmitted and backscattered specific intensities.

We will compare accuracy, computational cost and other related issues from among the two classes of methods mentioned above. Our initial results show that the best method (minimal work for a given accuracy requirement) to use will depend on the matrix sizes, parameter values (albedo and asymmetry of phase function) and the layer thickness. In particular, the eigen-function expansion method with scaling is good for wide ranges of optical thickness provided that the problem fits in core. For large matrices that do not fit into the computer memory, numerical solution of the vector Riccati equations together with the doubling method is a better choice since they can be implemented quite efficiently with out-of-core matrix multiplication/inversion algorithms.

**A SPURIOUS TLM MODE  
AND ITS EFFECT ON EQUIVALENCE OF THE FDTD AND TLM METHODS.**

Malgorzata Celuch - Marcysiak, Wojciech K.Gwarek  
Institute of Radioelectronics, Warsaw University of Technology,  
Nowowiejska 15/19, 00-665 Warszawa, Poland.

We present a new version of the theorem of equivalence of the FDTD and expanded node TLM methods for emulating physical modes in electromagnetic analysis of microwave circuits. In extension to the previous version (*Eur.Microwave Conf., Stuttgart 1991*) it explains the nature of supplementary information in TLM and susceptibility of TLM to spurious modes. We consider TLM and FDTD based on the same set of cells of arbitrary shape and filling. We discuss a general 3D case decomposed into a set of 2D nodes. We obtain a mesh of nodes connected by branches. The FDTD method provides voltages (corresponding to the electric field) at nodes and currents (magnetic fields) in branches. From TLM pulses we can extract data on two grids: grid  $\mathcal{S}$  (voltages at nodes, currents in branches) and grid  $\mathcal{F}$  (currents at nodes, voltages in branches).

In the theorem we prove that:

- Information on grid  $\mathcal{S}$  in TLM is physical and identical to FDTD.
- All boundary conditions and discontinuities can be equivalently described using only grid  $\mathcal{S}$  (or FDTD notation).
- The information available on  $\mathcal{F}$  can simplify calculations of S-parameters but it can be contaminated by a spurious mode of frequency  $f=0.5/\Delta t$  (where  $\Delta t$  is simulation time-step).
- From quantities on  $\mathcal{S}$  (or in FDTD) we can uniquely reconstruct average of quantities on  $\mathcal{F}$  in two consecutive iterations. To obtain instantaneous values on  $\mathcal{F}$ , we can locally supplement standard FDTD by an additional equation.

As a result of the above theorem we formulate the following statements which contradict the claims made by some authors:

- The FDTD and expanded node TLM methods provide the same accuracy in analysing microwave circuits of arbitrary shape and filling.
- There can be no superiority of either method in terms of the speed of convergence to the final solution, if equivalent sources of excitation are used.
- Any special features of one of the methods like particular sources of excitation, curved boundary models, graded mesh, higher order algorithms or subgridding can be transformed into the other method applying simple conversion rules.

During the presentation of the paper we will demonstrate these rules in the form of tables. We will also show how the theorem and the rules can be used in combining experience of both methods to improve curved boundary representation and models of sources, accelerating the convergence of algorithms and eliminating the TLM spurious modes.

## Numerical Restrictions for a Green's Function Solution

M. Y. Andrawis\*

South Dakota State University  
Electrical Engineering Department  
Brookings, SD 57007-0194

W. A. Davis

Virginia Polytechnic Institute and State University  
Bradley Department of Electrical Engineering  
Blacksburg, VA 24061-0111

This paper develops a basic Green's function solution for two coupled regions. The Green's function solution may be obtained by expanding the Green's functions in both regions in terms of the modes of the structures respectively. Applying field continuity over the aperture or coupling surface, the method of moments will be used to solve for a magnetic current source imposed at the aperture, effectively applying the mode-matching method. This solution method is applied to a reflection cavity structure designed to adapt to APC-7 connectors of frequency domain measuring instruments such as the HP 8510B network analyzer. A full field analysis for this cavity structure, referred to as the wideband dielectric-filled cavity structure, may be used for the evaluation of the dielectric properties of the dielectric material enclosed within it, based on knowledge of the sample geometry and the measured S-parameters of the filled cavity [*Wideband Dielectric Characterization Using a Dielectric Filled Cavity Adapted to the End of a Transmission Line*], Saed, Riad, and Davis, *IEEE Trans. on Instrum. and Meas.*, Vol. 39, No.3, June 1990].

To examine the accuracy of the solution due to truncation of higher order modes in the Green's function expansion, the fields for the full cavity problem will be computed in both regions for typical cavity dimensions and frequencies of interest. The fields at the aperture should agree in both regions and the tangential electric field at the cavity walls should be identically zero. The number of terms retained in the series representation of the Green's function in the cavity region determines the limitations on the ability to match both the aperture fields and the zero electric field at the conductor walls, as well as achieve convergence in the reflection properties in the transmission line. The number of modes in the transmission line region will be related to the number of modes in the cavity region in order to ensure solution convergence.



MONDAY PM URSI-A SESSION M-U9

Room: Savery 249

ANTENNA MEASUREMENTS

Chairs: C.F. Stubenrauch, NIST; I.J. LaHaie, Environmental Research Institute of Michigan

- 1:20 International Intercomparison of Horn Gain at X-Band 102  
*\*C.F. Stubenrauch, A.C. Newell, National Inst. of Standards and Technology*
- 1:40 A High Temperature Superconducting Leaky Wave Antenna 103  
*J. Poosarla, J.T. Williams, D.R. Jackson, Univ. of Houston*
- 2:00 Theory of Ultrawideband Three-Dimensional Sources and Their Application to High Range Resolution (HRR) Tracking Antennas 104  
*A.J. Devaney, E. Marengo, Northeastern Univ.; \*E. Heyman, Tel-Aviv Univ.*
- 2:20 Probe-Corrected Algorithm for Predicting Far Zone Scattering from Bistatic Spherical Near-Field Measurements 105  
*\*J.W. Burns, Environmental Research Inst. of Michigan*
- 2:40 Algorithm for Determining Waterline RCS of a High Aspect Target Using SNFFFT 106  
*\*J.W. Burns, I.J. LaHaie, Environmental Research Inst. of Michigan*
- 3:00 Break
- 3:20 Extrapolation of Far Zone Scalar RCS from Spherical Near Zone Monostatic Measurements 107  
*\*I.J. LaHaie, J.W. Burns, Environmental Research Inst. of Michigan*
- 3:40 Equivalence of the Far Field Monostatic-Bistatic Theorem and the Reflectivity Distribution Model for Scalar Fields 108  
*\*I.J. LaHaie, Environmental Research Inst. of Michigan*

## International Intercomparison of Horn Gain at X-band

Carl F. Stubenrauch\*, Allen C. Newell,  
Andrew G. Repjar, Katie MacReynolds  
National Institute of Standards and Technology  
Electromagnetic Fields Division  
Boulder, Colorado 80303

An international intercomparison of horn gain and polarization measurements at X-band has recently been completed. There were seven participating laboratories with the National Institute of Standards and Technology serving as the pilot laboratory. Two X-band pyramidal standard gain horns with a nominal gain of 22 dB served as the travelling standards. Quantities measured included on-axis fixed frequency gain at 8, 10, and 12 GHz, swept frequency gain between 8 and 12 GHz and polarization characteristics at the three fixed frequencies. All laboratories performed the fixed frequency gain measurements. The swept frequency and polarization measurements were optional, with four laboratories performing swept frequency measurements and four laboratories measuring polarization.

The results of the gain measurements generally agreed within the reported uncertainties which were of the order of 0.1 dB or less. Detailed results of the intercomparison will be presented as well as a brief description of the measurement techniques employed at the various laboratories.

## A HIGH TEMPERATURE SUPERCONDUCTING LEAKY WAVE ANTENNA

Jagannath Poosarla, Jeffery T. Williams,  
and David R. Jackson

Applied Electromagnetics Laboratory  
Department of Electrical Engineering  
University of Houston  
Houston, TX 77204-4793

Due to the low level fields associated with many millimeter-wave communication systems it is necessary to have sensitive, low noise figure components in the front end of the receivers and detectors. By integrating a monolithic, high gain antenna into these systems the overall performance and flexibility can be improved. Conventional high gain monolithic antennas suffer from high ohmic losses at millimeter-wave frequencies, primarily due to losses in the feed network. Designs which compensate for these losses are generally quite complex, thereby introducing inherent reductions in reliability. Since the physical scale of these structures is small at millimeter-wave frequencies, electrically large traveling-wave and leaky-wave antennas are feasible. These antennas are desirable in many applications due to their extremely high directivity.

In this presentation we will discuss a new superconducting antenna design suitable for millimeter-wave communication applications. This antenna consists of a conductor-backed substrate which is covered by a thin film of superconductor. When excited from below by a waveguide feed the structure acts as a leaky radial-waveguide. By appropriately selecting the geometric and electrical parameters of the antenna, extremely high gain performance can be realized. The basic nature of this new antenna is similar to multiple-layer dielectric leaky-wave antennas that have been previously studied; however, the design is more suitable for low profile, monolithic applications. It is interesting to note that such high gain performance cannot be realized by replacing the superconductor with a thin film of normally conducting material, regardless of the conductivity of the normal metal, because of an inherently low radiation efficiency. The new leaky-wave antenna design requires that the thin cover layer be superconducting due to the unique properties of these materials. More specifically, the superconductor can be modeled, in a macroscopic sense, with a complex conductivity. For a good superconductor, away from the critical temperature, the conductivity is large and dominated by the negative imaginary part, which leads to the high gain performance in this antenna design. The efficiency of this leaky-wave antenna increases substantially when operated below the critical temperature of the superconductor, therefore it is necessary to use high temperature superconducting materials in order to obtain high gain performance at a reasonable operating temperature.

THEORY OF ULTRAWIDEBAND THREE-DIMENSIONAL SOURCES  
AND THEIR APPLICATION TO  
HIGH RANGE RESOLUTION (HRR) TRACKING ANTENNAS

Anthony J. Devaney and Edwin Marengo  
Northeastern University, Dept. of Electrical and Computer Engineering  
Boston, MA 02115

and

Ehud Heyman\*  
Tel-Aviv University, Dept. of Electrical Engineering — Physical Electronics  
Tel-Aviv 69978, Israel

This talk presents recent results obtained in a study whose overall goal is to investigate the use of three-dimensional source distributions for the purpose of generating ultrawideband electromagnetic signals. The work reported in the talk focuses on the use of such distributions as models for antenna arrays in high range resolution (HRR) tracking radar applications. The motivation behind the work is the well known observation that the spatial distribution of a coherent source has a pronounced effect on the spectral character of its radiated field. In particular, by shaping the spatial profile of a source having a fixed spectrum it is possible to optimize the radiated spectrum  $S(\omega, \hat{\mathbf{r}})$  both as a function of direction  $\hat{\mathbf{r}}$  and frequency  $\omega$ . An important application of this procedure is HRR tracking radar where the goal is to generate a pulse having high energy and very short duration in the forward direction ( $\hat{\mathbf{r}} = \hat{\mathbf{z}}$ ) and low energy and very long duration in all other directions. In this talk it is shown that three-dimensional sources of compact support exist that yield optimal performance (in the sense of the maximum likelihood estimate of range and track direction) and that these sources can be approximated by finite sized discrete antenna arrays. The talk includes a review of the mathematical formulation of the problem as well as computer simulated examples.

PROBE-CORRECTED ALGORITHM FOR PREDICTING FAR ZONE  
SCATTERING FROM BISTATIC SPHERICAL NEAR-FIELD  
MEASUREMENTS

Joseph W. Burns

Signal Processing and Electromagnetics Laboratory  
Environmental Research Institute of Michigan  
P.O. Box 134001  
Ann Arbor, MI 48113-4001

Techniques for predicting the far zone radiation pattern of antennas from spherical near-field measurements have been developed over the last two decades. An excellent overview of the technology is provided in the book by J.E. Hansen (*Spherical Near-Field Antenna Measurements*, Peter Peregrinus Ltd., London, 1988). Comparatively little research has been done to develop means of predicting electromagnetic scattering from spherical near-field measurements. P.F. Wacker (IEEE Trans. Antennas Propagat., vol. AP-29, no.2, pp. 342-351) has described a general approach to the formulation, and M.G. Cote and R.M. Wing (*Proc. 15th Annual AMTA Mtg.*, pp 191-197, 1993) have recently demonstrated a non probe-corrected transmission formula with experimental data.

The Environmental Research Institute of Michigan is working to develop practical methods of predicting far zone radar cross-section (RCS) of targets from spherical near-field measurements. As a first step in this study, an exact probe-corrected spherical near-field to far-field transform (SNFFFT) algorithm for computing the far zone RCS of a target from bistatic spherical near-field measurements was developed and will be described in this presentation. In the accompanying paper, a simplified method of evaluating the algorithm to obtain a practical measurement system for high aspect targets will be discussed.

The derivation of the SNFFFT algorithm basically consists of three steps. First, an expression is deduced for the bistatic, near-field scattering data measured using a separate transmitter and receiver. The formula, referred to as the reflection formula, represents the scattering behavior of the target in the form of a spherical wave scattering matrix. Next, the reflection formula is inverted using the orthogonality properties of the spherical wave functions to obtain an expression that specifies the elements of the spherical wave scattering matrix in terms of the near-field measurements. Finally, an expression is given for the bistatic, far zone scattering in terms of the spherical wave scattering matrix elements. The combined results are then written in a matrix format that directly relates the measured near-field data to the desired far-field data.

The general approach to the discrete implementation of the algorithm will be presented, and estimates of the data collection requirements for a full bistatic measurement system will be discussed.

ALGORITHM FOR DETERMINING WATERLINE RCS  
OF A HIGH ASPECT TARGET USING SNFFFT

Joseph W. Burns\* and Ivan J. LaHaie

Signal Processing and Electromagnetics Laboratory  
Environmental Research Institute of Michigan  
P.O. Box 134001  
Ann Arbor, MI 48113-4001

The Environmental Research Institute of Michigan is developing practical methods of predicting the far zone radar cross-section (RCS) of a target from spherical near-field measurements. As a first step in this study, an exact probe-corrected spherical near-field to far-field transform (SNFFFT) algorithm for computing the far zone RCS from bistatic spherical near-field measurements was developed and is described in the accompanying presentation. A drawback of the general algorithm is that it requires the bistatic near-field scattering of the target to be measured over the entire surface of a sphere enclosing the target. For most targets, this type of data collection is impractical.

In the spherical near-field antenna literature, it is known that it is not necessary to measure the near-field radiation of an antenna over the entire surface enclosing the antenna if the far field radiation is only desired in a limited set of directions. A measurement scenario of interest is to determine the "waterline" radar cross-section (RCS) of a high aspect target from bistatic near-field measurements made in a circle about the target. In this presentation, the simplified evaluation of the general SNFFFT algorithm to obtain a practical measurement system for a high aspect target will be discussed.

We define a high aspect target as one having one dimension, such as its height, that is much smaller than its length. The waterline RCS is measured in a plane passing through the long dimension of the target, and in this discussion the plane will be taken to be the equator of the measurement sphere. It will be shown that, at a sufficient measurement radius, it is possible to predict the waterline RCS using the SNFFFT algorithm and bistatic near-field measurements collected only over equator of the measurement sphere. An interesting result is that the polarimetric components of the field are decoupled in the near-field to far-field transform for the waterline case. The reduction in required near-field measurements results from the shape of the target. The radius of the measurement sphere at which this is possible is deduced using the data truncation principle discussed in Hansen (*Spherical Near-Field Antenna Measurements*, Peter Peregrinus, Ltd., London, 1988, Section 6.6).

An algorithm for determining the far zone RCS from bistatic near-field measurements in the equatorial plane is then described. The discrete implementation of the algorithm will be discussed, and numerical simulations illustrating the performance of the algorithm will be presented.

## Extrapolation of Far Zone Scalar RCS from Spherical Near Zone Monostatic Measurements

Ivan J. LaHaie\* and Joseph W. Burns  
Signal Processing and Electromagnetics Laboratory  
Environmental Research Institute of Michigan  
P.O. Box 134001  
Ann Arbor, MI 48113-4001

It is well-known that the far zone scattered field, and hence, radar cross-section (RCS), of a target can be extrapolated from near zone measurements on a planar (M.A. Dinallo, Proc. AMTA, 1984) or spherical scanning surface (P.F. Wacker, IEEE Trans. Ant. Prop., AP-29, pp. 342-351, 1981). An explicit algorithm for the latter is derived in another presentation in this symposium (J.W. Burns, IEEE AP-S/URSI Symposium, 1994). However, the transformation algorithms require complete bistatic data which is impractical to collect and process in reasonable amounts of time.

As part of our research to develop practical spherical near field-to-far field transformations (SNFFFT) for scattering measurements, a scalar SNFFFT which requires only monostatic measurements is described. The algorithm is based on a scattering model commonly used in synthetic aperture radar (SAR) and inverse synthetic aperture radar (ISAR) imaging applications, wherein the target scattering is attributable to a three-dimensional reflectivity distribution which, for the purposes of mathematical derivation, is assumed to be independent of the frequency and aspect angle of the incident field. The algorithm itself does not require formation of an image, however. Instead, it is shown that the scattering problem can be converted to an equivalent near field radiation problem by taking the frequency derivative of the near field data. Consequently, measurements are needed at only two adjacent frequencies rather than over a broad bandwidth, as is normally required for imaging applications. The algorithm does not include probe-compensation, as this will be addressed as part of a generalization to vector fields in future.

The practical implications of the reflectivity assumption are discussed, and example results for a simplified version of the algorithm applicable to one-dimensional great circle (as opposed to 2-D spherical) measurements will be presented. In the companion presentation, it is shown that the reflectivity model is completely equivalent to a target satisfying the far field monostatic-bistatic theorem.

## **Equivalence of the Far Field Monostatic-Bistatic Theorem and the Reflectivity Distribution Model for Scalar Fields**

Ivan J. LaHaie  
Signal Processing and Electromagnetics Laboratory  
Environmental Research Institute of Michigan  
P.O. Box 134001  
Ann Arbor, MI 48113-4001

In our continuing effort to develop practical near field-to-far field transformations (NFFFT) for predicting far zone radar cross-section (RCS) for near zone scattered field measurements, it is important to understand under which conditions the monostatic near fields provide sufficient information to predict the monostatic far fields. In general, complete bistatic near field measurements are required, but these are impractical from hardware, collection time, and data processing considerations.

In the preceding presentation, it was shown for scalar fields that if the target scattering can be described using a reflectivity distribution model commonly utilized in radar imaging, then a NFFFT algorithm can be derived which requires only monostatic near field measurements. In this presentation, it is shown that satisfaction of the monostatic-bistatic theorem (MBT) by the far zone scattered fields is a necessary and sufficient condition for validity of the reflectivity distribution assumption. In fact, an explicit expression for the reflectivity distribution in terms of the three-dimensional Fourier transform of the far zone monostatic fields as a function of frequency and aspect angle is derived.

Mathematically, the equivalence requires that the far fields satisfy the MBT over all aspect angles and for all frequencies less than the measurement frequency. The presentation concludes with a discussion of the practical ranges of frequencies and aspect angles over which the MBT must hold for successful application of the monostatic NFFFT.

**MONDAY PM URSI-B SESSION M-U10**

Room: Savery 211

**HIGH FREQUENCY METHODS**

Chairs: R. Marhefka, The Ohio State University; R.G. Olsen, Washington State University

- 1:20 The Relationship Between Different Equivalent Current Formulations 110  
*\*J. H. Meloling, R. J. Marhefka, The Ohio State Univ.*
- 1:40 A Three Dimensional Solution for the Diffraction of an Inhomogeneous Plane Wave by a Wedge 111  
*\*G. Manara, Univ. of Pisa; P. Nepa, R.G. Kouyoumjian, The Ohio State Univ.*
- 2:00 Radiation Due to a Convex Curvature Discontinuity of a Dielectric Coated Perfect Conductor 112  
*\*D.H. Monteith, R.G. Olsen, Washington State Univ.*
- 2:20 Diffraction Catastrophes, Lips Events, and the Unfolding of Glory Scattering by Dielectric Spheroids: Analysis and Observations 113  
*P.L. Marston, G. Kaduchak, Washington State Univ.; H.J. Simpson, Naval Research Laboratory*
- 2:40 High-Frequency Analysis of Whispering-Gallery Mode Radiation from the Aperture of a Conducting Concave Boundary 114  
*K. Goto, \*T. Ishihara, National Defense Academy*
- 3:00 Break

1994 URSI Radio Science Meeting (Seattle)

**THE RELATIONSHIP BETWEEN DIFFERENT  
EQUIVALENT CURRENT FORMULATIONS**

J. H. Meloling\* and R. J. Marhefka  
The Ohio State University ElectroScience Laboratory  
Department of Electrical Engineering  
1320 Kinnear Rd.  
Columbus, Ohio 43212-1191

Two main theories are used to calculate the radiation and scattering at high frequencies. First, the Geometrical Theory of Diffraction (GTD) and its uniform version (UTD) use diffracted fields to correct the Geometrical Optics (GO) fields. Although the UTD does correctly remove the discontinuities along the shadow boundaries, it does not predict the correct fields in caustic regions. The second main theory is the Physical Theory of Diffraction (PTD) which is based on the GO current (PO). The PO field is continuous at the shadow boundaries and caustics. The PTD also uses non-uniform currents to correct the GO current near the edges of plates.

In both of these methods, various types of equivalent currents have been developed to predict the diffracted fields in caustic regions. The equivalent currents used with the GTD are found by comparing the field diffracted by an edge with the field radiated by a line source and solving for the electric and magnetic currents. These GTD equivalent currents are derived from a field point of view. The fringe equivalent current used in conjunction with the PTD is derived by dividing the non-uniform current on a wedge into narrow strips. These strips are then integrated up to the edge. This is then compared to the radiation integral and solved for the electric and magnetic currents. These fringe equivalent currents are derived from a current point of view. Another recently proposed formulation is the Incremental Theory of Diffraction (ITD). This formulation is based on a Fourier transform pair relation which is used to determine the field diffracted from an infinitesimal length of a wedge. These ITD fields are derived from a field point of view.

Here, a unifying approach is discussed which allows for the derivation of most of the commonly used equivalent current formulations. The field based GTD equivalent currents and ITD diffracted fields are derived from a current point of view. It is shown that all of these formulations are based on the same basic physical phenomena and are therefore directly related to one another.

## A THREE DIMENSIONAL SOLUTION FOR THE DIFFRACTION OF AN INHOMOGENEOUS PLANE WAVE BY A WEDGE

G. Manara\*, P. Nepa

Dept. of Information Engineering, University of Pisa, Italy

R. G. Kouyoumjian

Dept. of Electrical Engineering, The Ohio State University, USA

A uniform, high-frequency solution was presented for the two dimensional scattering of an inhomogeneous plane wave by a perfectly conducting wedge (R.G. Kouyoumjian et al., IXth Italian National Meeting on Electromagnetics, Assisi, Italy, 1992). The same two dimensional procedure has been more recently extended to analyze the diffraction of an inhomogeneous plane wave by a wedge with different impedance faces (G. Manara et al., URSI Radio Science Meeting, Ann Arbor, Michigan, 1993). In this paper, the more general case of the scattering of an inhomogeneous plane wave obliquely incident on the edge of a wedge is considered.

Either soft or hard boundary conditions may be imposed on the faces of the wedge. Since these conditions are uniform along the edge direction, an equivalent two dimensional problem can be defined. This is obtained by projecting the real and imaginary components of the wave vector on to the plane transverse to the edge. When the medium surrounding the wedge is lossless, the imaginary component of the wave vector can be arbitrarily oriented in a plane normal to the direction of propagation; however, the transverse projections of the real and imaginary components of the wave vector are not perpendicular in general. Consequently, the medium surrounding the wedge appears to be lossy. The problem can be solved by introducing an equivalent lossy medium and then using the method of solution for this case. The location of the shadow and reflection boundaries are determined, and the displacement of these boundaries from their position in the case of homogeneous plane wave incidence is discussed. The dependence of the displacements on actual losses in the medium surrounding the wedge is also described, together with the shape and location of the transition regions. The solution is interpreted in terms of the uniform GTD. The diffracted field properly compensates the discontinuities in the incident and reflected fields at their respective shadow boundaries. The expression for the diffracted field contains the uniform GTD transition function but its argument is complex.

Several numerical results will be presented both to show the continuity of the total field across the shadow boundaries, and to demonstrate the accuracy of the asymptotic expressions through comparisons with the corresponding eigenfunction solution.

**RADIATION DUE TO A CONVEX CURVATURE DISCONTINUITY  
OF A DIELECTRIC COATED PERFECT CONDUCTOR**

David H. Monteith\* and Robert G. Olsen  
School Of Electrical Engineering and Computer Science  
Washington State University  
Pullman, WA 99164-2752

It is known that surface waves radiate energy at curvature discontinuities. By reciprocity, surface waves will be excited by plane waves incident upon such a discontinuity. Here, the problem of radiation due to a surface wave incident upon the discontinuity formed by a flat dielectric coated perfect conductor which changes abruptly into a cylindrical dielectric coated perfect conductor is considered. The radius of the cylinder considered is large compared to the wavelength. The dielectric is assumed to be homogeneous, isotropic and linear. Of particular interest is determining the radiation characteristics as a cutoff frequency of the flat surface waveguide is approached. The problem is formulated as an integral equation over the vertical aperture formed at the abrupt change in curvature. It is formulated in terms of Green's functions of a flat and a cylindrical coated conductor. In the case for large radius of curvature, this integral equation can be simplified by the use of regular perturbation theory. From these an iterative approximate solution to the integral equation is obtained. Results as cutoff is approached and as the surface approaches an impedance surface are presented. These latter results are compared to published results for an impedance surface.

**Diffraction catastrophes, lips events, and the unfolding of glory scattering by dielectric spheroids: analysis and observations.** P. L. Márston and G. Kaduchak (Physics Dept., Washington State University, Pullman WA 99164-2814) and H. J. Simpson (Naval Research Laboratory, Code 7136, 4555 Overlook Ave. S. W., Washington DC, 20375).

High-order caustics associated with the merging of more than two rays can be described with catastrophe theory; the associated wavefields are known as diffraction catastrophes. Such caustics are known to exist in the far-field scattering of light by acoustically levitated oblate drops of water [P. L. Marston and E. H. Trinh, *Nature (London)* **312**, 529-531 (1984)] and in the light scattered by oblate bubbles rising through water. Investigation of these caustics is applicable to understanding the high frequency scattering for other ranges of refractive index and to other situations generating far-field high-order caustics. Scattering by a spheroid is a sufficiently well defined situation that the analysis of the caustics and associated wavefields illustrates the construction of smooth transformations needed for the application of catastrophe theory to scattering problems [P. L. Marston, "Geometrical and catastrophe optics methods in scattering," *Physical Acoustics* **21**, 1-234 (1992)]. Our observations emphasize situations where 3, 4, and 6 rays merge at a far-field caustic associated with transverse cusp, hyperbolic umbilic, and symbolic umbilic ( $E_6$ ) diffraction catastrophes. The transverse cusp wavefield can be described with a Pearcey function. We also examine the effects on backscattering by spheroids from the unfolding of the glory for a small oblateness and from the collapse of a lips shaped caustic. The former unfolding results from distortion of outgoing toroidal wavefronts due to the oblateness. The backscattering enhancement for a sphere having a refractive index of 2 has also been analyzed as well as the rainbow-enhanced backward glory scattering that occurs for spheres having refractive indices of approximately 1.180 and 1.089. These enhancements are associated with rays having one, two, and three internal reflections, respectively.

# HIGH-FREQUENCY ANALYSIS OF WHISPERING-GALLERY MODE RADIATION FROM THE APERTURE OF A CONDUCTING CONCAVE BOUNDARY

K.Goto and T.Ishihara\*  
Dept. of Electrical Engineering,  
National Defense Academy,  
Hashirimizu, Yokosuka, 239, JAPAN

Radiation fields of whispering-gallery (WG) modes from the aperture of the semicylindrical conducting concave boundary are analyzed asymptotically in the cylindrical  $(\rho, \phi, z)$  coordinate systems. By extending the range of the  $\phi$  coordinate from the physical periodic domain  $0 \leq \phi \leq 2\pi$  into an infinite domain  $-\infty < \phi < \infty$  and modeling the concave boundary as the surface  $\rho=a$  extending from  $\phi=0$  to  $\phi=-\infty$ , the integral representation of the radiation fields, excited by the WG modes, can be obtained explicitly by the Fourier transform method and the Wiener-Hopf technique [M.Idemen and L.B.Felsen, IEEE Trans. Antennas & Propag., AP-29, 4, pp.571-579, 1981] analogous to those applied in the half-plane problem.

The integrand of the integral representation of the radiation fields has the simple pole singularity near the isolated first-order saddle point. Thus, by applying the asymptotic analysis to the integral valid uniformly as the saddle point approaches the pole singularity, we obtain the beam field representation or the radiation field representation consisting of the geometrical ray and the edge diffracted ray. The modal ray congruences of the WG mode incident on the aperture of the concave boundary are converted into the geometrical rays in the free space. The diffraction coefficient for the modal ray congruence striking the edge of the cylindrical boundary is represented by using the Fresnel integral, which agrees with the result obtained by R.G.Kouyoumjian and P.H.Pathak [Proc. of the IEEE, 62, 11, pp.1448-1461, 1974].

Numerical comparisons with the reference solution calculated from the Fresnel-Kirchhoff diffraction formula reveal the validity and the utility of the uniform asymptotic representation valid in the transition regions near the reflection and the shadow boundaries. Of special interest is the physical interpretation of the beam field representation that comprises the mixture of geometrical ray and diffracted ray.

MONDAY PM URSI-B SESSION M-U11

Room: Savery 211

PROPAGATION AND ANTENNAS

Chairs: S.A. Saoudy, Memorial University of Newfoundland; R. G. Olsen, Washington State University

- 3:20 Scattering from Buried Dielectric Objects in the Presence of an Air-Earth Interface: A Method of Moments Technique 116  
*\*G.A. Ellis, I.C. Peden, Univ. of Washington*
- 3:40 Evaluation of Sky-Wave Propagation Characteristics at Cape Race, Newfoundland 117  
*F. Davis, S.A. Saoudy, Memorial Univ. of Newfoundland*
- 4:00 The Radiation Characteristics of an HF Log-Periodic Monopole Array Antenna for Ground Wave Propagation 118  
*\*S.A. Saoudy, Memorial Univ. of Newfoundland*
- 4:20 Numerical Procedure for Antenna Analysis and Synthesis 119  
*\*A.M.E.S. Casimiro, J.A.R. Azevedo, A.J.V. Grilo, Universidade da Madeira*
- 4:40 Linear Antenna Statistical Synthesis by the Given Radiation Pattern 120  
*\*Y.S. Shifrin, V.V. Dolzhikov, Kharkov State Technical Univ. of Radio Electronics*
- 5:00 Non-Linear Effects in Active Phased Arrays 121  
*\*Y.S. Shifrin, A.I. Luchaninov, A.S. Posokhov, Kharkov State Technical Univ. of Radio Electronics*
- 5:20 Side Lobe Limiting Level of Antenna Arrays with Sources Fluctuations 122  
*\*Y.S. Shifrin, Kharkov State Technical Univ. of Radio Electronics*

SCATTERING FROM BURIED DIELECTRIC OBJECTS IN THE PRESENCE OF AN AIR-EARTH INTERFACE: A  
METHOD OF MOMENTS TECHNIQUE

Grant A. Ellis and Irene C. Peden  
Department of Electrical Engineering FT-10  
University of Washington  
Seattle, WA 98195  
(206) 543-2150 (tel)  
(206) 543-3842 (fax)

**Abstract**

Modeling of complex geological structures in the presence of an air-earth interface is the focus of this paper. It presents method-of-moments formulations in two-dimensions, utilizing cylindrical pulse basis functions and point matching, to compute the scattering from buried dielectric objects near the air-earth interface for both TE and TM incident fields. The objects themselves may take on any geometrical cross-sectional form and may have any complex permittivity values. A Sommerfeld Green function is used to represent the effect of the air-earth interface. Both the co- and cross-polarized scattered electric fields are calculated for the TE case. Several examples are given for a tunnel-like target at depths that vary from one wavelength below the air-earth interface to depths at which this interface becomes insignificant. A cross-borehole configuration of target, source and receiver is assumed. When the transmitted signal is horizontally polarized, it is found that the cross-polarized (vertical) fields demonstrate less sensitivity to the presence of the interface than do the co-polarized (horizontal) fields. Experimental results utilizing a 1/40th laboratory scale model have been measured and are found to be in good agreement. Results for the case of TM incidence agree well with those of a related problem to be found in the literature.

The technique enables the user to investigate electromagnetic scattering from a variety of complex buried objects whose dimensions are typically in or below the resonance region.

**EVALUATION OF SKY-WAVE PROPAGATION  
CHARACTERISTICS AT CAPE RACE, NEWFOUNDLAND**

F. Davis and S.A. Saoudy

Centre for Cold Ocean Resources Engineering  
Memorial University of Newfoundland  
St. John's, Newfoundland, Canada A1B 3X5

The Northern Radar prototype Over-The-Horizon (OTH) Ground Wave Radar (GWR) which was built at Cape Race, Newfoundland, operates in the HF frequency band. Its maximum potential range for detecting ships and low flying objects is 450 km from the coast. The GWR employs the ground wave mode in its operation. The radar's scattered signals from the ionosphere act as an internal interference source leading to the reduction of both the reception quality and the radar's maximum detection range. The external interference source is caused by outside sources, such as broadcasting stations.

In this work, the properties of the ionosphere at the GWR site are examined using the computer package ICEPAC (F.G. Stewart, "The Ionospheric Communications Enhanced Profile Analysis and Circuit Prediction Program (ICEPAC)", NTIA, U.S. Dept. of Comm., Boulder, Colorado 80303, 1992). The first step in using the ICEPAC modelling scheme is to verify its validity for Canadian regions. This was successfully done by correlating ICEPAC's predicted ionograms with actual ionograms received from a Digital Ionosonde System for two regions; Manitoba and Ontario.

From analysis of the external interference, it was found that external interference is predominant during the nighttime, due to overseas broadcasting stations. It was found that with the use of a vertical antenna at Cape Race and a horizontal transmitting antenna in London, England, minimum interference was observed. For internal interference, vertically polarized antennas are ideal for ground wave transmission due to their antenna gain pattern. However, internal interference signals, reflected off the ionosphere are still received by the radar.

Different antenna radiation patterns have been tried in order to reduce the amount of internal interference in the radar system. This was done by using simulated antenna patterns in conjunction with ICEPAC. The simulated antenna patterns were made by lowering the gain level in the vertical and near vertical directions. This created a deep null towards the ionosphere which reduced the amount of self-generated sky-wave propagation off the ionosphere. It is found that in order to reduce the amount of internal interference significantly, it is necessary to design antennas with deep null in the vertical and near vertical directions.

**THE RADIATION CHARACTERISTICS OF AN HF  
LOG-PERIODIC MONOPOLE ARRAY ANTENNA  
FOR GROUND WAVE PROPAGATION**

S.A. Saoudy

Centre for Cold Ocean Resources Engineering  
Memorial University of Newfoundland  
St. John's, Newfoundland, Canada A1B 3X5

Vertical log-periodic dipole array (VLPDA) antennas can be used as transmitting antennas in a Ground Wave Radar (GWR) system. Specially designed VLPDA can offer the following desirable radiation characteristics: a wide operational bandwidth; a high power rating and directivity; a wide azimuth beamwidth; a high front to back ratio; and a deep null in the vertical direction. GWR systems employing VLPDA have the potential to detect over-the-horizon surface based and low flying objects out to 450 Km.

GWR operate in the lower HF frequency band since the lower the frequency becomes, the higher the maximum detection range will be. The height of the VLPDA which is at least  $\lambda_{max}/2$ , results in high costs in construction (tower and guy wires) and maintenance (winds, snow and ice accumulation). At 3 MHz, the height of the tower supporting the VLPDA must be at least 150 metres.

Replacing the VLPDA by a Vertical Log Periodic Monopole Array (VLPMA) would reduce the necessary height of the tower by one half. This would reduce the tower construction and maintenance costs considerably. A number of VLPMA configurations over perfect ground were reported (D.G.Berry and F.R.Ore, IRE Int. Conv. Rec., Part 1, pp. 76-85, 1961, and C.E.Smith, Log Periodic Antenna Design Handbook, Smith Elec. Inc., Ohio, 1966). In present work, these VLPMA configurations are quantitatively investigated for their suitability to GWR applications over perfect and imperfect ground.

The radiation characteristics are calculated using the Numerical Electromagnetics Code (NEC-2) which employs the moment method. Changes in the VLPMA characteristics due to the following will be reported: 1) the relative location of the tower with respect to the elements, 2) the height above ground of the entire VLPMA, and 3) the relative location of the lower tip heights of the elements over ground.

## NUMERICAL PROCEDURE FOR ANTENNA ANALYSIS AND SYNTHESIS

\*António Manuel E.S. Casimiro  
Joaquim A.R. Azevedo  
Alberto J.V. Grilo  
Grupo de Comunicações  
Universidade da Madeira  
Colégio dos Jesuítas  
9000 FUNCHAL  
PORTUGAL

### Abstract:

The possibility, facilities and problems of using the FFT (Fast Fourier Transform) to make the synthesis and analysis procedures between the radiating source distribution and the far field radiation pattern are presented.

In previous papers it was shown that, usually, it is possible to describe the radiation pattern of an antenna, as an window in the inverse Spatial Fourier Transform of source distribution in the antenna, if the variables involved are conveniently described.

All the procedure is based on the Theorem of the Small Complex Translation meaning that if we can represent all the radiating source distribution by complex translations of a reference source placed in the origin, the far field pattern and the radiating source distribution are related by the Fourier Transform.

For some cases, although the radiating source distribution or the desired far field pattern are in the conditions to use the Fourier Transform, the geometry of the distribution makes impossible or difficult to use analytical procedures to deal with the analysis or synthesis of radiation patterns.

The use of the FFT can overcome this difficulty, using a computational approach to find the far field pattern of a given source distribution or to find the approximate distribution that generates a desired far field pattern inside the useful window.

The sampling rate either in the spatial domain or in the radiation pattern domain, needs to be carefully chosen to avoid errors produced by the limitation to an window in the radiation pattern domain.

**LINEAR ANTENNA STATISTICAL SYNTHESIS BY THE GIVEN  
RADIATION PATTERN**

Y.S. Shifrin\*, V.V. Dolzhiikov  
Kharkov State Technical University of Radioelectronics

The complex radiation pattern (RP) of the linear continuous antenna in the presence of the sources fluctuations can be written as

$$f(u) = \frac{1}{2\pi} \int_{-a}^a A(x) \exp\{B(x) + j[\varphi(x) + ux]\} dx \quad (1)$$

where  $u = \pi L \sin \theta / \lambda$ ;  $L$  - the length of antenna;  $\theta$  - the angle from the normal to the antenna axis;  $\lambda$  - the wavelength;  $A(x)$  - the amplitude-phase distribution (APD) without fluctuations;  $x = 2z/L$ ;  $z$  - the coordinate along the antenna;  $B(x)$ ,  $\varphi(x)$  - random functions presenting the sources amplitude level and phases fluctuations.

The statistical synthesis problem consists in finding  $A(x)$  minimizing the mean square deviation of the realized RP  $f(u)$  from the given complex RP  $F(u)$ , with allowance for the specified sources fluctuations

$$ME^2 = M \int_{-a}^a |f(u) - F(u)|^2 du \quad (2)$$

where  $M$  is a mean value sign,  $a = \pi L / \lambda$ .

The given RP and the sought APD are presented as series by eigenfunctions of finite Fourier transform  $\psi_n$

$$F(u) = \sum_{n=0}^{\infty} d_n \psi_n, \quad A(x) = \sum_{n=0}^{\infty} b_n \psi_n \quad (3)$$

Coefficients  $d_n$  are defined by  $F(u)$  and  $b_n$  are the sought values. The terms in the series for  $A(x)$  can be regarded as the APD space harmonics giving its own partial RP. With  $n \leq 2a/\pi$  the partial RP maximum is in the visible region, with  $n > 2a/\pi$  - in the invisible region. Respectively, we have active and reactive harmonics. Substituting the expression for  $A(x)$  into (2) and equating  $ME^2$  variation to zero, it is possible to find coefficients  $b_n$  (i.e. the optimal APD) and  $(ME^2)_{\min}$ .

These values are expressed through the given RP and numerical parameters of the sources fluctuations.

As the computations show the accounting of sources fluctuations always present in the real antennas (even with their rather small values) results in a sharp limitation of reactive (high-oscillating) harmonics contribution into the optimal APD and hence in suppression of the superdirectivity effects possible in the RP deterministic synthesis.

## Non-Linear Effects in Active Phased Arrays

Y.S. Shifrin,\* A.I. Luchaninov, A.S. Posokhov  
Kharkov State Technical University of Radio Electronics

### Abstract

One of the characteristic features of modern antenna technique development is a wide introduction of active phased arrays (APA). As a rule active elements in such arrays must operate in the linear regime. But often the APA operate in such a condition that the active elements' nonlinearity begins to manifest itself. This results in emergence of some parasitic effects decreasing appreciably the APA characteristics and hampering the EMC problems solution.

This report presents the general method of nonlinear effect analysis in the APA developed by the authors. Its first stage consists in creation of a generalized mathematical model suitable for a wide class of antennas with nonlinear elements. The use of this model leads to the state equation system describing the APA stationary regime. This system solution is the second, the most difficult, state of the treated methods. A very effective algorithm for the state equation solution is proposed. It is based on the decomposition idea. Its essence consists in dividing the nonlinear elements on separate groups depending on the degree of their coupling with each other. Its separate groups depending on the degree of their coupling with each other. This allows to realize the multilevels iteration procedure for fast solution of the state equation system. The indicated algorithm also takes into account the possible types of symmetry in the array and in the exciting field. The last stage of the treated method consists in defining the output vector and finding the APA external parameters on this basis.

The proposed general method has been applied to nonlinear effect analysis of some receiving APA.

The main attention is given to such nonlinear effects as spurious radiation and side receiving channels if a strong noise is present along with a useful signal. It is shown that in this case the radiation pattern (RP) of the receiving APA on the main frequency depended both on the noise parameters (its level and arrival direction) and on the arrays characteristics on the noise frequency. In some cases the presence of power noise can completely destroy the RP of the APA on the main frequency.

It is noted that nonlinear effects in the APA, their extent and their manifestation peculiarity depended significantly on the array construction, mutual influence of the radiators, the parameters of linear and nonlinear elements, their position, the antenna operating conditions etc. The corresponding plots are given.

**SIDE LOBE LIMITING LEVEL OF ANTENNA  
ARRAYS WITH SOURCES FLUCTUATIONS**

Y.S. Shifrin  
Kharkov State Technical University of Radioelectronics

The sources fluctuations, always present in the real antennas, limit the capabilities to reduce their side-lobe level (SLL). Three approaches to estimating the minimal attainable (limiting) SLL are possible. The first is based on the mean radiation pattern (RP) analysis. The second, a more profound approach, rests on the study of the field amplitude fluctuations in the side lobe (SL) region. The third, the most correct one, is connected with finding the probability whether all RP in the given sector does not leave a definite level.

The aim of the given work is to compare the limiting SLL obtained in three different approaches.

Linear Dolph-Chebyshev array with small phase errors independent in separate radiators is treated. For every of three cases the dependence of the real SLL (denoted as  $V$ ) on their nominal (without fluctuations) Dolph-Chebyshev  $F$  level is defined. In the first case the mean SLL is taken as  $V$ , in two other cases the value  $V$  is such a level, that the probability of its non-exceeding by the field amplitude in the direction of one of the SL (the second case) or by all SL in the given sector (the third case) equals to the given value  $P$ . It is shown that in all three cases the real level decreases appreciably slower than the nominal one, reaching with a some low level  $F$  the minimum  $V_{lim}$  different for three cases. The values  $V_{lim}$  are close to the values  $V_{bin}$  corresponding to the binomial amplitude distribution, with which the nominal SL are absent. This allows to obtain simple estimations for  $V_{lim}$ :

$$V_{lim1} = \sigma S^{1/2}; \quad V_{lim2} = \eta V_{lim1}; \quad V_{lim3} = \mu V_{lim1}. \quad (1)$$

Here  $\sigma$  is a mean-square value of phase fluctuations;

$S = \sum_{n=1}^N A_n^2 / \left[ \sum_{n=1}^N A_n \right]^2$ ;  $\eta = 1,52 \sqrt{\lg[(1-P)^{-1}]}$ ;  $\mu$  - root of equation  $\Phi(\mu) = P^{1/2m}$ ,  $N$  - number of radiators;  $A_n$  - binomial coefficients;  $\Phi$  - probability integral;  $m$  - a number of SL in the half of given angle symmetrical sector.

For 8-element array with  $\sigma = 0,25$  ( $16^\circ$ ),  $P = 0,99$  and  $m = 3$  from (1) we have  $V_{lim1} = -18,8$  dB;  $V_{lim2} = -12,2$  dB;  $V_{lim3} = -11,9$  dB. With the increase of  $N$  the values  $V_{lim}$  decrease, but the gap between the correct estimation of the limiting SLL and the mean SLL insufficiently increases. Thus with the change of  $N$  from 8 to 40 this gap increases (with  $P = 0,99$ ;  $m = (N-2)/2$ ) from 6,9 to 8,6 dB.

**MONDAY PM URSI-D SESSION M-U12**

Room: HUB 200

**CIRCUITS AND DEVICES FOR MICRO AND MILLIMETER WAVES**

Chair: A.R. Mickelson, University of Colorado at Boulder

- 1:20 Toward Unified CAD for Active Microwave and Millimeter Wave Circuits and Radiating Systems 124  
*B. Houshmand, B. Jalali, T. Itoh, Univ. of California at Los Angeles*
- 1:40 A Review of High-Frequency Techniques for the Modeling of Passive Circuits 125  
*\*L.P.B. Katehi, Univ. of Michigan*
- 2:00 FDTD Supercomputing Computational EM for Dual Use Electronics and Optical Technology 126  
*\*M. Picket-May, Univ. of Colorado at Boulder*
- 2:20 AIM-Spice-A Circuit Simulator with New Device Models Including TFT and Deep Submicron FET Models 127  
*T. Ytterdal, T.A. Fjeldly, Univ. of Trondheim; M. Shur, Univ. of Virginia*

**Toward Unified CAD for Active Microwave and Millimeter Wave Circuits and Radiating Systems**

B. Houshmand, B. Jalali and T. Itoh  
Electrical Engineering Department  
UCLA  
Los Angeles, CA 90024-1594

In the past several decades, a considerable amount of effort has been expended in the area of analysis and characterizations for microwave integrated circuits, antennas and solid state devices with a view to developing CAD programs. In most cases, the effort has been spent without interlinking the approaches for different entities. For instance, the solid state device has been either analyzed numerically to find the I-V curves, extracts the RF characteristics, etc. without interacting with the ambient circuits. Numerous analysis and characterization computer programs have been developed for antennas including the integrated antennas. In the area of MMIC, CAD programs has been refined substantially from the quasi-static analysis and curve fit formula toward the EM simulator. However, they are typically limited to passive structures. In order to design active circuits, a number of nonlinear modeling and analysis programs have been developed such as the harmonic balance and Volterra series which are found to be useful for design based on the microwave network and equivalent circuit.

Recent trend in the complex microwave circuits and component design requires further advances in characterization and modeling techniques. For instance, active antennas need to be analyzed coherently for the antenna, active devices and passive circuits which cannot be separated. Their environment and packaging effect also need to be included. Further, many advanced circuits have very tight intra-chip coupling and there may exist multi-mode conditions. As such, classical network-based approach may not be sufficient. It is desirable to develop a unified CAD program which addresses characterizations of the entire microwave circuit. In this manner, it is possible, e.g., to find out what material parameters in the active device need to be modified in order to change the scan rate of an active antenna array by five degrees. Another example which requires this type of analysis is quasi-optical amplifiers and oscillators. These are large electrical circuits and can be operated in a multi-mode condition.

This talk will review some of the traditional approaches for circuit design for both passive and active circuits. Several key issues will be addressed which need to be explored. They include better device characterizations including the local heating effects, visualizations of the packaging and interconnect effect, multi-mode situations in an electrically large circuits, device-circuit interactions.

Some recent attempts toward alleviating these problems are presented. Examples include the full wave analysis of the tightly coupled active antennas under the large signal operating condition. Although the present status is far from the ideal CAD for the next generation, the approaches reported here are believed to pave a way toward such a goal, particularly with the advent of advanced computational techniques.

\* This work was supported by ARO and Joint Services Electronics Program.

# **A REVIEW OF HIGH-FREQUENCY TECHNIQUES FOR THE MODELING OF PASSIVE CIRCUITS**

by

Linda P.B. Katehi  
The University of Michigan

The electrical simulation of circuits operation in the microwave, millimeter and sub-millimeter wave region is increasingly becoming a step of critical importance to design procedures. The high-frequency modeling of circuits started in the 70's and grew considerably in the 80's to a research area of substantial interest. During this twenty-year period a number of full-wave formulations were developed and explored intensively to provide a variety of approaches. All of these techniques resulted in numerical treatments which were based on a direct or indirect solution of the Maxwell's equations and involved an extensive discretization of part or of the whole volume of interest. These techniques are divided into three major categories: integral equations or integral transform techniques, mode matching techniques and finite element of finite difference techniques.

Each one of these groups of techniques is characterized by its own sensitivities, inherent numerical errors and ability to selectively address specific physical phenomena. Furthermore the discretization procedures followed by each group resulted in a linear systems of equations with very different stability criteria, numerical error functions and error-control capabilities. In addition, the formulations themselves led the corresponding techniques to specific groups of problems thus making other classes of geometries impossible to handle.

This presentation will provide a critical review of frequency-domain formulations that belong to the three previously mentioned categories and will place emphasis on these techniques which have been designed specifically of the passive circuit modeling. Advantages and disadvantages of these techniques in terms of accuracy, error estimation and control stability, computer efficiency and memory requirements will be extensively discussed. Furthermore, this presentation will address present needs in circuit modeling and the requirements these needs impose on the modeling methodologies. Hybrid combinations of the above techniques which have been developed in response to these needs will be presented and their applications to specific problems will be discussed.

While frequency domain techniques have provided primarily the means of circuit modeling, state of the art applications require explicit use of the time domain. Techniques have also shown capability in effectively characterizing complex monolithic circuit geometrics. The recent success of time domain techniques inevitably raise the issue of time domain vs. frequency domain. This presentation will conclude with an attempt to critically look at the potential offered by the two domains and will discuss their capability to complement each other, thus providing the most complete information to circuit designer.

## FDTD Supercomputing Computational EM for Dual Use Electronics and Optical Technology

Melinda Picket-May  
University of Colorado at Boulder  
Boulder, CO 80309-0425

This paper summarizes advances in supercomputing solutions of Maxwell's equations that are permitting significant contributions to dual-use electronics and optical technology. Key application examples include complex nanosecond digital electronic circuits, microwave circuits and antennas, and femtosecond nonlinear optical devices. Note that dual use is inherent in the FDTD modeling process itself as well as the applications of this modeling process. This is because FDTD is so robust that merely "turning on" a few auxiliary differential equations permits the article being modeled to be switched from a jet fighter to a digital electronic circuit to a photonic device. The augmentation of FDTD in this manner gives it enormous capability in modeling nonlinear electronic and photonic phenomena that are central to ultrahigh-speed device behavior.

The following current capabilities in FDTD electromagnetic wave modeling will be considered:

1. Jean-Pierre Berenger's major advance in ABC / RBC theory, the "perfect matched layer" split-field nonphysical absorber (*Journal of Computational Physics*, in press). For both 2-D and 3-D FDTD grids, these absorbers have been demonstrated to have less than 1/3000 the reflectivity of any previous ABCs or RBCs used in the FDTD community (Mur, Liao, super absorption, etc.). This increases in the maximum possible dynamic range of FDTD modeling by more than 50 dB to an overall level of more than 90 dB. We are implementing this technique to generate ultra wideband terminations for striplines and waveguides in the FDTD mesh.

2. Incorporation of the lumped-circuit behavior of linear and nonlinear active devices into 3-D FDTD. We are developing a generalized FDTD software called "FDTD-SPICE" that provides a unified, user-friendly capability for dynamic, full-wave EM modeling of passive interconnects along with the physics of the nonlinear characteristics of the connected transistors and logic devices. FDTD-SPICE implements Local software links between the FDTD Maxwell's equations code and SPICE kernels. We believe that FDTD-SPICE is the very first simulation tool for electrical engineers to obtain dynamic (time-domain) simulations of analog and digital nonlinear circuits directly from Maxwell's equations in three dimensions. We expect a wide range of digital and analog applications well into microwave frequencies for this new simulation software, including modeling the logic functions of complex GHz-regime digital assemblies mounted in 3-D multilayer circuit board and MCM geometries, including all electromagnetic "artifacts" of the circuit embedding.

3. Incorporation of active nonlinear devices to excite phased array antennas. We are applying FDTD-SPICE specifically to model the excitation of phased array antennas by microwave transistor devices. Two examples will be presented: 1) Monopole phased array used to develop optimal hyperthermia power deposition in near surface tumors 2) An eight element array of crossed-pair Vivaldi quads working in the frequency range 6-18 GHz. These studies permit direct computation of the impulsive excitation of these antennas self consistently taking into account the element to element interactions with the nonlinear characteristics of the exciting transistors.

4. Incorporation of nonlinear optical properties of materials at femtosecond time scales. We report our latest results in modeling, fabricating, and testing millimeter-scale, femtosecond all-optical logic gates constructed of gallium aluminum arsenide. Here, the first such devices to be designed by applying FDTD Maxwell's equations solutions of nonlinear optical pulse interactions were built at the Cornell National Sub-Micron Facility. These devices are currently being tested for their effectiveness in switching femtosecond optical pulses, and the results are being compared to the FDTD simulations.

We believe that the theory and application of FDTD modeling of high speed microwave, millimeter wave, and optical devices is rapidly advancing. CAD/CAM tools are now emerging in this area for GHz regime analog and digital circuits. It is only a matter of time until similar tools are developed and used across the EM spectrum, all the way to optical frequencies.

The author would like to acknowledge the contributions of Mike Jones and Vince Thomas at Los Alamos National Lab, Kevin Thomas and Roger Grävrok at Cray Research, and Allen Taflove, Rose Joseph, and Chris Reuter at Northwestern University.

## AIM-Spice - A Circuit Simulator with New Device Models Including TFT and Deep Submicron FET Models.

T. Ytterdal<sup>+</sup>, T. A. Fjeldly<sup>+</sup>#, and M. Shur<sup>#</sup>,

<sup>+</sup>Department of Physical Electronics, Norwegian Institute of Technology, Trondheim, University of Trondheim, N-7034 Trondheim, Norway  
<sup>#</sup>Department of Electrical Engineering, University of Virginia, Charlottesville, VA 22903-2442, USA

### Abstract

The device feature size for both Si and GaAs based systems has been scaled down into the deep submicron range, and we can expect that a 0.25  $\mu\text{m}$  feature size will become typical only a few years from now and that a 0.1  $\mu\text{m}$  feature size will be used in VLSI by the start of the new century. This is a great challenge for device and circuit engineers, and new device models have become vital for accurate prediction of circuit and system performance. Unfortunately, conventional simulators lack good device models for thin-film transistors (TFTs) and deep submicron devices. The most widely used MOSFET SPICE models in industry today are level 2, 3 and the BSIM models (BSIM1 = level 4 and BSIM2 = level 5) from Berkeley. However, all these models have drawbacks. In particular, level 3 and BSIM have convergence problems owing to discontinuities. Furthermore, BSIM uses a large number of parameters - nearly a hundred for BSIM2 - rendering the model impractical for many applications. On the other hand, level 2 and 3 are often too simple for accurate simulations. Consequently, we developed our own circuit simulator, called AIM-Spice<sup>1, 2</sup> and included new advanced device models for a number of devices such as MOSFETs, MESFETs, HFETs, amorphous silicon thin film transistors, and polysilicon thin film transistors. The FET models are based on unified charge control models which allow us to obtain an accurate description of the transition between the above threshold and below threshold regimes, and to simulate deep submicron devices. Our device models have been applied to a number of different devices and technologies. In this paper, we present a number of simulation examples involving short channel devices, GaAs circuits, and TFT applications. We also show results from a comparison between two of our MOSFET models and existing models in terms of computing speed and accuracy. We conclude that our models give increased accuracy and computing speed, and in particular, that our models have excellent convergence properties owing to the unified charge control models.

### References:

- 1 K. Lee, M. Shur, T. A. Fjeldly, and T. Ytterdal, Semiconductor Device Modeling for VLSI, p. 309, Prentice Hall, New Jersey (1993)
- 2 A limited version of AIM-Spice can be downloaded from [sdl.sun4.ee.virginia.edu](http://sdl.sun4.ee.virginia.edu) using *ftp*.



**MONDAY PM URSI-B SESSION M-U13**

Room: Savery 243

**TIME DOMAIN ANALYSIS I**

Chairs: L. Carin, Polytechnic University; A.K. Bhattacharyya, New Mexico State University

- 1:20 Improving the Resolution of the Wave-Oriented STFT Processing of Time-Domain Dispersion 130  
*S.U. Pillai, L. Carin, D. Kralj, W.C. Lee, L.B. Felsen, Polytechnic Univ.*
- 1:40 K-Space Formulation for Electromagnetic Scattering Problems in Time Domain 131  
*\*Q.-H. Liu, Schlumberger-Doll Research*
- 2:00 Transient Scattering by Conducting and Resistive Bodies of Revolution 132  
*\*R.D. Graglia, Politecnico di Torino; P.L.E. Uslenghi, Univ. of Illinois at Chicago; U.F. D'Elia, R. Vitiello, Alenia*
- 2:20 Time-Domain Electromagnetic Scattering from Complex Objects with Arbitrary Surface Impedance: Solution by TDUTD 133  
*\*A. K. Bhattacharyya, New Mexico State Univ.*
- 2:40 Comparative Study of Spectral Estimation Techniques for Time-Domain Numerical Methods 134  
*\*C. Eswarappa, W. J. R. Hoefer, Univ. of Victoria*

## **Improving the Resolution of the Wave-Oriented STFT Processing of Time-Domain Dispersion**

S.U. Pillai, L. Carin, D. Kralj, W.C. Lee, and L.B. Felsen

Department of Electrical Engineering  
Polytechnic University  
Six MetroTech Center  
Brooklyn, NY 11201

We have previously investigated time domain (TD) wave phenomenology from pulsed plane-wave scattering data generated by structural dispersion associated with truncated periodic and quasi-periodic strip gratings. We have shown that the transient scattered fields from such gratings can be represented in terms of TD Floquet modes (FM), each with characteristic time-dependent frequencies. We have sought to develop wave-oriented processing strategies which extract these wave objects from TD scattering data. In those studies time-frequency  $(t, \omega)$  phase space distributions have been developed by the Gaussian windowed Short Time Fourier Transform (STFT) which sorts out the wave physics -- truncated TD FM -- with minimal contamination by anomalies but not necessarily with optimal resolution. For improved resolution in selected  $(t, \omega)$  windows, we subject the TD data here to various multi-resolution and super-resolution algorithms. The multi-resolution algorithms include time and frequency domain wavelet transforms, and the super-resolution algorithms include windowed ARMA and MUSIC transforms. It is found that the super-resolution schemes home in exceptionally well on the  $(t, \omega)$  dispersion curves for the various truncated TDFM, whereas the other algorithms yield bands of various widths surrounding the curves. The various algorithms are also tested when white Gaussian noise is added to the data, and it is shown that the super-resolution algorithms remain accurate with signal-to-noise ratios up to -3dB.

## K-SPACE FORMULATION FOR ELECTROMAGNETIC SCATTERING PROBLEMS IN TIME DOMAIN

QING-HUO LIU  
SCHLUMBERGER-DOLL RESEARCH  
OLD QUARRY ROAD  
RIDGEFIELD, CT 06877

The k-space formulation in frequency domain originated by Bojarski has found many applications in the solution of electromagnetic scattering problems. In contrast, very little attention has been paid to the k-space method in time-domain electromagnetic scattering problems, partly because of the complexities involved in the formulation.

In this work we propose a formulation for the time-domain k-space method for electromagnetic scattering problems. In frequency domain, the integral equation for the electric field is

$$\mathbf{E}_s(\mathbf{r}, \omega) = \int_V d\mathbf{r}' \overline{\mathbf{G}}(\mathbf{r}, \mathbf{r}') \cdot [k^2(\mathbf{r}') - k_0^2] \mathbf{E}(\mathbf{r}') - \int_V d\mathbf{r}' \overline{\mathbf{G}}(\mathbf{r}, \mathbf{r}') \cdot [\mu(\mathbf{r}') \nabla' \mu^{-1}(\mathbf{r}') \times \nabla' \times \mathbf{E}(\mathbf{r}'),$$

where  $\overline{\mathbf{G}}$  is the dyadic Green's function in  $\mathbf{r}$ - $\omega$  space for the homogeneous background medium ( $\epsilon_0, \mu_0$ ), and  $\mathbf{E}_s$  is the scattered field. First, we find a closed-form solution for the dyadic Green's function in  $\mathbf{k}$ - $t$  space. Then, the integral equation in  $\mathbf{k}$ - $t$  space is discretized. We can show that the time-domain k-space algorithm for non-magnetic media is given by:

$$\left\{ \begin{array}{l} \mathbf{E}_a(\mathbf{m}, n) = \mathcal{F}_m^{-1} \tilde{\mathbf{E}}_a(\mathbf{m}, n) \\ \mathbf{J}_e(\mathbf{m}, n) = (1 - \frac{\epsilon_0}{\epsilon}) [\mathbf{E}_a(\mathbf{m}, n) + \mathbf{E}_i(\mathbf{m}, n)], \quad \tilde{\mathbf{J}}_e(\mathbf{m}, n) = \mathcal{F}_m \mathbf{J}_e(\mathbf{m}, n) \\ \tilde{\mathbf{E}}_a(\mathbf{m}, n+1) = -\tilde{\mathbf{E}}_a(\mathbf{m}, n-1) + 2\tilde{\mathbf{D}} \cdot \tilde{\mathbf{J}}_e(\mathbf{m}, n) + \tilde{P}(\mathbf{m}) [\tilde{\mathbf{E}}_a(\mathbf{m}, n) - \tilde{\mathbf{D}} \cdot \tilde{\mathbf{J}}_e(\mathbf{m}, n)] \end{array} \right.$$

where the auxiliary field  $\mathbf{E}_a = \mathbf{E} + \mathbf{J}_e - \mathbf{E}_i$ , and  $\tilde{P}(\mathbf{m})$  is the propagator in  $\mathbf{k}$ - $t$  space. The indices  $\mathbf{m}$  and  $n$  are for spatial and temporal discretizations, respectively. The discrete Fourier transform is obtained by FFT.

The time-domain k-space algorithm presented in the above is a simple time-stepping algorithm, alternating between  $\mathbf{r}$ - $t$  space and  $\mathbf{k}$ - $t$  space. The advantages of this algorithm versus the explicit finite-difference method is that the dispersion error caused by the discretization is evenly distributed in space. For a problem with  $N$  spatial points, the number of complex multiplications in each time step is of order  $N \log_2 N$ , and the storage is of order  $N$ . Numerical examples will be shown to illustrate the use of the algorithm.

## TRANSIENT SCATTERING BY CONDUCTING AND RESISTIVE BODIES OF REVOLUTION

Robert D. Graglia\*

Dipartimento di Elettronica, Politecnico di Torino, Italy

Piergiorgio L.E. Uslenghi

Department of Electrical Engineering and Computer Science  
University of Illinois at Chicago, Box 4348, Chicago, IL 60680

Ugo F. D'Elia and Roberto Vitiello

Alenia, Rome and Fusaro, Italy

The scattering of a plane Gaussian pulse axially incident on a conducting body of revolution (BOR) is considered. The problem is formulated in terms of an integral equation for the unknown surface current density. Both the surface current and the bistatic scattered field at a large finite distance from the BOR are evaluated numerically.

Special attention is devoted to the self-cell contribution and to the truncation of the front and rear of the pulse. Although the treatment is valid for an arbitrary BOR, several numerical examples are given for convex and concave bodies whose profiles in a semiplane through the symmetry axis consist of combinations of straight segments and arcs of circles, i.e. for BORs consisting of combinations of cones, cylinders and spheres. Additionally, cases are considered where resistive sheets are added to the solid BOR. This study represents an extension to three dimensions of the previous two-dimensional work by Damaskos et al. (IEEE Trans. AP, **33**, 21-25, 1985), and an extension to resistive surfaces of the work done for perfectly conducting surfaces by Bennett and Mieras (Radio Sci., **16**, 1231-1239, 1981) and by Rao et al. (North-American Radio Sci. Meet., Quebec, June 1980), among others.

The bistatic RCS obtained via FFT of the time-domain far field is compared with frequency-domain results obtained with other computer codes. Conclusions are drawn on the efficiency of our time-domain code vis-a-vis previously developed frequency-domain codes.

**TIME-DOMAIN ELECTROMAGNETIC SCATTERING FROM  
COMPLEX OBJECTS WITH ARBITRARY SURFACE IMPEDANCE:  
SOLUTION BY TDUTD**

Asoke K. Bhattacharyya

Tel: (505) 522-9468

Research Center

Physical Science Laboratory

New Mexico State University

Las Cruces, NM 88003-0002

**Abstract:** The recently developed *time - domain uniform theory of diffraction* for arbitrary surface impedance has been applied to the problem of scattering from stationary complex objects such as a cone-cylinder and an aircraft model. The total bistatic TD field at any point, as in a frequency domain study, consists of the incident field, the reflected field and the contributions from scattered and creeping wave components all in TD. The second order components are the scattered-scattered, reflected-scattered and reflected-reflected and creeping-reflected et cetera. The time-domain reflected field from any surface with arbitrary principal radii of curvature has been used. The early and late time responses have been determined. The effect of imperfect conductivity of the object surface and thin RAM coating has been discussed. TD scattering from the objects due to different types of the incident wave such as a rectangular FD waveform transformed to TD and a TD *Gaussian beam* have been studied. The effect on TD scattering of different parameters, such as, dimensions of the objects, surface impedance, incident bandwidth, aspect angle and polarization.

## COMPARATIVE STUDY OF SPECTRAL ESTIMATION TECHNIQUES FOR TIME-DOMAIN NUMERICAL METHODS

Channabasappa Eswarappa\* and Wolfgang J. R. Hoefler

NSERC/MPR Teltech Research Chair in RF Engineering, Department of  
Electrical and Computer Engineering, University of Victoria, Victoria,  
B.C. V8W 3P6, CANADA

### ABSTRACT

Time domain numerical methods such as the Transmission Line Matrix (TLM) and Finite Difference-Time Domain (FD-TD) methods are becoming increasingly popular for the analysis of complex microwave structures. The frequency domain results over a wide frequency spectrum can be obtained with just one time domain simulation. However, they require a very large computer CPU time and memory. The shorter the input excitation pulse, larger is the time required to reach the convergence. Also the narrow band structures such as filters require larger number of iterations to converge because of multiple reflections. Recently, the spectral estimation techniques have been applied in conjunction with the time domain numerical methods to reduce the CPU time. The idea is to predict the future time samples from the past time samples, or, to estimate the transfer functions from the knowledge of a lesser number of time samples. The widely used spectral estimation techniques are the harmonic decomposition methods such as Prony, Pisarenko, MUSIC and the methods based on autoregressive (AR), moving average (MA) and ARMA models. The performance of these techniques in various kinds of microwave structures will be presented in this paper. The comparative study in terms of the implementation of the algorithm, accuracy of the results, and the limitations, etc., will be presented.

MONDAY PM URSI-B SESSION M-U14

Room: HUB 309

SCATTERING II

Chairs: V.V. Liepa, The University of Michigan; T. Cwik, California Institute of Technology

1:20	Modification of the Integral Equations for Smooth Conducting Objects Using Fock Functions <i>*P. Soudais, ONERA; P.L.E. Uslenghi, Univ. of Illinois at Chicago</i>	136
1:40	Electromagnetic Scattering by Resonant Low-Frequency Structures <i>W. Wu, *A.W. Glisson, D. Kajfez, Univ. of Mississippi</i>	137
2:00	Applications of the Mutual Interaction Method to a Class of Two Scatterer or Radiator Systems <i>*H.D. Ngo, C.L. Rino, Vista Research Inc.</i>	138
2:20	Electromagnetic Scattering from a Jet Engine Inlet Including a Compressor <i>*H.T. Anastassiou, J.L. Volakis, Univ. of Michigan</i>	139
2:40	Time/Frequency Analysis of Two Sphere Scattering <i>*C. McCormack, V.V. Liepa, W. Williams, Univ. of Michigan; R. Haupt, United States Air Force Academy</i>	140
3:00	Break	
3:20	Simulaton Study of Bistatic Scattering from Parallel Strips <i>H.E. Raemer, Y. Lou, Northeastern Univ.</i>	141
3:40	Scattering by 2-D Strips Using an Asymptotic Hybrid (Method of Moments)-(Physical Optics) Technique <i>A. Sullivan, Wright Laboratory; L. Carin, Polytechnic Univ.</i>	142
4:00	Scattering of EM Waves by Discontinuity in Trilayered Media Separated by Planar Interface <i>J. Song, *J. Qian, D. Nyquist, K.M. Chen, E. Rothwell, Michigan State Univ.</i>	143
4:20	Application of the Coupled Finite Element-Combined Field Integral Equation Technique (FE/CFIE) to Electromagnetic Radiation Problems <i>*V. Jamnejad, T. Cwik, V. Zuffada, California Inst. of Technology</i>	144
4:40	Characterization of Low-Frequency Pylon-Target Electromagnetic Interactions <i>S. Castillo, R. Jedlicka, S. Omick, New Mexico State Univ.; W. Leeper, T. Conn, EG&amp;G Management Systems, Inc.</i>	145

**MODIFICATION OF THE INTEGRAL EQUATIONS FOR  
SMOOTH CONDUCTING OBJECTS USING FOCK FUNCTIONS**

Paul Soudais (+)\*  
ONERA, BP72, 93322 Chatillon Cedex, France

P.L.E. Uslenghi  
Department of Electrical Engineering and Computer Science  
University of Illinois at Chicago, Box 4348, Chicago, IL 60680

The numerical solution of the integral equations of scattering theory (EFIE, MFIE or CFIE) via the method of moments requires the inversion of dense matrices. This problem becomes computationally intractable for bodies whose dimensions are very large compared to the wavelength. In an effort to simplify the problem, we introduce a first estimate of the surface current density on a large, smooth conducting body, that is based on Fock's asymptotic theory of diffraction, as improved by others (Cullen, 1958; Goodrich, 1959; Logan and Yee, 1962; etc.). For a given incident plane wave, the total surface current density is written as the sum of the known Fock asymptotic current and of a perturbation current.

Since Fock's current tends to the geometrical optics current on the well-illuminated portion of the scatterer and to the creeping waves current on the shadowed portion of the scatterer, the perturbation current (i.e., the difference between the true current and Fock's asymptotic estimate), is expected to be negligibly small over most of the scatterer's surface, with the exception of those portions of surface located near caustics of the optical rays.

The above physical interpretation constitutes the basis of our numerical treatment. First, we rewrite the integral equations with the perturbation current as the unknown. Second, for any given primary wave, we develop ray tracing on the scatterer surface and identify the caustics. Third, we assume that the perturbation current is nonzero only near the caustics and use this assumption as a first guess in an iteration scheme to determine the perturbation current. A discussion of the numerical efficiency of this procedure compared to a straightforward MoM implementation is given. Extensions of this technique to bodies with surface singularities are proposed.

(+) Presently on leave as a Visiting Researcher at the University of Illinois, Chicago.

## ELECTROMAGNETIC SCATTERING BY RESONANT LOW-FREQUENCY STRUCTURES

W. Wu, Allen W. Glisson\*, and D. Kajfez  
Department of Electrical Engineering  
University of Mississippi  
University, MS 38677

The analysis of problems involving electromagnetic scattering by objects of arbitrary shape whose maximum extent is comparable to the excitation wavelength can be readily performed using the method of moments and a triangular patch model of the scatterer. The problems associated with the application of the Electric Field Integral Equation (EFIE) to model conducting scatterers in the low-frequency regime and some solutions to these problems are available (D. R. Wilton and A. W. Glisson, *Spring URSI Meeting Digest*, p. 24, June 1981, J. R. Mautz and R. F. Harrington, *IEEE Antennas Propagat.*, vol. AP-32, pp. 330-339, 1984). Recently, an adaptation of the triangular patch model has been presented for low-frequency scattering problems (J. S. Lim, S. M. Rao, and D. R. Wilton, *URSI Meeting Digest*, p. 322, June 1993). In this recent approach a combination of divergence-free and curl-free basis and testing functions is used. For some geometrical configurations, however, an alternate formulation, which utilizes the divergence-free basis and testing functions along with a subset of the original triangular patch basis and testing functions, appears to have some computational advantages (W. Wu, A. W. Glisson, and D. Kajfez, to be presented, 1994 ACES Symposium, March 1994).

In this work we apply the method of moments and the two recently developed low-frequency approaches to investigate the problem of electromagnetic scattering and/or radiation by conducting objects that are small in comparison to the wavelength, but are nevertheless resonant structures. The formulation permits modeling of complex structures involving multiple bodies and bodies with closed loops. Conductivity of the metallic structure is included in the formulation to model conductor losses. Comparisons are provided between the two methods for several resonant structures and for some specific geometries in the very low frequency range where approximate models are reasonably accurate.

# Applications of the Mutual Interaction Method to a Class of Two Scatterer or Radiator Systems

Hoc D. Ngo\* and Charles L. Rino  
Vista Research, Inc.  
100 View Street, P.O. Box 998, Mountain View, CA 94042

The mutual interaction among many objects separable by parallel planes can be characterized exactly by a system of difference equations whose unknowns are the total fields that propagate away from these planes. These equations make use of the known scattering characteristics of each scatterer, which is represented by a scattering function. This function expresses the scattered wave field as a function of the incident and scattered wave vectors for a unit-amplitude incident plane wave scattering from the object in isolation:

$$\hat{\mathbf{E}}_{sc}(\mathbf{K}; z) = \exp\{ik_z(K)z\} \iint \hat{\mathbf{S}}(\mathbf{K}, \mathbf{K}') \cdot \hat{\mathbf{E}}_{inc}(\mathbf{K}', 0) \frac{d\mathbf{K}'}{(2\pi)^2}$$

The scattering function,  $\hat{\mathbf{S}}$ , can be derived completely from the scattered far-field of the object in isolation with the help of analytic continuation. For a two-scatterer system the mutual interaction equations reduce to a single vector Fredholm integral equation of the second kind, which can accommodate the case where one scatterer is a uniform semi-infinite medium. It turns out that analytic solutions are tractable for those scattering functions that are Dirac deltas or a sum of products of separable functions of the incident and scattered wave vectors. Scattering functions for a uniform semi-infinite medium, isotropic scatterers, as well as electric and magnetic dipoles all possess this property. The exact scattering functions agree with results obtained by analytic continuation. Analytic solutions can be derived for any pair of scatterers such as isotropic scatterers, electric dipoles, magnetic dipoles, and for any of the said scatterer above a dielectric or conducting plane. Because the results are exact, the effects of near-field interactions can be assessed as long as the separation is large compared to the physical dimensions of the relevant isotropic or dipole scatterers. The same method of solution can be used to compute the mutual interaction between a radiating object and a scatterer.

Evaluating the solutions to a pair of scatterers for a unit-amplitude incident plane wave will result in the two-object scattering function. This function can be used to solve the mutual interaction between the pair and a third object. The procedure can be repeated to solve the many-scatterer problem.

# ELECTROMAGNETIC SCATTERING FROM A JET ENGINE INLET INCLUDING A COMPRESSOR

Hristos T. Anastassiou \* and John L. Volakis  
Department of Electrical Engineering  
and Computer Science  
University of Michigan  
Ann Arbor MI, U.S.A.

The general problem of scattering by jet engine inlet terminations can be analyzed by means of the Mode-Matching technique, provided the fields in each section of the engine can be characterized by some mode representation. Although this is indeed possible for configurations where the blades lie on constant  $\phi$ -angle planes (Fig. 1), typical engine compressors are much more complex. Nevertheless, we have found that it is possible to construct an analytical representation of the fields within blade configurations that are engine-like (Fig. 2). Specifically, mode-field representations can be constructed for geometries where the location of the blades attached to the inner hub can have an arbitrary dependence on the longitudinal coordinate  $z$ . Since all blades are in practice identical, the gaps between each pair of blades are the same for any constant  $z$  cut. This observation can be exploited to construct mode representations within a real engine blade configuration as a perturbation of the known representation for blades arrangements which have no variation in  $z$ . The Generalized Telegraphist's Equations (G.T.E.) (G. Reiter, Proc. I.E.E., vol. 106B, suppl. 13, 54-57, 1959) can then be employed for propagating the modes through the non-uniform waveguide structure formed by the pair of two adjacent blades. It is interesting to note that for a linear dependence on  $z$  of the blades' angular position, the solution of the G.T.E. can be found in closed form.

In this paper we will present the application of the Mode-Matching technique in the scattering characterization of engine-like structures such as those described above. Comparison of results will also be presented with a hybrid Finite Element-Modal formulation.



Figure 1



Figure 2

## Time/Frequency Analysis of Two Sphere Scattering

Chris M<sup>c</sup>Cormack\*, Valdis Liepa, William Williams  
Department of Electrical Engineering and Computer Science  
University of Michigan  
Ann Arbor, MI 48109

Randy Haupt  
Department of Electrical Engineering  
United States Air Force Academy  
Colorado, 80840-5701

We address the problem of scattering by two spheres positioned close to each other. The spheres tested ranged from small (with Rayleigh scattering) to large (where the RCS approaches optical approximations). Both measured and numerically calculated cases were considered. Three different techniques were used to perform time/frequency analysis of the data; traditional spectrograms, reduced interference distributions (RID), and wavelets. Through time/frequency analysis of the measured data, we can examine scattering mechanisms for the interacting targets. By identifying the scattering mechanisms, we hope to develop rules for target classifications.

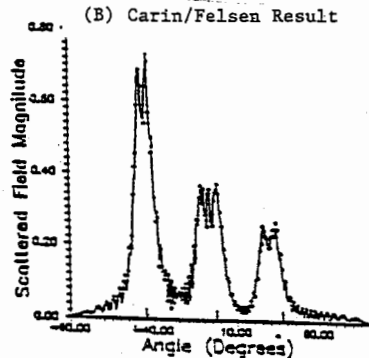
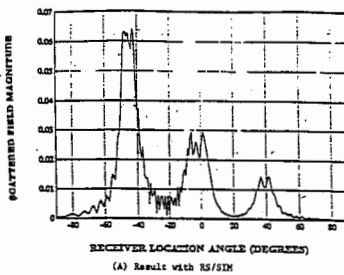
We also measured and analyzed a sphere that had been modified with a circumferential cavity backed slot to reduce its radar cross section by 30 decibels. Such impedance loading is a narrowband radar cross section reduction technique. Here we look at the loaded sphere's scattering in a broadband regime using the previously mentioned time/frequency analysis techniques.

## SIMULATION STUDY OF BISTATIC SCATTERING FROM PARALLEL STRIPS

H. E. Raemer and Y. Lou  
Northeastern University  
Center for Electromagnetics Research and ECE Dept.  
Boston, MA 02115

### ABSTRACT

The authors have developed a very comprehensive program for modelling and simulation of radar target and clutter scenarios based on coherent superposition of vector-phasor returns from all scattering material within the radar's field of view. This includes both natural terrain patches and discrete objects. The program is named RS-SIM. As a means of validating the various options available in the program, comparisons have been made between its results and those of studies made with other techniques. One such comparison was with studies of bistatic scattering from arrays of infinitely long-thin metallic strips conducted by L. Carin, L. Felsen [IEEE Microwave and Guided Wave Letters, Vol. 2, No. 9, Pp. 367-369] and M. McClure at New York Polytechnic Institute [MS Thesis, 1992]. Their techniques, based on MOM-derived currents on the strips, (implying that interactions between strips is automatically accounted for), produced a set of results for various geometries reported in the references cited above. We have run simulations of the same geometries with RS-SIM using simple algorithms characteristic of the usual radar analysis, eg. physical optics solutions for single scattering from flat rectangular plates. The agreement with the more rigorous Carin, Felsen, McClure results is excellent for virtually all of the comparisons made to date. A number of these results will be shown in the presentation. One of them is shown below. It is the case of a linear array of horizontal strips a wavelength wide whose centers are separated by 1.5 wavelengths. Refinements available in RS-SIM, eg. accounting for diffraction due to edges and multiple scattering between strips were not implemented in this run. Later runs including some of those features did not have a major effect on the results.



## **Scattering by 2-D Strips Using an Asymptotic Hybrid (Method of Moments)-(Physical Optics) Technique**

Anders Sullivan  
Wright Laboratory  
Eglin Air Force Base, Florida 32542

Lawrence Carin  
Department of Electrical Engineering  
Polytechnic University  
Brooklyn, NY 11201

TE and TM plane-wave scattering by perfectly conducting two-dimensional strips of various sizes is analyzed in the frequency domain. A hybrid formulation is applied which combines the method of moments (MOM) and physical optics to obtain the equivalent currents. Over electrically large regions of the strip scatterer the physical optics approximation is used for the induced current while near corners and edges a subsectional MOM expansion is applied. Such a scheme has been used by others to calculate the scattered fields from electrically large bodies. The new feature of this study is that asymptotic techniques are used to evaluate many of the highly oscillating integrals which constitute the MOM impedance matrix. The (endpoint)-(stationary point) asymptotics yield analytic approximations for many of the impedance-matrix elements, significantly reducing computational time. The simple asymptotic techniques used for the evaluation of the integrals yield remarkably accurate results. The induced surface currents and scattered fields from our algorithm are compared with results from other efficient MOM algorithms, validating the algorithm's accuracy. More importantly, we show that the present method reduces computational time by an order of magnitude compared to the most efficient MOM algorithms in the literature. The technique is shown here for relatively simple targets but it can be extended for more complicated two and three-dimensional perfectly conducting targets.

# SCATTERING OF EM WAVES BY DISCONTINUITY IN TRI-LAYERED MEDIA SEPARATED BY PLANAR INTERFACE

Jiming Song\*, Jian Qian<sup>†</sup>, Dennis Nyquist  
Kun-Mu Chen and Edward Rothwell

Department of Electrical Engineering, Michigan State University  
East Lansing, MI 48824

<sup>†</sup>Department of Information Physics, Nanjing University  
Nanjing, 210008, P. R. China

The two-dimensional interaction of electromagnetic (EM) waves with a discontinuity in an infinite sheet on a lossy material, which are all characterized by complex permittivity  $\epsilon$  and complex permeability  $\mu$ , is considered. Initially, the problem is decomposed into two parts by the use of superposition principle. One component is the incident EM field without the discontinuity, the other is the scattered EM field  $\vec{E}_s$  and  $\vec{H}_s$ , excited by the equivalent electric current  $\vec{j}^{eq}$  and magnetic current  $\vec{j}_m^{eq}$  in the discontinuity region. A set of coupled electric/magnetic field integral equations (EMFIE's) for the electromagnetic field in the discontinuity region is then derived based on dyadic Green's functions for the field produced by induced electric and magnetic polarization currents. Impressed electromagnetic fields consist of either plane waves incident from space upon the slab or surface waves supported by that structure. Both TE and TM polarizations are considered.

The Green's functions are derived by a direct field approach and expressed in terms of the inverse Fourier transformation over spatial frequency (Sommerfeld integral). By means of the duality theorem, magnetic Green's functions are derived from electric Green's functions. Computation of the inverse transformations is performed by integrating numerically along a deformed path above the real axis.

The EMFIE is solved via Galerkin's method with pulse basis functions. The scattered fields maintained by equivalent induced electric and magnetic polarization currents include surface waves and radiation fields in the space region; both are formulated, the latter by the steepest-descent integration approximation. Numerical results are shown for a rectangular discontinuity in both perfect and lossy dielectric and magnetic slabs. The validity of all the formulae and the numerical implementation are verified by comparing the results with some prior published results.

\*Current address: Department of Electrical and Computer Engineering  
University of Illinois at Urbana-Champaign, IL 61801

## Application of the Coupled Finite Element- Combined Field Integral Equation Technique (FE/CFIE) to Electromagnetic Radiation problems

Vahraz Jamnejad\*, Tom Cwik, and Cinzia Zuffada

**Jet Propulsion Laboratory  
California Institute of Technology  
Pasadena, CA 91109**

A coupled finite element-combined field integral equation (FE/CFIE) technique was originally developed for solving scattering problems involving inhomogeneous objects of arbitrary shape and large dimensions in wavelength. The method incorporated an exact integral equation outside an arbitrary surface of revolution (SOR), very near the object and circumscribing it (T. Cwik, V. Jamnejad, and C. Zuffada, IEEE-APS Symposium, June 1993). This technique can also be applied to the problems where sources are present, in which case the problem to be solved is that of radiating sources in the presence of the material bodies. This is the classic antenna radiation problem.

The development proceeds in a fashion similar to that for the original coupled technique for scattering problems. Of the three equations for the coupled approach formulation only one, namely the one involving the finite elements is changed. Starting with the Maxwell's Equations with electric and magnetic current sources  $J_e$  and  $M_s$ , the wave equation for H (or E) field can be written with source terms present. By multiplying the wave equation with a testing function, integrating over the volume of interest that should include the material bodies as well as the sources and some additional manipulation, the finite element equation with source is obtained. This equation is given as

$$j\eta_0 \iiint_V \left[ \frac{1}{\epsilon_r} (\nabla \times \vec{H}) \cdot (\nabla \times \vec{T}^*) - k_0^2 \mu_r \vec{H} \cdot \vec{T}^* \right] dv + k_0 \iint_{\partial V} (\vec{E} \times \hat{n}) \cdot \vec{T}^* ds = j\eta_0 \iiint_V \frac{1}{\epsilon_r} \vec{J}_s \cdot (\nabla \times \vec{T}^*) dv + k_0 \iint_V \vec{M}_s \cdot \vec{T}^* dv$$

Following the discretization of the equations by expanding the source terms in finite-element basis functions as is the case for the magnetic or electric field inside the volume, the general coupled approach matrix equation is obtained:

$$\begin{bmatrix} \mathbf{K} & \mathbf{C} & \mathbf{0} \\ \mathbf{C}^T & \mathbf{0} & \mathbf{Z}_0 \\ \mathbf{0} & \mathbf{Z}_M & \mathbf{Z}_J \end{bmatrix} \cdot \begin{bmatrix} \mathbf{H} \\ \mathbf{M} \\ \mathbf{J} \end{bmatrix} = \begin{bmatrix} \mathbf{V}_s \\ \mathbf{0} \\ \mathbf{V}_i \end{bmatrix}$$

The right-hand side vector now includes two terms involving sources: one for electric and magnetic source currents in the finite element volume,  $V_s$ , and the other for the outside incident field,  $V_i$ . Typically, for scattering problems the  $V_s$  term is zero and only an incident field exists which enters the matrix equation via the  $V_i$  term, while in antenna problems only the  $V_s$  term is present and the  $V_i$  term is zero. Of course, in general, both terms can be present and the problems of radiation and scattering can be solved simultaneously. The critical step in the source formulation involves the representation of current sources (volume and/or surface) by the same edge element basis functions over the mesh used in the representation of the H (or E) field inside the volume. Some examples of typical sources such as dipoles, microstrip antenna feeds, etc., are presented which show the suitability of this method for a variety of complicated antenna problems.

## CHARACTERIZATION OF LOW-FREQUENCY PYLON-TARGET ELECTROMAGNETIC INTERACTIONS

Steven Castillo, Russell Jedlicka and Steven Omick  
New Mexico State University  
Dept. 3-O, Box 30001  
Las Cruces, NM 88003

Captain Sam McKenzie  
U.S. Air Force  
46th Test Group  
Holloman AFB, NM 88330

William Leeper  
6540 Loblolly Dr.  
Huber Heights, OH, 45424

Timothy Conn  
EG&G Management Systems, Inc.  
Building 7000, P.O. DRAWER U  
Holloman AFB, NM 88330

As high-frequency signature reduction techniques are reaching maturity, engineers and scientists are faced with the remaining problems of VHF and UHF signature control. The Radar Target Scatter (RATSCAT) facility is the government's premier static Radar-Cross-Section (RCS) test and evaluation range chartered with signature characterization from .1 to 95 GHz. With VHF and UHF signature control progress continuing, RCS test ranges are challenged to provide instrumentation, signal processing, and target support structures which are congruent with accurate signature characterization at these lower frequencies.

Electromagnetic scattering at lower frequencies has some characteristics which are different from those at higher frequencies. At longer wavelengths the electromagnetic signature is due to reradiation by induced currents which are spatially distributed rather than localized to discrete scattering centers. For this reason the low-frequency phenomena are characterized by higher levels of coupling, penetration, and mutual interaction between adjacent bodies. This is the underlying reason for both the difficulty of radar signature control and of signature measurement at VHF/UHF. One area where this is of concern is the problem of electromagnetic interaction between a radar target and its support structure in static RCS testing. At VHF/UHF frequencies the target can interact strongly with its support, perturbing the desired free-space scattering signature measurement.

In this study, we have characterized the nature of pylon-target electromagnetic interactions at VHF/UHF frequencies using a combination of experimental and numerical tools. The swept frequency response is obtained both experimentally and numerically for a set of targets including a scale model of the 95 foot RAMS pylon at RATSCAT. These results were used to calculate the frequency response and the impulse response of targets with and without an attached pylon. Both a Finite-Difference Time-Domain (FDTD) code and an E-field integral equation code (Carlos-3D) were used to conduct the numerical study of these same target-pylon combinations. The results have been used to characterize the interactions in both the time and frequency domains, and to establish the perturbation these interactions introduce into RCS measurements. In this paper, we present these results and suggest methods for reducing pylon-target interactions for scattering measurements.



## TUESDAY AM JOINT SPECIAL SESSION T-J2

Room: HUB 310

### ROUGH SURFACE SCATTERING I

Chairs: G. Brown, Virginia Polytechnic Institute and State University; S. Broschat, Washington State University

Organizers: S. Broschat, Washington State University; A. Ishimaru, University of Washington

- 8:00 A New Solution for Scattering from Perfectly Conducting Surfaces with One Dimensional Roughness 148  
*A. Garcia, R.E. Collin, Case Western Reserve Univ.*
- 8:20 The Small Slope Approximation for Rough Surface Scattering 149  
*\*S.L. Broschat, Washington State Univ.; E.I. Thorsos, Univ. of Washington*
- 8:40 Small-Slope Approximation for Scattering of EM Waves at the Rough Boundary of Dielectric Halfspaces 150  
*\*A. Voronovich, NOAA/ERL*
- 9:00 Accuracy of Several Alternative Forms of the Operator Expansion Solution for Scattering from 1-D Randomly Rough Dirichlet Surfaces AP-S  
*\*P.J. Kaczowski, E.I. Thorsos, Univ. of Washington*
- 9:20 Perturbation Theory for Rough Surface Scattering with the Neumann Boundary Condition 151  
*\*E.I. Thorsos, Univ. of Washington*
- 9:40 Applications of Manifestly Reciprocal Representations of Scattering Theory 152  
*\*D. Wurmser, Naval Research Laboratory*
- 10:00 Break
- 10:20 Some Asymptotic Considerations in Low Grazing Angle Scattering from Rough Surfaces 153  
*\*G.S. Brown, Virginia Polytechnic Inst. and State Univ.*
- 10:40 Correlation Effects in Rough Surface Shadowing 154  
*\*D. A. Kapp, G. S. Brown, Virginia Polytechnic Inst. and State Univ.*
- 11:00 A Smoothing Approach to the Scattering of Electromagnetic Waves by Penetrable Random Rough Surfaces 155  
*C. Baylard, J.-J. Greffet, Ecole Centrale Paris*
- 11:20 Optimization of the Mueller [M] and Kennaugh [K] Power Density and the Covariance [ $\Sigma$ ] Matrices for Analyzing Incoherent Rough Surface Scatter 156  
*W.-M. Boerner, Univ. of Illinois at Chicago; E. Lüneburg, German Aerospace Research Establishment; Y. Yamaguchi, Niigata Univ.*
- 11:40 Some Features of Electromagnetic Scattering from Bounded Rough Surfaces 157  
*\*A.I. Timchenko, Ukrainian Academy of Sciences*

A NEW SOLUTION FOR SCATTERING FROM PERFECTLY  
CONDUCTING SURFACES WITH ONE DIMENSIONAL ROUGHNESS

A.Garcia-Valenzuela and R.E.Collin  
Electrical Engineering and Applied Physics Dept.  
Case Western Reserve University  
Cleveland, OH 44106

In this paper we will present a new first order rough surface scattering theory that has been obtained using a local spectral expansion method similar to that used in the full wave theory but following a different procedure. The new theory gives the following expression for the incoherent scattering cross sections:

$$\langle \sigma_{cs} \rangle = \ell \int_{-\infty}^{\infty} \{ S_1^2 e^{-v_y^2 \sigma^2} (e^{v_y^2 \sigma^2 C} - 1) \pm 2 S_1 S_2 e^{-(v_y^2 + u_y^2) \sigma^2 / 2} [e^{v_y u_y \sigma^2 C} - 1] + S_2^2 e^{-u_y^2 \sigma^2} (e^{u_y^2 \sigma^2 C} - 1) \} e^{j v_x \ell \bar{x}} d\bar{x}$$

where  $u_y = k_0 (\cos \theta_i - \cos \theta_s)$ ,  $v_y = k_0 (\cos \theta_i + \cos \theta_s)$ ,  $\ell$  is the surface height correlation length in wavelengths,  $\sigma$  is the RMS surface height, and  $C$  is the correlation function given by  $e^{-\bar{x}^2 / \ell^2}$  with  $\bar{x} = x / \ell$ . The scattering coefficients are given by  $S_1 = [1 + \cos(\theta_i + \theta_s)] / (\cos \theta_i + \cos \theta_s)$  and  $S_2 = [1 - \cos(\theta_i - \theta_s)] / (\cos \theta_i - \cos \theta_s)$ . The parameter  $v_x$  is given by  $k_0 (\sin \theta_s - \sin \theta_i)$ . The negative sign applies for horizontal polarization and the positive sign for vertical polarization. This new solution has the following properties:

1. It reduces to the small perturbation results when  $v_y \sigma$ ,  $u_y \sigma$ , and the correlation length are small.
2. When the scattering angle  $\theta_s$  equals the angle of incidence  $\theta_i$  the new solution agrees with the regular full wave and Kirchhoff solutions.
3. For horizontal polarization the incoherent cross section vanishes when the scattering angle approaches grazing values.
4. When the Kirchhoff solution is valid for horizontal polarization (except at grazing angles) the new solution agrees with the Kirchhoff solution. For vertical polarization the new solution agrees with the regular full wave solution at grazing angles.
5. The new solution for horizontal polarization agrees quite well with Thorsos' integral equation numerical solution for surface parameters that span the small perturbation and Kirchhoff regimes.

## **The Small Slope Approximation for Rough Surface Scattering**

**Shira Lynn Broschat \***

Electrical Engineering & Computer Science  
Washington State University  
Pullman, WA 99164-2752  
(509)335-5693, shira@eeecs.wsu.edu

**Eric I. Thorsos**

Applied Physics Laboratory  
College of Ocean and Fishery Sciences  
University of Washington  
Seattle, WA 98105  
(206)543-1369, eit@apl.washington.edu

In recent years there has been much interest in several new theories for rough surface scattering. Included among these is the Small Slope Approximation (SSA) introduced by A.G. Voronovich in the mid-1980s [Sov. Phys. JETP 62, 65-70, 1985]. Since its introduction, the SSA has been extended to a number of different problems, and numerical studies have demonstrated the usefulness of the SSA for acoustic scattering from fluid-solid, one-dimensional (1-D) interfaces [D.H. Berman, JASA 89, 623-636, 1991; T. Yang & S.L. Broschat, to be published in JASA, 1994] and TE-polarized (Dirichlet boundary condition) EM scattering from both 1-D and 2-D perfectly conducting surfaces [S.L. Broschat & E.I. Thorsos, ICO Topical Meeting Digest, 103-106, Florence, 1991; T. Yang & S.L. Broschat, IEEE Trans. Antennas Propagat. 40, 1505-1512, 1992]. In this paper we review the SSA for the Dirichlet problem and present numerical results for 1-D, Dirichlet surfaces satisfying a Gaussian surface roughness spectrum. The SSA reduces analytically to first-order perturbation theory and to the Kirchhoff approximation in the appropriate limits. By comparison with exact Monte Carlo integral equation results for scattering cross sections, we show this numerically as well. In addition, we compare the zeroth-, first-, and second-order SSA cross sections, discuss their regions of validity, and discuss the usefulness of the SSA for this type of problem.

## Small-Slope Approximation for Scattering of EM waves at the Rough Boundary of Dielectric Halfspaces

A.Voronovich

NOAA / ERL / Environmental Technology Laboratory, 325 Broadway, Boulder, CO, 80303

Small-slope approximation (SSA) is developed for description of wave scattering at rough interface of two homogeneous halfspaces. This method bridge the gap between two classical approaches to the problem: method of small perturbation and Kirchhoff (or quasi classical) approximation. In contrast to these theories the SSA is applicable irrespective of the wavelength of radiation provided that slopes of roughness are small as compared to the incidence and scattering angles. Both first and second order versions of the theory (with respect to slopes of elevations) are considered.

The resulting expressions of the SSA are given for the entries of S-matrix which represent scattering amplitudes of plane waves of different polarization interacting with the rough boundary. These formulas are quite general and are valid in fact for waves of different origin. Apart from the shape of the boundary some functions take place in these formulas which are coefficients of expansion of S-matrix into common power series in elevation. These roughness independent functions are determined by specific scattering problem. In this work they are calculated for the case of EM scattering at the interface of two dielectric halfspaces. Both reflected and transmitted field are considered in details.

*A priori* symmetry relations (reciprocity and energy conservation) which this scattering problem should obey are formulated in terms of S-matrix. Moreover, some new expression which relates the inverse of the S-matrix with changing sign of elevation is presented.

Statistical moments of scattering amplitudes are immediately related to the mean reflection coefficient and scattering cross-sections which are usually determined experimentally. Explicit formulas are given for the case of Gaussian space-homogeneous statistics of roughness. Corresponding cross-sections can be represented as a Fourier transform of some function of horizontal coordinates which is related in simple but non-linear manner with correlation function of elevations.

**Perturbation**

Applied  
College of Oceanography  
University of Washington  
Seattle, WA 98195  
(206)543-1369, eit@apl.washington.edu

Lowest-order perturbation theory has been quite useful for treating rough surfaces when  $kh \ll 1$ , where  $h$  is the rms surface height and  $k$  is the wavenumber. In the case where the rough surface obeys the Dirichlet condition it has been possible to extend the accuracy of perturbation theory to values of  $kh$  as high as 0.5 by taking perturbation theory beyond lowest order [B. Thorsos & D.R. Jackson, JASA 86, 261-277, 1989]. Here we consider a similar extension for the case of the Neumann boundary condition. For this case, however, the expression obtained for the scattering cross section diverges when standard perturbation theory methods are used beyond lowest order [J.M. Soto-Crespo, M.Nieto-Vesperinas, & A.T. Friberg, JOS A 7, 1185, 1990]. The low grazing angle behavior of the standard lowest order result also turns out to be fundamentally incorrect. These problems are related to the fact that surface roughness can support the propagation of surface waves for the Neumann boundary condition. Renormalization techniques are necessary in order to reformulate the perturbation series and correct the deficiencies of the standard series. The approach taken in this paper is based on renormalized perturbation theory developed by A.A. Maradudin and co-workers [see, for example, G. Brown et al., Phys Rev B 31, 4993-4998, 1985] specialized to the Neumann boundary condition case. Scattering cross section expressions will be presented which are free of the deficiencies of standard perturbation theory. The numerical implementation of the self energy (mass operator) solution of a non-linear integral equation for the renormalized perturbation theory has been studied by making comparisons with exact integral equations based on a Monte Carlo method. Results will be presented showing that renormalized theory is accurate for  $kh$  up to 0.5.

**Manifestly Reciprocal  
Calculations of Scattering Theory**

Daniel Wurmser  
Naval Research Laboratory  
Code 7144  
Washington, D.C. 20375-5350

In a previous collaboration with Roger Dashen (UCSD), a new approach for calculating scattering from rough surfaces was developed. At the heart of this approach are exact new expressions for the scattering amplitude, which manifestly exhibit time-reversal symmetry. A straightforward method was outlined where these expressions were used to obtain totally symmetric Composite Model and Small Slope approximations without the use of ad hoc arguments or involved derivations using Green's functions. Because of the fields, including electromagnetic radiation and (recently) elastic waves, and for various boundary conditions, these results were new. Other researchers symmetry of these approximate expressions, the effects of shadowing and multiple scattering can be incorporated in a natural way. Because of the have used our results to obtain new insights concerning ocean radar scattering at low grazing angles. In a previous publication by Dashen, Henyey and Wurmser, this formalism was used to show conclusively that the enhanced acoustic cross-sections observed in ocean scattering experiments cannot possibly come from the rough air-sea interface alone. This led others to investigate alternate mechanisms for near surface scattering, resulting in the determination that scattering from bubble clouds is often dominant. The d has also been applied to the problem of scattering from a layer of scatterers near the surface, or equivalently a variable sound speed profile of an effective surface roughness. The formalism has recently been Wurmser and A. Abawi to examine the scattering from planar objects, and finite objects. This work suggests a new approach for calculating the

## **Perturbation Theory for Rough Surface Scattering with the Neumann Boundary Condition**

**Eric I. Thorsos**

Applied Physics Laboratory  
College of Ocean and Fishery Sciences  
University of Washington  
Seattle, WA 98105  
(206)543-1369, eit@apl.washington.edu

Lowest-order perturbation theory has been quite useful for treating scattering from rough surfaces when  $kh \ll 1$ , where  $h$  is the rms surface height and  $k$  is the radiation wavenumber. In the case where the rough surface obeys the Dirichlet boundary condition it has been possible to extend the accuracy of perturbation theory to values of  $kh$  as high as 0.5 by taking perturbation theory beyond lowest order [E.I. Thorsos & D.R. Jackson, *JASA* 86, 261-277, 1989]. Here we consider a similar extension for the case of the Neumann boundary condition. For this case, however, the expression obtained for the scattering cross section diverges when standard perturbation theory methods are used beyond lowest order [J.M. Soto-Crespo, M.Nieto-Vesperinas, & A.T. Friberg, *JOSA* A7, 1185, 1990]. The low grazing angle behavior of the standard lowest order result also turns out to be fundamentally incorrect. These problems are related to the fact that surface roughness can support the propagation of surface waves for the Neumann boundary condition. Renormalization techniques are necessary in order to reformulate the perturbation series and correct the deficiencies of the standard series. The approach taken in this paper is based on renormalized perturbation theory developed by A.A. Maradudin and co-workers [see, for example, G. Brown et al., *Phys Rev B* 31, 4993-5005, 1985] specialized to the Neumann boundary condition case. Scattering cross section expressions will be presented which are free of the deficiencies of standard perturbation theory. The numerical implementation of these expressions involves the solution of a non-linear integral equation for the self energy (mass operator), and the method used will be described. The accuracy of the renormalized perturbation theory has been studied by making comparisons with exact integral equation results based on a Monte Carlo method. Results will be presented showing the renormalized theory is accurate for  $kh$  up to 0.5.

## Applications of Manifestly Reciprocal Representations of Scattering Theory

Daniel Wurmser  
Naval Research Laboratory  
Code 7144  
Washington, D.C. 20375-5350

In a previous collaboration with Roger Dashen (UCSD), a new approach for calculating scattering from rough surfaces was developed. At the heart of this approach are exact new expressions for the scattering amplitude, which manifestly exhibit time-reversal symmetry. A straightforward method was outlined where these expressions were used to obtain totally symmetric Composite Model and Small Slope approximations without the use of ad hoc arguments or involved derivations using Green's functions. For several types of fields, including electromagnetic radiation and (recently) elastic waves, and for various boundary conditions, these results were new. Because of the symmetry of these approximate expressions, the effects of shadowing and multiple scattering can be incorporated in a natural way. Other researchers have used our results to obtain new insights concerning ocean radar scattering at low grazing angles. In a previous publication by Dashen, Henyey and Wurmser, this formalism was used to show conclusively that the enhanced acoustic cross-sections observed in ocean scattering experiments cannot possibly come from the rough air-sea interface alone. This led others to investigate alternate mechanisms for near surface scattering, resulting in the determination that scattering from bubble clouds is often dominant. The method has also been applied to the problem of scattering from a layer of point scatterers near the surface, or equivalently a variable sound speed profile near the surface. It was shown that these problems can be reformulated in terms of an effective surface roughness. The formalism has recently been used by Dashen and A. Abawi to examine the scattering from planar objects, edges and corners. This work suggests a new approach for calculating the scattering from finite objects.

SOME ASYMPTOTIC CONSIDERATIONS IN LOW GRAZING ANGLE  
SCATTERING FROM ROUGH SURFACES  
Gary S. Brown, Bradley Dept. of Electrical Engineering  
Virginia Polytechnic Institute and State University  
Blacksburg, VA 24061-0111

The problem of long range detection and tracking by ground-based radar is driven by in large by clutter from the rough surface between the radar and the target. The modeling and prediction of scattering from rough surfaces near grazing angles of incidence presents a very difficult problem from an analytical and numerical point of view. One of the very first things that should be done is to obtain as much insight into the asymptotic behavior as possible. The purpose of this talk is to point out how ones physical intuition can be reconciled with some of the asymptotic theory and how the latter must be carefully applied very near grazing incidence.

It is well known that as grazing incidence is approached, the coherent or average field scattered in the specular direction increases at the expense of the fluctuating field in all other directions. However, if one considers the case of high frequency so that the integral equation for the current on the rough surface can be solved asymptotically, one obtains the result that the induced surface current will go to zero as grazing incidence is approached. If the current goes to zero, the scattered field will also go to zero in all directions. Of course one can correctly argue that asymptotic shadowing theory should not be used at grazing incidence because the assumptions in the method are not satisfied. On the other hand, one can use the theory close to grazing incidence and the predictions of a vanishing current still would seem to persist. One then tries to go into the details of the asymptotic shadowing theory to determine if there are local points or areas on the surface where the approximations breakdown. Indeed, one finds that these points do exist and they are the points of local grazing incidence. However, a careful examination of the vector direction of the current in the vicinity of these points shows that for horizontal polarization the current will be zero while for vertical polarization the current is directed back along the ray of incidence which implies that there is little or no contribution in the backward or forward scattering directions. The conclusion is that at the points where the stationary phase approximation breaks down, the current or its effect is small. Clearly something else is amiss!

The source of difficulty here is the neglect of diffraction along with the fact that the shadow of every hump or bump on the surface is finite in its length. Pure geometrical optics predicts that the shadow will extend for an infinite distance; diffraction theory says that for any nonzero wavelength, the shadow zone will be finite in length. Thus there will be a subset of the total surface area which is illuminated by the bending of the incident field into the optical shadow zone by diffraction. Even though this diffraction illuminated area is not the entire surface, it is sufficient to give rise to an infinite contribution to the specularly scattered field. Furthermore, since the height plays little or no role very near grazing incidence, the surface appears to be specular in this limit.

## Correlation Effects in Rough Surface Shadowing

David A. Kapp\* and Gary S. Brown

The Bradley Department of Electrical Engineering  
Virginia Polytechnic Institute and State University, Blacksburg, VA 24061-0111

The effects of correlation between shadowing and shadowed points are studied using a truncated infinite series of integrals representation. This approach allows a comparison between the approximate analytical results of Wagner and Smith and the series with no approximations other than the truncation. We show that each term in the series can be related to the number of upcrossings of the surface with an incoming ray of radiation; thus, the surface statistics and backscattering angles are chosen to make the truncated terms negligible. We also show that the second and third terms in the series correspond to the lower and upper bound of the shadowing function, respectively. We compare our results with two shadowing functions given by Wagner which make an approximation to a density function (of the distance from the shadowed point to the first intersection of the surface with an incoming ray of radiation) which is needed to calculate shadowing. Additionally, the first of these functions neglects correlation between the shadowing and shadowed point while the second attempts to account for this correlation through a Taylor series expansion of the autocorrelation function. We also compare our results to Smith's shadowing function, which also neglects the above mentioned correlation, but contains an additional "normalization" term due to a different approximation to the density function mentioned above. Differences between our numerical results with Wagner's and Smith's are shown to increase as one moves toward grazing incidence. Contrary to what was expected, the second shadowing function of Wagner, which attempts to include the effects of correlation, showed the greatest disagreement. The possible causes of this discrepancy will be discussed. We also show that when we neglect correlation between all shadowing points with each other and with the shadowed point our infinite series of integrals reduces to Wagner's first result in which correlation between the first shadowing point and the shadowed point is neglected. Thus, we conclude that the approximation to the density function that was made in Wagner's results, prior to the approximations made regarding the correlation between the first shadowing point and the shadowed point, is equivalent to the neglect of correlation between all shadowing points with each other and the neglect of correlation between shadowing points (other than the first) with the shadowed point.

**A smoothing approach to the scattering of electromagnetic waves by  
penetrable random rough surfaces**

C. Baylard, Jean-Jacques Greffet  
Laboratoire EM2C, UPR 288 du CNRS, Ecole Centrale Paris  
92295 Châtenay -Malabry Cedex

The goal of the paper is to develop a new approximate technique to deal with the scattering of electromagnetic waves by random rough surfaces. We consider an incident monochromatic field that illuminates a 2D surface ( $z=S(x,y)$ ) separating two penetrable media. The starting point is an integral equation for the Fourier transform of the transmitted field established ( J.-J. Greffet, Phys. Rev. B **37**, 6436-6441,1988) under the Rayleigh hypothesis. The field is split in the coherent and incoherent components. The smoothing technique (G. S. Brown, IEEE AP-**32**, 1308-1312,1984) is used to solve the problem for the coherent component. Note that unlike the work reported by Brown, we use the smoothing technique for the solution of an integral equation in k-space rather than in direct space.

To assess the validity of the technique, we have developed a numerical simulation (Greffet et al. , Opt. Lett. **17**, 1740-1742, 1992) that allows to evaluate the neglected terms. It is based on the same integral equation in k-space and is solved using a series solution and a MonteCarlo averaging. In order to establish the range of validity of the technique, we compare the transmitted and reflected coherent terms with a numerical simulation for 2D surfaces based on the coupled integral equation as developed by Thorsos. Finally, we compare the first order perturbation results for penetrable media and the Kirchhoff theory with this approach. The first order perturbation results are derived from the reduced Rayleigh equations (Toigo et al. , Phys. Rev. B **15**, 5618-565626, 1977) for both s and p-polarization.

OPTIMIZATION OF THE MUELLER [M] AND KENNAUGH [K] POWER DENSITY  
AND THE COVARIANCE [E] MATRICES FOR ANALYZING INCOHERENT ROUGH  
SURFACE SCATTER

Wolfgang-M. Boerner<sup>(1)</sup>, Ernst Lüneburg<sup>(2)</sup> and Yoshio Yamaguchi<sup>(3)</sup>

- (1) University of Illinois at Chicago, UIC-EECS/CSL, M/C 154,  
840 W. Taylor St., SEL-4210, Chicago, IL/USA 60607-7018
- (2) German Aerospace Research Establishment, Oberpfaffenhofen,  
DLR-IHFT, M[un]chener Str 20, D-82234 OPH/Postamt Wessling, FRG
- (3) Niigata University, Information and Sensing Engineering,  
Ikarashi Campus, 2 Nocho 8050, Niigata-Shi, 850-21 JAPAN

Basic principles of polarimetric radar metrology are introduced for a complete coherent dual orthogonal (A,B) transmit/receive antenna system of high channel isolation and sidelobe reduction. The purely monostatic dual polarization channel transceiver system is considered for recovering the  $2 \times 2$  coherent Sinclair matrix [S], the  $4 \times 4$  real Kennaugh power density matrix [K] and the complex  $3 \times 3$  polarimetric covariance matrix [E].

Separate matrix optimization procedures are introduced for determining the characteristic set of five pairs of optimal polarizations plus associated degrees of polarization. The derived optimization algorithms are verified for the case of incoherent backscatter from rough surface and volumetric meteorologic backscatter utilizing experimental data sets collected with DLR-POLDI-RAD (dense cloud scatter) and with the NU POL(FMCW)RAD snow surface scatter with volumetric underburden.

## **Some Features of Electromagnetic Scattering from Bounded Rough Surfaces**

**A.I. Timchenko**

Institute for Radiophysics and Electronics  
Ukrainian Academy of Sciences  
Proscura 12, Kharkov, 310085, Ukraine  
Phone: 7-0572-44-84-29 Fax: 7-0572-44-10-12

### **Abstract**

In the theory of electromagnetic scattering the infinite rough surface model usually is considered. In this case the average over the ensemble of randomly rough surfaces or infinite area is used. However, some natural objects have finite sizes and various mean values, measured from an experiment, often correspond to the integration over finite rough surface.

The objective of this work is to consider the scattering of two waves with a different wave vectors from the finite rough surface. Two incident wave model may be arisen in the case of transparent rough boundaries, two-frequency scattering, etc. Using the perturbation theory we have calculated the correlation functions by statistical and dynamic averaging. The angular distribution of these functions are examined for various incident angles, rms. height, correlation length and surface sizes. The numerical calculations were made for the intensity in the case of backscattering.

The theoretical expressions show that the dynamic and statistical averaging give different values for correlation functions, and both ones differ from the correlation function for an infinite surface. In both cases the scattered field contains the several terms describing the process of scattering for a various spectral component of the surface.

We have shown that a new effect of coherent interaction between some scattering waves leads to the complicated diffraction phenomena in the scattering process.

The theoretical results may be applied to determine with high accuracy such characteristics as sizes of small investigated objects from information about angular dependencies of the backscattering coefficients.



TUESDAY AM URSI-B SESSION T-U15

Room: Kane 130

ABSORBING BOUNDARY CONDITIONS AND MEI

Chairs: J.L. Young, University of Idaho; T.K. Sarkar, Syracuse University

8:20	Application of the Finite Element Methods and the "MEI" Method for the Solution of Electrostatic Problems <i>*G.K. Gothard, S. M. Rao, Auburn Univ.; T. Roy, T. K. Sarkar, A. R. Djordjevic, Syracuse Univ.; M. Salazar, Polytechnique Univ. of Madrid</i>	160
8:40	On Time Domain Measured Equation of Invariance <i>*K.K. Mei, Y. Liu, Univ. of California, Berkeley</i>	161
9:00	Application of the Measured Equation of Invariance to Structures of Planar Dielectric Media <i>Mark D. Prouty, *K.K. Mei, S.E. Schwarz, Y. Liu, Univ. of California, Berkeley; R. Pous, Universitat Politècnica de Catalunya</i>	162
9:20	The Measured Equation of Invariance: A Proof for the Postulates and a New Formulation as a Sparse Matrix Integral Equation Method <i>*J.M. Ruis, J. Parrón, R. Pous, A. Cardama, Universitat Politècnica de Catalunya</i>	163
9:40	Some Problems Associated with "MEI" Method and a Hybrid Method (DSRSR) That Eliminates Them <i>A. R. Djordjevic, *T. K. Sarkar, T. Roy, Syracuse Univ.; M. Salazar, Polytechnique Univ. of Madrid; S. M. Rao, Auburn Univ.</i>	164
10:00	Break	
10:20	Efficiency of Numerical Absorbing Boundary Conditions for Finite Element Applicatons <i>*R. Stupfel, R. Mittra, Univ. of Illinois</i>	165
10:40	Evaluation of New Vector ABC's for Conformal Printed Antennas <i>*L.C. Kempel, S. Bindiganavale, J.L. Volakis, Univ. of Michigan</i>	166
11:00	Validation and Extension of the Berenger Absorbing Boundary Condition for FD-TD Meshes <i>*D. S. Katz, Cray Research, Inc.; E. T. Thiele, A. Taflove, Northwestern Univ., McCormick School of Engineering</i>	167
11:20	On the Use of Absorbing Boundary Conditions in Finite Difference Time Domain Solution of Unbounded Geometry Problems <i>*O.M. Ramahi, Digital Equipment Corporation</i>	168
11:40	The Performance of FDTD Absorbing Boundary Conditions for Buried Scatterers <i>*K. Demarest, R. Plumb, Z. Huang, Univ. of Kansas</i>	169

**APPLICATION OF THE FINITE ELEMENT METHODS AND THE "MEI"  
METHOD FOR THE SOLUTION OF ELECTROSTATIC PROBLEMS**

Griffin K. Gothard\* and Sadasiva M. Rao  
Department of Electrical Engineering  
Auburn University, Auburn, Alabama 36849

Tanmoy Roy, Tapan K. Sarkar, and Antonije R. Djordjevic  
Department of Electrical and Computer Engineering  
Syracuse University, Syracuse, New York 13244

Magdalena Salazar  
Department of Electrical Engineering  
Polytechnique University of Madrid  
Madrid, Spain

Finite element techniques for solution of differential form of Maxwell's equation are well known. However, when applied to open region problems, the termination of the mesh at a finite distance from the object generally poses problems. In this work, while utilizing the finite element technique to open region problems, the mesh is terminated close to the object using a truncation condition based on MEI (Measured Equation of Invariance) concept. The MEI concept is based on the integral equation approach using Green's function which automatically enforces the radiation condition. Utilizing this novel approach leads to an increased computational efficiency of the finite element method. The major advantage of the present scheme is the significant reduction in the number of unknowns yet retaining the sparsity of the generating matrix even though an integral equation utilizing the Green's function is used to terminate the mesh.

In this method the triangular shaped finite elements are used to approximate the object of interest and the surrounding space. The triangular elements enable us to model any arbitrary contour accurately and efficiently. The scheme to terminate the mesh is an extension of "MEI" condition developed for finite difference technique. This procedure results in retaining all the advantages of finite element/finite difference methods such as sparsity of the matrix, ease of data specification and so on. Thus the present method generates a very efficient solution with a significant reduction in memory than conventional methods. Typical numerical results are presented for the solution of two-dimensional Laplace's equation to illustrate the accuracy of the technique.

## ON TIME DOMAIN MEASURED EQUATION OF INVARIANCE

Kenneth K. Mei\* and Yaowu Liu

Department of Electrical Engineering  
and Computer Sciences  
University of California  
Berkeley, CA 94720

The measured equation of invariance (MEI) is a technique to terminate the finite difference/element equations at mesh boundaries without invoking an absorbing boundary condition or a global integration. The concept of MEI is based on the postulate that the local linear relation between neighboring nodal fields are invariant to excitations. Based on this postulate as a first principle, the linear equations at the mesh boundaries are found without finite differencing the differential equation, which fails at the mesh boundary. MEI is a new concept in field computation, in that it breaks away from the traditional approach of deriving discrete nodal equations from differential equations, rather it derives the discrete equations from a set of solutions, which are associated to the object solution by geometry. MEI has been successfully applied to scattering, antennas and microstrip structures in frequency domain.

In this paper it is shown that the same postulates used in the frequency domain are applicable to time domain as well, i.e., we can terminate the FDTD mesh very close to the object boundary by linear equations retrieved from known solutions, via measuring functions and metrons. It is shown that using time domain MEI on a rectangular metal scatterer the FDTD mesh can be terminated at only two space segments away from the object boundary, where all conventional absorbing boundary conditions fail.

The time domain MEI is not only a contribution to make the FDTD method faster and leaner, but is also a potentially new venue to treat boundary configurations difficult for conventional approaches, such as mesh terminations crossing material interfaces or crossing obliquely with a transmission line.

## APPLICATION OF THE MEASURED EQUATION OF INVARIANCE TO STRUCTURES ON PLANAR DIELECTRIC MEDIA.

Mark D. Prouty, K. K. Mei\*, S. E. Schwarz, Y. Liu  
Department of Electrical Engineering and Computer Science  
and the Electronics Research Laboratory  
University of California, Berkeley, CA 94720

R. Pous  
Universitat Politecnica de Catalunya  
Barcelona, Spain.

The Measured Equation of Invariance (MEI) method, first proposed by K. K. Mei, [URSI Digest, p. 544, APS/URSI Joint Symposium, Chicago, 1992], is a means of applying boundary conditions at the edges of a finite-difference or finite-element mesh. The method works for meshes terminated extremely closely to the objects of interest, and can even account for the presence of conductors (such as ground planes) completely outside of the mesh. It has been applied previously to scattering problems and to transmission line problems without dielectric. In this work we analyze a variety of structures built on planar dielectric media.

Finite-difference equations are written in terms of the magnetic vector potential. All three components of this potential may be present. The analysis is a rigorous full-wave solution to Maxwell's equations. Currents are allowed in all 3 dimensions. The Sommerfeld's integrals are used to calculate the Green's function, which is used in the method to find conditions which are obeyed at the edges of the computational domain.

One key advantage to this method is its great flexibility. Aside from the calculation of the Green's functions, no other manual analyses need be performed. Other methods often require singular integrations, calculation of basis functions and their transforms, or other manipulations which might be specific to the geometry being studied. With this method, one simply digitizes the metal structure and solves the problem in the same manner regardless of the structure. Great flexibility is allowed in the means of excitation as well.

Results are presented for a variety of microstrip discontinuities (bends, open-ends, stubs), and antenna structures (flat dipoles and patches).

THE MEASURED EQUATION OF INVARIANCE:  
A PROOF FOR THE POSTULATES AND A NEW FORMULATION  
AS A SPARSE MATRIX INTEGRAL EQUATION METHOD

Juan M. Rius\* , Josep Parrón, Rafael Pous, Angel Cardama  
Dept. Teoria del Senyal i Compuncacions  
Universitat Politècnica de Catalunya  
Apdo. 30002, 08080 Barcelona, Spain

Electromagnetic scattering and radiation problems in the frequency domain usually involve the solution of the wave equation with some boundary conditions. Discretization of the wave equation results in a finite difference or finite element mesh which extends over the whole domain of the differential equation. For open problems, such as antenna radiation, radar cross section computation, etc., this domain is infinite and the solution must satisfy the Sommerfeld radiation condition at the infinite. In practice the finite difference or finite element mesh is truncated at a finite distance of the scatterer, and thus some radiation boundary conditions must be formulated at the mesh truncation boundary. However, these radiation boundary conditions either require a mesh volume much larger than the antenna or scatterer under consideration or, when formulated near the surface of the object they are not robust and they cannot be applied to concave surfaces.

The Measured Equation of Invariance (MEI) was presented by Mei and Pous at IEEE AP-S 1992 and 1993 Symposia as a mesh truncation condition for the finite difference and finite element methods in the frequency domain. The validity of the MEI was based on three postulates, which were not proved. This communication presents a proof for the postulates and, which is more important, a new conception of the MEI as a weighted residual integral equation method that produces an sparse impedance matrix with the same number of unknowns as the method of moments (MoM). As a consequence, it will be demonstrated that the mesh truncation condition of Mei and Pous is, in fact, a hybrid finite difference - boundary element approach in which an integral equation formulation is used to terminate the finite difference mesh.

Some results for the MEI applied as an integral equation method at the scatterer boundary will be presented for two-dimensional problems, with emphasis on the CPU and memory savings compared to method of moments.

SOME PROBLEMS ASSOCIATED WITH "MEI" METHOD AND A  
HYBRID METHOD (DSRSR) THAT ELIMINATES THEM

Antonijé R. Djordjevic, Tapan K. Sarkar\* and Tanmoy Roy  
Department of Electrical and Computer Engineering  
Syracuse University; Syracuse, New York 13244

Magdalena Salazar  
Department of Electrical Engineering  
Polytechnique University of Madrid  
Madrid, Spain

Sadasiva M. Rao  
Department of Electrical Engineering  
Auburn University  
Auburn, Alabama 36849

Abstract: The measured equation of invariance (MEI) combines features of both differential and integral based methods. However, there are convergence problems, particularly associated with the choice of proper metrons. It is easy to show that for the electrostatic problems if the charge distribution on the structure is not a proper combination of the proper metrons, then the method fails to converge. Examples will be presented where one will invariably run into convergence problems, for the solution of Laplace's equation. An alternate method is proposed which does not suffer from convergence problems and the absorbing conditions are numerically "exact". The new technique (DSRSR) method is also a hybrid method but imposes "exact" boundary conditions which evolves iteratively as the solution progresses. The DRSR method is also based on the Green's functions for the integral equations, however it is iterative in nature. The proposed technique will be illustrated through the solution of a two dimensional electrostatic problems for which the MEI method is known to fail.

It will be shown that for this type of finite element solutions of Maxwell's equations that the results are closer to the solution of the boundary element (integral equation approach) if the mesh is terminated close to the outer boundary, than when the mesh is terminated away from the boundary. This implies that to obtain more accurate results, the mesh must be terminated close to the boundary surface. When the mesh termination is far away, the results are of a worse accuracy than when the mesh is terminated closed to the surface. Even when the MEI method provides acceptable results for the capacitance, the charge distribution is still not correct. Examples, will be presented to illustrate the application of the new technique.

**EFFICIENCY OF  
NUMERICAL ABSORBING BOUNDARY CONDITIONS  
FOR FINITE ELEMENT APPLICATIONS**

Bruno Stupfel<sup>†§</sup> and Raj Mittra<sup>§</sup>

<sup>†</sup> Centre d'Études de Limeil-Valenton, Commissariat à l'Énergie Atomique.  
94195 Villeneuve St Georges cedex, France.

<sup>§</sup> Electromagnetic Communication Laboratory, University of Illinois.  
Urbana, IL 61801-2991

It has been shown (Stupfel and Mittra, URSI Symposium, 1994) that the following numerical absorbing boundary conditions (NABCs) for terminating a finite difference or a finite element mesh proposed by Mei, Pous, Chen and Liu, viz.,

$$u(M_0) = \sum_{i=1}^N c_i u(M_i) \quad (1)$$

and that suggested by Li, Cendes and Yuan

$$\partial_n u(M_0) = \sum_{i=0}^{N-1} c_i u(M_i) \quad (2)$$

become analytically equivalent to many existing absorbing boundary conditions in the limit the mesh size  $h$  tends to zero. In (1) and (2), the coefficients  $c_i$  are computed by solving a linear system of equations derived by using test waves that may be either plane waves or those radiated by line sources.

We show in this paper that the numerical accuracy of these NABCs can be limited. When  $h$  is small, the number of coefficients  $N$  which can be accurately calculated is limited by the finite number of significant digits available on the computer. Also, for fixed values of  $N$  and  $h$ , this accuracy can be improved by using double instead of a single layer of nodes on the boundary  $S$ .

Next, following the usual procedure in the time domain, we evaluate the numerical efficiency of the above two NABCs by computing the reflection coefficient for plane and cylindrical incident waves for an arbitrary boundary  $S$ . We show that the efficiencies of the two NABCs are essentially the same, and that they are higher for test waves that are line sources. It is hoped that these results would be useful for defining the guidelines for the implementation of these NABCs in the finite element codes.

# 1994 URSI Radio Science Meeting (Seattle)

## EVALUATION OF NEW VECTOR ABCs FOR CONFORMAL PRINTED ANTENNAS

Leo C. Kempel\*, Sunil Bindiganavale, and John L. Volakis  
Radiation Laboratory  
Department of Electrical Engineering and Computer Science  
University of Michigan, Ann Arbor, MI 48109-2122

### Abstract

We propose a new approach for modeling printed antennas with inhomogeneous radome configurations (see figure 1). The approach couples the finite element (FE) method with recently introduced conformal vector absorbing boundary conditions (A. Chatterjee and J.L. Volakis, *Microwave and Optical Tech. Letters*, 6, No. 16, pp. 886-889, Dec. 20 1993). We will evaluate the performance of these ABCs by comparison with a finite element-boundary integral (FE-BI) formulation which includes the presence of a planar dielectric superstrate. Another approach which has been suggested is to use a sheet condition to model a thin, lossy superstrate. A comparison will be made between this approximation and the rigorous FE-BI approach. The FE-ABC method will be used to evaluate the effect of multilayer superstrates on radiation by conformal antenna elements which are embedded in both planar and cylindrical surfaces. The FE method permits rather general inhomogeneous super/substrate configurations which will allow an optimal trade-off between the Radar Cross Section (RCS) and the antenna gain. Additionally, the FE method permits tremendous geometrical flexibility which will be exploited in designing multiple cavity-backed antennas which afford greater bandwidth than conventional single cavity designs permit. In addition, the use of multiple cavities behind the patch can be exploited for miniturization purposes.

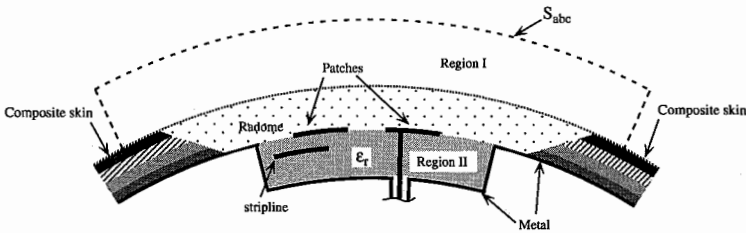


Figure 1: Coated cavity-backed patch antenna with ABC mesh termination.

## Validation and Extension of the Berenger Absorbing Boundary Condition for FD-TD Meshes

Daniel S. Katz\*  
Cray Research, Inc.  
c/o Jet Propulsion Laboratory  
MS 301-455, 4800 Oak Grove Drive  
Pasadena, CA 91109-8099

Eric T. Thiele  
Allen Taflove  
EECS Department  
McCormick School of Engineering  
Northwestern University  
Evanston, IL 60208

Berenger has recently published a novel absorbing boundary condition (ABC) for FD-TD meshes in two dimensions, with substantially improved performance relative to any earlier technique (J. P. Berenger, *Jour. Comp. Phys.*, in press). This approach, which he calls the "perfectly matched layer for the absorption of electromagnetic waves," is based upon a decomposition of electric or magnetic field components in the absorbing boundary region with the possibility of assigning losses to the individual split field components. The net effect of this is to create a non-physical absorbing medium adjacent to the outer FD-TD mesh boundary that has a wave impedance independent of the angle of incidence and frequency of outgoing scattered waves. Berenger reported effective reflection coefficients for his ABC  $1/3000^{\text{th}}$  that of the standard 2<sup>nd</sup> and 3<sup>rd</sup> order ABCs (i.e., Mur). Further, he reported total grid noise energies reduced to  $10^{-7}$ th the level produced by conventional ABCs.

In this paper, we report confirmation of these remarkable claims, and two extensions of the Berenger ABC. First, we reproduced his claimed reflection coefficients and total grid noise reductions for the two-dimensional TE and TM grid cases. Furthermore, we found that the Berenger ABC can be easily adapted to provide a reflection-less grid boundary when the interior region is filled with a uniform dielectric with non-unity relative permittivity.

In the major contribution of this paper, we have extended the Berenger ABC to three-dimensional Cartesian FD-TD meshes. We will show results for measurements of grid noise due to imperfect ABCs that are on the order of  $1/100^{\text{th}}$  that of the standard second-order Mur ABC. The implication of these findings is that the effective dynamic range of FD-TD modeling (as limited by imperfect ABCs) is increased by 40 dB by this implementation. This will allow modeling antennas and scattering objects having pattern dynamic ranges of 80 dB or more.

ON THE USE OF ABSORBING BOUNDARY  
CONDITIONS IN FINITE DIFFERENCE TIME DOMAIN SOLUTION  
OF UNBOUNDED GEOMETRY PROBLEMS

*Omar M. Ramahi*  
*Digital Equipment Corporation*  
*146 Main Street*  
*Maynard, MA 01754-2572*

When using the finite difference time domain or finite element methods to solve open region radiation or scattering problems, it is necessary to truncate the mesh region with an absorbing boundary condition (ABC) whether the geometry under study is finite or unbounded in size. For the class of open region problems involving finite size geometries, such as scattering from a sphere, one can always enforce the ABC at a comfortable distance away from the scatterer to ensure that the spurious reflections are kept to a minimum. For the class of geometries where the structure is infinite, such as microstrip structures, cavities embedded in infinite ground planes and microwave circuits, no matter how far the truncating boundary from the primary radiating structure is, there will always be spurious reflections arising not only from the use of the ABC itself, but also from the part of the structure where the truncation takes place. Although many earlier works have addressed the use of ABC in open region problems, little attention has been paid to the optimum choice of ABC when analyzing infinite size structures.

In this work, several ABCs were used in the finite difference time domain method to study the behavior of microstrip antennas and cavities. It was found that the Liao's absorbing boundary condition to be especially well-suited for truncating ground planes mostly encountered in microwave circuits. The distinguishing feature of the Liao's ABC from other common ABCs such as the Ingquest-Majda, Mur, Lindman, Bayliss-Turkel, ...etc., lies in its being an axial operator in the sense that it does not involve tangential derivatives. Numerical results and animated displays of the progression in time of field intensity will be presented for several 2-D and 3-D radiating structures. The results demonstrate how an axial absorbing boundary operator can be used to effectively eliminate reflections caused by structure truncation, even if the truncating boundary was chosen at a distance very close to the radiating structure.

## **The Performance of FDTD Absorbing Boundary Conditions for Buried Scatterers**

Kenneth Demarest\*, Richard Plumb, Zhubo Huang  
Radar Systems and Remote Sensing Laboratory  
Department of Electrical Engineering and Computer Science  
University of Kansas  
Lawrence, Kansas 66045

Recent advances in ground-penetrating radars and imagers have created a renewed interest in calculating the scattering characteristics of buried objects. In many ways, the finite-difference time-domain (FDTD) technique is ideally suited for calculating the scattering characteristics of objects buried in a lossy ground. Unlike integral equation techniques, where the presence of the large lossy-dielectric (ground) would demand an enormous increase in the number of unknowns necessary to solve the problem, FDTD can incorporate the characteristics of a lossy ground directly in the field advance equations of the half-space where the ground exists.

In spite of the obvious advantages of FDTD for modeling buried scatterers, one computational problem remains: the field advance equations along the outer boundary of the solution space. Unfortunately, the absorbing boundary conditions that are typically used in FDTD codes work best when the outer boundaries of the solution space are far enough away from the scattering centers of the geometry being analyzed so that the scattered fields behave locally like plane waves at the outer boundary. This usually poses no problem for scatterers in free space, since the distance from the outer boundary to the scatterer can be made large simply by increasing the size of the solution space.

For buried scatterers, however, the lossy ground is also a scatterer, at least as far as the FDTD field-advance equations are concerned. This means that a half-space ground will always extend to the outer boundary of the FDTD solution space, no matter how large the solution space is made. Hence, a 'blind' use of the usual absorbing boundary conditions near the interface between the air and the lossy-ground would be expected to produce non-physical reflections that corrupt the calculations.

In this presentation we will discuss the performance of absorbing boundary conditions when used for buried scatterers. Suggestions for improved performance will also be offered.



TUESDAY AM URSI-A SESSION T-U16

Room: Savery 249

EM FIELD MEASUREMENTS

Chairs: G. E. Miller, Boeing Defense and Space Group; D. Hess, Scientific Atlanta Inc.

8:20	Characterization of Sweeping Channel Nonlinearity for a Sampling Oscilloscope <i>W. Su, S.M. Riad, Virginia Polytechnic Inst. and State Univ.</i>	172
8:40	High Tc Superconductor Microwave Lines: Coplanar Waveguide Versus Microstrip Line <i>*M.A. Megahed, S. Shahpar, J. Pyon, S.M. El-Ghazaly, Arizona State University</i>	173
9:00	A Measure for the Quality of Anechoic Chambers <i>R.R. DeLyser, Univ. of Denver; *C.L. Holloway, National Center for Atmospheric Research</i>	174
9:20	A New 8-Term Error Model and Correction Equation for RCS Extraction <i>*A.S. Ali, United States Air Force Academy</i>	175
9:40	Utilization of Multiple Polarization Data for Aerospace Target Identification <i>*H.-J. Li, J.-Y. Lan, National Taiwan Univ.</i>	177
10:00	Break	
10:20	Development of a Full Scene Computer Model for Aircraft Landing <i>*P.A. Ryan, M.J. Gary, B.H. Hudson, J.M. Trostel, Georgia Inst. of Technology</i>	178
10:40	A New Technique for Calibration of Polarimetric Coherent-on-Receive Scatterometers <i>*A. Nashashibi, K. Sarabandi, Univ. of Michigan</i>	179
11:00	An Accurate Calorimetric Thermal Voltage Converter with Built-In Tee <i>*R.F. Clark, D.C. Paulusse, National Research Council</i>	180

**Characterization Of Sweeping Channel Nonlinearity  
For A Sampling Oscilloscope**

Wansheng Su and Sedki M. Riad  
Virginia Polytechnic Institute and State University  
Blacksburg, Virginia 24060, USA  
(Phone: +1-703-231-4469, FAX: +1-703-231-3362)

In a sampling oscilloscope, the nonlinearity of the time axis is directly related to the measurement accuracy of the transient parameters, such as transient time, pulse duration and time interval. The main difficulty in characterizing the sweeping channel nonlinearity is separating the nonlinearity of the signal channel from that of the sweeping channel. This paper presents an approach to characterize the sweeping channel nonlinearity by measuring standard sinusoidal signals.

In order to separate the nonlinearities from the two channels, two sinusoidal signals, one sine wave and one cosine wave, are used in this characterization. The assumption for this method is that the nonlinearity of the signal channel is relatively small. By neglecting the second order effects, the sweeping channel nonlinearity can be separated from the signal channel nonlinearity. For quality sampling oscilloscopes, this assumption usually holds true. The nonlinearity of the signal channel is only a few percent.

The method has been applied to characterize the sweeping channel nonlinearity for an HP54124 and a Tektronix 11801 sampling oscilloscope. Satisfactory results have been demonstrated by the method.

## High $T_c$ Superconductor Microwave Lines: Coplanar Waveguide Versus Microstrip Line

Mohamed A. Megahed\*, Shahpar Shahpar,  
Jung Pyon, and Samir M. El-Ghazaly  
Department of Electrical Engineering  
Arizona State University  
Tempe, Arizona 85287-5706

The potential advantages of high  $T_c$  superconductors, used in planar waveguiding structures, is the reduced losses of the lines, as compared to the normally conducting metal strips. The coplanar waveguide and the microstrip line are common planar structures used in both hybrid and monolithic microwave integrated circuits. Losses inside the high  $T_c$  superconductors and non-linearity need to be addressed, (M. Megahed et al., IEEE AP-S International Symposium, 1993).

Using a full wave analysis, the coplanar waveguide transmission line is compared to the microstrip line in terms of conductor loss and dispersion characteristics. The finite difference technique is used in the analysis presented in this paper. The method accounts for all the physical aspects of the superconducting materials, as well as satisfies the required electromagnetic boundary conditions. The field penetration effect is taken into consideration, which is especially needed when evaluating the losses for the propagating wave inside the superconducting guided structure. This approach fits the need for accurate computation of the dispersion characteristics of a superconducting transmission line. The solution is obtained by solving the eigenvalue problem for the finite difference set of equations. A comparison between the attenuation constant and the phase constant for the microstrip line and the coplanar waveguide will be presented. The aim of this paper is to assess the optimal microwave planar structure that exploits the interesting characteristics of high  $T_c$  superconductors and is convenient for specific applications.

Commission A

## A Measure for the Quality of Anechoic Chambers

Ronald R. DeLyser  
University of Denver  
Department of Engineering  
2390 S. York St., Denver, Co. 80208-0177

and

Christopher L. Holloway\*  
Remote Sensing Facility  
National Center for Atmospheric Research  
P.O. Box 3000, Boulder, CO 80307-3000

Return loss as a function of frequency and angle of incidence is typically studied to determine the quality of the absorbing material used in an anechoic chamber. This alone is not enough to determine the quality of an anechoic chamber, or to compare the quality of one anechoic chamber to another. While the information gained from return loss calculations and measurements as a function of angle is valuable, an overall measure of anechoic chamber effectiveness is necessary in order to compare different chamber designs. In this presentation, we discuss a new *chamber quality factor* based on the average of the reflection coefficient (or return loss) over all possible angles of incidence. We will show calculations of the reflection coefficients for typical materials used in these chambers. These calculations for the reflection coefficients are based on the models developed by Holloway and Kuester (EMC Symposium 1989 and EMC Trans. 1994). We will also show calculations and comparisons of this *chamber quality factor* for anechoic chambers with different types of absorbing materials.

## **A NEW 8-TERM ERROR MODEL AND CORRECTION EQUATION FOR RCS EXTRACTION**

Azar S. Ali  
Department of Electrical Engineering  
2354 Fairchild Drive, Suite 2F6  
United States Air Force Academy, CO 80840

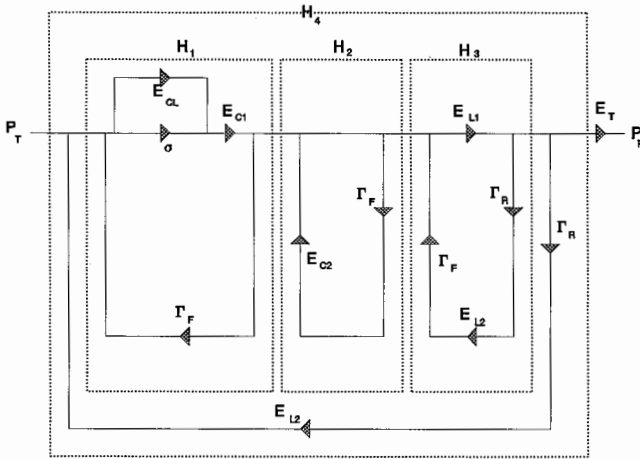
This paper presents a new 8-term error model and correction equation for extracting the radar cross section (RCS) of targets being measured in an enclosed radar range. It is more complete than the 2-term model in wide usage today.

In measuring the radar cross section of targets in an enclosed radar range, one gets errors. The errors increase as the target RCS increases. These errors are present in each of the typical range calibration measurements and manifest themselves as an increased noise floor in the image domain. The resultant elevated noise floor masks the RCS of smaller targets and often makes it impossible to distinguish one target from another.

At present, the RCS metrology community uses a 2-term error model in conjunction with a 2-term error correction equation to extract the RCS of the target under test. The 2-term error model incorporates the tracking and clutter terms. It does not account for many of the reflection induced errors. The mechanism for these increased errors is based on multiple reflections which occur between the target, the enclosed range, and the subsystems of the radar. For example there is always some degree of mismatch at the feed antenna and the receiver. There is also some loss in the cable between the feed antenna and receiver. These mechanisms are not accounted for by the 2-term error model presently being used.

While all of the reflection induced errors are difficult, if not impossible, to characterize, an improved 8-term error model and its corresponding error correction equation are developed. In addition to the tracking error and the target independent clutter, the new 8-term model accounts for the reflection coefficient at the receiver, the reflection coefficient of the receive antenna, the RF cable loss between the feed antenna and the receiver, the range transfer function for a target in the quiet zone, and a second major clutter source such as a subreflector.

The new 8-term error model and its correction equation are used to reduce the effects of reflection induced errors. This new pair provides a more accurate measure of the true RCS of the target when tested in an enclosed radar range. Specific techniques which can improve RCS measurement accuracy are also suggested.



Flow graph of improved error model for RCS measurements.

## UTILIZATION OF MULTIPLE POLARIZATION DATA FOR AEROSPACE TARGET IDENTIFICATION

\*  
Hsueh-Jyh Li and Jong-Yuan Lan  
Department of Electrical Engineering  
National Taiwan University  
Taipei, Taiwan, R. O. C.

Aerospace target identification with range profiles as the feature vector representations has been discussed in [1,2], where range profiles of a single polarization combination were used as the data base and two identification approaches, the matching score (MS) approach and the neural network (NN) approach, were employed to identify the targets. It is well known that fields from different polarization combinations (for examples, vertical - vertical V-V, vertical - horizontal V-H, horizontal - vertical H-V, and horizontal - horizontal H-H ) can carry or enhance certain important information. If data measured from all polarization combinations can be fully utilized to identify a target, it is expected that the recognition rate can be increased due to the increase of information contained.

In this paper five airplane models are chosen as the known targets. Their measured V-V, V-H, H-V, and H-H range profiles are used as the feature vector representation. When an unknown target is present and its 4 polarization combination range profiles are measured, we use several different decision rules: a majority vote rule, a maximum isolation distance rule, and a rule combining the above two rules, to determine the target class. Recognition performance obtained by different approaches (the MS approach and the NN approach) and different decision rules are compared. Effect of Gaussian noise on the recognition rates using the MS approach and the NN approach is also studied and compared. We have found that the MS approach is more robust to the Gaussian noise contamination.

### Reference

1. H. J. Li and S. H. Yang, IEEE-AP, 41, pp. 261-268, 1993
2. H. J. Li and V. Chiou, J. of EM Waves and Applications, 7, p.873-893, 1993

## Development of a Full Scene Computer Model for Aircraft Landing Applications

Patricia A. Ryan\*, Molly J. Gary, Brian H. Hudson, and John M. Trostel  
Georgia Tech Research Institute  
Georgia Institute of Technology  
Atlanta, Georgia 30332

A computer model for predicting the Millimeter Wave (MMW) radar return from an airport setting is in development to aid in quantifying the hardware requirements for MMW imaging radar for aircraft landing applications. In the Synthetic Vision Technology Demonstration (SVTD) Sensor Tower Test, 35 GHz and 94 GHz real aperture imaging radars were used to collect measured image data of an airport setting in clear weather, fog and rain conditions. This presentation discusses the scene geometry and reflectivity model development. Simulated imagery is compared to measured imagery for model evaluation.

A terrain class grid and a terrain elevation profile for the scene were constructed using Georgia Tech's GTVISIT program. Inputs included a map of the scene, photographs and observations from a site visit. Georgia Tech radar models are used to compute the radar returns as seen from an isotropic source of the scene geometry described by the terrain class map, terrain elevation profile and discrete object facet models. Z-buffering techniques are used to compute object on terrain, terrain on object, and terrain on terrain shadowing. As the mean depression angle to the scene is 3 degrees, Barton's Constant Gamma model developed for ground based radar (D. K. Barton, Proc. of the IEEE, 2, 198-204, 1985.) is used to compute the mean reflectivity from the terrain areas. A Weibull distribution is used to model the spatial distribution of the terrain returns. Currently, weather effects are included as a global scene attenuation factor.

The modeled scene imagery is compared to the measured imagery based on visual inspection, received power profile at constant range and runway/surrounding grass contrast as a function of range. A series of rectangular patches that extend into the surrounding grass is defined along the runway for computation of the runway/surrounding grass contrast. The model correctly predicts the runway width as being 6 cells, however the Weibull distribution for terrain returns does not predict the cell to cell variation in received power for the grass regions.

For making hardware design tradeoffs, the terrain model must represent the spatial and temporal variations of terrain return. Also, the weather model should account for particle drop size distribution and scattering. An improved weather and obscurant model that accounts for scattering and attenuation are in development at Georgia Tech. Analysis of the measured data to define critical image metrics will aid in the development of better terrain and weather models.

## **A New Technique For Calibration Of Polarimetric Coherent-On-Receive Scatterometers**

Adib Nashashibi\*, Kamal Sarabandi, and Fawwaz T. Ulaby  
Radiation Laboratory  
Department of Electrical Engineering and Computer Science  
The University of Michigan Ann Arober, MI  
Ann Arober, MI 48109-2122

### **Abstract**

Coherent-on-receive (COR) technique is the only reliable method for measurement of polarimetric backscatter response of distributed targets at millimeter wavelengths. The receiver of a COR scatterometer is capable of measuring coherently the two orthogonal components of the scattered fields in response to any transmitted polarization. Therefore, the scattered stokes vector corresponding to any transmitted polarization can be computed from which the Mueller matrix of a distributed target is constructed. The standard method for calibration of a COR scatterometer requires the use of an odd-bounce target with known RCS, in addition to a wire grid polarizer positioned in front of the receiving antenna at three different sequential orientations. This technique is usually limited by the cross-polarization isolation of the wire grid polarizer and its accuracy is hampered by the near field interaction of the wire grid polarizer with the receiving antenna.

In this paper, an accurate and convenient calibration technique for COR scatterometers is proposed. In this method the systematic errors are taken into account using an error model which include the cross-talk factors of the transmitting and receiving antennas, channel imbalances, and phase characteristics of the transmitter polarizers. A metallic sphere and any depolarizing target are required to be measured at four different polarizations in order to determine the system distortion parameters. The knowledge of the scattering matrix of the depolarizing target is not needed. Once the antennas cross-talk factors, which are time invariant parameters, are determined, only a single sphere is needed for characterizing the other distortion parameters.

Validity of the new calibration technique is examined using two COR scatterometers operating at 35 and 94 GHz. The Mueller matrix of independent point targets with known scattering matrices are compared to those measured by the scatterometers. This method is also extended so that the differential Mueller matrix of distributed targets can be measured accurately by characterizing the radar distortion parameters over the entire radiation pattern.

## AN ACCURATE CALORIMETRIC THERMAL VOLTAGE CONVERTER WITH BUILT-IN TEE

Richard F. Clark\* and David C. Paulusse  
Institute for National Measurement Standards  
National Research Council  
Ottawa, Canada K1A 0R6

Coaxial calorimeters constructed for use as microwave power standards have been used for many years as standards for voltage measurement at high frequencies. They have good characteristics for use at lower frequencies but the uncertainties associated with the input connector combined with the low input impedance of the calorimeter result in an unacceptably high uncertainty at a frequency such as 1 MHz. This problem can be solved by constructing a standard calorimetric thermal voltage converter with an integral Tee to be used for feeding input voltage into the standard and the thermal converter which is being calibrated. If, in addition, the coaxial input to the load resistor is made of thin-walled tubing, as is usual for coaxial calorimeters, the losses over the frequency range from d.c. to 1 MHz are virtually constant and so do not cause an appreciable ac-dc difference.

As shown in Fig. 1, the thermally insulating input coaxial line to the terminating resistor has an inner conductor of 304 stainless steel with outside diameter 0.065" and wall thickness 0.0025". The outer conductor has an inside diameter 0.173" and a wall thickness of 0.0035" and is made of the same material. The center conductor of the input feed line to the Tee is also stainless steel tubing with O.D. 0.032" and wall thickness of 0.002". The cylindrical resistor has a beryllium oxide dielectric for good thermal conductivity and is connected to the outer conductor by a 0.002" thick copper disc. The thermopile is made from a wound spiral of 0.001" diameter constantan wire 3/4 plated with copper. The thermopile is electrically insulated from the outer conductor of the resistive termination with a thin beryllium oxide washer. The cold junction of the thermopile is a composite of various copper blocks designed to support the thermopile and to permit assembly of the Tee. Copper block B provides partial support of the two flanged connectors (an SMA-female for the input to the Tee and a type N-female for connection of the thermal converter to be calibrated) and allows the open soldering of the center-conductor junction of the Tee.

A calculation of the expected voltage variation between the center of the Tee and the resistor was made for two values of resistance. The ac-dc difference due to the combination of resistive line loss, standing-wave and resistive loss in the 0.002" thick copper end plate would be +0.11 ppm at 1 MHz rising to +1.0 ppm at 3 MHz for a 250 ohm termination while the ac-dc difference for a 50 ohm resistor would be -0.15 ppm at 1 MHz and -1.4 ppm at 3 MHz.

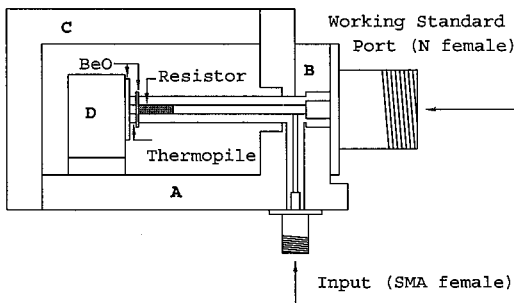


Fig. 1 Stylized view of the calorimetric thermal voltage converter.  
A, B, C, and D are copper blocks.

TUESDAY AM URSI-D SESSION T-U17

Room: HUB 200

MICROWAVE AND MILLIMETER WAVE DEVICES I

Chairs: L.P. Katehi, G.M. Rebeiz, The University of Michigan

8:20	Broadband Tunable Quasi-Optical Oscillators <i>*R.M. Weikle, II, Univ. of Virginia</i>	182
8:40	Monolithic 60 GHz PHEMT Oscillator <i>*M.J. Vaughan, R.C. Compton, Cornell Univ.; S. Weinreb, Martin Marietta Laboratories</i>	183
9:00	Development of a New Miniature Ring Hybrid and Its Application in a Balanced Mixer <i>*C. Nguyen, Texas A&amp;M Univ.</i>	184
9:20	A 4 GHz Image Reject Mixer Utilizing a Custom Monolithic GaAs IC <i>*E. Kpodzo, M. Suthers, G. Rabjohn, N. Reed, G. Boucher, B. Syrett, Bell-Northern Research Ltd.</i>	185
9:40	Four-Element Integrated Receiver Array for Digital Beamforming <i>*P. Jarmuszewski, McMaster Univ.; Y. Shen, Harris Farinon Canada; C. Laperle, Universite Laval; J. Litva, McMaster Univ.</i>	186
10:00	Break	
10:20	An Ultra Low Cost and Miniature 950-2050 MHz GaAs MMIC Downconverter <i>*T.H. Hsieh, H. Wang, T. Wang, National Chiao-Tung Univ.; T.H. Chen, Y.C. Chiang, S.T. Tseng, A. Chen, Y.E. Chang, Hexawave Photonic System, Inc.</i>	187
10:40	Mixed Lumped and Distributed Models for HEMT Devices Up to 100 GHz <i>*E.M. El-Rabaie</i>	188
11:00	Limitation of Using the Compact DC Models of GaAs MESFET for Large Signal Computer Calculations <i>*E.M. El-Rabaie</i>	189
11:20	Low Cost Dual-Mode Discriminators for Narrowband Microwave Receivers <i>M.M. Mosso, A. Podcameni, Catholic Univ. of Rio de Janeiro</i>	190
11:40	Chaotic Instabilities of Gunn-Diode Circuits <i>D. M. Vavriv, Cukurova Univ.</i>	191

## BROADBAND TUNABLE QUASI-OPTICAL OSCILLATORS

Robert M. Weikle, II

Department of Electrical Engineering  
University of Virginia  
Charlottesville, VA 22903-2442 U.S.A.

*Abstract*— Over the past several years, quasi-optical power combining has been shown to be a feasible and attractive alternative to traditional power combining methods based on waveguide technology. In addition, quasi-optical arrays, or grids, can be designed to perform many of the functions associated with more conventional microwave circuits, including frequency multiplication, detection and mixing, and amplification. The advantages of the quasi-optical approach are numerous and well-documented. The distribution of power over a large number of devices results in a corresponding increase in dynamic range. Waveguide sidewalls and their associated losses and machining tolerances are eliminated. Quasi-optical arrays are compatible with planar IC fabrication technology, making large-scale power combining possible. Furthermore, it is possible to model many quasi-optical arrays using simple transmission-line circuits, thus allowing grids to be designed using standard microwave circuit techniques and the wide variety of computer-aided engineering software packages now available.

Unfortunately, the performance and flexibility of power combiners based on planar grids is somewhat limited by their narrow tuning bandwidths (typically only a few percent). The narrow frequency tuning range is mainly a result of the physical configuration of the array. The planar grid into which devices are embedded is essentially a frequency selective surface. As a result, the impedance presented to devices in the array is a strong function of frequency. This impedance, which governs the behavior of the devices and determines the grid's overall performance as an oscillator, depends on the geometry of the array and is not readily adjustable.

In this paper, we discuss a new planar grid oscillator design which includes GaAs FET's and integrated varactor tuners. The varactor diodes permit the impedance of each transistor to be tuned. Simulations using a grid equivalent circuit model indicate that tuning bandwidths of over 50% can be achieved. The design and preliminary results for a 16-element 10-18 GHz planar oscillator array will be presented.

## Monolithic 60 GHz PHEMT Oscillator

M. J. Vaughan\* and R. C. Compton  
*School of Electrical Engineering*  
*Cornell University, Ithaca, NY 14853*

S. Weinreb  
*Martin Marietta Laboratories*  
*1450 South Rolling Road*  
*Baltimore, MD 21227*

This paper presents a first-pass 60 GHz monolithic oscillator based on a pseudomorphic High Electron Mobility Transistor (pHEMT). Measurements have shown 9 mW of CW output power at a dc-to-rf efficiency of 5%. With variation of the dc bias voltages and operating temperature, output frequencies from 58.4 GHz to 59.2 GHz are observed. The variations of the operating characteristics with changes in bias conditions are correlated with non-linear simulations based on a small-signal equivalent circuit model of the FET combined with dc I-V measurements.

The circuit was designed using a pseudo-linear technique that relies on modifying small-signal FET s-parameters for simulating large-signal operating conditions. Coplanar-waveguide (CPW) is used for the transmission lines on the 100  $\mu\text{m}$ -thick substrate, with a "resonant-tee" structure incorporated for frequency stabilization. The output power is coupled from the chip into rectangular waveguide via an integrated CPW-to-waveguide transition (E-plane probe).

Measurements of operating frequency versus temperature suggest a simple means of stabilization against temperature variation. Over the measured 25°–95°C range the frequency changes linearly with temperature with negligible hysteresis. Consequently, with a voltage-controlled-oscillator (VCO) version of this circuit, which could be constructed using another FET as a varactor, frequency stabilization can be provided utilizing feedback from an integrated diode temperature sensor.

# DEVELOPMENT OF A NEW MINIATURE RING HYBRID AND ITS APPLICATION IN A BALANCED MIXER

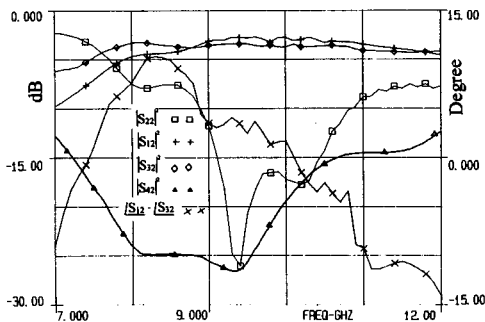
CAM NGUYEN

Department of Electrical Engineering  
Texas A&M University  
College Station, Texas 77843-3128

## ABSTRACT

180-degree hybrids are important building blocks in many balanced microwave circuits such as amplifiers, mixers, oscillators, and multipliers. Among them, the ring hybrid or rat-race is perhaps one of the most commonly used components due to its simplicity. This circuit has a circumference of one and a half wavelengths at the design center frequency and is, thus, relatively large. Hybrids of smaller geometry are needed to achieve compact microwave integrated circuits (MICs), especially microwave monolithic integrated circuits (MMICs) where real estate is very expensive.

In this paper, we report a newly developed compact 180-degree ring hybrid. As compared to the conventional ring hybrid, this component has only one wavelength in circumference and, consequently, occupies a smaller circuit area. Simple equations characterizing the scattering (S) matrix are derived. Design information as well as performance of a fabricated ring at X-band (8-12 GHz) are presented, which confirms the 180-degree hybrid nature. To demonstrate its use in balanced circuits, we also built and tested a microstrip singly balanced diode mixer using the new ring at X-band. Its measured performance, less than 6.5-dB conversion loss and more than 25-dB LO-RF isolation, is comparable with those using conventional ring hybrids. The new ring provides an alternative yet compact structure to the conventional ring and should be useful for realizing compact balanced MICs and MMICs.



Measured performance  
of the new ring.

## A 4 GHz Image Reject Mixer Utilizing a Custom Monolithic GaAs IC

E. Kpodzo\*, M. Suthers, G. Rabjohn, N. Reed, G. Boucher and B. Syrett  
Bell-Northern Research Ltd., Box 3511 Stn. C, Ottawa, Ont., Canada K1Y 4H7

### Abstract

The design of an image reject mixer covering 2.7 to 5.7 GHz is described. The mixer consists of two mirror image double balanced diode mixers with integral LO buffers on a single GaAs MMIC. A thin film Lange coupler is connected to the LO ports to obtain LO phase quadrature between the two mixers while the two RF ports are connected via a thin film Wilkinson coupler to achieve splitting or combining of the RF signal. A conventional IF hybrid is connected externally to the IRM to complete image reject mixing. The mixer exhibits a flat 7.0 dB conversion loss and image rejection in excess of 25 dB over a 1 dB bandwidth from below 3.5 GHz to over 5.5 GHz and the P1dB point is over +6 dBm for Pout, with phase rotation less than 3 degrees at this signal level. The complete device fits into a butterfly package with dimensions of 1.0 X 0.75 X 0.25 inches. The IRM is presently in production at Northern Telecom Electronics Limited for the 512 QAM Digital Microwave SONET Radio RNS 4/40.

FIG. 1

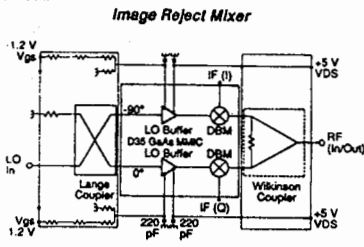


FIG. 2

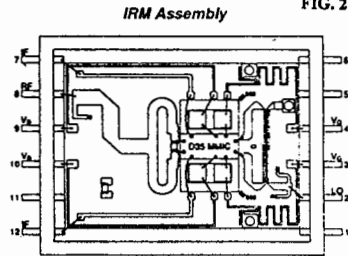
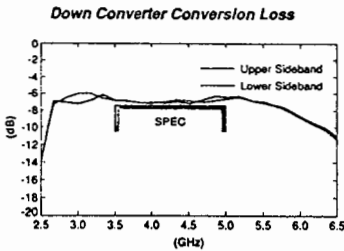
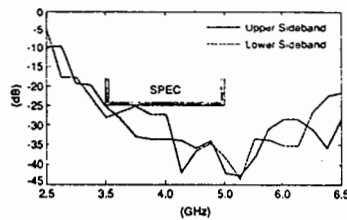


FIG. 3



**Up Converter Image Rejection**

FIG. 4



## Four-Element Integrated Receiver Array for Digital Beamforming

*P. Jarmuszewski\*, Y. Shen\*\*, C. Laperle\*\*\*, J. Litva  
Communications Research Laboratory, McMaster University  
Hamilton, Ontario, Canada, L8S 4K1*

*\*\* Harris Farinon Canada, Montreal, Canada*

*\*\*\* Department de genie electrique, Universite Laval, Quebec, Canada*

The advantages of digital beamforming for radar and communications have been recognized for many years. Advantages include improved adaptive pattern nulling and multiple beams where all of the information available at the aperture is preserved. The technology needed to implement a compact digital beamformer has not been available until recently. The speed and density of integrated circuits has advanced to the stage where it is feasible to design an integrated digital beamforming system. This paper will describe a recent digital beamforming (DBF) receiver array system.

A C-band multi-layer four-element integrated receiver array for DBF has been designed and implemented. Each receiver in the array uses double-down conversion and is IF sampled. The layers of the array are shown in Fig. 1. The receiver circuitry is integrated with the antenna by directly placing it under the antenna elements. Received signals are detected at the element level and are converted to digital outputs using A/D converters. The resulting digital signals are processed via a computer to form the desired beam. Fig. 2 shows the beam pattern of the array, the incident signal in this case is normal to the plane of the array. As a means of achieving precise pattern control (low sidelobes, adaptive nulling and high resolution) over large bandwidths and large dynamic ranges, the use of self-calibration techniques were studied and evaluated. Simulations based on Omnisys for single receiver elements are also discussed. Finally, preliminary measurement results of the array will be presented.

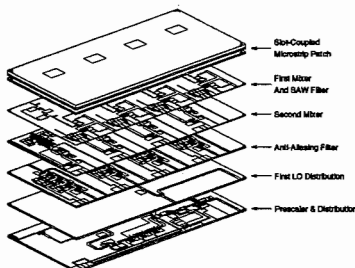


Figure 2: Receiver Array

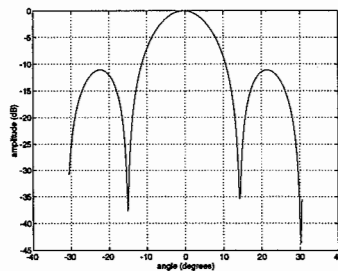


Figure 2: Beam Pattern

## **An Ultra Low Cost and Miniature 950-2050 MHz GaAs MMIC Downconverter**

T.H. Hsieh\*, H. Wang, Tahui Wang

Department of Electronics Engineering & Institute of Electronics  
National Chiao-Tung University, Hsin-Chu, Taiwan, R.O.C.

T.H. Chen, Y.C. Chiang, S.T. Tseng, Andy Chen, and Y.E. Chang

Hexawave Photonic System, Inc.  
Hsin-Chu, Taiwan, R.O.C.

Frequency conversion of RF signals is usually required in microwave systems. A down-converter performing this function may consist of a mixer, an oscillator, several amplifiers, and possibly a variable gain controller. Recent advances in GaAs material and processing have made it possible to integrate many of these functions on a single chip. The benefits of monolithic integration include reduced assembling cost, increased reliability, and reduced weight and size of receiver components. For high volume consumer applications, such as direct broadcast satellite (DBS) and cable television (CATV) converter, cost is the major concern.

The objective of this work is to develop a 950-2050 MHz cost-effective down-converter for satellite receivers. The monolithic downconverter is fabricated using a 1- $\mu\text{m}$  gate-length, ion-implanted GaAs MESFET process technology without through substrate via hole. Such a simple fabrication process can be of great advantage of the cost and throughput. A 950-2050 MHz RF input signal of the downconverter is converted by a 1430-2530 MHz LO to an IF signal of 480 MHz. This chip is highly integrated, including an RF LNA, a dual gate FET mixer, a varactor tuned oscillator, and an IF variable gain amplifier. The chip size is 1.4x1.5x0.18 mm<sup>3</sup>.

The primary design goals for this downconverter include the following: (1) 50-dB conversion gain, (2) 4-dB noise figure, (3) more than 40-dB gain control range, and (4) 50-dBc third-order intermodulation distortion. The performance meets the DBS receiver requirements. The design and performance of each component as well as the downconverter integration will be presented in the meeting.

# **Mixed Lumped and Distributed Models for HEMT Devices up to 100 GHz**

**Dr. S. El-Rabaie, Senior Member, IEEE**  
Faculty of Electronic Engineering  
32952 Menouf, Egypt

## **Abstract**

In this paper a mixed lumped and distributed model for HEMT devices up to 100 GHz is presented. The parameters of the proposed model can readily be evaluated either by the standard software packages or by the more recent published extraction techniques. The proposed model not only exactly fits the measured parameters in the range of the system measurement accuracy, but also it predicts with a high degree of accuracy the device parameters up to 100 GHz.

## **Limitations of Using the Compact DC Models of GaAs MESFET for Large Signal Computer Calculations**

**Dr. S. El-Rabaie, Senior Member, IEEE**  
Faculty of Electronic Engineering  
32952 Menouf, Egypt

### **Abstract**

In the literature a large number of compact DC models of GaAs MESFET and HEMT for large signal computer calculations. It becomes very hard for writers of nonlinear simulators to choose the proper model that fits the required application. In this letter we show by numerical investigations on the more recent published models in the literature, that the lack of coincidence of the simulation and experimental results for the sever nonlinearities (multiplier and mixer applications) is mainly due to the improper choice of the appropriate compact DC model.

**LOW COST DUAL-MODE DISCRIMINATORS  
FOR NARROWBAND MICROWAVE RECEIVERS**

Marbey M. Mosso and Abelardo Podcameni

CETUC - Catholic University of Rio de Janeiro

225 Marques de Sao Vicente - Rio de Janeiro - 22453-900 - Brazil

FAX - +(55-21) 294-5748

Narrowband Microwave Receivers are useful for VSAT, TVRO-SAT, remote sensing and mobile communications. In all cases, low cost is at a premium. Here, it will be described an FM low-cost homodyne narrowband microwave receiver which uses an original dual-mode frequency or phase discriminator for demodulation, as shown in Figure 1, where the cavity is loaded with a dielectric resonator.

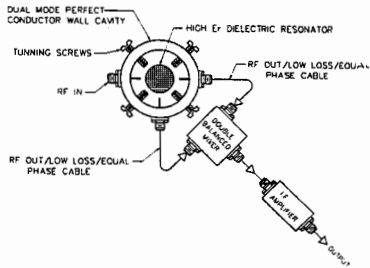


**Figure 1 - Simplified View of the Dual-Mode Receiver**

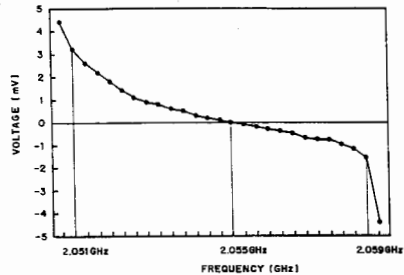


**Figure 2 - Discriminator Output Voltage x Signal Input Frequency**

At Figure 1, when the incoming RF is fed from antenna and LNA to the dual-mode cavity, at the  $HE_{11}$  resonant frequency, the 45 degree tuning screws will generate two orthogonal signals. The double balanced will furnish a null, at this frequency. When the incoming signal is a narrowband frequency swept one, the mixer output will be a cosine; the pair cavity-mixer perform the role of a frequency or phase discriminator. The demodulated signal is readily available.

A practical receiver was implemented at 2 GHz, using low-loss Trans-Tech Dielectric Resonator. An useful bandwidth from 8 to 40 MHz is easily achieved according to the in/out probes penetration, which varies the cavity loading. At Figure 2 it is seen the discriminator voltage with respect to the incoming frequency, with the discriminator settled for 8 MHz bandwidth.

The described configuration yields a reliable, easily-integrated and low-cost microwave receiver.

## CHAOTIC INSTABILITIES OF GUNN-DIODE CIRCUITS

Dmitry M. Vavriv  
Institute of Radio Astronomy, 4 Krasnoznamenaya St.,  
310002 Kharkov, UKRAINE

**SUMMARY.** The main regularities of the arising of chaotic instabilities in millimeter wave Gunn-diode circuits are summarized. We have found that the dynamical chaos can produce strong effect on the circuits stability, their output noise level. This fact is illustrated by the results of theoretical and experimental studies of Gunn-diode amplifiers and synchronized oscillators. The conditions and mechanisms of the instabilities arising, the properties of excited oscillations are also discussed.

**RESULTS.** The two main factors are responsible for the initiation of chaotic instabilities in Gunn-diode circuits: at first, the reactive nonlinearity of the majority of real mm-devices and, secondly, the interaction of several independent frequencies excited in a circuit. These independent frequencies can be, for example, some spectral components of amplified signal. The results indicate, that the stable amplifier operation at a harmonic input signal does not guarantee that it will work in the same way with real, multi-frequency signals. The most dangerous excitation (from the point of view of the stability) is that with distance between signal spectral components equal to the width of the mode absorption line. The increasing of the degree of reactive nonlinearity and the quality factor of the mode leads to the sharp decreasing of the chaos threshold with respect to the amplitude of the external force. The conditions of the instabilities arising do not qualitatively depend on the type of a diode as well as the external signal: amplitude, frequency, or phase modulated.

Chaotic instabilities of Gunn-diode oscillators can be caused by a variety of factors. They can arise, for example, as the result of the interaction of high-frequency oscillations as well as low- and high-frequency ones, or due to the interaction of an active mode with other modes. We have studied in more details the synchronized oscillators wherein the spectrum of the synchronizing signal includes a "parasitic" frequency component as well as the influence of low-frequency hindrance in the diode supply circuit.

The theoretical studies were carried out simultaneously with experiments on investigation of the chaotic instabilities of the circuits in the 8-mm wavelength band with different types of diodes. We have found that most of amplifiers and oscillators exhibit chaotic oscillations in finite regions of control parameters. The qualitative and quantitative relationship between theoretical and experimental results have been revealed. The principal result is that the conditions for the chaotic instabilities arising are not very stringent and they can manifest itself in a great number of practical situations.

We have to conclude that present knowledge of Gunn-diode circuits dynamics should be thoroughly revised and the most adequate description of such circuits must take into account possibilities of the chaos initiation.



TUESDAY AM URSI-B SESSION T-U18

Room: HUB 309

SCATTERING III

- Chairs: R. Haupt, U.S. Air Force Academy; R.J. Chiavetta, Boeing Defense and Space Group
- 8:20 Hybrid Analysis (MM-UTD) of EM Scattering by Finned Objects 194  
*\*M. Hsu, P.H. Pathak, The Ohio State Univ.*
- 8:40 Induced Current Extrapolation: A Technique for Solving Scattering Problems at High Frequencies 195  
*\*Z.G. Figan, R. Mittra, A. Boag, E. Michielssen, Univ. of Illinois*
- 9:00 Variational Method for Computing Scattering from Finite Sections of Dielectrically-Loaded Cylinders with Airfoil Profiles 196  
*\*R.J. Chiavetta, Boeing Defense and Space Group*
- 9:20 Hybrid Geometrical Optics/Physical Optics Applied to Structures Containing Penetrable Surfaces 197  
*J.R. Newhouse, D.H. Friedman, \*R.T. Brown, Lockheed Advanced Development Company*
- 9:40 Hybrid Geometrical Optics/Physical Optics Scattering by Complex Objects Involving Multiple Interactions 198  
*J.R. Newhouse, \*D.H. Friedman, R.T. Brown, Lockheed Advanced Development Company*
- 10:00 Break
- 10:20 Implementing the Hybrid Ray-FDTD Method for Computing the RCS of 3-D Open-Ended Waveguide Cavities 199  
*\*T. T. Chia, R. Lee, The Ohio State Univ.*
- 10:40 A New High Frequency Extrapolation Technique for RCS Computation of Complex Scatterers 200  
*\*S. Vermersch, D. Bouche, CEA/CESTA Laboratories; R. Mittra, Univ. of Illinois*
- 11:00 A Progressive Physical Optics Algorithm for Computing the EM Scattering by Jet Inlet Cavities 201  
*\*R.J. Burkholder, The Ohio State Univ.*
- 11:20 First Order Wedge Diffraction Associated with Repeatedly Interacting Surfaces 202  
*\*J.R. Newhouse, R.T. Brown, Lockheed Advanced Development Company*
- 11:40 Scattering from a Perfectly Conducting Wedge with a Small Aperture in a Face 203  
*A. Monorchio, \*G. Manara, Univ. of Pisa; R. Coccioli, G. Pelosi, Univ. of Florence*

## HYBRID ANALYSIS (MM-UTD) OF EM SCATTERING BY FINNED OBJECTS

Mimi Hsu\* and Prabhakar H. Pathak  
The Electrosience Laboratory  
Department of Electrical Engineering  
The Ohio State University  
Columbus, Ohio 43212

A hybrid combination of the method of moments (MM) and the uniform geometrical theory of diffraction (UTD) has been developed for treating electrically large, perfectly conducting, convex scatterers containing appendages which can be modeled by a set of perfectly conducting plates. Such a hybrid technique is useful for analyzing the high frequency radiation/scattering from complex aerospace vehicles in a far more efficient and tractable fashion than is possible by either the MM or the UTD alone. In this hybrid scheme, the integral equation for the currents induced on the scatterer by an external source involves a recently developed closed-form, UTD-based Green's function in the kernel. This Green's function, which was a result of being able to extend the UTD to predict the scattering due to near field sources, accounts for an arbitrarily-located source and observer in the presence of the large convex scatterer. As a consequence, in the hybrid MM-UTD scheme, the unknown surface currents are restricted to the region of the appendages. Therefore, when the MM is used to solve the integral equation for these currents, the resulting MM impedance matrix is significantly smaller than that in the conventional MM approach which uses the free-space Green's function, and which therefore requires the unknown currents to reside on the entire finned object rather than only on the fins. In the MM procedure, overlapping piecewise sinusoids are chosen as the basis functions for expanding the unknown surface currents on the appendages. These basis functions are particularly well-suited for use with the UTD Green's functions in this hybrid scheme.

These generalized UTD solutions together with the MM will be used to treat the electromagnetic radiation and scattering from elongated convex cylindrical objects with multiple fins attached which are electrically small in comparison with the main cylindrical body. Numerical results based on this hybrid analysis will be compared with those based on the conventional MM procedure and measurements where possible.

## INDUCED CURRENT EXTRAPOLATION: A TECHNIQUE FOR SOLVING SCATTERING PROBLEMS AT HIGH FREQUENCIES

Z. Gürkan Figen \*, Raj Mittra, Amir Boag and Eric Michielssen  
 Electromagnetic Communications Laboratory  
 University of Illinois, Urbana, Illinois 61801

A novel approach to the solution of the problem of high-frequency scattering from PEC bodies is presented in this paper. Numerically rigorous techniques, such as the Method of Moments (MoM), Finite Element Method (FEM), or Finite Difference Time Domain Method (FDTD) are extremely useful for solving electromagnetic scattering problems provided the size of the scattering body is not large compared to the wavelength. At high frequencies, the memory and CPU time can become prohibitively large and one typically resorts to asymptotic techniques such as, the GTD, UTD, and PTD. However, at intermediate frequencies, asymptotic techniques often do not offer the desired accuracy, and it becomes necessary to seek alternate methods that might bridge the gap between the low and high frequency regimes. In this paper, we present an induced current extrapolation technique that begins with the solution derived by using one of the numerically rigorous methods, e.g., the Method of Moments. The current density distribution on the scatterer is initially computed over a range of the wave number  $k$ , up to the highest frequency possible. The diffracted currents in the lit and shadow regions, which when added to the physical optics current yield the total current, are then expressed for each  $k$ , in terms of a superposition of exponentials. Next, inspired by the form of asymptotic solutions of associated canonical problems for the geometry of interest, the frequency behaviors of the weight coefficients of these exponentials are curve-fitted with functions of the type  $Ak^n$  or  $A+kn$ , by solving for the constants  $A$  and  $n$ . Finally, the frequency behaviors of these functions are extrapolated to yield the currents at higher frequencies for which the problem may be too big to be solved directly. Fig. 1 shows the comparison between the direct-numerical and extrapolated solutions for the induced current, derived by applying the procedure described above to an elliptic cylinder which is obliquely ( $45^\circ$ ) illuminated by a TM plane wave. The companion figure, Fig. 2, exhibits a similar comparison for the bistatic radar cross-section. The agreement between the two solutions is seen to be very good for this test problem. Also, it is found that the error current, defined as the difference between the direct-numerical and extrapolated currents, radiates little in the far field and, hence, the far-field results are even more accurate than those for the diffracted currents.

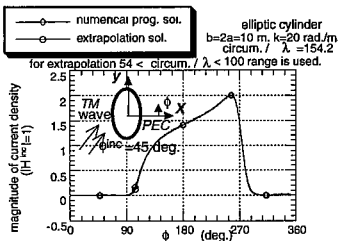


Fig. 1.

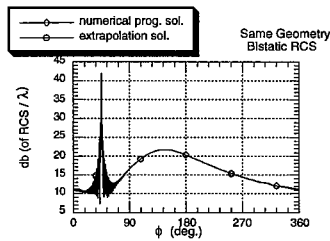


Fig. 2.

VARIATIONAL METHOD FOR COMPUTING SCATTERING FROM  
FINITE SECTIONS OF DIELECTRICALLY-LOADED CYLINDERS WITH  
AIRFOIL PROFILES

Robert J. Chiavetta  
Boeing Defense and Space Group  
P.O. Box 3999; Mail Stop 82-11  
Seattle, Washington (98124)

This paper addresses the development of improved non-computationally-intensive scattering models for cylindrically-extruded sections of airfoil profiles. Present non-moment method techniques for treating scattering from these bodies are based on the Uniform Theory of Diffraction (UTD) or Physical Theory of Diffraction (PTD) for scattering by airfoil-shaped profiles in two dimensions, and applied to cylindrically-extruded sections in three dimensions. Primarily perfectly-conducting bodies are considered; attempts to account for attenuation by absorbing materials or dielectric-loading are accounted for through the use of empirical reflection coefficients or "scale factors". The extension to three dimensions from the canonical two-dimensional scattering theory is carried out through multiplication by the appropriate " $\sin x/x$ " factor to account for the finite illuminated length and the oblique scattering geometry. It is shown in this paper with accompanying data that this approach is inadequate for finite length sections with dielectric loading.

A method for computing bistatic scattering from cylindrically-extruded airfoils with dielectric loading is described. The method is based on the variational formulation and Rayleigh-Ritz method, and is applicable at low and high frequencies to bodies whose length along the direction of cylindrical symmetry is large compared to their profile characteristic dimensions. At lower frequencies, the trial functions for the equivalent electric and magnetic currents on the surface of the body are obtained from *two-dimensional* moment method solutions. At high frequencies, the trial functions are based on equivalent line currents.

The method was validated by application to oblique scattering from homogeneous dielectric cylinders for which scattering data is available. Additional computations were made for a finite section of dielectric airfoil with NACA profile.

# Hybrid Geometrical Optics/Physical Optics Applied to Structures Containing Penetrable Surfaces

James R. Newhouse, Daniel H. Friedman and \*Robert T. Brown  
Lockheed Advanced Development Company  
Dept. 25-52, Bldg. 311, Plant B-6  
P.O. Box 250  
Sunland, California 91041

Hybrid geometrical optics beamtracing/physical optics algorithms that have been developed for calculating multiple interaction contributions to high-frequency scattering have been successfully extended to the case of faceted bodies containing penetrable surfaces. The basic hybrid GO/PO approach consists of specular reflection between interacting surfaces, with a bistatic PO contribution to the scattered field calculated from each illuminated surface that is also visible to the receiver. Full geometric shadowing is employed, so at each reflection the ongoing beam may be redefined based both on the illuminated portion of the target facet, and the portion of the incident beam intercepted.

In the extension to penetrable surfaces, in addition to specular reflection plus bistatic physical optics at each surface, transmission may occur. The incident beam will penetrate a surface having a finite transmission coefficient, leading to further beams proliferation. The algorithm thus consists of geometrical optics reflection, transmission if necessary, and bistatic physical optics scattering at each surface as required. The method has been validated against a finite Salisbury screen consisting of a square metal plate and a resistive sheet, shown in Fig. 1, and other simple cases with known solutions.

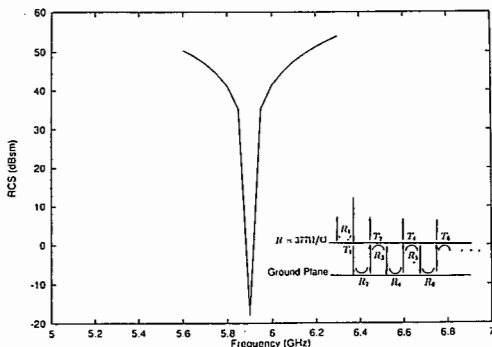


Figure 1: Calculated backscatter from a finite Salisbury screen.

# Hybrid Geometrical Optics/Physical Optics Scattering by Complex Objects Involving Multiple Interactions

James R. Newhouse, \*Daniel H. Friedman and Robert T. Brown  
Lockheed Advanced Development Company  
Dept 25-52, Bldg. 311, Plant B-6  
P.O. Box 250  
Burbank, California 91041

The methods of physical optics combined with the physical theory of diffraction (PO/PTD) have proven extremely valuable in predicting electromagnetic scattering from electrically large targets. However, these methods have several well-known limitations. They are generally useful only for convex structures, in which multiple interactions can be neglected. In addition, the basic theory is valid only for impenetrable surfaces. This paper will describe the development of hybrid geometrical optics/physical optics (GO/PO) methods which are found to give excellent results for a large variety of complex geometries. Scattering surfaces may be perfectly conducting, may be described by an IBC, or by complex reflection coefficients. Reflection coefficients may be calculated from multilayer coating descriptions in the local plane-parallel approximation, read from an input file, or based on an equivalent IBC obtained from a MoM calculation.

The methods have been validated against a large number of test cases, including electrically large cavities, both conducting and with coated surfaces. In most cases the results obtained with the methods described here are in excellent agreement with either measured data, exact modal solutions, or in-principle exact solutions such as the method of moments. The number of multiple interactions to be considered may be set by the user, or controlled by a threshold contribution to the scattered field. For a 60° dihedral or a 90° trihedral it has been found that triple bounces are the highest that make a significant contribution. For rectangular cavities, on the order of 100 bounces must be considered at incidence angles far from normal. Since the most computationally intensive part of the calculation consists of a large number of simple beam-tracing interactions, the method is very fast. Typical run times for a large cavity are a few minutes on a Silicon Graphics work station. The beam-tracing portion of the calculation is also frequency independent, allowing a set of frequencies to be covered in much less than the time required to carry out the calculations separately.

**IMPLEMENTING THE HYBRID RAY-FDTD METHOD  
FOR COMPUTING THE RCS OF  
3-D OPEN-ENDED WAVEGUIDE CAVITIES**

T. T. Chia\* and R. Lee

ElectroScience Laboratory  
Department of Electrical Engineering  
The Ohio State University  
1320 Kinnear Rd.  
Columbus, Ohio 43212-1191

A hybrid method which combines the Generalized Ray Expansion (GRE) method with the finite difference time domain (FDTD) method has recently been introduced to analyze the electromagnetic scattering from the interior of two-dimensional (2-D) open-ended waveguide cavities (R. Lee & T. T. Chia, *IEEE Trans. Antennas Propagat.*, Nov. 93). This hybrid ray-FDTD method combines the efficiency of the GRE method with the modeling flexibility of the FDTD method and has been shown to produce accurate radar cross-section (RCS) results for electrically large 2-D cavities with complex terminations.

In this paper, we describe the implementation of the hybrid ray-FDTD method for analyzing the scattering from 3-D cavities and provide some representative results. The implementation in 3-D provides a new set of issues to be dealt with. For example, the number of unknowns in the FDTD grid and the number of rays used in going from a 2-D geometry to a 3-D geometry increase tremendously. Moreover, the second order Mur's absorbing boundary condition and the different schemes for coupling GRE and FDTD used in the 2-D case may not be effective or efficient for use in 3-D.

In the 3-D implementation of the hybrid method, the modeling of the ray and FDTD sections of the cavity are decoupled so that the two sections can be characterized independent of one another. For the FDTD section, waveguide modes are used to characterize the termination in terms of a modal reflection matrix. In addition, a pulsed time variation is used so that multiple reflection matrices can be obtained for a wide range of frequencies. For the ray section, a "fire-and-forget" approach is used to track each ray from the aperture to the interface between the ray and FDTD sections of the cavity. The "incident" field on the interface due to each ray is expressed in terms of modes via an efficient numerical gridding scheme. From the "incident" modal coefficients and the reflection matrix, the scattered field can be obtained via the modal form of the termination reciprocity integral.

## A NEW HIGH FREQUENCY EXTRAPOLATION TECHNIQUE FOR RCS COMPUTATION OF COMPLEX SCATTERERS

S. Vermersch\*<sup>†</sup>, D. Bouche<sup>†</sup> & R. Mittra<sup>††</sup>

<sup>†</sup>CEA/CESTA Laboratories, Le Barp, France

<sup>††</sup>EMC Laboratory, University of Illinois, Urbana, IL, U.S.A.

The computation of radar cross-section of electrically large objects is a challenging task because the asymptotic techniques are often not as accurate as desired, and the numerically rigorous techniques are severely limited by the cpu time and available memory of the present computers. Two recent papers by Bouche, Mittra, Vermersch, Gay and Leroy (1993 AP-S Digest, pp. 1420-1423), and R. Mittra and D. Bouche (1993 URSI Abstracts, p. 76), have proposed ways to circumventing this problem by using different types of extrapolation techniques, and have presented some numerical examples illustrating the application of these techniques.

In this paper, we take another look at the problem and present a new extrapolation-based approach for computing the RCS of complex targets at high frequencies. In common with the two previous techniques referred to above, the first step in the process is still the computation of the scattering characteristics of the target by using a numerically rigorous scheme over a relatively narrow range of frequencies. Next, the bright points on the object are identified, numerically, from the Fourier transform of the computed bistatic RCS vs. frequency characteristics of the object. The bistatic RCS calculation is carried out in the usual manner by first solving for the induced current on the scatterer and then computing, for a fixed angle of incidence, the scattered far field for a range of observation angles. Once the locations of the bright points have been determined, a parametric model for the frequency variation of the weight coefficients of the bright points is constructed by employing a nonlinear Kalman filtering algorithm. In some cases, it is possible to verify the results derived from this model with the known asymptotic behaviors of these weight coefficients. It should be noted, however, that a strictly asymptotic procedure cannot be used to determine the bright points and their weight coefficients for many complex targets of practical interest, because the diffraction coefficients associated with these points are unavailable for all but a few canonical geometries.

As a final step in the present approach, the parametric model for the numerically-extracted bright points are used to extrapolate the RCS results over a wide frequency range, encompassing high frequencies well beyond the reach of numerically-rigorous algorithms. Numerical results illustrating the application of the extrapolation procedure, the validation of the scheme for some test targets, and a discussion on the scope and limitations of the method are included in the paper.

## A PROGRESSIVE PHYSICAL OPTICS ALGORITHM FOR COMPUTING THE EM SCATTERING BY JET INLET CAVITIES

Robert J. Burkholder

The Ohio State University ElectroScience Laboratory  
Department of Electrical Engineering  
1320 Kinnear Road, Columbus, Ohio 43212

The electromagnetic (EM) scattering from electrically large and complex jet inlet cavities is computed using an algorithm based on the high-frequency asymptotic principles of physical optics (PO). The problem is broken up into a hybrid combination of three interconnected sub-problems: (1) the *coupling* of the external incident fields into the cavity interior via the aperture at the open end, (2) the *propagation* of the fields from the open end down the inlet to a cross-section  $S_T$  in front of the engine termination, and (3) the *reflection* of the fields from the termination back to  $S_T$ . Once the fields are known at  $S_T$ , a reciprocity integral is used to obtain the externally scattered fields (P.H. Pathak & R.J. Burkholder, *IEEE Trans. MTT*, 41(4), 702-707, 1993). The coupling from the exterior region is modeled by placing equivalent currents in the aperture which radiate into the cavity. The propagation down the smoothly varying aerodynamic inlet section is computed using a progressive PO (PPO) algorithm which is being introduced here. The reflection from the complex engine termination may be found using a numerical solution, such as the method of moments or the finite element method, but PO will be used here as an approximate solution.

In the PPO method, a magnetic field integral equation (MFIE) is derived for the equivalent electric currents which replace the walls of the duct section. The MFIE is solved by iteration, starting with the first order wall currents which are excited by the equivalent currents in the aperture. The first order currents are integrated according to the MFIE to give a new set of currents which are then substituted back into the MFIE and integrated, etc. In principle, the number of iterations necessary for convergence is directly related to the expected number internal reflections of importance. However, this may be a large number for long ducts, and the numerical integration of the MFIE may be very time consuming for electrically large ducts. The PPO algorithm reduces this process to a single integration by using the fact that the fields only need to be tracked one-way down the duct to  $S_T$ . The currents are integrated progressively, starting at the open end and marching down the duct towards  $S_T$ , such that each current element only radiates to points on the wall that are closer to  $S_T$ . The cumulative wall currents are then integrated to give the fields at  $S_T$ .

# First Order Wedge Diffraction Associated with Repeatedly Interacting Surfaces

\*James R. Newhouse and Robert T. Brown  
Lockheed Advanced Development Company  
Dept 25-52, Bldg. 311, Plant B-6  
P.O. Box 250  
Burbank, California 91041

Hybrid geometrical (GO) and physical (PO) optics methods applicable to multiple scattering from complex faceted surfaces have recently been developed based on exact geometrical beam tracing and shadowing algorithms. These algorithms begin by determining which facets of the surface have normals pointing opposite the incident plane wave direction. The algorithm returns unshadowed regions of the facets and then loops over these regions and again loops over all facets to determine regions that receive specular reflections from unshadowed regions. If a facet is found to receive a reflection from an unshadowed region then another loop over all facets is performed to determine unshadowed regions receiving a reflection due to intervening facets. The final step in the GO computation is to loop over all facets and compute portions of the region receiving a reflection visible to the observer. At each region visible to the observer a bistatic PO calculation determines the contribution to the scattered field.

Improvements to the GO/PO result may be obtained using first order physical theory of diffraction (PTD) equivalent current solutions with illuminated edge lengths determined by similar beam tracing and shadowing algorithms. For example, complex scatterers may consist of acute interior wedge structures. Scatterers with such features generally require three or more facet-beam interactions for solution convergence. Such facet-beam interactions may cause the same edge to repeatedly generate unique first order diffracted field contributions. While higher order multiple diffractions between edges are neglected in this approach, the more important first order PTD diffractions generated by reflected planar beams interacting with edges are precisely modeled. In support of this approach, it should be recalled that if  $n$  is the order of diffraction the approximate importance of the diffraction goes as wavelength to the  $(n + 1)/2$  power. Approximations associated with the un-physical nature of beam-edge interactions will be discussed and predictions compared with method of moment solutions.

## SCATTERING FROM A PERFECTLY CONDUCTING WEDGE WITH A SMALL APERTURE IN A FACE

A. Monorchio, G. Manara\*

Department of Information Engineering, University of Pisa  
Via Diotisalvi 2, I-56126 Pisa, Italy

R. Coccioli, G. Pelosi

Department of Electrical Engineering, University of Florence  
Via C. Lombroso 6/17, I-50134 Florence, Italy

The electromagnetic scattering from cavity-backed apertures in conductive surfaces is a problem of considerable interest in a large class of applications. For instance, the evaluation of field contributions from gaps and cracks, where two component structures are joined has recently gained a great attention in the context of radar scattering analyses [T.B.A. Senior *et al.*, IEEE Trans. AP, no. 7, 1990]. In this communication, the influence on the scattered field of the presence of a small aperture in a face of a perfectly conducting wedge is analyzed, in the case of plane wave illumination. When the hypothesis of small dimensions with respect to the wavelength is met, the opening can be modeled by introducing localized impedance boundary conditions. Consequently, the solution can be derived in the context of a perturbative method, by interpreting the equivalent impedance patch as a perturbation of the boundary condition for a perfect electric conductor on the pertinent wedge face.

Recently, a perturbative procedure has been presented for the diffraction of a plane wave by a planar junction between a perfectly conducting and a periodically loaded impedance surface [G. Pelosi *et al.*, IEEE Trans. AP, no. 11, 1993]. Here, a different approach is followed which allows to evaluate the first-order perturbative correction by performing a simple numerical integration, without resorting to a spatial harmonic decomposition of the impedance profile. The solution obtained can be applied to configurations with arbitrary exterior wedge angles. Moreover it allows to recover all higher-order perturbative contributions by applying a simple numerical integration procedure.

Extensive numerical results are presented and discussed. The limit of application of the procedure is determined by comparisons with data obtained via an hybrid technique which combines the Finite Element Method and the uniform GTD or the eigenfunction expansion of the field [G. Pelosi *et al.*, COMPEL, no. 2, 1994].



TUESDAY PM JOINT SPECIAL SESSION T-J3

Room: Kane 110

WAVE PROPAGATION AND SCATTERING (HONORING AKIRA ISHIMARU)

Chair: S. Broschat, Washington State University

Organizer: S. Broschat, Washington State University

- 1:25 Introductory Remarks  
*Shira Lynn Broschat (Ph.D. 1988), Washington State Univ.*
- 1:40 Wave Propagation and Scattering in Random Media 206  
*\*L. Tsang, Univ. of Washington*
- 1:55 The Non-Random World of Profession and Colleagues 207  
*\*I.C. Peden, Univ. of Washington*
- 2:10 Complex Density Tensor in Ultrasonic Heating of Composite Materials 208  
*\*R.A. Sigelmann (Ph.D. 1964), Univ. of Washington*
- 2:25 Electromagnetic Theory Applied to Insect Eyes 209  
*\*G.D. Bernard (Ph.D. 1964), Boeing Commercial Airplane Group*
- 2:40 Remote Sensing of the Solar Wind with Radio Scattering and Scintillation Measurements 210  
*\*R. Woo (MSEE 1964), California Inst. of Technology*
- 2:55 A Practical Approach to Proving "Goldbach's Conjecture" 211  
*\*F.P. Carlson (Ph.D. 1967), Carlson Consultants, Inc.*
- 3:10 A Novel Conformal Array Antenna for a Joined Wing Surveillance Aircraft 212  
*R.J. Coe (Ph.D. 1969), G.E. Miller (Ph.D. 1986), D.B. Peterson, M.J. Taylor, Boeing Defense and Space Group*
- 3:25 Break
- 3:35 Microwave Ablative Surgery for Treatment of Cardiac Arrhythmia 213  
*\*J.C. Lin (Ph.D. 1971), Univ. of Illinois at Chicago*
- 3:50 Hyperthermia for Cancer Therapy 214  
*\*C.K. Chou, City of Hope National Medical Center*
- 4:05 Optical Trans-Body Imaging of Physiological Functions 215  
*\*K. Shimizu, M. Mouri, K. Yamamoto, Hokkaido Univ.*
- 4:20 Discovery of Backscattering Enhancement from Densely Distributed Non-Tenuous Particles 216  
*\*Y. Kuga (Ph.D. 1983), Univ. of Washington*
- 4:35 Velocity Profile in the Normal Human Blood Vessel: A Comparison of Theoretical Results and In Vivo Data 217  
*\*Q. Ma (Ph.D. 1989), Siemens Medical Systems, Inc.; J. Gattinella, Advanced Technology Laboratory*

## WAVE PROPAGATION AND SCATTERING IN RANDOM MEDIA

Leung Tsang  
Department of Electrical Engineering, FT-10  
University of Washington  
Seattle, Washington 98195

This paper discusses the various contributions of Professor Akira Ishimaru in the area of wave propagation and scattering in random media and rough surfaces.

We first review the work before 1978 as documented in his two-volume monograph, *Wave Propagation and Scattering in Random Media*, Academic Press, 1978. This includes transport theory, diffusion approximation, beam wave and pulse propagation, correlation functions in stationary and moving particles, relations between ladder approximations, and Twersky's integral equation.

We then discuss the work since 1978. This includes wave propagation in dense media, pair-distribution functions, backscattering enhancement in discrete random media, ladder and cyclical terms, and diffusion approximation. Backscattering enhancement is a coherent effect in multiple scattering. It predicts a larger scattering cross section than classical radiative transfer theory based on independent scattering. The dense media effects show that correlated scattering and mutual coherent interaction of scatterers are important.

Ishimaru's works include both theoretical prediction and experimental confirmation in backscattering enhancement and dense media effects. Backscattering enhancement of random rough surfaces is also discussed as well as the second-order Kirchhoff theory with shadowing corrections. The shadowing corrections are important for energy conservation. The paper will review both the fundamentals of wave scattering and the applications, particularly in remote sensing.

---

Special Session in Honor of Professor Akira Ishimaru  
Organized by Shira Broschat

## **THE NON-RANDOM WORLD OF PROFESSION AND COLLEAGUES**

**Irene C. Peden  
Department of Electrical Engineering  
University of Washington  
Seattle, WA 98195**

An important companion to the technical and professional excellence that is normally present in the truly outstanding is their willingness to donate their time and energy to advancing the stature of the overall profession as well as increasing its knowledge base. Such individuals can also be generous to their professional colleagues and friends and to their students, extending the aura of goodwill to help them grow and prosper. Professor Ishimaru is a shining example of that kind of human excellence. His many contributions to both the IEEE Antennas and Propagation Society and URSI are reviewed, together with the broader reach of his professional activities, and many of the recognitions that have been accorded him are touched upon. Less well known, but still important to the overall pattern of his professional life, is the service he has provided over the years to the University of Washington and to its faculty and students. In identifying some of these activities, his role as a valued departmental colleague, dedicated teacher, friend and mentor will be emphasized. Personal perspectives sprinkled with a few anecdotes characterize this tribute by Professor Peden to a favorite colleague.

**Complex Density Tensor in Ultrasonic Heating  
of Composite Materials**

**Rubens A. Sigelmann**  
Professor Emeritus  
Dept. of Electrical Engineering  
University of Washington  
Seattle, WA 98195

It is shown in this paper, that deposition of heat due to an ultrasonic wave in a homogenous material depends on the mechanical losses. These losses are characterized by complex components of the stiffness or compliance tensors. For this case, the deposition of heat can be formulated in terms of the velocity of the particle only. In viscous composite materials, a model was developed where the heat deposition is characterized by an equivalent complex density tensor. For this case, it is also shown that heat deposition can be formulated in terms of the displacement of the particle. In the most general case, complex density tensor and stiffness or compliance tensors must be used. As an illustration of this model, theoretical results for a layered system consisting of fat, muscle and bone are presented.

## **ELECTROMAGNETIC THEORY APPLIED TO INSECT EYES**

**Gary D. Bernard  
Boeing Commercial Airplane Group  
Enabling Research & Development  
Advanced Sensors Laboratory**

An insect compound eye is a sophisticated sensory system that provides to the brain processed information concerning the form, color, polarization, and movement of surrounding objects. It contains optical components that function as broadband anti-reflection coatings, GRIN lenses, anisotropic fiber-optic detectors, waveguide attenuators, and interference filters.

Because each insect species has special visual requirements dictated by peculiarities of their lifestyle, one finds an amazing diversity among insects in these optical structures. Electromagnetic theory of interference, diffraction, and guided waves is necessary but not sufficient for understanding the value of these structures for visual information processing. Interdisciplinary collaboration with specialists in behavior, physiology, ecology, and evolution of insects is also necessary. I shall show results from such collaborations, comparing eyes of honeybees to those of butterflies. Both insects have globally non-uniform photo-detector arrays, but are non-uniform in very different ways.

The bee eye is divided into two zones. One zone contains an array of twisted fiber-optic detectors that analyzes form, color, and motion but lacks sensitivity to polarized light. The other zone contains a smaller array of straight detectors that extracts directional information from polarized skylight, but lacks sensitivity to color and form. Most bee species have similar eyes with about the same color-vision system.

Butterfly species, on the other hand, have great diversity in their color vision systems. Both global and local spectral organization of their detector arrays is driven in large part by differences in coloration of wings and host plants. Their eyes contain a novel lens/GRIN-lens arrangement for excitation of each detector waveguide, and a non-uniform multi-layer interference reflector that optically terminates each detector waveguide. Neither structure is found in bees.

## REMOTE SENSING OF THE SOLAR WIND WITH RADIO SCATTERING AND SCINTILLATION MEASUREMENTS

R. Woo  
Jet Propulsion Laboratory  
California Institute of Technology  
Pasadena, CA 91109

The solar wind is highly complex and exhibits structure and phenomena varying over an extensive range of spatial and temporal scales. Although our knowledge and understanding of the solar wind has improved with the enormous quantity of in situ measurements returned by numerous spacecraft missions since 1962, it is far from complete. Exploration continues with Ulysses on its way out of the ecliptic plane, and the Voyager and Pioneer spacecraft searching for the outer reaches of the heliosphere. Although measurements in the region near the Sun are crucial for understanding the evolution of the inner solar wind, direct measurements have not yet been possible inside 0.3 AU. In the mean time, we must rely on indirect remote sensing measurements, of which measurements based on radio propagation through the turbulent solar wind plasma have played a major role.

Recent progress in the analysis of radio scattering and scintillation measurements with monochromatic spacecraft radio signals has resulted in significant new information on structure and properties of the near-Sun solar wind. The purpose of this paper is to briefly review the remote sensing capabilities of these radio scattering observations, and to show how they have been exploited to obtain details of the global large-scale structure in the solar wind and its evolution with heliocentric distance. The solar wind results are exciting, because they bridge the gap between solar and in situ solar wind observations, and reveal features that can be related to features in both solar and in situ plasma measurements beyond 0.3 AU.

## A Practical Approach to Proving "Goldbach's Conjecture"

F. Paul Carlson, Ph.D.  
Carlson Consultants, Inc.  
1201 Pacific Avenue, Suite 1450  
Tacoma, WA

The recent excitement about the proof of Fermat's Theorem ( $x^n + y^n = z^n$ ,  $n \leq 2$ ) by Andrew Wiles, a British mathematician from Princeton University, has also raised again real interest in Goldbach's Conjecture, the unproved statement by the 18th-century Prussian. The conjecture states that every even number greater than two is the sum of two prime numbers. Mathematicians have long said there is no obvious way to start playing with this statement in order to lead to a proof.

As a tribute to Professor Ishimaru's tenacious pursuit of unresolved conjectures from a practical perspective, I would like to offer a practical approach to proving this conjecture. The basic strategy to this proof is to create sum and difference conjectures and then develop a particular sum that identifies the path to the conjecture proof.

A restatement of the Conjecture could be as follows:

**Th:** An even number,  $E > 2$ , can be written as  $E = n + l$ , where  $n$  and  $l$  are different members of a set of all prime numbers.

Proof:

Cor.1: Every prime number is an odd number. If this were not so, a number 2, an even number, could be factored from this prime number.

Cor.2: The difference of two odd numbers is an even number. A deductive examination of any paired sequence of odd numbers shows this corollary.

Th.1: The difference of two prime numbers is an even number. This follows the combination of Cor.1 and Cor.2 above.

Cor.3: The sum of two odd numbers is an even number. Again, a deductive examination of any paired sequence of odd numbers demonstrates this corollary.

Th.2: The sum of two prime numbers is an even number. This follows from the combination of Cor.1 above and Cor.3.

Cor.4: The sum of the difference of two prime numbers,  $n$  and  $m$ , and the sum of two prime numbers  $l$  and  $m$  is an even number,  $E$ , i.e.  $(n-m) + (l+m) = n+l = E$ .

**Th/QED:** An even number,  $E > 2$ , can be written as  $E = n + l$ , where  $n$  and  $l$  are different members of a set of all prime numbers.

## **A Novel Conformal Array Antenna for a Joined Wing Surveillance Aircraft**

R.J. Coe, G.E. Miller, D.B. Peterson and M.J. Taylor  
Electromagnetics Technology  
Research and Technology Division  
Boeing Defense & Space Group  
Seattle, WA

The Boeing Defense & Space Group has, over the past several years, undertaken an effort to mature a naval airborne surveillance system concept for a follow-on to the E-2C aircraft. The system concept is based upon a joined wing airframe and uses electronically scanned conformal array antennas on each of the four joined wings to provide 360 deg coverage in azimuth. One of the unique aspects of this program deals with the fact that the aircraft platform has been designed to accommodate the radar. Previous and existing surveillance system designs have centered on designing the radar system to accommodate the airframe.

Each conformal phased array antenna for the E-X concept consists of two linear arrays - one conformal to the top of the wing surface and the other conformal to the bottom wing surface. Each linear array is comprised of 28 stick elements which, in turn, are made up of three element, end-fire, microstrip patch arrays. Polarization of the arrays is vertical with respect to the wing surface. Amplitude tapering of the linear arrays is used to control the sidelobe performance of the arrays. The frequency of operation of the system is in the UHF radar band (400-450 MHz).

In this paper we will present the design trades which resulted in the selected array configuration. Analysis performed to optimize the excitation of the end-fire sticks for minimization of the wing leading and trailing edge diffraction effects will also be discussed. Scale model measurement data, used to validate the design concept, will be presented.

## **MICROWAVE ABLATIVE SURGERY FOR TREATMENT OF CARDIAC ARRHYTHMIA**

James C. Lin  
Department of Electrical Engineering (M/C 154)  
University of Illinois at Chicago  
851 South Morgan Street  
Chicago, IL 60607-7053

A minimally invasive surgical modality using transcatheter microwave energy is described for treatment of abnormal cardiac rhythms. The absorption of microwave energy in biological tissue is governed by the source frequency, antenna configuration, as well as tissue geometry and permittivity. The distribution of absorbed energy can be controlled by judicious design of the antenna. Also, by taking advantage of the wavelength contraction that takes place in tissue medium, antennas can not only be designed to provide greater penetration of microwave energy into tissue, but also allow discrete localization of microwave energy absorption. The absorbed energy is converted into heat by dielectric loss. Therefore, it is possible to titrate, in a stepwise manner, the quantity of microwave energy delivered to cause varying degrees of tissue modifications.

A microwave system consisting of four major components: a microwave power source, switch assembly, catheter antenna, and control circuits has been designed. It is currently used in animal tests to ascertain its effectiveness and efficacy. The microwave power source is of low cost and is capable of delivering up to one hundred watts of power. It is interfaced through an electrocardiogram and microwave power switch to a flexible, coaxial transmission line catheter antenna combination that is necessary for percutaneous and transcatheter operations. The digital control circuits provide measured amount of power delivery and to set treatment duration. A critical element in the design of a minimally invasive microwave therapeutic system is the catheter antenna.

Investigations to date have shown that substantial quantities of microwave energy could be transported via miniature flexible coaxial transmission lines and catheter antennas to produce localized tissue modifications. It has also been demonstrated that percutaneous treatments of a number of abnormal rhythm diseases are amenable to catheter-based, minimally invasive thermal microwave therapy.

## Hyperthermia for Cancer Therapy

C.K. Chou, Ph.D.  
Department of Radiation Research  
City of Hope National Medical Center  
Duarte, California 91010, U.S.A.

In reviewing 15 years of efforts in clinical hyperthermia, much progress has been made. There are improvements of equipment based on medical demands, and technological progress has fulfilled many clinical requirements. However, a single piece of equipment will not satisfy all clinical requirements for patient treatments. Depending upon the location and vascularity of the tumor and adjacent tissues, and the general physical condition of the patient, physicians need to have the option of choosing the most appropriate equipment.

To date, most clinical studies of hyperthermia have been concerned with feasibility and toxicity of various heating methods. Unfortunately, due to the limited penetration of electromagnetic energy and the reflections of ultrasound at tissue/air and bone interfaces, it has been impossible to heat large and deep tumors effectively. Thus, trials of hyperthermia plus radiation have been investigated mainly for superficial small nodules. Although hyperthermia and radiation schedules varied, and the temperature distributions produced in tumors were not well characterized, such studies consistently showed an advantage for radiation plus hyperthermia compared to radiation alone. Improved duration of tumor control as a result of the combined treatment has also been demonstrated in some studies. Such results cannot be achieved without careful attention to the technical quality of the treatment. If the tumor is inadequately heated, the treatment will result in little benefit.

The temperature rise in tumors is determined by the energy deposited in the tissue and the physiological responses of the patient. When electromagnetic energy is used, the power deposition is a complex function of frequency, intensity, polarization of the applied fields, geometry and size of the applicator, as well as dielectric properties, geometry, size and depth of the tumor. The final temperatures in the exposed tissues are not only dependent on the energy deposition but also on blood flow and thermal conduction in tissues. Thermal dosimetry and treatment planning with microwave and radiofrequency fields is far from adequate in present hyperthermia research. Further clinical applications cannot proceed fully without the prerequisite knowledge of how heat is to be delivered in various clinical situations. Recent efforts on intracavitary hyperthermia and radiation for esophageal cancer treatment and whole body hyperthermia will be presented.

## Optical Trans-body Imaging of Physiological Functions

Koichi Shimizu\*, Mitsuhiro Mouri and Katsuyuki Yamamoto

Department of Bioengineering, Faculty of Engineering,

Hokkaido University, Sapporo, 060, Japan.

( Phone:+81-11-716-2111 (Ext.6857), Fax:+81-11-757-2485 )

There has been increasing interest in imaging through dense random media. Attempts were made to visualize the functional change inside a living biological body using a transillumination technique. With a near-infrared light, the transillumination images of a human hand, a mouse abdomen and a rat brain were obtained. To examine the feasibility of functional imaging, a localized hypoxia was made in each of above body parts. Fig.1 illustrates the experiment. Fig.2 shows one of a kidney which was made hypoxic by stopping the renal circulation. It was visualized using transillumination images of multiple wavelengths of light. With a rat brain, the change of the image was investigated in various conditions. The physiological change of a rat was made by changing the oxygen fraction of inhalation gas or by occluding the carotid artery to change the brain circulation. It was found that the changes in the brain blood volume and in the brain oxygenation state could be detected noninvasively. In this way, the spatial distribution of these changes could be visualized in the transillumination images of a living body. Through this study, the feasibility of optical trans-body imaging of physiological functions was verified.

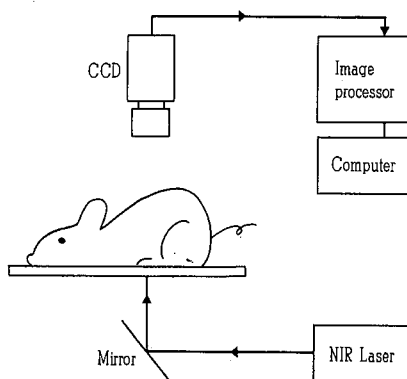


Fig.1 Experimental setup

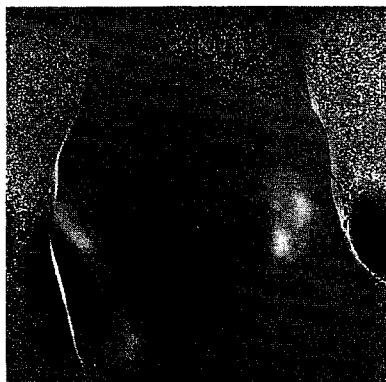


Fig.2 Imaging of hypoxic part in mouse abdomen (right kidney)

**Discovery of Backscattering Enhancement from Densely  
Distributed Non-Tenuous Particles**

Yasuo Kuga  
Department of Electrical Engineering  
University of Washington  
Seattle, WA 98195

During the past ten years significant experimental and theoretical progress has been made in the understanding of backscattering enhancement effects from randomly distributed particles, rough surfaces, and turbulence. The first observation of backscattering enhancement was reported by Kuga and Ishimaru in 1984 in *JOSA*. The original data for this paper were obtained in 1982 when we were studying the backscattering peak suggested by de Wolf (*Wave Propagation and Scattering in Random Media*, A. Ishimaru, p. 311, 1978). However, the observed peak in the back direction was much smaller than the expected value  $(kD)^{-1}$  and we did not understand the reason. Professor Ishimaru was very cautious, and we redid the experiments three to four times checking for all possible errors. Finally, we were convinced that our data were new and not previously published. In 1983, Professor Tsang joined the University of Washington and suggested that the peak may be due to the multiple scattering effects. He obtained the backscattering peak by studying the bistatic cross section of randomly distributed isotropic scatterers. To our surprise, physicists were also studying the backscattering enhancement, also called photon localization, and similar experimental data were published in *Phys. Rev. Lett.* in 1985.

# **VELOCITY PROFILE IN THE NORMAL HUMAN BLOOD VESSEL:**

**A comparison of theoretical results and in vivo data**

Qinglin Ma  
Siemens Medical Systems, Inc.  
Ultrasound Group  
Issaquah, WA 98027

Judy Gattinella  
Advanced Technology Laboratory  
Bothell, WA 98041

## **ABSTRACT**

This paper presents the blood flow velocity profiles in normal human blood vessel versus the cardiac cycle. The profiles are obtained by Womersley's pulsatile flow theory using the in vivo mean velocity waveform obtained by an ultrasonic beam which encompasses the entire vessel cross sectional area. The theoretically predicted velocity profile is then used to calculate the mean velocity waveform through the cardiac cycle for a narrow beam, which can be entirely placed within the vessel. Finally, the theoretical mean velocity waveform is compared with the measured data. The comparison shows that they are consistent with each other. This agreement suggests that the pulsatile flow theory may be used to predict the blood flow profile which can not be easily measured.



TUESDAY PM URSI-B SESSION T-U19

Room: Kane 220

MICROSTRIP ANTENNAS

Chairs: A. Kishk, University of Mississippi; Ke Wu, École Polytechnique-Montréal

- 1:20 Active Millimeter-Wave Microstrip Patch Antenna Sub-Array 220  
*\*M.G. Keller, Y.M.M. Antar, Royal Military College of Canada; D. Roscoe, A. Ittipiboon, Communications Research Centre*
- 1:40 Analysis of a Two-Layered Microstrip Patch Antenna Using Triangular-Domain Basis Functions 221  
*\*H. A. N. Hejase, Instituto Tecnológico y De Estudios Superiores De Monterrey, Campus Edo. De México; S. D. Gedney, Univ. of Kentucky*
- 2:00 On Modeling a Coaxial-Fed Microstrip Antenna 222  
*D.C. Chang, Arizona State Univ.; G. Jankovic, D.I. Wu, Boulder Microwave Technologies*
- 2:20 Experimental Check of Microstrip Gap Results Obtained with the Excess Charge Method 223  
*J. Martel, \*F. Medina, R.R. Boix, M. Horno, Univ. of Seville*
- 2:40 Conformal Multifunction Antenna for Automobile Application 224  
*\*J.J.H. Wang, V.K. Tripp, J.K. Tillery, C.B. Chambers, Wang-Tripp Corporation*
- 3:00 Break
- 3:20 Studies of Stacked Electromagnetically Coupled Patch Antennas 225  
*W. Chen, \*K. F. Lee, Univ. of Toledo; R. Q. Lee, NASA Lewis Research Center*
- 3:40 Linear Microstrip Array with a Simple Transmission Line Feed 226  
*C. S. Lee, Southern Methodist Univ.; \*V. Nalbandian, F. Schwering, US Army CECOM*
- 4:00 Suppression of Surface Waves in a Thick Microstrip Antenna by Parasitic Elements 227  
*\*T. -H. Hsieh, C. S. Lee, Southern Methodist Univ.; V. Nalbandian, US Army CECOM*
- 4:20 Microstrip Wrap Around Antenna on a Conical Surface 228  
*\*P. F. Wahid, Univ. of Central Florida; P.S. Neelakanta, Florida Atlantic Univ.*
- 4:40 Evaluation of Radiation Loss from Microstrip Line Discontinuities Using a Multiport Network Modeling Approach in MM Wave Microstrip Antenna Arrays 229  
*\*A. Sabban, Haifa Israel*

## **Active Millimeter-Wave Microstrip Patch Antenna Sub-Array**

**+M.G. Keller\*, +Y.M.M. Antar, ++D. Roscoe,  
++A. Ittipiboon**

**+Royal Military College of Canada  
Kingston, Ontario K7K 5L0, Canada**

**++Communications Research Centre  
P.O. Box 11490, Station H, Ottawa, Ontario K2H 8S2 Canada**

Distributed amplification in planar arrays with spatial power combining is an attractive alternative for some radar and satellite communications applications. Recently, results were reported on the integration of active devices in the feedlines of aperture-coupled patch antenna elements (Y. Shen et al., AP-S Symposium, pp. 1390-1393, Jul 1993) and on a monolithic aperture-coupled antenna element at millimeter-wave frequencies (H. Ohmine et al., ISAP, pp. 1105-1108, Sep 1992). These configurations utilize the well documented advantages of the aperture-coupling feed mechanism. However, the multilayered configuration adds complexity to the assembly processes especially at millimeter-wave frequencies. At these frequencies electrical challenges related to the design and integration of the amplifier and antenna occur. In addition, mechanical problems arise due to the small dimensions and the resultant difficulty associated with obtaining satisfactory physical alignment of the feed, slot, and patch.

This paper reports on the results of a sub-array composed of 42 GHz aperture-coupled microstrip patch antenna elements individually fed by MMIC amplifiers. The effects of fabrication tolerances of the antenna elements and of gain variation of the amplifiers on the performance of the sub-array are discussed. The presented results will provide design information useful for the large scale integration of such an active sub-array configuration.

## **ANALYSIS OF A TWO-LAYERED MICROSTRIP PATCH ANTENNA USING TRIANGULAR-DOMAIN BASIS FUNCTIONS**

**Hassan A.N. Hejase\*, IEEE member  
Dept. of Electrical Engineering  
Instituto Tecnológico y De Estudios Superiores De Monterrey  
Campus Estado De México, México**

**Stephen D. Gedney, IEEE member  
Dept. of Electrical Engineering  
University of Kentucky  
Lexington, KY 40506**

This work studies the effect of substrate thickness and dielectric constants on the radiated emissions from arbitrarily shaped two-layered microstrip patch antennas. The microstrip patch is discretized into triangular sub-domains which are capable of conforming to any geometrical surface or boundary. The conducting patch is assumed to have zero resistance and zero thickness. The method of moments is used to solve a mixed-potential integral equation where the unknown currents are expanded using vector-current basis functions associated with the triangular patch edges. The elements of the impedance matrix in the resulting MOM matrix equation contain double integrals over adjacent triangular patch pairs; the integrand being Sommerfeld-type integrals that represent the vector and scalar potential Green's functions. The vector and scalar Green's functions are computed using a method similar to that proposed by Mosig and co-authors. The 2-D integration over the triangular patch domains is performed using normalized area coordinates with Gaussian Quadrature interpolation. This analysis can also be applied to study scattering from microstrip patches, and to compute the scattering parameters of microstrip discontinuities. Of particular interest, for EMC applications, is the study of radiated emissions from printed circuit traces due to common-mode currents on the transmission-line structure, caused by the asymmetrical positioning of voltage sources between parallel traces. Numerical results for the radiated far-fields and gain as a function of the dielectric constants and thicknesses of the two layers will be presented and compared to results available in the literature.

## On Modeling a Coaxial-fed Microstrip Antenna

David C. Chang  
College of Engineering  
Arizona State University  
Tempe, AZ 85287-5506

George Jankovic and Doris I. Wu  
Boulder Microwave Technologies  
2336 Canyon Blvd, #102  
Boulder, CO 80302

Coaxial probes are commonly used by antenna designers to feed microstrip patch antennas. Occasionally, reactively-loaded probes are also used for providing impedance matching or frequency selectivity. The inner conductor, in this case, is connected from underneath to the microstrip, while the outer conductor is flush-mounted to the ground plane. The impedance of these probes are then described by what it is seen by the coaxial transmission-line. The question, then, is how to accurately account for the structurally-induced reactance in the local vicinity of the probes.

A conceptually most rigorous approach is to formulate a set of coupled integral equations for solving simultaneously the current distributions on the microstrip structure, on the probe, and the aperture field distribution across the coaxial opening by assuming an incident TEM-mode field in the coaxial region. Such an approach is tedious, as well as unsatisfying because much of the computational effort is expended on matters which are local in nature and thus, unrelated to the dynamic nature of the antenna itself.

A common approach is to assume a known magnetic frill current corresponding to the TEM-mode at the coaxial opening. This approach ignores the capacitive effect resulted from a charge accumulation at the aperture. Furthermore, the computation is still quite extensive because the detail distribution of current on the probe has to be modeled.

Further simplification can be achieved by using a constant current source to replace the probe, and thus, eliminates the need to find the current distribution on the probe altogether. Such an approach can still retain the inductive effect of a conductor, but not the capacitive effect resulted from the non-uniform charge distribution near the corner where the probe and the microstrip intersect. The approach is also somewhat awkward to implement in an integral-equation formulation, since the "voltage" is not the natural outcome of the process.

In this talk, we shall discuss the significance of end corrections, and how the concept can be used to simplify the computational scheme, while still allow us to retain the required numerical accuracy. An explicit expression for the end-correction network of lumped elements is derived when a constant-current assumption is used in conjunction with the integral-equation formulation.

## Experimental Check of Microstrip Gap Results Obtained with the Excess Charge Method

J. Martel, F. Medina\*, R. R. Boix, M. Horno  
Microwaves Group. Department of Electronics and Electromagnetics  
University of Seville  
Avda. Reina Mercedes s/n 41012 SEVILLA (SPAIN)

Because of the importance of the end-to-end coupling of resonators in some microstrip filter configurations, the correct characterization of this effect is essential to accurately predict the filter frequency response. Recently, some of the authors of this communication have focused their attention on the accurate calculation of the equivalent circuit parameters employed to characterize symmetric, asymmetric and offset microstrip gap discontinuities (J. Martel et al., IEEE-MTT, 39, 1623-1629, Sep. 1991, J. Martel et al., MOTL, 6, 277-280). The method applied in those works was the excess charge technique in the spectral domain. Although this analysis is electrostatic in nature, it has been reported that the frequency dependence of the equivalent circuit parameters is not very strong (V. Rizzoli et al., IEEE-MTT, 29, 655-660, Jul. 1981, Y. C. Chiang, IEE pt-H, 139, 376-384, Aug. 1992). The goal of this work is to demonstrate the validity of the excess charge technique in addition to the presentation of new experimental results of asymmetric microstrip gap discontinuities on two layer substrates. The experimental technique we have employed is a slight modification of the resonant technique proposed by C. Gupta et al., IEEE-MTT, 26, 649-652, Sep. 1978. The basis structure consists of two straight resonators (lengths approximately equal to  $\lambda/2$ ) in which even and odd modes are excited. The measurement of the resonant frequencies of both even and odd modes in conjunction with the second resonant frequency of the same structure without gap lets us to establish equations for the equivalent excess length of each mode. These excess electrical lengths are obtained by subtracting the measured total lengths. The advantage of the subtraction is that we eliminate the inaccuracy associated to the measurement of the lengths of the resonators (T. C. Edwards, IEEE-MTT, 24, 506-513, Aug. 1976). This length is required for the experimental determination of the effective dielectric constant,  $\epsilon_{eff}$ , at the measurement frequency (R.K. Hoffmann, *Handbook of MIC*, Artech House 1987). However, the impact of the inaccuracy of this length on the calculation of  $\epsilon_{eff}$  is roughly two orders of magnitude below its influence on the determination of the excess lengths. The measured  $\epsilon_{eff}$  has been used in conjunction with the theoretical gap parameters to simulate the behaviour of the gap discontinuity. It has been found excellent agreement between calculated and measured excess lengths for a wide range of operating frequencies.

1994 URSI Radio Science Meeting (Seattle)

**Conformal Multifunction Antenna  
for Automobile Application**

J. J. H. Wang<sup>\*1,2</sup>, V. K. Tripp<sup>1,2</sup>, J. K. Tillery<sup>1</sup>, and C. B. Chambers<sup>1</sup>

<sup>1</sup> Wang-Tripp Corporation

1710 Cumberland Point Drive, Suite 17, Marietta, Georgia 30067

and

<sup>2</sup> Georgia Tech Research Institute

Georgia Institute of Technology

Atlanta, Georgia 30332

With the proliferation of wireless electronic systems on cars, trucks, boats, aircraft, and missiles, and the limited availability of surface area on a vehicle suitable for antenna mounting, the need for antennas that can handle two or more systems (and thus are called *multifunction antennas*) has been recognized for more than a decade. However, there have been very few documented reports on the development of the multifunction antenna, in particular the vehicular multifunction antenna. This is probably due to the requirements that a multifunction antenna must generally have (1) a wide, though not necessarily continuous, frequency bandwidth, (2) radiation pattern diversity, and that in the case of the vehicular multifunction antenna, the antenna must also be conformable and low-profile.

The spiral-mode microstrip (SMM) antenna (J. J. H. Wang and V. K. Tripp, *IEEE AP Trans.* 39, 332-335, 1991; patents pending), is among the very few antennas that meet all the three requirements, and has been developed at Wang-Tripp Corporation (WTC) for automobile multifunction applications. This antenna is of the shape of a flat panel less than 1-inch thick and with a surface area of about 2 ft X 2.5 ft, and thus can be integrated into the rooftop of a passenger car as a "hidden" antenna. It handles AM, FM, remote keyless entry, cellular phone, and other mobile and satellite communications and geolocation systems (such as the GPS) below about 2.2 GHz. Connections between the antenna and the receivers/ transmitters are mainly by a multiplexing feed network. The feed network is on a microstrip substrate and uses mainly lumped elements. The different pattern requirements among the various systems are met by spiral modes of the mode numbers 0, 1, and 2.

The performance of this antenna was tested by anechoic chamber pattern measurements as well as by sensitivity tests in outdoor ambient signal environments. The multifunction antenna's performance is found to be comparable to that of existing stand-alone automobile antennas in spite of the insertion loss in multiplexing in the multifunction antenna; this is probably due to the fact that stand-alone automobile antennas are generally not optimum, being either electrically small or not well matched with the vehicle or the wave.

STUDIES OF STACKED ELECTROMAGNETICALLY COUPLED PATCH  
ANTENNAS

Wei Chen and Kai Fong Lee\*

Dept. of Electrical Engineering, University of Toledo,  
Toledo, OH

R.Q. Lee

NASA Lewis Research Center, Cleveland, OH

The stacked two-layer electromagnetically coupled patch (EMCP) antenna consisting of one fed patch and one parasitic patch on another layer has been found experimentally to be capable of providing an impedance bandwidth which is significantly larger than the single patch. Although several groups of authors have reported theoretical analysis of the EMCP antenna, much remains to be studied. In this paper, we report our continual theoretical investigation of this antenna using the spectral domain moment method analysis and computer code which we developed for probe-fed multi-layer multi-patch antennas (W. Chen and K.F. Lee, PIER '93 Proceedings, p. 404). The model, valid for electrically thick substrates, includes a proper attachment mode to ensure current continuity at the patch-probe junction and uses multiple expansion modes on the probe current to allow for both longitudinal and azimuthal variations. Results to be reported include the variation of input impedance with feed position, dielectric cover effect, effect of an offset of the parasitic patch on bandwidth, parasitic size effect, and comparison of the half-power beamwidths of two-layer EMCP antennas with the single patch.

Recognizing that it is time-consuming and expensive for antenna engineers who do not have the computer code to design EMCP antennas, we have also embarked on a program to develop computer-aided design (CAD) formulas which are capable of predicting the essential characteristics based on curve fitting the data obtained from moment method analysis. Our efforts in attempting to obtain CAD formulas which are useful for the design of these antennas will also be described in the meeting.

# 1994 URSI Radio Science Meeting (Seattle)

## LINEAR MICROSTRIP ARRAY WITH A SIMPLE TRANSMISSION LINE FEED

Choon Sae Lee  
Electrical Engineering Department  
Southern Methodist University  
Dallas, Texas 75275

Vahagn Nalbandian\* and Felix Schwering  
US Army CECOM  
Fort Monmouth, New Jersey 07703

Single microstrip patches have a large beamwidth. In order to have a narrower beamwidth as well as a scanning capability, an array structure is needed. In this presentation, a new linear microstrip array with a simple transmission line feed is introduced. The proposed device is simple and inexpensive to fabricate. The antenna consists of two layers as shown in Figure 1. The top layer contains microstrip patches, each radiating at its own resonant frequency. The bottom layer is a microstrip transmission line which has slots under the microstrip patches. These slots feed the radiating patches above. The width of the transmission line is the same as that of the radiating elements. In this way, the impedance matching procedure is greatly simplified and a relatively wide frequency band is obtained. The separation between two slots is designed to be about one wavelength so that radiation from the microstrip patches interferes constructively near the zenith. The length of the radiating patches is about a half wavelength at the resonant frequency for a maximum radiation. This design is possible when the lower layer has a higher dielectric constant than that of the upper layer. The resultant structure is a combination of patch and slot arrays. The radiation comes from the region of a lower dielectric constant and the feed power propagates in the region of a higher dielectric constant. The proposed array can be mass-produced at a low unit cost by using the printed-circuit techniques because all the structure is planar. Also the simple feeding scheme makes the frequency scanning possible. The gap size and location critically determine the coupling between the radiating patch and the transmission line. Results for an optimum design will be presented.

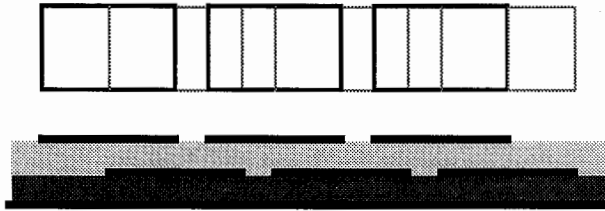


Figure 1. Microstrip array with a transmission line feed

1994 URSI RadioScience Meeting (Seattle)

## Suppression of surface waves in a thick microstrip antenna by parasitic elements

Tung-hung Hsieh\*, Choon Sae Lee  
Electrical Engineering Department  
Southern Methodist University  
Dallas, Texas 75275  
and  
Vahakn Nalbandian  
US Army CECOM  
Fort Monmouth, New Jersey 07703

It is well known that microstrip antennas are narrow bandwidth devices. One simple way to improve the narrow-bandwidth behavior is to increase the thickness of dielectric substrate. However, surface waves will become highly excited as the thickness increases. This excitation is out of control and will reduce the radiation efficiency. Furthermore, the unwanted radiation through the surface waves will interfere with the main beam, usually to degrade the radiation quality. To improve the narrow bandwidth without reducing the radiation efficiency of microstrip antennas, a novel design is presented. In the proposed design, two parasitic strips are placed near the two radiation edges of a microstrip antenna to suppress the surface-wave propagation. The patch antenna is fed with a coaxial probe, although other feeds could be employed equally well. This microstrip antenna is easy to manufacture. The surface waves can be eliminated by placing a conducting strip perpendicular to the ground plane, as in cavity backed microstrip antennas. However this device is difficult to fabricate, especially, in a large quantity. On the other hand, the proposed antenna can be produced cheaply by using the printed-circuit technology because all the antenna structures are planar. The numerical analysis is performed by a moment method in spectral domain. Our results in both theory and experiment indicate that the parasitic elements are highly effective to reduce the surface waves. A major portion of the surface waves is either diffracted to the space wave or falls back into the resonating cavity of the microstrip antenna. In this presentation, the design scheme will be presented for an optimum configuration of the parasitic elements as a function of the length of the parasitic strips, the distance from the main patch and the location of the strips between the plane of the main radiation patch and the ground plane.

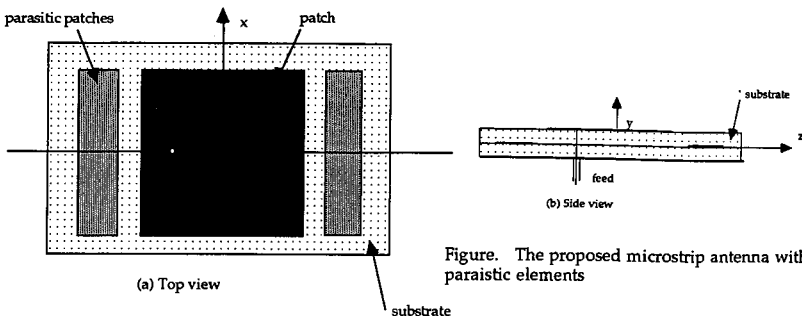


Figure. The proposed microstrip antenna with parasitic elements

## MICROSTRIP WRAP AROUND ANTENNA ON A CONICAL SURFACE

P. F. Wahid\*  
Electrical and Computer Engineering Department  
University of Central Florida  
Orlando Florida 32816

P. S. Neelakanta  
Electrical Engineering Department  
Florida Atlantic University  
Boca Raton, Florida 33431

Microstrip antennas on cylindrical and conical surfaces are of importance due to their applications in air and space vehicles. Microstrip wrap around antennas on conical surfaces which are suitable for such applications have not been investigated. This work deals with a wrap around microstrip antenna on a conical surface with the thickness of the microstrip antenna being negligibly small. The losses due to surface waves are neglected. The radiation characteristics of the microstrip antenna are studied using the cavity model. With the aid of the equivalence theorem, the far field radiation patterns are obtained through a knowledge of the equivalent current density on the conical surface. The effect of the microstrip parameters on the radiation pattern are analyzed. The radiation patterns are presented for various conical structures.

EVALUATION OF RADIATION LOSS FROM MICROSTRIP LINE DISCONTINUITIES USING  
A MULTIPOINT NETWORK MODELING APPROACH IN MM WAVE MICROSTRIP ANTENNA ARRAYS

ALBERT SABBAN

RAFAEL, P.O.B 2250 Haifa, Israel,31021.

ABSTRACT

This paper presents a convenient method for incorporating radiation losses from microstrip line discontinuities in the design of mm wave microstrip antenna arrays.

Microstrip antennas possess attractive features such as low profile, light weight, small volume and low production cost. In addition, the benefit of a compact and low cost feed network may be attained by integrating the microstrip feed structure with the antenna on the same substrate. However, the open nature of the microstrip configuration suffers from radiation originating at various geometrical discontinuities. This radiation phenomenon in mm wave microstrip antenna arrays causes additional signal loss in the microstrip antenna feed network and undesired interactions between different parts of the feed network because of external electromagnetic coupling. These phenomena become significant in mm wave microstrip antenna arrays, more bends and other discontinuities are introduced in the feed network and spurious electromagnetic coupling and radiation losses increase considerably. As an example a right angled bend in a 50 ohm line on a 10-mil duroid substrate with  $\epsilon_r=2.2$ , the radiation loss is 0.1dB at 30 GHz and 0.17 dB at 40 GHz. These results point out that radiation losses need to be taken into account for accurate microstrip antenna array design at mm wave frequencies.

In this paper a planar multipoint network model and the segmentation method are used to evaluate radiation losses in a 64 and 256 patches array at 35 GHz. Design considerations and computational results will be presented.



## TUESDAY PM URSI-B SESSION T-U20

Room: HUB 310

### ANTENNAS I

- Chairs: E. Altshuler, Rome Laboratory-U.S. Air Force; R.D. Nevels, Texas A & M University
- 1:20 Airborne Radar for the 21st Century: The Space-Time Adaptive Array 232  
*\*R.L. Fante, The MITRE Corporation*
- 1:40 Analysis of Rectangular Waveguide Radiating Element for Use in a Wide-Angle Scanning Phased Array Antenna 233  
*R. G. Schmier, S. Geibel, Westinghouse Electric Corporation*
- 2:00 Synthesis of Shaped Beam Antenna Patterns Using Implicitly Constrained Non-Uniformly Spaced Current Elements 234  
*\*M.J. Buckley, Westinghouse Electric Corporation*
- 2:20 Beamforming with Spiral Antennas 235  
*\*N. Sangary, C. Wu, T. Lo, J. Litva, McMaster Univ.*
- 2:40 A Broad Band Characterization of Active Planar Antennas 236  
*J. Plet, M. Drissi, R. Gillard, J. Citerne, LCST/IINSA*
- 3:00 Break
- 3:20 The Method of Lines for the Analysis of Planar Antennas 237  
*R. Pregla, L. Vietzorreck, Fern Universität*
- 3:40 Field Patterns of Resonant Noncircular Closed-Loop Arrays 238  
*\*G. Fikioris, Department of the Air Force, Rome Laboratory (AFMC)*
- 4:00 A Double-Folded Monopole for Hemispherical Coverage 239  
*\*E. E. Altshuler, Department of the Air Force, Rome Laboratory (AFMC)*
- 4:20 Pattern Synthesis of Phased Array Antennas Using Linear Superposition of the FDTD Simulated Fields 240  
*\*C.E. Reuter, E.T. Thiele, A. Taflove, Northwestern Univ.; M. Picket-May, Univ. of Colorado; A.J. Fenn, Massachusetts Inst. of Technology*
- 4:40 A Solution of the Dielectric-Loaded Infinite Array Antenna Problem by a Method of Factorization with Interpolation 241  
*E. Baradit, F. Miranda, Universidad del Bio-Bio; V. Volman, The Hebrew Univ. of Jerusalem*

Airborne Radar for the 21<sup>st</sup> Century:  
The Space-Time Adaptive Array

by

Ronald L. Fante  
The MITRE Corporation  
Bedford, MA 01730

In this paper we will discuss the characteristics and limitations of space-time adaptive radar. We will illustrate how space-time adaptive degrees of freedom can be used to detect small targets, even in the presence of heavy ground clutter, jammers, and jammer multipath. The limitations on performance imposed by internal motion of the ground clutter, radar-platform crabbing, electromagnetic interaction of the antenna with the radar platform, channel equalization, jammer multipath, etc., will be evaluated. Suboptimum architectures will be proposed and discussed.

1994 URSS Radio Science Meeting (Seattle)

## Analysis of Rectangular Waveguide Radiating Element for Use in a Wide-Angle Scanning Phased Array Antenna

Robert Schmier and Steven Geibel  
Westinghouse Electric Corporation  
Baltimore, Maryland

In this paper the analysis and performance of an iris-loaded rectangular waveguide radiating element used in a phased array antenna is discussed. Construction of the antenna employing this type of element centers around a conductive plate, or faceplate, with rectangular holes milled in it in a predetermined grid pattern. The plate is milled from both sides such that a thin rectangular iris, which represents an inductance, is recessed in the waveguide aperture. This iris helps to match the radiating element over a wide range of scan angles. A thin sheet of mylar is used to seal the waveguide apertures. Subarrays containing phase shifters and manifolds are bolted to the faceplate to form the complete antenna.

This paper will describe the design of this radiating element which began with a complete electromagnetic analysis employing a spectral moment method solution of the magnetic field integral equation, rigorously taking into account various dielectric layers and waveguide fillers. The key to the analysis of this element is setting up an equivalent problem. In the equivalent problem, the aperture formed by the iris is replaced by a perfect conductor and a sheet of magnetic current is placed on top of the conductor on both sides of the aperture. The currents on opposite sides of the aperture are of equal magnitude and opposite sign. By employing this equivalent problem, the analysis can be conveniently separated into three distinct regions - free space to the left side of the aperture, a waveguide region in the faceplate, and a waveguide region which terminates in the phase shifter. The analysis allows for any number of stratified dielectrics in all three regions.

Comparisons will be shown between calculated performance, based on a numerical analysis computer code generated as a result of the analysis, and data measured from a Ku-band phased array antenna.

Synthesis of Shaped Beam Antenna Patterns using Implicitly  
Constrained Non-Uniformly Spaced Current Elements

Michael J. Buckley  
Westinghouse Electric Corporation  
P. O. Box 746 Mail Stop 55  
Baltimore MD 21203

Ground mapping airborne radars typically use a variation of a  $\text{csc}^2$  shaped beam. A technique for the synthesis of shaped beam patterns of a linear array using implicitly constrained non-uniformly spaced current elements is presented. The current elements must be constrained in order to realize physically producible patterns. Implicitly constraining the current elements avoids the use of explicitly constrained algorithms. Both element magnitude and spacing are implicitly constrained. Using a non-uniformly spaced linear array rather than a uniformly spaced linear array reduces pattern ripple in the shaped region. The initial starting point for the algorithm is a current distribution with uniform magnitude and spacing and elements phase shifted such that beam maximum coincides with the desired shaped beam maximum. This choice of starting point ensures convergence to a global minimum. In contrast with conventional methods the zeroes of the pattern function in the side lobe region are not constrained to lie on the unit circle. In order to assess the utility of the proposed technique, a comparison is made with previously published results. Compared to conventional approaches, the resulting current element-to-element variation is significantly less which minimizes mutual coupling difficulties. Both traveling wave and center fed designs are possible with the technique outlined in this paper.

# 1994 URSI Radio Science Meeting (Seattle)

## Beamforming With Spiral Antennas

Nagula Sangary\*, Chen Wu, Titus Lo, John Litva

Communication Research Laboratory, McMaster University  
Hamilton, Ontario, Canada L8S 4K1

The use of Spiral Antennas is becoming wide spread in the area of personal communications, in the past the spiral antennas were built with an absorbing cavity backing, this was done in order to maintain the frequency independent property of the antenna. Although these antennas were wide band, the efficiency is low. Therefore in order to increase the efficiency, the use of reflector plane instead of the absorbing cavity has become popular, even with the reflector plane the spiral antennas are wide band. Along with wide band operation, the other interesting feature is the different modes of operation. That is, when the spiral arms are fed with a different phase (0 to 180 degrees), the radiation pattern will be unique to this differential feed. Although , for beam forming this type of antennas will not give high accuracy as a large array antenna, the simplicity and low cost will find a good application in personal communications.

A unique feed structure was developed to feed the Two-Arm Archimedean Spiral Wire (thin line on the substrate) to have a variable differential feed, the following figures show radiation pattern obtained at 5GHz with two differential phase of 60 and 180 degrees. The axial ratio were fairly good (less than 2dB), the pattern is same for all plane cuts that are normal to the spiral plane. The measurement results were in close proximity of the theoretical predication, the technique used in the analysis was the Moment Method. The detail of the variable feed structure and more measurement results will be presented at the conference.

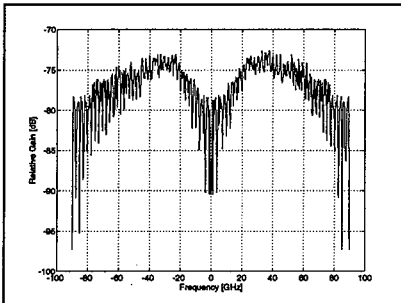


Figure 2: Differential Feed 60 degrees

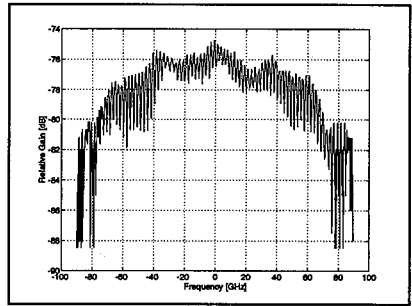


Figure 1: Differential Feed 180 degrees

## A BROAD BAND CHARACTERIZATION OF ACTIVE PLANAR ANTENNAS

J. PLET, M. DRISSI, R. GILLARD and J. CITERNE  
LCST/INSA, URA CNRS 834, 35043 RENNES CEDEX FRANCE

Recent research have shown that the concept of active planar antennas is very attractive to improve the bandwidth and the gain of the radiating element around its resonant frequency.

In the present work, the integral equation technique associated with the theory of loaded scatterers and solved by the Method of Moments is used to characterize active microstrip antennas in a large frequency range.

The studied structure is a microstrip dipole electromagnetically coupled to a microstrip feeding line on which a MMIC amplifier (AVANTEK MSA-0835) is implemented as shown in Fig 1 (R. Gillard, H. Legay, J.M. Floch', J. Citerne "Rigorous modelling of receiving active microstrip antenna" Electronics Letters, December 1991 Vol. 27, N°25 page 2357).

Fig 2 presents that the maximum of relative power is obtained at the resonant frequency 2.4 GHz. The difference between the active and the passive antennas at 2.4 GHz gives approximately the gain of the amplifier (18 dB for the present case). This result shows also that when the frequency decreases, the relative power of the active antenna remains constant compared to the passive one which decreases rapidly.

Fig 3 presents the relative power as a function of  $\delta c$  for different frequencies. This result shows that for each frequency it's possible to obtain a constant relative power if the amplifier is sufficiently far from the radiating element.

When they get closer, a large amount of the incident power is directly coupled to the radiating element. As a result the total radiated power decreases. Only such a global analysis can exhibit this phenomenon.

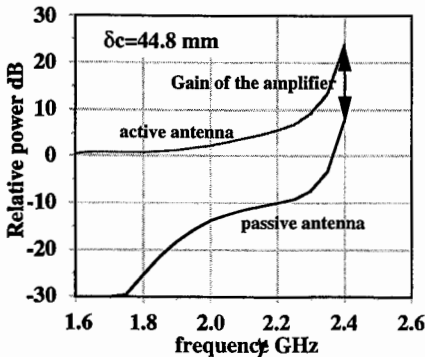
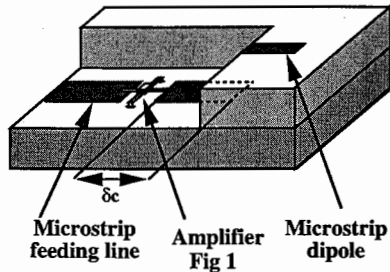


Fig 2

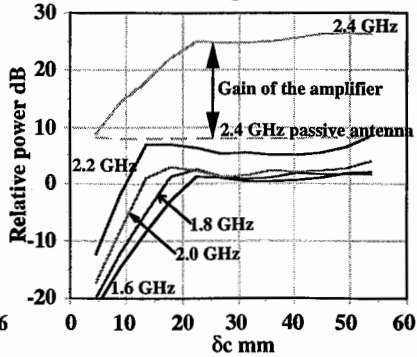


Fig 3

# The Method of Lines for the Analysis of Planar Antennas

Reinhold Pregla\* and Larissa Vietzorreck

Allgemeine und Theoretische Elektrotechnik, FernUniversität, D-58084 Hagen, Germany

## Abstract

The method of lines (MoL) – a special finite difference method – is one of the methods for the analysis of planar multilayered waveguide structures as used for microwave and millimeter wave integrated circuits. The MoL does not yield spurious modes and the relative convergence phenomenon is not observed. Because of the semianalytical approach the numerical effort is comparatively small. To model open structures absorbing boundary conditions are introduced, which take into account the radiated fields. A combination of the absorbing boundary conditions with the source method (S.B.Worm, MTT-38, No.10, 1510-1514, 1990) allows the analysis of planar antennas which are fed directly or indirectly by a microstrip line (see Fig.1).

In this contribution it will be demonstrated how the input impedance of such structures can be calculated. For that purpose the discretized field near the enclosing boundary, which crosses the feedline (s. Fig. 2), is separated into an incoming and an outgoing part. The difference operators for both parts are constructed differently. The absorbing boundary conditions are applied to the outgoing waves, which result from the reflection at the discontinuity, whereas the incoming field distribution can be calculated by analyzing the one-dimensional line problem.

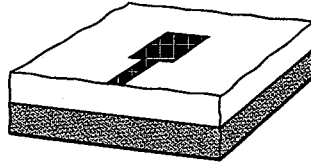


Fig.1: Example of a planar antenna

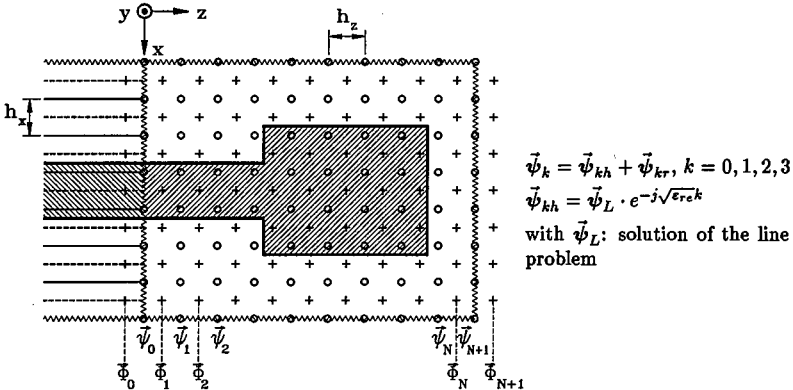


Fig.2: Discretization in z-direction

The separation of the discretized field leads to an inhomogeneous wave equation for the reduced part  $\psi_r$ , which contains near the boundary only the reflected components and the whole field in the remaining part of the calculation window. This wave equation can be solved analytically according to R.Pregla and W.Pascher ('The MoL' in T.Ittoh 'Numerical Techniques ...', 381-446, Wiley, 1989).

## FIELD PATTERNS OF RESONANT NONCIRCULAR CLOSED-LOOP ARRAYS

George Fikioris  
Rome Laboratory  
Electromagnetics and Reliability Directorate  
Hanscom AFB, MA, 01731

Recent studies have been made of large circular antenna arrays consisting of many vertical, non-staggered, perfectly conducting cylindrical dipoles. The following have been shown: 1) If only one of the  $N$  ( $N \gg 1$ ) dipoles is driven and the rest are parasitic, the circular array possesses a series of very narrow resonances as the frequency is varied. Each resonance is characterized by a large integer parameter  $m$ . 2) The currents on all the elements are large and of the same order of magnitude. The radiation field (obtained by summing over the discrete elements) is asymptotically the same if the  $N$  currents are replaced by a continuous distribution  $\cos m\phi'$  on the circle. This distribution of current may be thought of as a standing wave around the underlying circle. 3) In the azimuth, the radiation field consists of  $2m$  pencil-like beams. 4) One may drive a second element in the array and generate a traveling wave of current  $e^{im\phi'}$  around the circle. The field pattern in the azimuth is now omnidirectional. (G. Fikioris, R. W. P. King, and T. T. Wu, "A Novel Resonant Circular Array: Improved Analysis", to be published in J. Electro. Waves Appl.).

Furthermore, the possibility of generating a highly directive field by a resonant *noncircular* closed-loop array has been proposed (R. W. P. King, IEEE AP Trans. 37, 178-186, 1989).

In the present paper, this possibility is investigated by studying field patterns of noncircular arrays. The current distribution around the underlying curve is assumed to be a continuous traveling wave as in the resonant circular array with two driven elements. In polar coordinates  $(\rho', \phi')$ , the equation of the class of closed curves under study contains a small parameter  $\epsilon$  and reduces to the equation for a circle when  $\epsilon = 0$ . Although the shape of the array remains nearly circular ( $\epsilon \ll 1$ ), it is shown that the radiation field is very different from the omnidirectional field of the corresponding circular array. The effect of changing  $\epsilon$  and the other parameters of the problem is discussed in detail, and it is shown that for proper choices of the parameters, the field pattern in the azimuth consists of a single narrow radiated beam.

## A DOUBLE-FOLDED MONOPOLE FOR HEMISPHERICAL COVERAGE

Edward E. Altshuler  
U.S. Air Force Rome Laboratory  
Electromagnetics and Reliability Directorate  
Hanscom AFB, MA. 01731-3010  
Phone: 617-377-4662, FAX: 617-377-5040

A traveling-wave distribution of current can be produced on a linear antenna by inserting a resistance of approximately 240 ohms one-quarter wavelength from its end. This antenna is very broadband and has directional properties that are useful for special applications. The main disadvantage of the resistive-loaded traveling-wave antenna is that it is only about 50% efficient because part of the input power is absorbed by the resistor. It is possible to replace the resistor with a resonant antenna having a radiation resistance approximately equal to that of the matching resistor. Thus the input section still has a traveling-wave distribution of current up to the inserted element, but now the power previously dissipated in the resistor is radiated.

The antenna that was initially used to replace the resistor was a modified folded dipole (E.E. Altshuler, IEEE Trans. AP-S 41-7, 871-6, 1993). By adjusting the length of this folded element accordingly, a radiation resistance of about 240 ohms could be obtained. The input impedance, current distribution and radiation patterns of a folded monopole over an infinite ground plane were computed using the Numerical Electromagnetics Code (NEC). Horizontally polarized patterns were similar to those of this horizontal dipole over a ground plane and vertically polarized patterns in a plane orthogonal to the folded element were similar to those of a monopole over a ground plane. In addition, coverage was also obtained in the zenith direction in the plane of the folded element, as long as it was not an integral number of half wavelengths above the ground plane. When the folded element was approximately 1 of a wavelength above the ground plane, near hemispherical coverage was achieved in the plane of the folded element.

The double-folded monopole consists of orthogonal modified folded dipoles in place of the resistor. This antenna has three orthogonal radiating elements and it is shown that it is possible to approach near hemispherical coverage by adjusting the elements accordingly. The polarization is elliptical over the hemisphere and approaches circular over a wide range of angles.

## Pattern Synthesis of Phased Array Antennas Using Linear Superposition of the FD-TD Simulated Fields

C. E. Reuter\*, E. T. Thiele, A. Taflove  
Department of Electrical Engineering and Computer Science  
Northwestern University, McCormick School of Engineering  
Evanston, Illinois 60208

M. Piket-May  
Department of Electrical and Computer Engineering  
University of Colorado  
Boulder, Colorado 80309-0425

A. J. Fenn  
Lincoln Laboratory, Massachusetts Institute of Technology  
Lexington, Massachusetts 02173

This paper explores the generalization of the linear superposition principle from circuit theory to 3-D vector field solutions of Maxwell's equations as obtained by the FD-TD method. We describe a technique to apply the linear superposition principle to FD-TD models of phased array antennas.

The basic procedure consists of exciting one array element using a recently-developed  $50 \Omega$  resistive source feed representation (Piket-May et al, *IEEE Trans. MTT*, 1994, in press). Short circuits are modeled at the remaining element feed locations. Data for the fields at the near-to-far field integration surface are stored for this run. This procedure is repeated for each array element. Thus, an array with 8 elements would require 8 separate FD-TD runs. A subsequent post-processing step, not requiring a Cray FD-TD run, would merely scale each set of stored data by an arbitrary magnitude/phase distribution, and then transform to the far field for the radiated pattern. In this manner, literally hundreds of amplitude/phase tapers across the phased array could be quickly examined. Or, a synthesis procedure involving adaptive nulling techniques (Fenn, *IEEE Trans. APS*, 38:173-185, 1990) could be utilized to optimally provide the magnitude/phase taper. It is believed that this linear superposition approach is novel relative to FD-TD modeling.

Computed data for two phased array antenna systems are presented. The first system is an experimental prototype device in use at Lincoln Laboratory. It is a non-invasive monopole phased array designed to heat cancerous tumors near the surface of the skin. The second system consists of crossed-pair Vivaldi flared horn antenna elements combined into linear array antennas. It is demonstrated that the linear superposition technique has broad applications in FD-TD-based pattern synthesis, adaptive nulling, and design of phased array systems.

A SOLUTION OF THE DIELECTRIC-LOADED INFINITE ARRAY ANTENNA  
PROBLEM BY A METHOD OF FACTORIZATION WITH INTERPOLATION.

Erik Baradit<sup>(\*)</sup> - Fernando Miranda<sup>(2)</sup> - Vladimir Volman<sup>(3)</sup>

(\*) Universidad del Bío-Bío, Casilla 5-C, Concepción, Chile.

(2) Universidad del Bío-Bío, Casilla 5-C, Concepción, Chile.

(3) The Hebrew University of Jerusalem.

ABSTRACT

The phased array antennas are one of the most used antennas today, and the ones formed by rectangular waveguides play an important role among them. However, the study of these is rather complex due to the large number of elements and to the dielectric materials that compound them. This is one of the reasons why there are so many papers about this topic and also why there is such a diverse amount of methods to solve the diffraction problem associated with this type of antenna. Among these we have the Ritz-Galerkin method, modified residue-calculus techniques, the generalized method of moments, the Wiener-Hopf method, etc. The majority of these methods do not give simple equations that facilitate the analysis of the physical phenomena that occur in the structure of the antenna.

In this work a new method is applied. This is the method of factorization with interpolation which deals with certain complex variable technique and transforms the diffraction problem into an interpolation problem. This method which has given good results in other problems give us simple expressions for the reflection and transmission amplitudes related to this type of antenna. These expressions allow us to easily analyze the resonance phenomena through an equivalent model of antenna, and to obtain a transcendental equation for the angular behavior and location of the nulls of the antenna depending on the electrodynamical and geometric parameters.

The equivalent model consists in a resonant cavity inside of a waveguide.



TUESDAY PM URSI-A SESSION T-U21

Room: Savery 249

IMPULSE RADAR MEASUREMENTS

Chairs: E. Walton, The Ohio State University; M. Kanda, National Bureau of Standards

1:20	A Family of Orthogonal Pulse Compression Waveforms <i>S. El Assad, I. Lakkis, Laboratory S2HF (Systèmes et Signaux Hautes Fréquences)</i>	244
1:40	Impulse Radar Signatures of 3D-Targets: Development of a TD- Measurement System <i>*M. Piette, Royal Military Academy Brussels</i>	245
2:00	Comparison of Impulse and Noise-Based UWB Ground Penetrating Radars <i>*E. Walton, F. Paynter, The Ohio State Univ.</i>	246
2:20	Simulation of Imaging Radar Scenarios <i>H.E. Raemer, Y. Lou, Northeastern Univ.</i>	247
2:40	Simulation Study of Radar Returns from Mountain Terrain <i>H.E. Raemer, Y. Lou, Northeastern Univ.</i>	248
3:00	Break	
3:20	A Novel Bistatic Scattering Matrix Measurement Technique Using a Monostatic Radar <i>*K. Sarabandi, A. Nashashibi, Univ. of Michigan</i>	249
3:40	Radar Target Discrimination Using Recurrent Dynamic Memory and Noise Tolerant Multi-Layer Feedforward Backpropagation Neural Networks <i>*C.Y. Tsai, K.M. Chen, E.J. Rothwell, Michigan State Univ.</i>	250
4:00	Data Storage Techniques for Use in Correlation-Based Early-Time Radar Target Discrimination <i>*Q. Li, E.J. Rothwell, K.M. Chen, D.P. Nuquist, J. Ross, R. Bebermeyer, Michigan State Univ.</i>	251
4:20	Aspect Angle Sensitivity of Ultrawide Band Target Scattering Data <i>*J.E. Ross, R. Bebermeyer, E.J. Rothwell, K.M. Chen, D.P. Nyquist, Michigan State University</i>	252
4:40	An Electromagnetic Field Study for the Design of a Radar Range <i>*C. H. Tang, The MITRE Corporation</i>	253

# A Family Of Orthogonal Pulse Compression Waveforms

S. EL ASSAD, I. LAKKIS

Laboratoire S2HF (Systèmes et Signaux Hautes Fréquences)  
IRESTE, La Chantrerie CP 3003, 44087 NANTES Cedex 03, FRANCE

Tél: 40 68 30 36 - Fax: 40 68 30 66 - e-mail: selassad@ireste.ireste.fr

Modern radars generally incorporate pulse compression waveforms to obtain the desired range resolution while avoiding pulses having large peak powers. Pulse compression waveforms are exemplified by the Barker, pseudorandom shift register, chirp, and the polyphase codes [3].

A family of orthogonal linear FM waveforms is derived here. These waveforms have potential applications in cancelling range-ambiguity in a medium or high pulse repetition frequency PRF, and in reducing mutual interference between radar in proximity to each other that are operating in the same frequency band.

In this paper exact mathematical formulations of the autocorrelation function  $\chi_{m,m}(t)$  and the crosscorrelation function  $\chi_{m,n}(t)$  are derived for a family of  $M$  segments. Analytical expressions are obtained for five segments which are mutually orthogonal. Numerical results are used to verify our relations. The auto and crosscorrelation functions obey equation (1)

$$\left\{ \begin{array}{l} \chi_{m,m}(t) = g_m(t) \otimes g_m^*(-t) \\ \chi_{m,n}(t) = g_m(t) \otimes g_n^*(-t) \\ |\chi_{m,m}(t)| \leq \varepsilon_1 \quad t \in \mathfrak{R} - \left[ -\frac{1}{B}, \frac{1}{B} \right] \\ |\chi_{m,n}(t)| \leq \varepsilon_2 \quad t \in \mathfrak{R} \end{array} \right. \quad (1)$$

with

$$\left\{ \begin{array}{l} g_m(t) = \frac{1}{\sqrt{N}} \sum_{p=0}^{N-1} h(t-pT, B_{m,p}, \Phi_{m,p}) \\ h(t, B, \Phi) = \frac{1}{\sqrt{T}} \text{Rect}\left[\frac{t}{T}\right] e^{j\pi \frac{B}{T} t^2 + j\Phi} \end{array} \right. \quad (2)$$

where  $g_m(t)$  ( $m = 0, 1, \dots, M-1$ ) is the transmitted pulse and  $h(t, B, \Phi)$  the linear FM waveform.

## References

- [1] I. LAKKIS, S. EL ASSAD and J. SAILLARD. "Diagrammes ambiguité des formes d'ondes optimales et orthogonales". Contrat DME/ST3S/ES Mai 1992.
- [2] A. W. RIHACZEK. "Principles of high-resolution radar". 1985 Mc Graw-Hill.
- [3] K. GERLACH and F. F. KRETSCHMER. "General forms and properties of zero crosscorrelation radar waveforms". IEEE AES, vol. 28, no. 1 January 1992.

## IMPULSE RADAR SIGNATURES OF 3D- TARGETS DEVELOPMENT OF A TD- MEASUREMENT SYSTEM

Marc PIETTE  
Royal Military Academy Brussels  
30, avenue de la Renaissance  
B-1040 Brussels, Belgium

In view of the growing interest in the Impulse Radar- a special case of the Ultra-Wide Band Radars- and its potential identification capabilities for non co-operative targets when used in conjunction with aspect independent techniques like the Extinction Pulse Technique, the Royal Military Academy Brussels/Department Microwaves & Opto-electronics has started the development of an indoor test facility aimed at measuring *directly in the time-domain* the impulse response of 3D-targets.

The system consists of five parts. On the transmitting side, a long conical antenna on ground plane is coaxially fed by a high voltage short duration step function generator (100V/200ps). A small-scale version of the target under test is put on the ground plane and is illuminated by the step function like and nearly transverse electromagnetic wave radiated by the antenna. On the receiving side, a broad band  $\hat{\epsilon}$ -sensor detects the response of the target and sends the time derivative of this, the impulse response, to a high sensitivity sampling scope through a broad band low noise amplifier (Fig.1).

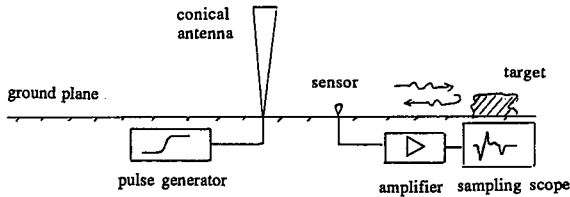


Fig. 1 View of the TD measurement system

The main effort of the current research is put into the design of the transmitting antenna because commonly used broadband antennae are unsuitable for radiating efficiently and without any distortion the step function waveform. After a thorough detailed theoretical study of the coaxially fed conical antenna under sub-nanosecond transient excitation (*modal analysis*), a conical antenna with a characteristic impedance of 200 Ohms was chosen and home-made (Fig.2). Special attention was paid to the design of the coaxial feeding point at the apex (Fig.3) and its effect on the input impedance, first theoretically and then experimentally by TDR with transients as short as 35ps.

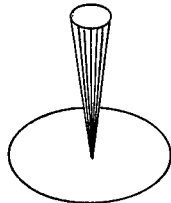


Fig. 2 200 Ohms conical antenna  
on ground plane

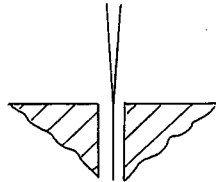


Fig. 3 Coaxial feeding point

## Comparison of Impulse and Noise-based UWB Ground Penetrating Radars

Eric Walton\* and Frank Paynter

The Ohio State University  
ElectroScience Laboratory  
1320 Kinnear Road  
Columbus, Ohio 43212-1191

The use of radar to locate and characterize underground objects has become important in recent years. Useful penetration occurs in the band below 800 MHz. In this band the underground propagation is dispersive, lossy and varies greatly as a function of the characteristics of the soil. These propagation and bandwidth limitations constrain the underground mapping (SAR) resolution and the use of classical high resolution imaging for classification of buried objects. The most successful classification technique has been to extract the resonance characteristics of detected objects from the frequency domain characteristics of the scattering. For these reasons, ground penetrating radars (GPR's) tend to cover as much of the frequency band below 800 MHz as possible. Two techniques for operation in this band will be compared here; the impulse radar and the noise radar.

Impulse radars transmit a short electromagnetic (EM) impulse; there is no carrier. We will show data from a system with an impulse duration of 2 ns. This system therefore has a bandwidth extending from DC to 500 MHz. Our antenna can radiate this impulse into the ground over the band from 50 to 500 MHz. The received signal is sampled at a 0.25 ns rate. We will show the received signals and demonstrate the signal processing required for underground mapping and resonance based target classification.

We will also show data from a radar based on correlation of wide-band noise (DC - 500 MHz). The bandwidth, antennas, average power and correlation time are comparable to that of the impulse system. We will show the experimental data and demonstrate the signal processing required for underground mapping and resonance based target classification.

The two radar systems will be shown to produce identical results under identical radiated power, bandwidth and equivalent integration times. Comparisons will be shown, especially under radio frequency interference (RFI) conditions.

## SIMULATION OF IMAGING RADAR SCENARIOS

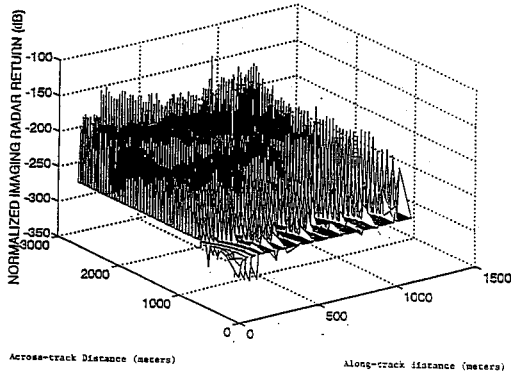
H. R. Raemer and Y. Lou  
Northeastern University  
Center for Electromagnetics Research and ECE Dept.  
Boston, MA 02115

### ABSTRACT

The authors have developed a very comprehensive program for modelling and simulation of radar target and clutter scenarios, based on coherent superposition of vector-phasor returns from all scattering material within the radar's field of view. This includes both natural terrain patches and discrete objects.

Recently the program has been used to simulate SAR-like imaging of terrain and objects on the terrain. For the initial run in this category, the antenna is a linear array of dipoles mounted on the fuselage of the aircraft with the array axis in the along-track direction. The dipole axis is also in the along-track direction to provide omnidirectional across-track coverage. Resolution in the across-track direction is obtained with a bank of narrow range gates. The result is a map of the relative intensities of the return from the patch of terrain illuminated by the radar, which can be displayed as a three-dimensional plot of intensity vs. x and y coordinates or as a contour plot in the x-y plane. A sample result is shown below and more results will be shown at the presentation.

We are currently enhancing the program to allow simulation of an actual SAR. The current results are for an unrealistically long real-aperture array that provides along-track resolution comparable to that attainable with SAR.



## SIMULATION STUDY OF RADAR RETURNS FROM MOUNTAIN TERRAIN

H. R. Raemer and Y. Lou  
Northeastern University  
Center for Electromagnetics Research and ECE Dept.  
Boston, MA 02115

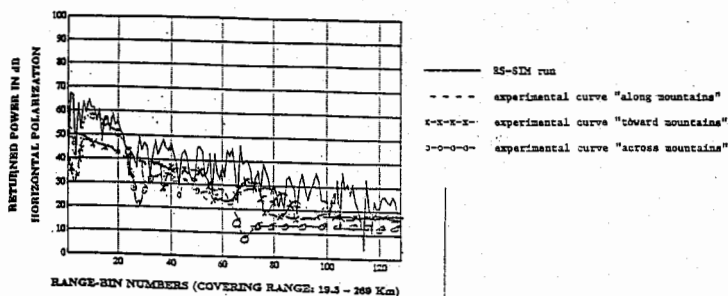
### ABSTRACT

The authors have developed a very comprehensive program for modeling and simulation of radar target and clutter scenarios, based on coherent superposition of vector-phaser returns from all scattering material within the radar's field of view.

We have run comparisons of the outputs of the program with results of field experiments. In this paper we focus on comparisons with results of airborne radar clutter measurements made by NRL in 1979 and 1980 in the Appalachian Mountain region. These measurements were at UHF with various geometries. Some of the experimental results were obtained with the antenna beam pointed horizontally in the direction of the mountains. The antenna was an array of half-wave dipoles mounted horizontally below the wing. The aircraft was flying at an altitude of about 16,000 feet.

In the absence of a terrain specific height profile, we generated a synthetic height profile designed to simulate a mountain range. We ran cases showing the return vs range over a region 270 km long, simulating the experimental conditions as closely as possible and using various options in the program for empirical and analytical terrain scattering models. We also tried different options for terrain material, eg. rocks and soil, vegetated terrain, snow covered terrain, etc., to characterize the composition of mountain terrain.

Some comparison results are shown below. The agreement between experimental and simulation results is quite good considering the uncertainties in the values of parameters needed to model the scattering from the terrain.



## A Novel Bistatic Scattering Matrix Measurement Technique Using A Monostatic Radar

Kamal Sarabandi\* and Adib Nashashibi

Radiation Laboratory

Department of Electrical Engineering and Computer Science

The University of Michigan Ann Arober, MI

Ann Arober, MI 48109-2122

### Abstract

Polarimetric bistatic RCS measurement of a point target have been, traditionally, conducted using two disjoint dual-polarized antennas. In this method often the transmitter and target are kept fixed and the receiver is moved on the surface of a sphere having the target at its center in order to measure the bistatic RCS at different bistatic angles. The complicated experimental setup and calibration procedure required for the bistatic measurement are the two major drawbacks of this technique.

In this paper a new technique for the bistatic scattering matrix measurement of point targets is introduced that circumvents the above mentioned difficulties of the standard method. The bistatic RCS measurement is performed using a wideband, fine resolution, polarimetric, monostatic radar in conjunction with a rotatable perfectly conducting ground plane positioned behind the target. Assuming that the distance between the target and the ground plane is larger than the radar resolution, the desired bistatic response (image contribution) can be isolated from the unwanted backscatter response. Since the radar operates in the backscatter mode, the measured cross-polarized responses, namely  $\sigma_{hv}$  and  $\sigma_{vh}$ , cannot be resolved. In order to resolve this ambiguity, additional independent measurements are required. The additional equation for the cross-polarized measurement is obtained by placing an anisotropic lossless slab on top of the perfectly conducting flat surface. Calibration of the measured data is accomplished by characterizing the radar distortion parameters over its entire mainlobe radiation pattern using the single target calibration technique (STCT). This information is then incorporated in an error model that takes into account the different transmit and receive signal paths in the bistatic measurement. The validity and accuracy of the bistatic measurement technique is demonstrated by measuring a number of point targets with known theoretical bistatic responses.

## **RADAR TARGET DISCRIMINATION USING RECURRENT DYNAMIC MEMORY AND NOISE TOLERANT MULTI-LAYER FEEDFORWARD BACKPROPAGATION NEURAL NETWORKS**

C.Y. Tsai\*, K.M. Chen and E.J. Rothwell  
Department of Electrical Engineering  
Michigan State University  
East Lansing, MI 48824

Radar target discrimination using the early-time transient response requires the efficient storage of target signatures at multiple aspect angles. A promising technique is to use a neural network which will recognize a target from an associated stored pattern under reasonable distortion. A variety of neural network techniques exist which can be adapted to target discrimination. We will examine Recurrent Correlation Memory (RCM), Recurrent Dynamic Memory (RDM) and noise tolerant backpropagation networks.

RCM networks store pattern information in a correlation matrix. When a measured target response is processed by the matrix, the output is the most likely associated partner. Since RCM's use a predetermined fixed order of correlation, they may require large resources if high orders are used, and may become inefficient or result in incorrect identification if low orders are used.

RDM networks use dynamic memory to accumulate information on the relationship between individual stored patterns and the input to the network. They adjust their dynamic memory based on correlation to gradually adapt to the pattern most similar to the input. Unlike a Hopfield network, or other RCM, an RDM network is adaptive in that it doesn't use a fixed order of correlation. This adaptability prevents the network from converging to unknown states or becoming trapped in local minima, as is often the case during the training of multi-layer networks.

Lastly, we will examine multi-layer feedforward backpropagation networks. These networks are usually noise sensitive, due to the fixed value of the activation parameter. Noise tolerance can be increased if a separate learning process is undertaken for individual layers, after the training of the entire network has converged. This increases the noise tolerance of each layer, and thus of the overall network.

Each of the above techniques will be demonstrated using the early-time responses of several scale model aircraft measured at multiple aspect angles.

## DATA STORAGE TECHNIQUES FOR USE IN CORRELATION-BASED EARLY-TIME RADAR TARGET DISCRIMINATION

Q. Li\*, E.J. Rothwell, K.M. Chen, D.P. Nyquist,  
J. Ross and R. Bebermeyer  
Department of Electrical Engineering  
Michigan State University  
E. Lansing, MI 48824

Several radar target discrimination techniques have been devised which use the early-time temporal response. Of these, probably the most straightforward are correlation-based schemes. The early-time responses of the expected targets are stored for a range of aspect angles, and the measured response of an unknown target is correlated with each stored response. The stored pattern which produces the maximal correlation is associated with the unknown target, and thus the target identified.

The difficulty with this approach is the rapid variation of early-time response with aspect angle, necessitating the storage of an enormous number of potential patterns. This paper describes three techniques for reducing the data storage through either a physical interpretation of early-time scattering, or through the use of an efficient signal representation algorithm.

Since the early-time response is dominated by specular reflections from target scattering centers, the response can be represented as a series of pulse responses. In this case it is only necessary to store the temporal positions of the scattering events and a limited amount of information about the scattering center impulse response. This information can be obtained either in the time domain, by fitting time-shifted pulses to the measured response, or in the frequency domain where the spectrum of the measured response can be modeled as a sum of complex exponentials. The arguments of the exponentials are related to the specular time positions and can be extracted using the E-pulse technique. An alternative technique uses wavelet basis functions to represent the measured data. It is found that only a small subset of the wavelet coefficients are needed to perform accurate target discrimination.

Discrimination among five different aircraft models will be demonstrated using each of the techniques for data storage. A "discrimination range" will be introduced to describe the range of aspect angles over which a correct decision is possible. This helps to determine the aspect angle discretization required for data storage.

## ASPECT ANGLE SENSITIVITY OF ULTRAWIDE BAND TARGET SCATTERING DATA

J.E. Ross\*, R. Bebermeyer, E.J. Rothwell, K.M. Chen, D.P. Nyquist  
Department of Electrical Engineering  
Michigan State University  
E. Lansing, MI 48824

Ultrawide band radar holds the promise of improved target detection as well as target identification. Much of this promise resides in the ability of the radar to exploit certain characteristics of the target scattering response.

In the case of target identification, differences in the received response due to target-to-target variations are used to make decisions. Recently, the early-time portion of the received response has been used in target identification. This portion of the response is composed of specular reflections from various parts of the aircraft fuselage, wings and engines. It provides a received signal that varies greatly from one target to another. Unfortunately, the signal also varies greatly depending on the aspect angle for a given target. The late-time portion of the response has also been used in target identification. The late-time has characteristic mode frequencies that are independent of aspect angle but amplitudes and phases that are aspect dependent. Thus, to assess the robustness of target identification methods, the variation of the received response with aspect angle must be investigated.

Recent improvements to the Michigan State University transient scattering range allow calibrated measurement of the scattering properties of scale model targets over the frequency range 0.2 to 18 GHz for all linear polarization combinations (hh, hv, vh, vv). Further, using a computer controlled rotation platform, the target aspect angle can be varied by as little as  $0.15^\circ$  between 0 and  $360^\circ$ . This measurement system is used to obtain data that is representative of both the early-time specular response as well as the late-time resonance response of the target models. Measured data from several scale model aircraft will be presented. The aspect angle sensitivity of the data will be examined for both the early-time and late-time. The possible impact of the aspect variations on target identification methods will be discussed.

## An Electromagnetic Field Study for the Design of a Radar Range

Chien H. Tang  
The MITRE Corporation  
Burlington Road  
Bedford, MA 01730

This paper discusses the design of a proposed radar range for end-to-end system integration testing of the Joint STARS radar system. Major radar test requirements include antenna beam pointing calibration, radar pulse stability check, isolation of various radar faults. The design of the range involves considerations of the mounting of a 24' by 2' phased array radar antenna and location of far-field towers for two-way line-of-sight testings.

An electromagnetic field study is performed to calculate the X-band radar radiated power density for human safety considerations and to evaluate the scattering effects of a preliminary site layout. Both the far-field and the nearfield (using the Fresnel field calculation) of the rectangular aperture antenna are carried out to describe the power density distribution. ANSI standard is used for configuring the range site safety provisions which include a security fence and a perimeter detection system.

For the evaluation of scattering effects of a given site layout, the following factors are considered:

- a. the Fresnel zones for given radar antenna and far-field tower heights and range separation,
- b. the "Glistening Surface" areas for different surface roughness, and
- c. the effects of antenna patterns on the ground reflection amplitude.

The local terrain profile and the associated surface features, obtained from the DMA database, are then used for the line-of-sight propagation selection. Details of the study will be highlighted.



TUESDAY PM URSI-B SESSION T-U22

Room: Savery 211

INVERSE PROBLEMS

Chairs: T. Habashy, Schlumberger Doll Research Center; G. Tricoles, GDE Systems Inc.

- 1:20 A Multiple Scattering Approach for Forward and Inverse Problems Involving Large Conductivity Contrasts 256  
*\*T.M. Habashy, C. Torres-Verdin, Schlumberger-Doll Research*
- 1:40 Time-Harmonic Electrical Impedance Tomography Using the T-Matrix Method 257  
*G.P. Otto, \*W.C. Chew, Univ. of Illinois*
- 2:00 Inverse Imaging with a Material Classification Technique 258  
*\*C.W. Manry, Jr., S.L. Broschat, Washington State Univ.*
- 2:20 Materials Characterization in Heterogeneous Media Using an Inverse Scattering Algorithm 259  
*K.J. Harker, D.G. Watters, D.G. Falconer, SRI International*
- 2:40 Analysis of Dispersive Radar Scattering by Data Preconditioning 260  
*\*E.K. Walton, M.J. Gerry, The Ohio State Univ.*
- 3:00 Break
- 3:20 Backpropagation and Time Domain Inverse Scattering Using Pulsed Beams 261  
*T. Melamed, Y. Ehrlich, \*E. Heyman, Tel-Aviv Univ.*
- 3:40 Target Discrimination Based on K-Pulse Technique Using Narrow-Band Data 262  
*\*G. Turhan-Sayan, Middle East Technical Univ.*
- 4:00 Distributed Neural Networks in Shape Recognition 263  
*M. Kuzuoglu, K. Leblebicioglu, Middle East Technical Univ.*
- 4:20 A New Parallel Algorithm for Diffraction Tomography 264  
*M. Kartal, \*B. Yazgan, Technical Univ. of Istanbul*
- 4:40 Emission Sources Finding Technique with Aperture Synthetic Method Combining Discrete Singularity Method 265  
*K. Murakawa, M. Takahasi, Y. Maeda, Y. Tokuda, NTT Telecommunication Networks Laboratories*

## A Multiple Scattering Approach for Forward and Inverse Problems Involving Large Conductivity Contrasts

Tarek M. Habashy\* and Carlos Torres-Verdín

Schlumberger-Doll Research, Old Quarry Road, Ridgefield, CT 06877

Forward and inverse scattering problems can be rigorously approached with finite-difference, finite-element or integral equation techniques. These simulation procedures can normally be rendered as accurate as possible with existing computer resources for very wide ranges of material properties and frequencies, but their main disadvantage is that they entail the inversion of a large stiffness matrix. The latter aspect is of serious consequences especially when the same operation is to be performed many times in the course of minimizing a cost function which defines an inverse scattering problem. In this paper, we report on accurate and efficient solutions to scattering problems suitable for large contrasts in conductivity and which do not require the inversion of a large matrix.

The EM scattering formulation presented here is based on a novel approach to multiple scattering which allows a closed-form renormalization of the infinitude of secular terms present in the Born series expansion and which otherwise render the Born approximation inaccurate. We call the resulting solution the *Localized Nonlinear Approximation*. In deriving such a solution, we start with the source-type integral equation that governs the total field. Next, we express the fields internal to the scatterers in a Taylor series expansion around the observation point. This results in a hierarchy of equations which are linear in the internal field and its higher-order gradients. Depending on the degree of smoothness assumed on the internal field, one can truncate this hierarchical set of equations allowing, in principle, a closed-form solution of the internal electric field. The ensuing renormalization has the effect of adjusting the background field (i.e., the field excited in the absence of the scatterers) by way of amplitude, phase, and cross-polarization corrections that result from frequency-dependent mutual coupling effects among scatterers. Hence, it accounts for a great deal of the multiple scattering among scatterers that is absent in the finite order Born series expansion.

By comparison with a finite-difference code, we demonstrate the range of validity of the Localized Nonlinear solution as a function of conductivity contrast, scatterer size, and frequency of operation. Furthermore, we show that the solution has a numerical efficiency comparable to that of a linear scheme such as the Born approximation and which is orders of magnitude faster than a finite-difference formulation.

We also develop a mathematical framework to approach nonlinear inverse scattering problems based on the Localized Nonlinear Approximation. This consists of the derivation of fast explicit formulas for the Jacobian matrix whose efficiency is demonstrated in the case of limited-angle, multi-frequency tomography experiments.

# Time-Harmonic Electrical Impedance Tomography Using the $T$ -Matrix Method

GREGORY P. OTTO AND WENG CHO CHEW\*  
ELECTROMAGNETICS LABORATORY  
DEPARTMENT OF ELECTRICAL AND COMPUTER ENGINEERING  
UNIVERSITY OF ILLINOIS  
URBANA, IL 61801

## Abstract

Many EIT theories exist, but currently, measurement systems have not been able to realize the resolution predicted by synthetic data. Measurement accuracy and electrode contact impedances have been identified as some of the limitations of the current methods. The measurement accuracy can be significantly improved by using the four-electrode method and optimal current injection methods. Also, an electrode contact impedance model has been appended to Yorkey's standard electrostatic model. Even using these modifications, there is substantial room for improvement. For example, in the frequency range of 10-100 KHz, the wavelength is on the order of meters if the conductivity is on the order of S/m. Thus, an electrostatic description may not be adequate. Instead, the system might be susceptible to finite frequency effects; the treatment of these effects requires an electrodynamic physical model. From another viewpoint, since the measurement accuracy has been found to be crucial to the resolution, one might reduce modeling error by improving the physical model to include frequency effects. This could increase the resolution since the signal to noise ratio is effectively increased when the errors due to physical modeling are reduced.

This paper solves the EIT inverse problem for two-dimensional inhomogeneous objects. This solution for the inverse problem details a new formulation that abandons the standard electrostatic impedance model for the full-wave  $T$ -matrix model. The goal of this work is to use an improved physical model to increase the resolution and invert higher contrast objects than other methods. Another advantage of this formulation is that a better gradient matrix is obtained, so the image reconstruction converges in fewer iterations. It will be shown that the use of this method has no additional computational cost, compared to the finite element solution.

## Inverse Imaging with a Material Classification Technique

Charles W. Manry, Jr.\*, and Shira L. Broschat

Electrical Engineering & Computer Science

Washington State University

Pullman, WA 99164-2752

cmanry@eecs.wsu.edu, (509)335-2348

shira@eecs.wsu.edu, (509)335-5693

In recent publications the inverse imaging problem has been solved using an iterative approach based on moment methods and either the Born or Distorted-Born approximation [Chew *et al.*, IEEE BME, 9, 218-225, 1990] and the Gauss-Newton method [Borup *et al.*, Ultrasonic Imaging, 14, 69-85, 1992]. These different imaging techniques assume that the scattering object is bounded inside a region of space but that no additional information is known. They consist of two steps. In the first step, the total field is computed for a given scattering object; in the second, the scattering object is updated using the measured scattered fields and the calculated total field. An iteration consists of a pass through both steps. In this paper, we discuss the use of a third step. If the scattering object is composed of a known set of materials, but with an unknown configuration, the convergence rate of the inverse solution can be increased using the *a priori* knowledge of the material characteristics.

In the third step, an attempt is made to classify a region of the scattering object as one of the known materials. When this material classification can be accomplished, a region is set equal to the appropriate material. When it cannot be accomplished, a region is left unmodified. In either case the object is passed back for the next iteration. The classification procedure is based on construction of a histogram of wavenumbers for the image with Gaussian curves fitted to it. Classification decisions are based on the overlap of these Gaussian curves. By identifying regions in the object as they become distinct, fewer iterations are needed to solve the problem. This technique can be applied in non-destructive testing to find known types of defects and in biomedical imaging if tissues types can be well characterized.

MATERIALS CHARACTERIZATION IN HETEROGENEOUS MEDIA  
USING AN INVERSE SCATTERING ALGORITHM

K.J. Harker, D.G. Watters, and D.G. Falconer  
SRI International, Menlo Park CA 94025

We have developed a numerical technique to solve the inverse scattering problem of determining the electrical and magnetic properties of unknown materials in an enclosure. It is assumed that the shapes of homogeneous regions within the enclosure are known, and it is desired to characterize the complex permittivity and permeability of each homogeneous region from a series of measurements of the scattered field. This technique may be useful for identifying materials within nonmetallic containers.

Our technique uses standard minimization routines and method-of-moments (MOM) scattering codes. The reference scattered field is first measured over a range of frequencies and monostatic scattering angles. Starting from a guess of the physical properties of the embedded bodies, the MOM code calculates the surface currents on each body and then computes the scattered field. Using the root mean square value of the phasor difference between the reference and calculated fields as a cost function, the permittivity and permeability of each embedded body is varied to obtain a minimum value for the cost function. The physical properties of each body at the minimum are assumed to be the problem solution. Although the technique is quite general, its application has been restricted thus far to bodies of revolution (BOR) consisting of non-magnetic linear isotropic dielectric (both lossy and lossless) materials. A BOR MOM code was used to calculate the scattered fields (JRBOR: "Computation of Scattering from a General Body of Revolution," Vol I and II, James R. Rogers, Technical Report JR-2, Revised, Atlantic Aerospace Electronics Corp., Greenbelt, MD, 1990.)

In the theoretical phase of this study we calculated the reference scattered field from a known set of permittivities for each homogeneous region in an enclosure. The heterogeneous body consisted of a lossless tenuous dielectric cylinder with a lossy dielectric torus and lossless dielectric sphere in its interior. Using a realistic guess for the permittivities, the minimization algorithm obtained a minimum value within 7% of the reference permittivities for frequencies corresponding to a body size of 0.2 to 2 wavelengths for the largest physical dimension. The introduction of Gaussian noise into the reference scattered field showed that convergence to 10% of the reference permittivities was robust for signal-to-noise ratios down to 20 dB.

In the experimental phase of this study we constructed a test body and placed it in our anechoic chamber. The test body consisted of a styrofoam cylinder with a lucite ring of square cross section and a delrin cylinder in its interior. All three materials are low loss dielectrics. Scattered field measurements were obtained over a frequency range of 0.4 to 18 GHz and a polar monostatic scattering angle range of 180 degrees. Using the scattered field at several frequencies and angles (greater than four) as the reference, the cost function was minimized. Good agreement between the reference and calculated permittivities was obtained.

## Analysis of Dispersive Radar Scattering by Data Preconditioning

Eric K. Walton\* and Michael J. Gerry

The Ohio State University  
ElectroScience Laboratory  
1320 Kinnear Road  
Columbus, Ohio 43212-1191

Radar scattering is made up of scattering from a number of specific subcomponents of the target. Spectral estimation techniques such as Fourier transforms or model based techniques such as autoregressive techniques (forward-backward linear prediction for example) or multiple sinusoid techniques (the MUSIC algorithm) may be used to transform from the frequency domain to the time domain.

We model the dispersive scattering from a subcomponent of the radar target as

$$S(f) = A (2 \pi f)^\alpha e^{-j (2 \pi f t)}$$

where the dispersive nature of the scatterer is given in terms of  $\alpha$ . The dispersive characteristics for various common radar scatterers are given in table 1

**Table 1. Scattering mechanisms and associated  $\alpha$  values.**

Points	0
Corner	-1
Edge	-0.5
Dihedral or Trihedral	+1
Cylinder (axial)	+1
Cylinder (broadside)	-0.5
Flat plate	+1

We have developed a technique where we pre-condition the data so that the inverse of the dispersive characteristic for various assumptions of  $\alpha$  is pre-multiplied by the original frequency domain data. Next, a model-based frequency domain to time domain transformation is performed. The result after a scan in  $\alpha$  is a mapping of the time domain response of a radar target into the down range versus  $\alpha$  domain. The response forms a peak when the value of  $\alpha$  is matched to the data.

Examples for both theoretical and experimental scattering will be given. It will be shown that if there are two scatterers with different  $\alpha$  values (even at the same down range location), then this new technique will actually differentiate between them.

## BACKPROPAGATION AND TIME DOMAIN INVERSE SCATTERING USING PULSED BEAMS

Timor Melamed, Yael Ehrlich and Ehud Heyman\*  
Tel-Aviv University, Dept. of Electrical Engineering — Physical Electronics  
Tel-Aviv 69978, Israel  
Fax: +972-3-6423508, E-mail: heyman@eng.tau.ac.il

With the trend toward increased bandwidth in radiating and detection systems, and the resulting gain in resolution, modeling algorithm *directly* in space-time can now be based on interrogation by well collimated short pulse wavepackets, also termed pulsed beams (PB). Such solutions furnish not only a complete basis for representation of arbitrary space-time signals, but also provide individually highly resolved wavelets for local probing of targets or of the propagation environment. The spatial-temporal resolution achieved under PB conditions furnishes an unambiguous measure of where the “physical” signal resides, in contrast to frequency domain procedures that must rely on more intricate phase discrimination.

We present two PB-based target interrogation and data processing schemes for imaging within the Born approximation. The first scheme deals with local data processing, backpropagation and imaging using PB as basis elements. For simplicity, the interrogating field is a (non-local) pulsed plane wave. The procedure starts with data processing using a local Radon transform that projects the data onto an appropriately parametrized phase space and localizes the regions wherein the “physical” signal resides. This local data defines a spectrum of pulsed beams that are then backpropagated and focused onto the image points. The other imaging scheme involves local interrogation. Here, the data is taken by scanning the target with pulsed beams. The image is obtained, again, by focusing backpropagated wavepackets onto the image points. Numerical results for imaging of a low contrast dielectric sphere will be presented.

**Target Discrimination Based on K-Pulse Technique  
Using Narrow-Band Data**

Gönül Turhan-Sayan, Associate Professor  
Department of Electrical and Electronic Engineering  
Middle East Technical University  
06531 Ankara, Turkey

The K-Pulse of an electromagnetic scatterer is a time-limited excitation waveform whose Laplace transform zeros coincide with the natural resonance frequencies of the object. Among all possible excitations, K-Pulse of the scatterer is the one which produces a target response waveform of finite support in time. In other words, based on pole-zero cancellations between the K-Pulse spectrum and the transfer function of the scatterer, the natural resonances are annihilated and the K-Pulse response of the object turns out to be a finite energy signal regardless of the aspect and the polarization of the excitation. Therefore, the K-Pulse technique suggests an aspect and polarization independent target discrimination method which is applicable to electromagnetic scatterers of arbitrary geometry but of finite size. This method is especially useful in applications where the backscattered measurement data are available for a single or a few (and quite possibly unknown) orientations of the target. The noise performance of the discrimination scheme has shown to be very satisfactory. Also, the required computation time for data processing is in the order of seconds provided that a library of K-Pulse waveforms for a set of candidate targets are already synthesized and stored in the system.

With all the features outlined above, the K-Pulse approach is found suitable for the radar target discrimination problem where the speed of discrimination process is as important as the accuracy of the discrimination result. However, in radar applications, the measured backscattered data are available only over a narrow spectral band at the radar frequencies at which the wavelength is a very small fraction of the overall target dimensions. Therefore, the K-Pulse spectrum zeros over this band must closely approximate the system poles falling into the same spectral band (without any extra zeros if possible) for accurate discrimination results. This calls for special modifications in the previously suggested K-Pulse synthesis technique. This paper presents K-Pulse waveforms and the results of various simulated radar target discrimination problems for geometrically simple targets such as conducting straight thin wires (high-Q scatterers) and conducting spheres (low-Q scatterers) using very narrow band spectral data. The test target geometries are intentionally chosen to be simple to eliminate the effects of target substructures in the K-Pulse synthesis and the target discrimination process.

## DISTRIBUTED NEURAL NETWORKS IN SHAPE RECOGNITION

Mustafa Kuzuoğlu      Kemal Leblebicioğlu

Middle East Technical University, Dept. of Elect. Eng., 06531, Ankara, Türkiye

The determination of the cross-sectional boundary  $\Gamma$  of infinitely-long perfectly conducting cylinders from scattered far-field data is a well-known inverse problem. The operator mapping the far field pattern to the boundary  $\Gamma$  is nonlinear and its explicit expression is not known in general. In this work, this operator is simulated by a distributed neural network architecture composed of  $N$  layers such that the equation governing the  $i$ -th layer is

$$x_i(\xi) = f\left(\int_0^1 w_i(\xi, \eta)x_{i-1}(\eta)d\eta + b_i(\xi)\right) \quad i = 1, 2, \dots, N \quad (1)$$

where  $f(\cdot)$  is a known nonlinearity, preferably a sigmoid.  $x_i$ 's are called the states of the neural network system and the corresponding equations in the form of equation (1) are referred to as state equations. The weight distributions  $w_i(\cdot, \cdot)$  and the threshold functions  $b_i(\cdot)$  are determined in terms of the training pairs  $(\Gamma_j, p_j)$   $j = 1, \dots, M$  where  $p_j$  is the far-field pattern corresponding to the boundary shape  $\Gamma_j$ . The problem is formulated as an infinite-dimensional constrained optimization problem, where a functional (related to the training pairs) is minimized subject to the equations satisfied at each layer. This problem can be transformed to an unconstrained optimization problem by augmenting the functional using the method of Lagrange multipliers. In this method, inner products of the state equations with Lagrange multiplier functions  $\lambda_i$   $i = 1, \dots, N$  are added to the original functional to form the augmented functional. During the training phase, using variational methods, the equations satisfied by the stationary points of the augmented functional are found. The expressions satisfied by  $\lambda_i$ 's turn out to be integro-difference equations similar to equation (1), and they are named as adjoint state equations, and  $\lambda_i$ 's as adjoint state variables. The coupled state-adjoint state equations are iteratively solved by using the steepest descent method. However, there is no guarantee for the convergence of the iterates to the global minimum. On the other hand, for successful training, it is sufficient to reduce the value of the functional below a certain value. The neural network is used in pattern recognition by identifying the boundary shape  $\Gamma$  from noisy measurements of the far field pattern. For this purpose, the network is trained by a finite set of data  $(\Gamma_j, p_j)$   $j = 1, \dots, M$  where each  $\Gamma_j$  is chosen to be a boundary curve which can be encountered in practical situations (e.g. circle, square, ellipse,  $\dots$ , etc.). Finally, it is shown that the method provides a fast and robust means for object recognition which may be a powerful alternative in pattern recognition problems in radar applications.

## A NEW PARALLEL ALGORITHM FOR DIFFRACTION TOMOGRAPHY

Mesut KARTAL    Bingül YAZGAN\*

Technical University of Istanbul, Electrical & Electronics  
Engineering Faculty 80626 Maslak, Istanbul Turkey

In this paper, we discuss a parallel multistage algorithm with forward-backward processing for microwave tomographic image reconstruction. In this technique, the matrix determined by the reconstruction algorithm is partitioned into submatrices, and a matrix-inversion method is applied to each submatrix independently. Using the method of moments, the scattered field at any point outside the object can be expressed in matrix form as

$$XW = U \quad (1)$$

$X$  is the  $N \times M$  Green matrix and in general,  $N$  is different from  $M$ .  $W$  is the  $M \times 1$  column vector whose components are proportional to the value of the object function in the cells and,  $U$  is a  $N \times 1$  column vector whose components are the scattered field values at points located outside the scatterer. The least-squares solution (LS) of Eq.(1) which maximizes the square-error  $\|o\|^2 - \|XW - U\|^2$  can then be written as  $\varpi - X^*U$ , where  $X^*$  is the generalized inverse of  $X$ . The new algorithm involves partitioning of the matrix equation and processing in a number of stages in a forward-backward scheme. The major advantage of the multistage algorithm is the reduced computational time when the stages are mostly implemented in parallel. For example the partitioning of the matrix equation (1) into two can be written as

$$\begin{bmatrix} X_1 & X_2 \end{bmatrix} \begin{bmatrix} W_1 \\ W_2 \end{bmatrix} = U \quad (2)$$

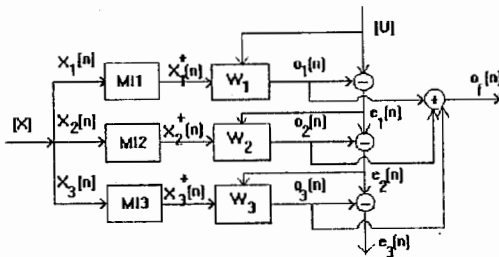
Processing in the two-stages is done by applying the LS solution to the each submatrix using a parallel algorithm. In forward-backward processing, the process is iterated by expressing the desired output of the first stage in terms of the actual output of the first stage and the error of the second stage. Then the process is repeated. The number of iterations are continued until convergence is obtained. Processing in the two-stages is done as follows:

**Stage 1:**  $X_1W_1 = U$ ,  $\varpi_1 = X_1^*U$ ,  $o_1 = X_1\varpi_1$ ,  $e_1 = U - o_1$

**Stage 2:**  $X_2W_2 = e_1$ ,  $\varpi_2 = X_2^*e_1$ ,  $o_2 = X_2\varpi_2$ ,  $e_2 = e_1 - o_2$

This process can be easily generalized to  $L$  stages with  $L > 2$ .

The multistage algorithm is found to be more robust against numerical errors and to yield more robust reconstruction in the presence of measurement noise as compared to a single-stage algorithm.



Flow graph of the 3-stage parallel system

## Emission Sources Finding Technique with Aperture Synthetic Method combining Discrete Singularity Method

Kazuo MURAKAWA, Masayuki TAKAHASI, Yuji MAEDA and Masamitsu TOKUDA  
NTT Telecommunication Networks Laboratories  
9-11, 3-chome, Musashino-Shi, Tokyo 180 Japan

### 1. INTRODUCTION

To find emission sources is available to simulate emission properties of equipment in near and far field and to countermeasure emission from equipment. In this paper, emission sources finding technique with aperture synthetic method combining discrete singularity method is proposed.

### 2. THEORETICAL AND EXPERIMENTAL RESULTS

Combining the aperture synthetic method[1] and the discrete singularity method[2] which are used to find emission source points, some problems in these two methods can be solved. To obtain the emission source points and levels, a following new norm is introduced.

$$I_N = \sum_{m=1}^M |E_m - \sum_{i=1}^N J_i * F_{mi}|^2 + M_s * \sum_{t=1}^T \sum_{m=1}^M |E_m - \sum_{i=1}^N J_i * F_{mt}| F_{mt} / |F_{mt}| \quad (1)$$

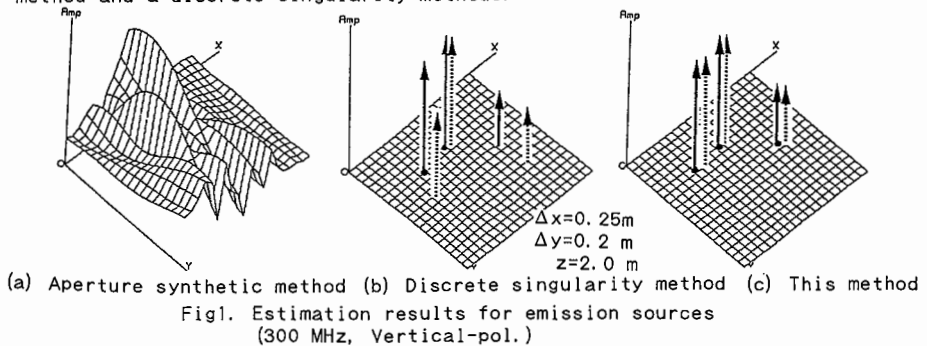
$$F_{mi} = \exp(-jkR_{mi})/R_{mi}, \quad F_{mt} = \exp(-jkR_{mt})/R_{mt} \quad (2)$$

where  $E_m$  is  $m$ -th measure electric field and  $J_i$  is  $i$ -th emission source current.  $R_{mi}$  is a distance between measurement point  $P_m$  and emission source point and  $R_{mt}$  is a distance between measurement point and emission source scanning point  $S_t$ .  $M_s$  is a weighting factor.  $k$  is a wave number.  $T$ ,  $M$  and  $N$  are total numbers of scanning points, measurements and emission source currents. By calculating the linear equation related to unknown point and levels of  $J_i$ , the emission source points and levels are obtained.

The emission source finding results are shown in Fig.1. In Fig.1, three emission sources (small dipole antennas) are located in semi-anechoic chamber. Fig.1 (a) shows a evaluation result for aperture synthetic method, and Fig.1 (b) shows a emission source points for a discrete singularity method and Fig.1. (c) show emission source points obtained by this method. In Figs.1 (b) and (c), a solid line shows an original emission source vector (point and level) and a broken line demotes an estimated one. From the result of this method, the emission sources are to coincide to the original emission source points compared to the other two methods.

### 3. CONCLUSION

In this paper, a new emission source finding technique combining with the aperture synthetic method and the discrete singularity method is proposed. Using proposed method, it is available to find emission source point and its level not considering some difficulties of the aperture synthetic method and a discrete singularity methods.



#### REFERENCES

- [1] W. F. Gabriel: "Spectral analysis and adaptive array supperresolution techniques", Proc. IEEE, Vol. 68, No. 6, pp. 654-666, 1980.
- [2] M. Nisimura et al: " A Numerical Analysis of Electromagnetic Scattering of Perfect Conducting Cylinders by means of discrete Singularity Method Improved by optimization Process", IEICE, Vol. J67-B, No. 5, pp. 552-558, 1994.

TUESDAY PM URSI-K SESSION T-U23

Room: Savery 241

PHYSICAL CHARACTERISTICS OF EM FIELD IN BIOLOGICAL MEDIA

Chairs: C. Ramon, University of Washington; Koichi Ito, Chiba University

1:20	Three-Dimensional Bidomain Modeling of Cardiac Tissue on a Massively Parallel Computer <i>*K.T. Ng, P.D. Claessen, H. Saleheen, R. Hart, New Mexico State University</i>	268
1:40	3D Analysis of Ion-Current Exposure on a Human Body <i>K. Shimizu, M. Yamashita, G. Matsumoto, Hokkaido Inst. of Technology</i>	269
2:00	Modeling Induced Currents in Biological Cells Exposed to Low Frequency Magnetic Fields <i>*M.A. Stuchly, W. Xi, Univ. of Victoria</i>	270
2:20	Induced Electric Currents in Man and Rodents Exposed to Magnetic Fields <i>*M.A. Stuchly, W. Xi, Univ. of Victoria; O. P. Gandhi, Univ. of Utah</i>	271
2:40	Noninvasive Biomagnetic Sensing of Biological Currents <i>*C. Ramon, P. Czapski, R.J. Marks II, H.C. Lai, S. Lee, Univ. of Washington</i>	272
3:00	Break	
3:20	A Simple Method to Incorporate the Effects of an RF Shield into MRI Antenna Analysis <i>*J. Jin, Univ. of Illinois</i>	273
3:40	Exposure System for ION Cyclotron Resonance Stimulation at 2.2 GHz <i>*I.D. Fitian, A.R. Liboff, Oakland Univ.; V.V. Liepa, Univ. of Michigan</i>	274

## **THREE-DIMENSIONAL BIDOMAIN MODELING OF CARDIAC TISSUE ON A MASSIVELY PARALLEL COMPUTER**

**K.T. Ng\*, P.D. Claessen, H. Saleheen, and R. Hart**

**Department of Electrical & Computer Engineering  
New Mexico State University  
Las Cruces, NM 88003**

Cardiac tissue modeling is important for understanding the mechanisms underlying the different phenomena occurring in the heart, e.g., fibrillation and electrical defibrillation. One model which has been used successfully to represent the cardiac tissue is the so-called bidomain model, which is a continuum model with electrical properties corresponding to those of the tissue averaged over many cells. Specifically the intracellular and interstitial regions of a tissue are modeled individually as an electrically conducting domain and current can flow from one domain to the other only through the membrane represented by a capacitance and an appropriate ionic current model, e.g., Beeler-Reuter model. Application of the bidomain model, however, has been limited in the past mainly to two-dimensional geometries or three-dimensional structures with simplified assumptions, due to the speed and memory constraints of conventional computers. As a step in extending the size and complexity of the problems that can be studied, we have implemented the bidomain model on a massively parallel computer, the Connection Machine. The large number of processors in the Connection Machine provides a high level of parallelism and the solution of large problems.

The elliptical equations for the intracellular and interstitial regions are first combined to obtain a single equation for the transmembrane potential. Spatial operators are discretized with the finite-difference technique and the transmembrane potential is updated at each time step with the forward Euler method. The equation for the intracellular or interstitial potential is then discretized also with the finite-difference method and the resulting system of equations is solved with the Jacobi technique with overrelaxation. The medium surrounding the cardiac tissue is modeled as a monodomain and discretized in a similar fashion. Current continuity conditions are enforced at the boundary between the bidomain and monodomain. A nodal assembly technique is used in which each virtual processor is responsible for all the calculations related to a node in the solution process. This allows an efficient mapping of the finite-difference grid to the processor array. Various models have been implemented for the ionic currents represented by Hodgkin-Huxley type equations, including the classical Beeler-Reuter model and the recent Luo-Rudy model for ventricular cardiac tissue. Development of a realistic bidomain model for the myocardium that incorporates measured geometry and fiber data will be discussed. Details of the numerical procedure will be presented together with various simulation results.

### 3D Analysis of Ion-Current Exposure on a Human Body

Koichi Shimizu\*, Masaji Yamashita\*\* and Goro Matsumoto\*\*

\* Department of Bioengineering, Faculty of Engineering,  
Hokkaido University, Sapporo, 060, Japan.

\*\* Hokkaido Institute of Technology, Sapporo, 006, Japan.

To study the biological effects of the ion-current commonly found under ultra-high voltage DC transmission lines, a technique was developed to evaluate the human exposure to the ion-current field. This technique is based on numerical analysis using the boundary element method. The difficulty of handling the space charge in the calculation was overcome by assuming a lumped source ion-current. This technique is applicable to a three dimensionally complex object such as a human body. In comparison with theoretical values, the accuracy of this technique was evaluated to be satisfactory for our purposes. It was then applied to a human body in an ion-current field. The distribution of the electric field along the body surface was obtained.

Fig.1 shows the manner of model division and the calculated results of surface electric field. The vectors show the orientation and the intensity of the field. The general characteristics of field distribution were essentially the same as in those without space charges. However, it was found that the strength of the field concentration was significantly enhanced by the space charges. Further, the field exposure when a human body was charged by an ion-current was evaluated. As the charged voltage increases, the position of field concentration moves from a human's head toward his legs. But the danger of current discharge increases. This technique provides a useful tool for the study of biological effects and safety standards of ion-current field.

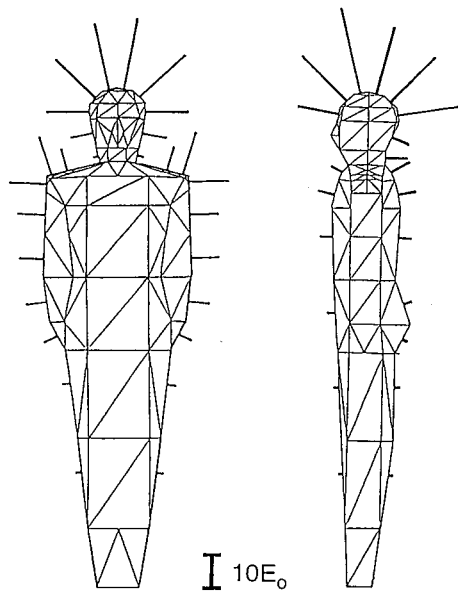


Fig.1 Field exposure in ion-current of  $10^{-7}$  C/m<sup>3</sup>

# 1994 URSI Radio Science Meeting (Seattle)

## MODELING INDUCED CURRENTS IN BIOLOGICAL CELLS EXPOSED TO LOW FREQUENCY MAGNETIC FIELDS

\*M.A. Stuchly and W. Xi, Department of Electrical and Engineering, University of Victoria, P.O. Box 3055, Victoria, British Columbia, Canada V8W 3P6

Interactions of low frequency magnetic fields with biological systems have been a subject of an intense scientific inquiry and public concern. Most of research has been done at power-line frequencies of 50 or 60 Hz. One of the key questions related to interactions of low-frequency magnetic fields with biological systems is which parameters of the exposure field are responsible for observed effects. It has been recognized that macroscopic and microscopic dosimetry are some of the tools that are useful in resolving the apparent contradictions and elucidating interaction mechanisms. Some experimental studies with cells in vitro indicate that the observed interactions depend on the induced electric field and current rather than directly on the applied magnetic field. At the same time, there has been paucity of information on the levels and spatial distribution of exogenously produced electric field and currents by the applied low frequency magnetic fields. Only very simplified modeling of current flow in cell suspensions has been performed, that practically neglects the influence of cells on the current flow.

We have analyzed two simplified, but more realistic, models of cells in culture exposed to 60 Hz magnetic fields. To evaluate induced currents and electric fields in models of biological cells the three dimensional (3D) impedance network method is used. In one of the models we consider different densities of cells in a conductive solution settled at the bottom of a cylindrical dish. Biological cells are represented by cubical volumes of zero conductivity. Since cell membranes have the conductivity of the order of  $10^{-5}$  to  $10^{-7}$  S/m such representation is justified as the first approximation. Cells are placed in a medium of the conductivity typical for cell suspensions, in this case of 1 S/m. The cells are only permitted to occupy positions at the bottom of an exposure container, e.g., petri dish. This simulates the behavior of cells forming a monolayer. Two representative threshold distributions of biological cells in the monolayer are considered and cell densities associated with them are estimated. In our model the biological cells are randomly placed (placement generated by computer) but there are restrictions on surface contact between them. In the first case, no contact between any two cells is permitted resulting in 17% cell density within the monolayer. In the second case, cells can make contact with other cells but only at their edges. Cell placement is also random as generated by a computer algorithm. The edge contact effectively obstructs the current flow. Under this condition an approximate cell density within the monolayer is 34% within the monolayer.

In the second model the effect of gap junctions connecting biological cells is investigated. The gap junctions are placed in the centre of the cell surfaces adjacent to the neighbouring cells. The area of the junctions is varied from approximately 0.4 to 5% of the total surface area of the membrane. The conductivity is varied from  $10^{-2}$  to 1 S/m. The selected parameters of the model gap junction are representative of those reported for actual gap junctions, i.e. conductivity up to 1 S/m and surface area up to 3%. The current density, particularly its maximum, is significantly affected by the presence of gap junctions, their size and conductivity.

# 1994 URSI Radio Science Meeting (Seattle)

## INDUCED ELECTRIC CURRENTS IN MAN AND RODENTS EXPOSED TO MAGNETIC FIELDS.

\*M. A. Stuchly<sup>1</sup>, W. Xi<sup>1</sup>, and O.P. Gandhi<sup>2</sup>. <sup>1</sup>Dept. of Electrical and Computer Eng., University of Victoria, Victoria, B.C. V8W 3P6. <sup>2</sup>Dept. of Electrical Eng., University of Utah, Salt Lake City, UT 84112.

Many physical characteristics of extremely low frequency magnetic fields appear to affect responses of biological systems. At least some interactions observed in various in vitro systems have been shown to have thresholds in terms of the induced electric field or current and to be dependent on the induced currents density. These interactions provided a motivation for computer simulations of current densities induced in models of man and rodents exposed to a uniform 60 Hz magnetic field. The objective of this research was to apply the impedance method to homogeneous and heterogeneous 3D models, and to compare the average and maximal current densities for the homogeneous vs. heterogeneous models, for various species and three orientations of the magnetic field. The impedance method was previously used and shown to be computationally effective. However, it is only suitable approximately up to  $10^6$  computational blocks. To be able to obtain finer spatial resolution (to handle a larger number of blocks), the computational algorithms have been modified, to enable use of a coarse mesh for the whole model of the biological body and a fine mesh for a selected subregion, e.g. the head. The computational methods have been verified using a double-layered sphere. Two heterogeneous models of man have been used, one consisting of 1.3 cm cubic blocks representing the tissue properties, and the other with cubes of 0.65 cm side dimension. Additionally homogeneous models of man, rat and mouse have been analyzed. The models had correct anatomical shapes (obtained for MRI scans) and average tissue conductivity.

For various human models (homogeneous, layered and heterogeneous) the average densities of induced currents have been found not to depend critically on the model, but the maximum values varied significantly. The differences depend on the orientation of the magnetic field with respect to the body. Differences by a factor of more than two have been observed.

The computed maximum current densities in the three species (in homogeneous models) can be used for scaling. It is interesting to note that the scaling coefficients are quite different than those previously used and calculated as ratios of the cube roots of the masses. For instance, scaling from man to mouse gives a factor of 2.5 from our computations, but a factor of 1.5 from the cube root of the ratio of masses.

An analysis with a finer computational mesh has indicated that both the induced current density and electric field are significantly different. Interestingly, higher maxima of both occur for finer mesh models, while the average values differ little. In the case of the induced electric field differences are of the order of three times.

Our computations confirm the earlier estimates that the induced currents and fields for environmental exposures are weak when compared to those endogenously produced. However, their spatial distributions in the body are very different.

## Noninvasive Biomagnetic Sensing of Biological Currents

C. Ramon<sup>\*1,2</sup>, P. Czapski<sup>2</sup>, R. J. Marks II<sup>2</sup>, H C. Lai<sup>3,1</sup>, S. Lee<sup>2</sup>

<sup>1</sup>Center for Bioengineering, <sup>2</sup>Department of Electrical Engineering and

<sup>3</sup>Department of Pharmacology

University of Washington, Seattle, WA 98195, U.S.A.

Biological currents flowing in the body produce magnetic fields that could be detected and mapped with cryogenic SQUID (Superconducting Quantum Interference Device) biomagnetometers. These are noninvasive noncontact measurements. By solving the biomagnetic inverse problem the current distribution in the tissue could be reconstructed. These techniques can also be applied for reconstruction of current distributions in isolated tissue samples in a conducting medium. A brief review of the reconstruction techniques and examples are given here.

Magnetic field produced by a current distribution is given by the Biot-Savart law. In matrix form it could be written as,  $[B] = [R] [J]$ , where  $B$  is the magnetic field,  $R$  is the distance between the source and field point where the magnetic field is sampled, and  $J$  is a planar current distribution consisting of several dipoles. Often the number of magnetic field measurements is less than the number of unknown dipoles in a current distribution, thus the inverse problem becomes under-determined. The current distribution could be solved by the generalized minimum norm solution techniques. It is given as:  $[J] = [R]^T \{([R][R]^T)^{-1}\} [B]$ . This provides an optimum estimate of the current distributions. In our reconstructions we found that there is always noise present based on the number of samples, and the size of sample and reconstruction space. A general shape of the current distribution is recognizable, but the reconstructed images are blurred. Thus image restoration becomes necessary. Making an assumption that all the current distribution are composed of line-like sources, we have used alternating projections techniques to restore the images. The procedure is to use the minimum norm solution as the initial guess and project it on a line-like space to obtain the next best estimate of the image. The iterative procedure is continued till the difference between two successive projections has reached the lowest limit.

These procedures were applied to the reconstructions of parallel conductors, circular current distribution, a complex pattern of current distribution in the shape of letters UWBC, dipoles in the brain, and an excitation pathway of the heart. In all the examples considered we were able to reconstruct the original shape of the current distribution.

## A SIMPLE METHOD TO INCORPORATE THE EFFECTS OF AN RF SHIELD INTO MRI ANTENNA ANALYSIS

Jianming Jin

Department of Electrical and Computer Engineering  
University of Illinois at Urbana-Champaign  
Urbana, IL 61801-2991

MR imaging scanners use a set of three gradient coils to obtain spatially selected information and a set of shim coils to achieve a high degree of homogeneity of the main magnetic field. These coils generally consist of multiple turns of wires with integrated length up to hundreds of meters. When RF fields, produced by an MRI antenna, impinge on these coils, numerous interactions occur which can degrade the performance of the MRI antenna. For example, the gradient and shim coils can cause losses to the antenna, resulting in a low signal-to-noise ratio in MR images. They can also give rise to spurious resonance which may displace and dampen the desired resonance of the antenna. Because of these, an MRI antenna is often partially enclosed in an RF shield to prevent the RF fields from penetrating into the gradient and shim coils, therefore reducing or eliminating the interactions between the antenna and the coils. Therefore, an accurate analysis of MRI antennas must include the effects of the RF shield.

An MRI antenna can be analyzed using the method of equivalent circuits, which amounts to model the distributed structure with lumped elements. This method is very simple and efficient, and has been used successfully to provide guidelines (field homogeneity and resonant frequencies) for MRI antenna design. However, there is no simple theoretical method (except for complicated moment method solutions) available to incorporate the effects of an RF shield into the analysis, especially for predicting the resonant frequencies of the antenna. The purpose of this paper is to present such a method.

In the proposed method, we employ the method of images to model the effects of the RF shield. In accordance with this method, the shield can be replaced with an image current running in the opposite direction of the original current. This is a well known fact, but the key point of the proposed method is to recognize that such an image current reduces the value of self inductance of the wire supporting the original current. This reduced inductance can be determined easily with the knowledge of the image's position. Similarly, the image current also reduces the mutual inductance between the original wire and other wires. Therefore, to incorporate the effects of an RF shield into the equivalent circuit analysis of MRI antennas, we only need to replace the self and mutual inductance (calculated without the shield) with the reduced self and mutual inductance without any further modifications. Although this method is very simple, it is effective and capable of predicting the resonant frequencies of an MRI antenna within 5% of measured values.

## EXPOSURE SYSTEM FOR ION CYCLOTRON RESONANCE STIMULATION AT 2.2 GHz

I.D. Fitian\* and A.R. Liboff  
Department of Physics, Oakland University, Rochester, MI 48309

V.V. Liepa  
Department of Electrical Engineering and Computer Science  
The University Of Michigan, Ann Arbor, MI 48109

A series of key experiments studying chick brain exposed to amplitude modulated RF has shown that a maximum change of Calcium occurs at very low modulating frequencies, approximately 14-16 Hz. Following the observation that the local magnetostatic field plays a role in the outcome, it was proposed that an ion cyclotron resonance mechanism may be involved. The present work aims at studying this effect, in particular the relative roles of the carrier and modulating component frequencies, as well as the effects of polarization.

An exposure system has been designed around a cavity resonator, consisting of a 8.6 cm ID brass cylinder, 19 cm in length. The carrier frequency, 2.2 GHz, is chosen to operate it in  $TE_{111}$  mode. Two coaxial inputs feed the cavity and are located halfway up the cylinder and displaced by 90 degrees circumferentially and 4.0 cm longitudinally. In addition nine small holes were drilled in the cavity walls for sampling the field. From a microwave signal generator, the (carrier) signal is split into two arms, containing variable attenuator, phase shifter, modulator, and amplifiers. Mixers are used as modulators with input at L port, output at R port, and modulating (ELF) signal at I port. An audio function generator provides modulation signal either in-phase or in quadrature.

With no modulation, and equal carrier amplitudes, but shifted by 90 degrees, the field in the cavity is uniformly distributed about perimeter of the cavity (a circularly polarized field). With in-phase modulation and equal carrier amplitudes shifted by 90 degrees, a circularly polarized amplitude modulated field is obtained. With modulating signals in quadrature and carrier signals in phase, a linearly polarized field that rotates at ELF rate is obtained.

One of the key objectives of this research is to study the effect of ion cyclotron resonance frequency modulation on high frequency carrier interactions with biological systems. Accordingly, the cavity is mounted coaxially in a long solenoid to provide highly uniform magnetostatic fields that can be adjusted for various desired ion cyclotron resonance conditions.

TUESDAY PM URSI-D SESSION T-U24

Room: Savery 243

MICROWAVE AND MILLIMETER WAVE DEVICES II

Chairs: Tatsuo Itoh, UCLA; C. Nguyen, Texas A&M University

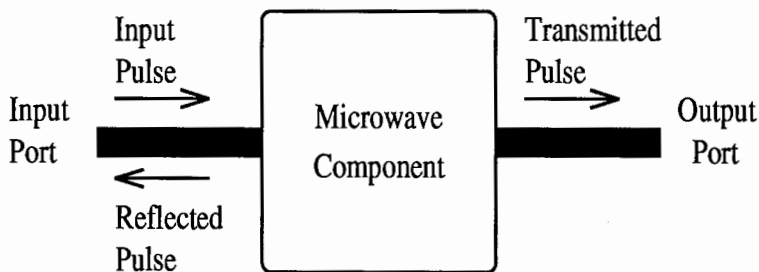
- 1:20 FDTD Analysis of BFN Microwave Components 276  
*\*P. Chung, C. Wu, J. Litva, McMaster Univ.*
- 1:40 Modeling of Diode Mounting Structures Using the Finite Difference Time Domain Method 277  
*E.M. Tentzeris, N.I. Dib, L.P.B. Katehi, Univ. of Michigan; J. Oswald, P. Siegel, JPL*
- 2:00 The Use of Negative Characteristic Impedances in Microwave Circuit Analysis and Design 278  
*C. Nguyen, R. Schwindt, M. Tran, Texas A&M Univ.*
- 2:20 Experimental Study of the CPW Phase Shift on Patterned Ground Planes 279  
*\*S. C. Wu, H. Grebel, New Jersey Inst. of Technology*
- 2:40 Vector Maxwell's Equations Modeling of Nonlinear Corrugated Semiconductor Waveguides with Application to Optical Switching 280  
*\*R.M. Joseph, S.T. Ho, A. Taflove, Northwestern Univ.*
- 3:00 Break
- 3:20 Effect of Dielectric Overlay on the Characteristics of 3db Hybrid Microstrip Directional Coupler 281  
*\*V. Puri, Shivaji Univ.*
- 3:40 Determination of Noise Semiconductor Devices Using the Monte Carlo Simulation 282  
*\*V. I. Yatskevich, Technische Universität Hamburg-Harburg*
- 4:00 Waveguides Theory as an Effective Tool for Analysis of Near-Earth Propagation of Nonsinusoidal Waves 283  
*\*L.V. Vavriv, V.V. Knyazev, Research and Engineering Inst. Molniya; A.E. Serebryannikov, Radio Astronomy Inst. of Ukrainian Academy of Science*
- 4:20 Vacuum Microelectronics Technology Applicaton for the Beginning of Microwave Tubes Second Life 284  
*Y. Romanstrov, V. Zhadan, The Radio Astronomy Inst. of Ukrainian Academy of Science*
- 4:40 Particularities of Electron-Wave Interaction in Power Clinotron-Type BWO of Millimeter and Submillimeter Wave Bands 285  
*V. Zhadan, Y. Romanstrov, The Radio Astronomy Inst. of Ukrainian Academy of Science*

## FD-TD ANALYSIS OF BFN MICROWAVE COMPONENTS

Paul Chung \*, Chen Wu, and John Litva  
Communications Research Laboratory  
McMaster University, Hamilton, Ontario, Canada

A method developed to numerically solve Maxwell's curl equations is called the Finite-Difference Time-Domain (FD-TD) technique. FD-TD is conceptually simple, robust, and provides highly accurate modelling predictions in the time domain. Of most importance, it is extremely flexible and can be applied to problems with much complexity — problems that can't be solved simply using other EM techniques.

This paper presents the FD-TD method applied to the analysis of microwave components used in satellite beam forming networks (BFNs). Examples will include couplers and phase shifters (see figure). Scattering parameters describing the characteristics of these components are obtained by a study of Gauss pulse propagation. An absorbing boundary condition is applied at the input and output port boundaries for mesh truncation. The time domain results are converted into the frequency domain by using the Fourier transform. Importance is placed on the sensitivity to finite difference mesh approximations to component geometries. By means of FD-TD based programs, it will be shown that numerical simulations can greatly enhance the design process of these components. Results comparing various simulated and measured characteristics are in good agreement over a wide frequency range of interest. The details will be reported at this symposium.

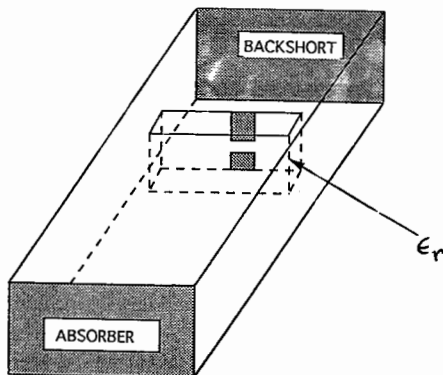


MODELING OF DIODE MOUNTING  
STRUCTURES USING THE  
FINITE DIFFERENCE TIME  
DOMAIN METHOD

E. M. Tentzeris, N. I. Dib and L. P. B. Katehi  
University of Michigan, Ann Arbor

J. Oswald and P. Siegel  
JPL

The finite difference time domain method is used in the RF characterization of diode mounting structures such as the one shown in fig. 1. A variety of excitation functions is considered and their effect on numerical convergence is studied. One of these functions, the Gabor function, offers a wavelet-like behavior and is used to provide the excitation for the waveguide mounting structure shown in the figure. This function is localized both in time and frequency domain and its characteristics can be chosen so that its spectral content is centered around a desired frequency. As a first step towards analyzing the geometry shown below, a number of single waveguide discontinuities are analyzed and the FDTD results are compared to data derived through the integral equation and finite element methods for validation purposes. The same excitation function has been applied to the diode mounting structure and the input impedance as a function at frequency has been evaluated and compared to measurements. A parametric study of this input impedance for a number of geometrical parameters has been performed and results will be presented and discussed.



**THE USE OF NEGATIVE CHARACTERISTIC IMPEDANCES  
IN MICROWAVE CIRCUIT ANALYSIS AND DESIGN**

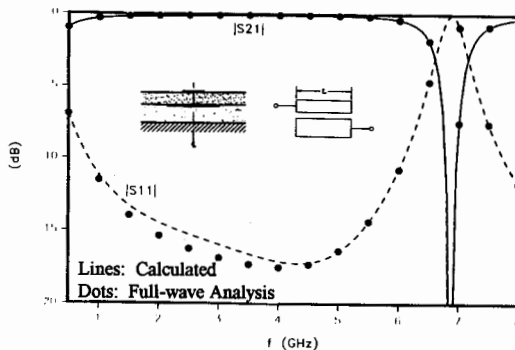
CAM NGUYEN\*, RANDAL SCHWINDT†, AND MICHAEL TRAN†

Department of Electrical Engineering  
Texas A&M University  
College Station, Texas 77843-3128

**ABSTRACT**

Parallel-coupled lines are used extensively in microwave circuits. Recently, an interesting phenomenon of negative mode characteristic impedances in parallel-coupled lines has been reported. However, the use of negative characteristic impedances in microwave circuit analysis and design has not been addressed. This has presented somewhat of a confusion for practical microwave engineers in utilizing the parallel-coupled structures having negative mode characteristic impedances in microwave circuits.

In this paper, we present results of negative characteristic impedances for multi-layer broadside-coupled microstrip lines and discuss the use of negative characteristic impedances in the analysis and design of microwave circuits. To demonstrate their applications, we have analyzed an open-circuited interdigital band-pass filter, consisting of broadside-coupled microstrip lines having negative mode characteristic impedances, by using the conventional chain matrix of the open-circuited interdigital section and by using a full-wave analysis of the actual filter's physical layout. The calculated frequency responses, as shown below, agree very well, which confirms the fact that the negative characteristic impedances are indeed physical and can be used in microwave circuit analysis and design as the positive characteristic impedances.



† Currently with Texas Instruments, Dallas, Texas 75265

# EXPERIMENTAL STUDY OF THE CPW PHASE SHIFT ON PATTERNED GROUND PLANES

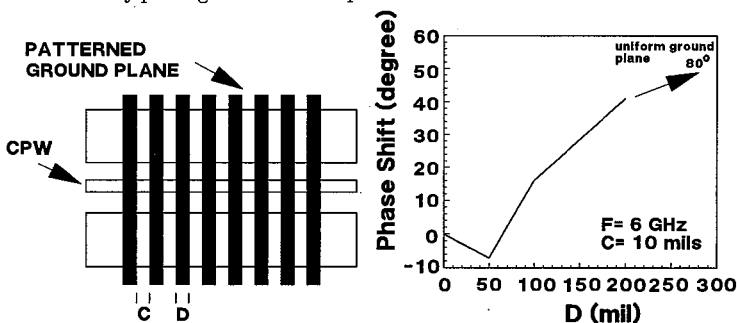
Shih-Chang Wu\* and Haim Grebel  
Department of Electrical and Computer Engineering  
New Jersey Institute of Technology  
Newark, NJ 07102

## Abstract

As the complexity of microwave systems increases, more multifunction MMICs rely on the controllable microwave devices to accomplish their objectives. In the coplanar waveguide applications, optically/mechanically controlled CPW phase shifters have been reported. The common method was to optically/mechanically alter the transmission-line boundary condition. This results in the change of the CPW dispersion characteristic to achieve a phase shift after constant distance of propagation. In these reports, the boundary condition was changed uniformly over the entire section of the device.

This paper describes the preliminary study of the phase shift characteristic of the CPWs with patterned ground planes. From the artificial dielectrics point of view, an effective permittivity of the patterned ground plane is controlled by the shape, size, and orientation of the conducting pattern. Consequently, the dispersion characteristic of the CPWs can be controlled freely without the restriction on the available dielectric material. In addition, a larger phase shift has been observed by switching the CPW boundary condition from the uniform ground plane to a needlelike conducting pattern than that to a plain dielectric.

We propose that these structures may play a role in passive, custom made delay lines. Moreover, if patterned Multiple Quantum Well (MQW) structures are considered, active optically controlled microwave devices may be realized by placing the needlelike planar conductive feature on the CPWs.



# **Vector Maxwell's Equations Modeling of Nonlinear Corrugated Semiconductor Waveguides with Application to Optical Switching**

R. M. Joseph\*, S. T. Ho and A. Taflove  
EECS Department  
McCormick School of Engineering  
Northwestern University  
Evanston, IL 60208

This paper considers detailed FD-TD models of optical propagation in corrugated waveguide structures fabricated of semiconductor materials. In such structures, the nonlinear response of the semiconductor can be exploited to achieve optical switching. At low optical power levels, the corrugated structure presents a stop band characteristic to the incident light beam. At high optical power levels, the nonlinear behavior of the semiconductor precipitates a change of refractive index within the structure sufficient to shift the edge of the stop band away from the optical signal frequency. This causes a switching of the structure from a reflecting state to a transmitting state.

In the optics community, such corrugated waveguide structures have traditionally been studied using perturbative analysis. However, when the depth of the corrugations is increased relative to the guiding layer thickness, the perturbative approach becomes invalid while a full-vector Maxwell's equations solver can provide accurate results. In this paper, we make comparisons between FD-TD and perturbative results for transmission and reflection characteristics of periodic waveguides for both TE and TM polarizations. This determines the regime of validity of the traditional perturbative models.

In addition, this paper presents large-scale computational studies of the dynamics of optical pulse switching within the nonlinear corrugated structure. The nonlinear FD-TD algorithm employed can incorporate the physics of dispersion, third-order nonlinearity and loss mechanisms such as two-photon absorption. Low-velocity Bragg solitons are observed within the periodic structure. A variety of periodic waveguide geometries are modeled and results are presented.

## EFFECT OF DIELECTRIC OVERLAY ON THE CHARACTERISTICS OF 3db HYBRID MICROSTRIP DIRECTIONAL COUPLER

VIJAYA PURI

Deptt. of Physics, Shivaji University, Kolhapur India 416 004

This paper reports the preliminary investigation on the effect of  $\text{Bi}_2\text{O}_3$ ,  $\text{Al}_2\text{O}_3$  and  $\text{MgF}_2$  overlays on symmetrical branch line microstrip directional coupler with 3db power split at 9.0 GHz. The changes in isolation and coupling with overlay thickness from 200  $\mu\text{m}$  to 3000  $\mu\text{m}$  were studied. The diameter of the overlay was such that it covered the coupling area completely. The three materials  $\text{Bi}_2\text{O}_3$ ,  $\text{Al}_2\text{O}_3$ ,  $\text{MgF}_2$  were chosen to study the effect of permittivity variations,  $\text{Bi}_2\text{O}_3$  and  $\text{MgF}_2$  having higher and lower dielectric const respectively as compared to the substrate ( $\text{Al}_2\text{O}_3$ ).

It was seen that for thinner overlays 200  $\mu\text{m}$  to 600  $\mu\text{m}$  there was a general band width broadening of  $\approx$  900 MHz where 3db power split was obtained. This broadening was irrespective of the overlay material used. The isolation also increased;  $\text{Bi}_2\text{O}_3$  showing the greatest increase of about 8db. Above 700  $\mu\text{m}$  an oscillatory behaviour was observed in the coupled ports with decrease in coupling after about 10.5 GHz. The isolation characteristic of the 3db hybrid coupler showed dependence on both thickness and permittivity of the overlay material.  $\text{Bi}_2\text{O}_3$  showed decrease in isolation between 960  $\mu\text{m}$  - 2000  $\mu\text{m}$  after which there is a sharp increase in isolation value, ZnS showed a steady decrease in isolation with increase in overlay thickness and  $\text{Al}_2\text{O}_3$  overlay of thickness greater than 2000  $\mu\text{m}$  decreased the isolation.

It is felt that by suitable choice of dielectric material with appropriate thickness, an improved broad band coupling and high isolation may be realized by simple overlay technique.

## DETERMINATION OF NOISE SEMICONDUCTOR DEVICES USING THE MONTE CARLO SIMULATION

Vitali I. Yatskevich

Arbeitsbereich Hochfrequenztechnik  
Technische Universität Hamburg-Harburg  
Postfach 90 10 52 , D-21073 Hamburg, Germany

The computer-aided simulation of physical processes in the semiconducting materials is rapidly gaining an increasing employment in the microwave engineering applications due to the fact that it enables one to determine the parameters of a semiconductor device at the early stage of design. The efficiency of semiconductor devices is critically dependent upon the noise factor of the semiconductor amplifying elements used. The previously known numerical methods for the evaluation of the noise factor involve essential calculational complexities and require intensive computation time to obtain an accurate result [ R.W.Hockney, J.W.Eastwood, Computer Simulation Using Particles, Adam Hilger, New York, 1989 ].

In this report, a novel simulation method for the determination of the noise level of semiconducting elements is described and the results of its validation are discussed. Physically, the proposed method invokes the notion of the noise temperature  $T_n$  which determines the noise level and is expressed in the following form :  $T_n = m^* V_t^2 / k$ . Here  $m^*$  is the mass of electron in the respective energy valley.  $V_t$  is the thermal velocity and  $k$  is the Boltzmann's constant. The aforementioned expression has been derived in the quasi-classical approximation under the assumption of maxwellian distribution for the electron velocity. It has been also assumed the existence of a non-equilibrium state due to difference between the grid temperature and the electron temperature [ V.L.Bonch-Bruevich, S.G.Kalashnikov, Physics of semiconductors, (in Russian), Nauka, Moskow, 1977 ].

The notion of noise temperature is widely used in microwave engineering. The proposed extension of this classical notion assures an opportunity to compare the parameters of the devices based on different physical principles, with the semiconductor devices inclusive.

In mathematical respect the simulation method exploits the Monte Carlo technique. The present author has applied this method to investigate the GaAs MESFET structures. For instance, it has been shown numerically that for a transistor with the gate length  $0.25 \mu\text{m}$  and the doping level  $1 \cdot 10^{24} \text{ m}^{-3}$  the lowest noise level equal to 21 K is provided in the case where the drain voltage equals 0.5 V and the gate voltage is -1 V.

## WAVEGUIDES THEORY AS AN EFFECTIVE TOOL FOR ANALYSIS OF NEAR-EARTH PROPAGATION OF NONSINUSOIDAL WAVES

Loudmila V. Vavriv\*, Vladimir V. Knyazev

Research & Engineering Institute Molniya, Kharkov, Ukraine

Andrey E. Serebryannikov

Radio Astronomy Institute of Ukrainian Academy of Science, Kharkov, Ukraine

The extended use of non sinusoidal waves in radar and radio communication on the one hand and the necessity of the solution of a number of electromagnetic compatibility problems on the other hand stimulate the development of effective methods used for the analysis of non sinusoidal waves' propagation. The principal peculiarity of the considered problems is the necessity of taking into account the scatterer.

The effective method that allows for the obtaining of different numerical results is a division of problem into two parts. At the first stage of solution the availability of scatterer is not taken into account. This assumption allows for the analysis of peculiarities of electromagnetic situation shaping in the areas of possible scatterer location. Thus, at the second stage we assume the incidence of the locally flat wave on the scatterer. This wave can be approximated by a flat wave or by a superposition of the limited number of flat waves. The solution of the first part of the problem using Sommerfeld integral method doesn't have an applied meaning, because it doesn't take into account the availability of ionosphere and complicates the consideration of scatterer. The waveguide model appears to be the most adequate to the natural conditions.

The problem on excitation of waveguide formed by two parallel plates and by nonstationary dipole source has been investigated in detail. In 2D approximation with the use of FD solution and Laplace transform we obtain the TD solution in a closed form, which is convenient for the analysis of non sinusoidal waves' propagation along the Earth surface. The expansion of excitation function into eigenfunctions of a waveguide has also been used. Naturally the problem is generalized for the case of arbitrary sources' system, for example, for the channel of lightning discharge. The finite conductivity can also be taken into account in this solution, if the condition of attached waves' absence is met (A.S. Il'inskiy, G.Ya. Slepian Oscillations and waves on dissipative electrodynamic systems. Moscow, 1984). Let us note, that the TD solution of a problem on natural nonstationary waves can be obtained in a closed form using the method of non complete variables' division in combination with the Riemann functions apparatus (V.V. Borisov. Nonstationary fields on waveguides. Leningrad, 1991). The powerful means are a Green function method including nonstationary one. The laminar composition of atmosphere can be taken into account using the Green function. The method of Green function or of partial domains' method is used at the second stage of problem solution depending on the scatterer geometry. In a number of cases it is possible to reduce the problem to the canonical one in the waveguide theory. The high development level of methods used for the analysis of sinusoidal processes in waveguides makes it expedient to use FD solutions in combination with the FFT algorithms. As an example the problem on scattering of pulsed electromagnetic field having the parameters peculiar for the fast transition lightning electromagnetic pulse on the perfectly conductive cylindrical scatterer located in the parallel-plate waveguide has been considered.

Vacuum Microelectronics Technology application  
for the beginning of microwave tubes second life

Yuri Romantsov and Vladimir Zhadan,  
Radio Astronomy Institute of Ukrainian Acad. of Sc. ,  
Department of Microwave Electronics  
4 Krasnoznamennaya st., Kharkov 310002 , The Ukraine

Vacuum Microelectronics Technology (VMT) is showing now great prospects for novel microwave electronic devices to be created with the applying of low voltage matrix field- emission electron sources (H.G. Kosmahl, *IEEE Tr. on E.D.*, V.36,n.11,Part II,,1989,pp.2726). One possibility is that the new generation of millimeter and submillimeter waves tubes such as Smith-Purcell FEL (Yu. Romantsov, Proc. of XXIV URSI G.A.,1993,p.157), twystron amplifiers and EIA, may be developed by using the phenomena of microwave modulation of field emission as well as the application of high density electron beams to be created using Field Emission Cathodes Array (FECA). With a matrix parking density of  $10^4$  picks per  $\text{mm}^2$  such cathodes allow to obtain current of an order  $10\div 100$  mA. It is significance that very small dimensions of such devices active branches make the process of field emission millimeter wave modulation of field emission current practically inenertionless and ,in addition, the point to emphasize is that FECA gives the principal possibility to increase the density of thin electron beams. This is very attractive because typical effective thickness of the beam  $a \approx 0.2\lambda * v_0 / c$  may amount the several percent of wave length  $\lambda$  in nonrelativistic case and thermocathodes can not ensure the current of an order 100 mA for such flow by the reason of technological and physical limitations.

These facts in connection with sharp slope of gated field-emitter current-voltage characteristics make FECA rather attractive for creation compact and highly efficient converters of millimeter band signal into modulation parameters of electron beam. The application of such devices can essentially simplify development of millimeter wave amplifiers and multipliers as in this case the total length of the tube, weight and overall dimensions of focusing magnets may be decreased. In the same time the gain of the order of  $20\div 40$  dB and efficiency  $\sim 30\div 50\%$  can be reached due to preliminary electron bunching by input signal and the possibility to optimize electron-wave interaction in output circuit.

In our report the new resonant and wide band tubes (Smith-Purcell FEL, twystron amplifiers, EIA, EIO and clinotron) of MM wave frequencies based on FECA application are represented. The fundamentals of the construction are discussed and the most promising designs are pointed out. On the basis of the developed theory the ultimate output parameters of the tubes are estimated.

Particularities of electron-wave interaction in power clinotron-type BWO  
of millimeter and submillimeter wave bands.

Vladimir Zhadan and Yuri Romantsov,  
Radio Astronomy Institute of Ukrainian Acad. of Sc. ,  
Department of Microwave Electronics  
4 Krasnoznamenaya St., Kharkov 310002 , The Ukraine

At the time due to the rapid development of the semiconductor industry such type oscillators of millimeter wave band supplant vacuum tubes in the low power field. However, in those fields, where higher output power and efficiency with high frequency stability are required the semiconductor devices of mm wave range appeared to be incapable of providing the required parameters. So, the perfection of vacuum tubes have a reason, because the potential of these devices still is not exhausted. Among them the BWO must be pointed due to wide range of electrical frequency tuning the ability to generate the oscillation of mm and submm bands of electromagnetic wave spectrum. But it is well known that the main problem in providing of high output power of such BWO like carcinotron is the decreasing of cross-section dimensions of the effective electron-wave interaction bunch with the shortening of the wave length of radiation. Thus the efficiency and output power of mm wave of carcinotrons are so low and tubes weight is too high due to application of powerful focusing magnets and high beam voltage.

The way to get rid of this shortcomings was pointed out by G. Levin (USSR). He offered the clinotron -- the BWO having the original construction where the thick electron beam fall on the slowing structure of a diffraction grating type under an angle. The devices of this type provide the output power level in the some time higher than the BWO having the parallel beam with slow-wave system. This phenomenon is explained by the next. Where the electron flow has an angle with a slowing structure, its upper layers enter also into the region of effective interaction with the surface wave of the system. In the classical BWO this layers take a small part in the energy interchange between a bunch and field. The achieved output power of the clinotrons -- 10 W in the mm range and 0.1 W in the submm one -- is the highest among devices of such a class.

We have made the theory of clinotron on the basis of the nonlinear self-concerted equations, which describe the nonlinear processes in clinotron qualitatively and quantitatively with a sufficient degree of precision. It allows to explain the principal physical processes and particularities of electron-wave interaction taking place in tube. By this theory one can to give the advice for improving the output parameters of clinotron.

The results of the numerical calculations are in the good correspondence with observed experimental data.



TUESDAY PM URSI-B SESSION T-U25

Room: HUB 106

TIME DOMAIN ANALYSIS II

Chairs: S. Castillo, New Mexico State University; R.K. Gordon, University of Mississippi

1:20	Characterization of Open and Using Finite-Difference Time-Domain Method <i>S.W. Chen, *K. Umashankar, Univ. of Illinois at Chicago</i>	288
1:40	FDTD Modeling of Chip-to-Package Interfaces in Very High Speed Digital Systems Using Physical Device Models for the Nonlinear Drivers <i>*Y.-S. Tsuei, A.C. Cangellaris, Univ. of Arizona</i>	289
2:00	Parallel RCS Benchmark Calculations with DSI3D <i>N.K. Madsen, G.O. Cook, Jr., Lawrence Livermore National Laboratory</i>	290
2:20	Application of Finite-Volume Time-Domain Method to Linear Antennas <i>*A. H. Mohammadian, W.F. Hall, V. Shankar, C. M. Rowell, Rockwell International</i>	291
2:40	An Efficient Time-Domain Taylor-Galerkin Finite-Element Formulation <i>S. Omick, S. Castillo, New Mexico State Univ.</i>	292
3:00	Break	
3:20	Time Domain Electromagnetic Scattering Computations with DS13D <i>*J.D. Collins, L. Takacs, Lockheed Advanced Development Company</i>	293
3:40	Unstructured Grid Generation for Large Time-Domain Simulations <i>*L.A. Takacs, J.D. Collins, Lockheed Advanced Development Company</i>	294
4:00	The Analysis of Three-Dimensional Microwave Circuits and Antennas Using a Parallel Finite Element Time-Domain Method <i>U. Navsariwala, S.D. Gedney, Univ. of Kentucky</i>	295
4:20	Iterative Analysis on a Parallel Computer of the Global Matrices Arising in Wavelet and Finite Element Methods <i>*R.K. Gordon, J. Brown, Univ. of Mississippi</i>	296
4:40	Computation of Resonant Frequencies of Rectangular Dielectric Resonators Using the Method of Finite Difference in Time-Domain <i>*T.K.C. Lo, A.K.Y. Lai, The Chinese Univ. of Hong Kong</i>	297

# Characterization of Open and Closed Type Waveguides using Finite-Difference Time-Domain Method

Shen W. Chen and Korada Umashankar\*  
Department of Electrical Engineering and Computer Science  
University of Illinois at Chicago  
Chicago, Illinois 60680

Current needs in the microwave and millimeter-wave engineering applications require straightforward analysis of arbitrary-shaped complex waveguide geometries to obtain mode propagation characteristics. Not only an accurate electromagnetic numerical models are becoming essential for computer-aided analysis and design program tools, there exists a great need for systematic and economical way to model and evaluate waveguide propagation phenomena. In order to describe the waveguide propagation characteristics completely, information concerning waveguide modes, cutoff frequencies, characteristic impedance and dispersion relationships should be known. Although the mode propagation characteristics for canonical geometries are widely addressed by many researchers, new close and open type waveguide geometries are getting more complicated, and a general numerical method that can deal with arbitrary waveguide structure is desired. Based on the full-wave analysis, without lack of generality, the finite-difference time-domain approach is extensively developed as an efficient numerical tool for the analysis of arbitrary-shaped complex close and open type waveguide geometries to obtain their mode propagation characteristics.

One of the important characteristics of any open or close type waveguide is the spectrum of discrete mode cutoff frequencies. The full wave equations simplify to their two dimensional form for cutoff conditions. Using a Gaussian impulsive excitation, the time history of an electric or a magnetic field component is determined and Fourier transformed to determine spectrum of mode cutoff frequencies. The results of the cutoff frequencies are rigorously validated for close type waveguides, such as hollow rectangular waveguide, partially dielectric filled rectangular waveguide and number of shielded microstrips lines. Extensions of this study are also presented for open optical waveguides. The dispersion characteristic is another important waveguide parameter. It gives relationship between the operating frequency and the corresponding mode propagation constant along the waveguide and it requires a three dimensional full wave analysis of the waveguide. A compact two dimensional technique along with number of validations are demonstrated to determine dispersion characteristic of open optical waveguide geometries. The finite-difference time-domain method gives the total field distributions containing all the modal fields. Efficient numerical technique are presented using band pass mode filters to determine the modal field distributions. The real power propagated and energy stored in the waveguide are calculated in terms of known field distributions to determine mode characteristic impedances.

FD-TD MODELING OF CHIP-TO-PACKAGE INTERFACES  
IN VERY HIGH SPEED DIGITAL SYSTEMS  
USING PHYSICAL DEVICE MODELS FOR THE NONLINEAR DRIVERS

Yuh-Sheng Tsuei\*, Andreas C. Cangellaris  
Center for Electronic Packaging Research  
Department of Electrical and Computer Engineering  
University of Arizona, Tucson, AZ 85721

A methodology is presented for the rigorous electromagnetic analysis of very fast pulse transmission through the chip-to-package interfaces in very high speed digital systems. The methodology combines a full-wave, vectorial, time-dependent Maxwell's equations solver with physical device models for the nonlinear drivers. The Maxwell's equations solver, based on the Finite-Difference Time-Domain (FD-TD) method, is used to facilitate the accurate modeling of the electromagnetic phenomena in the system, while the basic semiconductor equations (consisting of Poisson's equation, the continuity equations for electrons and holes, and the current relations for electrons and holes) are used to model the physics of the nonlinear drivers.

Clearly, our objective is to develop a methodology for the electromagnetic analysis of very high speed digital electronic circuits for which equivalent circuit (SPICE-like) models of the nonlinear devices are unavailable or very difficult to develop. Indeed, equivalent circuit models of semiconductor devices that are valid at very high frequencies are very difficult to extract and, in those cases that are available, their validity is subject to specific constraints. This is especially true for large-signal operation of the devices. The problem is more severe with new devices that are currently being developed for use in both electronic and optoelectronic computer and communication systems.

The proposed methodology circumvents the use of SPICE models for the semiconductor devices since it works directly with the basic semiconductor equations. The presentation will focus on how the device equations interact with Maxwell's equations in the context of the FD-TD algorithm. To demonstrate its validity results obtained using the proposed methodology will be compared with those calculated using SPICE and S-PISCES simulators.

## Parallel RCS Benchmark Calculations with DSI3D

Niel K. Madsen and Grant O. Cook, Jr.  
Lawrence Livermore National Laboratory  
L-23  
Livermore, CA 94551

The parallel electromagnetics computer program, DSI3D, has been extended to be able to compute the radar cross section (RCS) of arbitrarily-shaped bodies. This program has been operational for several years on some parallel computers. It uses some new discrete surface integral (DSI) methods for solving Maxwell's equations in the time-domain. The primary advantage of these methods is their ability to employ a computational mesh that conforms to the electromagnetic scattering objects in the domain. Another important attribute of these DSI methods is their conservation of charge: they locally preserve the divergence of the magnetic field.

We have recently extended DSI3D to efficiently compute radar cross sections of large and complex objects. To accomplish this, we first implemented two kinds of second-order absorbing boundary conditions. The first of these was the standard second-order Mur condition on a rectangular outer boundary. Secondly, a stabilized second-order Liao condition was added. This Liao boundary condition can be applied on any mesh boundary that has four layers of uniformly thick zones and collinear evaluation points for each boundary point. Next, the technique of (Luebbers, R. J. et al, IEEE Trans. **AP-39**, 429-433, 1991) was used to find the far-field vector potentials from which cross sections with respect to any orientation are computed. However, this technique cannot be directly applied to DSI3D since only the primary mesh edge values of the E field and the dual mesh edge values of the H field are found by its standard solution strategy. To efficiently solve this problem, we developed a solver that finds all components of the E and H fields that are needed by the surface integrals for the vector potentials. Since the number of far-field evaluation points can be large, leading to extremely large memory requirements for the time histories of the vector potentials, these potentials are placed in secondary storage as they are developed, and a postprocessing code computes the cross sections in a stand-alone fashion. Extensions to DSI3D material treatments are in progress to model lossy, anisotropic, and nonlinear materials.

From the parallel computation point of view, each of these extensions to DSI3D requires special attention so as to take into account the spatial coupling of each algorithm on the computational mesh, and to facilitate the sharing of required data between nodes on the parallel computer that are performing the field updates in adjacent spatial regions.

In order to validate this code, several benchmarks from the Electromagnetics Code Consortium have been run. The parallel speedups for these will be shown.

## **Application of Finite-Volume Time-Domain Method to Linear Antennas**

A. H. Mohammadian\*, W. F. Hall, V. Shankar, and C. M. Rowell  
Rockwell International Science Center  
1049 Camino Dos Rios  
Thousand Oaks, California 91360

Linear antennas have long been a subject of great interest to researchers in the area of applied electromagnetics and antennas. This is perhaps best exemplified by such classic books as "Linear Antennas" by R. W. P. King or "Advanced Antenna Theory" by A. A. Schelkunoff, and also by the development of large computer codes such as NEC, one of whose major task is to numerically solve general linear antennas. In recent years, differential equation solvers in the time domain have proven themselves as strong contenders in dealing with many difficult electromagnetic problems.

The Finite-volume time-domain (FVTD) method of solving Maxwell's equations in the differential form in the time domain has been very successfully applied to many complex real life objects in order to predict the scattering of electromagnetic waves off these objects. It has been also shown that this method can be used to model a variety of radiating structures such as waveguides, horns, etc., and arrays of these radiators.

In the present work, we show that the FVTD method may be efficiently applied to linear antennas without having to appeal to approximate models for these antennas or to idealize the feed mechanism. Moreover, the change in the input impedance due to finite ground planes or to the presence of near-by structures may be predicted without a substantial increase in either the complexity of the problem or the computation time.

It should also be noted that much of the contribution to linear antennas has been for the time harmonic excitation, even though some attempts have been made to obtain closed form solutions for the current distribution due to a pulse excitation in some idealized cases. Integral equation formulations in the time domain for linear antennas have been used in the past and have been generally successful when dealing with a stand-alone antenna, subject to the usual feed approximation. A time domain method such as the FVTD can provide valuable information for linear antennas excited by a pulse in the real life environment.

In the past, some attempts have been made to use an approximate model for a thin wire in the context of the Yee's algorithm, in order to avoid the ultra fine gridding of the computational domain dictated by the sub-wavelength dimensions of the cross section of a thin wire as well as by the uniform gridding approach. However, based on what has so far been published, it is not clear if this approach can adequately solve the practical problems involving this class of antennas, even though the formalism may be adequate in some scattering problems involving thin wires.

## AN EFFICIENT TIME-DOMAIN TAYLOR-GALERKIN FINITE-ELEMENT FORMULATION

Steven Omick  
Steven Castillo  
New Mexico State University  
Dept. 3-O, Box 30001  
Las Cruces, NM 88003

The formulation of a time-domain finite-element algorithm offers the advantages of modeling curved and irregular surfaces. This advantage is often offset by temporal inaccuracy and the high computational complexity of finite-element codes. In the Taylor-Galerkin formulation, the temporal variation is approximated with a Taylor Series approximation carried out to the third-order term. The time derivatives in the series are replaced with the corresponding curl and wave equations. The resulting spatial derivatives in the Taylor series are then approximated with a non-staggered Galerkin finite-element discretization. The resulting set of equations are solved with a sparse L-U decomposition and forward and back substitution at the first time step. For each successive time step, only the right-hand side changes so that no further LU decompositions must be performed.

The Taylor-Galerkin finite-element approach is very similar to the Lax-Wendroff finite-difference method with an additional term left in the Taylor series. The third-order term in the finite difference context would lend additional accuracy to the time discretization but with the result being a fully implicit finite-difference algorithm. In the finite-element context, the equations are already implicit due to the spatial discretization so that the additional temporal accuracy comes with negligible computational cost.

In this paper, accuracy comparisons between the Taylor-Galerkin finite-element algorithm on a rectangular grid, the Lax-Wendroff finite-difference algorithm, and the staggered Yee finite-difference algorithm will be given using a modified equation approach. This modified equation technique will show that the phase and magnitude accuracy of the Taylor-Galerkin finite-element algorithm to be better than the Yee finite-difference algorithm and at the same time having the same stability limit. A code using this technique as been implemented with a Liao absorbing boundary condition for open-region problems and can be used in conjunction with flux-corrected transport for additional phase accuracy. Results will be presented for both free-space propagation as well as scattering from a right circular cylinder and compared with both exact results and results obtained from codes using Yee's algorithm and a Lax Wendroff algorithm.

# Time Domain Electromagnetic Scattering Computations with DSI3D

Jeffery D. Collins\* and Laszlo Takacs  
Lockheed Advanced Development Company  
Dept. 25-52, Bldg. 311, Plant B-6  
P.O. Box 250  
Sunland, California 91041

DSI3D is a time domain electromagnetics code currently under joint development between Lawrence Livermore National Laboratory and Lockheed ADC. It is based on the Discrete Surface Integral Method (DSI) (N.K. Madsen, AP-S/URSI Symposium, Chicago, Ill., 1992), which is a generalization of the FDTD method to nonorthogonal unstructured grids. DSI is a divergence preserving approach and when applied to a rectilinear grid, recovers the Yee FDTD stepping equations.

DSI3D supports a wide variety of element types, from structured hexahedrons to unstructured tetrahedrons, wedges and pyramids. This lends great flexibility when modeling complex structures. To reduce computation time and storage, grids may be formed from mostly orthogonal elements, leaving non-orthogonal elements only near interfaces. In any case, no need exists for special case elements at interfaces.

For facilitate scattering computations, the stabilized Liao boundary condition is implemented in DSI3D (D. Steich, R. Luebbers & K. Kunz, *1993 Joint IEEE APS/URSI Symposium Digest*, vol. 1, pp. 6-9, 1993) to truncate the computation region. The scattered fields are computed via the near-to-far zone transformation (R. Luebbers, K. Kunz, M. Schneider & F. Hunsberger, *IEEE Trans. Ant. Prop.*, vol. 39, p.429, 1991) modified for non-rectangular integration surfaces.

Several examples will be presented to demonstrate the capabilities of the code. Curved inhomogeneous structures will be emphasized, particularly ones with wide dynamic range. Some realistic structures will be included as well. Issues of accuracy, storage, and run time will be addressed for each target considered.

# Unstructured Grid Generation for Large Time-Domain Simulations

\* Laszlo A. Takacs and Jeffery D. Collins  
Lockheed Advanced Development Company  
Dept. 2552, Bldg. 311, Plant B-6  
P.O. Box 250  
Sunland, California 91041

The technique of volumetric time-domain simulation has been slowly growing in popularity as a way of obtaining engineering answers to complex electromagnetic problems. There several reasons for this. First is the growing capacity of supercomputers to perform the enourmous computations required. Second is the recent development of highly accurate body-fitted time-stepping algorithms such as the work of N. K. Madsen, (AP-S/URSI Symposium, Chicago, Ill., 1992). Third is the realization that wideband field information is useful and interesting in its own right.

The practical day-to-day use of the technique requires that very large volumetric grids be easily and routinely generated. Furthermore the generated grid must meet several quality criteria in order to allow an efficient and accurate simulation. Simple minded discretizations of the space will usually result in an unviable simulation.

There are no fully automatic techniques today that produce good unstructured electromagnetic time-domain grids. There are however many techniques utilizing various degrees and stages of manual effort that can produce grids suitable for use with the time domain solvers. Because the simulation targets are geometrically complex, sophisticated computer modeling tools must be used before a grid generation process can be started. Usually a solid modeling system is the most appropriate starting point.

This presentation will address some of the issues surrounding the practical generation of unstructured grids containing 10 million or more elements around complex realistic targets.

## The Analysis of Three-Dimensional Microwave Circuits and Antennas Using a Parallel Finite Element Time-Domain Method

Umesh Navsariwala\* and Stephen D. Gedney\*  
 Department of Electrical Engineering,  
 University of Kentucky,  
 Lexington, KY

In this paper a parallel Finite Element Time-Domain (FETD) method for the analysis of printed microwave devices is presented. The FETD method is based on a variational solution of Maxwell's curl equations. To this end, the volume is discretized using an unstructured three-dimensional grid. Throughout the discrete volume, the electric field is approximated using first-order vector edge elements and the magnetic flux density is approximated using first-order vector face elements. From Faraday's and Ampere's Laws, a variational expression is obtained. Approximating the time-derivatives using central difference approximations leads to an implicit time-domain solution. In discrete form, this is expressed as [Mahadevn, et. al., IEEE AP Symposium Digest, pp. 1680-1683, 1993]

$$\begin{aligned} \bar{E}^{n+1/2} &= \bar{E}^{n-1/2} + \left( \frac{1}{c_o \Delta t} M_\epsilon \right)^{-1} (\eta_o X_\mu \bar{B}^n - M_\sigma \bar{E}^{n-1/2}) \\ \bar{B}^{n+1} &= \bar{B}^n - \frac{c_o \Delta t}{\eta_o} A_b \bar{E}^{n+1/2} \end{aligned} \quad (1)$$

where  $M_\epsilon$ ,  $M_\sigma$ ,  $X_\mu$ , and  $A_b$  are sparse matrices. Note that each time iteration requires the inversion of  $M_\epsilon$ . Since  $M_\epsilon$  is real, positive-definite, iterative methods such as the conjugate gradient method converge rather quickly.

The FETD algorithm has a number of advantages over other time-domain techniques such as the Finite-Difference Time-Domain (FDTD) method. Initially, by using unstructured grids, accurate models of devices with complex geometries are easily obtained using automatic grid generation techniques. Furthermore, the numerical grid is non-dispersive, unlike the FDTD, and it is not bound by the Courant Stability criterion. As a result larger time steps and spatial discretizations can be used as compared to traditional explicit methods such as the FDTD method. The disadvantage of unstructured grids is that the numerical grid and the sparse matrices must be stored. However, this can be greatly relaxed by exploiting symmetries in the model. When treating stratified planar devices a two-dimensional grid can be used to model the circuit device, and a regular grid is assumed for the third-dimension. Furthermore, due to the assumed regularity along the third-dimension the sparse matrices for only one-layer of cells need be stored. This greatly reduces the overall memory requirements.

The parallel algorithm is based on a spatial discretization of the unstructured grid. The decomposition is performed using the Greedy algorithm which provides excellent load balance. Since the Greedy algorithm is not a power of two algorithm, it can be used across many platforms. Then, by treating the sparse matrices as subassemblies of matrices interior to each subdomain, the matrix inversion and the matrix-vector multiplications are efficiently performed in parallel leading to a highly scalable algorithm.

The analysis of a number of planar microwave circuit devices using the parallel FETD algorithm will be presented. Performance analyses will also be presented for the implementation of this algorithm on the Intel Delta, and the iPSC/860.

Iterative Analysis on a Parallel Computer of the Global Matrices Arising in Wavelet  
and Finite Element Methods

Richard K. Gordon\* and Joel Brown  
Department of Electrical Engineering  
University of Mississippi  
University, MS 38677

It has been recently shown that using simple diagonal preconditioning it is possible, using a wavelet method, to obtain a global matrix the condition number of which is bounded by a constant as the number of points of discretization is increased (S. Jaffard, SIAM J. Numer. Anal., pp. 965-986, August 1992). This contrasts sharply with the situation that arises when the finite element or finite difference method is used; in either of these cases the usual preconditioning methods make the condition number  $O\left(\frac{1}{h}\right)$ ; and if simple diagonal preconditioning is used the condition number will go to infinity as, at best,  $\frac{C}{h|\log h|}$  as the number of points of discretization is increased, i.e., as  $h$  goes to zero. This is important because when iterative algorithms are employed, ill conditioning can lead to numerical instabilities or slow convergence.

In this paper, a wavelet method and a finite element method for solving a Dirichlet type boundary value problem will be discussed in detail. The global matrices arising in both of these analyses will be presented. The iterative solution of several problems using these methods will be discussed; a comparison of the rates of convergence observed and cpu times required in each case will be presented.

The numerical implementation of these techniques on both serial and parallel processors will be discussed. Numerical results obtained from the University of Mississippi's Cray X-MP and the San Diego Supercomputer Center's 400 node Paragon will be presented. Details on the parallelization of these algorithms will be provided along with a discussion of such issues as speed-up and interprocessor communication.

Computation of Resonant Frequencies of Rectangular Dielectric Resonators Using the Method of Finite Difference in Time-Domain

Terry K. C. Lo\*, Albert K. Y. Lai  
 Dept. of Electronic Engineering, The Chinese University of Hong Kong

The numerical method of finite difference in time-domain (FDTD) has been applied, coupled with the fast Fourier Transform (FFT), to determine the resonant frequencies of the TE to z modes of free rectangular dielectric resonators of size 3cm times 3cm times 1.5cm with different  $\epsilon_r$ . This method can be used to compute the field quantities in different modes in a single computation process and allows faster computation of the field distribution on the frequency spectrum. Assume at  $t = 0$ , a Gaussian point source is started at the center of the rectangular dielectric resonator. The width of the Gaussian point source must be chosen carefully so as to include a wide range of frequencies. The whole geometry can be covered by the rectangular finite difference grid with an appropriate spatial and temporal increment. In accordance with discretized Maxwell's curl equations, the field components can be computed through the Yee's time-stepping algorithm. Mur's second order absorbing boundary condition has been employed for the truncation of the computational domain. A spatial point is chosen inside the rectangular dielectric resonator and the field variation  $\{\phi^n(I, J, K)\}$  at that point at successive time step,  $n$ , is obtained. The field distribution on the frequency spectrum can be found by applying the FFT to the time series  $\{\phi^n(I, J, K)\}$ . Since the magnitude of the field quantities will be maximum when resonance occurs, the frequency values at which the magnitude of  $\Phi^n = \mathcal{F}\{\phi^n(I, J, K)\}$  acquires a local absolute maximum correspond to the resonant frequencies at different modes and the corresponding harmonics. The maxima of 4 different spectra, as shown in Fig 1, corresponding to 4 different dielectric resonators have been identified and compared with the first order approximation in (A. Okaya & L. F. Barash, Proc. of IRE, 2081-2092, 1962.) and they are in reasonable agreement. The results are listed in Table 1. The value of  $\Delta f$  used is 84.514 MHz and  $\Delta t$  is 2.889 ps. The analysis of the spatial field pattern for different modes on the rectangular dielectric resonator and its radiation pattern as an antenna are in progress.

			$\epsilon_r = 8.9$		$\epsilon_r = 12.8$		$\epsilon_r = 15.2$		$\epsilon_r = 17.1$	
l	m	n	Theory	FDTD	Theory	FDTD	Theory	FDTD	Theory	FDTD
0	1	0	2.094	2.113	1.746	1.775	1.602	1.690	1.510	1.606
0	1	1	3.745	3.634	3.123	3.042	2.866	2.873	2.702	2.704

Table 1 The comparison between Okaya's 1st order approximation & FDTD results  
 (All values are in GHz)

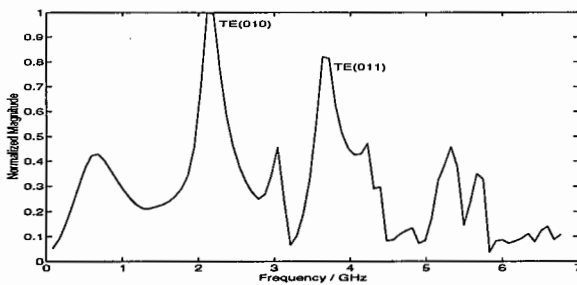


Fig 1 Frequency Spectrum with  $\epsilon_r = 8.9$  obtained from the FFT of the time series of  $E_y$



**WEDNESDAY AM PLENARY SESSION W-P1**

Room: Kane 130

**PLENARY SESSION**

Moderator: Irene Peden, University of Washington

8:30 Welcoming Remarks

8:40 Space-borne Remote Sensing of Earth and Planetary Surfaces and Atmospheres  
*Charles Elachi, Jet Propulsion Laboratory*

9:10 Intelligent Cellular Communication Systems  
*William C.Y. Lee, Vice President and Chief Scientist, PacTel*

9:40 Influences of Electromagnetics Technology on Aerospace Products — A Fifty Year Look  
*Theodore L. Johnson, Vice President, Research & Engineering, Boeing Defense & Space Group*

10:10 Break

10:30 Electromagnetic Interactions in Biological Systems  
*James C. Lin, Chairman of Bioengineering, Univ. of Illinois at Chicago*

11:00 Virtual Reality  
*Maxwell Wells, Associate Director, Human Interface Technology Laboratory, Univ. of Washington*



WEDNESDAY PM JOINT SPECIAL SESSION W-J4

Room: HUB 310

ROUGH SURFACE SCATTERING II

- Chairs: Z.H. Gu, Surface Optics Corporation; E. Rodriguez, California Institute of Technology
- Organizers: S. Broschat, Washington State University; A. Ishimaru, University of Washington
- 2:00 Theoretical and Experimental Studies of Millimeter-Wave Scattering from Well Characterized Two-Dimensional Rough Surfaces 302  
*\*C. Le, A. Ishimaru, Y. Kuga, P. Phu, Univ. of Washington*
- 2:20 Broadening of Gaussian Pulses Scattered by Rough Surfaces 303  
*\*L. Ailes-Sengers, A. Ishimaru, D. Winebrenner, Univ. of Washington*
- 2:40 The Scattering of Light from Guided Wave-Supporting Structures Possessing Random Surfaces 304  
*J.A. Sánchez-Gil, A.A. Maradudin, Univ. of California at Irvine; J.Q. Lu, Surface Optics Corporation; V.D. Freilikher, M. Pustilnik, I. Yurkevich, Bar-Ilan Univ.*
- 3:00 [Paper withdrawn]
- 3:20 Coherent Light Scattering from a One-Dimensionally Rough Metal Surface 305  
*\*T.R. Michel, California Inst. of Technology*
- 3:40 Break
- 4:00 Spectral Correlation Measurements of Light Propagating through Multiple Scattering Media 306  
*T. Okamoto, T. Asakura, Hokkaido Univ.*
- 4:20 Combined Volume and Surface Scattering in a Channel Using a Modal Formulation 307  
*M.J. Beran, S. Frankenthal, The Catholic Univ. of America*
- 4:40 High Frequency Acoustic (Scalar Field) Forward Scattering from Gaussian Spectrum, Pressure Release, Corrugated Surfaces Producing Clusters of Caustics: Catastrophe Theory Modeling and Experimental Comparisons 308  
*\*K.L. Williams, Univ. of Washington; J.S. Stroud, P.L. Marston, Washington State Univ.*
- 5:00 Effects of Reflection from an Uneven Surface on a Chirp Radar 309  
*\*S. Mudaliar, Department of the Air Force*
- 5:20 Radar Scatter Cross Sections for Two-Dimensional Random Rough Surfaces with Different Roughness Scales AP-S  
*\*E. Bahar, B.S. Lee, Univ. of Nebraska, Lincoln*
- 5:40 Examination of Large Radius of Curvature Approximation for Rough Surface Scatter Cross Sections AP-S  
*\*E. Bahar, M. El-Shenawee, Univ. of Nebraska, Lincoln*

## Theoretical and Experimental Studies of Millimeter-Wave Scattering from Well Characterized Two-Dimensional Rough Surfaces

Charles Le, Akira Ishimaru, Yasuo Kuga, and Phillip Phu

Department of Electrical Engineering, FT-10  
University of Washington  
Seattle, Washington 98195

We present experimental results and analytical solutions to the scattering of electromagnetic waves from two-dimensional rough surfaces with Gaussian surface roughness statistics. The first-order analytical solution was obtained by using the Kirchhoff approximation and the geometric optics approximation. The conventional solution for the first-order Kirchhoff solution is complicated because of the vector nature of the electromagnetic fields. To simplify the derivation, the cross products were substituted by anti-symmetric matrices and the solution was expressed as a product of matrices. The advantage of using matrices is that the analytical expressions are easier to read so that physical interpretations of the solution can readily be made. Furthermore, the computation becomes straightforward with the matrix multiplication software such as MATLAB.

The first-order analytical solution was compared with experimental results. The rough surfaces with Gaussian surface correlation functions were fabricated by means of a computer-numerical-controlled milling machine. The surface statistics are precisely controlled. We conducted the bistatic scattering experiments with two different surfaces. The first surface has a rms height  $\sigma=3$  mm ( $1\lambda$  at 100 GHz) and correlation length  $l=6$  mm ( $2\lambda$  at 100 GHz), corresponding to a rms slope  $m=0.71$ . The characteristics of the second surface are  $\sigma=3$  mm and  $l=12$  mm, yielding a rms slope  $m=0.35$ . The bistatic scattering cross section was obtained for the frequency between 75 and 100 GHz, and the observation angle from  $-70^\circ$  to  $70^\circ$ . Good agreement was obtained between measurements and the analytical solution for the surface with  $m=0.35$ . However, some significant discrepancies were shown between the first-order Kirchhoff solution and the experimental data for the surface with  $m=0.71$ . In particular, backscattering enhancement and a large amount of cross-polarization which were observed in the experimental data are missing in the first-order Kirchhoff approximation. To include both backscattering enhancement and cross polarization in the analytical solution, the second-order Kirchhoff approximation with shadowing correction needs to be considered.

## BROADENING OF GAUSSIAN PULSES SCATTERED BY ROUGH SURFACES

\*Lynn Ailes-Sengers, Akira Ishimaru and Dale Winebrenner  
Department of Electrical Engineering  
University of Washington  
Seattle, WA 98195 USA

Recently, there has been an increasing interest and need for understanding pulse broadening and coherence bandwidth of acoustic and electromagnetic waves scattered from rough surfaces. For example they are useful in characterizing ocean acoustic scattering channels and in SAR remote sensing of earth surfaces. This paper presents a study of pulse scattering by rough surfaces in the region of surface parameters where backscattering enhancement takes place. This is the case where the rms slopes are close to one.

We present analytical expressions for the two-frequency mutual coherence function of the scattered wave based on the first and second order Kirchhoff approximation with shadowing. For narrowband, the scattered pulse shapes in the time domain are calculated as the convolution of the incident pulse shape and the Fourier Transform of the two-frequency mutual coherence function. We present scattered pulse shapes for several incident pulse widths where the incident pulse is Gaussian. The relationship between Gaussian pulse width and coherence bandwidth will be discussed. When the pulse is ultra-wideband, the two-frequency mutual coherence function can no longer be assumed independent of the center frequency. We present results from millimeter wave scattering experiments and Monte Carlo simulations on one dimensional rough surfaces which show good agreement with the analytical results.

The results show that the coherence bandwidth depends on the illumination area as well as the incident and scattered angles and the surface characteristics. Both the analytical and experimental two-frequency mutual coherence function show that the frequency correlation function is maximum at the center frequency and drops rapidly towards zero as the frequency moves away from the center frequency. This results in a finite coherence bandwidth. The inverse of this bandwidth is the pulse broadening. The broadening of the scattered pulse is minimum in the specular direction due to the minimum travel time and increases as the observation angle deviates from the specular region. It is interesting to note that in the region of the enhanced backscattering, multiple scattering takes place due to the double bounce of the wave on the surface, and that this extra propagation distance on the surface yields a long pulse tail in the enhanced backscattering direction.

The Scattering of Light From Guided Wave-Supporting Structures  
Possessing Random Surfaces

J. A. Sánchez-Gil and A. A. Maradudin

Department of Physics and Institute for Surface and Interface Science

University of California

Irvine, CA 92717, U.S.A.

Jun Q. Lu

Surface Optics Corporation

P. O. Box 261602, San Diego, CA 92126 U.S.A.

V. D. Freilikher, M. Pustilnik, and I. Yurkevich

The Jack and Pearl Resnick Institute of Advanced Technology

Department of Physics

Bar-Ilan University

Ramat-Gan 52900, Israel

**Abstract**

By perturbation theory and by a computer simulation approach we have studied the incoherent scattering of s-polarized light, incident from the vacuum side, onto a randomly rough, one-dimensional, surface of a thin dielectric film deposited on a planar, perfectly conducting surface. The thickness of the dielectric film is such that in the absence of the roughness the scattering system supports two guided wave polaritons. As a consequence, each multiply-scattered light wave is now degenerate. The coherent interference of each of these degenerate waves with the waves obtained from them by time-reversal produces two satellite peaks in the angular dependence of the intensity of the incoherent component of the scattered light, in addition to the enhanced backscattering peak. These satellite peaks occur at scattering angles  $\theta_s$  that are related to the angle of incidence  $\theta_0$  by  $\sin \theta_s = -\sin \theta_0 \pm (c/\omega)(q_2(\omega) - q_1(\omega))$ , where  $q_1(\omega)$  and  $q_2(\omega)$  are the wave numbers of the two guided wave polaritons supported by the scattering system at the frequency  $\omega$  of the incident light. These peaks are present in the results of both the perturbation and simulation calculations. They are shown to be multiple-scattering effects, and not a single-scattering phenomenon.

# Coherent Light Scattering from a One-dimensionally Rough Metal Surface.

T.R. Michel

Jet Propulsion Laboratory  
California Institute of Technology  
Pasadena, California 91109

The coherent scattering of light from a one-dimensional, randomly rough surface on a metal is studied using simulation calculations based on the extinction theorem. The reduced Rayleigh equations are solved numerically for small roughness heights, and a method of moments with a periodic Green's function is used for roughness heights comparable to the incident wavelength. The profile of the random roughness is described by a Gaussian process having a Gaussian correlation function. The dependence of the coherent scattering on the angle of incidence, the incident wavelength, the roughness parameters, and polarization are considered. A pseudo-Brewster angle is observed near grazing incidence for wavelengths in the infra-red, or for perfectly conducting surfaces when the roughness height is comparable to the incident wavelength. Similar observations have been recently reported in an experimental study, and the calculations are compared with these experimental results. For weak roughness heights the simulation calculations are compared with a self-energy method. Finally, when a segment of surface is illuminated by a beam of finite width, strong fluctuations in the angular or frequency dependence of the unaveraged specular intensity may be associated with the excitation of surface plasmon polaritons.

## Spectral Correlation Measurements of Light Propagating through Multiple Scattering Media

Takashi Okamoto and Toshimitsu Asakura  
Research Institute for Electronic Science, Hokkaido University,  
Sapporo 060, Japan  
Phone: +81-11-716-2111 (ext.2646), Fax: +81-11-758-3173  
E-mail: okamoto@hikari.hokudai.ac.jp

### Introduction

In the field of laser speckle, the spectral-correlation method has been used for characterizing rough surfaces. The speckle pattern produced by a diffuse object changes its spatial structure with the wavelength of light illuminating the object. Since this decorrelation of speckle patterns depends strongly on the scattering properties of the surface, measurements of surface roughness can be made on the basis of this principle. The light propagating through a relatively dense scattering medium also gives rise to a speckle pattern, but its spectral-correlation properties have not been fully explored yet. In this paper, we apply this correlation method to a weakly multiple-scattering medium and investigate the relationship between the characteristics of the medium and the resultant intensity correlation of speckle fluctuations.

### Experiments

In the present experiment, aqueous suspensions of polystyrene spheres with various diameters were used as scatterers. A sample cell containing the scatterer was illuminated by a polychromatic Ar-ion laser beam and was moved perpendicularly to the optical axis to examine the interaction between number fluctuations and phase fluctuations. The scattered light was collected by a camera lens of the relatively small  $f$ -number, and time-varying intensities of the light with two different wavelengths were detected separately by two photomultipliers. The cross-correlation function of the signals was then measured by an FFT analyzer.

### Results

Experimental results have revealed that the correlation coefficient of intensity fluctuations with different wavelengths depends not only on the optical thickness of the sample but also on the number density of the particles. This is due to the fact that the temporal variations in the intensity detected are not just 'speckle' fluctuations, but are attributed to number fluctuations as well. For the dynamical aspect of cross-correlated intensity fluctuations, it is shown that the reciprocal value of their correlation time is linearly proportional to the translating velocity of the particles. This result clearly indicates that the diffusive motion, which affects significantly the correlation time obtained by a conventional autocorrelation method, is sufficiently suppressed.

Combined volume and surface scattering in a  
channel using a modal formulation

by

Mark J. Beran\*  
and  
Shimshon Frankenthal\*

The Catholic University of America

In previous work a modal approach was used to study random volume scattering in a shallow channel (M.J. Beran and S. Frankenthal, J. Acoust. Soc. Am., 91, 3203-3211, 1992). Here we shall show how the effects of a rough channel surface may be included in the formulation. To include the effects of the rough surface the modes are taken to be dependent on the range and transverse coordinates in addition to the depth coordinate. The range coordinate is taken to be along the mean direction of the propagation of energy and the parabolic approximation is used.

The propagation is studied in terms of the ensemble-averaged two-point coherence function. The equation governing the coherence function is derived by segmenting the propagation-direction coordinate  $z$  into a sequence of intervals of length  $\Delta z$ . An interval  $\Delta z$  is chosen to be small enough so that the diffraction and scattering effects may be considered independently and the scattering effects may be treated by perturbation theory in each interval. The general method is given in detail in the above reference for volume scattering. Here it is shown how the surface scattering terms may be treated in this approach.

The two-point coherence function is expressed as the sum over both self-modal and cross-modal coherence functions. The difference between the self-modal coherence functions and the cross-modal coherence functions is discussed. Conditions are given when the cross-modal coherence functions may be neglected. An example is considered in which the sound-speed profile within the channel may be neglected.

\*Permanent address: Tel Aviv University

**High frequency acoustic (scalar field) forward scattering from Gaussian spectrum, pressure release, corrugated surfaces producing clusters of caustics: Catastrophe theory modeling and experimental comparisons.** K. L. Williams (Applied Physics Laboratory, University of Washington, 1013 NE 40th St., Seattle, WA, 98105), J. S. Stroud, P. L. Marston (Washington State University, Physics Dept., Pullman WA 99164)

Exact integral equations for the acoustical pressure scattered from a rough pressure release surface can be solved numerically; however analytical progress, gained at the expense of various approximations, can lend physical and geometrical insight not as evident from numerical studies. With this motivation, a high frequency approximation will be presented for the pressure (scalar field) forward scattering by Gaussian spectrum, pressure release (free surface), corrugated surfaces. The emphasis is on the intensity fluctuations associated with random caustics and on the transition to farfield scattering. The approximation is also pertinent to vector field scattering. To include diffraction, the analysis uses ideas and results from catastrophe theory [M. V. Berry and C. Upstill, *Prog. Opt.* **18**, 258-346 (1980); P. L. Marston, *Physical Acoustics* **21**, 1-234 (1992)]. Catastrophe theory allows one to write down the scattered pressure in terms of a finite set of diffraction catastrophe and stationary phase contributions. The catastrophe theory results will be compared to numerical integration and experimental results for an individual rough surface to demonstrate their validity and the insight they supply. The second moment of intensity will also be examined as a function of distance away from the scattering surface. The non-Gaussian statistics seen near the surface will be interpreted via catastrophe theory as will the time-domain features of transient echoes. [Work supported by the U.S. Office of Naval Research.]

## EFFECTS OF REFLECTION FROM AN UNEVEN SURFACE ON A CHIRP RADAR

Saba Mudaliar  
Rome Laboratory  
Hanscom AFB, MA 01731

Scattering of waves from an uneven surface is encountered in many problems related to radar detection and tracking. It is primarily in this connection theoretical studies on scattering from rough surfaces have progressed so much during the past few decades. However, theoretical analyses have always made simplifying assumptions which may not truly represent the practical situation. For instance, one often assumes the incident signal to be a monochromatic continuous wave. But several radars use different types of pulsed signals. With this in mind, we study in this paper the effects of reflection from a rough surface on a chirp radar.

The chirp radar under consideration consists of a transmitter which sends out a linearly swept frequency modulated pulse. The receiver contains an associated matched filter. The object is to achieve a higher peak power and resolution without stretching the peak power handling capacity of the transmitter [Klauder et al., *B.S.T.J.*, 39, 745-808, 1960].

The surface we consider is a randomly uneven surface whose mean is a plane. The surface has gentle undulations and its fluctuations about the mean is assumed to be normally distributed. Both the transmitter and the receiver are assumed to be in the far zone. The primary quantity of interest in this paper is the average signal power at the receiver. The reflection from the uneven surface is calculated using the Kirchhoff method. Using the Green's theorem the reflected wave is expressed as an integral in terms of the field on the surface. The surface field is then computed assuming that the surface is locally flat. The reflected wave is thus calculated and an analytical expression is obtained for the average received power. Two special cases are considered for discussion. Finally, numerical examples are provided to examine the distortion of the received signal.



WEDNESDAY PM JOINT SPECIAL SESSION W-J5

Room: Kane 220

NONLINEAR ELECTROMAGNETISM

Chairs: I.M. Besieris, Virginia Polytechnic Institute and State University; R.W. Ziolkowski, University of Arizona

Organizer: P.L.E. Uslenghi, University of Illinois at Chicago

- 2:00 Physical Models of Nonlinear Susceptibilities for FDTD Implementation 312  
*J.M. Arnold, Univ. of Glasgow; \*R.W. Ziolkowski, Univ. of Arizona*
- 2:20 An Overview of Wave Propagation in Random Nonlinear Media 313  
*\*I.M. Besieris, Virginia Polytechnic Inst. and State Univ.*
- 2:40 Chaos in Multi Pendular Optical Resonators 314  
*G. Franceschetti, Univ. of Napoli; V. Pierro, I.M. Pinto, Univ. of Salerno*
- 3:00 NL-FDTD Simulations of Dielectric Waveguide, Ultrashort Optical Pulse Output Couplers Formed by Linear and Nonlinear Corrugated Sections 315  
*\*R.W. Ziolkowski, J.B. Judkins, Univ. of Arizona*
- 3:20 Steady-State Electromagnetic Analysis of 2D Nonlinear Frequency-Dispersive Structures 316  
*G. Ghione, R.D. Graglia, Politecnico di Torino*
- 3:40 Break
- 4:00 Nonlinear Microwave Circuit Analysis 317  
*\*S. Mas, Nonlinear Technologies, Inc.*
- 4:40 Numerical Analysis of Nonlinear Advection-Diffusion Partial Differential Systems Arising in Hydrodynamic Transport Models for High-Frequency Semiconductor Devices 318  
*\*G. Ghione, Politecnico di Torino*
- 5:20 Discussion on the Future of Nonlinear Electromagnetism  
*Moderator: P.L.E. Uslenghi, Univ. of Illinois at Chicago*

## PHYSICAL MODELS OF NONLINEAR SUSCEPTIBILITIES FOR FDTD IMPLEMENTATION

J. M. Arnold<sup>1</sup> and R. W. Ziolkowski<sup>2\*</sup>

<sup>1</sup>Department of Electronics & Elect. Eng., University of Glasgow, Glasgow, Scotland, UK

<sup>2</sup>Department of Elect. & Comp. Eng., University of Arizona, Tucson, Arizona, USA

The problem of the accurate numerical modelling of nonlinear integrated optics devices has been subject to increasing interest in recent years, for potential applications in all-optical switching and integrated semiconductor lasers. Since the most interesting nonlinear phenomena are transient, and superposition is not available, it is natural to try to carry out this modelling directly in the time-domain, and for this reason the finite-difference time-domain (FDTD) method is receiving intensive study (see, for example, Ziolkowski and Judkins, *J. Opt. Soc. Am. (B)*, **10**, 186, 1993). In contrast to the case for frequency-domain linear analysis, a single value of 'permittivity'  $\epsilon$  is completely inadequate to describe nonlinear time-dependent phenomena, and it is essential to model the interaction of the electromagnetic field with the material medium. This in turn requires quantum-mechanical descriptions of the electronic states available in the medium. Physical models incorporate all propagation effects such as dispersion and nonlinearity, with the proper physical linkages between them. As the size of optical devices is reduced to the size of an optical wavelength, the need for more exact materials and response models is a precondition to the successful design and fabrication of those devices. Most current simulation models are based on known macroscopic, phenomenological models that avoid issues dealing with specific microscopic behavior of the materials in the NLO devices. Inaccuracies in the simulation results are then exacerbated as the device sizes shrink to subwavelength sizes and the response times of the excitation signals surpass the response time of the material. Quantum mechanical effects begin to manifest themselves in this parameter regime; the simulation models must incorporate this behaviour to be relevant. In this paper we review some quantum-mechanical models of electromagnetic polarisation which, while being relatively simple, are extremely useful in FDTD implementations of the modelling.

Several examples will be presented which will illustrate the advantages of the self-consistent microscopic materials and macroscopic electromagnetics response model represented by coupling Maxwell's equations and the quantum mechanical Schrodinger equation together. These will include configurations that produce self-induced transparency (SIT) effects. These problems depend intimately upon the quantum-mechanical effects associated with the two-level atomic system model; the SIT results are not realizable with purely phenomenological macroscopic materials models. The one-dimensional versions of these problems have known solutions which can be used to guide and validate the numerical analysis. Device and simulation complexity will be introduced by considering multi-dimensional effects. Behaviour which results from the vector nature of our simulations will be emphasized.

## AN OVERVIEW OF WAVE PROPAGATION IN RANDOM NONLINEAR MEDIA

Ioannis M. Besieris  
The Bradley Department of Electrical Engineering  
Virginia Polytechnic Institute and State University  
Blacksburg, Virginia 24061

Nonlinear stochastic theory pertains to the derivation of statistical information (e.g.,  $n$ th order moments, the "local" energy spectrum, etc.) in the presence of nonlinearity, initial, boundary and parametric random fluctuations, as well as deterministic channel properties, such as absorption, dispersion and inhomogeneities.

Random nonlinear problems are traditionally linked with hydrodynamic and plasma turbulence, the kinetic theory of gases and fluids, etc. More recently, however, an urgent need has emerged for a stochastic generalization of nonlinear wave propagation. This has been dictated by specific physical problems, such as the transmission of a thermally stressed laser beam in a turbulent atmosphere, the utilization of optical channels created from laser-induced evaporation of water drops in dense clouds and mists, optical propagation in soliton fibers, microwave propagation in nonlinear transmission lines with random perturbations, etc. Stochastic nonlinear problems arise, also, in connection with the development of schemes for neutralizing the effects of turbulence (e.g., adaptive optics or phase conjugation). The relevance of localization, chaos, critical phenomena and universality theory to turbulence, as well as in deterministic systems (e.g., dynamical chaos of rays in a waveguide with longitudinal periodic inhomogeneities or irregular cross section) is becoming important and is being studied intensively.

Exact solutions for representative stochastic nonlinear problems arising in physical applications are practically impossible. As a consequence, a serious effort has been made to develop asymptotic or perturbative techniques which yield reasonable approximate solutions. For the most part, these methods are formal and cannot easily be validated, either analytically or numerically. There exists, however, the possibility for full statistical characterization for certain special sets of stochastic nonlinear equations; also, multi-scale methods provide a systematic approach for deriving evolution equations for nonlinear waves in random media, even in cases where the statistical fluctuations are large.

In this talk, an overview will be provided of characteristic stochastic nonlinear phenomena arising in electromagnetic wave propagation. A critical assessment will also be made of the available methods for studying the relevant stochastic nonlinear equations.

# Chaos in Multi Pendular Optical Resonators

G. Franceschetti

(Dip. Ing. Elett. I Univ. Napoli e CNR-IRECE, Napoli, Italia)

V. Pierro, I.M. Pinto

(Dip. Ing. Info. ed Ing. Elett., Univ. Salerno, Salerno, Italia)

## Abstract

Multistability and chaos in optical resonators as effects of medium nonlinearity have long since been known (K. Ikeda, Opt. Commun, 30, 257, 1979). Multistability in pendular Fabry Perots due to nonlinear radiation pressure was also predicted and observed (P. Meystre et al., J. Opt. Soc. Am. B2, 1830, 1985). In view of a general theorem (see Lichtenberg and Liebermann, *Regular and Stochastic Motion*, Springer, 1983) chaos requires a phase space with dimension higher than two to show up. Hence, it cannot occur in single-pendular Fabry Perots, unless light propagation delays are included (Ph. Tourrenc and N. Deruelle, Ann. Phys. Fr., 10, 241, 1985). Most Fabry Perots employed in interferometric sensors of very small displacements, including gravitational wave antennas (V. Pierro and I.M. Pinto, Phys. Lett., A185, 14, 1994) are multi-pendular for efficient insulation from seismic noise, and thus can be chaotic even if light propagation delays are negligible. We present the results of an extensive study of chaotic dynamics in multi-pendular FPs. As a representative result, the statistical density of Sinai entropy (sum over positive Lyapounov exponents) obtained by evolving a system with two equal arms (1 m long) and masses (400 Kg each), optical cavity length 3Km,  $\lambda = 514 \text{ nm}$  (laser wavelenght),  $P = 25W$  (laser power) and  $\rho = .995$  (half transparent mirror reflection coefficient) is displayed in *fig. 1* over an integration time of  $\sim 15'$ , starting from a regular lattice of  $10^4$  initial conditions in the phase space box  $|\xi_i| \leq 0.005$ ,  $|\eta_i| \leq 0.005$ ,  $\xi_i$  being the pendular displacements in units of the laser wavelenght, and  $\eta_i$  the corresponding canonically conjugate momenta. The reciprocal of Sinai entropy gives an estimate of the time after which the system becomes unpredictable (Pesin theorem). It is seen that the system can develop chaos within a typical operation time with significant probability.

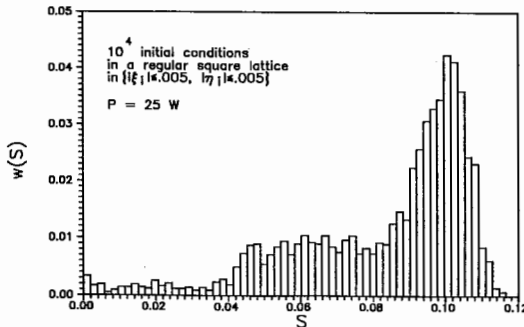


Fig. 1 - Statistical density of Sinai entropy

**NL-FDTD SIMULATIONS OF DIELECTRIC WAVEGUIDE,  
ULTRASHORT OPTICAL PULSE OUTPUT COUPLERS FORMED  
BY LINEAR AND NONLINEAR CORRUGATED SECTIONS**

*Richard W. Ziolkowski\* and Justin B. Judkins*

Electromagnetics Laboratory  
Department of Electrical and Computer Engineering  
The University of Arizona  
Tucson, AZ 85721 USA  
(602) 621-6173 (office) (602) 621-8076 (fax)  
ziolkowski@ece.arizona.edu

With the continuing and heightened interest in linear and nonlinear semiconductor and optically integrated devices, more accurate and realistic numerical simulations of these devices and systems are in demand. Such calculations provide a testbed in which one can investigate new basic and engineering concepts, materials, and device configurations before they are fabricated. The time from device conceptualization to fabrication and testing should therefore be enormously improved with numerical simulations that incorporate more realistic models of the linear and nonlinear material responses and the actual device geometries. It is felt that vector and higher dimensional properties of Maxwell's equations that are not currently included in existing scalar models, in addition to more detailed materials models, may significantly impact the scientific and engineering results.

In this paper we describe numerically obtained, multi-dimensional, full-wave, vector Maxwell's equations solutions to problems describing the interaction of ultrashort, pulsed beams with complex structures filled with either a linear material or a dispersive, nonlinear material having a finite response time. The numerical solutions of the nonlinear material structures have been obtained in two space dimensions and time with a nonlinear finite difference time domain (NL-FDTD) method which combines a generalization of a standard, FDTD, full-wave, vector, linear Maxwell's equations solver with a Lorentz linear dispersion model, a nonlinear Raman model, and an instantaneous Kerr nonlinear model.

We will specifically present NL-FDTD results obtained for the interaction of ultrashort pulses propagating in corrugated waveguide sections filled with either linear or nonlinear materials. Interest in this problem follows from our desire to design of nonlinear guided wave couplers and beam steerers. The corrugations modeled can be dielectric (an extension of the dielectric waveguide) or metallic (deposited into or on top of the dielectric waveguide). Expected conversion efficiencies from the guided mode energy to the radiated field energy have been observed in the linear case. The nonlinear waveguiding structures are presenting interesting challenges in their analysis and interpretation. A variety of *TE* and *TM* cases with metallic corrugations will be presented to illustrate the desired nonlinear beam steering effects. Since the electric field behavior near the edges of these metallic corrugations is significantly different between the two polarizations, the resulting radiated field structures reflect this difference. Output beam characteristics depending on the medium response time, the polarization, and the material parameters, have been studied and will be reported. Particular emphasis will be given to pulses whose time-record length is approximately the size of the corrugation region. It is found that even pulses that are short in comparison with the corrugation region can be effectively used to beam steer.

-----  
This work was supported in part by the Lawrence Livermore National Laboratory under the auspices of the U. S. Department of Energy under contract W-7405-ENG-48.

# Steady-State Electromagnetic Analysis of 2D Nonlinear Frequency-Dispersive Structures

Giovanni Ghione and Roberto D. Graglia  
Politecnico di Torino, Dipartimento di Elettronica,  
Corso Duca degli Abruzzi 24, 10129 Torino, Italy.

We investigate the time-domain steady-state electromagnetic field scattered by a nonlinear, frequency-dispersive magnetic or dielectric arbitrarily shaped cylindrical structure excited by a normally incident plane wave.

In order to allow for a general kind of nonlinear and frequency-dispersive material behavior, we solve the time-domain system of Maxwell curl equations for the electric and magnetic fields coupled to the constitutive equations that relate the fields to the corresponding flux densities.

The steady-state incident and scattered fields are expanded in Fourier-Bessel series on a circle surrounding the scatterer cross section in terms of unknown scattering coefficients to be determined. Within the bounded circular scatterer region, the differential problem is formulated through the Finite Element method applied to the transversal and longitudinal parts of the curl equations.

Tangential basis functions are used to discretize the transverse components of the  $\underline{E}$  and  $\underline{H}$ , so as to guarantee the boundary conditions in the presence of material parameter discontinuities, whereas the longitudinal components are assumed as piecewise constant, according to a consistent edge-element formulation; thus, the formulation of the longitudinal problem is weak.

After the spatial discretization has been carried out, the resulting time-domain nonlinear algebraic-differential system is analyzed by means of fast algorithms for the steady-state solution of nonlinear systems under periodic excitation based on time-domain approaches, such as the shooting and extrapolation methods. Some case studies are carried out for both the dispersionless and dispersive cases, and the method is applied to the analysis of strongly nonlinear materials.

# Nonlinear Microwave Circuit Analysis

Stephen Maas

**Nonlinear Technologies, Inc.**

PO Box 7284, Long Beach, CA 90807, USA

## Abstract

This paper describes the dominant methods for the analysis of nonlinear microwave circuits: time domain, Volterra-series, and harmonic-balance methods. We examine briefly the history and technology of these methods, and identify those that hold the most promise for present and future systems and components. We also discuss limitations that must be overcome before these techniques can be considered mature; these include numerical accuracy of Fourier transforms, methods for accurate modeling of both linear and nonlinear circuit elements, selection of frequency components.

Because of the broad range of frequencies generated by nonlinear circuits, nonlinear analysis puts severe demands on the modeling of linear elements such as transmission line discontinuities. Although much progress has been made in the modeling of linear circuit elements, models that are accurate and suitable for computer circuit analysis are still few and immature. Of course, there is still a great need for accurate models of nonlinear devices. Most existing models are sufficiently accurate for only a limited range of applications.

Nonlinear circuit analysis is used for the design of a wide range of microwave components. It is indispensable for the design of mixers, power amplifiers, frequency multipliers, and low-distortion amplifiers, especially those realized as monolithic circuits. Many types of systems benefit significantly from advances in this technology, especially those that are unusually sensitive to interference and nonlinear distortion: radar, wireless applications, personal communications, and electro-optical systems.

# Numerical analysis of nonlinear advection-diffusion partial differential systems arising in hydrodynamic transport models for high-frequency semiconductor devices

Giovanni Ghione

Dipartimento di Elettronica, Politecnico di Torino,  
Corso Duca degli Abruzzi 24, Torino, Italy

The numerical simulation of semiconductor devices is today an indispensable tool for the computer-aided design of integrated circuits, both at low frequency and in the domain of (Monolithic) Microwave Integrated Circuits (MMIC's) made on compound semiconductors (GaAs, InP, GaAlAs).

Numerical device simulation is based on three steps: the choice of an appropriate physical model, its spatial and/or time-domain discretization and the solution of the resulting nonlinear time-domain differential system in the several possible operating conditions (DC, small signal, large-signal). A physical model is obtained by coupling an electromagnetic model (often Poisson's equation only, due to the quasi-static hypothesis implied by the small dimensions of solid-state devices) to a transport model describing the behaviour of electron and holes in the presence of electric fields and concentration gradients. The simplest of these models, called the drift-diffusion model, in which the carrier velocity depends on the local electric field, is often inadequate to the simulation of advanced devices like the short-channel MESFET or HEMT and the heterojunction bipolar transistor (HBT). More refined transport models can be directly derived from the Boltzmann transport equation, that is from an exact semi-classical picture of carrier transport. In this way one obtains the so-called hydrodynamic models, which describe the conservation of the carrier populations and of their average energy and momentum.

The spatial discretization can be performed, as a matter of principle, through conventional finite-element or finite-differences schemes based e.g. on polynomial basis functions on triangular or rectangular domains. This choice is adequate for Poisson's equation but leads to spurious spatial oscillations when applied to the conservation equations of the transport models, unless the mesh spacing is extremely small. The reason for this failure is well known from the field of computational fluid dynamics, where transport equations arise in which *drift* or *advection* terms are present together with *diffusive* terms. These equations are structurally (and also physically) similar to the conservation equations arising in device modelling, and their discretization has been addressed through intrinsically stable discretization schemes, known as *upwinding* or UFEM (Upwind Finite Element Method) schemes.

The paper presents a review of the finite-element like numerical discretization schemes applied to hydrodynamic semiconductor device models, with the aim of highlighting both their computational properties and the impact of these on the simulation results. Starting from the classical Scharfetter-Gummel scheme applied to the continuity equation within the framework of a finite-box approach, the extension to energy and transport momentum equations will be discussed, together with their rigorous treatment through UFEM schemes. Numerical results and examples will be presented at the Symposium.

WEDNESDAY PM URSI-B SESSION W-U26

Room: HUB 106

TIME DOMAIN ANALYSIS III

Chairs: L. Gurel, IBM; N.K. Madsen, Lawrence Livermore National Laboratory

- 2:00 Analysis of Dispersive Medium by FDTD Methods for Vector Potential and Hertz Vector 320  
*\*N. Yoshida, Hokkaido Univ.*
- 2:20 Comparison of Dispersive Media Modeling Techniques in the Finite Difference Time Domain Method 321  
*\*D.F. Kelley, R.J. Luebbers, The Pennsylvania State Univ.*
- 2:40 A Full FDTD Formulation for Radio Propagation in Linear Dispersive Media 322  
*\*J. L. Young, Univ. of Idaho*
- 3:00 Dispersion Analysis of Multiconductor Waveguiding Systems Using a Mixed Compact 2D-FDTD and Point-Matched Time-Domain Finite Element Method 323  
*\*W. Pinello, A.C. Cangellaris, Univ. of Arizona*
- 3:20 A Full FDTD Formulation for Radio Propagation in a Warm Plasma 324  
*\*J. L. Young, Univ. of Idaho*
- 3:40 Break
- 4:00 A Hybrid FDTD/Spectral Method for the Modeling of Electromagnetic Wave Guidance in Three-Dimensional Periodic Structures 325  
*\*M. Gribbons, A.C. Cangellaris, Univ. of Arizona*
- 4:20 A Comparison of Two Conformal Methods for FDTD Modeling 326  
*\*M.W. Steeds, S.L. Broschat, J.B. Schneider, Washington State Univ.*
- 4:40 Embedding Unstructured Meshes into Uniform Grid Finite-Difference Time-Domain Codes 327  
*D.J. Riley, C.D. Turner, Sandia National Laboratories; C.C. Carson, Jr., Rice Univ.*
- 5:00 Parallelization of FDTD Algorithm Using Parallel Virtual Machine [PVM] 3.2 328  
*\*V. Varadarajan, R. Mittra, Univ. of Illinois*
- 5:20 Parallel and Serial Computing Comparison for Finite Difference Time Domain 329  
*\*W.V. Andrew, D.M. Kokotoff, C.A. Balanis, R.A. Renaut, Arizona State Univ.*

# ANALYSIS OF DISPERSIVE MEDIUM BY FD-TD METHODS FOR VECTOR POTENTIAL AND HERTZ VECTOR

Norinobu Yoshida  
Department of Electrical Engineering  
Hokkaido University, Sapporo 060 Japan

I have already proposed the three-dimensional and time-dependent formulation of the vector potential [N.Yoshida: "Unified Treatment of Scalar and Vector Potential Fields with Lorentz Gauge Condition by Spatial Network Expression", *Int. J. of Microwave and Millimeter-Wave Computer-Aided Engineering*, 3, 3, pp.165-174 (1993)] and the Hertz vector [N.Yoshida: "Treatment of Hertz Vector in 3-Dimensional Lattice Network of Spatial Network Method", *Abstract of 1990 URSI Radio Science Meeting*, 56 (1991)]. So far, these formulation has been presented for the Spatial Network Method because of easiness to prove the realization of the wave field in each equivalent network. For the formulation, the following characteristic equations are defined by using the magnetic potential  $A$  and electric potential  $S$ , and the electric Hertz vector  $\Pi$  and magnetic Hertz vector  $\Pi^*$ ;

$$\begin{aligned} \nabla \times A &= \sigma^* S + \mu \frac{\partial S}{\partial t} & (1a) & \quad \nabla \times \Pi = -\sigma^* \Pi^* - \mu \frac{\partial \Pi^*}{\partial t} & (2a) \\ \nabla \times S &= -\sigma A - \varepsilon \frac{\partial A}{\partial t} & (1b) & \quad \nabla \times \Pi^* = \sigma \Pi + \varepsilon \frac{\partial \Pi}{\partial t} & (2b) \end{aligned}$$

These equations to be similar to the Maxwell's equation can be directly applied to the FD-TD method by arranging their each component in the Yee's lattice as the same manner for the electromagnetic field component. The correspondence of each component to that in the Maxwell's equation is shown in Table. Hence, such formulation by the full components has the same advantage of the conventional FD-TD method that the medium condition including dispersive mediums can be treated at each lattice points. In Figure, the results of dispersive characteristics of the orientation polarization medium computed by both proposed FD-TD methods show the good agreement with analytical ones and also with each other.

Electric Node		Magnetic Node	
Component Equations	Variables	Component Equations	Variables
A.	$\frac{\partial^2 S_x}{\partial t^2} - \frac{\partial^2 S_x}{\partial x^2} = c_0 \frac{\partial^2 F_x}{\partial t^2}$ $\frac{\partial^2 S_y}{\partial t^2} - \frac{\partial^2 S_y}{\partial y^2} = c_0 \frac{\partial^2 F_y}{\partial t^2}$ $\frac{\partial^2 S_z}{\partial t^2} - \frac{\partial^2 S_z}{\partial z^2} = c_0 \frac{\partial^2 F_z}{\partial t^2}$	E <sub>y</sub> A <sub>y</sub> H <sub>y</sub>	F. $\frac{\partial^2 A_x}{\partial t^2} - \frac{\partial^2 A_x}{\partial x^2} = c_0 \frac{\partial^2 F_x}{\partial t^2}$ $\frac{\partial^2 A_y}{\partial t^2} - \frac{\partial^2 A_y}{\partial y^2} = c_0 \frac{\partial^2 F_y}{\partial t^2}$ $\frac{\partial^2 A_z}{\partial t^2} - \frac{\partial^2 A_z}{\partial z^2} = c_0 \frac{\partial^2 F_z}{\partial t^2}$
D.	$\frac{\partial^2 S_x}{\partial t^2} - \frac{\partial^2 S_x}{\partial x^2} = c_0 \frac{\partial^2 F_x}{\partial t^2}$ $\frac{\partial^2 S_y}{\partial t^2} - \frac{\partial^2 S_y}{\partial y^2} = c_0 \frac{\partial^2 F_y}{\partial t^2}$ $\frac{\partial^2 S_z}{\partial t^2} - \frac{\partial^2 S_z}{\partial z^2} = c_0 \frac{\partial^2 F_z}{\partial t^2}$	E <sub>x</sub> A <sub>x</sub> H <sub>x</sub>	B. $\frac{\partial^2 A_x}{\partial t^2} - \frac{\partial^2 A_x}{\partial x^2} = c_0 \frac{\partial^2 F_x}{\partial t^2}$ $\frac{\partial^2 A_y}{\partial t^2} - \frac{\partial^2 A_y}{\partial y^2} = c_0 \frac{\partial^2 F_y}{\partial t^2}$ $\frac{\partial^2 A_z}{\partial t^2} - \frac{\partial^2 A_z}{\partial z^2} = c_0 \frac{\partial^2 F_z}{\partial t^2}$
E.	$\frac{\partial^2 S_x}{\partial t^2} - \frac{\partial^2 S_x}{\partial x^2} = c_0 \frac{\partial^2 F_x}{\partial t^2}$ $\frac{\partial^2 S_y}{\partial t^2} - \frac{\partial^2 S_y}{\partial y^2} = c_0 \frac{\partial^2 F_y}{\partial t^2}$ $\frac{\partial^2 S_z}{\partial t^2} - \frac{\partial^2 S_z}{\partial z^2} = c_0 \frac{\partial^2 F_z}{\partial t^2}$	E <sub>x</sub> A <sub>x</sub> H <sub>x</sub>	C. $\frac{\partial^2 A_x}{\partial t^2} - \frac{\partial^2 A_x}{\partial x^2} = c_0 \frac{\partial^2 F_x}{\partial t^2}$ $\frac{\partial^2 A_y}{\partial t^2} - \frac{\partial^2 A_y}{\partial y^2} = c_0 \frac{\partial^2 F_y}{\partial t^2}$ $\frac{\partial^2 A_z}{\partial t^2} - \frac{\partial^2 A_z}{\partial z^2} = c_0 \frac{\partial^2 F_z}{\partial t^2}$

Table Correspondence in Yee's Lattice

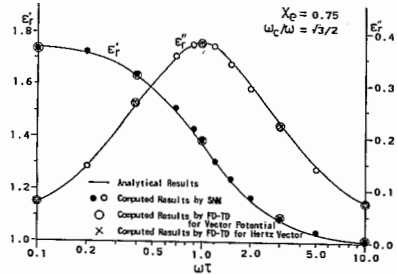


Figure Dispersion Property of Orientation Polarization

## **COMPARISON OF DISPERSIVE MEDIA MODELING TECHNIQUES IN THE FINITE DIFFERENCE TIME DOMAIN METHOD**

**David F. Kelley\* and Raymond J. Luebbers**  
**Department of Electrical Engineering**  
**The Pennsylvania State University**  
**University Park, Pennsylvania 16802**

Several methods for incorporating dispersive media into finite difference time domain (FDTD) calculations are compared with respect to accuracy, stability, computer memory requirements and computational speed. Most methods that have been developed so far can be classified into two general approaches. The first approach employs recursion to update a numerical approximation to the convolution in time of the electric field and the dielectric susceptibility function. The second involves the solution of an auxiliary differential equation relating the electric flux density to the electric field via the frequency-dependent permittivity. These two general approaches will be referred to as the recursive convolution method and the differential method. Within each category several methods with subtle differences have been proposed. The comparisons presented here will demonstrate the trade-offs in computational performance inherent in each approach.

Another important area of comparison to be examined is the ease with which the two methods can incorporate extensions to media with more than one pole in the susceptibility function. Most of the literature on treating dispersive media in FDTD solutions focuses on media that can be characterized by one first-order pole (Debye media) or one second-order pole (Lorentz media). Methods that employ recursive convolution already exist that can treat the case of media with multiple poles; however, similar extensions have not been demonstrated for the differential method. Techniques for extending the differential method to allow analysis of media characterized by multiple poles will be examined here, along with the performance trade-offs that result by adding this capability.

A FULL FDTD FORMULATION  
FOR RADIO PROPAGATION IN LINEAR DISPERSIVE MEDIA

Jeffrey L. Young  
Department of Electrical Engineering  
University of Idaho  
Moscow, ID 83843

It is well known that the finite difference time domain (FDTD) method, as first put forth by Yee and further developed by Taflov, is an effective and robust numerical tool that predicts the propagation and scattering characteristics of an electromagnetic field. Unfortunately, when the media is temporally dispersive it is not sufficient to just discretize Ampere's and Faraday's curl equations; one must also consider the convolution integral that relates the displacement vector to the electric field vector. Even though the convolution integral implies a storage of the complete time history of the electric field, Luebbers *et al.* [e.g. *IEEE Trans. Ant. Propagat.*, 1993] have developed schemes, bearing the acronym (FD)<sup>2</sup>TD, that employ recursive techniques and hence, schemes that minimize computational memory.

As reported in this presentation, there exists an alternative method to that of Luebbers's. For example, if the medium is characterized by a relative permittivity of the form

$$\epsilon_r(\omega) = 1 + \frac{\omega_p^2}{\omega_1^2 + j\omega\nu - \omega^2}$$

( $\omega_1$ ,  $\nu$  and  $\omega_p$  are the resonant, collision and plasma frequencies, respectively) then there exists a set of first order equations in space and time that are compatible with the Yee cell and with the standard leap-frog time integrator. Given this, the scheme is thus seen to be second order accurate in time and space, memory parsimonious and highly robust. Moreover, the extension to  $N$ th-order media requires little to no additional effort, whether programming or analytical. Aspects such as these are discussed in further detail, numerical dispersion relationships are deduced and numerical results are given that lend credence to the proposed method.

DISPERSION ANALYSIS OF MULTICONDUCTOR WAVEGUIDING SYSTEMS  
USING A MIXED COMPACT 2D-FDTD AND  
POINT-MATCHED TIME-DOMAIN FINITE ELEMENT METHOD

W. Pinello\* and A.C. Cangellaris  
Center for Electronic Packaging Research  
Department of Electrical and Computer Engineering  
University of Arizona  
Tucson, AZ 85721, USA

This paper presents a numerical scheme that combines point-matched time-domain finite element concepts (Cangellaris, et al, IEEE Trans. Antennas Prop., Oct. 1987) with a compact 2D-FDTD scheme (Asi and Shafai, Electronic Lett., vol. 28, p. 1451, 1992), for the extraction of the propagation characteristics of multiconductor waveguiding systems in multi-layered, inhomogeneous, anisotropic substrates. Such waveguiding systems are encountered frequently in dense interconnect packages for high-speed digital and RF/microwave integrated circuits. The proposed method is essentially an extension of the aforementioned compact 2D-FDTD scheme. The point-matched finite-element method is introduced to discretize the hyperbolic system of Maxwell's equations on a grid that conforms to the arbitrary shapes of the metallic conductors as well as any nonplanar media interfaces formed by the substrate and insulating media. This finite element grid exists only in the vicinity of the conductor cross sections. The rest of the cross section is discretized using the compact 2D-FDTD grid.

The method takes advantage of the fact that for propagating modes the field variation along the axis of the waveguide,  $x$ , is of the form  $\exp(-jpx)$ , where  $p$  is the propagation constant. Thus, in Maxwell's time-dependent curl equations the  $x$ -derivatives are replaced with  $(-jp)$  and the numerical discretization is restricted only on the cross section of the waveguide. The remaining spatial derivatives are approximated using standard finite-element procedures over the staggered electric and magnetic field grids used in the point-matched, time-domain finite element method. The standard finite difference approximations are used on the FD-TD grid. A methodology that preserves the 2nd-order accuracy of the overall numerical scheme will be presented for handling nodes at the interface between the two grids. The fully discrete system is integrated in time as follows. First, a desirable value of the propagation constant  $p$  is selected, along with some initial value for the field distribution over the cross-section of the guide. Next, a leap-frog scheme is used and the equations are integrated in time until a steady state is reached. Subsequently, the time histories of the fields are Fourier transformed to obtain the frequencies at which the various propagating modes exhibit the selected propagation constant. These frequencies correspond to the peaks in the Fourier spectra. In addition to the detailed presentation of the method, the paper introduces ways to improve the speed of convergence of the algorithm by appropriate selection of the initial value for the field distributions and special processing of the time histories of the fields using a specific correlation integral.

A FULL FDTD FORMULATION  
FOR RADIO PROPAGATION IN A WARM PLASMA

Jeffrey L. Young  
Department of Electrical Engineering  
University of Idaho  
Moscow, ID 83843

A finite difference time domain (FDTD) methodology that is applicable for radio wave propagation in a warm plasma is presented. The scheme considers the coupled, governing equations of Maxwell and Euler in their first order form (i.e. first order derivatives in time and space). To accomplish the spatial discretization, a finite difference cell is postulated that is compatible with the central difference approximation of the curl, gradient and divergence operators that appear in the four governing equations. Moreover, by collocating the components of the velocity and electric vectors, we effect a natural coupling between the acoustical and electromagnetic equations. With respect to the temporal discretization, a leap-frog methodology is employed. Hence all of the key attributes of Yee's original method [Yee, *IEEE Trans. Ant. Propagat.*, 1966] – namely, second order accuracy and robustness – are retained in this new methodology. Data are provided that compare the FDTD data with IFFT results of closed-form, frequency-domain solutions; the comparison is seen to be excellent.

Since an isotropic warm plasma can support two modes of propagation, two independent dispersion relationships are derived that quantify the numerical artifacts of the dispersive and anisotropic kind. These relationships also provide valuable information on the numerical stability of the algorithm, which is different from the standard stability requirement of Courant, Friedrichs and Lewy. Plots are given that detail these numerical effects.

A HYBRID FD-TD/SPECTRAL METHOD FOR  
THE MODELING OF ELECTROMAGNETIC WAVE GUIDANCE  
IN THREE-DIMENSIONAL PERIODIC STRUCTURES

M. Gribbons\* and A. Cangellaris

Department of Electrical and Computer Engineering  
University of Arizona, Tucson, AZ 85721

This paper presents a hybrid FD-TD/spectral method developed for the efficient electromagnetic analysis of three-dimensional structures with periodicity in one or two dimensions. The method obtains the propagation characteristics and mode profile of electromagnetic waves in non-homogeneous, anisotropic, open geometries. The method retains the simplicity of modeling of complex geometries associated with FD-TD, and exhibits the benefit of increased accuracy due to the introduction of a spectral technique.

A summary of the proposed method follows. The fundamentals of the mathematical formulation and application to two-dimensional closed periodic waveguiding structures can be found in Cangellaris et. al, IEEE Microwave and Guided Wave Lett., Oct. 1993. The spatial and temporal discretization of Maxwell's time-dependent curl equations over a single cell of the periodic structure is performed according to the standard FD-TD method except for the following modification. From Floquet's theorem, we know that the fields have a pseudo-periodic character. To take advantage of this, the Fourier series representation, implemented through the efficient FFT, is used for the calculation of the spatial derivatives of all field components along the axes of periodicity of the structure. In other words, the derivatives along the axes of periodicity of the structure are computed spectrally at each time step. This way, not only are the periodic boundary conditions enforced exactly but some of the spatial derivatives are calculated with exponential accuracy characteristic of spectral methods. The other spatial and the temporal derivatives are calculated by the standard central differencing scheme associated with FD-TD. Since the propagation constant needs to be assumed known for the calculation of the Floquet expansions, the frequency becomes the eigenvalue quantity and is obtained from the solution of the hyperbolic system as an initial value problem. In addition, since the propagation constant is known, a second order Mur RBC of high accuracy can be implemented for the simulation of open structures.

The details of the mathematical formulation along with the modifications of the FD-TD lattice for periodicity in one and two dimensions, which are necessary for the correct implementation of the spectrally calculated derivatives, will be presented. The numerical stability and numerical dispersion of the method will be discussed. In order to examine the applicability of the method, results will be presented for structures which are periodic in one and two dimensions, as well as structures which are generally anisotropic.

## A Comparison of Two Conformal Methods for FDTD Modeling

Mark W. Steeds\*, Shira L. Broschat, and John B. Schneider

Electrical Engineering & Computer Science

Washington State University

Pullman, WA 99164-2752

msteeds@eecs.wsu.edu, (509) 335-0903

shira@eecs.wsu.edu, (509) 335-5693

schneidj@eecs.wsu.edu, (509) 335-4655

Since the advent of powerful computers, the Finite-Difference Time-Domain (FDTD) algorithm, originally proposed by Yee [IEEE Trans. Antennas Propagat. AP-14, 302-307, 1966], has been widely used in electromagnetic scattering applications. However, it has been shown that the Yee algorithm is incapable of modeling many curved surfaces accurately unless a relatively dense grid is used. Inaccuracy is caused by the stair-step approximation of curved surfaces inherent in the Yee algorithm. Two proposed conformal methods for improving Yee's FDTD algorithm for the modeling of curved surfaces are considered. The first, proposed by Jurgens *et al.* [IEEE Trans. Antennas Propagat. 40, 357-366, 1992], uses the contour path method. The second, proposed by Yee *et al.* [IEEE Trans. Antennas Propagat. 40, 1068-1075, 1992], uses overlapping grids. Electromagnetic scattering from a perfectly conducting circular cylinder is used to test each method's ability to model a curved surface. Electromagnetic scattering from a perfectly conducting rotated rectangular cylinder is used to test each method's ability to model corners and edges. The advantages and disadvantages of both methods are given based upon accuracy, complexity of implementation, and actual improvement over Yee's original algorithm.

## EMBEDDING UNSTRUCTURED MESHES INTO UNIFORM GRID FINITE-DIFFERENCE TIME-DOMAIN CODES

Douglas J. Riley and C. David Turner  
Radiation and Electromagnetic Analysis Department  
Sandia National Laboratories  
Albuquerque, New Mexico 87185

Charles C. Carson, Jr.  
Rice University  
Houston, Texas 77030

Finite-difference time-domain (FDTD) codes are based upon rectangular grids that often use the same spatial step for all three dimensions. To model fine detail such as wires and apertures, special algorithms are generally required. In addition, surface curvature can only be modeled with a "staircase" approximation. However, FDTD codes are mature with regard to radiation boundary conditions and near-to-far-field transformations; consequently, it is desirable to take advantage of these and other existing features when extending the overall capabilities of the FDTD method.

This paper addresses the use of an embedded unstructured, non-orthogonal 3D grid within a traditional FDTD code. The unstructured region is defined to terminate on a rectangular surface with specified node locations. This surface constitutes the boundary between the non-orthogonal and orthogonal regions. The Yee algorithm is applied in the orthogonal region along with standard near-to-far-field transformations and radiation boundary conditions. A modified finite-volume algorithm is used in the unstructured region. The Sandia developed CUBIT software package is used to generate the unstructured grid with the desired termination properties. Zoning the computational volume in this manner leads to a formulation that is efficient, accurate, and general. Multiple unstructured regions can be embedded within the same computational volume. Three additional routines plus a mesh data file provide uniform-grid FDTD codes with an unstructured grid capability. Radar cross section predictions for spheres, cylinders and ovoids are presented.

## Parallelization of FDTD Algorithm using Parallel Virtual Machine [PVM] 3.2

V. Varadarajan\* and Raj Mittra

Electromagnetic Communication Laboratory

University of Illinois at Urbana-Champaign, IL 61801

The Finite Difference Time Domain (FDTD) calculations have been parallelized using PVM [Parallel Virtual Machine] 3.2 to utilize the collective computational power of a group of workstations. Representative large problem sizes that have been parallelized involve  $75 \times 75 \times 150$  cells,  $75 \times 75 \times 300$  cells,  $100 \times 100 \times 640$  cells, and  $140 \times 140 \times 320$  cells. It has been found that the speedup factors can approach the maximum achievable values for large problem sizes if the computation-to-communication ratios are maintained at values significantly greater than unity. Furthermore, in order to achieve linear speedups, the problem sizes should be increased with the number of processors while adequate computation-to-communication ratios are maintained in individual processors. As an example, the speedups achieved for a rectangular cavity problem with two different fixed number of cells, viz.,  $75 \times 75 \times 150$  and  $75 \times 75 \times 300$  and also with  $100 \times 100 \times 80$  cells per processor are illustrated in Figure 1 as a function of the number of HP-735 workstations. For the later problem the speedup is given at two different rates of computation, viz., at 14 and 24 MFLOPs. With parallelized Ethernet communications, good speedups can be achieved for large problem sizes in all three coordinate directions. The achieved speedup, communication-to-computation ratios and turnaround times for various problem sizes demonstrate the potential of parallel distributed computing using the software PVM 3.2.

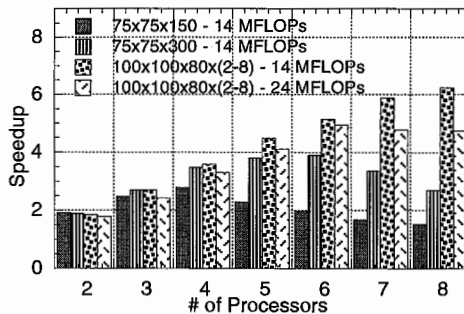


Figure 1: Speedup with  $75 \times 75 \times 150$  cells (total),  $75 \times 75 \times 300$  cells (total), and  $100 \times 100 \times 80$  cells (per processor); the last at 14 MFLOPs and at 24 MFLOPs

# Parallel and Serial Computing Comparison for Finite Difference Time Domain

William V. Andrew\*, David M. Kokotoff,  
Constantine A. Balanis and Rosemary A. Renaut

Telecommunications Research Center  
Arizona State University  
Tempe, AZ 85287-7206

The objective of this project was to investigate the applicability of a massively parallel computing architecture to the solution of a two dimensional electromagnetic scattering problem using the Finite-Difference Time-Domain (FDTD) method. A serial two-dimensional FDTD FORTRAN 77 code was translated to FORTRAN 90 using the VAST code conversion utility on the MasPar machine at Arizona State University. The converted code was then analyzed and optimized by hand to improve the parallel code's efficiency. The effectiveness of both the VAST converted code and the optimized FORTRAN 90 code was measured by comparing the accuracy of the solution to published results and by comparing computational speed of the FORTRAN 90 parallel codes run on the MasPar to the serial version of the code run on a Sun IPX workstation. Also, scaling the problem by increasing the size of the computational workspace and varying the number of processors used on the MasPar was performed to determine the relative increase in speed between the serial machine, and the VAST translated and "optimized" software on the parallel machine. It was found that large computational gains can be realized by using a massively parallel machine like the MasPar over a "standard" serial machine for the two dimensional FDTD code. The VAST translation utility was a useful tool to parallelize a FORTRAN 77 code, but significant improvements in efficiency were realized by optimizing the FORTRAN 90 output of the VAST program. Finally, a recommendation will be made as to whether or not a three dimensional implementation of the FDTD method could be solved on ASU's MasPar machine. Figure 1 shows the comparative processing speed for the "optimized" FORTRAN 90 code run on the MasPar versus the serial code run on a Sun IPX workstation. Cases 1 through 4 are computational spaces of increasing size: (1)60x60, (2)90x90, (3)120x120 and (4)240x240 cells.

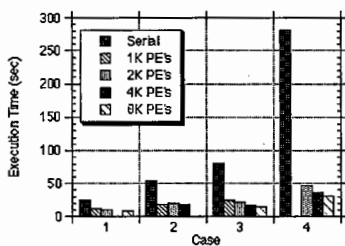


Figure 1: Execution times for "optimized" code vs. serial code for 4 different problem sizes on 4 different configurations of the MasPar processing array.



WEDNESDAY PM URSI-B SESSION W-U27

Room: Savery 249

WAVEGUIDES I

Chair: To be arranged

- 2:00 Vector Finite Element Solution of Ferrite Loaded Waveguides 332  
*B.C. Anderson, Z.J. Cendes, Carnegie Mellon Univ.*
- 2:20 Investigation of the Resonances of Open Rectangular Cavities 333  
*\*L. Gürel, S. Daijavad, B.J. Rubin, IBM Research Division*
- 2:40 Leakage Behavior of Planar Waveguides Investigated with the Method of Lines 334  
*\*A. Dreher, Fern Universität*
- 3:00 Finite-Difference Analysis of Circular Dielectric-Loaded Waveguides 335  
*J.-M. Guan, National Tsinghua Univ.; D.-C. Chang, Private China Junior College of Technology*
- 3:20 Horizontal Gaussian Beams-Vertical Modes in Three-Dimensional Multimode Irregular Waveguides 336  
*\*N. N. Zernov, Univ. of St. Petersburg*
- 3:40 Break
- 4:00 Oscillating System for Millimeter-Wave Magnetron with Optimal Q-Factor 337  
*D.M. Vavriv, \*A.E. Serebryannikov, Radio Astronomy Inst. of Ukrainian Academy of Science*
- 4:20 An Experimental Method for the Design of Reentrant Cavity Filters 338  
*P. R. Aragón, \*K. Shamsaifar, Alcatel Espacio*
- 4:40 Hybrid Analysis of EM Scattering by Large Open Cavities Including Effects of Aperture Shape and Interior Obstacle 339  
*C.W. Chuang, \*P.H. Pathak, R.J. Burkholder, The Ohio State Univ.*
- 5:00 Computer Aided Design of Dielectric Open Waveguides by Boundary Element Method of GMEIE's 340  
*K. Tanaka, M. Tanaka, H. Tashima, Gifu Univ.*

# Vector Finite Element Solution of Ferrite Loaded Waveguides

Brian C. Anderson & Zoltan J. Cendes  
 Carnegie Mellon University  
 Pittsburgh, PA 15213

**Abstract:** Ferrite loaded waveguides are used in a number of microwave devices including circulators and isolators. The analysis of these structures is complicated by the fact that ferrite materials are characterized by an Hermitian permeability tensor that results in non-reciprocal behavior.

Analytic solutions are known only for a few geometries when the waveguide contains ferrite material. To provide a more general capability, recent work has focused on numerical methods for modeling ferrite devices. In particular, Dillon, Gibson and Webb (IEEE Trans. MTT, 41, 803-8) have recently published a finite element solution of ferrite loaded waveguides using co-variant projection elements. Results are calculated for the case where the DC bias is parallel to propagation.

This report describes a new method for finding the propagation constants for ferrite loaded waveguides using triangular vector finite elements. It provides a direct extension to the work done by Lee, Sun and Cendes (IEEE Trans. MTT, 39, 1262-71) for waveguides containing isotropic media. The vector finite element method described by Lee, et. al. results in a matrix that can be solved by the Lanczos method. This method for finding the eigenvalues of a large, sparse, symmetric is extended here to solve the Hermitian matrices encountered in the ferrite case. The transverse DC bias case results in a quadratic eigenvalue problem. A method is developed which reduces the quadratic problem to a linear problem not quite twice as large. The symmetric form of the matrices is preserved during the reduction so that the efficient Lanczos method can still be applied.

The finite element solutions are compared to analytic solutions that are known. Accurate results are computed for DC bias parallel and transverse to the direction of propagation. Figure 1 shows the propagation constant of the dominant mode for DC bias transverse, partially filled rectangular guide.

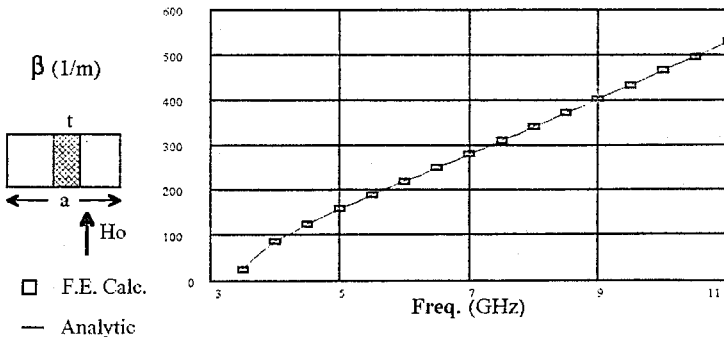


**Figure 1**  
 $\beta$ /Frequency

$H_0 = 200$  Oe  $M_s = 2000$  Gauss  $\epsilon = 9$   $a = .022$  m  $t = .004$  m  $\gamma = \gamma_L$

# Investigation of the Resonances of Open Rectangular Cavities

*Levent Gürel\*, Shahrokh Daijavad and Barry J. Rubin*  
*IBM Research Division*  
*P.O. Box 218*  
*Yorktown Heights, NY 10598*

The resonances excited in conducting rectangular cavities, with one or more walls removed or with openings on their walls, are investigated. These open cavities are formed by the separation between two conducting plates, two boxes (closed cavities), two other open cavities or any combination thereof. The case of multiple cavities formed by the separations among an array of boxes is also considered. The excitation of the resonances by using different source types (e.g., dipoles and loops), different source locations (sources inside or outside the cavity) is studied. Open cavities are also excited by the resonances of other nearby cavities.

A full-wave electromagnetic analysis program, based on the method of moments formulation, is used for the modeling of the cavity geometries. All of the resonances obtained through computational simulations are identified by comparing their resonant frequencies to those obtained from closed-form expressions valid for ideal cavities, where the open faces of the cavities are modeled with idealized magnetic walls. Plots of current distributions on the cavity walls at the resonant frequencies are also helpful in the identification and classification of the cavity modes.

Elimination of the open cavity resonances by placing conducting pins inside the cavity is studied. Containment of the radiation of open cavity resonances is also investigated.

# LEAKAGE BEHAVIOR OF PLANAR WAVEGUIDES INVESTIGATED WITH THE METHOD OF LINES

A. Dreher  
FernUniversität  
Fachbereich Elektrotechnik  
D-58084 Hagen, Germany

In printed or integrated circuits for high frequency applications (MMIC), cross talk and coupling of lines is an undesired effect and subject of investigation in electromagnetic compatibility (EMC). A significant contribution to these phenomena is caused by the leakage of surface waves in coplanar waveguide structures or higher order modes of a single microstrip line. Due to the radiation of energy, the propagation constant becomes complex. It has been emphasized, that these solutions are often not included in a full-wave analysis (H. Shigesawa, M. Tsuji, A. A. Oliner, *Radio Sci.* 2, 559-564, 1991), but in recent years some research work has also been performed by means of the integral equation method in spectral domain which yields the desired results (W. E. McKinzie & N. G. Alexopoulos, *IEEE MGWL*, 2, 65-66, 1992).

It is the objective of this paper to demonstrate, that leakage behavior of planar waveguide structures is included in the analysis with the method of lines (MoL) in combination with absorbing boundary conditions (ABC). The complex propagation constants of single microstrip lines as well as coplanar waveguides (CPW) and conductor-backed coplanar waveguides (CBCPW) are computed and compared to available results from the literature. The energy flow in the near field is depicted by a plot of the Poynting vector. This makes it possible to study the coupling effects due to radiation in detail.

It should be mentioned, that leakage behavior of a single microstrip line has already been observed while investigating the applicability of absorbing boundaries in the method of lines (A. Dreher & R. Pregla, *IEEE MGWL*, 6, 138-140). Unfortunately, these results have remained unpublished.

## Finite-Difference Analysis of Circular Dielectric-Loaded Waveguides

Jenn-Ming Guan<sup>+</sup> and Da-Chiang Chang<sup>\*</sup>

<sup>\*</sup> Private China Junior College of Technology, Taipei, Taiwan

<sup>+</sup> Department of Electrical Engineering, National Tsinghua University, Hsinchu, Taiwan

Dielectric-loaded waveguides of circular symmetry are commonly used in many microwave systems. The general configurations which can be analyzed in present investigation are shown in Fig. 1. with the piecewise-continuous dielectric constant distributions  $\epsilon(r)$ . The whole structures are assumed to be lossless. The matrix eigenvalue problems resulting from the finite-difference method to the governing differential equations are solved by the modified simultaneous iteration with the Chebyshev acceleration method (C. C. Su & J. M. Guan, IEEE MTT, to appear). This algorithm for sparse matrix eigenproblems involves no operations corresponding to matrix inversions. As a result, very fine discretizations associated with finite-difference method can be done and hence accurate results can be obtained efficiently. The complex modes in this lossless waveguide can also be treated by the present approach if they exist. Compared to the standard approach by solving the complicated characteristic equations (H. Lin & K. A. Zaki, IEEE MAG, 2950-2952, 1989), the present finite-difference method is more convenient especially when multilayer structures are considered.

Using the two transverse magnetic fields (C. C. Su, IEEE MTT, 328-332, 1986), the governing equations for the guided modes with the azimuthal dependence  $e^{-jm\theta}$  are :

$$\Psi'(r) + \frac{1}{r}\Psi'(r) + \left[ \epsilon(r)k_0^2 + \gamma^2 - \frac{(1+m^2)}{r^2} \right] \Psi(r) - \frac{2m}{r^2}\Phi(r) - \frac{\epsilon'(r)}{\epsilon(r)} \left[ \Psi'(r) + \frac{\Psi(r)}{r} + \frac{m}{r}\Phi(r) \right] = 0 \quad (1a)$$

$$\Phi'(r) + \frac{1}{r}\Phi'(r) + \left[ \epsilon(r)k_0^2 + \gamma^2 - \frac{(1+m^2)}{r^2} \right] \Phi(r) - \frac{2m}{r^2}\Psi(r) = 0, \quad (1b)$$

where  $\Psi = H_\theta$ ,  $\Phi = jH_r$ , and the propagation constant  $\gamma = \alpha + j\beta$ . The associated boundary conditions at the permittivity discontinuity are the continuity condition of the fields  $H_z$  and  $E_z$  by using the divergent and curl equations of the magnetic field, respectively. For the azimuthally invariant modes ( $m=0$ ),  $\Psi$  and  $\Phi$  are uncoupled. Hence, (1a) and (1b) are the governing equations for the TM and TE modes, respectively. A standard matrix eigenvalue problem can be obtained by applying the finite-difference method to the equations (1). The numerical results for the dispersion characteristics of the first ten modes with  $m=2$  are shown in Fig. 2. with  $a=0$ ,  $b=0.4$  in,  $c=0.6$  in,  $\epsilon(a < r < b) = 35.59$ , and  $\epsilon(b < r < c) = 1$ . These results are in good agreement with those in the literature (C. Chen & K. A. Zaki, IEEE MTT. 1455-1457, 1988).

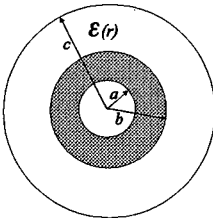


Fig. 1

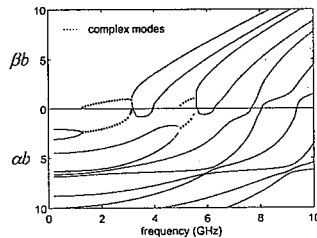


Fig. 2

## Horizontal Gaussian Beams-Vertical Modes in Three-Dimensional Multimode Irregular Waveguides

Nikolay N. Zernov  
Institute of Physics, University of St.Petersburg, Russia

There has been developed the method for the description of higher-order modes of three-dimensional irregular multimode waveguides in (Zernov, N., Radio Sci., 28, 339-350, 1993). The idea of the method is that in the case of a slow range dependence of the electrical properties of the waveguide and a mode of a large index excited, the total number of coupled modes is much less than the excited mode's index. In this case the coefficients of waveguide equations can be expanded into a series by powers of the difference of indexes. Taking the linear terms of the expansions into account only and making use of the convolution theorem by the difference of indexes one can obtain a partial differential equation with a greater number of variables instead of the waveguide equations. This new equation, which we call below as the main equation, can be then solved by different methods.

The choice of the method depends on the correlation between the spatial scale of the waveguide inhomogeneity and the Fresnel zone size on the path of propagation from a source to a point of observation. When the spatial scale is greater than the Fresnel zone size diffraction effects are negligible, and geometrical optics approximation is valid. In the opposite case, when the diffraction is essential, the full-wave type solution has been constructed in the form of an integral representation by component waves, taking diffraction effects into account (Zernov N., Radio Sci., 28, 339-350, 1993).

While considering geometrical optics approximation for the main partial differential equation one can use different sorts of solutions of the eikonal equation and main transport equation. We have used ray solution and an integral representation by the ray-type waves (oscillatory integral) as well as gaussian beams (Zernov, N., Radio Sci., 28, 339-350, 1993).

The goal of the present report is to discuss the gaussian beam-type solutions of the main equation. Geometrical optics set of equations for waveguide modes obeys the terms, taking into account coupling effects. For the slow range dependence coupling can be described by perturbation theory. Then the zero-order approximation equations are for the adiabatic modes, and their solution can be easily constructed as the gaussian beams in two-dimensional inhomogeneous media. To take the transverse mode coupling into account the first-order geometrical optics equations have been considered. As the result the horizontal gaussian beams including vertical mode coupling have been constructed of two types: the first one constructed in the local ray-centered variables (without ray pencil divergence), and the second one constructed in the orthogonal trajectory coordinate system or normal coordinate system. Amplitude of this type of beams diverge at caustics. For the case of the gaussian beams in ray-centered variables the integral representation by gaussian beams is given and discussed too.

## OSCILLATING SYSTEM FOR MILLIMETER-WAVE MAGNETRON WITH OPTIMAL Q-FACTOR

Dmitry M. Vavriv, Andrey E. Serebryannikov\*

Radio Astronomy Institute, Ukrainian Academy of Science, Kharkov, Ukraine

One of the main problems of calculation and design of millimeter-wave magnetrons is a search of optimal characteristics providing a highest value of Q-factor. The influence of geometrical characteristics to the Q-factor of oscillating system (OS) of magnetron having sectorial resonators have been investigated using the strict electrodynamic model. At the first stage we use the expansion of the fields in the interaction space (IS) and in the resonators by eigenfunctions of Helmholtz operator. Using the approximation of perfectly conducting walls of OS is allows to solve self-conjugate boundary problem. The initial problem is reduced to the infinite second kind systems of linear algebraic equations. Single equations' sets have been used both for frequencies spectra calculation and for estimation of natural waves' amplitudes. The derivation of equations' sets is quite identical in case of TE and TM waves.

At the second stage the numerical integration has been used for the eigen Q-factor calculation. We assumed, that using of the boundary conditions of the "perfectly magnetic walls" are possible at the end-faces of the OS and that the dissipation in the IS is negligibly small comparing to the dissipation in the walls of OS.

The problem of the correct choice of a number of considered natural wave in the IS and in the resonators was investigated numerically in dependence from the requiring accuracy for various sets of geometrical parameters. Highest influence to dynamics of a changing of a Q-factor value exert so parameters as  $R_c/R_a$  (where  $R_c$  is a cathode radius and  $R_a$  is anode radius), number and azimuthal size of resonators.

The analytical solution for eigen Q-factor have been founded taking into account only principal waves both in the IS and in the resonators. It has been represented through the integrals of Lommel. Limits of useful of these expressions have been grounded basing on numerical results for the wide domain of geometrical parameters of the OS. Let us note, that the analytical solution is independent from the values of waves' amplitudes. Use of the analytical expressions provide requiring accuracy in much practical cases. It was established that the approximation of "principal wave" produces no qualitative influence on accuracy of the Q-factor estimation.

As a result, we founded an existence of optimal in sense of maximization of Q-factor values of OS geometrical parameters. Use of optimal regimes allows to compensate for decreasing of Q-factor value by using an open OS instead a closed one. This circumstance permits to use so advantages of open OSs as more homogeneous axial distribution of the field in the IS and simpler technology of manufacturing of an open OS comparing to a closed one.

Besides, the possibilities of the use of equivalent boundary conditions have been investigated; comparison of Q-factor of magnetron OS with it one of smooth-walls coaxial resonators have been carried out. The various practical recommendations for the choice of OS geometry and choice of working mode have been given up on the basis of calculation results.

## AN EXPERIMENTAL METHOD FOR THE DESIGN OF REENTRANT CAVITY FILTERS

Pilar Ruiz Aragón, Khosro Shamsaifar (\*)

Alcatel Espacio, Einstein 7, Tres Cantos (PTM)  
(Madrid), SPAIN

An experimental design of a bandpass reentrant cavity filter is presented at S-band. Two important features make reentrant cavities very attractive for the development of S-band filters: small size and large tuning range. Being a hybrid structure composed of a lumped capacitance and a distributed inductance, the resulting size is considerably reduced. The resonant frequency can be easily tuned in a wide range by simply varying the capacitive gap acting on a tuning screw. In addition, it offers relatively high quality factor, as well as, the possibility of realizing various transfer functions, such as elliptical or asymmetric response. This structure, therefore, seems to be quite suitable for space applications where factors such as low insertion loss, and low volume and weight are usually sought.

In order to study the main characteristics of the reentrant cavity filter, such as resonant frequency, input/output couplings, intercavity couplings, quality factor, spurious modes, etc., an experimental characterization procedure was carried out.

A first kit was manufactured to characterize the single cavity parameters, i.e., resonance parameters and access couplings. Input and output couplings are through capacitive probes. It was observed that a vertical probe (parallel to the post) will couple more energy to the cavity, hence a larger bandwidth. The quality factor was measured and also the frequencies of the first and second spurious modes. Design curves for the resonant frequency and the coupling coefficient as functions of dimensions were obtained.

Design curves for intercavity couplings were also obtained using a second kit which consisted of two cavities and a set of interchangeable irises to place between them.

Using the set of design curves, a five cavity Tchebyscheff filter was designed. Measured response of this filter validates the characterization method used. These curves can be used to design filters with different transfer functions and parameters, such as, return loss, bandwidth, etc. Although the characterization has been performed at a given frequency, it has been observed that the design curves could still be used in about 15% around this frequency by minor adjustments.

## Hybrid Analysis of EM Scattering by Large Open Cavities including Effects of Aperture Shape and Interior Obstacle

C.W. Chuang, P.H. Pathak\* and R.J. Burkholder  
The Ohio State University ElectroScience Laboratory  
1320 Kinnear Road, Columbus, Ohio

A hybrid procedure is developed for predicting the electromagnetic (EM) scattering by large open metallic cavities illuminated by an external source. The open end being illuminated is considered to have a rectangular cross-section in the present study; however, the method is applicable to other cross-sectional shapes. The rectangular open end has a scarf; furthermore, this scarfing could be serrated. In addition, the cavity can continuously and smoothly vary in its cross-sectional shape from rectangular at the open front end to a circular one near an interior complex obstacle deep inside the cavity. Also, the cavity can have a smooth S-bend along its length. Such a cavity can be modeled by a super-ellipse (and the present super-ellipse model is based on a computer subroutine provided by Prof. S.W. Lee of the Univ. of Illinois). For some direction of the source, the aperture surface  $S_a$  may be partly shadowed by the scarfing and hence the often-used Kirchhoff approximation is not valid to find the equivalent source of the fields which couple into the cavity. Therefore, a uniform geometrical theory of diffraction (UTD) analysis is employed to find the fields diffracted by the edges of the scarfed aperture, in addition to the direct illumination contribution when it exists, to then provide the equivalent sources at some conveniently chosen interior cavity cross-section  $S_0$  behind the scarfing (these UTD fields are found via a computer subroutine provided by Dr. Z. Al-Heikal and Prof. W.D. Burnside of The Ohio State University). The equivalent sources on  $S_a$  then generate the fields which propagate to the interior cavity obstacle. The generalized ray expansion (GRE) is employed to find the fields coupled into the cavity by launching a dense grid of ray tubes radially out from a periodic array of points in  $S_a$ . These ray tubes are then tracked individually via reflections at the interior cavity wall using the principles of geometrical optics (GO). The fields of these ray tubes are evaluated over a conveniently chosen mathematical surface  $S_T$  near the interior obstacle where they are expanded into a discrete set of plane waves, or local waveguide modes. The effects of the scattering from the interior obstacle is then taken into account via a plane wave or a modal scattering matrix for the smaller cavity-obstacle region beyond  $S_T$  which for the hemispherical hub is found here via a moment method (MM) solution of the governing integral equation.

Numerical results based on this hybrid UTD-GRE-MM analysis will be presented for some useful cavity shapes and compared in one case with measured results for a specific scarfed cavity model.

## **Computer Aided Design of Dielectric Open Waveguides by Boundary Element Method of GMEIE's**

**Kazuo Tanaka, Masahiro Tanaka and Hisamitsu Tashima**  
Department of Electronics and Computer Engineering,  
Gifu University  
Gifu City, Yanagido 1-1, Japan 501-11

Several numerical methods based on exact theory such as finite-element method and boundary-element method (BEM) have been applied to the analysis of dielectric open waveguide circuits. These numerical method proposed so far must be combined with normal-mode expansion techniques of open waveguide structures and this process will be very complicated in the application of computer aided design (CAD) software for various open waveguide circuits of complicated configuration. New boundary integral equation method for CAD of open dielectric waveguide circuits have been found in 1989. New integral equations can be called guided-mode extracted integral equations (GMEIE's) (K. Tanaka and M. Kojima, *J. Opt. Soc. Am. A* 6, 667-674, 1989). The basic idea of GMEIE's is the decomposition of total fields in the waveguide circuits into guided-mode field and other field called disturbed field. Disturbed field must vanish in at points far away from discontinuities in dielectric waveguides. Under these conditions, we can derive new type of integral equations (GMEIE's) which must be satisfied by disturbed fields. GMEIE-method gives an exact method for the analysis of open dielectric waveguide circuits and does not employ normal-mode expansion techniques. So, we can treat the dielectric waveguide discontinuity problems like the scattering by the isolated finite-sized dielectric object in the GMEIE-method. Furthermore, since the structure of GMEIE's is similar to that of conventional boundary integral equations, they can be solved them numerically by the conventional moment-method or BEM. In our laboratory, an CAD system for two-dimensional open dielectric waveguide circuits by BEM based on GMEIE-method have been developed. In this presentation, we show many examples of computer aided design of dielectric open waveguide circuits performed by our system. If we give parameters of waveguide circuits, we can calculate power transmission coefficient, power reflection coefficient, radiated power and radiation pattern by the system. Results can be checked by the energy conservation law and reciprocity of the circuits. Numerical results presented in this presentation satisfied the energy conservation law within an accuracy 1%.

WEDNESDAY PM URSI-B SESSION W-U28

Room: Savery 241

WEDGES AND SPHEROIDS

Chairs: P. Pathak, The Ohio State University; R. Rojas, The Ohio State University

- 2:00 On the Existence of Edge Wave Resonances Along an Impedance Wedge 342  
\*D.H. Koppel, M. Orman, Riverside Research Inst.
- 2:20 Radiation/Scattering of Complex Material Body of Arbitrary Shape in the Presence of an Impedance Wedge 343  
\*M. F. Otero, R. G. Rojas, The Ohio State Univ.
- 2:40 Diffraction of an E-Polarized Plane Wave by Two Adjoining Right-Angle Dielectric Wedges 344  
\*C. Bergljung, Lund Univ.; S. Berntsen, Univ. of Aalborg
- 3:00 Transient Image Theory for 2nd and 3rd Conducting Wedge Problems 345  
\*K. I. Nikoskinen, M. E. Ermutlu, I. V. Lindell, Helsinki Univ. of Technology
- 3:20 Time Domain Version of the UTD for a Curved Wedge 346  
\*P.R. Rousseau, P.H. Pathak, The Ohio State Univ.
- 3:40 Break
- 4:00 A Further Comparison of the Impedance Boundary Condition Formulation and Exact Solution for a Coated Prolate Spheroid 347  
\*J.D. Koulski, Sandia National Laboratories
- 4:20 Electromagnetic Scattering by a System of Two Uniformly Lossy Dielectric Prolate Spheroids in Arbitrary Orientation 348  
S. Nag, \*B.P. Sinha, Memorial Univ. of Newfoundland
- 4:40 On the Computation of the Prolate Spheroidal Radial Functions of the Second Kind for Thin Prolate Spheroidal Radiators 349  
T. Do-Nhat, R. H. MacPhie, Univ. of Waterloo
- 5:00 On the Computation of Infeld's  $r_n(h, \xi)$  Function Used in Evaluating the Admittance of Prolate Spheroidal Dipole Antennas 350  
T. Do-Nhat, R. H. MacPhie, Univ. of Waterloo

## ON THE EXISTENCE OF EDGE WAVE RESONANCES ALONG AN IMPEDANCE WEDGE

D. Koppel\*, M. Orman  
Riverside Research Institute  
330 West 42nd Street  
New York, NY 10036

Prominent maxima (e.g., Peters' lobes) in the backscattering RCS by bodies with edges have been ascribed to "edge waves". These are waves that are launched at a corner, and then propagate along an edge until they are shed and/or reflected at the next corner. However, a clear theoretical description of these waves does not seem to exist. In particular, they could either be waves that propagate along an edge with the free-space wavenumber, or resonances whose wavenumber depends on the material properties of the edge. To determine if resonant edge waves exist we study their possible initiation by a plane wave obliquely incident on a infinite wedge with impedance boundary conditions. The wedge has a  $90^\circ$  interior angle, one face being a perfect conductor and the other satisfying impedance boundary conditions (T.B.A. Senior and J.L. Volakis, *IEEE Trans. Antennas Propagat.* AP-34, May 1986). The solution is represented by a contour integral in the plane of a complex angle. This contour integral may be explicitly evaluated for the fields in two limiting cases: near the edge itself (within a wavelength) and far from the edge (compared with a wavelength). In the latter case, the contour integral in the complex plane must be deformed to include several poles, which are interpreted for normal incidence to represent the incident wave, the specular reflection, and surface waves. For oblique incidence there does not seem to be any additional poles which could be interpreted as edge wave resonances. For the field near the edge, the usual electrostatic singularity is recovered when both sides of the wedge are perfect electric conductors. However, if one side satisfies an impedance boundary condition, the field has a greater degree of singularity (though still satisfying the Meixner boundary condition), and propagates along the edge with the projected free-space wavenumber. Thus, for plane wave incidence on an impedance wedge, we do not find any evidence of a resonance that could be interpreted as an "edge wave". This does not, however, preclude the possible existence of such resonances for more general forms of excitations or for finite-length impedance wedges.

## **RADIATION/SCATTERING OF COMPLEX MATERIAL BODY OF ARBITRARY SHAPE IN THE PRESENCE OF AN IMPEDANCE WEDGE**

Michael F. Otero\* and Roberto G. Rojas  
The Ohio State University ElectroScience Laboratory  
Columbus, Ohio 43212-1191

A two-dimensional Green's function for a wedge whose faces satisfy the Leontovich boundary conditions has been developed which is very efficient for numerical computations (R.G. Rojas & M.F. Otero, 1992 URSI Digest, pg. 444). The present paper discusses the use of this Green's function to solve scattering as well as radiation problems. The scattering problem involves the diffraction of an incident plane wave by a two-dimensional material body of arbitrary shape which is in the vicinity of or attached to the tip of the wedge. Allowing the faces of the wedge to have impedance boundary conditions allows for the modeling of surfaces which may have a thin material coating or a surface roughness. The analysis will allow for a material body that has a very general configuration which may be inhomogeneous, anisotropic, as well as chiral. This enables the modeling of a material body that may be constructed of fairly complex materials such as honeycomb structures, fiber loaded resins, etc. The radiation problem involves the study of the radiation of two-dimensional slot antennas mounted on the faces of the impedance wedge. As in the scattering problem, the effect of the material body on the radiation pattern of the antennas will be investigated. For the scattering problem, the material body can be used to reduce the component of the field which diffracts from the wedge vertex, therefore, methods for reducing the echo width of wedge shaped objects will be studied. Lossy materials as well as chiral ones would be especially useful for this purpose.

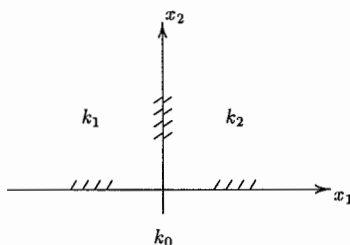
The method of analysis is the Moment Method/Green's function scheme where a set of integral equations with as few unknowns as possible has been developed. Since the Green's function that is used is the one that satisfies the boundary conditions on the faces of the impedance wedge, the only unknown to be solved for is the field within the material body. Note that due to the presence of the material body, which couples the various components of the electric and magnetic fields, it is important to obtain integral equations with this property; otherwise the resulting matrix equation becomes too large for practical applications. Several examples will be shown illustrating the effect of the impedance values of the faces of the wedge as well as the shape and material parameters of the material body on the scattering and radiation problems discussed above.

## DIFFRACTION OF AN *E*-POLARIZED PLANE WAVE BY TWO ADJOINING RIGHT-ANGLE DIELECTRIC WEDGES

Christian Bergljung\*  
Lund University, P. O. Box 118  
S-221 00 LUND, Sweden

Svend Berntsen  
Univ. of Aalborg, Fredrik Bajers vej 7  
DK-9220 Aalborg Øst, Denmark

A solution to the problem of diffraction of an *E*-polarized plane wave by two adjoining right-angle imperfectly conducting dielectric wedges is given. The geometry of the problem is depicted in the figure below. The medium in the half-space  $x_2 < 0$



is characterized by the constant wavenumber  $k_0$ , while the analogous constants for the quarter-spaces ( $x_1 < 0, x_2 > 0$ ) and ( $x_1 > 0, x_2 > 0$ ) are  $k_1$  and  $k_2$ , respectively. The incident field is polarized such that the only component of the electric field is parallel to the common edge of the wedges.

The solution obtained is represented in an implicit form in terms of solutions to integral equations for the Fourier transforms of the surface fields. The physical interpretation of the integral equations is clear. The optical field can be deduced completely from the residues at the poles of the Fourier transform of the surface field.

The integral equations are solved by using an iterative method. The convergence of the iterative method is investigated by using numerical methods. When the incident field is illuminating the double wedge configuration from below, the successive approximations of the iteration scheme converge to the unique solution of the diffraction problem provided that the value of  $|k_1^2 - k_2^2|$  is not too large. A better convergence can be achieved if the wedge media are dissipative, that is, for  $\text{Im } k_1 > 0$  and  $\text{Im } k_2 > 0$ .

An explicit approximation to the scattered far field is also given. This approximation is good for small values of  $|k_1^2 - k_2^2|$ . When the value of  $|k_1^2 - k_2^2|$  is sufficiently small, the explicit approximation is superior to the far-field approximation obtained from Maliuzhinets' solution, which is based on impedance boundary conditions. If the magnitude of the refractive indices of the wedge media  $|k_n/k_0| > 4$ ,  $n = 1, 2$ , then Maliuzhinets' solution is a reasonable approximation to the field in the region  $x_2 < 0$ .

## TRANSIENT IMAGE THEORY FOR 2D AND 3D CONDUCTING WEDGE PROBLEMS

Keijo I. Nikoskinen\*, Murat E. Ermutlu, Ismo V. Lindell  
Electromagnetics Laboratory,  
Helsinki University of Technology,  
Otakaari 5, 02150 Espoo, Finland

Recently a new image solution for the canonical scattering problem from a conducting wedge was found, (M.E. Ermutlu & al., *JEWA* 7, 971-986, 1993). In that paper a time-harmonic line source excitation was studied and the diffraction field from the edge of the wedge was interpreted as arising from a quasi-physical image source that is partly located in complex space whereas the geometrical optics field remained its standard representation as arising from point images whose positions can be obtained from geometrical arguments. The major advantage of this image approach is that knowing the image current of the original source, the field computation can be accomplished like in free space without taking into account the additional boundary conditions due to the wedge, i.e. Green function for this geometry is known. The image source that is forcing the correct boundary conditions at the conductor appeared to be very simple one, a combination of trigonometric functions. Its field can be calculated as usually in 2-D problems by convolving Hankel function and the current source.

In the present paper this new solution is exploited in the derivation of field solutions for an impulsive line and dipole sources with same boundary conditions. This can be done straightforwardly with Fourier transform from the frequency domain to the time domain. Because the time-harmonic image current does not depend on frequency, the Fourier integral operates only on the frequency domain free space Green function giving thus the corresponding time domain Green function that is a function of time and the coordinates of the source and the observation points. Because the time-harmonic image source is located in complex space the Fourier transform yields Green function in which the "distance" between the source and the observer is allowed to be complex. The imaginary part in the distance function opens up interesting questions about the reality and the causality of the field radiated by point current source that has a complex position. This problem is partly passed in the present paper since the diffraction images due to the wedge are current distributions whose radiation fields are superposed over the extended source. These integrated fields appear to be real and causal.

## TIME DOMAIN VERSION OF THE UTD FOR A CURVED WEDGE

Paul R. Rousseau\* and Prabhakar H. Pathak

ElectroScience Laboratory  
The Ohio State University  
Department of Electrical Engineering  
Columbus, Ohio 43212

The development of a time domain version of the uniform geometrical theory of diffraction (UTD) for a perfectly conducting curved wedge will be presented. The wedge may have a curved edge, curved faces and the incident wavefront (which is a geometrical optics (GO) field in the frequency domain) may possess two distinct principal radii of curvature. This time domain UTD (TD-UTD) is valid for early to intermediate times with respect to the arrival of the different wavefront (GO and diffracted) contributions. Such a TD-UTD solution provides a progressing wave picture for the transient scattering and diffraction effects, and it therefore provides essentially the same physical insight into these effects as does the corresponding frequency domain UTD ray solution.

The TD-UTD formulation is obtained by analytically transforming the frequency domain UTD for a curved wedge (Kouyoumjian & Pathak, Proc IEEE, pp. 1448-1460, Nov. 1974) into the time domain. The TD-UTD presented here is a generalization of the results obtained for a straight wedge in (Veruttipong, IEEE Trans.-AP, pp. 1757-1764, Nov. 1990). The TD-UTD is an approximation to the impulse response of the curved wedge and therefore a convolution must be performed to obtain the time domain response for any particular incident time waveform. An inversion of a frequency domain UTD solution into the time domain can lead to a non-causal result if a UTD ray has transversed through caustics; therefore, it is necessary to provide information into the TD-UTD solution keep it causal. A prescription to keep the present TD-UTD wedge solution causal will be indicated; such information is especially useful when predicting the transient response of a pulse excited complex realistic geometry containing edges.

Some specific geometries have been analyzed using the TD-UTD to illustrate its usefulness. In particular, the scattering from a two dimensional parabola with a flat strip extension will be presented. The determination of the "turn on" times for the reflected and diffracted field transient responses will be demonstrated with this geometry.

A Further Comparison of the Impedance Boundary Condition  
Formulation and Exact Solution for a Coated Prolate Spheroid

J. D. Kotulski  
Sandia National Laboratories  
Radiation and Electromagnetic Analysis Department  
MS 1166  
PO Box 5800  
Albuquerque, NM 87185-1166

Previously, the exact solution of a coated spheroid has been compared to the impedance boundary condition formulation of the coated spheroid. These problems are solved using an eigenfunction expansion due to the separable nature of the prolate spheroidal coordinate system. For the coated spheroid the fields are expanded in prolate spheroidal wavefunctions in the different regions and the boundary conditions between the regions are applied to solve for the unknown coefficients. Alternatively, the impedance boundary condition can be used to replace the coating region with a surface impedance. The surface of the prolate spheroidal scatterer can be varied to examine two limiting cases -- the wire and the sphere.

The purpose of this paper is to extend the comparison of the solution of a coated conducting spheroid using two different techniques that account for the coating on the conductor. The coating can be magnetic or dielectric with conductivity or loss. To simplify the problem the conducting spheroid is excited at an equatorial gap. The input admittance values obtained using both methods are compared as well as the fields on the surface of the coating. The poles of the input admittance are examined in the complex  $s$ -plane to allow a closer look at the resonance structure. Previous work considered the  $n=1$  mode of the structure and a limited class of coatings. The results are extended to include higher-order modes and additional coatings. The limiting cases for these higher-order modes will also be considered (the wire and the sphere) and will be compared to the previous results.

## Electromagnetic Scattering by a System of Two Uniformly Lossy Dielectric Prolate Spheroids in Arbitrary Orientation

Soumya Nag and B. P. Sinha\*

Faculty of Engineering and Applied Science  
Department of Electrical Engineering  
Memorial University of Newfoundland  
St. John's, NF, A1B 3X5, Canada.

By means of modal series expansions of electromagnetic fields in terms of prolate spheroidal vector wave functions, an exact solution is obtained for the scattering by two uniformly lossy dielectric prolate spheroids in arbitrary orientation embedded in free space, the excitation being a monochromatic plane electromagnetic wave of arbitrary polarization and angle of incidence. Since the dielectric medium of the scatterers is complex in nature, complex eigenvalues have been evaluated for the spheroidal scalar wave function of transmitted components of  $E$ -field and  $H$ -field expansions.

$\vec{M}^{(a)}$  vectors for  $E$ -field expansion and  $\vec{N}^{(a)}$  vectors for  $H$ -field expansion [  $\vec{M}^{(a)} = \vec{\nabla} \psi(h; \xi, \eta, \phi) \times \hat{a}$ ;  $\vec{N}^{(a)} = (1/k) \vec{\nabla} \times \vec{M}^{(a)}$ ,  $\hat{a} = (\hat{x}, \hat{y}, \hat{z})$  ] have been used in the present problem together with Rotational-Translational Addition Theorems for scalar spheroidal wave functions (R. H. MacPhie, J. Dalmas and R. Deleuil, *Quart. Appl. Math.*, 44, No. 4, pp. 737-749, 1987) and Rotational-Translational Addition Theorems for vector spheroidal wave functions (J. Dalmas, R. Deleuil and R. H. MacPhie, *Quart. Appl. Math.*, 47, No. 2, pp. 351-364, 1989; M. F. R. Cooray and I. R. Ciric, *COMPEL*, 8, No. 3, pp. 151-166, 1989). A vector spheroidal wave function defined in one spheroidal coordinate system  $(h; \xi, \eta, \phi)$  has been expressed in terms of a series expansion of vector spheroidal wave functions defined in another spheroidal coordinate system  $(h'; \xi', \eta', \phi')$ , which is rotated and translated with respect to the first one.

By applying appropriate boundary conditions, the field solution is obtained in the form  $\underline{\mathcal{L}} = [G]\underline{\mathcal{I}}$ , where  $\underline{\mathcal{L}}$  and  $\underline{\mathcal{I}}$  are respectively the column vector of the unknown coefficients of the series expansions of the scattered and transmitted fields taken together and the column vector of the known coefficients of the series expansions of the incident field.  $[G]$  is the system matrix which depends only upon the geometries of and spacing between the scatterers. The solution in the above form eliminates the need for repeatedly solving a new set of simultaneous equations in order to obtain the unknown expansion coefficients of scattered and transmitted fields for a new angle of incidence. Numerical results in the form of curves for the bistatic and monostatic radar cross sections are given for a variety of two-body system of uniformly lossy dielectric prolate spheroids in arbitrary orientation having resonant or near resonant lengths and having different distances of separation.

## On the Computation of the Prolate Spheroidal Radial Functions of the Second Kind for Thin Prolate Spheroidal Radiators

T. Do-Nhat and R. H. MacPhie  
 Dept. of Elect. & Comp. Eng., University of Waterloo  
 Waterloo, Ontario, Canada, N2L 3G1

The series expansion of the prolate spheroidal radial functions of the second kind expressed in terms of the spherical Neumann functions converges very slowly when the eccentricity of the spheroid is large (when  $\xi \rightarrow 1$ ). A sophisticated method which approximate the sum as an integral was developed to sum the Neumann series (B. P. Sinha & R. H. MacPhie, *J. Math. Phys.*, 16, 2378-2381, 1975). However, since the method basically depends on a curve fitting parameter, it cannot be reliable for  $\xi$  very close to 1, and/or large order  $n$ . In this paper we obtain an analytical series expansion in power of  $(\xi^2-1)$ , which converges very rapidly. This is accomplished by expanding the associated Legendre functions of the first and second kinds in terms of powers of  $(\xi^2-1)$ . For instance, for symmetrically excited prolate spheroidal radiators, their odd radial functions of the second kind are expressed as follows:

$$R_{1n}^{(2)}(h, \xi) = \frac{1}{2} \frac{\kappa_{1n}^{(1)}(h)}{\kappa_{1n}^{(2)}(h)} R_{1n}^{(1)}(h, \xi) \ln\left(\frac{\xi+1}{\xi-1}\right) - \frac{1}{\kappa_{1n}^{(2)}} \xi \sum_{r=0}^{\infty} \delta_r (\xi^2-1)^{r-\frac{1}{2}}, \quad n: \text{ odd} \quad (1)$$

where the joining factors  $\kappa_{1n}^{(1)}(h)$ ,  $\kappa_{1n}^{(2)}(h)$  are defined in Flammer's monograph (C. Flammer, Stanford U.P., Stanford, Calif., 1957), and  $h$  is the spheroid semi-interfocal length multiplied by the wavenumber. All the  $\delta_r$  coefficients are expressed in closed forms, and in terms of the  $d_{2l}^{1n}$ , and  $d_{p|2l}^{1n}$  coefficients defined in Flammer's monograph. The first two terms of the above power series expansion are given by the following expressions:

$$\delta_0 = \sum_{l=1}^{\infty} d_{2l}^{1n}(h) \quad (2)$$

$$\delta_1 = \sum_{l=0}^{\infty} d_{2l}^{1n}(h) \left[ \frac{l}{2}(2l+3) + (l+1)(2l+1) \left\{ 2 \sum_{k=0}^l \frac{1}{2k+1} + \sum_{k=0}^l \frac{1}{k-2l-1} - 1 \right\} \right. \\ \left. - \sum_{l=0}^{\infty} (l+1)(2l+3) d_{p|2l+4}^{1n} \right] \quad (3)$$

There also exists the recursion relation among these  $\delta_r$  coefficients. In the numerical results, by using the above expansion given by eq.(1) for the radial spheroidal wave function of the second kind, we can compute  $R_{1n}^{(2)}(h, \xi)$  with a double precision accuracy. Using the Wronskian test, this accuracy has been verified for  $\xi = 1.000000000002$  (extremely thin spheroid) and/or very large  $n$ . This newly developed expansion will be very useful for the rapid and accurate computation of the near fields of thin spheroidal radiators.

**On the Computation of Infeld's  $r_n(h, \xi)$  Function Used in  
Evaluating the Admittance of Prolate Spheroidal Dipole Antennas**

T. Do-Nhat and R. H. MacPhie  
Dept. of Elect. & Comp. Eng., University of Waterloo  
Waterloo, Ontario, Canada, N2L 3G1

In the computation of the admittance of thin prolate spheroidal dipole antennas of finite feed gap length (J.R.Wait, Antenna theory (Ed.:R.E.Collin & F.J.Zucker),1,13,523-559,McGraw-Hill,1969) we encounter the problem of the slow convergence of the input susceptance, expressed as an infinite sum of outgoing prolate spheroidal wave functions, and their derivatives. More specifically, each term in the summation includes the following function, introduced by Infeld (L. Infeld,Quar.Appl.Math.5,2,1947):

$$r_n(h, \xi) = \frac{(\xi^2 - 1)^{1/2} R_{1n}^{(4)}(h, \xi)}{\frac{d}{d\xi} [(\xi^2 - 1)^{1/2} R_{1n}^{(4)}(h, \xi)]} \quad (1)$$

where  $R_{1n}^{(4)}(h, \xi)$  is the prolate spheroidal wave function of the 4th kind (C. Flammer, Spheroidal wave functions, Stanford univ. press, 1957), and  $h$  is the semi-interfocal length multiplied by the wavenumber. We now show how to find the asymptotic expression of the function  $r_n(h, \xi)$  for large  $n$ . It can be shown that  $r_n(h, \xi)$  satisfies exactly the following Riccati differential equation:

$$\frac{dr_n(h, \xi)}{d\xi} + r_n^2(h, \xi)(\xi^2 - 1)^{-1}(\lambda_{1n} - h^2\xi^2) = 1 \quad (2)$$

where  $\lambda_{1n}$  is the eigenvalue of the prolate spheroidal wave functions. Infeld obtained the approximate Riccati differential equation (Eq.(2) without the term  $h^2\xi^2$ ). By using the perturbation method (J.Kevorkian & J.D. Cole, Perturbation methods in applied mathematics, Springer-Verlag, 1980) the asymptotic solution to the above differential equation can be expressed as an inverse power series of  $(\lambda_{1n} - h^2)$ , i.e.,

$$r_n(h, \xi) = \frac{(\xi^2 - 1)^{1/2}}{(\lambda_{1n} - h^2)^{1/2}} \sum_{m=0}^{\infty} (\lambda_{1n} - h^2)^{-m/2} h_m(h, x) \quad (3)$$

where  $x = (\xi^2 - 1)^{1/2} / \xi$ . The functions  $h_m(h, x)$  are independent of the eigenvalue  $\lambda_{1n}$  and can be expressed in closed forms. For instance  $h_0(h, x) = -1$ ,  $h_1(h, x) = -1/(2x)$  and  $h_2(h, x) = 1/4 + 1/(8x^2) - h^2x^2/(1-x^2)$ . Infeld obtained only one term  $h_0(h, x) = -1$ . It can be shown that there exists a recursion relation among the  $h_m(h, x)$ . The asymptotic condition of  $r_n(h, \xi)$  is given by the inequality  $N_c = (\xi^2 - 1)^{1/2} n > 1$ . If  $N_c = 3$ , and if we use 7 terms in the asymptotic series of Eq.(3) we obtain about 5 significant figures of accuracy. If  $N_c$  is increased, fewer terms are required to obtain the same accuracy.

WEDNESDAY PM URSI-D SESSION W-U29

Room: Savery 243

ELECTRONIC DEVICES AND WAVEGUIDES

Chair: A.R. Mickelson, University of Colorado at Boulder

- 2:00 Graded-Index Silicon Oxynitride Optical Waveguides 352  
*\*K. Remley, J.J. Marlia, T.K. Plant, A. Weisshaar, J.C. Wu, M.N. Wybourne, Univ. of Oregon*
- 2:20 Finite Difference Time Domain Simulation of a Subpicosecond GaAs Semiconductor Optical Switch 353  
*J. He, S.M. Riad, A. Elshabini-Riad, Virginia Polytechnic Inst. and State Univ.*
- 2:40 Pulse Compression Characteristics of Magnetostatic Wave Soliton in Non-Uniform Magnetic Field 354  
*\*M. Tsutsumi, V. Priye, Kyoto Inst. of Technology*
- 3:00 Low-Intrusive Optical Sensor for Remote Electric Field Sensing 355  
*K. Daneshvar, Univ. of North Carolina; L. Hales, Weapons Sciences Directorate*
- 3:20 Super-cholesteric Materials 356  
*\*W. S. Weiglhofer, Univ. of Glasgow; A. Lakhtakia, Pennsylvania State Univ.*

## Graded-Index Silicon Oxynitride Optical Waveguides

Kate Remley\*, J. John Marlia, Thomas K. Plant, and Andreas Weisshaar  
 Department of Electrical and Computer Engineering  
 Oregon State University  
 Corvallis, Oregon 97331  
 and

Jong C. Wu and Martin N. Wybourne  
 Physics Department  
 University of Oregon  
 Eugene, Oregon 97403

Planar SiON optical waveguides have been fabricated using a computer-controlled plasma-enhanced chemical vapor deposition (PECVD) system. Waveguides with both homogeneous and inhomogeneous refractive index profiles were produced.

In the PECVD system, calibrated flow rates of three gases, Silane ( $\text{SiH}_4$ ), Nitrogen ( $\text{N}_2$ ), and Nitrous Oxide ( $\text{N}_2\text{O}$ ), are used to deposit the  $\text{SiO}_x\text{N}_y$  film on the substrate. The flow rate of  $\text{N}_2\text{O}$  can be varied in small steps, resulting in constant index layer thicknesses as small as 10 angstroms. One advantage of this system is the ability to easily and precisely vary the refractive index of the waveguide, allowing production of arbitrary inhomogeneous index profiles between the refractive index values of 1.46 to 2.0.

Grating couplers with 0.5  $\mu\text{m}$  period were fabricated on each waveguide using electron beam lithography. The procedure left a layer of polymethyl methacrylate (PMMA) on the waveguide except where the e-beam had "written" the grating pattern.

Using a HeNe laser as a light source, the angles corresponding to guided modes were measured, and the corresponding effective index,  $n_{\text{eff}} = \beta/k_0$ , of each guided mode was calculated. The measurement error is approximately  $\pm 0.25^\circ$ . As an example, Table I gives measured and theoretical values of the coupling angles and corresponding effective mode indices for an inhomogeneous waveguide with refractive index profile shown in Figure 1. As seen in Table I, the theoretical and experimental values are in close agreement. A similar accuracy was obtained for a guide with 58 layers approximating a linear refractive index profile.

Inhomogeneous Waveguide				
Mode	Experimental		Theoretical	
	$\theta$	n eff.	$\theta$	n eff.
TE0	25.5	1.6961	26.0	1.7042
TE1	18.5	1.5829	18.0	1.5744
TE2	---	---	12.9	1.4881
TM0	25.5	1.6961	25.6	1.6976
TM1	17.5	1.5663	17.9	1.5730
TM2	---	---	12.6	1.4833

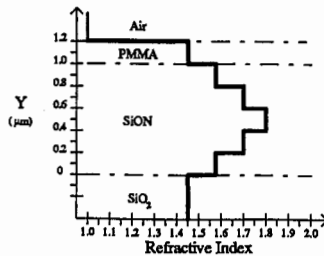


Table 1. Experimental and theoretical coupling angles and corresponding effective index values.

Figure 1. Refractive index profile of a five-layer inhomogeneous waveguide.

## **Finite Difference Time Domain Simulation of A Subpicosecond GaAs Semiconductor Optical Switch**

Jianqing He, Sedki M. Riad, and Aicha Elshabini-Riad  
Virginia Polytechnic Institute and State University  
Blacksburg, Virginia 24060, USA  
(Phone: +1-703-231-4469, FAX: +1-703-231-3362)

A subpicosecond pulse can be generated by a device called an optical switch. The structure of the device consists of a planar microstrip line with a gap at the center of the line and a semi-insulating GaAs semiconductor substrate on which the conductor strip is deposited. An optical pulse with a transition time in the order of tens of femtoseconds is injected into the gap and an electrical pulse is generated due to optical absorption in semiconductor. The electrical pulse then propagates along the microstrip line. Simulation of such a device was reported using finite difference time domain (FDTD) technique and a computationally intensive Monte Carlo method [1]. In this paper, a more efficient approach is presented.

The approach introduced is to use the FDTD technique to simulate the propagation of the electrical pulse and to solve the balance equation with energy and momentum relaxation time approximations to simulate the dynamic carrier transport in the semiconductor. More specifically, the FDTD technique is used to numerically approximate the time dependent Maxwell's equations. In GaAs, drift velocities of the optically-generated carriers are nonlinear, field and time dependent in the subpicosecond time scale. To obtain the carriers dynamic transport characteristics, the electrons energy and momentum balance (conservation) equations are solved by the finite difference numerical method. The energy and momentum relaxation times appearing in the balance equations are approximated by the electrons steady-state values of energy and velocity versus applied electric field. The steady-state values (or curves) are obtained by the Monte Carlo simulation. The Monte Carlo simulations of the steady-state values are much less computationally intensive than the Monte Carlo simulations of carriers dynamic transport as reported in [1].

The simulations using this approach were carried out on an optical switch with typical geometrical dimensions. The simulations resulted in the propagating pulse generated by the device, revealing the pulse features such as overshoots and nonlinearities in the subpicosecond time scale. The simulation results were compared with the experimental data reported in [2] and found to have good agreement, indicating that the approach is accurate as well as efficient.

### **References:**

- [1] S. M. El-Ghazaly, R. P. Joshi, and R. O. Grondin, " Electromagnetic and Transport Considerations in Subpicosecond Photoconductive Switch Modeling," IEEE Trans. on Microwave Theory and Tech., vol. MTT-38, no. 5, pp. 629 - 637, May 1990.
- [2] K. Meyer, M. Pessot, and G. Mourou, " Subpicosecond Photoconductivity Overshoot in Gallium Arsenide Observed by Electro-optic Sampling," Appl. Phys. Lett., vol. 53, no. 23, pp 2254 - 2256, Dec. 1988.

## Pulse compression characteristics of magnetostatic wave soliton in non-uniform magnetic field

Makoto Tsutsumi\* and Vishnu Priye  
 Department of Electronics and Information Science  
 Kyoto Institute of Technology, Matsugasaki  
 Sakyo-ku, Kyoto 606, Japan.

1. **Introduction:** Recently, magnetostatic wave (MSW) solitons have attracted much attention because of the new pulse compression phenomena observed in microwave region under moderate input power levels. This phenomena may lead to applications in microwave signal processing such as pulse compression of radar signals. This paper discusses the studies on the pulse compression phenomenon of magnetostatic volume wave bright solitons and surface wave dark soliton in non-uniform magnetic field.

2. **Experiment:** Experiments were carried out for the two MSW volume modes (MSFVW and MSBVW) and a surface mode (MSSW) in a 20  $\mu\text{m}$  YIG thick film. To enhance the MSW soliton behavior the bias magnetic field is non-uniformly distributed in the YIG film using concave magnetic pole pieces in the MSW delay line experiments as shown in Fig. 1. (Tsutsumi et al., IEEE Trans. Magnetics, 22,5, (1986) p 853-855.)

The power dependence of the dispersion characteristics are measured using cw microwave signal at S-band (2-4 GHz) for three types of the MSW modes. The nonlinearity parameter  $N (= \frac{\partial \omega}{\partial |U|^2})$  is estimated, the sign of which gives a criterion to form an envelope soliton. Here  $\omega$  is the angular frequency of a given MSW mode and  $|U|^2$  is proportional to the microwave power. The frequency dependence of the delay time is also measured upto the pulsed microwave power of 500 mW. The dependence of the delay time of the MSW on the phase constant is estimated which gives the value of  $D = \frac{d^2 \omega}{d\beta^2}$ . The sign of D gives the other criterion to form envelope soliton.

The nonlinear Schrödinger equation is estimated to get the MSW soliton from the sign of N and D for the three MSW modes. The bright soliton for the two volume modes and dark soliton state for the surface mode are confirmed. Experiments on the MSW soliton are carried out using non-uniform magnetic field as shown in Fig. 1. The pulse compression of about 80% are observed with a 100 ns input pulse and few hundred mW of microwave power. The pulse compression phenomenon is studied in detail by changing the frequency or the magnetic field. Some characteristic features observed are given in Table 1. This pulse compression is weak for uniform magnetic field even at high power and significantly increases for the non-uniform magnetic field.

3. **Conclusion :** The pulse compression phenomenon of the MSW are examined experimentally in a YIG film magnetised by a non-uniform magnetic field. The pulse compression increases in a non-uniform magnetic field and higher compression ratio is expected for the low magnetic loss  $< \Delta H = 0.5 \text{ Oe}$ .

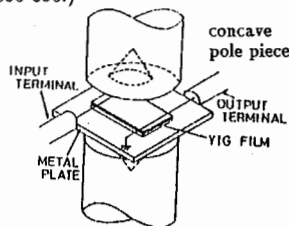


Fig. 1 MSW delay line with non-uniform magnetic field.

Mode	Soliton form	Compression ratio	Insertion loss	Optimum delay time
MSFVW	bright	5.0	moderate	80ns
MSBVW	bright	4.0	large	150ns
MSSW	dark	4.1	moderate	70ns

Table 1 : Observed pulse compression characteristics of MSW soliton.

## Low-intrusive Optical Sensor for Remote Electric Field Sensing

*K. Daneshvar, University of North Carolina, Charlotte, NC 28223 and L. Hales, Weapons Sciences Directorate, Redstone Arsenal, AL 35898-5248*

It is well known that it is impossible to make a measurement without disturbing the quantity that is being measured and that this distortion causes errors in measurement. As a result of this fact, absolute measurement of many things is not possible. While this measurement error is insignificant in most cases, it is of prime importance in others. Specifically, the metallic probing device in high frequency electromagnetic field measurement normally results in a considerable distortion in the field to be measured at the location of measurement. The sources of error are absorption which depends on the dielectric properties of the sensing element and re-radiation which distorts the field to be measured.

Electro-optical sensors have been investigated for electric field sensing at various field intensities and frequencies. Generally the electro-optic sensors are dielectric and introduce lesser distortion in the field at the location of measurement compared to conductive probes. This is due to the fact that the dielectric probes are low-reflective and the electromagnetic wave scattering is elastic, i.e., conserves electromagnetic energy. The operation of these devices relies on the modulation of the optical field by the external electric field to be measured. Generally, the optical path length in the electro-optic medium changes according to the intensity of the external field. The resulting phase change due to optical path difference is linearly proportional to the external electric field strength over a certain range of electric field strength. The phase changes can result in optical intensity variation which can be detected by several methods. These include interferometry and modulation of phase or intensity. The field strength to be measured and its distribution are the major considerations in selecting an optical approach for a sensing application.

Optical sensors for low-intrusive, non-contact, and remote measurement of a free space field have been developed. These sensors can be constructed to occupy a small space and allow mapping of a localized field distribution around a relatively small object. The sensor consists of an optical waveguide which is constructed on an electro-optic crystal substrate. The external field is detected by a tapered resistive load antenna which is patterned by an argon laser on a high resistive polymeric thin film. The field detected by the antenna induces a voltage across the waveguiding region. The waveguide is excited by a singly polarized light from a polarization maintaining fiber. This fiber, while used to deliver and receive the light intensity to the sensor, is also used as a polarizer and analyzer. After the light travels the length of the waveguide, it is reflected from a dielectric mirror which is deposited at the other end of the waveguide. The reflected light that enters the fiber has a polarization which is shifted corresponding to the field to be measured. The portion of the reflected light which enters the fiber is beam split by a polarization maintaining coupler and is detected by an avalanche photo detector. The experimental results, applications, and limitations of this sensor are discussed and compared with several other electro-optical methods that have been proposed for low-intrusive electric field sensing.

## Super-cholesteric Materials

W S Weiglhofer<sup>1\*</sup> and A Lakhtakia<sup>2</sup>

<sup>1</sup> Department of Mathematics, University of Glasgow, Glasgow G12 8QW  
Scotland, Great Britain; email: werner@maths.glasgow.ac.uk

<sup>2</sup> Department of Engineering Science and Mechanics,  
Pennsylvania State University, University Park, PA 16802-1401, USA

In this contribution we are describing a way to fabricate a new type of material and we will discuss its potential applications in a variety of optical technologies. The new *super-cholesteric material* combines the properties of cholesteric liquid crystals with those of particulate composites of electrically small uniaxial scatterers. It is well known that cholesterics are locally uniaxial and homogeneous at length scales not exceeding  $40\text{ nm}$ , and because optical wavelengths typically exceed  $400\text{ nm}$  in free space, we are able to construct a Maxwell Garnett model for macroscopic electromagnetic field behaviour in a super-cholesteric material at optical and suboptical frequencies. Thus the fabrication of this material is envisioned as a two-step process: first, identical, electrically small inclusions characterised by uniaxial polarisability dyadics are randomly dispersed in an isotropic host medium, all inclusions being aligned parallel to one another, to form a composite. The composite is effectively a bianisotropic uniaxial medium, its uniaxial nature expressed through an optical director fixed in space. Second, layers of such uniaxial composites are stacked on top of each other such that the optical director varies from layer to layer in a helicoidal way so that the typical periodically inhomogeneous structure of a cholesteric liquid crystal emerges.

A comparison of ordinary cholesteric liquid crystals with the envisioned super-cholesteric materials will be presented and application of super-cholesteric materials as novel polarisers, phase shifters, circulators and microstrip substrates at microwave and infrared frequencies will be discussed.

WEDNESDAY PM URSI-B SESSION W-U30

Room: HUB 309

**MICROSTRIP ANALYSIS**

Chairs: L. Shafai, University of Manitoba; Glenn Smith, Georgia Institute of Technology

- |      |   |     |
|------|---|-----|
| 2:00 | Pulse, Sinusoidal, or Wavelet? A Comparative Study of Various Basis Functions for the Analysis of Microstrip Antennas<br><i>*X.H. Yang, L. Shafai, Univ. of Manitoba.</i> | 358 |
| 2:20 | Analysis of Printed Patch Arrays Using a Space Domain Approach<br><i>A. K. Skrivervik, J. R. Mosig, Ecole Polytechnique Fédérale de Lausanne</i>                          | 359 |
| 2:40 | Efficient Computation of Green's Functions for Multi-Layer Microstrip Structures<br><i>*A. Hoorfar, Villanova Univ.; D.C. Chang, Arizona State Univ.</i>                  | 360 |
| 3:00 | Analysis of Corner Fed Microstrip Antennas Using the Multiport Network Model<br><i>S.P. Dholakia, *A. Sebak, Univ. of Manitoba</i>  | 361 |
| 3:20 | Analysis of Slot-Lines Using Closed-Form Green's Functions<br><i>*G. Dural, Middle East Technical Univ.; M.I. Aksun, Bilkent Univ.</i>                                    | 362 |
| 3:40 | Break   |     |

**Pulse, Sinusoidal, or Wavelet ?**  
**A Comparative Study of Various Basis Functions**  
**for the Analysis of Microstrip Antennas**

X. H. Yang and L. Shafai

Department of Electrical and Computer Engineering  
University of Manitoba, Winnipeg, Manitoba, Canada R3T 2N2

As it is known, the basis function types are important in applications of the method of moments. They influence the computation time and storage requirements and the effort needed to evaluate each term. When the method of moments is applied in the spectral domain to analyze microstrip antennas, the spectrum bandwidth of the basis function is also important for evaluation of the spectral domain integrals.

Various basis functions have been used in the spectral domain moment method to analyze microstrip antennas. Typical examples are the entire domain basis functions and the subsectional sinusoidal or rooftop basis functions. These basis functions are defined over finite regions in the space domain, which are classified as the domain based basis functions, and have infinite bandwidth in the spectral domain. The domain based basis functions should have narrow effective bandwidth in the spectral domain to save computation time. A comparative study of various basis functions will be presented and the possibility of using wavelet as domain based basis functions will also be discussed.

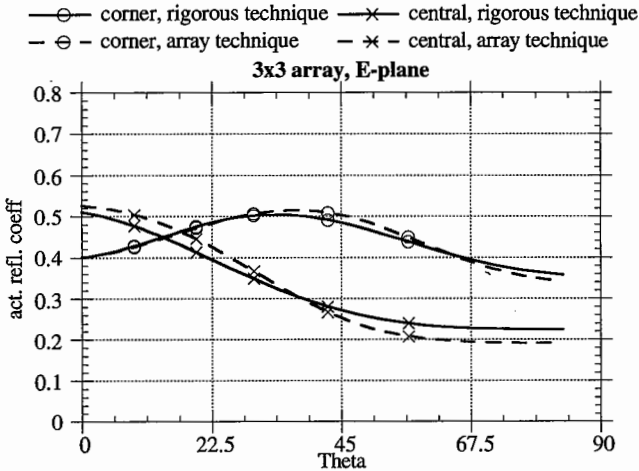
A domain based basis function is usually defined over a regular region so that its Fourier transformation over this region can be performed explicitly. Obviously, such a function will not be suitable for an arbitrary shaped patch. Therefore, a type of nodal based basis function is proposed to analyze microstrip antenna with arbitrary shaped patches. Numerical examples will be discussed in the presentation.

## ANALYSIS OF PRINTED PATCH ARRAYS USING A SPACE DOMAIN APPROACH

A. K. Skrivervik and J.R. Mosig  
 Laboratoire d'Electromagnétisme et d'Acoustique  
 Ecole Polytechnique Fédérale de Lausanne, Switzerland

Phased arrays of printed antennas have been of great interest during the last years, particularly in conjunction with the development of MMIC, where the radiators and phase shifters are integrated on the same substrate. Usually, finite arrays are studied either using an "element by element" approach (if there are not too many elements), or using the infinite array approximation for large arrays. The edge effects for finite arrays can be taken into account by combining the latter method with a convolution technique in the spectral domain (IEEE Trans. on AP, vol. AP-41, pp. 1105-1114, Aug. 1993). As the required convolutions are performed numerically, the behaviour of the infinite array has to be analyzed for many points in the spectral domain, i.e. for many scan angles in order to satisfy the sampling law. This difficulty can be avoided by working in the space domain instead of the spectral domain. Doing so, the convolution integrals become simple multiplication and the cumbersome sampling is avoided. The drawback is that using a space domain integral equation technique for printed antennas implies the computation the Green's functions for layered media (Sommerfeld integrals). However, this is not a major problem, as very efficient tools are nowadays available for the numerical evaluation of these integrals (J. R. Mosig, F.E. Gardiol, pp. 139-133 in Electronics and Electron Physics, vol. 59, P.W. Hawkes ed. Academic Press, 1982). This contribution presents the space domain analysis technique, and results for several single and multilayered arrays of various sizes.

As an example, the figure shows the modulus of the active reflection coefficient as a function of the scan angle for the central and the corner elements of a 3x3 array, computed using a rigorous full wave element by element analysis and using the finite array method described here. The radiators are 20 x 20 mm microstrip patches, the permittivity of the substrate is 2.33, its thickness 1.57 mm, the array spacing is 28.5 in both directions and the considered frequency 4.65 GHz. The results obtained by both methods agree well, but the finite array technique was about 10 times faster and required 50 times less memory space than the rigorous element by element approach. The gain of time and memory space with respect to the element by element approach increases drastically with the array size, and the method presented here can easily handle large arrays (tests have been made up to 50 x 50 elements).



## EFFICIENT COMPUTATION OF GREEN'S FUNCTIONS FOR MULTI-LAYER MICROSTRIP STRUCTURES

Ahmad Hoorfar\*  
Dept. of Electrical and Computer Eng.  
Villanova University, Villanova, PA 19085

David C. Chang  
College of Eng. and Applied Sciences  
Arizona State Univ., Tempe, AZ 85287

In the electromagnetic modeling of microstrip circuits and antennas, using the mixed-potential integral equation technique, one has to numerically evaluate the Green's functions of electric and magnetic types,  $G_e$  and  $G_m$ , that appear as the Kernels of the integral equation. These Green's functions are of the Sommerfeld integral type and have the form,

$$G(\rho) = \int_0^{\infty} \tilde{G}(\lambda) J_0(k_0 \rho \lambda) d\lambda \quad (1)$$

For a multi-layer substrate the (surface-wave) poles of  $\tilde{G}$  are located on or below the real axis of the complex  $\lambda$ -plane, in the region  $1 < \lambda < n_{\max}$ , where  $n_{\max}$  corresponds to the largest refractive index of the dielectric layers. One general integration scheme well-suited for the case of a multi-layer structure is to deform the contour of integration above the real axis, in order to avoid the surface-wave poles, and then back to the real axis to infinity. Due to the oscillatory behavior of the Bessel function when  $k_0 \rho \lambda \gg 1$ , the latter part of the integration is very time consuming and usually accounts for about 40-50% of the total computation time even when the integral averaging technique is used. In addition, in a typical solution process using the Galerkin method, the integral in (1) has to be evaluated for a large number of  $k_0 \rho$  values.

In this work we have developed a scheme which reduces the computation time for the real-axis integration by a factor of 3 or higher. The outline of the scheme is as follows: we first extract out the static,  $1/k_0 \rho$  singularity of  $G$ ; the remaining portion of the integrand is then monotonically decreasing and asymptotically behaves as  $1/\lambda^2$  as  $\lambda$  is increased. The numerical integration is now performed using an adaptive marching scheme in which we divide the integration range into small pieces. The range in each interval is chosen so that  $\tilde{G}$  can be well approximated by the first two terms in its Taylor-series expansion in  $\lambda^{-2}$ . Consequently, the integration in each interval can be evaluated analytically resulting in,

$$\int_{\lambda_m}^{\lambda_{m+1}} \tilde{G}(\lambda) J_0(k_0 \rho \lambda) d\lambda = \frac{A_m}{k_0 \rho} [Q_0(\tau_m) - Q_0(\tau_{m+1})] + B_m k_0 \rho [Q_{-2}(\tau_m) - Q_{-2}(\tau_{m+1})] \quad (2)$$

where  $\tau_m = k_0 \rho \lambda_m$  and the functions  $Q_0$  and  $Q_{-2}$  can be expressed in closed forms in terms of Bessel and Struve functions;  $A_m = \tilde{G}(1/\lambda_m^2) - (1/\lambda_m^2) \tilde{G}'(1/\lambda_m^2)$  and  $B_m = \tilde{G}'(1/\lambda_m^2)$ . We note that  $Q_0$  and  $Q_{-2}$  are functions of distance  $\rho$  only and independent of the dielectric layers' thicknesses and material properties. Therefore once the constants  $A_m$  and  $B_m$ ,  $m=1, 2, \dots$ , are computed and stored, the expression in (2) can be evaluated for all values of  $\rho$  at once; this results in a substantial reduction in the CPU time. Detailed comparison with the integral averaging technique for 2 and 3 layer structures will be given in the presentation.

## ANALYSIS OF CORNER FED MICROSTRIP ANTENNAS USING THE MULTIPOINT NETWORK MODEL

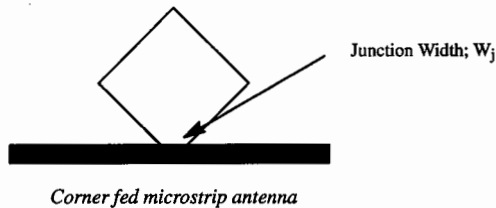
S. P. Dholakia and A. Sebak\*  
Department of Electrical and Computer Engineering,  
University of Manitoba,  
Winnipeg, Manitoba  
R3T 5V6 Canada

Two port rectangular corner fed microstrip patches are strong candidates of series fed arrays. The power radiated by individual patches is often controlled by varying the junction width between the patch and the microstrip feed line. A step by step procedure for the analysis and design of corner fed and linear array antennas, using Multipoint Network Model (MNM) method, is proposed here. The Green's function approach, for the analysis and design of a microstrip antenna, employs the impedance Green's function for segments with magnetic wall boundaries. In this method, the antenna is modelled as a multipoint resonator.

The MNM uses separate network models to represent the fields underneath the patch and the fields outside the patch. To obtain the internal field network, the  $Z$ -matrix is computed using the two dimensional Green's function for each segment. To obtain the fields outside the patch, mutual coupling and the radiation conductance are calculated. Network methods are used to match the external and internal fields at their interface. The analysis yields the input impedance and edge voltages for a given input excitation, which are used for evaluating the radiated field.

Investigation has been carried out to study the different properties and the transmission characteristics of the corner fed antennas. The Analysis procedure is extended to linear arrays of corner fed patches. A standard design procedure is established for linear arrays and applied for the design of an array with  $-20\text{dB}$  sidelobe levels.

Modeling details, results and verification will be presented.



## ANALYSIS OF SLOT-LINES USING CLOSED-FORM GREEN'S FUNCTIONS

Gülbin Dural\*  
Middle East Technical University  
Dept. of Electrical & Electronics Eng.  
06531 Ankara Turkey

M. Irsadi Aksun  
Bilkent University  
Dept. of Electrical & Electronics Eng.  
06533 Ankara Turkey

Slot-lines have broad spectrum of applications either as transmission lines or radiating elements. The most commonly used numerical technique for analyzing the slot-line geometries is the Method of Moments (MoM) which can be applied either in the spatial domain or in the spectral domain. Although the MoM is preferred over the differential equation methods because it is relatively efficient in terms of the computation time, it is still time consuming because of the slow convergence and the oscillatory nature of the integrals involved. One approach to overcome these difficulties is to employ the closed-form Green's functions in the spatial domain, that can speed up the computation of the MoM matrix elements by several orders of magnitude as compared to the numerical evaluation of the Sommerfeld integral or the conventional spectral domain method.

In this paper, the Galerkin's MoM analysis of the slot-line geometries in multilayered media has been developed in conjunction with the closed-form Green's functions of the vector and scalar potentials in the spatial domain. The tangential component of the magnetic field along the line is expressed in terms of an equivalent magnetic current density,  $\vec{J}^m$ , and the vector and scalar Green's functions for a horizontal magnetic dipole, HMD, (M. I. Aksun & G. Dural, IEEE-AP Symp. Proc., 354-357, 1993) as,

$$H_x = -j\omega G_{xx}^F * J_x^m + \frac{1}{j\omega} \frac{\partial}{\partial x} (G_x^{qm} * \nabla \cdot \vec{J}^m)$$

where  $J_x^m$  is the longitudinal component of the current density  $\vec{J}^m$ , and  $G_{xx}^F$  and  $G_x^{qm}$  are the Green's functions of the vector and scalar potentials for an  $x$  oriented HMD, respectively. In the calculation of the MoM matrix elements, the convolution integrals over the Green's functions are transferred over the testing and basis functions, which are chosen such that the convolution integrals involving these functions can be carried out analytically. It has been observed that the use of closed-form Green's functions increased the computational efficiency of the MoM matrix elements significantly in the analysis of the slot-line geometries.

WEDNESDAY PM URSI-B SESSION W-U31

Room: HUB 309

RADIO WAVE PROPAGATION FOR PCS

Chairs: Glenn Smith, Georgia Institute of Technology; L. Shafai, University of Manitoba

- |      |  |     |
|------|--|-----|
| 4:00 | Interaction of an Electromagnetic Wave with the Acoustic Field of a Traveling Point Source of Sound--Part I: Theory<br><i>*J.S. Asvestas, Grumman Corporate Research Center</i>                                | 364 |
| 4:20 | Interaction of an Electromagnetic Wave with the Acoustic Field of a Traveling Point Source of Sound--Part II: Application in a Standard Atmosphere<br><i>*J.S. Asvestas, Grumman Corporate Research Center</i> | 365 |
| 4:40 | Simulation and Measurement of Radio Wave Propagation in Urban Environments<br><i>*Y.H. Qi, Z.L. Cai, C. Wu, J. Chen, B.W. Currie, J. Litva, McMaster Univ.</i>   | 366 |
| 5:00 | Estimation of Signal Strength in Urban Microcellular Environment<br><i>*J. Chen, Y.H. Qi, C. Wu, Z.L. Cai, J. Litva, McMaster Univ.</i>  | 367 |
| 5:20 | Investigations of Wave Propagation Characteristics in Microcell Environments for PCS Applications<br><i>*Z.L. Cai, C. Wu, Y.H. Qi, J. Chen, N. Sangary, J. Litva, McMaster Univ.</i>                           | 368 |
| 5:40 | Experimental Investigations of Radio Wave Propagation in Some Special Environments<br><i>*C. Wu, Y. Qi, K. Cai, J. Chen, B. Currie, J. Litva, McMaster Univ.</i>   | 369 |

Interaction of an electromagnetic wave with the acoustic field of a traveling point source of sound. Part I: Theory

John S. Asvestas  
Grumman Corporate Research Center  
Mail Stop A01-26  
Bethpage, NY 11714-3580

It has been known for some time that the passage of a sound wave through a fluid causes the permittivity of the fluid to vary in both time and space. As a result, an electromagnetic (EM) wave traveling in the fluid scatters in all directions.

There is a large body of literature on this subject, and in most of it the sound source is stationary. We consider here the interaction of a plane EM wave with the field of an acoustic point source traveling along a straight line. The infinite medium has constant permittivity, permeability equal to that of free space, and conductivity equal to zero. Both waves are harmonic in time, with the point source traveling at a constant, subsonic speed, and with its direction of travel making an arbitrary angle with that of the plane EM wave.

We look at the variation in permittivity as a small perturbation about its constant value, and we compute the backscattered far field of the first correction term to the EM plane wave. We find that this term comprises two distinct waves. One is due to the interaction with the part of the acoustic wavefronts traveling in the backscattering direction. The other is due to the part of the acoustic wavefronts traveling away from it. The first of these waves is shifted up in frequency by an amount equal to the acoustic frequency, and the second is shifted down by the same amount. For each wave we define a backscattering cross section and we show that, for the right combination of parameters, a Bragg-type condition obtains and causes the cross section to form a sharp peak. The magnitude of this peak is further increased as Mach 1 is approached, and as the direction of travel becomes coincident with the direction of propagation of the plane EM wave.

Interaction of an electromagnetic wave with the acoustic field of  
a traveling point source of sound. Part II: Application in a  
standard atmosphere

John S. Asvestas  
Grumman Corporate Research Center  
Mail Stop A01-26  
Bethpage, NY 11714-3580

Elsewhere in this Program we develop the theory for the interaction of a plane electromagnetic (EM) wave with the acoustic field of a traveling point source of sound. In this talk we concentrate on the medium being a standard atmosphere.

We first discuss the variation of permittivity with pressure and, from it, we obtain a numerical value for the perturbation parameter. We also show how to compute the atmospheric acoustic absorption coefficient as a function of pressure, humidity, and frequency. We use these findings to analyze the backscattering cross section of the first two interaction waves in the resonance region. We assume that the frequency of the sound source is below 4 KHz. This puts an upper limit of about 18 GHz to the EM frequency.

Under typical atmospheric conditions we find that the resonance peak of the cross section can be substantial but, also, that both the EM and acoustic 3dB bandwidths of the resonance lobe are very narrow. This indicates that, if the acoustic frequency is unknown, it may be very hard to locate the EM resonance frequency; moreover, even when the EM resonance frequency can be located, a slight drift in the acoustic frequency may ruin the resonance effect. The sharpness of the acoustic resonance lobe indicates that an acoustic source with bandwidth will appear to the EM wave as being monochromatic, thus doing away with the need for studying the broadband case separately. We conclude by showing that, if the acoustic power is spread is spread through a 1/3-octave band, then we need an EM system with a 23.16% bandwidth to capture it.

## **Simulation and Measurement of Radio Wave Propagation in Urban Environments**

Y.H. Qi\*, Z.L. Cai, C. Wu, J. Chen, B.W. Currie, and J. Litva

Communications Research Laboratory

McMaster University, Hamilton, Ontario, Canada

Tel: 905-525-9140 Ext. 27141 E-mail: qi@aerostar.eng.mcmaster.ca

### **Abstract**

Pico- and micro-cellular systems will be very useful for providing future Personal Communication Services (PCS) in densely populated areas in commercial urban environments. The purpose of our research is to develop models and simulation software for urban street PCS applications. Models for recessed doorways, and the effects of vegetation, pedestrians, and vehicle traffic are given. A ray tracing method is used to carry out the simulation. Future PCS systems will make use of low antenna heights and low radiation powers (typically 10 mW) to achieve base station coverage over pico- and micro-cell areas. For such small cells, the antenna height and pattern are critical parameters in assuring good radio wave coverage and minimal interference. The software treats the base station antenna height and location as design parameters, and treats the antenna pattern, street width, recessed doorway geometry, vegetation geometry (tree spacing), and traffic distribution as input parameters. Both line-of-sight (LOS) and non-LOS paths can be predicted. The simulation software has been verified using measurements carried out in downtown Hamilton, and in densely populated streets in China. Simulation and measurement results are compared, using a Yagi transmit antenna at various heights.

# ESTIMATION OF SIGNAL STRENGTH IN URBAN MICROCELLULAR ENVIRONMENT

J. Chen\*, Y.H. Qi, C. Wu, Z.L. Cai, J. Litva

Communication Research Laboratory  
McMaster University  
Hamilton, Ontario, L8S 4K1, Canada

The deployment of personal communications services (PCS), geared towards mass market communications, is currently in the pipeline in North America. A directly related problem in the PCS is the prediction of signal strength in the microcellular environments. To acquire a knowledge of radio propagation characteristics in microcellular environment, simulation analysis as well as measurements are carried out in a typical urban area – street intersection. The emphasis is on the non-line of sight (LOS) propagation. In the simulation analysis, both reflection and diffraction of rays is considered. The reflections occur at the fronts of buildings along the streets. The diffracted rays come from building wedges as well as rooftops. By considering three dimensional diffraction, we can investigate the effect of base station antenna height, which is a very critical design parameter in the PCS system. We can also estimate the coverage of the radio wave signal by using non-LOS analysis. When applying ray tracing, a certain threshold is set to select the effective number of rays. Our software takes into account antenna height, antenna pattern and antenna polarization. In the measurements, a typical intersection in downtown Hamilton is selected to verify the simulation result. A high gain Yagi antenna is used as the transmitting antenna and the base station is set up at several different heights. The comparison will be made between measurements and the simulation. Some conclusions and suggestions for the PCS applications will be given.

# Investigations of Wave Propagation Characteristics in Microcell Environments for PCS Applications

Z. L. Cai\*, C. Wu, Y. H. Qi, J. Chen, N. Sangary and John Litva  
Communications Research Lab., McMaster University  
Hamilton, Ont., Canada L8S 4K1

Tel. 905-529-7070 ext. 27267 email: cai@aerostar.Eng. McMaster. CA

In order to study the wave propagation characteristics over a short transmission paths (less than 1km) and certain area coverage for Personal Communications Service (PCS) applications, a series of narrowband measurements at 960MHz were made on line-of-sight (LOS) and non-LOS paths on campus of McMaster University. The test site is shown in Fig. 1. A high gain directive Yagi antenna, instead of a conventional omni-directional antenna, was used as a base station transmitting antenna. It was mounted at different heights, namely, 6.5m, 15.8m and 31.0m (at the point O in Fig. 1), respectively, to investigate the dependance of attenuation characteristics on transmitting antenna heights and the coverage area of the base station. The height of the receiving antenna was 1.6m and its position was moved along the depicted routes OA, OB, OC, OD, OE, OF, OG, OH and OK (Fig. 1) at a space step 2m. The one-second signal average data are obtained by receiving vertically polarized transmitting signals. A propagation prediction model combined with UTD method, which can account for the diffraction effect from buildings, for transmitter/receiver heights, polarizations, antenna patterns and building structures which relate signal strength to the log of distance will be introduced. The comparison between measurement and theoretical results will be presented. Some conclusions and suggestions for the PCS system applications based on microcell environments will be given during the presentation.

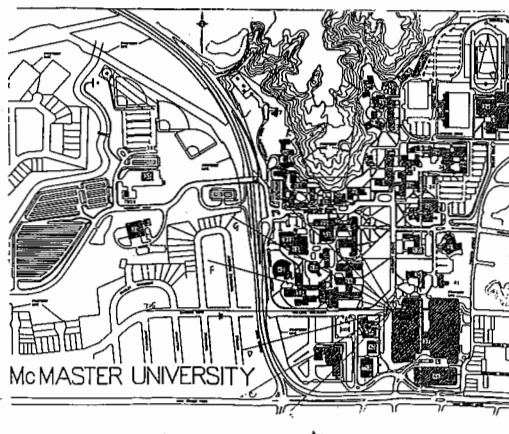


Fig. 1 Test Site of Measurements

## **Experimental Investigations of Radio Wave Propagation in Some Special Environments**

**Chen Wu\*, Yihong Qi, Kerry Cai, Ji Chen, Brian Currie and John Litva**  
**Communications Research Laboratory, McMaster University,**  
**Hamilton, Ontario, Canada L8S 4K1**  
**Tel: 905-529-7070 ext 27272**  
**E-mail: wuchen@mcmaster.ca**

Extensive studies for wave propagation in microcell environment have been published and good modelling has been developed to predict field distribution. Understanding wave propagation in picocell environments is another interested topic at present, because there is a requirement for the deployment of base stations and the setup of wireless communication networks for present and future Personal Communication Services (PCS). In this paper, we concentrate more on radio wave propagation over distances of a few hundred meters. Experimental studies and statistical models will be used to investigate and describe wave propagation characteristics in following special environments:

1. Wave propagation along a downtown shopping-street, which has a lot of stores along the street, and with a number of moving and fixed objects;
2. Wave penetration into a student dormitory, when the transmitter antenna is located outside the building;
3. Wave penetration into a residential apartment building, when the transmitter antenna is located outside the building;
4. Wave propagation along a street, which is covered by a tree-formed canopy;
5. Wave propagation in a wooded area consisting of pine trees, when the transmitter antenna height is 4 meters above the ground.

The investigations in all above scenarios are narrowband measurements at 960 MHz. A Yagi antenna is used as the transmitter antenna and transmitting power is 10 mW. The results have been obtained in these measurements provide good examples for obtaining a better understanding of wave propagation in these scenarios. More information will be presented at the conference.



THURSDAY AM JOINT SPECIAL SESSION TH-J6

Room: HUB 310

ROUGH SURFACE SCATTERING III

Chairs: C. Rino, Vista Research Corporation; J.B. Schneider, Washington State University

Organizers: S. Broschat, Washington State University; A. Ishimaru, University of Washington

- 8:20 The FDTD Method for Scattering from Rough Surfaces: Oblique Incidence 372  
*\*F.D. Hastings, S.L. Broschat, J.B. Schneider, Washington State Univ.*
- 8:40 Fast Solution of Scattering from Periodic Randomly Rough Infinite Surfaces AP-S  
*\*M.A. Nasir, W.C. Chew, Univ. of Illinois*
- 9:00 An Improved Numerical Simulation of Electromagnetic Scattering from Perfectly  
Conducting Random Surfaces AP-S  
*\*Y. Oh, K. Sarabandi, Univ. of Michigan*
- 9:20 A BMIA/FFT Algorithm for the Monte Carlo Simulations of Large Scale Random Rough  
Surface Scattering: Application to Grazing Incidence AP-S  
*L. Tsang, C.H. Chan, \*K. Pak, H. Sangani, Univ. of Washington*
- 9:40 The MEI Method Applied to Random Rough Surfaces 373  
*\*J.B. Schneider, S.L. Broschat, Washington State Univ.*
- 10:00 Break
- 10:20 Numerical Solution of Random Rough Surface Scattering with Low Dielectric Contrast  
Using Extinction Theorem 374  
*\*R.T. Marchand, Virginia Polytechnic Inst.*
- 10:40 Investigation of Shadowing in Rough Surface Scattering at Small Grazing Angles AP-S  
*\*J.C. West, Oklahoma State Univ.*
- 11:00 Comparison of Near-Grazing Ocean Scattering Calculations with Experimental Results 375  
*\*E. Rodriguez, Y. Kim, T. Michel, California Inst. of Technology; D. Trizna, M. Sletten,  
Naval Research Laboratory*
- 11:20 Range-Resolved Ocean Backscatter Simulations 376  
*\*C.L. Rino, H.D. Ngo, Vista Research Inc.*
- 11:40 Radar Backscatter from the Ocean at Low Grazing Angles 377  
*\*D. Kasilingam, Univ. of Massachusetts, Dartmouth*

## **The FDTD Method for Scattering from Rough Surfaces: Oblique Incidence**

**Frank D. Hastings\*, Shira L. Broschat, and John B. Schneider**

Electrical Engineering and Computer Science

Washington State University

Pullman, WA 99164-2752

fhasting@eecs.wsu.edu, (509)335-0903

shira@eecs.wsu.edu, (509)335-5693

schneidj@eecs.wsu.edu, (509)335-4655

The problem of modeling scattering from randomly rough surfaces has been approached through approximate and exact numerical methods. Both approaches have limitations: Approximate solutions are typically restricted to specific regions of validity and exact numerical solutions are hindered by the computational requirements inherent in the problem. Recently, the Finite Difference Time Domain (FDTD) method has been used to model rough surface scattering. This approach produces results at low computational cost.

In an earlier paper, results were presented for the normal incidence excitation of one-dimensional Dirichlet surfaces with Gaussian statistics satisfying a Gaussian roughness spectrum [Hastings *et al.*, submitted to IEEE Trans. Antennas Propagat., Aug. 1993]. Monte Carlo simulations were used to compute the scattering cross sections as a function of scattered angle. In this paper, we extend our work to oblique incidence, which requires the use of different absorbing boundary conditions (ABCs). Numerical results for the Monte-Carlo averaged cross sections are presented for various rms surface heights and correlation lengths, and the ABCs are discussed.

## The MEI Method Applied to Random Rough Surfaces

John B. Schneider\* and Shira Lynn Broschat

School of Elec. Eng. and Comp. Sci.

Washington State University

Pullman, WA 99164-2752

The Measured Equation of Invariance (MEI) method has received considerable attention recently. Unlike more traditional solution techniques, MEI solutions are obtained by inversion of a relatively small *and* sparse matrix. Therefore, the MEI method can potentially provide a solution much more quickly than other techniques. To date, the MEI method has been applied primarily to discrete objects. In this paper, the application of the MEI method to randomly rough surfaces is discussed. An implementation suitable for scattering from randomly rough surfaces is explained. Because accuracy is required over a range of about 60 dB, modifications to the originally proposed algorithm are required. These modifications include the use of a scheme where the metrons (the assumed source currents) are updated iteratively. These algorithm enhancements are not restricted to the rough surface scattering problem and can be used in problems with discrete scatterers. Monte Carlo simulations are used to obtain the scattering cross sections for one-dimensional, perfectly conducting surfaces. Results are compared with those from other techniques, and excellent agreement is demonstrated.

# Numerical Solution of Random Rough Surface Scattering With Low Dielectric Contrast Using Extinction Theorem

Roger T. Marchand  
Bradley Department of Electrical Engineering  
Virginia Polytechnic Institute, Blacksburg VA, 24061

## *Abstract*

The method of moments has seen widespread use in the numerical solution of random rough surface scattering. This technique has proved valuable, as it is valid over a large range of surfaces when the incident angle is not near grazing. However, special care must be taken when the scattering surface presents a low dielectric contrast, since the reflection from such surfaces may be comparable to the numerical error.

In this study, the method of moments was used in combination with the extinction theorem to numerically calculate the scattering from both random rough and flat surfaces. It will be shown that for flat surfaces, the solution error does not change significantly regardless of the dielectric contrast and is actually greatest for a dielectric ratio of 1:1. For an unknown spacing of  $0.1\lambda$  with an  $80\lambda$  flat surface, the solution is valid for a dielectric ratio of roughly 1:1.2.

The above analysis is possible because the exact solution for flat surfaces is known. There is no exact solution for random rough surfaces. However, the error might be approximated by the solution of the 1:1 dielectric ratio. It will be shown that if such an approximation is accepted, the numerical solution remains valid over roughly the same ratio as the flat surface.

## COMPARISON OF NEAR-GRAZING OCEAN SCATTERING CALCULATIONS WITH EXPERIMENTAL RESULTS

Ernesto Rodriguez\*, Yunjin Kim, Thierry Michel  
Jet Propulsion Laboratory  
California Institute of Technology  
Pasadena, CA 91109

Dennis Trizna, Mark Sletten  
Naval Research Laboratory  
Washington DC

Near grazing scattering from the ocean surface has many curious features which are not present in other incidence angle regimes. Two of the most unusual features are the anomalous statistics of the backscatter return and the horizontal to vertical polarization cross section ratio which, unlike the intermediate incidence angle regime results, can be close to, or greater than, one for intermittent spiking events. In our previous work, we have shown that, using ocean models which did not include capillary waves or wave breaking, the anomalous statistics could be reproduced by numerical scattering experiments. However, we were unable to reproduce the intermittent, spiking behavior.

We proceed in two ways to obtain better agreement with experimental results. First, we have experimentally obtained wave tank sea surface profiles from which numerical scattering calculations may be performed. This data was collected simultaneously with radar scattering data so that a comparison may be performed between the numerical and experimental scattering results. In this paper, we present and contrast these results and examine the relationship between specific surface features and the near and far scattered fields.

To extend these results to the open ocean, we have simulated realistic ocean surfaces, including capillary waves and nonlinear interactions, using the hydrodynamic model advocated by West et al. (JGR, 92 (NC11), 1987) to generate ocean surface realizations for a variety of ocean conditions. The results of these calculations are compared against the open ocean data in the literature as well as against the wave tank experiments.

## Range-Resolved Ocean Backscatter Simulations

Charles L. Rino\* and Hoc D. Ngo

Vista Research, Inc.

100 View Street, P. O. Box 998, Mountain view, CA 94042

Ocean surface backscatter at low to moderate grazing angles is evidently dominated by the returns from the region of the wave crests. The space-time dispersion characteristics of the radar returns and their Doppler spectra are readily associated with known properties of ocean surface waves; however, the precise origin of the backscatter appears to be polarization sensitive. That is, horizontally polarized backscatter responds to the faster moving structures near the wave crests, whereas vertically polarized backscatter responds to slower moving structures below the crests of the dominant surface wave structure. To model these phenomena, the range-resolution process must be considered in conjunction with an accurate representation of the wave crest region. The latter is a hydrodynamics problem that is currently receiving considerable attention.

In this paper we will describe the results from numerical simulations of the backscatter from one-dimensional surface realizations that have been constructed with varying degrees of hydrodynamic consistency. Time-domain methods have been used to calculate range-resolved backscatter, but most radars use pulse-compression or synthetic pulse techniques. It happens that standard frequency-domain techniques based on method-of-moments computations are particularly well suited to modeling synthetic-pulse radars because the simulation is not affected by range ambiguities. As a consequence, a coarse frequency sampling can be used to minimize the computation requirements.

Our current results show that the measured polarization characteristics are sensitive to the range-resolved location on the surface realization, however the polarization Doppler sensitivity observed in real data has not been reproduced by surfaces that were available at the time this abstract was submitted. We will review our most recent results and discuss the interpretation of range-resolved backscatter in the presence of wavelength-scale surface structure and multiple scattering.

## RADAR BACKSCATTER FROM THE OCEAN AT LOW GRAZING ANGLES

Dayalan Kasilingam  
University of Massachusetts, Dartmouth  
North Dartmouth, MA 02747-2300

Sea clutter is one of the factors that limit the performance of radars operating at low grazing angles. At these incidence angles, sea clutter is more sporadic than clutter at moderate incidence angles. The large spikes that occur due to this sporadic nature can significantly increase the false alarm rate in target detection. There is a real need to accurately characterize sea clutter at low grazing angles. However, modeling sea clutter at low grazing angles has been difficult, because the mechanisms that determine sea clutter at these incidence angles are significantly different from those at moderate incidence angles. Measurements at low grazing angles have found that the statistical properties, the Doppler signatures and the polarimetric signatures of sea clutter to be quite different from those at moderate incidence angles. It is found that the standard two-scale resonant model does not adequately explain all the observations at low grazing angles. Effects of shadowing and multiple scattering are invariably present at low grazing angles, but are generally negligible at moderate incidence angles. An exact scattering model is developed to describe scattering from two-dimensional rough surfaces that consist of periodic waves. The model is based on the space harmonic method for analyzing scattering from periodic surfaces. The surface is assumed to be perfectly conducting. The surface currents induced by the incident radiation is estimated for various angles from near-nadir incidence to grazing incidence angles. The estimates at near-nadir and moderate incidence angles are used to verify existing models for backscatter at these angles. It is shown that multiple scattering is negligible at these incidence angles. Using this model to estimate the currents, the effects of shadowing and multiple scattering at low grazing angles are also studied. The distribution of the currents are used to assess the levels of shadowing and multiple scattering. The effects of shadowing and multiple scattering are calculated for various combinations of wavelengths, amplitudes and wave directions. These results are then extended to low grazing angle backscatter from the ocean surface. Approximate results are obtained for the various properties of backscatter in the different sea states. The theoretical estimates are compared with a variety of experimental data sets. It is concluded that multiple scattering plays a significant role in the properties of backscatter at low grazing angles and it is crucial that it be properly described in any model.



THURSDAY AM URSI-B SPECIAL SESSION TH-U32

Room: Kane 130

A TRIBUTE TO ROGER F. HARRINGTON

Chair: Chalmers Butler, Clemson University

Organizers: A.T. Adams, Syracuse University; Chalmers Butler, Clemson University; Don Wilton, University of Houston

8:20	Roger and Me <i>*R.G. Kouyoumjian, The Ohio State Univ.</i>	380
8:40	Why You See Roger Harrington's Footprint on My Back <i>*C.M. Butler, Clemson Univ.; *D.R. Wilton, Univ. of Houston</i>	381
9:00	Field Equivalence Principles in Electromagnetic Theory <i>*R.E. Collin, Case Western Reserve Univ.</i>	382
9:20	The Method of Moments: The Last Twenty-Five Years <i>*A.T. Adams, B.J. Strait, Syracuse Univ.</i>	383
9:40	Use of the Method of Moments to Obtain Variational Solutions <i>*J.R. Mautz, Syracuse Univ.</i>	384
10:00	Break	
10:20	How to Improve Computational Efficiency of Large Problems Solved by Method of Moments <i>R. S. Adve, *T. K. Sarkar, Syracuse Univ.; S.M. Rao, Auburn Univ.</i>	385
10:40	Multiconductor Transmission Line Research at Syracuse University <i>*R.G. Plumb, Univ. of Kansas</i>	386
11:00	E-Field Integral Equations and the Method of Moments <i>*R.F. Harrington, Syracuse Univ.</i>	387

## Roger and Me

Robert G. Kouyoumjian  
Dept. of Electrical Engineering  
The Ohio State University  
Columbus, Ohio

Professor Roger Harrington and I first met over forty years ago at The Ohio State University, where we were graduate students in the Antenna Laboratory (now the ElectroScience Laboratory). We were both Ph.D. students, and it is ironic that a part of his dissertation was concerned with edge diffraction, whereas my dissertation was concerned with the variational method and the reaction concept, which are closely related to the moment method. In later years we exchanged these areas of interest. I remember Roger as being well-organized and very able (he graduated a year earlier than I did); however he also was a modest, cordial person with whom I formed a lasting friendship.

In the early 1970's Roger became interested in the uniform geometrical theory of diffraction (the UTD), and we corresponded on the subject. He used the UTD to calculate the scattering from polygonal cylinders, and compared the results with scattered patterns obtained from a moment method solution. Generally speaking, the two calculations were in close agreement. However there were discontinuities in the UTD patterns of some of the smaller cylinders. The erroneous discontinuities were the result of double diffraction which occurs when the second edge is illuminated by a transition region field from the first edge. This motivated Professor Roberto Tiberio and me to derive improved expressions for double diffraction which could correct this type of error.

The moment method is frequently employed to check the accuracy of a UTD solution. If the two compare closely, the accuracy of the UTD solution can be expected to increase with increasing frequency. However there are also direct connections between the two methods which are advantageous when a part of the radiating structure is large. In the hybrid method of Thiele and Newhouse the UTD is employed to augment the impedance matrix, whereas Burnside, Yu and Marhefka have used the UTD to develop high-frequency basis functions (physical basis functions) which greatly reduce the computational effort in the moment method solution.

No discussion of Professor Harrington's contributions would be complete without mentioning his two very fine books: Time Harmonic Electromagnetic Fields and Field Computation by Moment Methods. The author of this paper has used them frequently in his teaching and research.

**WHY YOU SEE  
ROGER HARRINGTON'S FOOTPRINT ON MY BACK**

Chalmers M. Butler,\* ECE Department  
Clemson University, Clemson, SC 29634-0915 USA  
and  
Donald R. Wilton,\* EE Department  
University of Houston, Houston, TX 77204-4793

The purpose of this presentation is to acknowledge the profound influence that Professor Roger F. Harrington and his work in electromagnetic theory and its applications have had on the authors and on many other researchers and educators. In the race to apply the power of computers to electromagnetic problems, for example, Professor Harrington not only established the rules, he also issued the challenge, set the pace, and left the imprint of his work on all those to follow. We draw attention to the many cases in which the foundations of our own work can be traced back to a fundamental contribution made earlier by him in a paper or in one of his books. We also attempt to relate incidences in which Roger's contributions to the literature have directly affected the work of others.

Without dwelling extensively on any one of Roger's contributions to our understanding of the fundamentals of electromagnetics and numerical techniques, we attempt to trace the development of those which have led us to a better understanding of the important principles. For example, we mention Roger's leadership in the use of vector and scalar potentials (as opposed to dyadic Green's functions) in formulating integral equations amenable to numerical solution. Also described are his popularization and pioneering elucidation of how to formulate aperture problems in terms of magnetic surface current, as opposed to employing more complex techniques based upon Green's theorems. And, of course, we will give appropriate focus to the power of the equivalence principle as expounded to the world by Roger Harrington.

If Roger actually slows down in retirement, the electromagnetics community will miss his intellectual stimulation and his warm friendship. And, in the event of true retirement, the authors hope that someone else comes to the fore and carries forth the Harrington method: think hard about a complex problem and reduce it to its simplest essentials so Butler and Wilton can understand it.

## FIELD EQUIVALENCE PRINCIPLES IN ELECTROMAGNETIC THEORY

R.E.Collin

Electrical Engineering and Applied Physics Department  
Case Western Reserve University  
Cleveland, OH 44106

This paper presents a short historical review of the development of field equivalence principles and their application in applied electromagnetic theory with particular emphasis on the contributions of Professor R.F.Harrington. The concept of equivalent secondary sources that can reproduce the electromagnetic field of a given set of primary sources originated with Huygens more than three centuries ago. Huygens' theory was a geometrical theory and treated light as a scalar wave field and ignored interference effects. Fresnel is credited with adding interference effects associated with time harmonic fields in 1818. Over the next 80 years important contributions were made by well known scientists such as Stokes, Helmholtz, and Kirchhoff. A rigorous mathematical development of equivalent sources on a closed surface was provided by Love in 1901. In the paper we also review the work of Larmor and Tedone, Kottler, Stratton and Chu, Schelkunoff, and Harrington which led to the modern form of the field equivalence principles expressed in terms of equivalent electric and magnetic current sheets. Professor Harrington provided a very concise and easily understood formulation of the field equivalence principles in his classic text "Time Harmonic Electromagnetic Fields".

By far the greatest stimulus to the use of field equivalence principles came about when Professor Harrington coupled their use with the method of moments which could provide solutions for the secondary sources. Professor Harrington and his colleagues have skillfully applied the use of field equivalence principles and the method of moments to solve a wide variety of problems in electromagnetic radiation and scattering. In the paper we will highlight the aperture coupling problem and the mutual interaction problem associated with the radiation from multiple waveguide apertures. These two problems are conceptually made much simpler by using the methods developed by Professor Harrington and provide a clear illustration of the great utility of field equivalence principles in applied work.

## THE METHOD OF MOMENTS: THE LAST TWENTY-FIVE YEARS

Arlon T. Adams\*  
Bradley J. Strait  
Department of Electrical and Computer Engineering  
Syracuse University  
Syracuse, NY 13244

For more than a quarter century Syracuse University researchers have been developing the "method of moments" and exploring its applications to practical problems in the field of electromagnetics. The method has been successfully used for both analysis and design in a) problems in electrostatics, b) treatment in the frequency domain and also in the time domain of problems involving radiation and scattering of electromagnetic waves by thin wires and rods, c) treatment in the frequency domain of problems involving radiation and scattering by two- and three-dimensional conducting bodies, d) problems of radiation and scattering by two- and three-dimensional material bodies, again treated in the frequency domain, e) frequency-domain coupling of electromagnetic energy through apertures in conducting bodies, and f) treatment of eigenvalue problems such as waveguides with arbitrary cross-sections. Most recently, the method has been applied to problems of wave propagation and coupling in multilayered dielectric media and analysis of microwave circuits and printed circuit antennas. This paper will summarize key research efforts and results in these areas and point out many of the well-documented computer codes that are readily available and that can be used to advantage by engineers working in the electromagnetics area. The paper will also point out some of the key milestones and contributions in the progress of this work of the past quarter century. In addition, some interesting historical aspects of the development of the method of moments will also be recounted.

## Use of the Method of Moments to Obtain Variational Solutions

Joseph R. Mautz  
Department of Electrical and Computer Engineering  
Syracuse University, Syracuse, NY 13244-1240

Consider  $\rho = \langle Lf, w \rangle$  where  $f$  and  $w$  satisfy

$$Lf = g \quad (1)$$

$$L^a w = h. \quad (2)$$

Here,  $L$  is a linear operator,  $L^a$  is the adjoint of  $L$ ,  $\langle Lf, w \rangle$  is the symmetric product of  $Lf$  with  $w$ , and  $g$  and  $h$  are known functions. A variational formula for  $\rho$  is a functional of two functions  $\tilde{f}$  and  $\tilde{w}$  that reduces to  $\rho$  when  $\tilde{f} = f$  and  $\tilde{w} = w$  and is stationary there. A variational formula is desirable because it gives a second order approximation to  $\rho$  when  $\tilde{f}$  and  $\tilde{w}$  are first order approximations to  $f$  and  $w$ , respectively.

Let  $\rho_v$  be a function of the three symmetric products  $\langle L\tilde{f}, \tilde{w} \rangle$ ,  $\langle L\tilde{f}, w \rangle$ , and  $\langle Lf, \tilde{w} \rangle$  where  $f$  is the exact solution to (1),  $\tilde{f}$  is an approximation to  $f$ ,  $w$  is the exact solution to (2), and  $\tilde{w}$  is an approximation to  $w$ . Viewing  $\rho_v$  as a functional of the functions  $\tilde{f}$  and  $\tilde{w}$ , one writes  $\rho_v = \rho_v(\tilde{f}, \tilde{w})$ . If

$$\rho_v(\tilde{f}, w) = \rho_v(f, \tilde{w}) = \rho_v(f, w) = \langle Lf, w \rangle \quad (3)$$

for arbitrary  $\tilde{f}$  and  $\tilde{w}$ , then one can show that  $\rho_v(\tilde{f}, \tilde{w})$  is stationary about  $(\tilde{f}, \tilde{w}) = (f, w)$ . Consequently,  $\rho_v(\tilde{f}, \tilde{w})$  is said to be variational.

Let  $\tilde{f}$  and  $\tilde{w}$  be moment approximations to  $f$  and  $w$ , respectively. The pair of moment solutions  $(\tilde{f}, \tilde{w})$  is a symmetric pair if the expansion and testing functions for  $w$  are respectively the testing and expansion functions for  $f$ . Although the simple formula  $\langle L\tilde{f}, \tilde{w} \rangle$  is not variational, one can show that if  $\tilde{f}$  and  $\tilde{w}$  are a symmetric pair of moment solutions, then the value of  $\rho_v(\tilde{f}, \tilde{w})$  is the same for any one of the class of variational formulas  $\rho_v$  that satisfy the conditions in the previous paragraph. Furthermore, this value is  $\langle L\tilde{f}, \tilde{w} \rangle$ . Therefore, one who seeks the most accurate approximation to  $\langle Lf, w \rangle$  afforded by a symmetric pair of moment solutions  $\tilde{f}$  and  $\tilde{w}$  will do just as well to bypass the whole class of variational formulas  $\rho_v$  described in the previous paragraph and use the "non-stationary" formula  $\langle L\tilde{f}, \tilde{w} \rangle$ .

## HOW TO IMPROVE COMPUTATIONAL EFFICIENCY OF LARGE PROBLEMS SOLVED BY METHOD OF MOMENTS

R. S. Adve and Tapan K. Sarkar  
Department of Electrical and Computer Engineering  
Syracuse University  
Syracuse, New York 13244-1240

Sadasiva M. Rao  
Department of Electrical Engineering  
Auburn University  
Auburn, Alabama 36849

**Abstract:** The objective of this presentation is to show how the principle of analytic continuation can be utilized effectively to solve large method of moment problems efficiently. To this end the method of Cauchy (Kottapalli et.al, IEEE Trans. on MTT, April 1991, pp. 682-687) has been utilized to interpolate/extrapolate an analytic function by a ratio of two polynomials. An information theoretic criteria based on the quality of the data has been utilized to select the parameters for the Cauchy's method. Cauchy's method involves approximating a function by a ratio of two polynomials. When values of the function and its derivative information is provided. Utilizing this method it has been possible to reduce computation time for large method of moments problems by at least two orders of magnitudes. Examples have been solved utilizing the Electric Field Integral Equation. Typical results involve scattering from arbitrary shaped 3-D structures. RCS results for a conducting sphere, plate, concave hemisphere and convex hemisphere are presented over a decade bandwidth utilizing this technique. Accompanying data will be presented to illustrate the accuracy and efficiency of this technique.

**Multiconductor Transmission Line Research at  
Syracuse University**

Richard G. Plumb  
Radar Systems and Remote Sensing Laboratory  
Dept. of Electrical Engineering and Computer Science  
University of Kansas  
Lawrence, KS 66045

In this paper we review the importance of multiconductor transmission line theory and the contributions made to this theory by researchers at Syracuse University. Published work performed by Professor Roger F. Harrington, his colleagues, and his graduate students at Syracuse University will be reviewed. Attention will be paid to the areas of quasi-static solutions, quasi-dynamic solutions and full-wave solutions for vias and cross-overs. Various techniques for computing the capacitance matrix and inductance matrix for transmission lines will also be covered. Finally, radiation for multiconductor connectors and pigtailed will be reviewed.

## E-FIELD INTEGRAL EQUATIONS AND THE METHOD OF MOMENTS

Roger F. Harrington  
Department of Electrical Engineering  
Syracuse University  
Syracuse, NY 13244, USA

We use the words "E-field integral equations" to emphasize that there are many forms that an EFIE may take. Furthermore, it is not a true integral equation, but rather an integro-differential equation. Finally, given any particular form of the E-field equation, there are many moment-method solutions to it.

First, consider the thin-wire mixed-potential EFIE. For a wire defined by the parametric variable  $\ell$ , this is  $Z(I) = E_t^i$  where  $E_t^i$  is the  $\ell$ th component of the impressed field and  $Z(I)$  is the operator which relates the current to the negative tangential component of the scattered field. Following the usual method of moments we obtain the matrix equation  $[Z] I = V$ , where the elements of  $[Z]$  are  $Z_{mn} = \langle w_m, Zf_n \rangle$ . Here  $f_n(\ell)$  are the expansion functions and  $w_m(\ell)$  are the testing functions.

Many ways of evaluating the  $Z_{mn}$  are possible. Perhaps the best one is to perform the inner-product integration by parts and obtain

$$Z_{mn} = j\omega\mu \int_0^L d\ell \int_0^L d\ell' w_m(\ell) f_n(\ell') G(\ell, \ell') \\ + \frac{1}{j\omega\epsilon} \int_0^L d\ell \int_0^L d\ell' \frac{dw_m}{d\ell} \frac{df_n}{d\ell'} G(\ell, \ell')$$

This results in the least singular integrals, since the Green's function  $G(\ell, \ell')$  is never differentiated. It also clearly shows that  $f_n$  and  $w_m$  should be functions whose  $\ell$ -derivatives exist. Other possibilities for evaluating  $Z_{mn}$  involve transferring derivatives to  $G(\ell, \ell')$ , which must be done with great care.

A similar procedure applies to the mixed-potential EFIE obtained for conducting surfaces. In this case  $Z_{mn}$  elements are obtained in terms of vector-valued expansion functions  $\underline{F}_n$  and vector-valued testing functions  $\underline{W}_m$ . The form of the equations for  $Z_{mn}$  show that  $\underline{F}_n$  and  $\underline{W}_m$  should be functions whose surface gradients exist.

Some possible choices for expansion and testing functions, and other forms for  $Z_{mn}$  will be discussed.



THURSDAY AM URSI-A SESSION TH-U33

Room: Savery 249

MEASUREMENTS FOR DIELECTRIC MEASUREMENTS

Chairs:	R.L. Moore, Georgia Institute of Technology; S.S. Stuchly, University of Victoria	
8:20	Free Space EM Measurement System <i>*P.G. Friederich, R.L. Moore, Georgia Inst. of Technology</i>	390
8:40	Effective Dielectric Constant for Composite Materials <i>K. Komisarek, N. Wang, A. Dominek, The Ohio State Univ.</i>	391
9:00	Dynamic Resonator Measurements of Metallic Surface Resistance and Complex Permittivity <i>*R.G. Geyer, J. Baker-Jarvis, National Inst. of Standards and Technology; J. Krupka, Instytut Mikroelektroniki i Optoelektroniki Politechniki Warszawskiej</i>	392
9:20	A Possibility of Wideband Dielectric Measurement Using the Coplanar Waveguide Technique <i>K. Wu, D. Maurin, C. Akyel, R.G. Bosisio, École Polytechnique</i>	393
9:40	Non-Destructive Measurement of EM Properties of Anisotropic Materials with a Waveguide Probe System <i>*C. W. Chang, K.M. Chen, J. Qian, Michigan State Univ.</i>	394
10:00	Break	
10:20	Dielectric and Magnetic Relaxation Models <i>J. Baker-Jarvis, R.G. Geyer, National Inst. of Standards and Technology</i>	395
10:40	Time Domain Method for Materials Characterization Using Microstrip Field Applicators <i>D.J. Infante, J. Ross, D.P. Nyquist, Michigan State Univ.</i>	396
11:00	Microwave Level Gauging System <i>*W. Guo, S.S. Stuchly, K. Caputa, Univ. of Victoria</i>	397

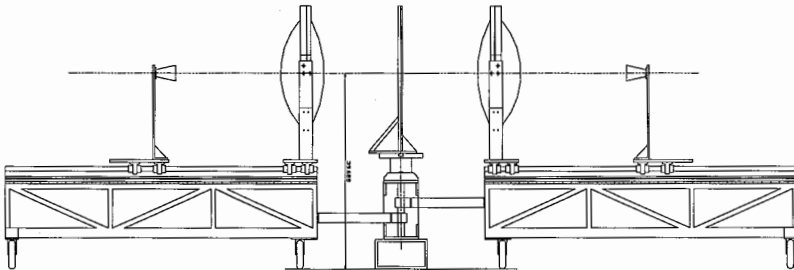
# Free Space EM Measurement System

**Paul G. Friederich\* and Rick L. Moore**  
**Georgia Tech Research Institute**

Prediction and control of the electromagnetic signature of an object requires knowledge of the constitutive properties of the materials composing the object. Georgia Tech researchers have implemented a variety of techniques to characterize such materials. One of the most versatile involves the use of focusing elements (lenses) with free space measurements. Two assumptions commonly made in the derivation of transmission and reflection coefficients as functions of material constitutive parameters are that the wavefront interacting with the sample is planar, and that all the energy of the wave interacts with the sample. Use of lenses to transform a spherical wave into one with a planar phase front, and to focus the energy, better satisfies these assumptions.

A Gaussian beam profile is achieved with lenses consisting of two plano-convex pieces with flat faces next to each other. The input lens half (closest to the horn antenna) is designed to collimate the beam and the output lens half focuses the beam. The lenses are mounted on booms which pivot around a point at which a sample is mounted. The sample holder, mounted on a mill turntable at the pivot position, accommodates up to 24" samples with precision positioning in either lateral direction and rotation around the vertical axis of the sample. This so-called "boom arch" arrangement, depicted below, allows the user to characterize the reflectivity of materials at various incident and reflected angles. Together with appropriate measurement calibration and data processing, the boom arch provides a means for measuring the complex permittivity, permeability, or sheet impedance of a material, as well as reflectivity, transmissivity, and bistatic scattering from particular samples. The facility has been used at frequencies from 2 to 100 GHz, and a similar arrangement has even been used to characterize the millimeter wave properties of ceramic foam panels at temperatures up to 1500°C.

Free-space algorithms used to calculate permittivity and permeability assume true plane-wave incidence. In order to assess their accuracy when used with focused beam illumination, the lenses have been characterized on a planar near field scanner to derive the plane wave spectrum of the lens output. Using the PWS data, the algorithm performance is being re-examined to assess the impact on derived values of constitutive parameters.



# Effective Dielectric Constant For Composite Materials

K. Komisarek, N. Wang and A. Dominek  
The ElectroScience Laboratory  
Department of Electrical Engineering  
The Ohio State University  
Columbus, OH 43212

## Abstract

Advanced fabrication practices employ composite materials in aerodynamic structures to achieve a variety of design goals. Some of these design goals assume the existence of an effective dielectric constant. The concept of an effective dielectric constant not only provides a mechanism to readily perform radiation and scattering calculations but more basically, the ability to characterize the electrical properties of composite material. The composite material of interest is formed by fibers embedded in a resin matrix. A variety of composite configurations will be evaluated to determine the validity of the effective dielectric constant concept. The evaluation is numerically performed by equating the reflection and transmission characteristics from generic composite structures to those of equivalent, uniform, isotropic material structures. Additionally, the issue of composite uniformity in the structure is also examined.

## DYNAMIC RESONATOR MEASUREMENTS OF METALLIC SURFACE RESISTANCE AND COMPLEX PERMITTIVITY

Richard G. Geyer\* and James Baker- Jarvis  
National Institute of Standards and Technology  
Electromagnetic Fields Division, 813.08  
325 Broadway, Boulder, CO 80303, U.S.A.

Jerzy Krupka  
Instytut Mikroelektroniki i Optoelektroniki Politechniki Warszawskiej  
Koszykowa 75, 00-662 Warszawa, Poland

Surface resistance measurements improve the accuracy of dielectric loss determinations made with metallic cavities by enabling better spectral characterization of wall losses. In addition, they are quite useful in many electromagnetic interference problems, where electronic systems are located within a metal enclosure and it is necessary to ascertain the shielding effectiveness of the enclosure. Accurate microwave measurements of metallic surface resistance may be conveniently performed by  $TE_{011}$  (or  $TE_{01\delta}$ ) mode excitation of a well-characterized very low-loss dielectric material, such as crystalline c-axis oriented quartz or sapphire. The measurement is made by placing this material between a metal plate whose surface resistance is known and a parallel plate consisting of the material under test. By changing the aspect ratio of the very low-loss dielectric material, it is possible to determine the surface resistance over a broad frequency spectrum.

In a similar fashion, accurate measurements of permittivity and dielectric loss tangent of low-loss dielectric materials may be performed. Given the dimensions of the dynamic resonator, the resonant frequency of the  $TE_{01\delta}$  mode, and the unloaded quality factor, both permittivity and dielectric loss can be resolved. Losses of the two parallel plates may be suitably accounted for. Although the  $TE_{011}$  mode is typically employed, higher-order TE and quasi-TE hybrid modes may be used, subject to positive identification of each resonant mode. Introduction of a small air gap between the sample under test and either of the metallic ground planes allows the fundamental TE resonant frequency at which the sample is tested to be changed. Applications of these techniques demonstrate that materials having relative permittivities as large as 100 or dielectric loss tangents as low as  $3 \times 10^{-6}$  can be measured. This measurement accuracy is not achievable with transmission line or free-space methods.

## A Possibility of Wideband Dielectric Measurement Using The Coplanar Waveguide Technique

Ke WU, David MAURIN, Cevdet AKYEL, Renato G. BOSISIO

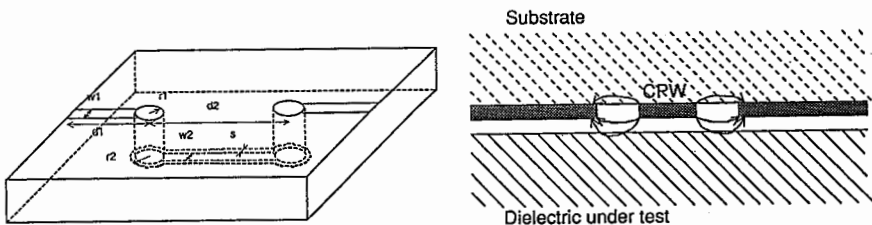
Groupe de Recherches Avancées en Microondes et en Électronique Spatiale  
(POLY-GRAMES)

Dept. de génie électrique et de génie informatique, École Polytechnique  
C. P. 6079, Succ. "Centre-Ville", Montréal, Canada H3C 3A7

Tel: 514-340-5991, Fax: 340-5892, e-mail: wuke@poly-hf2.grmes.polymtl.ca

### Abstract

A large variety of techniques has been proposed for characterizing dielectric materials. These measurements are essentially accomplished by using various electromagnetic sensors such as open coaxial lines, waveguides, six-port reflectometers, horn lens antenna, etc. These techniques, however, suffer from the requirement of either a wideband RF/microwave operation or a large range of measurement capability in terms of material parameters under test. This is mainly due to the limited sensibility and field saturation. We attempt to propose a possibility of overcoming these difficulties. This novel technique uses a quasi-TEM planar cell for wideband measurements of dielectric materials including highly lossy films. It consists of a coplanar waveguide (CPW) interconnected with two backside microstrips through via-holes. As shown in the following figure, the wideband high sensibility is achieved through the use of contact or non-contact procedure between the sample-under-test and the CPW surface. The electromagnetic field interacting with the sample is "modulated" by the unknown dielectric parameters over certain length of wave propagation, thereby giving appropriate information on reflection and transmission coefficients. These parameters can be extracted through the measured complex coefficients once the equivalent circuit model is established. Our preliminary theoretical and experimental results indicate that good transitions of the microstrip-CPW-microstrip can be made over wideband frequency range. Measurements of different material samples are presented to demonstrate a promising wideband sensitivity of the proposed CPW cell.



## NON-DESTRUCTIVE MEASUREMENT OF EM PROPERTIES OF ANISOTROPIC MATERIALS WITH A WAVEGUIDE PROBE SYSTEM

C.W. Chang\*, K.M. Chen and J. Qian  
Department of Electrical Engineering  
Michigan State University  
E. Lansing, MI 48824

A non-destructive measurement of electromagnetic (EM) properties of anisotropic materials using an open-ended waveguide probe has been conducted. The probe consisting of an open-ended rectangular waveguide with a large flange can be placed against a material layer to be measured. As the dominant mode of wave in the waveguide is incident upon the material layer, a part of it penetrates the material layer and the rest of it is reflected back to the waveguide due to the discontinuity present at the waveguide aperture. Since electric and magnetic fields of the dominant mode are orientated in specific directions, the reflected dominant mode of wave should be dependent on the anisotropic parameters of the material. Thus, by measuring the reflection coefficient of the dominant mode at various orientations of the waveguide with respect to a reference axis of the material layer, the tensor permittivity of the anisotropic material can be determined.

To analyze this waveguide probe for material measurement, the EM fields inside the waveguide near the waveguide aperture is expressed as the sum of incident and reflected dominant modes plus higher-order modes. The EM field inside the material layer is expressed in terms of eigenmodes for the anisotropic material case and Hertz potentials for the isotropic case. When the tangential components of electric and magnetic fields in the waveguide and the material layer are matched at the waveguide aperture, two coupled electric field integral equations (EFIE) with transverse components of the aperture electric field as unknowns can be derived. After the transverse components of the aperture electric field are solved from the coupled EFIE by Galerkin's method, the reflection coefficient of the dominant mode can be determined. Since the reflection coefficient of the dominant mode is an implicit function of tensor permittivity, we can inversely determine the tensor permittivity if the reflection coefficient of the dominant mode in the waveguide is measured experimentally.

An experimental setup was constructed with a waveguide system terminated on a large conducting flange on which a material layer can be placed. The reflection coefficient or the input impedance of the dominant mode of the waveguide terminated on a material layer is measured at the X-band using a network analyzer (HP 8720B). The measured reflection coefficient is then used to inversely determine the EM parameters of the material.

## DIELECTRIC AND MAGNETIC RELAXATION MODELS

James Baker-Jarvis and Richard G. Geyer  
National Institute of Standards and Technology  
Electromagnetic Fields Division, MS 813.08  
Boulder, CO 80303

Relaxation is observed in a wide variety of processes, for example, in response to magnetic, nuclear, and mechanical driving fields. Relaxation is a result of microscopic transitions between internal states and of an interaction with a thermal reservoir. If an external field, such as an electric field, is applied to a material, the material responds by adjusting the position of dipoles, higher multipoles, and free charge. At low frequencies, dipoles in a material respond with the applied field, whereas at higher frequencies the response lags the field. The resultant motion, the basis of dielectric relaxation, is analogous to a driven, damped harmonic oscillator. Energy is removed from the driving source by internal friction and by energy storage in the dielectric. Dipolar orientation can be altered by both driving field interactions and thermal effects. When simultaneous fields such as electric and magnetic are applied, the problem becomes more complex. A study of electrodynamic relaxation phenomena requires the analysis of ensembles of particles, and is based on Langevin or Fokker-Planck equations.

In this paper we examine dielectric and magnetic relaxation models, starting with Debye and Bloch equations and gradually increasing the complexity of the underlying assumptions. Generalizations of the Debye and Bloch equations of motion are presented which include memory effects. The generalized equations are shown to consist of reversible and irreversible components. The irreversible terms increase the entropy of the system, whereas the reversible terms do not directly influence the entropy. Using the algebra of Poisson brackets, expressions are derived for the reversible components in terms of field quantities.

**TIME DOMAIN METHOD FOR  
MATERIALS CHARACTERIZATION USING MICROSTRIP  
FIELD APPLICATORS**

D. Infante, J. Ross and D. P. Nyquist  
Department of Electrical Engineering  
Michigan State University  
E. Lansing, MI 48824

Microstrip and stripline field applicators have found increasing use for broadband measurement of the electromagnetic properties of materials. Frequency-domain calibration methods for field applicators have been developed which require measurements of a short located at three different positions within the applicator, and two measurements of the empty applicator.

Recently there has been an increased interest in high temperature measurements of the electromagnetic properties of materials at microwave frequencies. Because of its simple design, the microstrip field applicator is well suited for making such measurements. However, due to the complex propagation-mode spectrum associated with the microstrip, use of the frequency domain method with the microstrip has been limited to characterizing low permittivity, low loss materials. In addition, the frequency domain calibration method becomes cumbersome and of questionable accuracy for high temperature measurements, requiring that the applicator be heated and cooled several times to allow placement of the various standards. Multiple heating/cooling cycles limit the lifetime of the applicator and increase measurement time and cost. It has therefore become desirable to perform calibrations using a minimum number of standards.

The number of standard measurements required for calibration can be reduced by taking advantage of the inherent properties of the time-domain response of the field applicator. By careful design of that applicator and use of time-domain windowing techniques, the applicator can be calibrated with the measurement of only one short and one measurement of the empty applicator. This greatly reduces calibration time and measurement uncertainties caused by misplacement of the shorts and sample materials. In addition, the use of time-windowing techniques may permit the characterization of a wider variety of materials using the microstrip applicator.

This paper will discuss a calibration method for microstrip field applicators using time domain principles and will provide a comparison of material properties measured using both the time domain method and the usual frequency domain method.

# Microwave Level Gauging System

W. Guo\*, S. Stuchly and K. Caputa

Department of Electrical and Computer Engineering

University of Victoria

Victoria, BC, Canada V8W 3P6

Measuring and controlling liquid level in storage tanks and processing vessels is becoming more and more important in modern industrial processes. The level measurement requirements in tanks often exceed those in ordinary process level measurements and several level measuring techniques have been developed. Recently, use of microwave techniques for this application has been studied by many workers and a few microwave level gauging system (MLGS) have been developed. Resistance to harsh environment, versatility of measuring schemes and high precision make MLGS advantageous over other methods.

The MLGS consists of two units: a processor and a transmission medium. The processor allows for transmitting EM wave as well as processing the received echo signal. Two basic transmission media have been used: free space and metallic waveguides. The advantages of free space are non-contacting monitoring and simplicity of hardware. Sensitivity to the parasitic reflections and the requirement of a narrow beam antenna are the disadvantages. Metallic waveguides are free of parasitic reflections, however, due to the closed boundary structure, the meniscus effect is inevitable.

A novel X band microwave level gauging system is presented. Two kinds of surface waveguides, dielectric rod and Goubau line, are used as the transmission media and multiple frequencies continuous wave (MFCW) technique is adopted in the processor. Being open boundary guided structures, surface waveguides are free of meniscus effect and insensitive to the parasitic reflections. By carefully choosing the dimension and dielectric materials of the structure, the propagation loss of surface waveguides can be made comparable to that of metallic waveguides. In this paper, the design aspects of the proposed MLGS are described. First, a brief review of the surface waveguides is presented. This includes the analysis of loss, power containment and the design of the launching devices for surface waveguides. It also includes the theoretical comparisons of the chosen surface waveguides with several other transmission lines. Then, the design aspects of experiment sets up and the measurement results are presented. The experiments are concentrated on the measurement of the propagation losses and the reflection coefficient at the interface of liquid surface and measurement environment atmosphere along the guiding structure. Finally, results of level measurements for various liquids with proposed approach is presented and the accuracy and error correction are discussed.



THURSDAY AM URSI-B SESSION TH-U34

Room: Kane 120

FINITE ELEMENT / BOUNDARY ELEMENT

Chairs:	Z.J. Cendes, Carnegie Mellon University; J.W. Parker, California Institute of Technology	
8:20	Tree-Cotree Methods for Electromagnetic Field Computation <i>*J. Manges, Z.J. Cendes, Carnegie Mellon Univ.</i>	400
8:40	On Feed Modeling of Cavity-Backed Antennas in the Context of the Finite Element Method <i>*J. Gong, J.L. Volakis, Univ. of Michigan</i>	401
9:00	Accuracy in EM Fields Calculations Using a Combined FE-IE Approach <i>*C. Zuffada, T. Cwik, V. Jamnejad, California Inst. of Technology</i>	402
9:20	Vector Finite Element Modeling of Purely Physical Modes in a Ferrite-Filled Cylindrical Cavity <i>*J. Parker, California Inst. of Technology</i>	403
9:40	Scattering Analysis of an Arbitrarily Shaped Material Cylinder (2D) Using FEM-BEM Method <i>*M.D. Deshpande, Vigyan Inc.; C.R. Cockrell, NASA Langley Research Center</i>	404
10:00	Break	
10:20	A Three-Dimensional Bymoment Method Approach for the Analysis of Electromagnetic Scattering <i>R. Lee, The Ohio State Univ.; Ü. Pekel, Univ. of Illinois</i>	405
10:40	Comparison of Electric and Magnetic Field Formulations in Finite Element Modeling <i>*T. Cwik, V. Jamnejad, C. Zuffada, California Inst. of Technology</i>	406
11:00	Analysis of a Multilayered, Doubly-Periodic, Frequency Selective Structure Using an FEFD Technique Based on Edge-Elements <i>*Ü. Pekel, K. Mahadevan, R. Mittra, Univ. of Illinois</i>	407
11:20	3D Hybrid Finite Element Analysis of Scattering and Radiation by a Class of Waveguide-Fed Structures <i>*J. Jin, Univ. of Illinois</i>	408
11:40	Accurate FEM Analysis of Quasi-TEM Transmission Lines with Field Singularities <i>*J.M. Gil, J. Zapata, Universidad Politécnica de Madrid</i>	409

## Tree-Cotree Methods for Electromagnetic Field Computation

John Manges\* and Zoltan J. Cendes  
Department of Electrical and Computer Engineering  
Carnegie Mellon University  
Pittsburgh, PA 15213

Edge elements are often used with finite element or finite difference methods to model electromagnetic field problems. These elements have the advantage of representing the nullspace of the curl-curl operator properly and thereby avoiding the problem of spurious modes that are generated by using conventional node-based elements. Although the nullspace of the curl-curl operator is modeled correctly with edge elements, these elements do not eliminate this nullspace. Consequently, the matrix representing the curl-curl operator is singular. This singularity is manifest in a large number of zero eigenvalues in the discrete matrix and in an attendant increased size and increased computational resources required to compute resonant frequencies. It also sometimes leads to slow convergence with iterative solvers such as the conjugate gradient method when computing driven problems. (The fact that the conjugate gradient method correctly solves the singular curl-curl matrix was established by Barton and Cendes (*J. Appl. Phys.*, 61,3919-3921,1987)).

Albanese and Rubinacci (*Int. J. Num. Meth. Eng.*, 26, 515-532, 1990) have shown that the nullspace of the curl-curl operator is correctly eliminated with edge based finite elements by partitioning the edges in the mesh into a tree-cotree structure. In magnetostatics problems where one is solving for the vector potential  $A$ , one can set the values of the vector potential on an arbitrary tree of the mesh to zero. This is because the gauge of the vector potential is undefined and setting values of  $A$  on the tree does not impose the curl of  $A$  on any face of any finite element. Consequently, the edge values on the cotree of the mesh provide the independent set of variables for the curl operator and are uniquely determined once the tree values of the vector potential are eliminated.

This paper extends the approach taken by Albanese and Rubinacci to compute electric and magnetic fields directly for high-frequency applications. In solving for the vector potential in magnetostatics, one is free to assign arbitrary values, including zero, to the vector potential on the tree. This is not possible when solving for the electric or magnetic field since field values are never arbitrary. Instead, the values of  $E$  or  $H$  on the tree are related by taking a linear combination to the values of  $E$  or  $H$  on the cotree. It is possible to eliminate the tree values of  $E$  or  $H$  in favor of the cotree values. One may then solve for the unique and linearly independent values of  $E$  or  $H$  on the cotree and, subsequently, evaluate  $E$  or  $H$  on the tree by taking a linear combination of the cotree values. We show that the finite element matrix equation is greatly reduced in size by this process and that the zero eigenvalues in the original discrete curl-curl matrix are eliminated. Computations show that imposing the relationship between fields on the tree and the fields on the cotree of the mesh eliminates the nullspace of the curl-curl operator and results in a nonsingular matrix.

1994 URSI Radio Science Meeting (Seattle)

## On Feed Modeling of Cavity-backed Antennas in the Context of the Finite Element Method

J. Gong\* and J. L. Volakis  
Radiation Laboratory  
Department of Electrical Engineering and Computer Science  
The University of Michigan  
Ann Arbor, Michigan 48109-2122

### Abstract

It has been demonstrated that the hybrid finite element method (FEM) is an accurate and efficient approach for scattering and radiation analysis of printed antenna configurations. For antenna applications, typically a transmission line or a simple probe model excitation is assumed for simplicity. However, the simple probe model for the coaxial cable feed is valid only for electrically thin substrates. For thick substrates, sophisticated techniques and models are needed. Also, a high-rate sampling around the feed is usually required for the FEM analysis. This is an undesirable choice, since for many configurations the system condition worsens and the number of iterations increases significantly. Most importantly, this usually leads to a prohibitively large calculation cost (in terms of CPU time or number of unknowns) even for some small physical problems. Some other techniques have been seen in the literature for coax feed modeling, unfortunately they are either inefficient, inaccurate or incompatible with FEM applications. However, the FEM itself offers new possibilities for feed modeling improvement, and in this presentation, an efficient feed model will be described in the context of the finite element method for radiation by a coax-fed microstrip antenna or arrays. Specifically, a special shape function simulating the physical coaxial cable mode will be employed for field expansion inside the cable. Both incident and reflected waves within the cable are taken into account in the formulation. A combination approach to associate the fields below and above the cable-cavity junction will also be discussed in the presentation.

The detailed formulation and numerical considerations will be presented in the meeting together with some validation examples.

## Accuracy in EM Fields Calculations using a Combined FE-IE Approach

Cinzia Zuffada \*, Tom Cwik and Vahraz Jamnejad

Jet Propulsion Laboratory  
California Institute of Technology

4800 Oak Grove Dr., Pasadena, CA 91109

### ABSTRACT

A hybrid finite element - integral equation (FE-IE) approach has been developed to calculate the EM fields scattered by inhomogeneous 3D-bodies of arbitrary shape. It couples a 1st-order edge-based FE representation in a volume containing the scatterers and bounded by a surface of revolution, to an IE on the surface, to properly account for the FE mesh truncation. Hence, it solves for the component of either H or E along each edge in the FE mesh, as well as both E and H tangential to the surface of revolution bounding the problem domain. The code has been validated for RCS calculations on several objects with good results. Its applicability to calculate accurate fields in the near-zone of and inside penetrable scatterers is investigated here. Starting with the solution for the tangential field components at the surface of revolution, the fields are calculated everywhere in the space surrounding the problem domain. Similarly, inside the mesh volume, starting with their values along the edges, a proper linear combination yields the fields at any location, according to the chosen FE representation. Issues such as the scatterer's geometry modeling, as well as the choice of mesh density and mesh geometry for accurate field description are discussed. In particular, the impact on accuracy of coupling the FE representation to the IE representation on the surface of revolution is analyzed. Specifically, the two (different) representations need to be consistent, in terms of modeling of field variation on the surface of revolution, especially about its poles. Examples are provided for a variety of scatterers for which either analytical results or alternative numerical results are available.

## VECTOR FINITE ELEMENT MODELING OF PURELY PHYSICAL MODES IN A FERRITE-FILLED CYLINDRICAL CAVITY

J. W. Parker, Jet Propulsion Laboratory, California Institute of Technology  
Pasadena, California, USA 91109

Modes of a fictitious ferrite-filled perfectly conducting cavity are obtained by modeling the fully 3-D electric fields using Whitney edge elements. The cavity is modeled by a tetrahedral mesh with unknowns linked with each lattice edge representing the component of the field tangential to that edge. The perfectly conducting walls are represented by setting the included tangential electric field values explicitly to zero. A Hermitian matrix  $[S]$  is computed by combining the curl of the testing function, curl of electric field, and the Hermitian magnetization tensor. We solve the generalized eigenvalue problem  $[S]d = k^2 [T]d$ , for eigenvalues  $k^2$  and electric field coefficient eigenvectors  $d$ , where  $[T]$  is the positive definite matrix formed by combining the testing function and the electric field directly.

The 20 lowest order physical eigenvalues ( $5 < k^2 < 25$ ) differ from an analytic/transcendental solution by  $< 3\%$  for the case where the cavity is an axially-magnetized cylinder of unit radius, two units altitude, with unit relative permeability on the diagonal,  $\pm 0.1j$  off diagonal, for finite elements with typical edge length 0.3 units ( $\sim 1700$  unknowns). In addition, a finite number of  $k^2 \sim 0$  modes are computed, corresponding to the infinite-dimensional space of zero-frequency zero-curl divergence fields admitted by the curl-curl operator. It is notable that these modes compute to values of  $k^2 < 10^{-5}$ , demonstrating that Whitney elements may be used to represent fields in ferrite media with near-perfect separation of physical and non-physical modes. This indicates the ability to model fields in ferrite device and scattering problems with no corruption from vector parasites.

## Scattering Analysis of an Arbitrarily Shaped Material Cylinder (2D) Using FEM-BEM Method

*M. D. Deshpandè\*, Vigyan Inc., Hampton, VA.,*

*C. R. Cockrell, NASA Langley Research Center, Hampton, VA.*

### Summary

This paper presents scattering characteristics of an arbitrarily shaped infinite material cylinder (2D) using Finite Element Method (FEM) in conjunction with the Boundary Element Method (BEM). The material cylinder is assumed to be excited by either TE or TM polarized plane wave at normal incidence.

For mathematical modeling, the first step is to assume the cylinder to be enclosed by a fictitious, conformal boundary slightly away from the outer boundary of the cylinder. The next step is to discretize the surface  $S$ , enclosed by the curve  $\Gamma$  into linear triangular subdomains as shown in figure. For the TM case, the total electric field inside the region enclosed by  $\Gamma$  is obtained by using the weak form of the wave equation given by

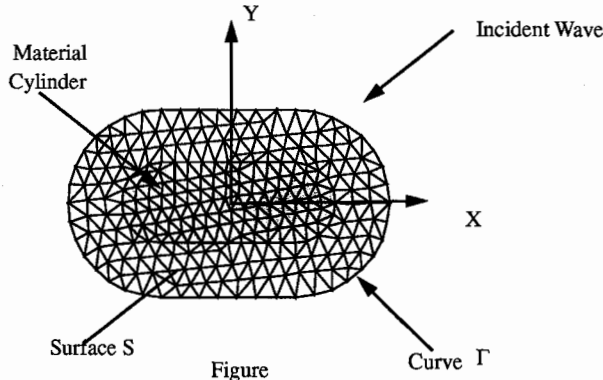
$$\iint \left[ \nabla T \cdot \nabla E_z^t - k_0^2 T E_z^t \right] ds = \int T \nabla E_z^t \cdot \hat{n} d\Gamma \quad (1)$$

where  $T$  is a testing function. The normal derivative of  $E_z^t$  over  $\Gamma$  required in equation (1) is obtained using BEM. The total field and its normal derivative over  $\Gamma$  are related through following variational equation

$$\frac{V_j}{2} = - \sum_{i=1}^P V_i \int \phi_i(\Gamma) q^* d\Gamma + \int \frac{\partial E_z^t}{\partial n} u^* d\Gamma \quad (2)$$

where  $V_j$  is the value of  $E_z^t$  at the  $j$ th node on  $\Gamma$ ,  $\phi_i(\Gamma)$  is a linear function,  $q^* = \frac{\partial u^*}{\partial n}$ , and  $u^*$  is the dominant solution of  $\nabla^2 u^* + k_0^2 u^* = \delta_{jj}$ . Substituting the normal derivative of  $E_z^t$  over  $\Gamma$  from equation (2) in (1), equation (1) is solved for  $E_z^t$ .

The computational code using the above mathematical model is first validated with earlier published data. The paper will include several examples of RCS computations of cylinders of various shapes.



## **A Three-Dimensional Bymoment Method Approach for the Analysis of Electromagnetic Scattering**

R. Lee  
ElectroScience Laboratory  
The Ohio State University  
1320 Kinnear Road  
Columbus, Ohio 43212

Ü. Pekel  
Electromagnetic Comm. Laboratory  
University of Illinois  
1406 W. Green Street  
Urbana, IL 61801

The finite element method (FEM) can be used to analyze two- or three-dimensional electromagnetic scattering problems in unbounded regions. However, the main difficulty that is encountered in the application of FEM to scattering problems is the fact that FEM is a differential-based method which must be formulated as a boundary value problem. This implies that one must define an artificial boundary surface of finite size at which the finite element mesh is truncated. The field solutions which are interior and exterior to the mesh must then be coupled in such a way that both the continuity conditions at the artificial boundary and the radiation condition at infinity are satisfied.

One can find various mesh truncation techniques in the literature, such as the ones which employ certain approximate absorbing boundary conditions (ABC's) on the artificial boundary surface, the hybrid finite element method (HFEM) technique, or the unimoment method approach. In this work, a three-dimensional bymoment method approach is developed for the FEM analysis of scattering problems (A.C. Cangellaris and R. Lee, *IEEE Trans. Antennas Propagat.*, AP-38, 1429-1437, Sept. 1990). The boundary truncation scheme of this approach focuses on two z-directed Hertz vector potentials instead of three Cartesian field components in order to decouple the interior and exterior region field solutions on the truncation boundary surface, which conforms geometrically to the surface of the scattering object. The boundary conditions for relevant field components are formulated on the truncation surface in terms of series of appropriate expansion functions which are weighted by unknown coefficients. The FEM field solutions, which pertain to these boundary conditions, are calculated in the interior region by treating the scattering problem as a Neumann-type boundary value problem. The FEM solutions are then subjected to a numerical "coupling" procedure, which is carried out on a second boundary surface that is conformal to the first one and is completely enclosed by it. Once the set of expansion coefficients is determined as a result of this procedure, it is used to express the total field solution as an appropriate linear combination of the interior region FEM field solutions. The three-dimensional bymoment method is a numerically efficient approach for the analysis of electromagnetic scattering from inhomogeneous, non-conducting, and geometrically complex objects. The numerical accuracy of this method is demonstrated by means of comparison to analytical results which are available for spherical scatterers, and to numerical results which have been obtained with alternative numerical techniques for other problem geometries.

## Comparison of Electric and Magnetic Field Formulations in Finite Element Modeling

*Tom Cwik\*, Vahraz Jamnejad, Cinzia Zuffada*

Jet Propulsion Laboratory  
California Institute of Technology  
Pasadena, CA 91109

A coupled finite element-integral equation technique has been developed for modeling fields scattered from inhomogeneous, three-dimensional objects of arbitrary shape. The method incorporates a finite element model of fields in and near the scatterer with an integral equation that models fields on an arbitrary surface of revolution very near and circumscribing the scatterer. The integral equation is used to truncate the computational mesh without approximation (T. Cwik, V. Jamnejad and C. Zuffada, IEEE-APS Symposium, June 1993). This method has been recently extended to include antenna radiators.

The formulation of this technique begins with the wave equation for either the magnetic or electric fields. Either field can be chosen in deriving a consistent set of equations that is a solution of Maxwell's equations. The choice of field is typically made depending on the materials present. For example, if the scatterer is a closed perfect conductor, using the magnetic field wave equation results in a natural enforcement of the boundary condition zeroing the tangential electric fields on the surface of the conductor. Yet, if the perfect conductor becomes electrically thin, or is a zero thickness plate, difficulties can arise in meshing the object and properly solving for the tangential magnetic fields on either side of the conductor. In this case it becomes expedient to use the electric field formulation and explicitly enforce the boundary condition zeroing tangential electric fields on the surface of the conductor. Explicit enforcement of this boundary condition requires modifications to the formulation not needed in the magnetic field formulation. Similar differences can arise when the scatterer consists of only dielectric or only magnetic materials, and again it can be preferable to use either the magnetic or electric field formulation.

This talk will present comparisons of the two formulations for scatterers composed of different materials. Numerical implementations based on vector, edge based tetrahedral elements and the coupled finite element-integral equation technique will be discussed. Results and necessary extensions of the formulation will be presented.

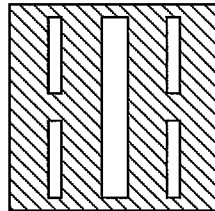
## Analysis of a Multilayered, Doubly-Periodic, Frequency Selective Structure using an FEFD Technique Based on Edge-Elements

Ü. Pekel\*, K. Mahadevan, and R. Mittra  
Electromagnetic Communication Laboratory  
University of Illinois, Urbana, IL 61801

The finite element method (FEM) can be applied to analyze a wide variety of problems in electromagnetics. In this work, a finite element frequency domain method (FEFD) is used to investigate the spatial filter characteristics of a frequency selective structure, which comprises several layers of lossless/lossy dielectric materials, and a perfectly-conducting, doubly-periodic screen of finite thickness which resides on these layers. The unit cell for this structure is shown in Fig. 1, where it is assumed that the slots in the conducting screen are filled with air. The FEFD technique that is employed to analyze the frequency selective structure is based on hexahedral edge-elements, and does not require the use of commercial mesh generation packages. The effect of the thickness of the screen on the transmission and reflection characteristics of the frequency selective structure is investigated over a frequency band ranging from 2.0 GHz to 8.0 GHz for an incident magnetic field that is polarized in the direction parallel to the slots in the screen. The results show that the finite screen thickness can indeed affect the characteristics of the frequency selective structure near the resonances, particularly in those cases where the screen thickness is large. Even for moderately thick screens, however, distinct differences are observed in comparison to the case of zero screen thickness, both in terms of the location of the resonances and the respective levels of the transmission and reflection coefficients. Consequently, for such frequency selective structures, one should be cautious when using MoM-type programs which are designed to analyze thin-screen FSS's, and do not account for the effect of finite screen thickness.



Side View



Top View

■ Epsr.=(11.812, -0.112)    ▨ Epsr.=(10.24, 0.0)    ▩ Epsr.=(9.333, 0.0)

Figure 1.

## 3D HYBRID FINITE ELEMENT ANALYSIS OF SCATTERING AND RADIATION BY A CLASS OF WAVEGUIDE-FED STRUCTURES

Jianming Jin

Department of Electrical and Computer Engineering  
University of Illinois at Urbana-Champaign  
Urbana, IL 61801-2991

Waveguide-fed structures are a class of important radiating structures found many applications in antenna and communication engineering. Such structures include horn and slot antennas and coaxial line-fed patch antennas, and are characterized by a waveguide with an opening(s) which radiates electromagnetic wave into free space through a transition region. To improve the radiation efficiency or protect the antenna, the transition region is often filled with some dielectric material, making its analysis rather difficult. The purpose of this paper is to present a three-dimensional hybrid finite element method for the analysis of the radiation and scattering properties of this class of structures.

In the proposed method, we divide the entire solution region into three regions: the exterior region, the transition region, and the waveguide region. The field in the exterior region is formulated using a boundary integral equation which is then converted to an exact global boundary condition for the field at the interface between the exterior and transition regions. The field in the waveguide region is formulated in terms of waveguide modes, from which an exact absorbing boundary condition is also derived for the field at the interface between the waveguide and transition regions. With a complete knowledge of the boundary conditions for the transition region, an equivalent variational formulation can be obtained for the field in the transition region. This variational problem is then solved using the finite element technique in conjunction with edge elements for a suitable expansion of vector fields. All antenna and scattering parameters can be calculated with a knowledge of the fields at the interfaces between the three regions.

The major advantages of this method are its versatility and accuracy. By virtue of the finite element technique, the method is applicable to the radiating structures consisting of a complicated transition region of arbitrary shape and material composition. Because of the employment of the exact boundary integral equation and waveguide absorbing boundary condition, the method is accurate except for numerical discretization errors. The accuracy of the method is particularly important for antenna characterization since antenna parameters are very sensitive to the errors in the near field calculation. Furthermore, since the waveguide absorbing boundary condition contains all high order modes, the interface between the waveguide and transition regions can be placed as close to geometry or material irregularities as possible, keeping the volume of the transition region to a minimum.

## ACCURATE FEM ANALYSIS OF QUASI-TEM TRANSMISSION LINES WITH FIELD SINGULARITIES

\* J.M.Gil, J.Zapata

Grupo de Electromagnetismo Aplicado y Microondas  
E.T.S.I.T de Telecomunicación U.P.M  
28040 Madrid Spain

Quasi-TEM structures consisting of a number of conducting strips with sharp edges, such as microstrips lines or coupled multiconductor lines, are commonly found in practice. In these configurations some of the field components become infinite at the edges producing a slow FEM convergence rate and inaccurate prediction of parameters such as characteristic impedance, couplings, etc. Inclusion of the known singular field behavior in the numerical method increases the rate of convergence and computation accuracy.

In microwave transmission lines with inhomogeneous dielectric and sharp metal edges, the order of field singularity depends on the relation between the dielectric permittivities, and it can be calculated from the Meixner's theory. On the other hand, the quasi-TEM model yields satisfactory results for the majority of the practical computations.

In this work, we describe a method to accurately cope with field singularities in the quasi-TEM analysis of multielectric and/or multiconductor transmission lines by using the Finite Elements Method. To achieve this goal, we employ singular elements which are introduced in the mesh surrounding singular points.

Additionally, a new transition element, able to approximate the field behavior when the singular point lays outside the element domain, will be proposed as an interface between singular and standard elements.

In order to assess the improvement on the rate of convergence of FEM and the approximation of fields near the singular point, several examples with different orders of field singularity have been analyzed, and results will be presented.



## THURSDAY AM URSI-B SESSION TH-U35

Room: Savery 243

### ANTENNAS II

Chairs: K.M. Luk, City Polytechnic of Hong Kong; M.D. Deshpande, Yigyan, Inc.

8:20	Radar Cross Section of a Ferrite Tuned Cavity Backed Slot <i>*D.M. Kokotoff, E.-B. El-Sharawy, J.T. Aberle, Arizona State Univ.</i>	412
8:40	Slot Antennas Backed by a Dielectric-Filled Cavity <i>*H. Ostner, T. Krems, J. Detlefsen, Technische Universität München</i>	413
9:00	Theoretical and Experimental Analysis of Surface Wave Excitation in Planar Slot Antennas <i>*M.O. Thieme, E.M. Biebl, Technische Universität München</i>	414
9:20	Numerical Study of Aperture Antennas Backed by a Rectangular Waveguide or Cavity <i>*H. Moheb, L. Shafai, Univ. of Manitoba</i>	415
9:40	The Method of Lines for the Analysis of Cylindrical Antennas <i>*R. Pregla, Fern Universität</i>	416
10:00	Break	
10:20	Radiation Characteristics of an Arbitrarily Shaped Aperture in Half Space Excited by a Rectangular Waveguide Using a Combined FEM/MOM Approach <i>*C.J. Reddy, M.D. Deshpande, C.R. Cockrell, F.B. Beck, M.C. Bailey, NASA-Langley Research Center</i>	417
10:40	FDTD Computation of Active Impedance of an Array of Vivaldi Quad Elements <i>E.T. Thiele, C.E. Reuter, A. Taflove, Northwestern Univ.; M. Piket-May, Univ. of Colorado</i>	418
11:00	Analysis of Aperture Coupled Rectangular Dielectric Resonator Antenna Using the FDTD Method <i>*S. M. Shum, K.M. Luk, City Polytechnic of Hong Kong</i>	419
11:20	FDTD Analysis of Rectangular Dielectric Resonator Antennas <i>*K.P. Esselle, Macquarie Univ.</i>	420
11:40	Analysis of Square Fed Patches with Different Feeding Excitation <i>H. Saboundji, J.P. Daniel, D. Thouroude, Univ. of Rennes I; S. Toutain, OEST ENSTBr (Brest)</i>	421
12:00	Optimization of Time-Domain Antennas <i>*J.-H. Wang, L. Jen, Southwest JiaoTong Univ.</i>	422

## Radar Cross Section of a Ferrite Tuned Cavity Backed Slot

David M. Kokotoff\*, El-Badawy El-Sharawy, and James T. Aberle  
Department of Electrical Engineering  
Telecommunications Research Center  
Arizona State University  
Tempe, Arizona 85287-7206

The cavity backed slot (CBS) antenna is an attractive candidate for aerospace applications due to its lightweight, low profile, and conformal attributes. However, conventional CBS antennas are usually limited to UHF and higher frequencies due to size constraints. The antenna size can be reduced by loading the cavity. Unfortunately, cavity loading reduces the antenna's bandwidth and increases its weight. An alternative approach is to load the cavity with ferrite. Besides reducing the size of the antenna, the material properties can be varied with the application of an external bias field.

The concept of magnetically tuning a ferrite loaded CBS antenna is not new. However, many investigators assume that the ferrite material is isotropic with a permeability that varies with the DC magnetic bias field, i.e. the permeability tensor is replaced with an effective permeability. This assumption simplifies the field equations, but ignores some gyromagnetic properties of ferrite. In this work, a *full wave* solution is utilized, which is an extension of our previous work for a two dimensional CBS antenna (Lopez, et. al., 1993 *IEEE AP-S Int. Sym. Dig.*, pp. 1175-8). Unlike previous work which concentrated on the effective permeability of the ferrite, this research focuses on exploitation of magnetostatic surface and volume wave modes. Use of these modes may allow the antenna to operate at much lower frequencies than predicted by the effective permeability of the ferrite.

The antenna comprises an aperture in an infinite ground plane backed by a cavity which is filled with various ferrite and dielectric layers. The structure is tuned by varying a DC magnetic bias field in the plane of the layers. The antenna is analyzed using the method of moments wherein the Green's functions are formulated using the spectral domain transmission matrix approach (El-Sharawy and Jackson, *IEEE Trans. MTT*, pp. 1071-9, June 1988).

By examining the scattering response of the antenna, one may determine resonant frequencies and qualitatively assess the antenna behavior. A discussion of dynamic, as well as, magnetostatic volume and surface wave mode resonances will be presented at the conference.

## SLOT ANTENNAS BACKED BY A DIELECTRIC-FILLED CAVITY

H. Ostner\*, T. Krems, J. Detlefsen

Lehrstuhl für Hochfrequenztechnik

Technische Universität München, 80290 München, Germany

There has been shown growing interest in planar slot antennas especially in the millimeter-wave frequency range due to the simplicity of fabrication and the possibility of monolithic integration of active devices. On the other hand it is well known that the efficiency of these slot antennas suffers from parasitic excitation of surface waves. Furthermore these surface waves can cause strong mutual coupling and eventually scan blindness in array configurations.

Up to now most of the investigations of planar active slot antennas have been directed to laterally open antenna configurations with or without backside metallization, without taking into account the finite substrate size. In this presentation we discuss planar slot antennas on an infinite ground plane backed by a dielectric-filled rectangular cavity. This seems to be a more appropriate design since chip area is expensive and therefore kept to a minimum especially when semiconductors such as silicon or gallium-arsenide are used to integrate active devices, e. g. Impatt-diodes, monolithically. In addition mutual coupling between adjacent elements can be prevented.

Using the equivalence principle the slot radiating in free space and the cavity are treated separately by spectral domain methods. This derivation is similar to that introduced by A. Hadidi and M. Hamid (IEE Proc., Pt. H, pp. 139-146, April 1989). In contrast to them we have focussed on full-wavelength slots providing low resistances in the center of the slots, the location of the active device. Additionally dielectric and ohmic losses of the dielectric-filled cavity and the ground plane are taken into account.

Calculated results will be presented showing input impedances in the case of silicon or gallium-arsenide filled cavities along with experimental results confirming the validity of the calculations. Further the influence of cavity depth and slot geometry on the input impedance will be discussed.

# THEORETICAL AND EXPERIMENTAL ANALYSIS OF SURFACE WAVE EXCITATION IN PLANAR SLOT ANTENNAS

Markus O. Thieme\* and Erwin M. Biebl

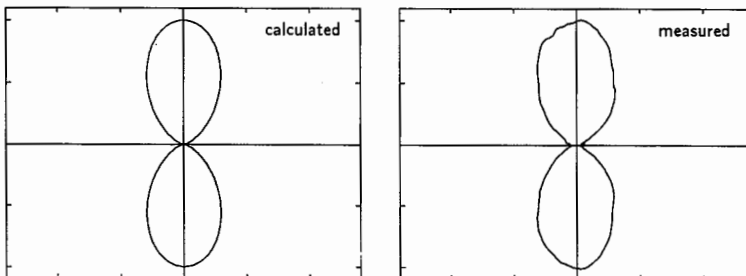
Lehrstuhl für Hochfrequenztechnik, Technische Universität München  
Arcisstr. 21, 80333 München, Germany

The radiation efficiency of planar antennas is mainly determined by the excitation of surface wave modes. In conductor backed planar slot antennas the TEM parallel plate waveguide mode is excited. This configuration is often chosen for monolithic millimeterwave integrated circuits, where the back conductor acts as a heat sink. The antenna impedance depends strongly on the substrate thickness (H. Ostner, E.M. Biebl, 1993 *AP-S Symp. Dig.*, pp. 612-615) indicating that the excitation of the TEM mode is also governed by this parameter. In this paper we report theoretical and experimental investigations of the excitation of the TEM modes in conductor backed planar slot antennas.

The magnetic currents in the aperture of the slot antenna are obtained by solving an integral equation using a MoM formalism in the spectral domain. Based on the magnetic current distribution, the radiation pattern of the antenna is calculated using a far field approximation of the Sommerfeld type integrals for both the radiation and TEM modes. The knowledge of the far field pattern of the TEM modes is important for the design of monolithic integrated circuits in order to minimize the mutual coupling between the circuit elements. The values of the power carried by radiation,  $P_r$ , and by the TEM mode,  $P_{TEM}$ , are calculated by integrating the Poynting vector over a hemisphere and a cylinder surface, respectively. Neglecting dielectric and conductor losses, the radiation efficiency is given by  $\eta = P_r / (P_r + P_{TEM})$ .

Far field patterns of the TEM modes are measured at X-band frequencies. A grounded dielectric slab is covered by a metal plate with the slot antenna. A tapered transition at the edge of the dielectric slab eliminates reflections. Port 1 of an HP8510 network analyzer is connected via a coaxial feed line at the center of the slot. The surface wave is measured using a coaxial probe, which is connected to port 2 of the analyzer. The separation between antenna and probe is 25 cm, and the azimuth angle is varied.

Sample calculated and measured far field patterns of a TEM mode excited by a full wave slot antenna are depicted in the figures below. With respect to the value of the main lobe the measured far field pattern is predicted within 5%. The dependence of the radiation efficiency and the radiation pattern on various geometrical and electrical parameters will also be presented.



**NUMERICAL STUDY OF APERTURE ANTENNAS  
BACKED BY A RECTANGULAR WAVEGUIDE OR CAVITY**

**H. Moheb\*, L. Shafai**

*Department of Electrical & Computer Engineering  
University of Manitoba, Winnipeg, Manitoba, Canada R3T 2N2*

The general problem of coupling through apertures have applications in slotted arrays, directional couplers, microstrip lines, etc. The coupling problem is usually formulated for the unknown tangential electric field in the aperture. Of these, the moment method is especially attractive because it inherently deals with apertures of arbitrary shape and size. It has been used extensively to examine the problems of two waveguides coupled through a rectangular slot, using pulse basis functions and point matching.

In this paper, we apply equivalence principle and the generalized network formulation [R. F. Harrington, and J. R. Mautz, *IEEE Trans., Antennas & Propagat.*, pp. 870-873, Nov. 1976] to model the tangential electric field of arbitrary apertures backed by a rectangular waveguide or cavity, in terms of equivalent magnetic currents. The result is an integral equation for the unknown aperture current. This integral equation is then reduced to a matrix equation using the method of moments [R. F. Harrington, *Field Computation By Moment Methods*, MacMillan, New York, 1968].

The formulation developed here allows the calculations of resonance frequency of an arbitrary aperture, the aperture admittance with guide dimensions appropriate for propagation of any mode, aperture gain, and its radiation characteristics. The aperture admittance can be easily calculated for different dielectric materials inside the waveguide, various number of slots, their shapes and also slot inclination angles.

The developed technique is then applied to several novel aperture antennas, such as crossed-slots, rectangular and square end-loaded, and centre-loaded crossed slot antennas backed by a waveguide or cavity. These antennas are easy to fabricate, are low loss, lightweight, and low cost. Their resonant frequency is a function of the physical dimensions of the waveguide and the slot, the shape of the slot, and the dielectric constant of the waveguide region.

For instance, one factor that affects the resonant frequency is the shape of the slot. Making the slot wider near the centre, increases its resonant frequency. On the other hand, loading the slot at both ends lowers its resonant frequency. The lower resonance frequency allows the use of smaller and/or air-filled cavities which results in wider antenna bandwidth and lighter weight. The slot shape also has direct effect on the radiation patterns and in particular the cross-polarized pattern. Therefore a study is undertaken to investigate their characteristics in particular the end-loaded and centre-loaded slots are reported in this paper. These antennas have potentials for M-SAT vehicle applications [F. Manshadi, *IEEE Symposium, APS*, vol. 3, 1991], and also are good radiators for use on high-speed aircrafts due to their low profile construction and weight [C. A. Lindberg, *IEEE Trans.*, *APS*, vol. 17, no. 5, sept. 1969].

# The Method of Lines for the Analysis of Cylindrical Antennas

Reinhold Pregla

Allgemeine und Theoretische Elektrotechnik, FernUniversität, D-58084 Hagen, Germany

## Abstract

In this paper a simple but very efficient and accurate procedure is described for the analysis of cylindrical antennas (Fig. 1). The fields will be calculated from the wave equation, which will be discretized in  $z$  direction to obtain an ordinary differential equation from the partial differential equation - as usual in the method of lines (MoL). Then the ODE is analytically solved on the discretization lines in  $\rho$  direction (see Fig. 1) in the source free regions. The solutions are Bessel (region I) and Hankel functions (region II). The arguments of these functions are complex because of the open structure, which is modelled by absorbing boundary conditions. The matching process with the source field in the slot gives the current distribution on the antenna and the input impedance. The conductivity of the dipole material needs not be ideal. Therefore loss resistances in the input impedances can be calculated. The behaviour of cylindrical antennas above a lossy plane (e.g. the not ideal earth) can be calculated, too. In Fig. 2 a diagram of the input impedance of a dipole is drawn. The results are compared with those given in Collin-Zucker: Antenna Theory (p. 366). Good agreement has been achieved. Taking into account losses for a dipole of copper with  $\kappa = 58 \Omega^{-1}\text{m/mm}^2$ , the dashed line curve was achieved. The loss resistance has the value of  $3 \Omega$  in the series type equivalent circuit for the  $2l = \lambda/2$  dipole and the value of  $151.8 \text{ k}\Omega$  in the parallel type equivalent circuit for the  $2l = \lambda$  dipole. Results for current distribution have been obtained, too. They are in best agreement especially with measured results because these calculations have taken into account the finite diameter of the dipole in a correct way.

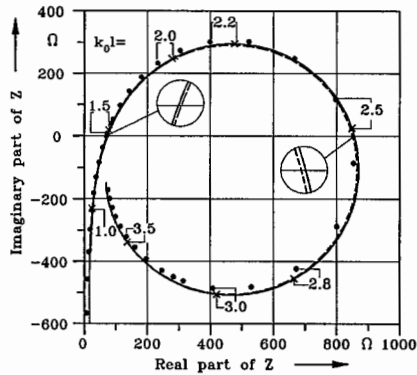
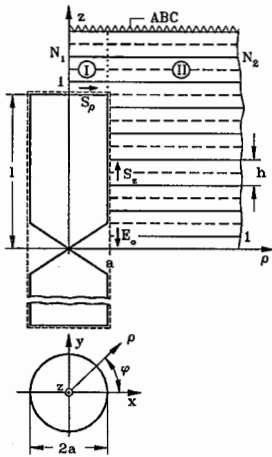


Fig. 2: Input impedance for a dipole as shown in Fig. 1  
 $a = 2.11 \text{ mm}$ ,  $l = 156.3 \text{ mm}$  ( $2 \ln l/a = 10$ )  
 $\times$  MoL     $\bullet$  King-Middleton (s. Collin-Zucker, p. 366)

Fig. 1: For the analysis of a cylindrical antenna - ABC: Absorbing Boundary Conditions  
 — Discretization lines for  $H_\phi, E_z, S_z$     - - - Discretization lines for  $E_\rho$

# RADIATION CHARACTERISTICS OF AN ARBITRARILY SHAPED APERTURE IN HALF SPACE EXCITED BY A RECTANGULAR WAVEGUIDE USING A COMBINED FEM/MoM APPROACH

C. J. Reddy\*, M. D. Deshpande, C. R. Cockrell, F. B. Beck and M. C. Bailey  
NASA-Langley Research Center, Hampton VA 23681, USA

## ABSTRACT

Radiation from rectangular waveguides opening onto a ground plane is of practical interest due to their applications in phased array antennas. Analysis of such antennas are restricted to apertures with regular shapes. In this paper a combined Finite Element Method and Method of Moments (FEM/MoM) technique is presented to analyze radiation from arbitrarily shaped aperture opening onto a ground plane, excited by a rectangular waveguide. The waveguide is assumed to be excited by the dominant  $TE_{10}$  mode. The Finite Element Method is employed to formulate the fields within the waveguide, and the fields external to the waveguide are expressed via the spectral domain radiation integrals over the aperture. The resulting equations are then combined using the boundary condition that the tangential fields across the aperture are continuous. The waveguide volume is discretized using tetrahedral elements, and hence, the aperture is automatically discretized by triangular patches. For the sake of numerical implementation, the length of the waveguide is assumed to be finite, but long enough, so that the reflected wave at the input plane consists of only the dominant  $TE_{10}$  mode. To validate the analysis, numerical data for radiation pattern of a rectangular waveguide opening onto a ground plane are calculated and compared with the available numerical data in the literature (C.A. Balanis, *Antenna Theory*, Harper & Row Publishers, 1982) and is presented in Figure 1. By virtue of the Finite Element Method and the Method of Moments, the present analysis is applicable to arbitrarily shaped apertures with or without dielectric loading. More numerical data with different aperture shapes will be presented at the conference.

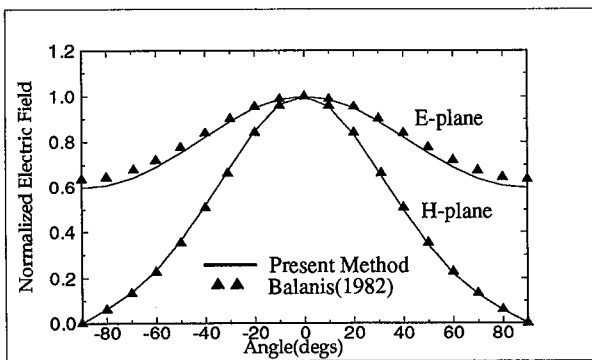


Figure 1

## **FD-TD Computation of Active Impedance of an Array of Vivaldi Quad Elements**

E. T. Thiele, C. E. Reuter, A. Taflove  
Department of Electrical Engineering and Computer Science  
Northwestern University, McCormick School of Engineering  
Evanston, Illinois 60208

M. Piket-May\*  
Department of Electrical and Computer Engineering  
University of Colorado  
Boulder, Colorado 80309-0425

This paper proposes a systematic means to obtain active impedance for arbitrary phased-array antennas using the finite-difference time-domain (FD-TD) approach. For antenna arrays, active impedance is defined as the input impedance of a given element when all other elements are excited. In many array configurations, the elements are near one another. This is true for the particular linear array of Vivaldi quad elements studied here. The closeness causes complex interactions to occur between all the elements, changing the current distribution of a given element relative to its distribution when it is isolated in free space. The degree or strength of this coupling is highly dependent upon the overall element geometry and the excitations of the various elements.

In this paper, we provide FD-TD computations of the active impedance and mutual coupling of a linear array of eight Vivaldi quad elements. Two different means of calculating the active impedance are used. In the first, the ratio between voltage and current is found at the element of interest while all other elements are driven. Here, the voltage is computed using a line integral between the stripline and ground plane, and the current is computed using a closed contour integral around the stripline. A discrete Fourier Transform is used to obtain frequency domain data for voltage, current, and impedance across a band of frequencies.

The second computation is a more involved, requiring a priori knowledge of the element self and mutual impedances as well as the calculation of the current on each element. This requires single-source runs for all possible mutual coupling geometries. Using symmetry for the Vivaldi array studied, the number of these geometries can be reduced by a factor of four to only eight, requiring eight single-source FD-TD runs. Once this is completed, full sourced array runs are made to determine the necessary currents to complete the computation. The benefit of this second method is the determination of the mutual coupling between antenna elements.

## ANALYSIS OF APERTURE COUPLED RECTANGULAR DIELECTRIC RESONATOR ANTENNA USING THE FDTD METHOD

S. M. Shum\* and K. M. Luk  
Department of Electronic Engineering  
City Polytechnic of Hong Kong  
83 Tat Chee Avenue, Kowloon, Hong Kong

### Abstract

Dielectric resonators (DR) with low permittivities can function as efficient radiators. Most efforts had been made on the studies of the cylindrical DR antennas due to their popularity. Rectangular DR antennas are easy to fabricate but have gained only limited attention in the past. The resonant frequencies of rectangular DR antennas have been estimated by using the perfect magnetic wall model but the discrepancy between theory and measurement is large (S. A. Long, M.W. McAllister & L. C. Shen, *Electron. Lett.*, 19, 218-219, 1983). Furthermore, only experimental results on the input impedance are available in the literature. Hence, to characterize rectangular DR antennas, more rigorous approaches should be considered.

The method of moments (MoM) has generally been regarded as a powerful and efficient method for solving electromagnetics problems. However, if the geometry involved contains many edge-shaped boundaries, as in the case of rectangular DR antennas, the formulation will be very complicated. On the other hand, with advances in computer technology, direct methods such as the finite-difference time-domain (FDTD) method are more attractive for dealing with complicated geometry. With the use of absorbing boundary conditions (ABCs), the applications of the FDTD method in antenna problems are feasible.

In this paper, we demonstrate how to use the FDTD method to analyze an aperture coupled rectangular dielectric resonator antenna. The excitation method chosen offers several advantages and is appropriate for MMIC applications. The results on resonant frequency, input impedance and radiation patterns will be presented and verified by experimental measurements.

## FD-TD Analysis of Rectangular Dielectric Resonator Antennas

Karu P. Esselle

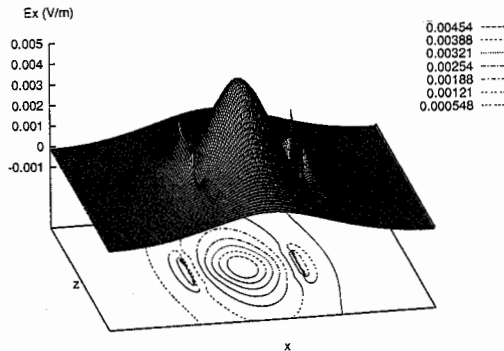
Electronics Department, Building E6A, School of MPC&E  
Macquarie University, Sydney, NSW 2109, Australia

Tel: 61 (02) 805 9141, Fax: 61 (02) 805 9128, Email: esselle@macadam.mpce.mq.edu.au

With the introduction of more accurate absorbing boundary equations and the availability of more and more powerful workstations and supercomputers, the FD-TD method has been receiving renewed attention in antenna analysis. It has been successfully used to obtain accurate results for simple antennas (J.G.Maloney *et al*, *IEEE Trans. AP-38*, 1059-1068, 1990) as well as more complicated antennas such as microstrip patches (A.Reineix & B.Jecko, *IEEE Trans. AP-37*, 1361-1369, 1989). This paper describes the use of FD-TD method for the analysis of rectangular dielectric-resonator (DR) antennas (A.Ittipiboon *et al*, *IEEE AP-S Symp.*, 604-607, 1993).

In this analysis, the dielectric resonator, the substrate, microstrip-line feed, the ground plane and the coupling aperture are accounted for. The substrate and the ground plane are assumed to be infinitely long in lateral directions. Thus they pass through the absorbing boundary (AB). Mur's second order absorbing boundary conditions (G.Mur, *IEEE Trans. EMC-23*, 377-382, 1981) are applied for most planar sections of the AB but the first order conditions are applied, diagonally, at the edges and corners of the AB. The far field is obtained by applying the Field Equivalence Principle directly in time domain; results are transformed into frequency domain later. The analysis package has been developed in FORTRAN77, with some FORTRAN90 extensions, and runs in a Cray YMP supercomputer.

For comparison with measurements, the rectangular DR antenna described by Ittipiboon *et al* was analyzed. Exactly the same dimensions were used for the DR antenna, the substrate and the aperture. The microstrip line was assumed to be 0.6mm wide. When excited by a sinusoidal source at 6.68 GHz, the  $E_x$  field component on a plane half-way across the DR and parallel to the ground plane, at a particular instant of time, is shown below. ( $x$  axis is from 0-4.5cm,  $z$  axis from 0-1.3cm; DR extends from 1.5-3cm in  $x$ -direction and .5-.8cm in  $z$ -direction.) The strong discontinuity of  $E_x$  at the dielectric boundary is clearly visible. Our results compare with the measurements favourably.



1994 URSS Radio Science meeting (Seattle)

**ANALYSIS OF SQUARE FED PATCHES WITH DIFFERENT FEEDING EXCITATION**

H.Saboundji, J.P.Daniel, D.Thouroude Univ of Rennes I CNRS URA 834.  
S.Toutain LEST ENSTBr (Brest) CNRS URA 1329.

The square patches shown on figures (1-a) and (1-b) have been previously analysed experimentally. It has been shown that these structures exhibit strong differences in term of the input impedance; the main idea was to determine theoretically the origin of this difference. The analysis was based on the segmentation technique taking into account the mutual coupling between radiating edges and the microstrip line. The multiport network model gives good results for rectangular patches fed by side when mutual coupling between radiating edges are taking into account.

The theoretical analysis of the patch fed at the corner needs to take into account both the (1,0) and (0,1) modes simultaneously. In that case the four edges are radiating energy and must be included in the multiport network model. The radiating conductance  $G_r$  is calculated from the radiated power of the circuit and distributed around the patch and the line.

In the table I, we present the input impedance  $Z_{in}$  at the resonant frequency of patches in plane  $\pi$  ( $\epsilon_r=2.2$ ,  $h=0.79$  mm and  $a=9$  mm) using the segmentation method compared to experimental results. For the patch of figure 1-b, the equivalent circuit is assumed to be a parallel impedance  $Z_{in}$  located at the center of the feedline. These results show us that the coupling effect between the patch and the feedline has an influence both on resonant frequency ( $Fr$ ) and the input impedance ( $Z_{in}$ ). The impedance obtained by configuration (b) is half than of configuration (a). Moreover, The choice of a non uniform distribution of the radiating conductance  $G_r$  gives better results than the usual uniform distribution.

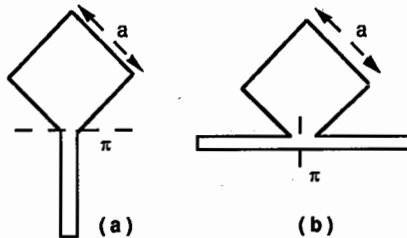


FIG 1 : Corner fed square patch

PATCH	measurements		segmentation using uniform distribution		segmentation non uniform distribution	
	Fr (GHZ)	Zin (Ω)	Fr (GHZ)	Zin (Ω)	Fr (GHZ)	Zin (Ω)
FIG 1-a	10,99	408	11,06	496	11.05	411
FIG 1-b	11,40	201	11,48	235	11,48	199

TABLE I : Comparison theory-measurement

## Optimization of Time-Domain Antennas

Jun-Hong Wang\*, Lang Jen  
 Institute of EM Theory and Microwave Technique  
 Southwest JiaoTong University, P. R. China

### Abstract

When designing time-domain antennas, we need to know the time-domain radiation characteristics of some antennas. Here we present the relationships between the maximum values of the front transient radiation fields  $E_{\max}$  (as shown in fig. 1) and the antenna structures. The configuration of an antenna is shown in fig. 1. The antenna is excited by Gauss pulse:  $V_{\alpha}(t) = \exp[-g^2(t-t_{\max})^2]$ . We use the time-stepping approach to calculate the radiation field and use the steepest descent method to optimize the antenna shape. Our objective is to find out the maximum value of the front transient radiation field. The results are shown in fig. 2 and fig. 3. From them we can see that the maximum value of the front transient radiation field is increasing with the Gaussian parameter  $g$  and the antenna length, meanwhile the optimum included angle is decreasing. Fig. 4 shows the waveforms of the transient radiation field of an antenna with parameters:  $L=1\text{m}$ ,  $\alpha = 112.34^\circ$ , and  $g=1.5 \times 10^9$ ,  $t_{\max}=1.43 \times 10^{-9}$ . From fig.4 we can see that the front radiation field is stronger than that of other directions.

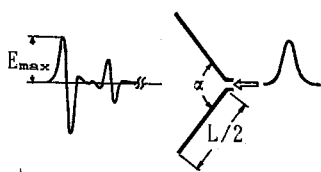


Fig. 1 Antenna structure and pulse waveforms

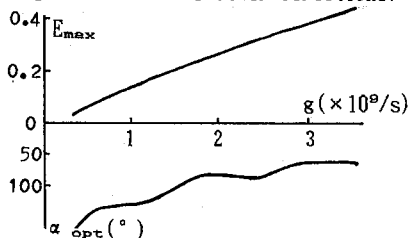


Fig. 2  $E_{\max}$  and  $\alpha_{\text{opt}}$  as functions of Gaussian parameter  $g$  ( $L=1\text{m}$ )

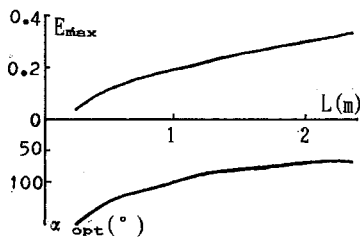


Fig. 3  $E_{\max}$  and  $\alpha_{\text{opt}}$  as functions of antenna length  $L$  ( $g=1.5 \times 10^9/\text{s}$ )

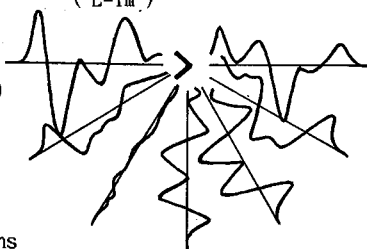


Fig. 4 Waveforms of transient radiation field

THURSDAY AM URSI-B SESSION TH-U36

Room: HUB 200 ABC

CHIRAL MEDIUM

Chairs:	I.V. Lindell, Helsinki University of Technology; K.W. Whites, University of Kentucky	
8:20	Green Dyadic of a Uniaxial Chiral Medium <i>*I.V. Lindell, Helsinki Univ. of Technology; W.S. Weiglhofer, Univ. of Glasgow</i>	424
8:40	Dyadic Green's Functions for Multi-Layered Uniaxially Anisotropic Media <i>*J.K. Lee, Y.H. Lee, Syracuse Univ.</i>	425
9:00	Electric Extremum or Magnetic Maximum? Strange Polarization Effects in Chiral and Bi-Isotropic Media <i>*A. Sihvola, Helsinki Univ. of Technology</i>	426
9:20	Optical Propagation in Helicoidal Bianisotropic Media <i>*W. S. Weiglhofer, Univ. of Glasgow; A. Lakhtakia, Pennsylvania State Univ.</i>	427
9:40	Computation and Physical Behavior of Bi-Isotropic Material Parameters for a Class of Lossy Inclusions <i>*K.W. Whites, Univ. of Kentucky</i>	428
10:00	Break	
10:20	Electromagnetic Scattering from Chiral Cylinder of Arbitrary Cross-Section <i>E. Arvas, *M. Alkanhal, Syracuse Univ.</i>	429
10:40	A General Scheme for the Electromagnetic Reflection and Transmission for Composite Structures of Complex Materials <i>*M. Norgren, S. He, Royal Inst. of Technology</i>	430
11:00	Estimates for the Effective Properties of Bi-Isotropic Composites with Helical Inclusions <i>*F. Guérin, P. Bannelier, Thomson-CSF Laboratoire Central de Recherches</i>	431
11:20	An Eigenvalue Theory of Circular Birefringence and Dichroism in a Chiral Medium Based on the Electric Quadrupole-Magnetic Dipole Multipole Approximation <i>*R.E. Raab, Univ. of Natal; J.H. Cloete, Univ. of Stellenbosch</i>	432
11:40	Reflection and Transmission in Uniaxial Chiral Omega Composites <i>S. A. Tretyakov, A. A. Sochava, St. Petersburg State Technical Univ.</i>	433

## GREEN DYADIC OF A UNIAXIAL CHIRAL MEDIUM

I.V. Lindell\* and W.S. Weiglhofer\*\*

\*Electromagnetics Laboratory  
Helsinki University of Technology  
Otakaari 5A, Espoo 02150 FINLAND

\*\*Department of Mathematics  
University of Glasgow  
Glasgow, G12 8QW, UNITED KINGDOM

In recent years, isotropic chiral media have been under intensive research because of their new and promising applications in antenna and microwave engineering. The basic electromagnetic problem was solved when the dyadic Green function corresponding to that medium was found by Bassiri, Engheta and Papas (*Alta Frequenza*, 55,83-88,1986). The problem of constructing the Green dyadic corresponding to a uniaxially chiral bianisotropic medium is treated in the present paper.

Such a medium can be obtained, e.g., by inserting similar metal helices, with their axes parallel to a certain direction, in an isotropic base material. Defining the axial direction by the unit vector  $\mathbf{u}_z$ , the constitutive equations of the medium can be written in first approximation as

$$\mathbf{D} = (\epsilon_t \bar{\bar{I}}_t + \epsilon_z \mathbf{u}_z \mathbf{u}_z) \cdot \mathbf{E} - j\kappa \sqrt{\mu_0 \epsilon_0} \mathbf{u}_z \mathbf{u}_z \cdot \mathbf{H},$$

$$\mathbf{B} = (\mu_t \bar{\bar{I}}_t + \mu_z \mathbf{u}_z \mathbf{u}_z) \cdot \mathbf{H} + j\kappa \sqrt{\mu_0 \epsilon_0} \mathbf{u}_z \mathbf{u}_z \cdot \mathbf{E},$$

with  $\bar{\bar{I}}_t = \mathbf{u}_x \mathbf{u}_x + \mathbf{u}_y \mathbf{u}_y$  denoting the two-dimensional unit dyadic transverse to the  $z$  axis. Plane wave propagation in such a medium was considered earlier by these and other authors and interesting polarization-transforming properties were found (A.J.Viitanen & I.V.Lindell, *Int.J.Infrared Millim.Waves*, 14,1993-2010,1993).

An explicit expression for the Green dyadic corresponding to the axially chiral uniaxial medium is derived through dyadic analysis. By avoiding the awkward Fourier transformation technique, the present derivation appears more straightforward than the previous ones also for the special case of nonchiral uniaxial anisotropic medium with  $\kappa = 0$ . The new Green dyadic expression serves as the basis for solving electromagnetic problems involving sources or equivalent sources and setting up integral equations in a medium of this kind. As an example, radiation from an axial electric dipole is considered and the result is seen to coincide with the one recently obtained through another analysis.

## DYADIC GREEN'S FUNCTIONS FOR MULTI-LAYERED UNIAXIALLY ANISOTROPIC MEDIA

Jay Kyoong Lee\* and Yun Hee Lee  
Department of Electrical and Computer Engineering  
Syracuse University  
Syracuse, New York 13244-1240, USA

Recently, because of wide applications of complex materials, many studies have been done with layered anisotropic media. The dyadic Green's functions for layered anisotropic media are very useful in solving problems of radiation and scattering of electromagnetic waves in layered anisotropic media. In studying uniaxially anisotropic medium, in most cases the optic axis has been assumed to be perpendicular (vertical) or parallel to the interface for simple analysis. Lee and Kong (*Electromagnetics*, vol. 3, 111-130, 1983) calculated the dyadic Green's functions for both unbounded and layered uniaxially anisotropic medium whose optic axis is tilted from the vertical axis.

In this paper, we consider the uniaxially anisotropic medium whose optic axis is arbitrarily oriented. First, the dyadic Green's function (DGF) for unbounded anisotropic medium is derived using the Fourier transform method. The DGF is expressed in compact dyadic form in terms of two characteristic waves, viz., the *ordinary wave* and *extraordinary wave*. Then we formulate the DGF's for multi-layered anisotropic media. The optic axis of each layer is assumed to be rotated by angles  $(\psi_i, \chi_i)$ ,  $i = 1, 2, \dots, n$  with respect to the  $z$ - and  $x$ -axes, respectively. In particular, the DGF's for three-layered anisotropic media are analytically obtained. Using the matrix method the coefficients of the three-layer DGF's are expressed in terms of half-space Fresnel reflection and transmission coefficients. Applying the boundary conditions of the continuity of the tangential electric and magnetic fields, the Fresnel reflection and transmission coefficients for anisotropic-anisotropic interface are also calculated.

## Electric Extremum or Magnetic Maximum? Strange Polarization Effects in Chiral and Bi-Isotropic Media

Ari Sihvola

Helsinki University of Technology, Electromagnetics Laboratory  
Otakaari 5 A, FIN-02150 Espoo, Finland

It is the purpose of this presentation to describe some qualitatively new aspects that appear in the wave-material interaction as there is chiral magnetoelectric coupling in the medium. The following constitutive relations, particularly well suited for the characterization of chiral media, between the electric ( $\vec{E}, \vec{D}$ ) and magnetic ( $\vec{H}, \vec{B}$ ) fields and flux densities

$$\vec{D} = \epsilon \vec{E} + (\chi - j\kappa) \sqrt{\mu_0 \epsilon_0} \vec{H}, \quad \vec{B} = \mu \vec{H} + (\chi + j\kappa) \sqrt{\mu_0 \epsilon_0} \vec{E}$$

contain the permittivity  $\epsilon$ , permeability  $\mu$ , chirality  $\kappa$ , and nonreciprocity  $\chi$  parameters of the material under discussion (I.V. Lindell, A.H. Sihvola, S.A. Tretyakov, and A.J. Viitanen: *Electromagnetic waves in chiral and bi-isotropic media*, Artech House, Norwood, Mass., to be published in 1994). Pasteur media ( $\chi = 0, \kappa \neq 0$ ) and Tellegen media ( $\chi = 0, \kappa \neq 0$ ) are special cases of general bi-isotropic media.

The effective properties of heterogeneous bi-isotropic and chiral media are often complicated functions of the electromagnetic parameters of the component phases, and also of the microscopic geometry of the material. The manner how bi-isotropic inclusions become polarized, in other words, how strong electric and magnetic dipole moments they generate, is essential in the analysis of the effective macroscopic properties of the medium.

Due to the fact that there is magnetoelectric coupling in the material, proportional to the material parameters  $\kappa$  and  $\chi$ , the polarizabilities of material inclusions are not as straightforward expressions as in the pure dielectric or magnetic cases. Two strange polarization effects will be described in this talk: the appearance of magnetic properties from nonmagnetic components, and an extremely strong polarization effect ECP (enhanced chiral polarization).

It seems counterintuitive that components with no magnetic properties (the permeability of all components in the mixture is that of free space,  $\mu_0$ ), mixed together, will create a medium with nonzero magnetic susceptibility. And even more; it is possible to tailor diamagnetic mixtures using only paramagnetic components (A.H. Sihvola and I.V. Lindell, *J. Electromagn. Waves Applic.*, 6(5/6), 553-572, 1992). And also the dual case is possible: chiral or bi-isotropic components that all have positive electric susceptibility, can form a mixture that has a negative susceptibility as a whole, i.e., its permittivity is less than  $\epsilon_0$ .

But the chiral coupling can also in some cases produce unexpectedly strong polarization in both electric and magnetic domains. The phenomenon I call here ECP. (The corresponding effect can also be predicted for nonreciprocal inclusions.) This, however, requires a rather strong magnitude of the chirality parameter. It will be shown that the amount of chirality needed for ECP is  $\kappa = \sqrt{\epsilon\mu/\epsilon_0\mu_0}$ , within the physical limits. Furthermore, the enhancement depends on the shape of the chiral inclusion in a sensitive manner. Due to the fact that the electromagnetic modeling of chiral materials is a very recent topic of study, it seems that ECP has neither been experimentally observed, nor even theoretically predicted.

# Optical Propagation in Helicoidal Bianisotropic Media

W S Weiglhofer<sup>1\*</sup> and A Lakhtakia<sup>2</sup>

<sup>1</sup> Department of Mathematics, University of Glasgow, Glasgow G12 8QW  
Scotland, Great Britain; email: werner@maths.glasgow.ac.uk

<sup>2</sup> Department of Engineering Science and Mechanics,  
Pennsylvania State University, University Park, PA 16802-1401, USA

In this contribution we will comprehensively investigate the problem of light propagation parallel to the helical axis of general classes of so-called helicoidal bianisotropic media (the *super-cholesteric* material proposed in a companion paper is an example of such a medium).

The objective of this paper is therefore to study propagation in an arbitrary helicoidal bianisotropic medium. The frequency-domain constitutive relations applicable to a helicoidal bianisotropic medium can be set down as

$$\begin{aligned}\mathbf{D} &= \epsilon_0 (\bar{\alpha}_{11}(z) \cdot \mathbf{E} + \bar{\alpha}_{12}(z) \cdot \mathbf{H}), \\ \mathbf{B} &= \mu_0 (\bar{\alpha}_{21}(z) \cdot \mathbf{E} + \bar{\alpha}_{22}(z) \cdot \mathbf{H}),\end{aligned}$$

where  $\bar{\alpha}_{mn}(z)$ ,  $m = 1, 2; n = 1, 2$  are the rotationally inhomogeneous constitutive dyadics of the medium. On implementing the above relations into Maxwell's equations, a system of partial differential equations is obtained which will be thoroughly studied for optical propagation parallel to the helical axis. Exact solutions will be obtained and their special features will be discussed. In addition, a procedure to obtain the response of a helicoidal bianisotropic medium slab to a normally incident plane wave will be presented.

Physical realizations of helicoidal bianisotropic media as liquid crystalline materials, solid thin films, and densely cross-linked polymers will be discussed. Finally, the analytical results obtained will be exemplified by application to: *cholesteric liquid crystals, super-cholesterics, gyrocholesteric dielectrics, ferromectics and cholesteric bianisotropic media.*

# Computation and Physical Behavior of Bi-isotropic Material Parameters for a Class of Lossy Inclusions

Keith W. Whites

Department of Electrical Engineering  
University of Kentucky  
Lexington, KY 40506-0046

An important component in the physical application of bi-isotropic materials is an understanding of the electromagnetic attributes and frequency dependence of their material parameters. While final confirmation of these quantities rests with laboratory measurement, numerical computation of these parameters has obvious advantages including the ease with which the inclusion shape, density and composition can all be changed. However, due to the inherently large number of inclusions and their small size, such numerical simulations have typically been relegated to simplified analytical models and/or ignoring the mutual interactions.

Recently, a full-wave simulation method has been developed which appears to overcome many of the short-comings inherent in the numerical computation of the effective constitutive parameters for bi-isotropic materials (*Digest of the 1993 URSI Radio Science International Symposium*, Ann Arbor, MI, p. 243, June 1993). This approach uses a Monte-Carlo technique to compute the averaged scattered fields from an ensemble of inclusions together with an analytical solution for the scattering by the volumetric shape in which the inclusions are suspended (with an assumed form of the constitutive model) in order to calculate the effective media parameters.

The aim of this work is to present an application of the previously derived full-wave simulation methodology to synthetic reciprocal chiral materials having lossy inclusions. In particular, the inclusion shape is restricted to the wire-helix class. To model the effects of lossy material wires, use is made of the resistive tube boundary condition (RTBC) which accurately predicts the scattering by lossy dielectric or magnetic wire shapes without a significant computational demand beyond that required for perfect electrically conducting wires (*Digest of the 1992 URSI Radio Science International Symposium*, Chicago, IL, p. 34, July 1992).

In this talk, a brief overview of the theory and computational implementation of the RTBC for material wires will be given followed by a presentation of the frequency dependence of the three effective constitutive parameters ( $\epsilon$ ,  $\mu$  and  $\beta$ ) for a number of handed wire inclusion geometries and varying loss. Phenomenological comparisons with the Drude equation predictions for the optical rotatory dispersion will also be shown.

# Electromagnetic Scattering from Chiral Cylinder of Arbitrary Cross-Section

Ercument Arvas and Majeed Alkanhal\*  
 Department of Electrical and Computer Engineering  
 Syracuse University, Syracuse, New York 13244-1240

A simple moment (MoM) solution is given for plane wave scattering by an arbitrary cross-section chiral cylinder. Electromagnetic chirality is found in materials characterized by the constitutive relations

$$\underline{D} = \epsilon \underline{E} - j\gamma \underline{B} \quad \text{and} \quad \underline{H} = (1/\mu) \underline{B} - j\gamma \underline{E} ,$$

where  $\epsilon$  is the permittivity,  $\mu$  is the permeability, and  $\gamma$  is the chirality admittance of the chiral medium. The chirality admittance  $\gamma$  is an indication of the degree of chirality of the medium.

The solution of the problem is begun by developing a simplified form of surface integral equations for scattering by chiral cylinders which is feasible to numerical computations. Then, surface equivalent problems of electric and magnetic surface currents radiating in free space and in an unbounded chiral medium are developed to replace the original problem of scattering by the chiral cylinder. The use of the chiral surface equivalence principle results in a set of two coupled vector integral equations for the surface electric and magnetic currents radiating in free space and in an unbounded chiral medium. Due to the coupling between the longitudinal and the transverse components of the fields in chiral media, both longitudinal and transverse components of the surface currents are considered in the scalarization of the coupled vector equations. The resulting coupled scalar equations are, then, solved by a pulse basis and point matching method of moments solution. Numerical results for circular chiral cylinders of different parameters show excellent agreement with the exact data found by eigen functions solution. The figure below compares the magnitudes of the computed and the exact internal E-fields for a circular chiral cylinder of the shown parameters.

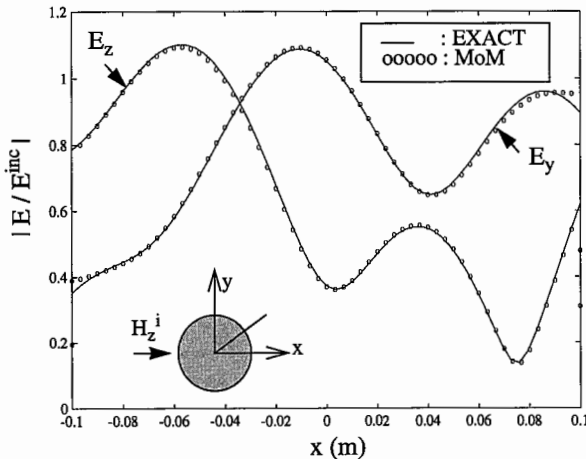


Fig. 1: The E-field internal to the circular chiral cylinder ( $\mu_r = 2.8$ ,  $\epsilon_r = 4.0$ ,  $\delta_e = 0.05$ ,  $\delta_m = 0.05$ ,  $\gamma = 0.002$ ,  $r = 0.1 \lambda_0$ ) along  $y=0$  axis illuminated by an incident  $TE_z$  plane wave.

# A general scheme for the electromagnetic reflection and transmission for composite structures of complex materials

Martin Norgren\* and Sailing He  
 Department of Electromagnetic Theory  
 Royal Institute of Technology  
 S-100 44 Stockholm, SWEDEN

## Abstract

A time-harmonic electromagnetic plane wave obliquely incident on a stratified composite structure consisting of complex (bianisotropic) materials is considered. The composite structure consists of multiple layers of different types of complex media. The parameters in each layer are arbitrary functions of the depth, which do not need to be continuous or differentiable. A modified invariant imbedding method is used to calculate the reflection and transmission, and the internal fields are calculated through a Green function approach. A characteristic feature of the approach is that it is based on a wave-splitting that is not related to the media which make up the composite structure, but is always defined with respect to vacuum. Any mismatch in the parameters makes no extra effect in the calculation using the present splitting. The advantages of this approach are identified and it is compared to other approaches. Numerical results for the co- and cross-polarized reflection and transmission coefficients for TE and TM modes for a composite structure consisting of a stratified chiral layer and a stratified  $\Omega$  layer are presented (cf. Figs. 1(a) and 1(b)).

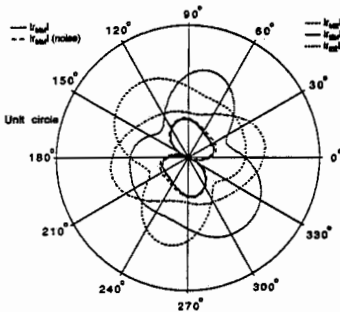


Fig.1(a): Reflection coefficients

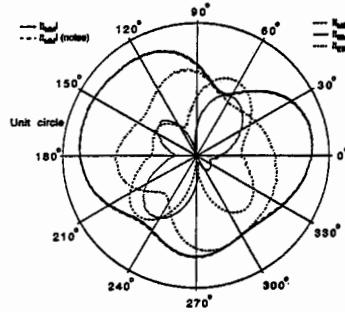


Fig.1(b): Transmission coefficients

## **Estimates for the effective properties of bi-isotropic composites with helical inclusions**

**Frédéric Guérin\***

**THOMSON-CSF Central Research Laboratories  
Domaine de Corbeville 91404 Orsay Cedex, France, and  
IRCOM, University of Limoges, 123 Avenue Albert Thomas  
87060 Limoges Cedex, France**

**Pierre Bannelier**

**THOMSON-CSF Radars and Countermeasures Division,  
La Clef de Saint Pierre, 78852 Elancourt Cedex, France**

Establishing a relationship between the microscopic features of a complex medium and its macroscopic, or "average", properties is a topic to which an appreciable research effort has been dedicated over the last decades. In electromagnetics, with the appearance of new classes of materials, the need for an appropriate tool aimed at predicting the effective properties of multiphased media has become even more pronounced.

The present paper is devoted to the study of composites consisting of a dispersion of asymmetric inclusions in a dielectric matrix. These materials belong to the class of bi-anisotropic media, an important subgroup of which is formed by reciprocal bi-isotropic, or chiral, substances. We will restrict our analysis to such substances, i.e. composites whose inclusions are randomly oriented metallic or dielectric helices; such materials have already been fabricated and experimentally characterized (F. Guérin, *PIERS Book Series Special Issue on Bi-Isotropic Media and Applications*, to appear in 1994).

Our model for predicting, or at least obtaining estimates for the effective properties of chiral composites is based on a finite-element computer code, *Antenna Design*, developed at Thomson-CSF Radars and Countermeasures Division. This software enables one to compute the electromagnetic field scattered in the forward and backward directions by a given object, in our case an helix, in a medium. The object can in general be made of a lossy magnetoelectric medium or a lossy metal, while the surrounding medium may be a lossy magnetoelectric one. Using the forward and backward vector scattering amplitudes, one can compute all 4 polarizabilities of an orientationally averaged helix (there are in fact only 3 independent polarizabilities, showing that the scatterer is reciprocal and the corresponding composite medium is chiral), provided that the quasi-static limit is applicable to the case. Once the polarizabilities are known, a Maxwell Garnett treatment leads to the effective constitutive parameters: permittivity, permeability, and chirality coefficient. Other variables of interest, such as the rotation angle, the ellipticity, or the scattering parameters, are then computed.

Numerical results relative to different types of inclusions will be presented. The effect of matrix permittivity and inclusion concentration on the effective properties will in particular be shown. Some comparison with experimental results will also be given. An analysis of the method will finally be performed, and further research directions will be discussed.

# An Eigenvalue Theory of Circular Birefringence and Dichroism in a Chiral Medium Based on the Electric Quadrupole-Magnetic Dipole Multipole Approximation

R.E. Raab\* and J.H. Cloete

Department of Physics, University of Natal, Pietermaritzburg 3200, South Africa  
and

Department of Electrical and Electronic Engineering,  
University of Stellenbosch, Stellenbosch 7600, South Africa.

Chiral effects occurring at optical frequencies in gases and crystals have been explained in the past by means of Maxwell's equations and constitutive relations which allow for induced electric quadrupoles and magnetic dipoles. The basis of this approach is that the relative magnitudes of the multipole contributions to an electromagnetic effect are ordered as (E.B. Graham, J. Pierrus, and R.E. Raab, "Multipole moments and Maxwell's equations," J.Phys. B, 25, 4673-4684, 1992)

$$\text{electric dipole} \gg \left\{ \begin{array}{l} \text{electric quadrupole} \\ \text{magnetic dipole} \end{array} \right\} \gg \left\{ \begin{array}{l} \text{electric octopole} \\ \text{magnetic quadrupole} \end{array} \right\} \gg \dots$$

Within the electric quadrupole-magnetic dipole approximation the  $\mathbf{D}$  field contains, in addition to the electric dipole moment density  $\mathbf{P}$ , a term in the electric quadrupole moment density  $\mathbf{Q}$ , which is a dyadic. The  $\mathbf{H}$  field is, consistent with the ordering shown above, truncated at the magnetic dipole moment density  $\mathbf{M}$ . The resulting constitutive relations are

$$\begin{aligned} \mathbf{D} &= \epsilon_0 \mathbf{E} + \mathbf{P} - \frac{1}{2} \nabla \cdot \mathbf{Q}^t + \dots \\ \mathbf{H} &= \mu_0^{-1} \mathbf{B} - \mathbf{M} + \dots \end{aligned}$$

A plane time-harmonic electromagnetic wave induces multipole moments in matter through its  $\mathbf{E}$  and  $\mathbf{B}$  fields and their space and time derivatives. When the constitutive relations are used with Maxwell's equations, a  $3 \times 3$  matrix eigenvalue equation is obtained. Its solution yields the polarization eigenwaves which the medium supports for a given direction of propagation, and their refractive indices,  $n$ , and absorption coefficients,  $k$ .

Although usually applied to crystals and gases, the theory also describes helices in a neutral substrate, where these simulate a crystal or a gas. The criteria for such a simulation are given. It is found that the expressions for the circular birefringence,  $n_R - n_L$ , and circular dichroism,  $k_R - k_L$ , contain an electric quadrupole term for uniaxial crystals but not for cubic crystals or gases. These expressions satisfy the essential requirements of being independent of the origin to which the multipole moments are referred, provided all electric quadrupole contributions are included.

## Reflection and transmission in uniaxial chiral omega composites

S.A. Tretyakov, A.A. Sochava

St. Petersburg State Technical University, Radiophysics Department  
195251 St. Petersburg, Russia

Electromagnetics of complex media attracts a lot of attention and efforts of researches. Isotropic chiral composites appear to be useful in microwave technology, antenna design and, especially, as perspective materials for anti-reflection coverings. Recently, more general bianisotropic materials such as composites with  $\Omega$ -shaped metal elements embedded in a dielectric matrix were studied. Especially, composites with uniaxial symmetry seem to offer good possibilities for applications. Here we study electromagnetic waves in more general reciprocal uniaxial materials with  $\Omega$  particles and with intrinsic handedness, i.e. in uniaxial chiral omega structures.

Corresponding material equations become uniaxial with the most general uniaxial dyadic coupling terms:

$$\overline{D} = \overline{\epsilon} \cdot \overline{E} + j\sqrt{\epsilon_0\mu_0}(-\kappa_t \overline{I}_t - \kappa_n \overline{z}_0 \overline{z}_0 + K \overline{J}) \cdot \overline{H},$$

$$\overline{B} = \overline{\mu} \cdot \overline{H} + j\sqrt{\epsilon_0\mu_0}(\kappa_t \overline{I}_t + \kappa_n \overline{z}_0 \overline{z}_0 + K \overline{J}) \cdot \overline{E}.$$

The dielectric permittivity  $\overline{\epsilon}$  and the magnetic permeability  $\overline{\mu}$  are uniaxial dyadics:

$$\overline{\epsilon} = \epsilon_0(\epsilon_t \overline{I}_t + \epsilon_n \overline{z}_0 \overline{z}_0), \quad \overline{\mu} = \mu_0(\mu_t \overline{I}_t + \mu_n \overline{z}_0 \overline{z}_0),$$

where  $\overline{z}_0$  stands for the unit vector along the axis and  $\overline{I}_t = \overline{x}_0 \overline{x}_0 + \overline{y}_0 \overline{y}_0$  is the transverse unit dyadic,  $\overline{J} = \overline{z}_0 \times \overline{I}_t = \overline{y}_0 \overline{x}_0 - \overline{x}_0 \overline{y}_0$  is the 90 degree rotator in the  $(x - y)$  plane. Additional coupling provided by the omega particles is measured by the dimensionless parameter  $K$ .

As is seen, introduction of chiral elements in omega structures makes the analysis much more involved. In non-chiral omega media, eigenwaves are linearly polarized  $TM$ - and  $TE$ -waves, whereas in isotropic chiral media eigenwaves are circularly polarized. In chiral omega structures eigenwaves, in general, have elliptical polarization patterns.

Here we study plane wave reflection and transmission phenomena in planar uniaxial bianisotropic layers. As it appears, such problems for complex media layers can be effectively treated by the vector transmission-line theory, where plane layers of a composite material are modelled by an equivalent transmission line with dyadic wave impedances and dyadic propagation factors. In general, the modelling line is non-symmetric, i.e., its wave impedances depend on the direction of the wave propagation.

Numerical examples demonstrate some interesting features of reflection and transmission phenomena in uniaxial layers. For example, low reflection from thin absorbing layer can be achieved in wide frequency ranges. Effects of chirality of the reflection and transmission coefficients are clarified.



THURSDAY AM URSI-B SESSION TH-U38

Room: HUB 106

PERIODIC SURFACES

- Chairs: Te-Kao Wu, California Institute of Technology; E.V. Jull, University of British Columbia
- 1:20 Analysis of Propagation and Scattering Characteristics of Material-Coated Periodic Gratings Using the Method of Lines 436  
*K. Wu, J.-J. Laurin, Ecole Polytechnique*
- 1:40 TM Blazing of Rectangular Groove Gratings at Non-Bragg Incidence 437  
*W. Chen, N.C. Beaulieu, N.C. Beaulieu, D.G. Michelson, \*E.V. Jull, Univ. of British Columbia*
- 2:00 Computer Modelling and Numerical Analysis of EM Scattering from Periodic Gratings of Lossy Conductors 438  
*\*H.A. Kalhor, State Univ. of New York*
- 2:20 Exact Solution of Helmholtz's Equation in Dielectric Gratings with Arbitrary Profiles 439  
*H. Mossallai, M.H. Rahnavard, H. Abiri, Shiraz Univ.*
- 2:40 Evaluation and Applications of Quasi-Optical Grids with Thin/Thick Rectangular Elements 440  
*\*T. K. Wu, California Institute of Technology*
- 3:00 Break
- 3:20 Design of Frequency Selective Surfaces Using Massively Parallel Genetic Algorithms 441  
*\*E. Michielssen, A. Boag, Univ. of Illinois; J.M. Sajer, CEA-CESTA Laboratories; R. Mittra, Univ. of Illinois*
- 3:40 Analysis of Frequency Selective Surfaces with Arbitrary Aperture Geometry 442  
*\*R.C. Hinz, C.H. Chan, Univ. of Washington; R.A. Kipp, DEMACO, Inc.*
- 4:00 Performance of Double Layered FSS with Complex Resonant Elements 443  
*\*J. Shaker, L. Shafai, Univ. of Manitoba*

# Analysis of Propagation and Scattering Characteristics of Material-Coated Periodic Gratings Using the Method of Lines

Ke WU and Jean-Jacques LAURIN

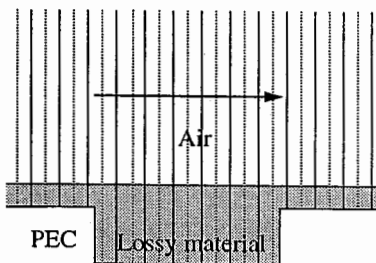
Groupe de Recherches Avancées en Microondes et en Électronique Spatiale  
(POLY-GRAMES)

Dept. de génie électrique et de génie informatique, École Polytechnique  
C. P. 6079, Succ. "A", Montréal, Canada H3C 3A7

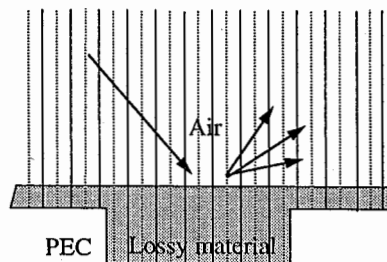
Tel: 514-340-5991, Fax: 514-340-5892, e-mail: wuke@poly-hf2.grmes.polymtl.ca

## Abstract

The method of lines is proposed for determining propagation and scattering characteristics of material-coated periodic gratings under the TE and TM illuminations. Periodic boundary conditions governed by Floquet theorem are formulated in terms of characteristic circulant matrix in the discretized space domain, thereby eliminating the need for field expansion in terms of Floquet harmonics, as required by the boundary integral techniques (e.g. J. Moore, H. Ling and C. S. Liang, IEEE Trans. on Antennas and Propagation, Vol. 41, Sept., pp. 1281-1288, 1993). The theoretical framework with nondistant discretization schemes is illustrated in the following figures for TE and TM analysis of both propagation and scattering problems. Compared to the boundary integral approaches, this technique presents simple formulation and monotonous convergence for multilayered material-coated periodic gratings. Owing to the nature of transmission-line expression upon the transform and decoupling procedure, the incident and scattered waves are easily determined in the space domain. As an example, complex propagation constant is calculated in the absence of incident fields for lossy material-coated periodic rectangular gratings to demonstrate the theoretical principle. Scattering and absorbing characteristics are also studied under the TE and TM illumination at arbitrary angle of incidence.



solid lines: electric lines



dotted lines: magnetic lines

## TM Blazing of Rectangular Groove Gratings at Non-Bragg Incidence

Wei Chen, N.C. Beaulieu, D.G. Michelson & E.V. Jull\*

Department of Electrical Engineering

University of British Columbia

Vancouver, B.C. V6T 1Z4

It is well known that perfect blazing to the  $n = -1$  order is possible for diffraction gratings under Bragg angle incidence. That is, the period  $d = \lambda / (2 \sin \vartheta_i)$ , where  $\lambda$  is the wavelength and  $\vartheta_i$  is the angle of incidence from the normal to the grating surface. High efficiency gratings are useful at millimeter wavelengths for multiplexers, demultiplexers and frequency-scanned reflector antennas. (eg. F.S. Johannsson, IEEE AP-38, 1491-1495, 1990) but 100% efficiency only for diffraction back in the direction of incidence is a serious inconvenience.

Perfect blazing for other than Bragg angle incidence, once thought impossible, has been observed numerically and experimentally with rectangular groove gratings (E.V. Jull and J.W. Heath, 1979 AP-S Symp. Dig. 515-518) and predicted for sinusoidal gratings (D. Maystre et al., Optica Acta 28, 457-470, 1981). In both instances it occurs only for TM polarization (magnetic field parallel to the grooves). It is a consequence of reciprocity that angles other than Bragg for which there is perfect blazing must occur in pairs. If between these angles specular reflection can be adequately suppressed, then high efficiency blazing over a wide angular range, or for a wide range of frequencies, has been achieved. Such high efficiency wideband diffraction gratings would be superior to any now available for multiplexers or frequency scanned antennas.

To establish design data for rectangular groove gratings with such desirable behavior a rigorous analysis by mode matching is being used with computer search routines for zeros in specular reflection. There is a very limited range of surface periods  $d/\lambda$  for which this unusual phenomena occurs. For example, with a groove width to period ratio of 0.5 the range is  $0.92 < d/\lambda < 0.98$  and the corresponding shallowest appropriate groove depths are  $0.20 < h/\lambda < 0.23$ . These results could not be predicted by any equivalence from those for sinusoidal gratings. Other grating widths are being investigated and the phenomena is observed also for the comb grating.

While the results apply to perfectly conducting surfaces, similar profiles may be expected to provide high efficiency wide-band optical gratings.

COMPUTER MODELLING AND NUMERICAL ANALYSIS OF EM SCATTERING  
FROM PERIODIC GRATINGS OF LOSSY CONDUCTORS

Hassan A. Kalhor  
Electrical Engineering Department  
State University of New York  
New Paltz, NY 12561

Metallic gratings of different groove shapes have many applications in the areas of optics and microwaves, because of their strong frequency dependent behavior. Many ingenious numerical methods have been developed for the analysis of such problems. Almost all of these analysis methods assume that the gratings are made of perfectly conducting materials. In practice, all scatterers are made of finitely conducting materials and in some applications the knowledge of losses becomes very important. The effects of finite conductivity in gratings with triangular groove shape have been previously calculated approximately ( H.A. Kalhor & A.R. Neureuther, JOSA, 63, 11, 1973 ) by using a surface impedance model.

In the present work, conductor losses are calculated exactly. The EM scattering problem is solved by a combined wave expansion and finite difference or finite element method which gives the fields within the material as well as the scattered fields. Conductor losses and their impact on the scattered fields can, therefore, be determined accurately. The losses are also calculated approximately by a perturbation method similar to that used in calculating the wall losses in waveguides. To demonstrate the method, a grating with rectangular grooves is considered, and it is assumed that the metal has infinite conductivity. This structure is easily amenable to solution by a mode matching technique. The scattered fields due to an incident plane wave are calculated inside and outside the grooves. The current distribution on the walls is then computed and conductor losses are determined. The results based on this approximate theory are then compared against those obtained by the exact method outlined above to show its limits of applicability.

# Exact Solution of Helmholtz's Equation in Dielectric Gratings with Arbitrary Profiles<sup>1</sup>

H.Mossallai, M. H. Rahnavard<sup>2</sup>, H. Abiri  
EE Department , School of Engineering,  
Shiraz University, Shiraz ,Iran

Based on an exact solution of the pertinent boundary-value problem, a method is presented for finding the electromagnetic fields radiated or guided by lossy dielectric gratings having arbitrary profiles. This method unifies the treatment of both perpendicular (TE) and parallel(TM) polarization by using the Boundary Element Method (BEM).

The computational method described in this paper relies on the numerical solution of the integral wave equation inside the grating region. For the problem at hand, the boundary conditions of the longitudinal interfaces of the grating layer are functionally known because of the Floquet expansion of the fields in the uniform layers above and below it. On the other hand, the boundary conditions for the interface between the periodic unit cell are naturally provided by Floquet's theorem and continuity requirements. Thus, the method can be applied in a rather straight forward way towards a rigorous solution of the periodic problem, without any a priori assumptions and to a user specified accuracy.

In this paper we calculate the electromagnetic fields and the radiation characteristics of a leaky dielectric waveguide with light-induced trapezoidal layer.

---

<sup>1</sup> This research was supported by Board of Research of Shiraz University, Shiraz, Iran.

<sup>2</sup>Presently at Electr. Eng. Department, Faculty of Engineering, University of Ottawa, Ont. on sabbatical leave from Shiraz University, Shiraz, Iran.

Evaluation and Applications of Quasi-Optical Grids  
with Thin/Thick Rectangular Elements

Te-Kao Wu  
Jet Propulsion Laboratory  
California Institute of Technology  
Pasadena, CA 91109

Quasi-optical grids consisting of periodic, thin/thick rectangular elements have been extensively used in high-pass, low-pass or band-pass filters (T.-K. Wu, Int. J. Infrared and Millimeter Waves, 14, 1017-1033, 1993.) Grids of this simple rectangular element type can be easily fabricated by the photo etching or lithography technique. Thus they have been extensively applied in many optical, millimeter and microwave systems.

These thin grids with rectangular elements has been analyzed by the accurate integral equation technique in the above mentioned reference. In this paper, the thick grids with finite or semi-infinite thickness (or open-ended waveguide array) were analyzed via the integral equation technique with the standard waveguide modes as the field expansion functions. The results matches very well with the HP's HFSS solutions for the case of an open-ended rectangular waveguide array. The integral equation technique is much more efficient than the HFSS. However, presently only the HFSS code can analyze a rhombic-shaped waveguide array, since it uses the finite triangular or tetrahedron elements to best fit the rhombic waveguide.

This paper will also describe the performance evaluation and interesting applications of these grids. They are the Far Infrared interference or coupling grids, beam splitters in many optical systems, sunshields for the space-craft antenna's thermal protection, and micro-switches for phased array beam steering.

## Design of Frequency Selective Surfaces Using Massively Parallel Genetic Algorithms

*E. Michielssen<sup>+</sup>\* A. Boag<sup>+</sup>, J.M. Sajer<sup>++</sup> and R. Mittra<sup>+</sup>*

*<sup>+</sup> Electromagnetic Communication Laboratory  
University of Illinois at Urbana-Champaign  
Urbana, IL 61801*

*<sup>++</sup> CEA - CESTA, le Barpe, France*

Frequency Selective Surfaces (FSSs) comprised of metallic patch or aperture elements supported by dielectric layers, find widespread applications as spatial filters over much of the electromagnetic spectrum. The filter characteristics depend upon the element shape and dimensions, as well as upon the thicknesses and permittivities of the dielectric layers. Few algorithms for systematically designing FSSs are currently available. As a consequence, one typically resorts to a tedious trial and error procedure to synthesize a filter with a desired frequency response. In this paper, an algorithm is presented for systematically synthesizing FSSs using a genetic algorithm (GA). GAs are stochastic optimization algorithms that mimic natural evolution. In contrast to traditional, gradient-based optimization algorithms which iteratively refine an initial guess, GAs operate on a large population of solutions, the members of which are processed stochastically and in a discretized form. Whereas GAs have been successfully applied to a variety of design problems across many disciplines, the development of GA-based algorithms for designing electromagnetic systems is still in an embryonic stage. This lack of progress in this area can be attributed to the computationally expensive nature of the objective functions that arise in the formulation of electromagnetic optimization problems.

The algorithm presented in this paper vastly improves upon a previously reported database-oriented GA synthesis technique ( E. Michielssen, J.M. Sajer and R. Mittra, 'Design of Multilayered Frequency Selective Surfaces and Waveguide Filters Using Genetic Algorithms,' AP-S Symposium Digest pp. 314-318, Ann Arbor, 1993 ). The database-oriented algorithm restricts the choice of the FSS element shape to a predefined set of elements. This restriction results in a significant speed-up of the GA search procedure, as it permits the pre-computation of the scattering matrices of the individual filter building blocks, which, in turn, allows for an efficient computation of the objective function during the execution of the GA. Unfortunately, the database-algorithm severely limits the GA search to a rather restricted class of structures. The new GA-based synthesis algorithm presented herein allows all aspects of the element shape to be optimized along with layer thicknesses and permittivities. This is accomplished by characterizing element shapes by a two-dimensional chromosomes, which represent full-blown pixel-based approximations of the elements. In order to offset the increased computational cost, the algorithm is implemented on a massively parallel computer (Connection Machine CM-5). The evaluation of the objective function within the GA framework belongs to the class of embarrassingly parallel problems, and a massively parallel implementation results in a significant reduction of the computational cost when compared to a sequential implementation. Several schemes for efficiently distributing the computational load over the available processors on a MIMD-configured CM-5 will be discussed for a variety of synchronous and asynchronous master-slave GA models. Numerical results illustrating the application of this technique will be provided in the presentation.

## Analysis of Frequency Selective Surfaces with Arbitrary Aperture Geometry

Robert C. Hinz\* and Chi H. Chan  
Department of Electrical Engineering, University of Washington  
Seattle, WA 98195

Robert A. Kipp  
DEMACO, Inc.  
100 Trade Centre Drive, Suite 303  
Champagne, IL 61820

A hybrid spatial/spectral technique for the analysis of frequency selective surfaces comprised of perfectly conducting patches embedded in a layered media has been reported recently. Each element for the MoM impedance matrix requires that 10 to 100 thousands of modes be summed to achieve convergence. The summation is accelerated by evaluating the potential at the FSS surface and subtracting an asymptotically identical potential that is just above the surface. A rapidly converging spectral summation which corresponds to the offset potential is added to recover the original summation. The spatial Green's functions for the layered medium are conveniently evaluated using complex images for an electric current source.

In this paper, a frequency selective surface (FSS) comprised of apertures embedded in a layered medium is analyzed using the hybrid spatial/spectral technique. The complex images, however, are modified for the magnetic current sources.

The magnetic currents associated with the shorted apertures of the frequency selective surface are defined in terms of arbitrary triangular basis functions. This allows a line segment approximation of the unit cell avoiding the staircase effect. The magnetic currents on the shorted apertures are computed by solving a mixed potential integral equation (MPIE). When the source and test triangular basis functions are sufficiently far apart, the double surface integral is replaced with evaluation at the centroids of the triangles. For sources near the test cell, integration of the entire triangular domain is required for computing the scalar potential. The scalar potential is dominant for near interactions, the vector potential does not contribute significantly to the result so it is approximated by the centroid method. The convergence of the hybrid spatial/spectral method is further improved by the use of Shanks transformation.

## **Performance of double layered FSS with complex resonant elements**

**J. Shaker\* and L. Shafai**

*Department of Electrical & Computer Engineering  
University of Manitoba, Winnipeg, Manitoba, Canada, R3T 2N2*

Frequency selective surfaces (FSS) have been used widely as filters for blocking undesired frequency bands, or, providing other filter characteristics in reflection and transmission of electromagnetic waves and in design of multi-reflector antennas. Our studies have concentrated on novel structures and geometries such as open or shorted rings, without or with loaded central conducting elements were investigated (J. Shaker & L. Shafai, *Electronic letters*, 1655–1657, 1993).

With single layer configurations the frequency selectivity can be controlled only by the resonance property of the single cell element. Since, these elements are two dimensional geometries, their performance is therefore limited by their complexity. This limitation can be overcome by adding other layers of conducting cells to generate three-dimensional structures, with additional flexibilities in the design of cell elements. The coupling between elements of different layers also acts as another parameter to increase the flexibility of the design. So far, however, we have investigated double layer etched on two sides of a dielectric slab. The formulation is based on dyadic Green's function in the spectral domain, which is solved using a moment method. Therefore, the coupling have been accounted for in the analysis.

Numerical simulation of an FSS, composed of two layers of square patches each of which etched on lower and upper interfaces of the slab, was performed to study the effects of coupling between them and the additional flexibility that have been introduced into the structure. The frequency dependence of the resulting structure's reflective properties is observed to be dictated by the layer that has larger square patches as its cell elements. In other words, it turned out the surface that has larger patches as its cell element either "blocks" or "electrically short" the one with smaller patches, depending on being etched on the upper or lower interface of the slab. However, for equal size square patches, there is a noticeable change in the resonant frequency of the structure compared to the single layer case.

To use the acquired flexibility one can etch different cell elements on the slab interfaces. As an example of such an undertaking, the case of FSS composed of open or short circuited square rings on the top and square patches on the lower interface was studied for different ring thickness and square sizes. The reflective properties of the resulting structure appears to vary between two extremes of ring or square, depending on their relative sizes with respect to each other.



THURSDAY PM JOINT SPECIAL SESSION TH-J7

Room: HUB 310

**RANDOM MEDIA & ROUGH SURFACE SCATTERING**

Chairs: S. Saatchi, California Institute of Technology; Y. Kim, California Institute of Technology

Organizers: S. Broschat, Washington State University; A. Ishimaru, University of Washington

- |      |   |      |
|------|---|------|
| 1:20 | Backscattering Enhancement of Volume-Surface Interaction of a Layer of Scatterers Overlying a Homogeneous Dielectric Half Space<br><i>*L. Tsang, Univ. of Washington; K.H. Ding, Massachusetts Inst. of Technology; G. Zhang, Univ. of Washington; C. Hsu, J.A. Kong, Massachusetts Inst. of Technology</i> | AP-S |
| 1:40 | Backscattering Enhancement from Discrete Scatterers Over a Rough Surface: Distorted Born Approximation<br><i>*R. H. Lang, The George Washington Univ.; N. S. Chauhan, D. M. Le Vine, NASA Goddard Space Flight Center</i>   | 446  |
| 2:00 | Enhanced Backscattering from Vacuum/Dielectric Interfaces<br><i>Z.H. Gu, J.Q. Lu, Surface Optics Corporation; A.A. Maradudin, Univ. of California; E.R. Mendez, Centro de Investigacion Cientifica y de Educacion Superior de Ensenada</i>  | 447  |
| 2:20 | Backscattering Enhancement by 2D Particles Deposited on a Planar Waveguide<br><i>A. Sentenac, J.-J. Grettet, UPR 288 C.N.R.S et Ecole Centrale Paris</i>  | 448  |
| 2:40 | Venusian Surface Roughness Inversion Using Two Scale Approximation<br><i>*Y. Kim, E. Rodriguez, S.S. Saatchi, California Inst. of Technology</i>  | 449  |
| 3:00 | Break   |      |
| 3:20 | Numerical Simulation of Scatterer Positions in a Very Dense Media<br><i>*P.R. Siqueira, K. Sarabandi, F.T. Ulaby, Univ. of Michigan</i>   | AP-S |
| 3:40 | Numerical Scattering Analysis of Two Dimensional Dense Random Media<br><i>*P.R. Siqueira, K. Sarabandi, Univ. of Michigan</i>   | AP-S |
| 4:00 | Numerical Analysis of Holographic Images Degraded by Turbulence in Consideration of the Double Passage Effect<br><i>*K. Fujisaki, M. Tateiba, Kyushu Univ.</i>  | AP-S |
| 4:20 | The Effective Permittivity of the Discrete Random Medium Composed of Dielectric Spheres and Homogeneous Space in the Region of Low to Resonance Frequencies<br><i>*Y. Nanbu, Sasebo National College of Technology; M. Tateiba, Kyushu Univ.</i>  | AP-S |

## **Backscattering Enhancement from Discrete Scatterers over a Rough Surface: Distorted Born Approximation**

by

Roger H. Lang\*  
The George Washington University  
Washington, DC 20052

and

Narinder S. Chauhan and David M. Le Vine  
NASA Goddard Space Flight Center  
Greenbelt, MD 20771

Bistatic scattering from a sparse distribution of discrete scatterers over a rough surface is investigated. The scatter is computed by employing the distorted Born approximation for the particle scatter along with a Kirchhoff treatment of the rough surface. The findings of this field based method are compared with the results of the first order transport theory. This comparison shows that there are coherent wave effects predicted by the distorted Born theory which are not present in the transport results. These wave effects contribute in the backscatter and the specular directions. These contributions are sometimes called enhancement effects.

In previous treatments of the problem where a flat interface has been assumed, enhancement effects have also been observed. In this case the backscatter is divided into: (1) direct or volume scatter, (2) direct-reflected or particle-ground interaction contributions and (3) reflected terms which scatter from the ground twice. In the case of the flat surface, enhancement terms arise from the forward and reverse going particle - ground interactions terms. When the interface is rough, the same enhancement terms arise as if from a flat interface at the mean level of the rough surface. For the rough surface case, other enhancement terms also occur. These terms result from forward and reverse interactions of waves which are bistatically scattered from particles and bistatically scattered from the surface.

The general results are applied to a layer of vegetation over a rough ground surface. The vegetation is modeled by dielectric discs and cylinders representing leaves and stems respectively. Backscatter results for P and L band frequencies will be given demonstrating the importance of each of the effects for typical values of plant and surface parameters.

# Enhanced Backscattering from Vacuum/Dielectric Interfaces

Zu-Han Gu and Jun Q. Lu  
Surface Optics Corporation, P.O. BOX 261602, San Diego, CA 92126, U.S.A.

Alexei A. Maradudin  
University of California, Physics Department, Irvine, CA92717, U.S.A.

E. R. Mendez  
Centro de Investigacion Cientifica y de Educacion Superior de Ensenada  
Apdo. Postal 2732, Ensenada, B.C., Mexico.

## ABSTRACT

One of the most interesting phenomena associated with the scattering of light from a randomly rough surface is that of enhanced backscattering. This is the presence of a well-defined peak in the retroreflection direction in the angular distribution of the intensity of the incoherent component of the light scattered from such a surface which is due primarily to the coherent interference of each multiple reflected optical path with its time-reversed partner.

It has been known for a few years that not only a rough metallic surface but also a rough dielectric surface can produce an enhanced backscattering peak. Due to the difficulty in fabricating one- or two-dimensional dielectric rough surfaces with a high index of refraction, no experiments have been able to reveal such a peak in scattering from a dielectric rough surface.

In this paper we will present recent theoretical analysis and experimental results that cover the enhanced backscattering from a characterized randomly rough 1-D free-standing dielectric film and a dielectric film on a dielectric substrate. We will also present the enhanced backscattering from a characterized randomly rough 1-D dielectric surface.

---

\* Submitted to The 1994 IEEE AP-S International Symposium (June 19-24, 1994 Seattle)

## Backscattering enhancement by 2D particles deposited on a planar waveguide

Anne Sentenac and Jean-Jacques Greffet

Laboratoire d'Energétique Moléculaire et Macroscopique, Combustion  
Ecole Centrale Paris, Centre National de la Recherche Scientifique  
92295 Châtenay-Malabry Cedex, France

Under certain conditions, the scattering of light by random rough surfaces exhibits a peak in the retroreflection direction. In the case of weakly rough surfaces, enhanced backscattering comes from the coherent interferences of multiple scattered surface waves, induced by the roughness, with its time-reversed partner. Actually this phenomenon has been primarily discussed for metallic structures which support surface polaritons (A. A. Maradudin et al., *Revista Mexicana de Fisica*, **38**, 343-397, 1992).

In this paper, we present another mechanism, involving multiple scattering of modes, that may lead to enhanced backscattering. We consider a homogeneous layer embedded in two semi-infinite homogeneous media enlightened by s or p-polarized plane wave. Small bidimensional defects (rods) are randomly placed on the illuminated surface of the film. We derive, in the Fourier space, an expression for the Green function, solution of the scattering of a dipole above the layer. Special care is taken to evaluate the poles, corresponding to the different modes (guided waves, plasmons) which appear in this formulation. Thanks to the Green function, the Heilmoltz differential equation is transformed into a volume integral equation (A. Sentenac et al., *J. Opt. Soc. Am. A*, **9**, 996-1006, 1992) that is solved by a classical moment method. A Monte-Carlo numerical simulation enables us to study the scattering of light by the structure. Backscattering enhancement is obtained for dielectric layers and metallic films. Its signification as a weak localization phenomenon of guided modes or long range surface plasmons respectively, is discussed.

## VENUSIAN SURFACE ROUGHNESS INVERSION USING TWO SCALE APPROXIMATION

Yunjin Kim\*, Ernesto Rodriguez, and Sasan S. Saatchi  
Jet Propulsion Laboratory  
California Institute of Technology  
Pasadena, CA 91109

Magellan was launched on May 4, 1989 on the Shuttle Atlantis in order to achieve global imaging of the Venus surface [R. S. Saunders et al., *J. Geophys. Res.*, vol. 95, pp. 8339-8355, 1990]. Since the Venusian surface is covered by a dense and optically opaque cloud layer, radar mapping is the best tool to obtain surface morphology and electrical properties. The Magellan radar operates in three different modes: altimeter, SAR, and radiometer. Using the altimeter data, the near nadir backscattering cross sections can be obtained. The SAR backscattering data provide the diffuse scattering cross section by small scale surface features. From the radiometer data, the emissivity of the Venus surface can be estimated.

In this paper, we present an algorithm which systematically estimates Venus' surface parameters using the two scale approximation. These surface parameters are the large scale spectral slope, dielectric constant, small scale surface rms height, and the small scale spectral slope, assuming that the surface power spectrum is a power-law spectrum. Our approach uses all three Magellan data sets (altimeter, SAR, and radiometer) and the resultant two scale predictions satisfy all the data sets simultaneously within the measurement error. As a test of our algorithm, we performed the surface parameter estimation using the Magellan data near Gula Mons. The estimated values are very close to the surface characteristics of the Playa lava flows on Earth. This and other examples will provide the effectiveness of the algorithm and the surface characteristics of some Venusian surfaces.



THURSDAY PM URSI-B SPECIAL SESSION TH-U37

Room: Kane 220

FUNDAMENTALS OF ACTIVE AND PASSIVE POLARIMETRY

Chairs: E. Pottier, IRESTE; Y. Yamaguchi, Niigata University

Organizer: W.-M. Boerner, The University of Illinois at Chicago

- 1:20 Basic Formulations of Wideband Polarimetric Vector Signal Processing 452  
*W.-M. Boerner, Univ. of Illinois at Chicago; E. Lüneburg, DLR-IHFT; Y. Yamaguchi, Niigata Univ.; J.Y. Dea, NCCOSC-NRaD*
- 1:40 Unsupervised Classification of Multipolarization SAR Images Using Competitive Neural Networks 453  
*E. Pottier, IRESTE*
- 2:00 The Development of Methods of Passive Radiopolarimetry in Russia: A Review. 454  
*A.I. Kozlov, A.I. Logvin, The Moscow State Technical Univ. of Civil Aviation*
- 2:20 Polarimetric Imaging of Complex Structured Radar Targets Using a Decomposition Theorem Founded on Geometrical Theory of Diffraction 455  
*F.A. Molinet, Société Mothesim*
- 2:40 Full Polarimetric Measurements of Targets and Environments by a V.H.F. Radar System 456  
*L. Challe, E. Pottier, J. Saillard, IRESTE*
- 3:00 Break
- 3:20 Nearfield Reflectance and Imaging of Underground Moisture: Effects of Polarization 457  
*G. Tricoles, P. Yasuhara, GDE Systems, Inc.*
- 3:40 Remote Sensing of the E-Region Ionospheric Magnetoplasma with a VHF Doppler Radar Polarimeter 458  
*G.C. Hussey, J.A. Koehler, G.J. Sofko, Univ. of Saskatchewan*
- 4:00 Experimental Results of the Measurement of Wind Velocity by Doppler Radars 459  
*A.I. Logvin, A.I. Kozlov, The Moscow State Technical Univ. of Civil Aviation*
- 4:20 Experimental Results of Rain-Backscatter Measurements with a Wideband Polarimetric Doppler Radar in the X-Band 460  
*W.-M. Boerner, A.P. Agrawal, G.D. Nesper, Univ. of Illinois at Chicago, P.P.S. Wei, Boeing DSG*

**BASIC FORMULATIONS OF WIDEBAND POLARIMETRIC VECTOR SIGNAL  
PROCESSING**

Wolfgang-M. Boerner, UIC-EECS/CSL, Chicago, IL/USA  
Ernst Lüneburg, DLR-IHFT, Oberpfaffenhofen, Bev./FRG  
Yoshio Yamaguchi, I&SE, Niigata University, N-Ikarashi, JAPAN  
Jack Y. Dea, NCCOSC-NRaD, Code 832, San Diego, CA/USA

The importance of complete vector signal description of electromagnetic wave radio emission as well object interrogation is analyzed covering the extrawideband (ULF-UV) spectral domain. First, it is shown that at ULF-ELF bands, it is essential to recover the complete (3-axis) magneto-metric and electro-metric as well as electromagneto-metric fields by implementing various 3-axis magnetometers, 3-axis electric field potential meters, and 3-axis loop antennas, respectively providing pertinent examples of polarimetric seismo-electromagnetology. Next, basic concepts LF/HF/UHF/EHF polarimetry and then IR, NIR-OPT-NUV polarimetry are introduced and compared. It is shown and verified that in high resolution electromagnetic sensing and imaging polarimetry plays an essential and crucial role.

1994 ISAP/URSI-NRSM, Seattle, WA  
Session: Fundamentals of Active and Passive Polarimetry

UNSUPERVIZED CLASSIFICATION OF MULTIPOLARIZATION SAR IMAGES  
USING COMPETITIVE NEURAL NETWORKS

E. POTTIER

Laboratory S2HF - IRESTE  
La Chantrerie - CP 3003  
44087 NANTES CEDEX 03  
FRANCE

Classification of earth terrain within a full polarimetric SAR image is one of the many important applications of Polarimetry. In previous publications Gaussian statistics have been assumed for the radar return signals to build the Bayes classifier. Among many non-Gaussian statistics, the K-distribution has proved to be very useful in characterizing the polarimetric distribution of electromagnetic earth echoes.

In such a case the Bayes classifier is very difficult to define, and another classification strategy has to be developed.

As the scattering matrix has the disadvantage of being dependent of the absolute phase, which means coherent addition, we prefer to use the Kennaugh matrix to perfectly describe the mixed target state. This matrix contains parameters which are dependent only of the relative phase, so it is possible to interpret independent objects which are added incoherently.

The approach to stationary target identification is to decompose the Kennaugh matrix into several matrices where one of them will be related to a pure state target. The way to proceed, consists in applying one of the most famous "target decomposition theorems" defined by Huynen, Cloude, Krogager and Barnes ...

Once the single averaged target, or the stationary target, has been obtained from one of the decomposition theorems, we show how it is possible to classify and identify the radar target by using a neural network method.

In previous publications, the author has shown how it was possible to classify such data using a supervised learned neural network. Now we deal with unsupervised neural network modelization, with training algorithms based on a competitive process (Hebbian Rule). This allows to develop a general classification process without any a priori knowledge about the number of the different classes, the specific features, etc ...

The decomposition and classification scheme is applied to fully polarimetric SAR data, and during the symposium, identification and classification results of real targets will be shown.

**The Development of Methods  
of Passive Radiopolarimetry in Russia.  
Review.**

Dr. Prof. A.I. Kozlov & Dr. Prof. A.I. Logvin  
The Moscow State Technical University of Civil Aviation

**Abstract**

Passive radiolocation in Russia (former USSR) began developing intensively in the mid-sixties when the first satellites designed for environmental studies were made. Considerable theoretical and experimental material on radio-thermal polarization measurement of the atmosphere and underlying surface is available. Among underlying surfaces the following ones have been studied intensively: fresh and sea water surfaces (of a river, lake, sea, ocean), fresh and sea ice, soil with plants at different ripening stages as well as soil without plants, forests (coniferous, foliage and mixed forests), tundra and marsh surfaces, etc.

Said measurements were carried out using both satellites and aircraft and special on-ground platforms. A great number of theoretical studies concerned with the application of radiopolarimetry methods in passive radiolocation have been carried out. These studies deal with solving problems of navigation, detection of ecological dangerous regions and territories, determining the humidity salinity of soils, drawing up ice maps in Arctic and Antarctic regions, solving tasks of different objects classification and identification, etc.

The summary of the main results of the studies obtained in Russia (USSR) in using passive polarimetry method for the environmental studies.

**POLARIMETRIC IMAGING OF COMPLEX STRUCTURED RADAR TARGETS UNSING  
A DECOMPOSITION THEOREM FOUNDED ON GEOMETRICAL THEORY OF DIFFRACTION**

Frédéric A. Molinet

Société MOTHEMIM, La Boursidière, 92357 Le Plessis-Robinson, France

In this paper, the decomposition of the scattered field of a complex closed form target into physical scattering mechanisms, as given by the Geometrical or Physical Theory of Diffraction, is used in order to establish new target decomposition theorems. Major emphasis is devoted to the symmetry properties of the Sinclair radar scattering matrix associated with single and multiply scattering phenomena.

The author has shown in previous publications [1, 2] that the monostatic Sinclair scattering matrix corresponding to  $N$  single reflection points on a smooth target can be decomposed into a symmetric target (sphere like-target) and a non symmetric target, the latter being of order  $1/k$  compared to the main term of the symmetric target,  $k$  being the wave number. This decomposition is independent of the reference frame. It has also been shown that for a target with edges, a similar decomposition can be performed. In this paper these results are extended to multiple interactions comprising double and triple bounce reflection, single reflection associated with single edge diffraction and double edge diffraction.

By taking into account the symmetry properties together with the order of magnitude with respect to the inverse powers of  $k$  of each diffraction mechanism, it is possible to separate the different contributions once the scattering matrix of a complex target is known.

Polarimetric ISAR images of missile-shaped targets are presented identifying separate and interactive images for each and several diffraction processes.

- [1] F.A. Molinet, Proceedings of the 2nd Int'l Conference on Electromagnetics in Aerospace Applications, Torino, Sept. 1991.
- [2] F.A. Molinet and al, eds, 2nd Int'l Workshop on Radar Polarimetry, Nantes, Sept. 1992.

## FULL POLARIMETRIC MEASUREMENTS OF TARGETS AND ENVIRONMENTS BY A V.H.F. RADAR SYSTEM

L. CHALLE-E. POTTIER-J. SAILLARD

Laboratory S2HF IRESTE  
La Chantrerie CP 3003  
44087 NANTES Cedex 03  
FRANCE  
tél.:(33) 40-68-30-64  
téléfax: (33) 40-68-32-33

At the present time, multifrequency multipolarization V.H.F. radar systems (20-100 MHz) are being used to study detection against stealthy behaviour of targets. These targets are easier to detect at V.H.F. because their dimensions are of the order of a wavelength (3-15 m) and so, the phenomena of electromagnetic resonances occur in reflection from targets. Moreover, the efficiency of absorbing materials and complex target shapes is reduced.

Radio-wave propagation at V.H.F. has the advantage of not being sensitive to atmospheric phenomena like snow, rain and clouds. But in this frequency band, we must take into account:

- The multipath propagation due to ground reflection effects.
- The curvature of the Earth, which becomes more important on the distance between target and antennas (10-300 km) increases.

The use of two polarizations simultaneously in reception and variable in transmission permits us to construct a full polarimetric received voltage matrix ( $2 \times 2$ ). From several different received voltage matrices, we shall show how it is possible to reconstruct the target backscattering matrix and determine the two Fresnel's coefficients  $R_H$  and  $R_V$  for the earth's surface.

During the symposium, we shall present results obtained by simulation and point out the limitations of such system (noise level, different architecture, number of antennas...).

## NEARFIELD REFLECTANCE AND IMAGING OF UNDERGROUND MOISTURE: SOME POLARIZATION EFFECTS

G. Tricoles and P. Yasuhara  
GDE Systems, Inc., P. O. Box 85310, San Diego, CA 92186-5310

In studies of radio wave systems for detecting and imaging leakage from buried pipes, we buried samples of wet soil and measured reflectance. A horizontal dipole antenna scanned parallel, horizontal lines over the sample region for phase and amplitude measurements at frequency 296 MHz. The sample was three plastic bags of wet soil and had overall a nearly rectangular contour; the longest dimension was in the antenna scan direction. Depth was 36 inches, or 0.9 wavelength. Measurements were made with the dipole first parallel and then orthogonal to the scan direction.

The measured, nearfield reflectance distribution depended on polarization; moreover, it spanned a region appreciably larger than the area of the buried sample. To understand the data, we dug the soil and found wet soil around the buried sample. The explanation was rain water that had entered the test region by seeping underneath a wall of the test facility's plastic tent. The moisture from the rain was not visible on the air-ground surface before digging. Reflectance contours coincided with the shape of the moist buried soil region, and they were larger for polarization parallel to its boundaries.

An image was formed by digitally processing the measured reflectance data. Polarization for this case was parallel to scan direction, which was orthogonal to the overall direction of underground water migration. Image calculation was based on Rayleigh-Sommerfeld diffraction theory. The angular spectrum of reflectance was backward propagated, with a measured value of dielectric constant for dry soil. The image contour agreed well with that of the sample and moist soil around it.

## **Remote Sensing of the E-Region Ionospheric Magnetoplasma with a VHF Doppler Radar Polarimeter**

**G.C. Hussey, J.A. Koehler, and G.J. Sofko**  
Institute for Space and Atmospheric Studies  
Department of Physics and Engineering Physics  
University of Saskatchewan  
Saskatoon, SK, Canada S7N 0W0  
(Fax: 306-966-6400; E-Mail: sofko@skisas.usask.ca)

### **Abstract**

Two bistatic 50 MHz Doppler radar links have been used to measure the polarization of scatter from a common ionospheric E-region target volume in two nearly orthogonal directions. The radar were operated during magnetically disturbed periods when scatter of high signal to noise ratio from the lower E-region (heights 100-120 km) was observed. Assuming as is usual that the coherent scattering is weak, the polarization changes should be due mainly to the propagation of the radar waves through the magnetoplasma to and from the scatterers. The 50 MHz waves are not expected to exhibit large polarization changes because the radar frequency is far above the electrom plasma frequency. However, the measured polarization parameters (intensity, polarization ratio, ellipticity and orientation) show rapid, large variations. Some of the polarization observations will be presented, and physical mechanisms such as Faraday rotation, Faraday dispersion and magnetoionic mode splitting will be proposed to explain the unexpected results.

## **Experimental Results of the Measurement of Wind Velocity by Doppler's Radar**

**Dr. Prof. A.I. Kozlov & Dr. Prof. A.I. Logvin**  
The Moscow State Technical University of Civil Aviation

### **Abstract**

The results of the experimental studies on the measurement of wind velocity by Doppler's radar operating in sm bandwidth at different kinds of polarization are given. The results of measurements by means of specially developed algorithms were directly displayed on PC in color-brightness image where different gradation of color correspondent to wind velocities which made it possible to see the dynamics of the development of wind processes with a high degree of accuracy. Considerable illustrating material on the results of the experiment and the respective analysis of the obtained images are given in this work.

Additionally, different mathematical models of the development of wind process have been considered and simulation on the basis of the formed models has been carried out.

Comparing the results of the simulation to real measurements has shown that the proposed mathematical models of the dynamics of the development of wind processes describe these processes quite adequately. Further ways for the development of experimental studies on measuring wind velocity from the viewpoint of increasing their accuracy for the purpose of more reliable description of the situation and for further forecasting the developments, i.e. detecting dangerous zones having a higher turbulence are shown.

**EXPERIMENTAL RESULTS OF RAIN-BACKSCATTER MEASUREMENTS WITH A  
WIDEBAND POLARIMETRIC DOPPELER RADAR IN THE X-BAND**

Wolfgang-M. Boerner, Amit P. Agrawal, Gerald D. Nespor,  
UIC-EECS/CSL, Chicago, IL/USA and P. Pax Sam Wei, Boeing DSG,  
Physics Division, Kent, WA/USA

The polarimetric backscatter from fluctuating distributed hydro-meteors is modeled utilizing basic properties of the coherency matrix  $[J]$ , the  $2 \times 2$  Sinclair  $[S]$ , the  $3 \times 3$  covariance  $[\Sigma]$  and the  $4 \times 4$  Kennaugh  $[K]$  matrices in order to formulate the Kennaugh target characteristic polarization theory for the time-dependent distributed scatterer case. A simplified shape-model for rain-drops based on the STAPOR-PRATT formulation (oblate and prolate spheroids) is implemented including an analysis of the associated polarimetric Doppler signatures of vibrating and oscillating hydro-meteors. Experimental data collected with the BAC polarimetric instrumentation X/K-band radars is utilized for verifying the validity of the model.

1994 ISAP/URSI-NRSM, Seattle, WA  
Session: Fundamentals of Active and Passive Polarimetry

THURSDAY PM URSI-B SESSION TH-U39

Room: Savery 249

WAVEGUIDES II

Chair: A.D. Yaghjian, Rome Laboratory (USAF)

- |      |   |     |
|------|---|-----|
| 1:20 | Field Pattern Computation of the Waveguides<br><i>*A. Asi, L. Shafai, Univ. of Manitoba</i>   | 462 |
| 1:40 | Waveguides Discontinuities - Multimode Moment Method Analysis<br><i>*A.K. Bhattacharyya, Hughes Space and Communications</i>  | 463 |
| 2:00 | On the Full-Wave Spectral Domain Analysis of Multiconductor Coplanar Waveguide Structures<br><i>G. Cano, *F. Medina, M. Horno, Univ. of Seville</i>   | 464 |
| 2:20 | An Algorithm for the Determination of the Roots of the Characteristic Equation for Corrugated or Dielectric Loaded Circular Waveguides<br><i>*L. Costa da Silva, Pontificia Universidade Católica do Rio de Janeiro</i> | 465 |
| 2:40 | Variational Analysis of Optical Waveguides with Arbitrary Cross-Section and Refractive Index Distribution<br><i>*J.R. Souza, Pontifical Catholic Univ. of Rio de Janeiro</i>  | 466 |
| 3:00 | Break   |     |
| 3:20 | Synthesis of a Curved Waveguide Evanescent Mode Filter<br><i>H. Tertuliano, P. Jarry, Bordeaux I Univ.; L.A. Bermudez, Brasilia Univ.</i>   | 467 |
| 3:40 | Studies on Radiation Patterns of Thinned and Normal Arrays of Waveguide Radiators<br><i>V.M. Rao, GITAM Engineering College; *G.S.N. Raju, K.R. Gottumukkala, Andhra Univ.</i>  | 468 |
| 4:00 | Transferred Power in an Asymmetrical Two-Dimensional Directional Coupler with Trapezoidal Corrugation<br><i>F. Mohajeri, H. Abiri, Shiraz Univ.; M.H. Rahnvard, Univ. of Ottawa</i>                                     | 469 |

# Field Pattern Computation of the Waveguides

Ali Asi\* and Lotfollah Shafai

Department of Electrical and Computer Engineering  
University of Manitoba, Winnipeg, Manitoba, Canada R3T-5V6

Finite difference has proven to be one of the most versatile techniques in dealing with waveguides of arbitrary cross-sections and profiles. The problem with conventional finite difference methods lays in the fact that they are usually formulated based on one vector field component. This poses an extra computational burden to calculate the other field components using the differential operators of Maxwell's equations. It can be easily verified that this procedure is prone to numerical inaccuracies especially in the presence of truncation error.

In this presentation, a novel finite difference scheme is proposed which is capable of evaluating all six vector field components at any arbitrary frequency of operation. It is based on a four directional expansion of finite difference form of Maxwell's equations. As the input of the algorithm, one has to specify the normalized frequency of operation  $\Delta l/\lambda$  and its corresponding eigenvalue, i.e. normalized wave number  $\beta \cdot \Delta l$ . The value of this eigenvalue can be extrapolated from dispersion curves of the waveguide or it can be easily evaluated using Compact FDTD, i.e. CFDTD (A. Asi, L. Shafai, IEEE AP-S symposium digest, vol.1, pp. 360-363, 1993).

One may still argue that the calculation of the field patterns can also be achieved using any of the conventional time domain methods. But, this new finite difference algorithm is even superior to those methods for the following reasons. First, the calculation of both time and axial derivatives are handled analytically, while in time domain methods one or both of these derivatives are taken numerically. Second, the field pattern calculation using time domain methods are based on either transient or steady state analysis. For the transient analysis, one has to take record of the evolution of the fields at each individual node of the mesh and then take the Fourier transform at all these nodes. Needless to say this is a rather tedious and wasteful approach, especially when the field patterns at few frequencies are of major concern, and not at all frequencies and all modes. For the steady state analysis, on the other hand, one has to excite the structure with a sinusoidal waveform and then after sufficient iterations, average the field absolute values at all nodes and for all field components. In addition to large number of iterations required to remove the transient response effect, this method suffers from another drawback. In fact, taking the absolute values of the field components simply suppresses all phase information of that component.

## Waveguide Discontinuities - Multimode Moment Method Analysis

Arun K. Bhattacharyya  
Hughes Space and Communications  
Bldg. S12, MS V348  
Los Angeles, CA 90009.

A number of techniques are available in the literature to analyze waveguide discontinuity problems. They include the variational method (R.F.Harrington, *Time-Harmonic Electromagnetic Fields*, McGraw-Hill, 1961), the Mode Matching Technique (MMT) (G.L. James, *IEEE Trans.*, MTT-29, pp. 1059-1066, 1981) and the Method Of Moments (MOM) (H. Auda and R.F. Harrington, *IEEE Trans.*, MTT-31, No. 7, 1983). The variational method provides fairly accurate results for an isolated discontinuity in a waveguide supporting only one propagating mode. The results become inaccurate if two consecutive discontinuities are close to each other, because of the higher order modes interaction. The MMT can incorporate the higher order modes interactions between discontinuities. In this method, the generalized scattering matrix of a discontinuity is determined from the continuity conditions of the electromagnetic fields. Because a large number of modes are generated by a discontinuity, the matrix size becomes large which requires large CPU time. The MOM analysis available in the literature is very similar to the MMT in terms of the CPU time.

In this paper we present a computationally efficient method for analyzing waveguide discontinuity problems. The method is based on Galerkin's MOM formulation. The modes that are generated by a discontinuity are divided into two categories, interacting modes and non-interacting modes. It is found that the size of the generalized scattering matrix is proportional to the number of interacting modes only. The non-interacting modes affects the elements of the matrix. A generalized equivalent network is constructed which gives physical insight to the problem. The method is found to be several times faster than MMT. The accuracy of the method will be demonstrated by comparing the numerical results with the measured return loss of a multisection iris-coupled filter.

## On the Full-Wave Spectral Domain Analysis of Multiconductor Coplanar Waveguide Structures

G. Cano, F. Medina\*, M. Horno  
Microwaves Group. Department of Electronics and Electromagnetics  
University of Seville  
Avda. Reina Mercedes s/n 41012 SEVILLA (SPAIN)

Coplanar waveguide transmission line is a type of planar structure that constitutes an interesting alternative to microstrip in hybrid and monolithic microwave circuit technologies. The advantages of this configuration have been already discussed elsewhere (e.g. R.W. Jackson, IEEE-MTT, 34, 1450-1456, Dec. 1986). The basic structure consisting of a strip centered between two (ideally infinite) ground planes has been exhaustively studied in the past under quasi-TEM and more rigorous approaches. During the last decade a number of papers have been published on the analysis of this type of line emphasizing the possible CAD suitability of the model. Most of this work has been done on the single conductor version of this line. However, coupled structures involving several lines are usual building blocks in microwave circuitry. The most popular technique to analyze with reasonable computational effort this type of configurations is probably the spectral domain approach. Unfortunately, this method, although very efficient, still requires remarkable computational effort if it is not implemented carefully.

During the last two or three years, some of the authors of this communication have devoted part of their attention to improve the numerical performance of the SDA by means of intensive analytical preprocessing. This work has given place to some interesting results in the quasi-TEM analysis of several planar structures (F. Medina et al., IEEE-MTT, 40, 1748-1756, Sep. 1992; E. Drake et al., IEEE-MTT, 41, pp. 260-267, Feb. 1993; E. Drake et al., Int. J. MiMiCAE, to appear). Starting from this experience, we have treated from the same perspective (to attain high accuracy and reliability and short CPU time) the intrinsically more involved problem of the dynamic (full-wave) analysis. Apart from techniques to speed up computations, which are essentially a translation of the previously developed for the quasi-TEM analysis, we have used a modified dispersion equation in order to improve the process of root searching in the complex plane. Some preliminary results for the single boxed coplanar waveguide embedded in a layered substrate were published in (F. Medina et al., 23rd EuMC, pp. 690-692, Madrid, Sep. 1993). In this communication we present the extension of the method to multiple coupled lines. A systematic algorithm to compute the dispersive modal impedances for an arbitrary stratified medium -thus avoiding the need of repeating the analysis for a different dielectric structure- is also provided. The final goal is to develop an algorithm to compute dynamic parameters of multiconductor coplanar waveguide structures which is accurate, reliable and quick enough to be considered a CAD tool.

AN ALGORITHM FOR THE DETERMINATION OF THE ROOTS OF THE  
CHARACTERISTIC EQUATION FOR CORRUGATED OR DIELECTRIC  
LOADED CIRCULAR WAVEGUIDES

Luiz Costa da Silva  
Pontificia Universidade Católica do Rio de Janeiro  
Rio de Janeiro-Brazil

An Algorithm is presented for the numerical computation of the roots of the characteristic equation for corrugated or dielectric loaded circular waveguides, with guaranteed identification of all the roots, real, imaginary or complex, in a given interval. In a 9121 IBM computer, 100 roots for a corrugated waveguide can be calculated in 1 second of CPU time.

Both characteristic equations under consideration can be put in the form:

$$F(x) = Cte$$

The zeros of the denominator of  $F(x)$  (discontinuities of the function) are easily determined, and the function has the shape shown in Fig. 1. An inspection of this figure leads to the following observations, that are the basis for the computation algorithm:

- i) In the first interval, from the origin to the first discontinuity of  $F(x)$ , if  $F(0) < Cte$  there is a real root; if not, the characteristic equation has an imaginary root.
- ii) In the remaining intervals, between discontinuities of  $F(x)$ , if  $F(x)$  changes sign, there is a real root. If not, and  $F(x_{min}) < Cte$ ,  $F(x_{min})$  being the minimum value of  $F(x)$  in the interval, there are two real roots; if  $F(x_{min}) > Cte$ , there are two conjugated complex roots, with real part close to  $x_{min}$ . In the search of the complex roots, it can be used, as initial values, the roots of the parabolic equation that fits  $F(x)$  in the neighborhood of  $x_{min}$ .

The real and imaginary roots are quickly computed by the method of Brent, and the complex roots by the method of Muller.

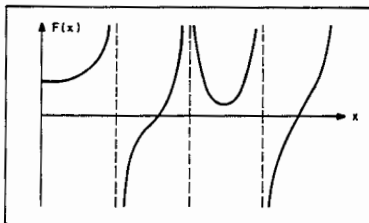


Fig. 1.  $F(x)$

## VARIATIONAL ANALYSIS OF OPTICAL WAVEGUIDES WITH ARBITRARY CROSS-SECTION AND REFRACTIVE INDEX DISTRIBUTION

J. R. Souza

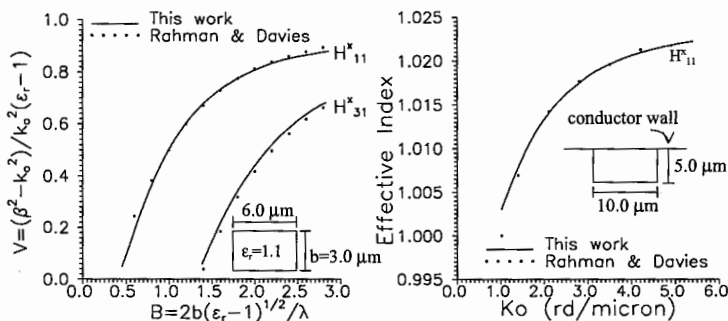
Center for Telecommunication Studies - Pontifical Catholic University of Rio de Janeiro  
Rua Marquês de São Vicente, 225 ~ 22453-900 Rio de Janeiro - RJ, Brazil

There has been an increasing interest in dielectric waveguides for application in optical communication systems. But the analysis of dielectric waveguides becomes very difficult if the cross-sectional shape is not a slab or circle, as in this case Maxwell's equations are not amenable to analytical solution, especially when the refractive index varies with position.

This paper presents a variational formulation for the analysis of optical waveguides with arbitrary cross-section and refractive index distribution. The formulation is based on the following formula, developed by A. D. Berk (in IRE Trans. A.P., Vol. 4, 104-111, 1956):

$$\omega^2 = \left[ \int (\nabla \times \mathbf{H}^*) \cdot \epsilon^{-1} \cdot (\nabla \times \mathbf{H}) d\Omega \right] \cdot \left[ \int \mathbf{H}^* \cdot \boldsymbol{\mu} \cdot \mathbf{H} d\Omega \right]^{-1} \quad (1)$$

where  $\omega$  represents the angular frequency and  $\mathbf{H}$ , the magnetic field vector.  $\Omega$  describes the region of interest. Although Berk's formula accommodates anisotropic material, only isotropic materials will be considered here. It is well known that (1) gives rise to spurious, nonphysical solutions, as the corresponding Euler equation does not satisfy  $\text{div } \mathbf{H} = 0$ . This condition is then enforced: the longitudinal component of  $\mathbf{H}$  is written in terms of the transversal ones, and (1) is modified accordingly. Next, the remaining  $\mathbf{H}$  components are expanded in a series of Hermite polynomials, which form a complete, orthonormal set in the infinite domain. The Rayleigh-Ritz procedure is then used, and a generalized eigen-value problem is obtained, whose eigen-values correspond to  $\omega$  and the eigen-vectors, to the expansion coefficients for the transversal components of  $\mathbf{H}$ . This formulation was implemented in a computer program, which allows the analysis of waveguides with arbitrary cross-section and refractive index distribution. Several types of waveguides were analysed, such as channel, rib, slab, image waveguides, including gradual refractive index distribution, with excellent agreement with other results of the literature. Sample results are shown below for slab and image waveguides, together with results obtained by the finite element method (Rahman & Davies, IEEE Trans. MTT, Vol. 32, 20-28, 1984).



# Synthesis of a Curved Waveguide Evanescent Mode Filter

H. TERTULIANO\*, P. JARRY\*, L.A. BERMUDEZ\*\*

\*Telecommunications Laboratory - ENSERB - Bordeaux I University - Bordeaux - France

\*\*Brasilia University -UnB - Brasilia - Brazil

## Abstract:

The curved type, evanescent mode filter is a type of waveguide filter that can be constructed using standard techniques. However the design of this kind of filter, must be based on accurate modeling of a bend waveguide's electrical properties. For the Fig.1 a study is made of the structure of the electromagnetic field in curved waveguide of rectangular section, and the expressions for the electromagnetic field and the propagation constants are derived. Using also the properties that relies the scattering matrix [S] with the voltage-current in the begin and in the end of the circuit the [ABCD] matrix, a synthesis procedure is determined.

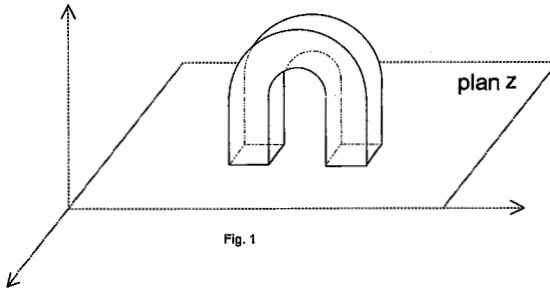
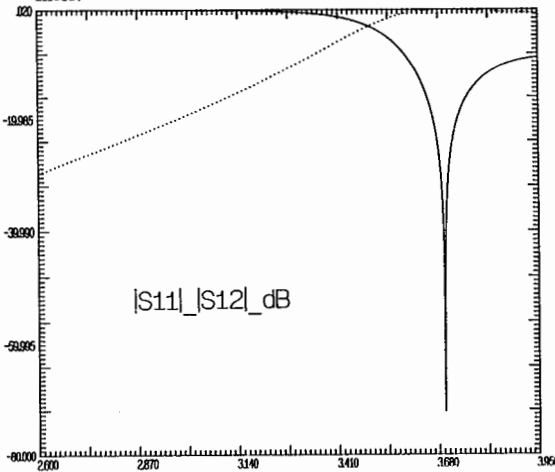


Fig. 1

Taking also in the other hand the choice of a fixed calculus of frequency: the filter's midband frequency, we present in Fig.2 the results obtained for one band-pass curved evanescent mode filter.



Final Results:	
Band-pass:	3.1 - 3.8 GHz
Number of poles:	1
Undulation in the band:	0.012dB
Width:	9.5mm
Height:	4.0mm
Curvature Ray:	33.2 mm
Total lenght:	13.867mm

**STUDIES ON RADIATION PATTERNS OF THINNED AND NORMAL  
ARRAYS OF WAVEGUIDE RADIATORS**

V.Malleswara Rao, Department of Electronics and Communication  
Engineering, GITAM Engineering College, Visakhapatnam-530 045  
G.S.N.Raju\*, K.R.Gottumukkala, A.U. College of Engineering  
Visakhapatnam-530 003, INDIA.

The radiation patterns for an array of isotropic radiators are evaluated from the finite summation of individual far-field components by considering the phase differences that are resulted from the phase distribution functions. When the elements of the array are non-isotropic the patterns are evaluated from the product of the element pattern and array factor. The element pattern, in general, varies from element to element, size to size and it also depends on its orientation.

When the elements are rectangular waveguides, it has been possible from the present work to thin the array without disturbing the pattern characteristics and parameters.

The radiation patterns are numerically computed for arrays of waveguide radiators for different inclinations,  $\delta$  of the radiators in the array. For the purpose of deciding minimum number of elements in the array for each inclination, the possible spacing is estimated and the results are presented in the following table for array length of  $10\lambda$  and  $\delta=10^\circ, 20^\circ, 30^\circ$ . It is found from the results that it is possible to keep 12, 11, 10 elements in the array of length  $10\lambda$  and with the inclination of  $10^\circ, 20^\circ, 30^\circ$  respectively. Reducing the number of elements further for the same length, grating lobes are found to appear.

It is interesting to note from the computed results that the radiation patterns of 12 and 20 elements of the array are almost the same. In other words, the overall pattern is not disturbed by thinning the array.

Length	$\delta$	Spacing	Number of Elements
$10\lambda$	10	2.60	12
$10\lambda$	20	2.71	11
$10\lambda$	30	3.00	10

## Transferred Power in an Asymmetrical Two-Dimensional Directional Coupler with Trapezoidal Corrugation<sup>1</sup>

F. Mohajeri, H. Abiri and M.H. Rahnavaard<sup>2</sup>  
EE Department, School of Engineering  
Shiraz University, Shiraz, Iran

Directional coupler is a 4-port device in which power can be applied to one of its ports and taken from the other ports. One of the methods of constructing this device is by using two parallel dielectric waveguides, in which the end of each guide plays the role of a port. The transferred power from one port to other is controlled by producing periodic corrugations at one or both adjacent surfaces of the two parallel waveguides. If the refractive index of the two sides of the waveguides aren't the same, coupler is called asymmetrical.

In this paper Finite Difference Time Domain (FDTD) method is used to obtain coupled waves between two waveguides of a directional coupler composed of the parallel dielectric waveguides with trapezoidal corrugation at one and at both adjacent surfaces. Using the obtained electric and magnetic fields, the transferred power from one waveguide to the other one is also computed.

1. This research was supported by Board of Research of Shiraz University, Shiraz, Iran.
2. Presently at Elec. Eng. Department, Faculty of Engineering, University of Ottawa, Ottawa, On., Canada, on sabbatical leave from Shiraz University, Shiraz, Iran.



THURSDAY PM URSI-K SESSION TH-U40

Room: Savery 241

**MEDICAL APPLICATIONS OF RADIOFREQUENCY FIELDS**

Chairs: J.C. Lin, University of Illinois at Chicago; M.A. Stuchly, University of Victoria		
1:20	Comparison of Homogeneous and Heterogeneous Tissue Models for Coil Optimization in Neural Stimulation *M.A. Stuchly, Univ. of Victoria; S. Pisa, Univ. of Rome; K. P. Esselle, Macquarie Univ.; G. D'Inzeo, Univ. of Rome	472
1:40	An Alternative Approach to EM Stimulation of Long Nerves R.P. Penno, D.D. Reuster, Univ. of Dayton	473
2:00	EM Wave Live-Detection System for Post Earthquake Rescue Operations *K.M. Chen, J. Kallis, Y. Huang, J. T. Sheu, A. Norman, C. S. Lai, A. Halac, Michigan State Univ.	474
2:20	Measurement of Cattle Fat Thickness Using a 1GHz Cavity Device *L.S. Taylor, Univ. of Maryland; N.L. Buck, U.S. Department of Agriculture	475
2:40	Hyperthermia Modeling for an Infinite Two-Layer Concentric Cylinder Using Matrix Optimization G. Kim, A. Ishimaru, Univ. of Washington	476
3:00	Break	
3:20	Performing the Spatial and Temporal Electromagnetic Fields on the Axis of a Lossy Cylinder - Torso or Limb K.A. Nabulsi, KAAU; *R.J. Wait, Consultant	477
3:40	Basic Characteristics of Coaxial-Slot Antennas for Interstitial Microwave Hyperthermia *K. Ito, M.-S. Wu, J.-I. Takada, H. Kasai, Chiba Univ.	478
4:00	Dipole and Concentric Ring Radiators for Tissue Ablation and Hyperthermia Applications *R.D. Nevels, Texas A&M Univ.	479
4:20	<b>Contrast Enhancement for Underwater Imaging Using a Polarization Differencing Technique Based on Biological Visual Systems</b> J.S. Tyo, M.P. Rowe, E.N. Pugh, Jr., N. Engheta, Univ. of Pennsylvania	480
4:40	Fundamental Study for CT Imaging of Biological Body with Light *K. Shimizu, M. Kitama, K. Yamamoto, Hokkaido Univ.	481
5:00	Near and Far Field Approaches for Non-Invasive Microwave Hyperthermia R.W.Y. Habash, A. Kumar, Indian Inst. of Science	482

## COMPARISON OF HOMOGENEOUS AND HETEROGENEOUS TISSUE MODELS FOR COIL OPTIMIZATION IN NEURAL STIMULATION

\*M.A. Stuchly<sup>1</sup>, S. Pisa<sup>2</sup>, K.P. Esselle<sup>3</sup> and G. D'Inzeo<sup>2</sup>, <sup>1</sup>Department of Electrical and Engineering, University of Victoria, P.O. Box 3055, Victoria, British Columbia, Canada V8W 3P6, <sup>2</sup>Department of Electronics, University of Rome, "La Sapienza", Via Eudossiana 18, 00184 Rome, Italy, <sup>3</sup>School of Mathematics, Physics, Computing and Engineering, Macquarie University, Sidney, Australia

2109

Stimulation of motor neurons by a magnetic field in humans for a diagnostic purpose was first reported by Barker and associates in 1985. Since that time the technique has gained acceptance as a clinical and research tool in medicine. In magnetic stimulation of long straight nerves reasonably far from their terminations, the parameter characterizing the interaction, the so called activation function, is the spatial derivative of induced electric field along the nerve. Considerable engineering efforts have been devoted to modeling electromagnetic problems associated with magnetic stimulation. The main motivation is provided by needs to control which nerve is stimulated, and the location of stimulation, to avoid stimulation of other nerves, and hyperpolarization of the text (desired) nerve between the stimulation point and the nerve connection to the muscle. It is also desirable to produce the strongest stimulus at the desired site from a given stimulator (for a constant voltage). In a broad sense one can consider this problem as an optimization of the stimulating coil.

Two methods of modeling magnetic field stimulation of a nerve in a cylindrical volume conductor representing a human forearm are compared. An analytical solution for a homogeneous tissue cylinder and a finite-difference numerical method for an anatomically correct heterogeneous tissue cylinder are considered. Various coils such as circular, square, double-square (DS) and quadruple square (QS) are considered. The main focus is on an evaluation of the applicability of the coil optimization performed for simplified, homogeneous models to the actual heterogeneous tissue structure.

In the analytical solution the potential inside the cylindrical volume conductor defined by Laplace's equation and the distance from a unit element of the stimulating coil are expanded in terms of modified (hyperbolic) Bessel functions. A closed form solution is obtained, and only integration needs to be done numerically. The numerical solution using 3D admittance method is applied to both the homogeneous model (the same as used in the analytical solution) and the heterogeneous (anatomically correct) model of a human arm. The tissue resolution is 2.5 mm.

A comparison of results obtained for the heterogeneous and homogeneous models of an arm confirms the usefulness of the simplified analysis (homogeneous models) in the optimization of stimulation coils. While for any type of coil the stimulus is weaker for the heterogeneous tissue than for the homogeneous one, the number and location of the stimulation regions are reliably predicated by the simplified analysis such as those developed earlier. The analysis described here applies only to straight long neurons. This assumption is reasonably well satisfied for peripheral nerves in the arm.

AN ALTERNATIVE APPROACH TO  
EM STIMULATION OF LONG NERVES

Robert P. Penno and Daniel D. Reuster

University of Dayton  
Department of Electrical Engineering  
Dayton, Ohio 45469-0226

Systems for Functional Neuromuscular Stimulation (FNS) of nerve tissue are a required element of neural prosthetic devices. These systems deliver an electromagnetic signal to nerve or muscle tissue, replacing the link originally performed by human nerve tissue. As recently as 1988 (W.J.Heetderks, F.T. Hambrecht, *IEEE Proceedings*, vol176, No.9, pp1115-1121), the point probe, or electrode, has been utilized for this purpose. Such a probe was used to inject current into the nerve fiber, or at least into the area adjacent to the target fiber. More recently, techniques using magnetic stimulation, or induction, with coils oriented to produce the dual of the electric probe have been employed (S. Nagarajan, D. Durand & E. Warman, *IEEE Trans.Biomed. Eng.*, vol 40, no.11, pp1175-1187, 1993). Analysis with these methods sometimes employ circuit models to approximate the effects of myelination.

As an alternative, it is suggested for stimulation of a long nerve fiber that a long, thin probe be oriented parallel to the nerve fiber. This probe would act as a traveling wave antenna source, with the nerve fiber as a traveling wave receiving antenna. Such an alignment would provide optimum coupling between the two and, hence, would maximize the coupling between probe and nerve fiber. Numerical analysis using Finite-Difference, Time-Domain (FDTD) techniques affords the use of a more rigorous electromagnetic fields model of the embedded nerve fiber, either with or without myelination.

FDTD is used to analyze the coupling between two infinite slabs, separated by material of permittivity,  $\epsilon$ . A CW signal is initiated upon one of the slabs, with subsequent coupling shown on the other. Effects of spacing, slab thickness, and permittivity are examined. Besides introducing a more efficient means of stimulating a long nerve fiber, insight is obtained into the coupling process itself via the use of time domain techniques.

## **EM Wave Life-Detection System for Post Earthquake Rescue Operations**

**K.M. Chen\*, J. Kallis, Y. Huang, J.T. Sheu,  
A. Norman, C.S. Lai, and A. Halac  
Department of Electrical Engineering  
Michigan State University  
E.Lansing, MI 48824**

An electromagnetic (EM) wave life-detection system operating at UHF range was constructed for the purpose of locating trapped victims under earthquake rubble.

The system operates on the principle that when an EM wave beam illuminates a trapped human subject, the reflected wave from him is modulated by the body movement which include heartbeat and breathing. Thus, when the reflected wave is received and properly demodulated, the heartbeat and breathing signals can be extracted. Since an EM wave at UHF range can penetrate walls and rubble to a great depth, it is possible to construct an EM wave life-detection system to locate passive victims trapped under a thick pile of rubble by measuring their heartbeat and breathing signals. Also from the recorded heartbeat and breathing signals, the physiological status of the victim can be determined.

The life-detection system consists of (1) a phase-locked generator which produces an EM wave at 450 MHz with a power of 100 mW, (2) a probing antenna which can penetrate into the rubble and a reflector antenna which can be placed on the rubble surface, (3) a microprocessor-controlled clutter cancellation unit, and (4) a signal processing and monitor system. The antenna is used to transmit the EM wave through the rubble and also to receive the reflected wave. The reflected wave received by the antenna consists of a large clutter signal reflected from the rubble and a weak signal reflected from the victim's body. The large clutter signal is cancelled by the automatic clutter cancellation unit which consists of a digitally controlled phase-shifter and attenuator. The uncancelled signal reflected from the victim's body is amplified and mixed with a reference signal so that low-frequency heartbeat and breathing signals can be extracted. The extracted signal is fed to a signal processing system to reduce background noise. The final output showing the heartbeat and breathing signals is displayed on a computer monitor.

Typical results showing the heartbeat and breathing signals from various human subjects lying under simulated earthquake rubble will be presented in the meeting.

## Measurement of Cattle Fat Thickness Using a 1GHz Cavity Device

Leonard S. Taylor\*, Electrical Engineering Department, University of Maryland, College Park, MD and Nelson L. Buck, Instrumentation and Sensing Laboratory, U.S. Dept. of Agriculture, Beltsville, MD.

Non-invasive measurement of the body fat layer of cattle is a problem of concern to beef producers, who wish to minimize production costs by eliminating the expense of feeding animals beyond the point at which the muscle tissue has become optimally marbled by fat. The thickness of the subcutaneous fat layer is one factor used in estimating body fat. S-band microwaves can penetrate the thick hides of cattle, and are responsive to the large difference in the dielectric properties of fat and muscle or hide. Thus, the wide-band measurement of the input impedance to a microwave contact applicator placed against the animal provides a possible means for determining the thickness of the subcutaneous fat.

A system using a modified one-gigahertz open-ended coaxial cavity has been designed and tested and found to provide a useful device for this application. (The design of the device was guided by a series of laboratory trials of a variety of cavity modifications.) The basis of the measurement is the resonant frequency and reflection coefficient at resonance of the cavity in contact with the animal. Although an exact theoretical calculation of the response of this type of device in contact with a multi-layered lossy medium has not been possible, a phenomenological description of the response is in agreement with the observed results and provides a basis for understanding the response characteristics. The results of laboratory (and available in vivo) testing of the system are described.

## HYPERTHERMIA MODELING FOR AN INFINITE TWO-LAYER CONCENTRIC CYLINDER USING MATRIX OPTIMIZATION

Gary Kim and Akira Ishimaru  
Electromagnetics and Remote Sensing Laboratory  
Department of Electrical Engineering, FT-10  
University of Washington, Seattle, WA 98195  
Telephone: (206)543-2159 Fax: (206)543-3842

The work presented here shows how the technique of matrix optimization can be used to find optimum surface field distribution patterns for the case of a lossy infinite two-layer concentric cylinder. The research has application in the area of hyperthermia array focusing.

The radii of the cylinders as well as their complex dielectric constants are chosen to model the muscle and bone of the human arm. For this idealized geometry, the method can be used to obtain a graph showing specific absorption rate (SAR) levels over a cross section of the cylinder. The TM case studied here becomes a scalar problem as only the  $z$  component of the electric field is represented for the infinite cylinder.

The optimization is done by choosing the largest eigenvalue of a Hermitian matrix. This approach, as it applies to the specific problem of maximizing intensity at a focal point within the cylinder with respect to the total surface power, is outlined here. The calculation of the specific integral equation required for this optimization is discussed. The integral equation relates the internal scalar field to the surface field.

Some graphs are presented illustrating the results of the technique. Peak surface intensities are reduced by setting all surface fields to uniform amplitude, while keeping the calculated phase. Focal points are chosen in both the inner and outer cylinders. Results showing the effect of a combination of a maximum and a minimum intensity point are shown. Data for three different biomedical microwave frequencies is included.

Finally, a procedure for extending the method to allow variation in the  $z$  direction, thereby providing focusing along the  $z$  axis, is described.

PREFORMING THE SPATIAL AND TEMPORAL  
ELECTROMAGNETIC FIELDS ON THE AXIS  
OF A LOSSY CYLINDER - TORSO OR LIMB  
Khalid A. Nabulsi, KAAU, ECE Dept.,  
Jeddah, 21413, POB 9027, Saudi Arabia  
James R. Wait,\* Consultant,  
2210 East Waverly, Tucson AZ 85719

The desire to control the spatial and temporal field distribution in a lossy medium arises in a number of areas. For example, in hyperthermic cancer therapy, it is important to focus the field at the location of the tumour, while controlling the exposure time so that the proper thermal dose is applied. To model a human torso or limb, in such a situation, we choose an homogeneous conducting cylinder of infinite length.

The model is also relevant in bioelectromagnetics where it has been shown that time-limited exposure to electromagnetic fields enhances the immune system of the human body. Also it has been indicated that such a behaviour for the immune system can be achieved or optimised by controlling the relative length and intensity of the exposure (Worldwide Non-ionizing Safety Standards, Capri, May, 1988).

It is clear, from the above, there is a need to control or prescribe the spatial and temporal electromagnetic field within the conducting body for therapy applications. But it should also be mentioned that in non-destructive testing of materials, it is often desirable to prescribe the spatial and temporal field distributions.

To simplify the analysis here, we pose the problem of determining the required external aperture field on the surface of the cylinder when the internal axial electric field has been prescribed both as a function of time and the  $z$  coordinate. The mathematical procedure is straight-forward but the numerical double Fourier transform inversion is simplified when we employ nice Gaussian space and time variations. In our example, we show that the scheme, as proposed, is validated by doing a forward analysis having idealized the source as a multi-slotted cylindrical array which encloses the torso, limb or sample.

## BASIC CHARACTERISTICS OF COAXIAL-SLOT ANTENNAS FOR INTERSTITIAL MICROWAVE HYPERTHERMIA

Koichi Ito\*, Meng-Shien Wu, Jun-ichi Takada and Haruo Kasai  
Department of Electrical and Electronics Engineering  
Faculty of Engineering, Chiba University  
1-33 Yayoi-cho, Inage-ku, Chiba, 263 Japan

Hyperthermia is a cancer treatment to heat tumors up to therapeutic temperatures (42 - 45 °C) without overheating the surrounding normal tissue. Microwave interstitial hyperthermia is considered to be an effective and practical technique to heat deep-seated or large-volumed tumors.

The authors *et al.* have proposed an interstitial antenna made of a thin semirigid coaxial cable with multiple coaxial slots, which will radiate microwave energy into a tumor. The antenna is loaded into a thin plastic catheter and then an array of the antennas is inserted into the tumor. The diameter of the normal antenna used is 0.86 mm and the catheter thickness is about 0.2 mm. Various heating experiments using agar phantoms and animals have confirmed that the coaxial-slot antenna is effective and useful.

Theoretical analysis of the antenna is necessary to understand its basic characteristics. The analysis is performed for the simplified antenna structure with a single slot. The antenna is covered with a dielectric catheter and penetrating the interface between the air and a lossy medium. The catheter around the antenna is replaced with an unknown equivalent polarization current. The moment method incorporated with the so-called complex-image method is employed to obtain electric current distributions on the antenna and the polarization current.

Antenna parameters, such as catheter thickness and distance between the slot and the antenna tip, have been varied to discuss their effects on the electric current distributions as well as SAR (specific absorption rate) distributions around the antenna. The dependence of the antenna insertion depth on the electric current and SAR distributions has also been calculated.

**Dipole and Concentric Ring Radiators  
for Tissue Ablation and Hyperthermia Applications**

R. D. Nevels  
Department of Electrical Engineering  
Texas A&M University  
College Station, TX 77843

Various types of probe radiators have been investigated for the purpose of removing either cancerous tumors or damaged tissue which can for example produce a heart abnormality known as cardiac arrhythmia. Because the probe must be inserted through a small catheter with a diameter of approximately 2mm and because frequencies are in the high megahertz to gigahertz range, the probe must generally be straight, narrow and fed by a coaxial line. Initially probes were dipole configurations fed either at the coaxial opening or through one or a series of circumferential slots. More recently the helical coil has become popular due to the uniformity of its heating pattern as well as its ability to radiate at the tip. Also it has been reported that dipole probe heating patterns are more sensitive to inhomogeneities in the surrounding medium than the helical coil. In particular, radiation from currents flowing on the outside of the feedline have been shown to produce heating 'hot spots' when the dipole probe is near the interface of two materials.

In this paper we present a finite-difference time domain analysis of several probe configurations which are extractions of the dipole design. Each will contain an impedance match produced by a quarter-wave trough surrounding the outside sleeve at the coaxial opening. In all cases the probes will be inside a catheter which will be inserted in a lossy medium or near the interface of two mediums which represent biological material. Probes will be: a single dipole, several dipole sections fed by slots and a multiple concentric ring waveguide. It will be shown that the concentric ring waveguide provides the most even heating pattern, mainly because it avoids the zero amplitude current conditions at the ends of a dipole. Overall characteristics of the concentric ring structure are similar to that of a helical coil, but because the ring height can be adjusted, radiation along the length of the device can be carefully controlled.

# CONTRAST ENHANCEMENT FOR UNDERWATER IMAGING USING A POLARIZATION DIFFERENCING TECHNIQUE BASED ON BIOLOGICAL VISUAL SYSTEMS

J. S. Tyo\*, M. P. Rowe†, E. N. Pugh, Jr.°, and N. Engheta\*

\* Moore School of Electrical Engineering  
University of Pennsylvania  
Philadelphia, PA 19104

† Institute of Neurological Sciences  
University of Pennsylvania  
Philadelphia, PA 19104

° Department of Psychology  
University of Pennsylvania  
Philadelphia, PA 19104

## Abstract

Inspired by biological visual systems of certain vertebrates we are studying an imaging system which is based on the hypothesis that these animals can generate "polarization-difference" neural images in their retinas. Many vertebrates and invertebrates are sensitive to polarization in the optical region of the spectrum [K. von Frisch, *Experientia*, 5:142-148, 1949; and T. H. Waterman, *Polarization Sensitivity*, in *Handbook of Sensory Physiology VII/6B*, H. Autrum (ed.) Springer, Berlin, 1981]. We hypothesize, based on anatomical and behavioral experiments [D. A. Cameron and E. N. Pugh, Jr. *Nature*, 353:161-164, 1991; D. A. Cameron and S. S. Easter, Jr. *Vis. Neurosci.* 10:375-384, 1993; and W. Saidel *et al. Nature*, 304:534-536, 1983], that one of the reasons that these species have evolved polarization sensitivity is to enhance the visibility of objects in scattering media. Specifically, it appears that polarization-sensitive vision systems improve contrast by computing the difference in responses of these visual systems to two orthogonal linear polarizations. We believe that the visual systems of these animals can serve as models for the reverse engineering of a system for enhancing image contrast under conditions of poor visibility, e.g., observation under water or in foggy weather. Our technique is to subtract out background light by obtaining two images which differ only in the orientation of a polarizer placed in front of the camera and digitally subtracting those two images. Our preliminary results show that polarization differencing can, under some circumstances, increase the visibility of targets in scattering media (compared with a system which did not take advantage of polarization differencing). The reason for this is that essentially all of the background light will tend to be polarized at the same angle across the visual scene as long as the scatterers are isotropic radiators, and the light striking them is principally from a single source. However, the light scattered from targets will tend to be polarized differently. Orthogonal polarizer positions can thus be found which will result in a finite signal emanating from the target, and minimal signal (other than noise) emanating from the background. We have examined this possibility by setting up a tank containing a low concentration of milk in aqueous suspension as the scattering medium and a metallic aluminum bar (with sanded patches on one of its face) immersed in this medium as a target. In this talk we present some preliminary results of our experimental investigation of an imaging system equipped with such polarization-difference coding and we show how this system can be used for enhancing image contrast of targets suspended in scattering media.

## Fundamental Study for CT Imaging of Biological Body with Light

Koichi Shimizu\*, Masataka Kitama and Katsuyuki Yamamoto  
Department of Bioengineering, Faculty of Engineering,  
Hokkaido University, Sapporo, 060, Japan.  
( Phone:+81-11-716-2111 (Ext.6857), Fax:+81-11-757-2485 )

With the progress of light sources and detectors, it has become possible to detect the light passed through a living body. A fundamental study was conducted to examine the feasibility of an optical CT with a CW light. The strong scattering in body tissues has been identified as a difficult problem to realize the CT imaging of a living body. A technique called "a scattering angle differential technique" has been newly developed to suppress the effect of scattering in the imaging through diffuse random media.

Fig.1 illustrates the principle of this technique. Two detectors are placed on and off the optical axis of a collimated beam of incident light. The scattered component in transmitted light is greatly reduced by subtracting the output of the

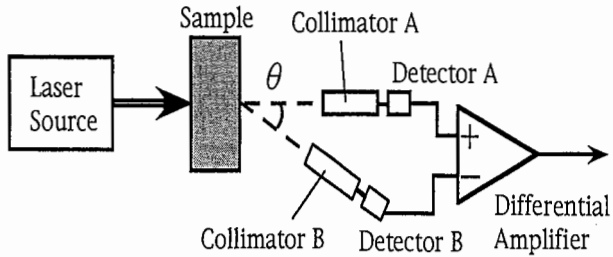


Fig.1 Scattering angle differential technique

off-axis detector from that of the on-axis detector. The effectiveness was confirmed in CT imaging of a model phantom. However, it was found in experiments that this technique alone was not effective with a living mouse. The problem was found to be the reflection and the refraction at the air-tissue interface. Another technique called "a contact technique" was newly developed to overcome this problem. A measurement system was developed to use both techniques simultaneously. Fig.2 shows this system schematically. Using this system, CT imaging of a mouse abdomen was attempted. Though the spatial resolution was poor, the existence of a liver and kidneys were recognized in the CT image of a living mouse.

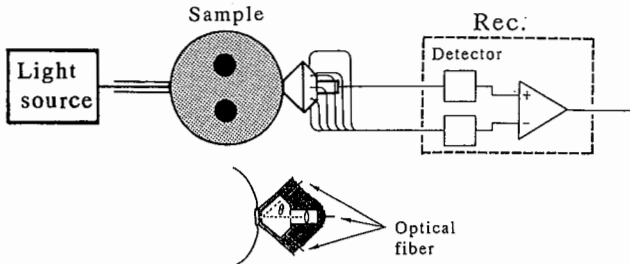


Fig.2 Measurement with differential and contact techniques

# Near and Far Field Approaches for Non-invasive Microwave Hyperthermia

R. W. Y. Habash and A. Kumar

E.C.E. Department, Indian Institute of Science, Bangalore-560 012, India.

## Abstract

The main challenge in hyperthermia is the ability to develop effective and focused, non-invasive applicators. For a considerable improvement of therapy, the field size and focusing ability have to be improved in order to focus the corresponding power within the tumour region. Among the techniques utilized to achieve that is employing the open-ended rectangular waveguide as a direct-contact applicator (ORWDA).

In this paper, we have considered three theoretical approaches, 1) plane wave, 2) single element ORWDA, and 3) linear and planar array of ORWDAs. The analysis is carried out in order to study the distribution of electromagnetic energy through the muscle tissue, in the far field zone for the first approach and in the near field zone for the second and third ones. Two frequencies, 915 and 2450 MHz at the ISM band are considered. It has been concluded that main drawback of the plane wave approach is excessive surface heating. While in the second and third approach, a very compact applicator may be obtained, where the compactness is further increased when a surface cooling is directly integrated in the applicator body. Two drawbacks are observed in the case of single ORWDA: namely, the excessive surface heating and the reduced penetration depth. For this reason, such applicator can be used only for treating tumours located near the surface. The planar array of ORWDAs has better performance than the linear array of ORWDAs. The only drawback of this planar array applicator is increased size. In addition, the adopted array applicator models, requires only a single oscillator and one measurement network. These models are simple and cheap compared to the phased array applicators which are widely used for localized hyperthermia.

The search for an ideal hyperthermic system is still on. Perhaps a combination of various approaches discussed in this study would lead to an approximate optimal system. We look forward to continued future research work in this regard.

THURSDAY PM URSI-B SESSION TH-U41

Room: Savery 243

ANTENNAS III

Chairs: M. Hamid, University of South Alabama; B. Houshmand, UCLA

- 1:20 Equivalent Circuit Model of Dipole Antenna 484  
*\*M. Hamid, Univ. of South Alabama*
- 1:40 A Full-Wave Model for the Transient Response of Linear Antennas in a Cylindrically Stratified Medium 485  
*\*J.J. Xia, T.M. Habashy, Schlumberger-Doll Research*
- 2:00 The Tapered Coplanar-Waveguide Antenna 486  
*\*M.A. Saed, State Univ. of New York, College at New Paltz*
- 2:20 Performance of the Generalized Multipole Technique (GMT/MMP) in Antenna Design and Optimization 487  
*\*R.Y.-S. Tay, Motorola, USA; N. Kuster, Swiss Federal Inst. of Technology (ETH)*
- 2:40 Decomposition of the Radiation Integral for Distorted Reflector Antennas 488  
*\*W.T. Smith, R.J. Bastian, Univ. of Kentucky*
- 3:00 Break
- 3:20 Quasi-Focusing Radiating System with an Elliptic Reflector Above a Lossy Dielectric Half-Space 489  
*Y. Chen, \*B. Beker, Univ. of South Carolina*
- 3:40 Loaded TEM Horn Antenna for Ultra-Wideband Signal Reception 490  
*\*M.A. Morgan, R.C. Robertson, Naval Postgraduate School*
- 4:00 Far Field Computation of Active Antennas 491  
*\*B. Houshmand, B. Toland, T. Itoh, Univ. of California, Los Angeles*
- 4:20 Parallel Algorithm for Near and Far Field Computations of Reflector Antennas 492  
*\*B. Houshmand, Univ. of California, Los Angeles*
- 4:40 Theoretical and Experimental Investigations on Corrugated Conical Horn 493  
*C.X. Zhang, W. Hong, \*Y.Y. Chen, W.T. Wang, J.Q. Wang, Southeast Univ.*
- 5:00 Using of Dual Polarization Radars for Studying Evolution Microphysic Characteristics of Clouds and Precipitation During Their Natural Development and Weather Modification 494  
*A.B. Shupiatsky, B.V. Antipovsky, L.A. Dinevich, I.P. Kapitalchuk, V.R. Megalinsky, Central Aerological Observatory*

## EQUIVALENT CIRCUIT MODEL OF DIPOLE ANTENNA

M. Hamid  
Department of Electrical Engineering  
University of South Alabama  
Mobile, Alabama 36688

The input impedance  $Z_{in}$  (or  $R_{in} + jX_{in}$ ) of a center-fed dipole as a function of frequency  $f$  (or radian frequency  $\omega = 2\pi f$ ) or electrical length  $2h/\lambda$  in wavelengths is an important property since it determines the efficiency of the antenna and facilitates the design of matching networks to the feedline. In a recent paper, Tang et al (IEEE Trans. on AP, 41, 100-103, 1993) presented a survey of previous attempts to synthesize  $Z_{in}$  with two and three-element equivalent circuits and proposed a new and more accurate four-element circuit. However, the values of their circuit elements are difficult to compute and their circuit is valid up to only  $2h/\lambda = 0.5$ . The purpose of this paper is to present a similar but more accurate four-element equivalent circuit valid up to  $2h/\lambda = 1$  but which could be extended to longer dipoles. The proposed procedure employs a given graph of  $Z_{in}$  vs  $\omega$  or  $2h/\lambda$  and permits the optimization of element values with the aid of standard computer software packages such as MICROCAP and MATHCAD. The proposed circuit consists of a capacitor  $C_0$  in series with a parallel RLC network. To evaluate the four unknown element values, four frequencies are identified as  $\omega_1$ ,  $\omega_2$ ,  $\omega_s$  and  $\omega_p$  at which  $2h/\lambda = 0.25$ ,  $R_{in} = X_{in}$ ,  $X_{in} = 0$  with  $2h/\lambda = 0.5$  (i.e. series resonance) and  $X_{in} = 0$  with  $2h/\lambda = 1$  (i.e. parallel resonance), respectively.  $C_0$  is determined from the condition  $-j/\omega_1 C_0 = X_{in}$  at  $\omega_1$ , while  $R$  is set equal to  $R_{max}$  or  $R_{in}$  at  $\omega = \omega_p$ . Furthermore, the parallel and series resonance conditions lead to the relations  $\omega_p^2 = 1/LC$  and  $\omega_s^2 R^2 LC_0 (1 - \omega_s^2 LC) = R^2 (1 - \omega_s^2 LC)^2 + (\omega_s L)^2$ , respectively. An auxiliary relation is also employed to find alternative values of  $L$  and  $C$  and is based on the condition that  $R_{in} = X_{in}$  at the 3-dB frequency  $\omega = \omega_2$  which leads to  $R_{in}(\omega = \omega_2) = \omega_2 L / (1 - \omega_2^2 LC)$ . Once these equations are solved simultaneously,  $Z_{in}$  vs  $f$  is plotted for the equivalent circuit and minor adjustments are made to ensure a best fit with the original graph. Examples are presented with and without these modifications to illustrate the accuracy and simplicity of the proposed method relative to previous results while cascaded parallel RLC networks are used to illustrate how the proposed method can be extended to equivalent circuits of dipoles of arbitrary length.

## **A Full-Wave Model for the Transient Response of Linear Antennas in A Cylindrically Stratified Medium**

Jake J. Xia\* and Tarek M. Habashy  
Schlumberger-Doll Research  
Old Quarry Road, Ridgefield, CT 06877

In geophysical survey, borehole radar is used to detect locations of formation discontinuities. The borehole radar consists of a linear transmitting antenna which sends out a probing pulse and a linear receiving antenna which detects formation reflected pulses. In this paper we describe a rigorous model for computing borehole radar tool responses. Such a forward model will provide the framework for inversion of the radar response for mapping formation heterogeneities.

The transmitting antenna is excited by a transient gap voltage. The currents on the transmitting and receiving antennas are then cast in terms of a surface integral equation with its kernel given by the Green function of a cylindrically stratified medium to account for a borehole. The surface integral equation is then solved using two approaches. The first approach is based on a moment method. The second approach is an approximation that explores the singular nature of the Green function. The advantage of the second approach is that it provides a fast way for computing the radar response that allows a rapid inversion. We present a comparison between the two approaches pointing out the limitations of the second approach.

One important issue in the approach using the method of moments is the treatment of the singularity of the Green function. We have devised two ways for dealing with this singularity. One way is to use the asymptotic expansion of the elliptical integral resulting from the static part of the Green function. The other is to use the properties of the equation governing the Green function.

Pulse propagation of the linear antennas in the presence of a borehole is studied. Under certain conditions, borehole modes may be excited. Coupling of the transmitting and receiving antennas result in a direct arrival pulse. Formation permittivity and conductivity in the near wellbore region can be inverted from certain attributes of these direct pulses.

Numerical examples will be presented for various pulse shapes, different geometries and borehole parameters.

## THE TAPERED COPLANAR - WAVEGUIDE ANTENNA

Mohammad A. Saed  
Electrical Engineering Department  
State University of New York  
College at New Paltz  
New Paltz, New York 12561

This paper presents the design, analysis, and testing results of the tapered coplanar - waveguide antenna. The center strip and ground plane on both sides of the strip in a coplanar waveguide are tapered to produce a radiating antenna. This tapered coplanar antenna is similar to the well known tapered slotline antenna (also known as the notch antenna or the Vivaldi antenna) which has seen considerable interest in the recent literature. The tapered coplanar and tapered slotline antennas are attractive because of their planar geometry which makes it easy to integrate other planar devices such as filters, transistors, Schottky diode mixers, ...etc. Also, since they are traveling wave antennas, they exhibit a relatively wide impedance bandwidth when compared to resonant antennas such as microstrip antennas. Because of these features, the slotline antenna has been used at microwave frequencies and, more recently, at millimeter and submillimeter wave frequencies with and without integrated active components. One disadvantage of the slotline antenna, however, is that it exhibits high cross polarization in the diagonal plane.

To the best of the author's knowledge, the coplanar - waveguide antenna has not been proposed or treated in the literature. In this paper, various versions of this antenna are analyzed using the finite-difference time-domain method. Results for input impedance, antenna gain, as well as radiation patterns will be presented. Comparisons will be made to the slotline antenna. The various versions of the antenna are fabricated using photolithographic etching. The numerical results are verified experimentally in the microwave frequency range.

## Performance of the Generalized Multipole Technique (GMT/MMP) in Antenna Design and Optimization

Roger Yew-Siow Tay<sup>\*1</sup> and Niels Kuster<sup>2</sup>

<sup>1</sup>Florida Electromagnetics Laboratory, MOTOROLA, USA

<sup>2</sup>Swiss Federal Institute of Technology (ETH), Zurich, Switzerland

During the last decade, the Generalized Multipole Technique (GMT) has been extensively studied, improved and applied to many electromagnetics problems such as bioelectromagnetics, optics, waveguides and Electromagnetic Compatibility (EMC), but little has been reported towards utilizing this method for antenna design and optimization. On the other hand, the few published examples of simple dipoles and helices in the close vicinity of lossy scatterers (e.g., N. Kuster, BME-40, 611-620, 1993) were suggesting a significant potential of GMT for antenna design purposes.

To study the advantages and limitations of the GMT based 3D Multiple Multipole (MMP) code, seven basic antenna configurations were simulated. These are Monopole, Loop, Axial Mode Helix, Normal Mode Helix, Inverted-L, Inverted-F and the Yagi-Uda array. The thin-wire expansion in combination with multipoles and roof top functions enable high flexibility in modeling. In addition, the most recently implemented expansion, "Curved Line Multipoles", extends the code's efficiency to non-thin-wire configurations (e.g., helix with small ratios of pitch to wire diameter).

Critical issues of modeling are the feed point area, matching points location and segment length-to-diameter ratio. Symmetries are used where possible, to minimize computation time without loss of generality as any antenna element may easily be assembled in non-symmetrical configurations with the block-iterative solver. These experiments revealed that the method's principally high accuracy on and in the extreme vicinity of the boundaries is a key advantage of this technique for antenna modeling. In order to achieve a confident base for more complex configurations, extensive studies were performed to increase efficiency and stability of modeling and will be discussed. At the same time, the numerical validation techniques are extended to satisfy the special requirements of antenna simulations.

For all configurations, radiation pattern, impedance, efficiency, radiated power, gain and directivity are computed and compared, if available, with results from experiment and/or published results by others using different techniques. The agreement is good to excellent but always within the uncertainties of the compared configurations.

These principal studies exhibit excellent potential of GMT/MMP for use in analysis, synthesis and design of antennas.

## DECOMPOSITION OF THE RADIATION INTEGRAL FOR DISTORTED REFLECTOR ANTENNAS

W. T. Smith\*, R. J. Bastian  
Department of Electrical Engineering  
University of Kentucky  
Lexington, Kentucky 40506-0046

This paper investigates the decomposition of the radiation integral for distorted paraboloidal reflector antennas. The physical optics / aperture integration (PO/AI) method is employed in this study. The distorted surface function is expanded into series of orthogonal basis functions which are used in the radiation integral decomposition.

This work was motivated by an earlier study on the use of neural network computing for electromagnetic reflector surface error compensation [Smith & Bastian, 1993 APS Digest]. In that study, the radiation integral of a distorted infinite parabolic cylinder reflector was decomposed into an approximate finite series of radiation integrals. Each series term corresponded to one of the orthogonal basis functions. In the expansion of the one-dimensional series, only the dc and linear terms were required. This decomposition was a necessary step in the implementation of a computationally efficient electromagnetic surface error compensation algorithm.

In this study, the radiation integrals for distorted paraboloidal reflector antennas are decomposed using series approximations. It is desired to achieve second-order accuracy by including the quadratic terms in the series. Including the second-order terms increases the complexity of the expansion as cross-terms that involve two basis functions must now be evaluated. In addition, the expansion functions are now bivariate.

In general, any series could be used for the decomposition. Several sets of orthogonal basis functions were evaluated for use in decomposing the radiation integral for a distorted reflector surface. Using orthogonal basis functions facilitates studying the sensitivity of the expansion to increasing the number of terms in the series without having to recompute the amplitudes of previously determined series terms. Candidate orthogonal basis functions were Bessel functions, modified Jacobi polynomials (reference [Galindo-Israel & Mittra, APS, vol. AP-25, Sept. 1977]) and a set of orthogonal basis functions developed for this study.

In this presentation, the decomposition of the radiation integral into a series approximation is outlined. The choice of basis functions for the decomposition is discussed.

# Quasi-Focusing Radiating System with an Elliptic Reflector Above a Lossy Dielectric Half-Space

Yinchao Chen and Benjamin Beker\*

Department of Electrical and Computer Engineering, University of South Carolina  
Columbia, SC 29208

A quasi-focusing radiating system, which employs an elliptic reflector antenna above a lossy or lossless dielectric half-space, is presented (see Fig. 1). The equivalence principle is used to formulate the radiation boundary value problem in terms of the combined-field surface integral equations (CFSIEs) for the electric current on the reflector as well as for electric and magnetic currents on the air-to-half-space interface, which for  $TM^z$  polarization are given by:

$$E_z^{\text{in}} = j\omega[A_{z1}(J_z^R) + A_{z1}(J_z^G)] + \hat{a}_z \cdot \frac{1}{\epsilon_0} \nabla \times \bar{F}_1(\bar{M}^G)$$

$$0 = j\omega[A_{z1}(J_z^R) + A_{z1}(J_z^G) + A_{z2}(J_z^G)] + \hat{a}_z \cdot \frac{1}{\epsilon_0} \left[ \nabla \times \bar{F}_1(\bar{M}^G) + \frac{1}{\epsilon_r} \nabla \times \bar{F}_2(\bar{M}^G) \right]$$

$$0 = j\omega \hat{a}_n \times [\bar{F}_1(\bar{M}^G) + \bar{F}_2(\bar{M}^G)] + \hat{a}_n \times \nabla [\psi_1(\bar{M}^G) + \psi_2(\bar{M}^G)] - \hat{a}_n \times \left[ \frac{1}{\mu_0} \nabla \times \bar{A}_1(J_z^R) \right]$$

The moment method is employed to solve CFSIEs and to determine the electric field within the lossy half-space that will be produced by this quasi-focusing system.

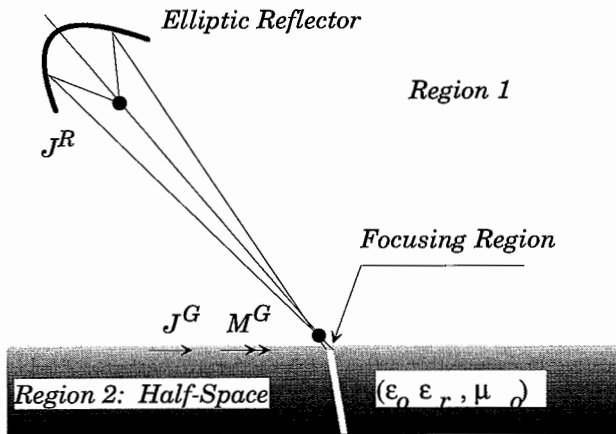


Fig. 1: Graphical illustration of the quasi-focusing principle.

## LOADED TEM HORN ANTENNA FOR ULTRA-WIDEBAND SIGNAL RECEPTION

Michael A. Morgan\* and R. Clark Robertson  
ECE Department, Naval Postgraduate School  
833 Dyer Road, Room 437, Monterey, CA 93943-5121

Requirements for low distortion short-pulse receiving antennas are compared with the those of conventional wide-band antennas. Central to this characterization is the behavior of the frequency-domain transfer function of the receiving antenna, known as the "sensitivity." An optimal sensitivity for high-fidelity impulse reception will have constant amplitude and linear phase shift over the passband of the incident signal. The sensitivity is dependent upon the behavior of the antenna's effective length as well as the impedance characteristics of both the antenna and the receiver. A special type of loaded TEM horn structure, developed at the National Institute for Science and Technology (NIST), provides a near-optimal sensitivity behavior for receiving impulsive waveforms.

Applying the NIST approach to our specific requirements, two identical resistively loaded, prototype TEM horns were designed, constructed and evaluated. The magnitude of the complex sensitivity function of the prototype antenna is theoretically flat to within 3dB (and with nearly linear phase) over a nominal passband of 70 MHz to 8 GHz. A new test procedure is described for measuring the transient response characteristics and the frequency domain complex sensitivity of the prototype antennas. Measured prototype antenna performance shows minimal distortion in receiving impulsive fields having a time duration of less than 100 ps. A current effort is described to extend the response of this class of antenna to cover both lower and higher frequencies, as well as to increase its sensitivity, while retaining similar physical dimensions.

## **Far Field Computation of Active Antennas**

B. Houshmand\*, B. Toland and T. Itoh

Department of Electrical Engineering  
University of California, Los Angeles  
Los Angeles, CA 90024-1594  
U. S. A.

### **ABSTRACT**

The FDTD algorithm is used for full wave simulation of active antennas. This analysis is capable of predicting the stable steady state behavior of the active devices and field distribution in the microwave structure. The field distribution is used to perform the far field pattern computation. The far field computation from the near field information is performed by the use a spatial Fourier Transformation. By virtue of the Huygens' principle, the far field is computed from the equivalent current distributions which enclose the radiating structure. One issue of importance is the choice of the E-Field, H-Field or a combination of both in order to compute the far field. While analytically the above three choices are equivalent, the computed results are different due to numerical inaccuracies. In this talk the issue of far field pattern computation is presented. By comparison to measurements, the relative accuracy of various equivalent current choices are presented.

## **Parallel Algorithm for Near and Far Field Computations of Reflector Antennas**

B. Houshmand

Department of Electrical Engineering  
University of California, Los Angeles  
Los Angeles, CA 90024-1594  
U.S.A.

### **ABSTRACT**

Fast computation of the radiated fields from reflector antennas is of interest for a number of applications such as antenna optimization and reflector shaping where a number of iterations on the field computation are required in the process of solution. In general the near field as well as the far field information is of importance in the optimization process. The far field pattern is computed for evaluation of reflector performance parameters such as side-lobe levels and beam shape. The near field of reflectors is computed for configurations such as multiple reflector systems and beam waveguides where the reflecting surfaces are situated in close proximity. In addition, the near field information is useful for antenna diagnostics. In this paper an algorithm is presented which computes both near and far radiated fields. In addition, the algorithm is formulated to be amiable to parallel computation. The field computation is performed by dividing the reflector surface into rectangular or triangular patches. The triangular patch representation is particularly useful for representing shaped reflector surfaces. The field computation is performed by coherent addition of the fields radiated by each patch element in its local coordinate system. The patch orientation is taken into account from the knowledge of the patch normal vector with respect to the global coordinate system. As such, the computation of the radiated field from a reflector surface is transformed into a summation of the contributions from each patch. In this talk the implementation of this algorithm on a cluster of computer nodes is presented. Representative results for computation of both near and far fields are illustrated which show excellent agreement with the physical optics formulation for the far fields and the spectral domain formulation for the near fields.

## THEORETICAL AND EXPERIMENTAL INVESTIGATIONS ON CORRUGATED CONICAL HORN

C.X. Zhang, W. Hong, Y.Y. Chen\*, W.T. Wang and J.Q. Wang\*  
*Dept. of Radio Eng., Southeast University, Nanjing 210018, P.R. China*

**SUMMARY:** In this paper, the corrugated conical horns as shown in Fig.1 are investigated. Inside of the conical horn, we first calculated the generalized scattering matrices of each corrugation element, then the total generalized scattering matrix of the corrugated conical horn is determined in terms of the cascade property. Outside of the horn, the fields are expanded with dual Fourier transformation. At the aperture, tangential fields continuity conditions are applied to match the inside and outside fields. After solving the matrix equation, the fields at the neck of the horn and at the aperture are then obtained. Based on the calculated fields, the input VSWR and the far field pattern are finally determined. Fig.2 shows a set of typical patterns of the horn as shown in Fig.1(b). It can be seen that the calculated results are in good agreement with the experimental data, where the number of slots is 53, frequency is  $5.925GHz$ , and the structure parameters of each slot are different. The VSWRs are also in good agreement with the experimental data.

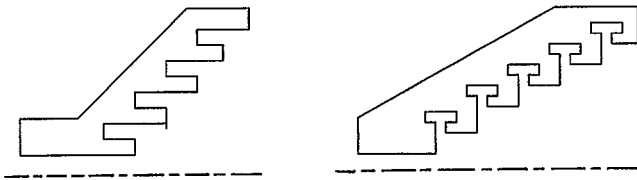


Fig.1 (a) Axial slot conical horn, (b) T-type ring slot conical horn

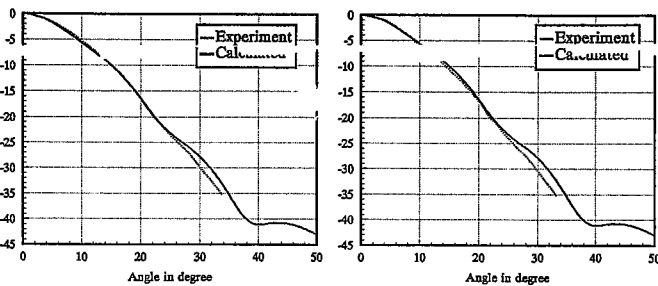


Fig.2 (a) E-plane pattern, (b) H-plane pattern

# Using of Dual Polarization Radars for Studying Evolution Microphysic Characteristics of Clouds and Precipitation During Their Natural Development and Weather Modification

A.B. Shupiatsky, S.V. Antipovsky, L.A. Dinovich, I.P. Kapitalchuk, V.R. Megalinsky  
Central Aerological Observatory  
Dolgoprudny, Moscow Region  
141700 Russia

## Abstract

The special advanced ground-sited and air-borne polarization weather radars possess the capability to change sequentially the polarization mode of transmitted pulse and the reception of the radars echoes.

The differential reflectivity, depolarization measurements on one channel and a digital signal processing permit to obtain the polarimetric parameter set during the period of hydrometeors quasi-stationary state with great accuracy.

The air-borne and ground-place dual polarization radars are presented.

Changing in a space and a time polarimetric set of the radar returns and the use of computerized data collecting and processing permit to calculate two-parameter size distribution of the cloud and precipitation microphysical characteristics in an operational time mode. These values are calculated by the equation system which is set the relation between the phase state of cloud and precipitation particles, ellipticality, spatial orientation, size and concentration on the one hand and measured radar reflectivity, depolarization, differential reflectivity and temporal and special correlations of orthogonal components of signal on the other hand.

The results of our study have shown that the above mentioned polarimetric characteristics of the radar signal give the possibility to distinguish the cumulonimbus clouds on their phase compound and development stages and to make the supershort-range forecast (about 10 min before the phenomenon) of the cloud transition to the hail state.

The depolarization, reflectivity and differential reflectivity quantities a hailfall region can be determined with sufficient degree of accuracy. Furthermore, on the differential reflectivity quantity zones of big supercooled drops concentrations in the cloud can be detected.

The location of these zones in the supercooled part of the cloud is connected with the updrafts regions and is an additional information for determining the seeding region in the hail suppression and artificial precipitation enhancement works. Using the correlation values permit to neutralize the signals from interfering objects and carry out polarization selection clouds and precipitation of different structure.

The typical vertical and horizontal sections of polarimetric and calculated microphysic parameters are presented for clouds during their natural development and weather modification.

## **Author Index**

Aberle, J.T.....	412	Besieris, I.M.....	313
Abiri, H. ....	439, 469	Bhattacharyya, Asoke K. ....	133
Adams, A.T. ....	383	Bhattacharyya, Arun K. ....	463
Adve, R.S. ....	385	Bhupal, A. ....	45
Agrawal, A.P. ....	460	Biebl, E.M. ....	414
Aguilera, J. ....	41	Bindiganavale, S. ....	166
Aguirre, G. ....	30	Boag, Amir.....	48, 73, 195
Ailes-Sengers, L.....	303	Boag, Alona.....	73
Aksun, M.I. ....	40, 362	Boag, A. ....	441
Akyel, C. ....	393	Boerner, W.-M. ....	156, 452, 460
Ali, A.S. ....	175	Boix, R.R. ....	223
Alkanhal, M. ....	429	Booton Jr., R.C. ....	91
Altshuler, E.E. ....	239	Bosisio, R.G. ....	393
Anastassiu, H.T.....	139	Bouche, D. ....	200
Anderson, B.C. ....	332	Boucher, G. ....	185
Andrawis, M.Y. ....	99	Boyse, W.E.....	20
Andrew, W.V. ....	329	Bracher, C. ....	4, 5
Andrews, L.C. ....	7, 8	Bridges, G.E. ....	50
Antar, Y.M.M. ....	220	Broschat, S.L. ....	149, 258, 326, 372, 373
Antipovsky, B.V. ....	494	Brown, G.S. ....	153, 154
Aragón, P.R. ....	338	Brown, J. ....	296
Arnold, J.M. ....	312	Brown, R.T. ....	197, 198, 202
Arvas, E. ....	429	Buck, N.L. ....	475
Asakura, T. ....	306	Buckley, M.J. ....	234
Asi, A. ....	462	Burkholder, R.J.....	201, 339
Asvestas, J.S. ....	364, 365	Burns, J.W. ....	105, 106, 107
Azevedo, J.A.R. ....	119	Butler, C.M. ....	94, 95, 96, 381
Bailey, M.C. ....	417	Cai, K. ....	369
Baker-Jarvis, J. ....	392, 395	Cai, Z.L. ....	366, 367, 368
Balanis, C.A. ....	329	Calamia, M. ....	54
Ballard, J.G. ....	3	Cangellaris, A.C. ....	16, 30, 32, 289
Bannelier, P. ....	431	.....	323, 325
Barabanenkov, Y.N. ....	62	Canning, F.X. ....	24
Baradit, E. ....	241	Cano, G. ....	464
Bastian, R.J. ....	488	Caputa, K. ....	397
Baucke, R.C. ....	53	Cardama, A. ....	163
Baylard, C. ....	155	Carin, L. ....	64, 130, 142
Beaulieu, N.C. ....	437	Carlson, F.P. ....	211
Bebermeyer, R. ....	251, 252	Carson Jr., C.C. ....	327
Beck, F.B. ....	417	Casimiro, A.M.E.S. ....	119
Beker, B. ....	489	Castillo, S. ....	145, 292
Beran, M.J. ....	307	Cavecey, K.H. ....	38
Bergljung, C. ....	344	Cecchini, R. ....	54
Bermudez, L.A. ....	467	Celuch-Marcysiak, M. ....	98
Bernard, G.D. ....	209	Cendes, Z.J. ....	29, 332, 400
Bertsen, S. ....	344	Challe, L. ....	456

Chambers, C.B. ....	224	Daneshvar, K. ....	355
Chan, C.H. ....	442	Daniel, J.P. ....	421
Chang, C.W. ....	394	Dashen, R. ....	6
Chang, D.-C. ....	335	Davis, F. ....	117
Chang, D.C. ....	222, 360	Davis, W.A. ....	99
Chang, H.-W. ....	97	Dea, J.Y. ....	452
Chang, Y.E. ....	187	DeLyser, R.R. ....	174
Chaudhuri, S.K. ....	92	Demarest, K. ....	169
Chauhan, N.S. ....	446	Dembart, B. ....	23
Chen, A. ....	187	Deshpande, M.D. ....	404, 417
Chen, J. ....	366, 367, 368, 369	Detlefsen, J. ....	413
Chen, K.M. ....	143, 394, 474, 250	Devaney, A.J. ....	104
.....	251, 252	Dholakia, S.P. ....	361
Chen, S.W. ....	288	Dib, N.I. ....	277
Chen, T.H. ....	187	Dinevich, L.A. ....	494
Chen, W. ....	225, 437	Djordjevic, A.R. ....	160, 164
Chen, Y. ....	489	Do-Nhat, T. ....	349, 350
Chen, Y.Y. ....	493	Dolzhirov, V.V. ....	120
Chew, W.C. ....	257	Dominek, A. ....	391
Chia, T.T. ....	199	Donnelly, R. ....	85
Chiang, Y.C. ....	187	Drake, E. ....	21
Chiavetta, R.J. ....	196	Dreher, A. ....	334
Chou, C.K. ....	214	Drissi, M. ....	44, 236
Chuang, C.W. ....	339	Dural, G. ....	362
Chung, P. ....	276	Durden, S. ....	59
Citeme, J. ....	44, 81, 236	Ehrlich, Y. ....	261
Claessen, P.D. ....	268	El Assad, S. ....	244
Clark, R.F. ....	180	El-Ghazaly, S.M. ....	173
Clayton, C. ....	61	El-Rabaie, E.M. ....	188, 189
Cloete, J.H. ....	432	El-Sharawy, E.-B. ....	412
Coccioli, R. ....	203	Ellis, G.A. ....	116
Cockrell, C.R. ....	404, 417	Elshabini-Riad, A. ....	353
Coe, R.J. ....	212	Elsherbeni, A.Z. ....	36
Collin, R.E. ....	148, 382	Engheta, N. ....	78, 480
Collins, J.D. ....	293, 294	Erez, E. ....	93
Colosi, J.A. ....	5	Ermutlu, M.E. ....	345
Compton, R.C. ....	183	Esselle, K.P. ....	420, 472
Conn, T. ....	145	Eswarappa, C. ....	134
Cook Jr., G.O. ....	290	Ewart, T.E. ....	3
Costa da Silva, L. ....	465	Ewe, H.T. ....	27
Currie, B.W. ....	366, 369	Falconer, D.G. ....	259
Cwik, T. ....	144, 402, 406	Fallai, M. ....	54
Czapski, P. ....	272	Fante, R.L. ....	232
D'Elia, U.F. ....	132	Felsen, L.B. ....	64, 130
D'Inzeo, G. ....	472	Fenn, A.J. ....	240
Daijavad, S. ....	333	Figani, Z.G. ....	195

Fikioris, G. ....	238	Halac, A. ....	474
Fitian, I.D. ....	274	Hales, L. ....	355
Fjeldly, T.A. ....	127	Hall, W.F. ....	291
Flatté, S.M. ....	4, 5, 6	Hamid, M. ....	484
Follet, T. ....	44	Hanna, V.F. ....	81
Franceschetti, G. ....	314	Harker, K.J. ....	259
Frankenthal, S. ....	307	Harrington, R.F. ....	387
Freilikher, V.D. ....	304	Hart, R. ....	268
Friederich, P.G. ....	390	Hastings, F.D. ....	372
Friedman, D.H. ....	197, 198	Haupt, R. ....	140
Gandhi, O.P. ....	271	He, J. ....	353
Garcia, A. ....	148	He, S. ....	430
Gary, J. ....	71	Hejase, H.A.N. ....	221
Gary, M.J. ....	178	Henderson, J.H. ....	75
Gattinella, J. ....	217	Heyman, E. ....	84, 104, 261
Gedney, S.D. ....	221, 295	Hill, D.A. ....	38
Geibel, S. ....	233	Hinz, R.C. ....	442
Gerry, M.J. ....	260	Ho, S.T. ....	280
Geyer, R.G. ....	392, 395	Hoefler, W.J.R. ....	134
Ghali, H. ....	81	Holloway, C.L. ....	174
Ghione, G. ....	316, 318	Hong, W. ....	493
Gil, J.M. ....	409	Hoorfar, A. ....	360
Gillard, R. ....	236	Hoppe, D. ....	83
Glisson, A.W. ....	90, 137	Horno, M. ....	21, 41, 42, 223, 464
Goggans, P.M. ....	90	Houshmand, B. ....	60, 124, 491, 492
Goldberg, A. ....	84	Hsieh, T. ....	227
Gong, J. ....	401	Hsieh, T.H. ....	187
Gordon, R.K. ....	296	Hsu, M. ....	194
Gothard, G.K. ....	160	Huang, Y. ....	474
Goto, K. ....	114	Huang, Z. ....	169
Gottumukkala, K.R. ....	468	Hudson, B.H. ....	178
Graglia, R.D. ....	132, 316	Hussey, G.C. ....	458
Grebel, H. ....	279	Infante, D.J. ....	39, 396
Greffet, J.-J. ....	155, 448	Ishihara, T. ....	114
Gribbons, M. ....	325	Ishimaru, A. ....	9, 302, 303, 476
Gridchin, S.I. ....	33	Ito, K. ....	478
Griolo, A.J.V. ....	119	Ito, S. ....	63
Gu, Z.-H. ....	447	Itoh, T. ....	124, 491
Guan, J.-M. ....	335	Ittipiboon, A. ....	220
Guérin, F. ....	431	Jackson, Darrell R. ....	66
Guillem, J. ....	17	Jackson, David R. ....	37, 103
Guo, W. ....	397	Jalali, B. ....	124
Gürel, L. ....	333	Jamnejad, V. ....	144, 402, 406
Gwarek, W.K. ....	98	Janaswamy, R. ....	74
Habash, R.W.Y. ....	482	Jankovic, G. ....	222
Habashy, T.M. ....	256, 485	Jarmuszewski, P. ....	186

Jarry, P. ....	467	Kumar, A. ....	482
Jedlicka, R. ....	145	Kuster, N. ....	487
Jen, L. ....	422	Kuzuoglu, M. ....	263
Jin, J. ....	273, 408	LaHaie, I.J. ....	106, 107, 108
Joseph, R.M. ....	280	Lai, A.K.Y. ....	297
Judkins, J.B. ....	315	Lai, C.S. ....	474
Jull, E.V. ....	437	Lai, H.C. ....	272
Kaduchak, G. ....	113	Lakhtakia, A. ....	79, 356, 427
Kajfez, D. ....	137	Lakkis, I. ....	244
Kalhor, H.A. ....	438	Lan, J. ....	177
Kalkan, M. ....	34	Lang, R.H. ....	446
Kallis, J. ....	474	Laperle, C. ....	186
Kapitalchuk, I.P. ....	494	Laurin, J.-J. ....	436
Kapp, D.A. ....	154	Laxpati, S.R. ....	18, 49
Kartal, M. ....	264	Le, C. ....	302
Kasai, H. ....	478	Le Menn, B. ....	44
Kasdepke, T. ....	28	Le Vine, D.M. ....	446
Kasilingam, D. ....	377	Leblebicioglu, K. ....	263
Katehi, L.P.B. ....	125, 277	Lee, C.S. ....	226, 227
Katz, D.S. ....	167	Lee, J.K. ....	425
Kawalko, S.F. ....	18, 49	Lee, K.F. ....	225
Keller, M.G. ....	220	Lee, Robert ....	199
Kelley, D.F. ....	321	Lee, R. ....	405
Kempel, L.C. ....	166	Lee, R.Q. ....	225
Kemptner, E. ....	55, 56	Lee, S. ....	272
Kendra, J.R. ....	58	Lee, W.C. ....	130
Kerestecioglu, F. ....	34	Lee, Y.H. ....	425
Kim, G. ....	476	Leeper, W. ....	145
Kim, Y. ....	375, 449	Leviatan, Y. ....	73, 93
Kipp, R.A. ....	442	Levinson, C.L. ....	94
Kitama, M. ....	481	Li, H. ....	177
Klement, D. ....	56	Li, Q. ....	251
Knyazev, V.V. ....	33, 283	Liboff, A.R. ....	274
Koehler, J.A. ....	458	Liepa, V.V. ....	140, 274
Kokotoff, D.M. ....	329, 412	Lin, J.C. ....	213
Komisarek, K. ....	391	Lindell, I.V. ....	345, 424
Kong, J.A. ....	27	Litva, J. ....	186, 235, 276, 366 367, 368, 369
Koppel, D.H. ....	342	Liu, Q.-H. ....	131
Kotulski, J.D. ....	347	Liu, Y. ....	161, 162
Kouyoumjian, R.G. ....	111, 380	Lo, T. ....	235
Kozlov, A.I. ....	454, 459	Lo, T.K.C. ....	297
Kpodzo, E. ....	185	Logvin, A.I. ....	454, 459
Kralj, D. ....	130	Lou, Y. ....	141, 247
Krems, T. ....	413	Lu, J.Q. ....	304, 447
Krupka, J. ....	392	Luchaninov, A.I. ....	121
Kuga, Y. ....	61, 216, 302		

Luebbers, R.J.....	321		
Luk, K.M. ....	419		
Lüneburg, E. ....	156, 452		
Ma, Q. ....	217		
Macaskill, C. ....	3		
MacPhie, R.H. ....	349, 350		
Madsen, N.K. ....	290		
Maeda, Y. ....	265		
Mahadevan, K. ....	407		
Mamischev, A.V. ....	31		
Manara, G. ....	111, 203		
Manges, J. ....	400		
Manry Jr., C.W. ....	258		
Maradudin, A.A. ....	65, 304, 447		
Marchand, R.T. ....	374		
Marengo, E. ....	104		
Marhefka, R.J. ....	110		
Markey, G.J. ....	27		
Marks II, R.J. ....	272		
Marlia, J.J. ....	352		
Marqués, R. ....	41		
Marston, P.L. ....	113, 308		
Martel, J. ....	223		
Mass, S. ....	317		
Matsumoto, G. ....	269		
Maurin, D. ....	393		
Mautz, J.R. ....	14, 384		
McCormack, C. ....	140		
McDonald, K. ....	59		
McGurn, A.R. ....	65		
McKenzie, S. ....	145		
Medina, F. ....	21, 223, 464		
Megahed, M.A. ....	173		
Megalinsky, V.R. ....	494		
Mei, K.K. ....	161, 162		
Melamed, T. ....	261		
Meloling, J.H. ....	110		
Mendez, E.R. ....	447		
Mesa, F. ....	42		
Michel, T.R. ....	305, 375		
Michelson, D.G. ....	437		
Michielssen, E. ....	48, 195, 411		
Miller, G.E. ....	212		
Miller, W.B. ....	7		
Miranda, F. ....	241		
Mitra, R. ....	40, 48, 72, 73, 165, 195, 200		
			328, 407, 441
Moghaddam, M. ....	59, 60		
Mohajeri, F. ....	469		
Mohamed, D.A. ....	74		
Mohammadian, A.H. ....	291		
Moheb, H. ....	415		
Molinet, F.A. ....	455		
Monorchio, A. ....	203		
Monteith, D.H. ....	112		
Moore, R.L. ....	390		
Morgan, M.A. ....	490		
Mosig, J.R. ....	359		
Mossallaii, H. ....	439		
Mosso, M.M. ....	190		
Mouri, M. ....	215		
Mudaliar, S. ....	309		
Murakawa, K. ....	265		
Muth, L. ....	71		
Nabulsi, K.A. ....	477		
Nag, S. ....	348		
Naibandian, V. ....	226, 227		
Naldini, A. ....	54		
Nashashibi, A. ....	179, 249		
Navsariwala, U. ....	295		
Neelakanta, P.S. ....	228		
Nepa, P. ....	111		
Nespor, G.D. ....	460		
Nevels, R.D. ....	31, 479		
Newell, A.C. ....	102		
Newhouse, J.R. ....	197, 198, 202		
Ng, K.T. ....	268		
Nghiem, D. ....	37		
Ngo, H.D. ....	138, 376		
Nguyen, C. ....	184, 278		
Nikoskinen, K.I. ....	345		
Norgren, M. ....	430		
Norman, A. ....	474		
Nyquist, D.P. ....	39, 143, 251, 252, 396		
Ogawa, T. ....	9		
Okamoto, T. ....	306		
Oliner, A.A. ....	37		
Olsen, R.G. ....	51, 112		
Ornick, S. ....	145, 292		
Orman, M. ....	342		
Ostner, H. ....	413		
Oswald, J. ....	277		

Otero, M.F. ....	343
Otto, G.P. ....	257
Pan, G.-W. ....	22
Pankaskie, T.A. ....	51
Parker, J. ....	403
Parrón, J. ....	163
Pathak, P.H. ....	194, 339, 346
Paulusse, D.C. ....	180
Paynter, F. ....	246
Pearson, L.W. ....	80
Peden, I.C. ....	116, 207
Pekel, Ü. ....	405, 407
Pelosi, G. ....	203
Penno, R.P. ....	473
Peterson, D.B. ....	212
Phu, P. ....	302
Pierro, V. ....	314
Piette, M. ....	245
Piket-May, M. ....	126, 240, 418
Pillai, S.U. ....	130
Pinello, W. ....	323
Pinto, I.M. ....	314
Pisa, S. ....	472
Plant, T.K. ....	352
Plaza, G. ....	42
Plet, J. ....	236
Plumb, R.G. ....	169, 386
Podcameni, A. ....	190
Poosarla, J. ....	103
Posokhov, A.S. ....	121
Pottier, I. ....	453, 456
Pous, R. ....	70, 162, 163
Pregla, R. ....	237, 416
Prince, J.L. ....	32
Priye, V. ....	354
Prouty, Mark D. ....	162
Pugh Jr., E.N. ....	480
Puri, V. ....	281
Pustilnik, M. ....	304
Pyon, J. ....	173
Qi, Y.H. ....	366, 367, 368, 369
Qian, J. ....	143, 394
Qiu, Z. ....	95
Raab, R.E. ....	432
Rabjohn, G. ....	185
Raemer, H.E. ....	141, 247, 248

Rahnavard, M.H. ....	439
Rahnavard, M.H. ....	469
Raju, G.S.N. ....	468
Ramahi, O.M. ....	168
Ramon, C. ....	272
Rao, S.M. ....	75, 160, 164, 385
Rao, V.M. ....	468
Raymat-Samii, Y. ....	83
Reddy, C.J. ....	417
Reed, N. ....	185
Remley, K. ....	352
Renaut, R.A. ....	329
Reuster, D.D. ....	473
Reuter, C.E. ....	240, 418
Riad, S.M. ....	172, 353
Rickett, B. ....	2
Ricklin, J.C. ....	7
Riley, D.J. ....	327
Rino, C.L. ....	138, 376
Robertson, R.C. ....	490
Rodriguez, E. ....	375, 449
Rojas, R.G. ....	343
Romanstrov, Y. ....	284, 285
Roscoe, D. ....	220
Ross, J.E. ....	251, 252, 396
Rothwell, E.J. ....	143, 250, 251, 252
Rousseau, P.R. ....	346
Rowe, M.P. ....	480
Rowell, C.M. ....	291
Roy, T. ....	160, 164
Rubin, B.J. ....	333
Ruis, J.M. ....	163
Ruppel, M. ....	55
Russell, B.D. ....	31
Ryan, P.A. ....	178
Saatchi, S.S. ....	59, 449
Sabban, A. ....	229
Saboundji, H. ....	421
Saed, M.A. ....	486
Said, R.A. ....	50
Saillard, J. ....	456
Sajer, J.M. ....	441
Salazar, M. ....	160, 164
Saleheen, H. ....	268
Sánchez-Gil, J.A. ....	304
Sangary, N. ....	235, 368

Saoudy, S.A. ....	117, 118	Stubenrauch, C.F. ....	102
Sarabandi, K. ....	58, 179, 249	Stuchly, M.A. ....	270, 271, 472
Sarkar, T.K. ....	160, 164, 385	Stuchly, S.S. ....	397
Schmier, R.G. ....	233	Stupfel, B. ....	17, 72, 165
Schneider, J.B. ....	326, 372, 373	Su, W. ....	172
Schwarz, S.E. ....	162	Suchy, K. ....	86
Schwering, F. ....	226	Sullivan, A. ....	142
Schwindt, R. ....	278	Sun, D. ....	29
Sebak, A. ....	50, 361	Sun, K. ....	43
Seidl, A.E. ....	20	Suthers, M. ....	185
Selleri, S. ....	54	Syrett, B. ....	185
Senior, T.B.A. ....	82	Taflove, A. ....	167, 240, 280, 418
Sentenac, A. ....	448	Takacs, L. ....	293, 294
Serebryannikov, A.E. ....	33, 283, 337	Takada, J.-I. ....	478
Shafai, L. ....	358, 415, 443, 462	Takahasi, M. ....	265
Shahpar, S. ....	173	Tanaka, K. ....	340
Shaker, J. ....	443	Tanaka, M. ....	340
Shamsaifar, K. ....	338	Tang, C.H. ....	253
Shankar, V. ....	291	Tashima, H. ....	340
Shen, Y. ....	186	Tassoudji, M.A. ....	27
Sheu, J.T. ....	474	Tay, R.Y.-S. ....	487
Shifrin, Y.S. ....	120, 121, 122	Taylor, D.J. ....	52
Shimizu, K. ....	215, 269, 481	Taylor, L.S. ....	475
Shum, S.M. ....	419	Taylor, M.J. ....	212
Shumpert, J.D. ....	96	Tentzeris, E.M. ....	277
Shupiatsky, A. ....	11, 494	ter Haseborg, J.L. ....	26, 28
Shur, M. ....	127	Tertuliano, H. ....	467
Siegel, P. ....	277	Thiele, E.T. ....	167, 240, 418
Sigelmann, R.A. ....	208	Thieme, M.O. ....	414
Sihvola, A. ....	426	Thorsos, E.I. ....	149, 151
Simpson, H.J. ....	113	Thouroude, D. ....	421
Sinha, B.P. ....	348	Tillery, J.K. ....	224
Skrivervik, A.K. ....	359	Timchenko, A.I. ....	67, 157
Sletten, M. ....	375	Tokuda, Y. ....	265
Smith, C.E. ....	36	Toland, B. ....	491
Smith, W.T. ....	488	Torres-Verdin, C. ....	256
Sochava, A.A. ....	433	Toutain, S. ....	421
Sofko, G.J. ....	458	Tran, M. ....	278
Song, J. ....	143	Tretyakov, S.A. ....	433
Soudais, P. ....	19, 136	Tricoles, G. ....	457
Souza, J.R. ....	466	Tripp, V.K. ....	224
Spring, C.T. ....	16	Trizna, D. ....	375
Steeds, M.W. ....	326	Trostel, J.M. ....	178
Stein, V. ....	56	Tsai, C.Y. ....	250
Strait, B.J. ....	383	Tsang, L. ....	206
Stroud, J.S. ....	308	Tseng, S.T. ....	187

Tsuei, Y.-S. ....	32, 289	Woo, R. ....	210
Tsutsumi, M. ....	354	Wu, C. ....	235, 276, 366, 367
Turhan-Sayan, G. ....	262	.....	368, 369
Turner, C.D. ....	327	Wu, D.I. ....	222
Tyo, J.S. ....	480	Wu, J.C. ....	352
Überall, H. ....	52	Wu, K. ....	393, 436
Ulaby, F.T. ....	58	Wu, M.-S. ....	478
Umashankar, K. ....	18, 288	Wu, S.C. ....	279
Uslenghi, P.L.E. ....	49, 132, 132	Wu, T.K. ....	440
Vakanas, L. ....	30	Wu, T.-L. ....	97
Varadarajan, V. ....	328	Wu, W. ....	137
Vaughan, M.J. ....	183	Wurmser, D. ....	152
Vavriv, D.M. ....	191, 337	Wybourne, M.N. ....	352
Vavriv, L.V. ....	283	Xi, W. ....	270, 271
Verma, A.K. ....	45	Xia, J.J. ....	485
Vermersch, S. ....	200	Yaghjian, A.D. ....	15
Vietzorreck, L. ....	237	Yamaguchi, Y. ....	156, 452
Vitiello, R. ....	132	Yamamoto, K. ....	215, 481
Volakis, J.L. ....	139, 166, 401	Yamashita, M. ....	269
Volman, V. ....	241	Yang, X.H. ....	358
Voronovich, A. ....	150	Yang, Y.E. ....	27
Wahid, P.F. ....	228	Yano, S. ....	9
Wait, R.J. ....	477	Yanovsky, F.J. ....	10, 11
Walton, E. ....	246, 260	Yasuhara, P. ....	457
Wang, G.-Y. ....	4, 6	Yatskevich, V.I. ....	282
Wang, H. ....	187	Yazgan, B. ....	264
Wang, J.-H. ....	422	Ying, Y. ....	36
Wang, J.J.H. ....	224	Yip, B. ....	23
Wang, J.Q. ....	493	Yoshida, N. ....	87, 320
Wang, N. ....	391	Young, C.Y. ....	8
Wang, R.W. ....	15	Young, J.L. ....	322, 324
Wang, T. ....	187	Yousefi, M. ....	92
Wang, W.T. ....	493	Ytterdal, T. ....	127
Watters, D.G. ....	259	Yuan, X. ....	29
Wei, P.P.S. ....	460	Yurkevich, I. ....	304
Weiglhofer, W.S. ....	79, 356, 424, 427	Zapata, J. ....	409
Weikle, II, R.M. ....	182	Zernov, N.N. ....	336
Weinreb, S. ....	183	Zhadan, V. ....	284, 285
Weisshaar, A. ....	352	Zhang, C.X. ....	493
Whites, K.W. ....	428	Zhu, X. ....	22
Williams, J.T. ....	37, 103	Ziolkowski, R.W. ....	85, 312, 315
Williams, K.L. ....	308	Zuffada, C. ....	144, 402, 406
Williams, W. ....	140	Zurk, L.M. ....	62
Wilton, D.R. ....	381		
Winebrenner, D. ....	303		
Wolf, F. ....	26		

## 1995 IEEE AP-S INTERNATIONAL SYMPOSIUM AND USNC/URSI RADIO SCIENCE MEETING

Newport Beach, California  
June 18-23, 1995

The 1995 AP-S International Symposium sponsored by the IEEE Antennas and Propagation Society and the URSI Radio Science Meeting sponsored by USNC Commissions A, B, D, E, F, G, and K of the International Union of Radio Science will be held at Newport Beach, California, June 18-23, 1995. The technical sessions, workshops, and short courses will be coordinated among the two symposia to provide a comprehensive, well-balanced program. Industrial exhibits will be open from June 19th through June 22nd.

- General information may be obtained from:

**Dr. William Imbriale**, Steering Committee Chair  
Jet Propulsion Laboratory 144-201, 4800 Oak Grove Drive  
Pasadena, CA 91109-8099  
tel: (818) 354-5172, fax: (818) 393-6743,  
e-mail: imbriale@voyager.jpl.nasa.gov

- IEEE-APS technical program inquiries should be directed to:

**Dr. Ronald Pogorzelski**  
Technical Program Committee Chair  
Jet Propulsion Laboratory T-1703, 4800 Oak Grove Drive  
Pasadena, CA 91109-8099  
tel: (818) 354-3835, fax (818) 393-0050,  
e-mail: pogo@ccmail.jpl.nasa.gov

- URSI inquiries may be directed to:

**Dr. Ross Stone**  
1446 Vista Claridad, La Jolla, CA 92037  
tel: (619) 459-8305, fax: (619) 459-7140,  
e-mail: 71221.621@compuserve.com

- Potential exhibitors may obtain detailed information from:

**Dr. Michael Thorburn**  
Jet Propulsion Laboratory 238-725, 4800 Oak Grove Drive  
Pasadena, CA 91109-8099  
tel: (818) 354-1843, fax: (818) 354-2825  
e-mail: thorburn@ccmail.jpl.nasa.gov



